



National Library
of Canada

Acquisitions and
Bibliographic Services Branch

395 Wellington Street
Ottawa, Ontario
K1A 0N4

Bibliothèque nationale
du Canada

Direction des acquisitions et
des services bibliographiques

395, rue Wellington
Ottawa (Ontario)
K1A 0N4

Your file *Votre référence*

Our file *Notre référence*

NOTICE

The quality of this microform is heavily dependent upon the quality of the original thesis submitted for microfilming. Every effort has been made to ensure the highest quality of reproduction possible.

If pages are missing, contact the university which granted the degree.

Some pages may have indistinct print especially if the original pages were typed with a poor typewriter ribbon or if the university sent us an inferior photocopy.

Reproduction in full or in part of this microform is governed by the Canadian Copyright Act, R.S.C. 1970, c. C-30, and subsequent amendments.

AVIS

La qualité de cette microforme dépend grandement de la qualité de la thèse soumise au microfilmage. Nous avons tout fait pour assurer une qualité supérieure de reproduction.

S'il manque des pages, veuillez communiquer avec l'université qui a conféré le grade.

La qualité d'impression de certaines pages peut laisser à désirer, surtout si les pages originales ont été dactylographiées à l'aide d'un ruban usé ou si l'université nous a fait parvenir une photocopie de qualité inférieure.

La reproduction, même partielle, de cette microforme est soumise à la Loi canadienne sur le droit d'auteur, SRC 1970, c. C-30, et ses amendements subséquents.

Canada

**NUMERICAL SOLUTION OF REACTING
LAMINAR FLOW HEAT AND MASS TRANSFER
IN DUCTS OF ARBITRARY CROSS-SECTIONS FOR POWER-LAW FLUIDS**

BY

MOHAMMAD ALI ISAZADEH

**A Thesis
Submitted to the Faculty of Graduate Studies and Research
in Partial Fulfilment of the
Requirements for The Degree of
Doctor of Philosophy**

**Department of Chemical Engineering
McGill University
Montreal, Quebec, Canada**

August 1993



National Library
of Canada

Acquisitions and
Bibliographic Services Branch

395 Wellington Street
Ottawa, Ontario
K1A 0N4

Bibliothèque nationale
du Canada

Direction des acquisitions et
des services bibliographiques

395, rue Wellington
Ottawa (Ontario)
K1A 0N4

Your file *Votre référence*

Our file *Notre référence*

The author has granted an irrevocable non-exclusive licence allowing the National Library of Canada to reproduce, loan, distribute or sell copies of his/her thesis by any means and in any form or format, making this thesis available to interested persons.

L'auteur a accordé une licence irrévocable et non exclusive permettant à la Bibliothèque nationale du Canada de reproduire, prêter, distribuer ou vendre des copies de sa thèse de quelque manière et sous quelque forme que ce soit pour mettre des exemplaires de cette thèse à la disposition des personnes intéressées.

The author retains ownership of the copyright in his/her thesis. Neither the thesis nor substantial extracts from it may be printed or otherwise reproduced without his/her permission.

L'auteur conserve la propriété du droit d'auteur qui protège sa thèse. Ni la thèse ni des extraits substantiels de celle-ci ne doivent être imprimés ou autrement reproduits sans son autorisation.

ISBN 0-315-94641-5

Canada

M. A. ISAZADEH THESIS TITLE (shortened):

NUMERICAL SOLUTION OF REACTING

LAMINAR FLOW HEAT AND MASS-TRANSFER

ABSTRACT

This study is concerned with the numerical analysis, formulation, programming and computation of solution of steady, 3D conservation equations of reacting laminar duct flow heat and mass transfer in ducts of arbitrary cross-sections. The non-orthogonal boundary-fitted coordinate transformation method is applied to the Cartesian form of overall-continuity, momenta, energy and species-continuity equations, parabolized in the axial direction. The boundary conditions are also transformed accordingly.

In the mathematical modelling of the system under consideration, variable physical and transport properties of fluid, viscous heat-dissipation and buoyancy effects are also considered. The non-Newtonian power-law constitutive equation is employed to express the rheology of the purely viscous fluids considered.

Applying a novel feature of the solution procedure, the contravariant velocity components are introduced into the transformed equations while the physical Cartesian velocity components are retained as dependent variables of the velocity field in the equations. This approach greatly simplifies the subsequent finite-difference formulation of the transformed equations. The latter equations are discretized by the control-volume finite-difference method in which a suitably-adopted staggered grid is employed using Patankar's B-type arrangement in the transformed plane. For discretization, the transformed equations are integrated over 3D control-volumes, followed by differencing the convective and diffusive terms employing upwind and central-difference schemes respectively. A modified version of the SIMPLER algorithm is introduced in the solution procedure and a line-by-line TDMA algorithm is employed for the solution of the discretization equations.

A computer-programme is developed for the generation of non-orthogonal grids corresponding to the B-type arrangement in the transformed plane. A general computer programme in Fortran is developed in this study for the solution of flow, heat and mass transfer problems for laminar reacting fluids in straight ducts of arbitrary cross-sections for Newtonian and purely viscous non-Newtonian fluids. The model and computer codes are validated by theoretical, experimental and numerical results from various sources.

The computer programmes are employed for studies in the analysis of hydrodynamics and heat transfer in the thermal entrance regions of ducts of arbitrary cross-sections for Newtonian and non-Newtonian fluids. Relevant results are documented for triangular, trapezoidal and pentagonal ducts. The computer programmes are ultimately employed for simulation of the production of polystyrene in arbitrary cross-sectional duct reactors.

RÉSUMÉ

Dans cette étude, on présente une modélisation numérique des équations de conservation de quantité de mouvement, d'énergie et de masse dans un écoulement laminaire en régime établi d'un fluide en réaction à l'intérieur d'une gaine tri-dimensionnelle dont la géométrie de la section est arbitraire. Un système des coordonnées curvilignes non orthogonales adaptées aux parois du domaine de solution est utilisé pour transformer les équations de base. Les conditions limites ont également été transformées en fonction du nouveau système des coordonnées.

Le modèle mathématique de solution tient compte de la variation des propriétés physiques de fluide, ainsi que des autres effets tel que la dissipation visqueuse et la flottaison dans le fluide. Des solutions sont présentées pour l'écoulement d'un fluide Newtonien, ainsi que pour un fluide non-Newtonien dont la viscosité varie selon la loi de puissance.

Dans la procédure de solution, une nouvelle approche a été adoptée, où les composants contravariant de la vélocité sont introduits dans l'équation transformée tandis que les composants contravariants de la vélocité sont introduits dans l'équation transformée tandis que les composants cartésiens de vitesse sont maintenus comme variables dépendants dans les équations de mouvement. Cette approche simplifie la formulation en différences finies des équations transformées de profil de vitesse. Ces équations sont discrétisées dans un nombre de volumes de contrôles et un réseau des noeuds déplacés en avant dans un arrangement de type B décrite par Patankar. Les équations de base sont intégrées sur chaque volume de contrôle, les termes représentant de la convection et de la diffusion sont convertis dans les équations des différences finies en utilisant la méthode des valeurs en amont et des différences centrales. Une version modifiée de l'algorithme SIMPLER est introduite et la solution des équations des différences finies est assurée par un balayage ligne-par-ligne et l'algorithme de AMTD.

Un logiciel a été développé pour la génération des coordonnées non-orthogonales qui correspond à un arrangement de type B dans le plan de transformation. Un deuxième programme en Fortran a été également écrite pour solutionner les problèmes de l'écoulement, transfert de chaleur et de masse dans un écoulement laminaire d'un fluide Newtonien et non-Newtonien en réaction à l'intérieur d'une gaine droite à section arbitraire. Le modèle et le logiciel ont été validés par des résultats théoriques et expérimentaux venant des sources variées.

Les logiciels ont servis pour étudier l'écoulement et le transfert de chaleur dans la section d'entrée dans une gaine à section variable d'un fluide Newtonien et non-Newtonien. Des résultats ont été documentés pour des gaines à section triangulaire, trapézoïdale et pentagonale. Les logiciels peuvent servir pour simuler la production de polystyrène dans des réacteurs utilisant des gaines à sections variables.

ACKNOWLEDGEMENTS

I wish to express my sincere appreciation to Professor Arun S. Mujumdar, my thesis supervisor, for his support of the study, encouragement and guidelines regarding research and development of the present subject.

I also wish to express my gratitude to Professor Mainul Hasan, my thesis co-supervisor, for his extensive support, useful discussions and guidance throughout this study.

I am also very grateful for the financial support from Abadan Institute of Technology (Iran) to pursue the present study.

The cooperation of the Computer Center of McGill University is acknowledged for allocating mainframe computing time on IBM3090 and IBM ESA 9000 machines.

TABLE OF CONTENTS

	PAGE
ABSTRACT	
ACKNOWLEDGEMENTS	
CHAPTER 1 LITERATURE REVIEW AND BACKGROUND	1-1
1.1 NEWTONIAN FLUIDS	1-1
1.2 NON-NEWTONIAN FLUIDS	1-4
1.3 THERMAL POLYMERIZATION OF STYRENE	1-6
1.4 CLOSURE	1-10
CHAPTER 2 MATHEMATICAL MODELLING IN CARTESIAN COORDINATES	2-1
2.1 INTRODUCTION	2-1
2.2 GENERAL CONSERVATION LAWS	2-3
2.3 CONSERVATION LAWS IN CARTESIAN COORDINATES	2-4
2.4 THE STRESS TENSOR	2-5
2.5 CONSIDERATIONS INTRODUCED IN THE CONSERVATION EQUATIONS	2-8
2.6 PARABOLIC APPROXIMATION	2-9
2.7 THE PARABOLIZED GOVERNING EQUATIONS IN CARTESIAN COORDINATES	2-11
2.8 THE BOUNDARY CONDITIONS	2-13
2.9 CLOSURE	2-15

TABLE OF CONTENTS (*Continued*)

CHAPTER 3	COORDINATE TRANSFORMATION AND NUMERICAL METHOD OF SOLUTION	3-1
3.1	INTRODUCTION	3-1
3.2	THE ORTHOGONAL AND NON-ORTHOGONAL COORDINATE SYSTEMS	3-2
3.3	CURVILINEAR TRANSFORMATION	3-3
3.4	NUMERICAL GRID GENERATION	3-5
3.5	TRANSFORMATION OF THE GOVERNING EQUATIONS	3-8
3.6	DISCRETIZATION OF TRANSFORMED EQUATIONS .	3-9
3.7	SOLUTION PROCEDURE	3-12
3.8	CLOSURE	3-18
CHAPTER 4	THE TRANSFORMATION AND DISCRETIZATION OF GOVERNING EQUATIONS AND BOUNDARY- CONDITIONS	4-1
4.1	INTRODUCTION	4-1
4.2	THE TRANSFORMED GOVERNING EQUATIONS . . .	4-2
4.3	THE EXPANDED SET OF TRANSFORMED GOVERNING EQUATIONS	4-5
4.4	THE DISCRETIZATION EQUATIONS	4-9
4.5	THE DISCRETIZED BOUNDARY CONDITIONS . . .	4-26
4.6	CLOSURE	4-32
CHAPTER 5	POLYMERIZATION OF STYRENE	5-1
5.1	INTRODUCTION	5-1
5.2	KINETICS OF THERMAL POLYMERIZATION OF STYRENE	5-2

TABLE OF CONTENTS (*Continued*)

	5.3	DATA FOR SYSTEM PROPERTIES	5-6
	5.4	PREDICTION OF MOLECULAR WEIGHT DISTRIBUTION	5-6
	5.5	THERMAL INSTABILITY	5-8
	5.6	CLOSURE	5-9
CHAPTER	6	THE SELECTED GEOMETRIES AND GRID GENERATION	6-1
	6.1	INTRODUCTION	6-1
	6.2	THE COMPUTER CODES FOR GRID GENERATION .	6-1
	6.3	GRID GENERATION PLOTS	6-2
CHAPTER	7	THE COMPUTER CODE FOR CONSERVATION EQUATIONS	7-1
	7.1	INTRODUCTION	7-1
	7.2	THE MAIN PROGRAMME	7-2
	7.3	SUBROUTINES	7-8
CHAPTER	8	RESULTS AND DISCUSSIONS	8-1
	8.1	INTRODUCTION	8-1
	8.2	FLUID FLOW	8-1
	8.3	HEAT TRANSFER	8-26
	8.4	MASS TRANSFER WITH CHEMICAL REACTION . .	8-39
	8.5	SIMULTANEOUS REACTING FLOW, HEAT AND MASS-TRANSFER	8-44
CHAPTER	9	CONCLUSIONS AND CONTRIBUTIONS TO KNOWLEDGE	9-1

TABLE OF CONTENTS (*Continued*)

	9.1 INTRODUCTION	9-1
	9.2 SUMMARY AND CONCLUSIONS	9-1
	9.3 CONTRIBUTIONS TO KNOWLEDGE	9-3
REFERENCES	R-1
NOMENCLATURE	N-1
APPENDIX A	DERIVATION OF TRANSFORMATION RELATIONS	A-1
	A.1 BASIC RELATIONS	A-2
	A.2 DERIVATION OF DERIVATIVE TRANSFORMATIONS	A-2
	A.3 DERIVATION OF RELATIONS ($\frac{\partial f}{\partial x}$ & $\frac{\partial f}{\partial y}$)	A-4
	A.4 TRANSFORMATION OF POISSON EQUATION	A-5
	A.5 DERIVATION OF DISCRETIZATION-EQUATION FOR GRID-GENERATION EQUATIONS	A-14
APPENDIX B	DERIVATION OF TRANSFORMED GOVERNING EQUATIONS	B-1
	B.1 THE OVERALL CONTINUITY EQUATION	B-2
	B.2 THE MOMENTUM EQUATIONS	B-3
	B.3 THE ENERGY EQUATION	B-10
	B.4 THE REACTANT CONTINUITY EQUATION	B-14
	B.5 THE TRANSFORMED FORM OF THE COMPONENTS STRESS TENSOR	B-17
	B.6 THE TRANSFORMED FORM OF "I" AND "M"	B-18
APPENDIX C	DERIVATION OF DISCRETIZATION EQUATIONS	C-1
APPENDIX D	MODELLING OF COEFFICIENTS OF DISCRETIZATION EQUATIONS IN I-J COORDINATES	D-1

TABLE OF CONTENTS (*Continued*)

	D.1 COEFFICIENTS FOR THE "U1" MOMENTUM EQUATION	D-2
	D.2 COEFFICIENTS FOR THE "U2" MOMENTUM EQUATION	D-9
	D.3 COEFFICIENTS FOR THE "W" MOMENTUM EQUATION	D-15
	D.4 COEFFICIENTS FOR THE ENERGY EQUATION	D-20
APPENDIX	E DERIVATION OF DISCRETIZED BOUNDARY CONDITIONS FOR REACTANT CONTINUITY EQUATION	E-1
APPENDIX	F DERIVATION OF RELATIONS OF PRESSURE-VELOCITY COUPLING IN TRANSVERSE DIRECTION	F-1
	F.1 DERIVATION OF PRESSURE-CORRECTION EQUATIONS	F-2
	F.2 DERIVATION OF THE PRESSURE-EQUATION FOR SIMPLER ALGORITHM	F-23
APPENDIX	G DERIVATION OF MISCELLANEOUS RELATIONS	G-1
	G.1 CONTRAVARIANT VELOCITIES	G-2
	G.2 CONTRAVARIANT VELOCITIES SATISFYING MASS CONSERVATION	G-4
	G.3 CONTRAVARIANT VELOCITIES NOT SATISFYING MASS CONSERVATION	G-6
	G.4 PHYSICAL VELOCITIES	G-6
	G.5 APPLICATION OF RELAXATION FACTORS	G-7
	G.6 PRESSURE-GRADIENT TERMS IN I AND J COORDINATES	G-10

TABLE OF CONTENTS (Continued)

G.7	DERIVATION OF PRESSURE-GRADIENT TERM FOR BOUNDARY CONTROL-VOLUMES (J=2 AND J=M2)	G-11
G.8	DERIVATION OF PRESSURE-GRADIENT TERM FOR BOUNDARY CONTROL VOLUMES (I=2 AND I=L2)	G-13
G.9	BUOYANCY-TERM IN y-MOMENTUM EQUATION	G-15
G.10	NUSSELT-NUMBER	G-17
APPENDIX H	COMPUTER SOFTWARE	H-1
H.1	INPUT DATA AND FILE ALLOCATIONS FOR GRID PROGRAMMES	H-2
H.2	SEQUENCE OF STEPS ON MUSIC-A OPERATING SYSTEM FOR GRID GERENATION	H-17
H.3	SEQUENCE OF STEPS ON MUSIC-A AND "OS" OPERATING SYSTEMS FOR SOLUTION OF DISCRETIZATION EQUATIONS	H-17
H.4	A BRIEF USER'S GUIDE (INPUT INSTRUCTION) FOR STAR30.FOR PROGRAMME	H-17
H.5	LIST OF COMPUTER PROGRAMMES	H-18

LIST OF FIGURES

FIGURE		PAGE
2.1	Arbitrary cross-sectional duct in Cartesian coordinates	2-2
3.1	Curvilinear transformation	3-19
3.2	Grid generation	3-19
3.3	Contravariant velocities	3-19
3.4	Non-staggered grid arrangement	3-20
3.5	Classical staggered grid arrangement	3-20
3.6	Grid arrangement adopted	3-21
3.7	Three dimensional control volume in transformed-plane	3-21
3.8	Physical velocities over the whole computational domain	3-22
4.1	Control volume for u_e and v_e	4-33
4.2	Control volume for u_n and v_n	4-33
4.3	Control volume for u_w and v_w	4-33
4.4	Control volume for u_s and v_s	4-33
4.5	Control volume for w_p , h_p and v_p	4-33
6.1	21 × 21 B-type grid for circular duct	6-4
6.2	21 × 21 B-type grid for square duct	6-4
6.3	21 × 21 B-type grid for triangular duct	6-4
6.4	21 × 21 B-type grid for trapezoidal duct	6-5
6.5	21 × 21 B-type grid for pentagonal duct	6-5
6.6	21 × 21 B-type grid for hexagonal duct	6-5
7.1	Marching sequence through a duct	7-3
7.2	Flow chart of the computer programme	7-3
8.1(a-d)	Centerline velocity development (Newtonian)	8-10
8.2(a-d)	d.l. press.-drop vs. d.l. axial dist. (Newtonian)	8-11

LIST OF FIGURES (Continued)

8.3(a-d)	Development of axial velocity profile (Newtonian)	8-12
8.4(a-d)	Centerline velocity development (non-Newtonian)	8-13
8.5(a-d)	d.l. press.-drop vs. d.l. axial dist. (non-Newtonian)	8-14
8.6(a-d)	Development of axial velocity profile (non-Newtonian)	8-15
8.7	d.l. press.-drop vs d.l. axial-dist. (Newtonian/circle)	8-16
8.8	Secondary flow velocity profiles for a square duct, Newtonian fluids, $Re = 900$, $(z/D_h)/Re = 0.0054$	8-17
8.9	Secondary flow velocity profiles for a square duct, non-Newtonian fluids, $(n=0.5)$, $Re = 128$, $(z/D_h)/Re = 0.0115$	8-17
8.10a & b	Secondary flow velocity profiles for a trapezoidal duct, Newtonian fluids, $Re = 900$, $(z/D_h)/Re = 0.0054$	8-18
8.11a & b	Secondary flow velocity profiles for a trapezoidal duct, non-Newtonian fluids, $(n=0.5)$, $Re = 128$, $(z/D_h)/Re = 0.0115$	8-19
8.12a & b	Secondary flow velocity profiles for a triangular duct, Newtonian fluids, $Re = 900$, $(z/D_h)/Re = 0.0054$	8-20
8.13a & b	Secondary flow velocity profiles for a triangular duct, non-Newtonian fluids, $(n=0.5)$, $Re = 128$, $(z/D_h)/Re = 0.0115$	8-21
8.14a & b	Secondary flow velocity profiles for a pentagonal duct, Newtonian fluids, $Re = 900$, $(z/D_h)/Re = 0.0054$	8-22
8.15a & b	Secondary flow velocity profiles for a pentagonal duct, non-Newtonian fluids, $(n=0.5)$, $Re = 128$, $(z/D_h)/Re = 0.0115$	8-23
8.16	Axial velocity contours, Newtonian fluids, square ducts, $Re = 900$ (@ F.D.)	8-24

LIST OF FIGURES (Continued)

8.17	Axial velocity contours, Newtonian fluids, triangular ducts, <i>Re</i> = 900 (@ F.D.)	8-24
8.18	Axial velocity contours, Newtonian fluids, trapezoidal ducts, <i>Re</i> = 900 (@ F.D.)	8-25
8.19	Axial velocity contours, Newtonian fluids, pentagonal ducts, <i>Re</i> = 900 (@ F.D.)	8-25
8.20	Nusselt number variation along the square duct (Newtonian) . . .	8-34
8.21(a-d)	d.l. temperature vs. d.l. axial-dist. (Newtonian)	8-35
8.22(a-d)	Development of temperature profile (Newtonian)	8-37
8.23(a-h)	Case # 1 mol. wt. distribution	8-50
8.24(a-h)	Case # 2 mol. wt. distribution	8-52
8.25(a-h)	Case # 3 mol. wt. distribution	8-54
8.26(a-h)	Case # 4 mol. wt. distribution	8-56
8.27(a-h)	Case # 5 mol. wt. distribution	8-58
8.28(a-h)	Case # 1 axial velocity profile	8-60
8.29(a-h)	Case # 1 temperature profile	8-62
8.30(a-h)	Case # 1 polymer concentration profile	8-64
8.31(a-h)	Case # 1 density profile	8-66
8.32(a-h)	Case # 1 viscosity profile	8-68
8.33(a-h)	Case # 2 axial-velocity profile	8-70
8.34(a-h)	Case # 2 temperature profile	8-72
8.35(a-h)	Case # 2 polymer concentration profile	8-74
8.36(a-h)	Case # 2 density profile	8-76
8.37(a-h)	Case # 2 viscosity profile	8-78
8.38(a-h)	Case # 3 axial-velocity profile	8-80

LIST OF FIGURES (Continued)

8.39(a-h)	Case # 3 temperature profile	S-82
8.40(a-h)	Case # 3 polymer concentration profile	S-84
8.41(a-h)	Case # 3 density profile	S-86
8.42(a-h)	Case # 3 viscosity profile	S-88
8.43(a-h)	Case # 4 axial-velocity profile	S-90
8.44(a-h)	Case # 4 temperature profile	S-92
8.45(a-h)	Case # 4 polymer concentration profile	S-94
8.46(a-h)	Case # 4 density profile	S-96
8.47(a-h)	Case # 4 viscosity profile	S-98
8.48(a-h)	Case # 5 axial-velocity profile	S-100
8.49(a-h)	Case # 5 temperature profile	S-102
8.50(a-h)	Case # 5 polymer concentration profile	S-104
8.51(a-h)	Case # 5 density profile	S-106
8.52(a-h)	Case # 5 viscosity profile	S-108
C.1	Typical derivation for " u_z "	C-7
D.1 to D.34	Modelling of coefficients of discretization equations	D-25 to D-39
E.1	Boundary condition on the physical plane	E-9
E.2	Boundary condition on the computational plane	E-9
E.3	Control volume @ J=M1 boundary	E-10
F.1	Derivation of pressure correction equation	F-2
F.2	Relations for pseudovelocities in I and J coordinates	F-25
F.3	Relations for pseudovelocities in I and J coordinates	F-26
G.1 to G.11	Related to derivation in Appendix "G"	G-19 to G-22

LIST OF TABLES

TABLE		PAGE
5.1	Fluid properties data	5-6
6.1	The optimum relaxation factor and number of iterations	6-2
6.2	List of the selected geometries	6-3
8.1	Results for centerline velocity and pressure gradient	8-3
8.2	Results for centerline velocity	8-3
8.3	Residual values (fluid flow)	8-4
8.4	Development length results (n=1)	8-5
8.5	Residual values (heat transfer)	8-27
8.6	$Nu_{z,T}$ variations for different geometries, Newtonian fluids, $Pr = 6.78$	8-28
8.7	$Nu_{m,T}$ variations for different geometries, Newtonian fluids, $Pr = 6.788$	8-28
8.8	Thermal entry length and limiting Nu_T results	8-29
8.9	Comparison of limiting Nusselt numbers	8-29
8.10	Comparison of Nusselt number, $Nu_{z,T}$ variations (n=1)	8-31
8.11	Comparison of Nusselt number, $Nu_{m,T}$ variations (n=1)	8-31
8.12	$Nu_{z,T}$ variations for square ducts	8-32
8.13	$Nu_{z,T}$ variations for triangular ducts	8-32
8.14	$Nu_{z,T}$ variations for trapezoidal ducts	8-33
8.15	$Nu_{z,T}$ variations for pentagonal ducts	8-33
8.16a	Chi-Chi Chen, Simulation results	8-40
8.16b	Present work simulation results	8-40
8.17a	Husain and Hamielec, simulation results	8-41
8.17b	Present work simulation results	8-41
8.17c	Present work simulation results	8-41
8.18a	Chi-Chi Chen, Simulation results	8-42

LIST OF TABLES (Continued)

8.18b	Present work simulation results	8-42
8.19a	C. Kleinstreuer and S. Agarwal, Simulation results	8-43
8.19b	Present work simulation results	8-43
8.20	Operating conditions	8-44
8.21	Residual values (mass transfer)	8-44
8.22	Diameter of circular ducts corresponding to non-circular geometries .	8-45
8.23	Simulation results of styrene polymerization at reactor exit (case # 1)	8-46
8.24	Simulation results of styrene polymerization at reactor exit (case # 2)	8-47
8.25	Simulation results of styrene polymerization at reactor exit (case # 3)	8-47
8.26	Simulation results of styrene polymerization at reactor exit (case # 4)	8-48
8.27	Simulation results of styrene polymerization at reactor exit (case # 5)	8-48

CHAPTER 1

LITERATURE REVIEW AND BACKGROUND

1.1 NEWTONIAN FLUIDS

Bosworth¹ studied the distribution of reaction times in laminar flow tubular reactors, the reaction being either homogeneously catalyzed or uncatalyzed. In laminar flow different filaments of the stream travel at different speeds as a result of the velocity profile so that the different sections of the fluid will have different reaction times. At any given rate of flow and given reaction vessel there is a population of reaction times exhibiting a certain distribution curve. He dealt first with the distribution under conditions of negligible molecular diffusion and later investigated the effect of molecular diffusion radially and longitudinally when it is taken into account. He also determined the conditions under which axial or radial diffusion effects can be neglected in evaluating the reaction rate data for reactors with noncatalytic walls. He concluded that the modifying effect of diffusion on the reaction time distribution curve is most pronounced in the smallest vessels. In liquid systems, however, there is wider range of possible reactor sizes for which the effect of diffusion is negligible. He also noted that since in chemical engineering circles it is regarded as a normal practice to make the length of a reaction vessel at least ten times the diameter, his condition for negligible longitudinal diffusion effect is usually automatically satisfied.

Denbigh² showed that for laminar flow the diffusion effect is often quite negligible in liquids provided that the departure from the parabolic velocity distribution is not

too large.

Cleland et al.³ studied diffusion and chemical reaction in viscous flow non-catalytic tubular reactors. They obtained a numerical solution in which only radial diffusion of the reactant was considered and the axial diffusion was neglected. The distribution of contact time in laminar flow causes a radial concentration gradient to be established which in turn tends to be diminished by molecular diffusion and under some conditions by free convection. Considering an isothermal liquid phase first order chemical reaction, steady state, axial symmetry, flow in axial direction only, no axial diffusion and no volume change on reaction, the mass balance equation for a chemical component was written with the velocity profile described by the Poiseuille's equation. A comparison of their theoretical predictions and experimental data showed satisfactory results. However, under certain circumstances, free-convection, which was not included in their solution, may have had important effects in laminar flow tubular reactor performance.

Lauwerier⁴ obtained an analytical solution for the concentration of a substance in a fluid in Poiseuille flow, under the following conditions: an irreversible first order homogeneous chemical reaction, steady state, isothermal condition, and constant physical properties. He neglected the axial diffusion. A separation of variables method was applied to obtain the solution of the partial differential equation describing the system while an orthogonal set of eigenfunctions were determined for the eigen-value problem. Also an asymptotic solution of the eigen-value equation was determined, valid for higher eigen-values.

Wissler et al.⁵ later performed a numerical solution of Lauwerier's formulation in which, the eigenvalues, the Fourier expansion coefficients, the norms and eigenfunctions were computed and tabulated. These numbers coupled with the analytical results obtained by Lauwerier allow one to determine the composition of the reacting specie as a function of position. They also tabulated the average concentration values determined by Cleland et al.³, and the results obtained in their work which showed excellent

agreement. They extended Lauwerier's method to deal with the case of consecutive first-order reaction $A \longrightarrow B \longrightarrow C$ etc. and obtained an analytical solution for this case.

Katz⁶ studied a reaction catalysed on the wall of a cylindrical tube for a process gas undergoing an axial flow with a pre-assigned radial pattern of axial velocity. He neglected axial diffusion compared to the main convective effect of the gas stream, thus the range of applications would likely be for Poiseuille flow and a correspondingly low molecular diffusivity. Considering steady isothermal situation he introduced the mathematical formulation of the physical system in question and then carried out a reduction to an integral equation. Applications to kinetic analysis and to reactor design was then discussed. A suitable eigenfunction expansion of the kernel of the integral equation was then developed.

Walker⁷ studied the performance of a tubular reactor including first-order homogeneous and heterogeneous reactions and Poiseuille flow, including both axial and radial diffusion. He showed that exact analytical solutions to such problems are impossible to obtain and numerical methods must be used.

Hsu⁸ obtained analytical solution for the problem previously solved by Cleland et al.³ numerically, using separation of variables method. He applied, however, numerical integration to the characteristic value problem to obtain the eigenvalues, eigenfunctions and relevant constants for a specific value of diffusion parameter. The main advantage of this method of solution is claimed to be the explicit expression of the reactant concentration, while using a numerical method for solving the partial differential equation, leads to solution through implicit difference schemes. Also, there is no need to worry about convergence and stability as is required for the numerical methods. Obviously these are advantages of any analytical solution to numerical solution.

Solomon et al.⁹ studied the interaction of irreversible, first order, simultaneous heterogeneous and homogeneous reactions in an isothermal tubular reactor under laminar

inar flow conditions. The irreversible reaction, $A \rightarrow$ products, is considered under steady state conditions. Assuming dilute solution, constant fluid properties, Poiseuille velocity distribution and no axial-diffusion, an analytical solution was obtained for the problem using the separation of variables approach for which the characteristic value problem was solved by the Galerkin method¹⁰, expanding the eigenfunctions in a complete set of trial functions. Ultimately, the values of the eigenvalues, eigenfunctions, coefficients and radial concentration profile were obtained for a dilute system. Further investigations were carried out to deduce the conditions under which the homogeneous reaction may be neglected in favor of the heterogeneous reaction and vice-versa. It was shown that the effect of heterogeneous reaction on the radial concentration profiles is negligible for low heterogeneous rates and for large homogeneous rates, that is, when the homogeneous reaction rate is the controlling factor. An alternate case was also studied viz. the heterogeneous reaction rate controlling. A limiting case of this problem is the classical Graetz problem for which accurate values of the eigenvalues and vectors were obtained numerically by Brown¹¹ and asymptotically by Sellars et al.¹².

1.2 NON-NEWTONIAN FLUIDS

The problem of homogeneous reaction in a purely viscous non-Newtonian fluid in laminar flow in a tubular reactor has several industrial applications. The thermal pasteurization of liquid food products is a typical example, where the liquid behaviour is non-Newtonian and the death rate of microorganisms is proportional to the population density of the microorganisms implying first-order kinetics¹⁷. The tubular polymerization reaction is another example with complex kinetics and variable physical properties.

Homsy et al.¹³ studied the problem of diffusion and chemical reaction in a tubular reactor for non-Newtonian fluids in laminar flow operating under isothermal and steady conditions using a first-order reaction. They assumed negligible axial diffusion of the reactant. The characteristic value problem resulting from the separation of variables

was solved by the method of Galerkin for various Ostwald de Waele (or power-law) and Prandtl-Eyring models.

Osborne¹⁴ developed a convective model for the laminar flow performance of a tubular reactor with a liquid reaction medium. Laminar flow severely restricts the application of the axial dispersion model so widely used under turbulent flow conditions. Levenspiel¹⁵ recommends a criterion for using the dispersion model in characterizing the tracer response of laminar flow reactors so that small molecular diffusivity of liquids limits the laminar flow application of the dispersion model to very long reactors. The conservation equation for laminar flow assuming axially symmetric, steady, fully developed incompressible flow with any order reaction was first introduced. Owing to the negligible effects of molecular diffusion as compared with the effects of the velocity profile, which has been shown by Bosworth¹ and Cleland et al.³, the diffusion terms were neglected to yield a pure convective model for the laminar flow reactor. A solution of the resulting differential equation for the displacement of non-reactive tracer injected into the reactor inlet can be used to relate average effluent concentrations to the inlet stimulus for step and impulse inputs. These effluent tracer concentration responses were used to evaluate the apparent velocity profile index which was related to the non-Newtonian laminar flow reactor performance. The model was then extended to a multiple reaction sequence, $A \longrightarrow B \longrightarrow S$.

Tsay et al.¹⁶ studied the unsteady and steady state Graetz problems for mass transfer with first order chemical reaction in the entrance region for fully developed laminar flow of power-law non-Newtonian fluids in a circular tube. They applied the instantaneous local similarity method to the unsteady state problem and local similarity method to the steady problem. The solutions of the first method, however, are restricted to small times and small axial distance from the entrance and the solutions of the second method are restricted to small axial distance from the entrance.

Venkatsubramanian et al.¹⁷ studied convective diffusion with reaction for develop-

ing flow of a non-Newtonian fluid in the entrance region of a round conduit. Using the approximate solution of Langhaar¹⁸ for the entrance velocity profiles, they obtained conversions for homogeneous bulk phase reactions and wall-catalyzed heterogeneous reactions. For a steady, two-dimensional flow with constant physical properties and for power-law fluids they solved the governing equations numerically. The equation for concentration was solved using the Crank-Nicolson scheme of finite-difference scheme. The resulting set of tridiagonal system of equations was then solved by the Thomas algorithm. They showed graphically the variation of bulk average concentration with normalized-distance for different values of Schmidt numbers and reaction-parameter for both Newtonian and non-Newtonian fluids. For a given value of reaction parameter, they observed that the influence of flow development is higher at lower Schmidt numbers. Typical non-Newtonian liquids are large Schmidt number fluids as they are rather viscous and the diffusivities are rather low. For high Schmidt number systems the calculations approach those of a fully-developed flow. Thus the flow development in non-Newtonian systems could be neglected and calculations could be based on those for fully developed conditions.

Cavatorta et al.¹⁹ used the orthogonal collocation method developed by Villadsen et al.²⁰ to solve the problem of isothermal tubular reactor with first-order chemical reaction for laminar flow for two types of non-Newtonian fluids: A power-law or Oswald de Waele model and a Prandtl-Eyring model. Comparison of the results with those obtained by Homsy et al.¹⁴ showed good agreement.

1.3 THERMAL POLYMERIZATION OF STYRENE

The reaction chosen for simulation in this study is the thermal bulk polymerization of styrene in a rectilinear tubular reactor. There are several articles in the literature dealing with thermally and chemically initiated tubular polymerization of styrene of which only a few papers of interest are selected here for discussion on thermal poly-

merization of styrene.

Sala et al.²² analyzed styrene polymerization by solving the steady, two dimensional conservation equations numerically using the upwind scheme for convective terms and the stream-function/vorticity approach. The finite difference equations were solved by Gauss-Seidel technique. The fluid was assumed to be Newtonian. Polystyrene, however, is a non-Newtonian fluid. Variable (temperature-dependent) physical properties were used. The viscous heat generation was disregarded. A simple first-order kinetics along with a constant molecular weight of 70,000 was employed. The influence of inlet feed concentration, inlet temperature, and feed-rate on the temperature distribution in adiabatic and isothermal tubular reactors was analyzed. It was concluded that adequate control of the polymerization can be achieved by maintaining the tube wall temperature below the inlet feed temperature to inhibit thermal runaway.

Wyman et al.²³ introduced an approximate model to calculate the number and weight-average molecular weights of the polymer being produced in a continuous steady-state tubular reactor from the zeroth, first and second moments of radical and polymer distributions. The partial differential equations describing temperature, velocity and composition were written considering axial symmetry and incompressible laminar flow in a cylindrical tube, allowing for variable viscosity and conductivity. The reaction rate constant was of Arrhenius type in which the so-called gel effect was also taken into account. The pressure drop in the tube was obtained from the equation of motion. Radial convection, axial conduction and viscous heating of polymer in the energy balance equation were neglected. The radial and angular components of velocity were ignored in the equation of motion. The partial differential equations were solved numerically using the classical explicit finite-difference method.

Husain et al.²⁴ made a computational study of bulk thermal polymerization of styrene in a tubular reactor in which the fluid rheology was represented by a power-law model. They considered the polymer to be a non-diffusing specie and neglected

radial velocities. They also neglected the axial diffusion of mass and energy. They took into account the gel effect following Hui et al.²¹. The system of differential equations was solved by finite differencing radially and solving the resulting equations using a fourth-order Runge-Kutta-Gill routine.

Valsamis et al.^{25,26} used piston flow and segregated flow models for the polymerization of styrene in tubular reactors. Experiments were performed in a helically coiled tube with a length of 14.6 m and a diameter of 0.46 cm. Running pure thermal styrene polymerization at 160 degrees Celsius yielded a conversion of 15% in 5.15 minutes residence time.

Chen et al.^{27,28} determined the residence time wash-out function theoretically by means of flow models and experimentally by inert tracer techniques. Introducing steady mass, momentum and energy transport equations for laminar axisymmetric flow in cylindrical coordinates using fully-developed velocity profile in axial direction. The mass diffusion and heat conduction in axial direction were ignored. The viscous heating effect was also ignored. The fluid was assumed Newtonian. The polymer was considered to be non-diffusing. The kinetic rate constants were obtained from Hui et al.²¹, while the physical property data were obtained from various sources. The partial differential equations were solved by the method of lines (MOL) in which the equations were approximated by a set of initial value problems (IVP) in ordinary differential equations which were then discretized using finite differences and solved by IVP solvers. The model predicted axial and radial velocity profiles which were subsequently used in a tracer model which consisted of the unsteady, two-dimensional convective diffusion equation. The solution of this model evaluated at the tube outlet provided the residence time wash-out function. Experimental measurements were made to verify the theoretical model for residence time distribution using toluene as a nonreactive inert tracer. The measured wash-out function confirmed the presence of velocity profile elongation. Molecular weight of polymer was also calculated using the approach based on

the zeroth, first and second moments of radical and polymer distributions.

Kleinstreuer et al.^{29,30} solved the two-dimensional equations governing the thermal polymerization of styrene at steady state in the laminar flow in a straight circular duct assuming axial-symmetry and power law model for liquid behaviour. They neglected the body force term but considered variable physical properties and a developing flow with parabolic velocity profile at inlet. They obtained the kinetic rate constants from Hui et al.²¹ and the data for physical properties from various sources. They employed control volume approach for discretization and used a software package using the SIMPLE algorithm to obtain the results. They analyzed a simple tube as a representation of the shell-and-tube type configuration. They generated stability plots by computer experimentation varying the effective system parameters and concluded that a small tube up to a radius of 2 cm could be effectively used to carry out styrene polymerization. However, as the tube radius increases, the problem of thermal runaway and flow elongation make the operation unfeasible.

Malkin and Zhirkov^{31,32} discussed the effect of viscosity growth on the macrokinetics features of the polymerization process and the influence of velocity profile distortion over the heat and mass transfer characteristics. Due to the velocity distribution and therefore the distribution of residence times along the radius, the liquid layers stay longer near the reactor wall than near the axis. Therefore they react more fully, and hence, the liquid viscosity near the wall becomes much higher compared to that near the axis. The more viscous liquid flows more slowly and remains inside the reactor for a longer period of time as a result of which the following flow structure forms: very viscous products near the wall and a much less viscous mixture of reactants and products in the axial zone. The most typical feature of such a flow are the highly elongated and deformed velocity profiles with a point of inflection and with the maximum velocity much higher than the average velocity.

1.4 CLOSURE

The above survey shows that for laminar flow tubular reactors, the axial diffusion effect is negligible for both Newtonian and non-Newtonian fluids. This conclusion is used later in the present analysis. The problem discussed in the above survey was solved under specific sets of assumptions, the most important of which are as follows:

- only one or two-dimensional flows are considered,
- generally fully-developed flow is assumed for velocity profile distribution,
- usually the tubular reactor is considered to be isothermal,
- mostly constant physical-properties are used,
- viscous heat generation is generally disregarded,
- possible free-convection effect is ignored,
- mostly simple first order reactions are considered,
- the problem is solved only for circular duct reactors and no attempt is made to analyze noncircular cross-section duct reactors.

It is therefore clear that a comprehensive study, formulation and solution of a 3-D reacting laminar flow problem in which velocity, temperature and concentration fields develop simultaneously, deserves attention. Furthermore, it is important to consider the effects of variable physical properties, viscous heat generation and free-convection effects in noncircular duct reactors.

CHAPTER 2

MATHEMATICAL MODELLING IN CARTESIAN COORDINATES (GOVERNING-EQUATIONS AND BOUNDARY CONDITIONS)

2.1 INTRODUCTION

The flow, heat and mass transfer phenomena of fluids are governed by the conservation equations of mass, momentum, energy and species. The conservation equations subjected to various simplifying assumptions may be solved analytically or numerically. Other than the assumption of negligible axial diffusion for the problems examined in this work, no other simplifying assumptions are needed. Analytical solution of the conservation equations is impossible for the case studied.

The strongly conservative form of the conservation equations will be presented in this chapter. The conservative form enhances subsequent treatment of the equations for numerical solution. The rheology of many purely viscous non-Newtonian fluids is adequately expressed by the power-law model for which the corresponding constitutive equations (shear-stress, strain relationships) are given in this chapter. It is the goal of this chapter to present the conservation equations in 3-D Cartesian coordinates in which the constitutive equations to be included and the boundary conditions are to be specified.

The latter equations and the boundary conditions are later transformed into curvilinear coordinates to handle arbitrary cross-sections. The coordinate axes selected for the Cartesian domain are shown in Figure 2.1.

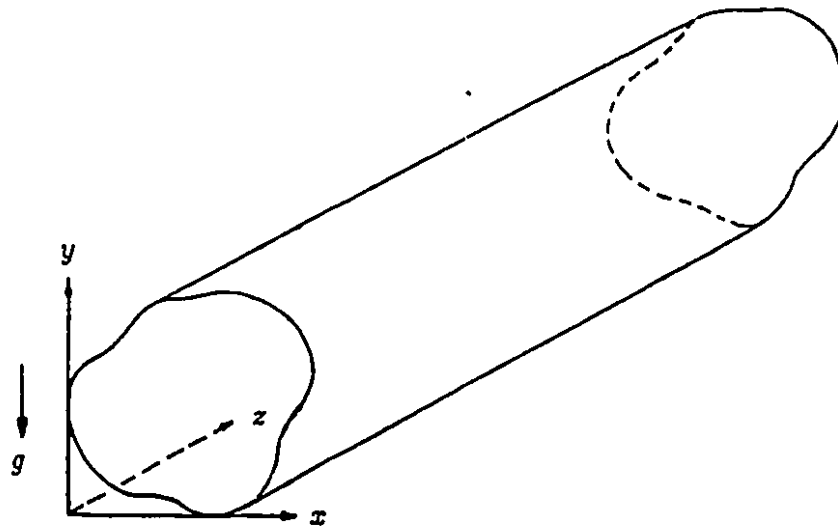


Figure 2.1 Arbitrary cross-sectional duct in Cartesian coordinates

2.2 GENERAL CONSERVATION LAWS

2.2.1 The Overall Continuity Equation

$$\frac{\partial \rho}{\partial t} + (\nabla \cdot \rho v) = 0 \quad (2.1)$$

2.2.2 The Momentum Equation

$$\frac{\partial(\rho v)}{\partial t} = -(\nabla \cdot \rho v v) - \nabla P - (\nabla \cdot \tau) + \rho g \quad (2.2)$$

2.2.3 The Energy Equation

$$\begin{aligned} \frac{\partial(\rho C_P T)}{\partial t} = & -(\nabla \cdot \rho C_P T v) - (\nabla \cdot q) - (\tau : \nabla v) + \left(\frac{\partial \ln V}{\partial \ln T} \right)_P \frac{DP}{Dt} \\ & + \rho T \frac{DC_P}{Dt} + Q_R \end{aligned} \quad (2.3)$$

2.2.4 The Reactant Continuity Equation

$$\frac{\partial(\rho \omega_A)}{\partial t} + (\nabla \cdot \rho \omega_A v) = (\nabla \cdot \rho D_A \nabla \omega_A) - R_A \quad (2.4)$$

2.3 CONSERVATION LAWS IN CARTESIAN COORDINATES

2.3.1 The Overall Continuity Equation

$$\frac{\partial \rho}{\partial t} + \frac{\partial(\rho u)}{\partial x} + \frac{\partial(\rho v)}{\partial y} + \frac{\partial(\rho w)}{\partial z} = 0 \quad (2.5)$$

2.3.2 The Momentum Equation

x-component

$$\frac{\partial(\rho u)}{\partial t} + \frac{\partial(\rho u^2)}{\partial x} + \frac{\partial(\rho uv)}{\partial y} + \frac{\partial(\rho wu)}{\partial z} = -\frac{\partial P}{\partial x} - \left(\frac{\partial \tau_{xz}}{\partial x} + \frac{\partial \tau_{yz}}{\partial y} + \frac{\partial \tau_{zx}}{\partial z} \right) + \rho g_x \quad (2.6)$$

y-component

$$\frac{\partial(\rho v)}{\partial t} + \frac{\partial(\rho uv)}{\partial x} + \frac{\partial(\rho v^2)}{\partial y} + \frac{\partial(\rho wv)}{\partial z} = -\frac{\partial P}{\partial y} - \left(\frac{\partial \tau_{xy}}{\partial x} + \frac{\partial \tau_{yy}}{\partial y} + \frac{\partial \tau_{zy}}{\partial z} \right) + \rho g_y \quad (2.7)$$

z-component

$$\frac{\partial(\rho w)}{\partial t} + \frac{\partial(\rho uw)}{\partial x} + \frac{\partial(\rho vw)}{\partial y} + \frac{\partial(\rho w^2)}{\partial z} = -\frac{\partial P}{\partial z} - \left(\frac{\partial \tau_{xz}}{\partial x} + \frac{\partial \tau_{yz}}{\partial y} + \frac{\partial \tau_{zz}}{\partial z} \right) + \rho g_z \quad (2.8)$$

2.3.3 The Energy Equation*

$$\begin{aligned}
 \frac{\partial}{\partial t}(\rho C_p T) + \frac{\partial}{\partial x}(\rho C_p T u) + \frac{\partial}{\partial y}(\rho C_p T v) + \\
 \frac{\partial}{\partial z}(\rho C_p T w) = \frac{\partial}{\partial x} \left(k \frac{\partial T}{\partial x} \right) + \frac{\partial}{\partial y} \left(k \frac{\partial T}{\partial y} \right) + \\
 \frac{\partial}{\partial z} \left(k \frac{\partial T}{\partial z} \right) - \left(\tau_{xx} \frac{\partial u}{\partial x} + \tau_{yy} \frac{\partial v}{\partial y} + \tau_{zz} \frac{\partial w}{\partial z} \right) - \\
 \left[\tau_{xy} \left(\frac{\partial u}{\partial y} + \frac{\partial v}{\partial x} \right) + \tau_{xz} \left(\frac{\partial u}{\partial z} + \frac{\partial w}{\partial x} \right) + \right. \\
 \left. \tau_{yz} \left(\frac{\partial v}{\partial z} + \frac{\partial w}{\partial y} \right) \right] + Q_R \quad (2.9)
 \end{aligned}$$

* In the energy equation, the Fourier's Law, $q = -k \nabla T$ is applied

2.3.4 The Reactant Continuity Equation

$$\begin{aligned}
 \frac{\partial}{\partial t}(\rho \omega_A) + \frac{\partial}{\partial x}(\rho \omega_A u) + \frac{\partial}{\partial y}(\rho \omega_A v) + \frac{\partial}{\partial z}(\rho \omega_A w) = \frac{\partial}{\partial x} \left(\rho D_A \frac{\partial \omega_A}{\partial x} \right) + \\
 \frac{\partial}{\partial y} \left(\rho D_A \frac{\partial \omega_A}{\partial y} \right) + \frac{\partial}{\partial z} \left(\rho D_A \frac{\partial \omega_A}{\partial z} \right) \\
 - R_A \quad (2.10)
 \end{aligned}$$

2.4 THE STRESS TENSOR

2.4.1 The Stress Tensor

The nine components of the stress tensor are as follows³⁴:

$$\tau = \begin{pmatrix} \tau_{xx} & \tau_{xy} & \tau_{xz} \\ \tau_{yx} & \tau_{yy} & \tau_{yz} \\ \tau_{zx} & \tau_{zy} & \tau_{zz} \end{pmatrix} \quad (2.11)$$

Consideration of the angular momentum shows that:

$$\tau_{yx} = \tau_{xy} ; \tau_{zx} = \tau_{xz} ; \tau_{zy} = \tau_{yz} \quad (2.12)$$

that is the stress tensor is symmetrical and the state of stress at a point is determined by six, rather than nine independent stress components.

2.4.2 The Rate of Strain Tensor

The rate-of-strain or rate-of-deformation tensor is symmetrical and has Cartesian components as follows³⁴:

$$\Delta = \begin{pmatrix} \Delta_{xx} & \Delta_{xy} & \Delta_{xz} \\ \Delta_{yx} & \Delta_{yy} & \Delta_{yz} \\ \Delta_{zx} & \Delta_{zy} & \Delta_{zz} \end{pmatrix} \quad (2.13)$$

where Δ_{xx} , Δ_{yy} , Δ_{zz} are lineal strain rates and Δ_{xy} , Δ_{yz} , Δ_{xz} are rates of shear deformation.

$$\Delta_{xx} = 2 \frac{\partial u}{\partial x}; \quad \Delta_{yy} = 2 \frac{\partial v}{\partial y}; \quad \Delta_{zz} = 2 \frac{\partial w}{\partial z} \quad (2.14)$$

$$\Delta_{xy} = \Delta_{yx} = \frac{\partial u}{\partial y} + \frac{\partial v}{\partial x} \quad (2.15)$$

$$\Delta_{yz} = \Delta_{zy} = \frac{\partial w}{\partial y} + \frac{\partial v}{\partial z} \quad (2.16)$$

$$\Delta_{xz} = \Delta_{zx} = \frac{\partial u}{\partial z} + \frac{\partial w}{\partial x} \quad (2.17)$$

2.4.3 The Power-Law Constitutive Equations

For power-law model the stress-tensor is related to the rate-of-strain tensor by the following relationship³⁴⁻³⁸:

$$\tau_{ij} = -\mu \left| \sqrt{\frac{1}{2}(\Delta_{ij} : \Delta_{ij})} \right|^{n-1} \Delta_{ij} \quad (2.18)$$

in which

$$\begin{aligned} \frac{1}{2}(\Delta_{ij} : \Delta_{ij}) = 2 \left[\left(\frac{\partial u}{\partial x} \right)^2 + \left(\frac{\partial v}{\partial y} \right)^2 + \left(\frac{\partial w}{\partial z} \right)^2 \right] + \left(\frac{\partial u}{\partial y} + \frac{\partial v}{\partial x} \right)^2 + \\ \left(\frac{\partial w}{\partial y} + \frac{\partial v}{\partial z} \right)^2 + \left(\frac{\partial u}{\partial z} + \frac{\partial w}{\partial x} \right)^2 \end{aligned} \quad (2.19)$$

if one denotes $\frac{1}{2}(\Delta_{ij} : \Delta_{ij}) = I$ then

$$\left| \sqrt{\frac{1}{2}(\Delta_{ij} : \Delta_{ij})} \right|^{n-1} = I^{(\frac{n-1}{2})} \quad (2.20)$$

using the values of the rate-of-deformation-tensor, one can write the components of the stress-tensor as follows:

$$\tau_{xx} = -2\mu \left(\frac{\partial u}{\partial x} \right) I^{(\frac{n-1}{2})} = -2M \left(\frac{\partial u}{\partial x} \right) \quad (2.21)$$

$$\tau_{yy} = -2\mu \left(\frac{\partial v}{\partial y} \right) I^{(\frac{n-1}{2})} = -2M \left(\frac{\partial v}{\partial y} \right) \quad (2.22)$$

$$\tau_{zz} = -2\mu \left(\frac{\partial w}{\partial z} \right) I^{(\frac{n-1}{2})} = -2M \left(\frac{\partial w}{\partial z} \right) \quad (2.23)$$

$$\tau_{xy} = \tau_{yx} = -\mu \left(\frac{\partial u}{\partial y} + \frac{\partial v}{\partial x} \right) I^{(\frac{n-1}{2})} = -M \left(\frac{\partial u}{\partial y} + \frac{\partial v}{\partial x} \right) \quad (2.24)$$

$$\tau_{xz} = \tau_{zx} = -\mu \left(\frac{\partial u}{\partial z} + \frac{\partial w}{\partial x} \right) I^{(\frac{n-1}{2})} = -M \left(\frac{\partial u}{\partial z} + \frac{\partial w}{\partial x} \right) \quad (2.25)$$

$$\tau_{yz} = \tau_{zy} = -\mu \left(\frac{\partial w}{\partial y} + \frac{\partial v}{\partial z} \right) I^{(\frac{n-1}{2})} = -M \left(\frac{\partial w}{\partial y} + \frac{\partial v}{\partial z} \right) \quad (2.26)$$

in which

$$M = \mu I^{(\frac{n-1}{2})} \quad (2.27)$$

where M is the apparent viscosity for a power-law fluid.

2.5 CONSIDERATIONS INTRODUCED IN THE CONSERVATION EQUATIONS

2.5.1 The Body-Force Terms in Momentum Equations

The body-force (the gravitational field) is applied only in the "y" direction, for the coordinate system selected (Figure 2.1).

2.5.2 The Buoyancy Term in the y-Momentum Equation

Whenever there is a temperature variation in transverse direction in the flow field, a buoyancy force is generated due to the presence of the body force field and causes a natural convection flow to be established³⁹⁻⁴¹. The buoyancy term is hence introduced in the y-momentum equation while the pressure field is modified. For derivation of the buoyancy term in the y- momentum equation refer to Appendix G.

2.5.3 Heat of Reaction in Energy Equation

This is expressed by $Q_R = (-\Delta H)R_A$ in which $\Delta H < 0$ for exothermic-reactions and $\Delta H > 0$ for endothermic reactions.

2.5.4 Steady State Condition

In practical applications, tubular reactors are operated in steady-state mode, hence, this condition is accepted here for the chemically-reacting duct flows in arbitrary geometries. Unsteady state situation is beyond the scope of the present study.

2.5.5 Variable Fluid Properties

The interdependence of fluid properties with temperature and other variables, if exists, are introduced through empirical equations for any specific fluid-reaction system. These properties are: density, viscosity, specific-heat *, thermal-conductivity, heat of reaction and mass-diffusivity. Refer to Chapter 5 for the specific relations regarding the fluid properties for reaction system under study.

2.5.6 The Reaction Rate Constant

The Arrhenius model or any empirically-obtained rate-law may be used for any reaction under consideration. The relations for the reaction under study are presented in Chapter 5.

2.6 PARABOLIC APPROXIMATION

2.6.1 Parabolic Space Coordinate

It is experimentally observed that in geometries which do not undergo radial changes in the primary flow direction, the downstream conditions exert little or no influence on upstream in the predominant flow direction⁴²⁻⁴⁷. Therefore the flow tends to be dominated by the upstream conditions and any small disturbance at a given point is not transmitted very far upstream of that point.

In this situation, the conditions in the main flow direction become a "one-way" coordinate, that is, the upstream conditions determine the downstream flow properties but not vice-versa.

* A constant specific heat is considered in the discretized energy equation ($h = C_p T$)⁶⁹ to employ control volume approach over the conservative form of the original energy equation. Specific heat is nearly constant for liquids within some specified temperature ranges.

2.6.2 General Conditions for the Parabolic Assumption

1. if there is a predominant direction of flow (no recirculation, no separation, no reverse flow or negative velocity in that direction),
2. if the diffusion of momentum, heat and mass is negligible in that direction,
3. if the downstream pressure-field has little influence on the upstream flow conditions (this condition results in a decoupling of the pressure-field).

2.6.3 Application of Marching Integration

A reasonable approximation to such a flow is by a stepwise integration in the direction of flow from a given set of upstream initial conditions.

2.6.4 Decoupling of Longitudinal and Lateral Pressure Gradients

In order to be able to march in the "z" direction, one must treat the pressure "P" in the axial momentum equation differently than the pressure in the transverse momentum equations^{42,43}. The decoupling in the pressure-field is expressed by writing the three-dimensional pressure-field as

$$P(x, y, z) = \tilde{P}(x, y; z) + \bar{P}(z) \quad (2.28)$$

where $\tilde{P}(x, y; z)$ and $\bar{P}(z)$ are the local and the average variations of the pressure in the cross-section respectively^{45,46}. The pressure \tilde{P} is a two-dimensional field, but changes with "z" as the solution is marched in stepwise manner. The pressure \bar{P} can be thought of as a form of space-averaged pressure over a cross-section.

The pressure-gradient term in the axial flow direction, $\frac{dP}{dz}$, is therefore decoupled from those in the other flow directions: $\frac{\partial P}{\partial x}$ and $\frac{\partial P}{\partial y}$. The gradient $\frac{dP}{dz}$ is referred to be a mean viscous pressure-drop which is a function of "z" only and is constant in the x-y plane.

2.6.5 Advantages of the Parabolic Approximation

The governing equations are elliptic in all three space-coordinates which require a great amount of storage and computation time. Assuming that there is no strong influence travelling from downstream to upstream of the duct, the governing equations are parabolized in the axial direction. The resulting equations are then elliptic in the two transverse space-coordinates and parabolic in the axial space coordinate. These equations are solved by marching integration in axial direction in stepwise manner, solving a two-dimensional elliptic problem at each cross-sectional plane. The dependent variables are needed only to be stored on the calculation plane and on the upstream plane due to which substantial economy of computer storage and computer time is possible.

2.6.6 Modification of Governing Equations with Parabolic Assumption

In order to parabolize the fully elliptic governing equations in axial direction, one should neglect the diffusion terms in the axial direction, therefore the terms $\frac{\partial \tau_{xx}}{\partial z}$, $\frac{\partial \tau_{xy}}{\partial z}$, $\frac{\partial \tau_{xz}}{\partial z}$, $\frac{\partial}{\partial z}(k \frac{\partial T}{\partial z})$ and $\frac{\partial}{\partial z}(\rho D_A \frac{\partial \omega_A}{\partial z})$ are neglected. Also the pressure-gradient in the axial-momentum equation, $\frac{\partial P}{\partial z}$ is decoupled from the other pressure gradient terms; $\frac{\partial P}{\partial x}$ and $\frac{\partial P}{\partial y}$ using $\frac{dP}{dz}$ in that direction.

2.7 THE PARABOLIZED GOVERNING EQUATIONS IN CARTESIAN COORDINATES

2.7.1 The Overall Continuity Equation

$$\frac{\partial}{\partial x}(\rho u) + \frac{\partial}{\partial y}(\rho v) + \frac{\partial}{\partial z}(\rho w) = 0 \quad (2.29)$$

2.7.2 The Momentum Equations

x-component

$$\frac{\partial}{\partial x}(\rho u^2) + \frac{\partial}{\partial y}(\rho v u) + \frac{\partial}{\partial z}(\rho w u) = -\frac{\partial P}{\partial x} - \left(\frac{\partial \tau_{xx}}{\partial x} + \frac{\partial \tau_{yx}}{\partial y} \right) \quad (2.30)$$

y-component

$$\frac{\partial}{\partial x}(\rho u v) + \frac{\partial}{\partial y}(\rho v^2) + \frac{\partial}{\partial z}(\rho w v) = -\frac{\partial P}{\partial y} - \left(\frac{\partial \tau_{xy}}{\partial x} + \frac{\partial \tau_{yy}}{\partial y} \right) - (\rho - \rho_a)g \quad (2.31)$$

z-component

$$\frac{\partial}{\partial x}(\rho u w) + \frac{\partial}{\partial y}(\rho v w) + \frac{\partial}{\partial z}(\rho w^2) = -\frac{d\bar{P}}{dz} - \left(\frac{\partial \tau_{xz}}{\partial x} + \frac{\partial \tau_{yz}}{\partial y} \right) \quad (2.32)$$

2.7.3 The Energy Equation *

$$\frac{\partial}{\partial x}(\rho C_p T u) + \frac{\partial}{\partial y}(\rho C_p T v) + \frac{\partial}{\partial z}(\rho C_p T w) = \frac{\partial}{\partial x} \left(k \frac{\partial T}{\partial x} \right) + \frac{\partial}{\partial y} \left(k \frac{\partial T}{\partial y} \right) + M \cdot I + (-\Delta H)R_A \quad (2.33)$$

2.7.4 The Reactant Continuity Equation

$$\frac{\partial}{\partial x}(\rho \omega_A u) + \frac{\partial}{\partial y}(\rho \omega_A v) + \frac{\partial}{\partial z}(\rho \omega_A w) = \frac{\partial}{\partial x} \left(\rho D_A \frac{\partial \omega_A}{\partial x} \right) + \frac{\partial}{\partial y} \left(\rho D_A \frac{\partial \omega_A}{\partial y} \right) - R_A \quad (2.34)$$

* Note that the right hand side of this equation is true only if C_p is a constant.

The pressure, P in the above equations is dynamic-pressure due to the introduction of buoyancy term in the “ y ” momentum equation. In cases of negligible buoyancy effect. P would be the total pressure defined as hydrostatic plus dynamic pressures. Refer to Appendix G for details. The term I in the energy equation expressed above, is the dissipation function for the power-law non-Newtonian fluid.

2.8 THE BOUNDARY CONDITIONS

2.8.1 Inlet (@ $z = 0$)

Axial Velocity

A uniform entrance velocity profile is specified at inlet:

$$w = w_{inlet} \quad (2.35)$$

Transverse Velocities

It is assumed that there is no secondary flow at inlet:

$$u = 0 \quad (2.36)$$

$$v = 0 \quad (2.37)$$

Temperature

A uniform temperature-profile is specified at inlet:

$$T = T_{inlet} \quad (2.38)$$

Reactant Weight Fraction

For an unconverted reactant at inlet:

$$\omega = 1 \quad (2.39)$$

2.8.2 Walls of the Duct

Axial Velocity

No slip-condition is assumed on the walls of the duct:

$$w = 0 \quad (2.40)$$

Transverse Velocities

$$u = 0 \quad (2.41)$$

$$v = 0 \quad (2.42)$$

Temperature

For a constant wall-temperature:

$$T = T_{wall} \quad (2.43)$$

Reactant Weight-Fraction

The material does not move through the wall:

$$\frac{\partial \omega}{\partial n} = 0 \quad (2.44)$$

2.8.3 Outflow Condition (@ $z = L$)

The complete conservation equations are elliptic, hence the geometrical domain under consideration must be closed; therefore for duct flow, the downstream boundary-conditions have to be specified. However for the parabolized governing equations used here no downstream boundary conditions are required.

2.9 CLOSURE

In this chapter the 3-D conservation equations of mass, momentum, energy and species are written in their strongly conservative form in Cartesian coordinates including the following considerations:

- constitutive equations corresponding to power-law non-Newtonian fluids,
- viscous heat dissipation effect in the energy equation,
- free-convection effect (the buoyancy term) in the y-momentum equation,
- the heat of reaction in the energy equation,
- variable fluid properties,
- arbitrary rate-law model for the reaction involved.

CHAPTER 3

COORDINATE TRANSFORMATION AND NUMERICAL METHOD OF SOLUTION

3.1 INTRODUCTION

The subjects in transport phenomena are modelled by nonlinear coupled partial-differential equations. These equations can be solved by several approximate solution methods for special cases such as asymptotic-expansion and perturbation methods, collocation and integral methods, finite-difference, finite-volume, and finite-element methods⁶³. In general, finite-difference, finite-volume and finite-element discretization techniques have been the most successful methods the use of which, however, requires to discretize the entire domain employing a mesh or a grid network.

The finite element method has been concerned with the treatment of irregular boundaries since its beginning, however this method requires excessive amount of computational time and storage⁶⁴.

In finite difference methods a convenient choice for a grid network is one composed of rectangles. The application of the method is therefore suitable to domains such as rectangular shapes whose boundaries coincide with the computational grid points. In earlier studies whenever the finite-difference method was applied to irregular-shape domains, special interpolation schemes were employed at the boundaries for discretization of the boundary conditions. However, this method can lead to large errors. In any boundary value problem, the boundary conditions exert a strong influence on the solution of the interior of the domain, so that greater accuracy is required in the representation of the difference equations at the boundaries than what is obtained by interpolation.

The inadequacy of the interpolation methods and the fact that an accurate expression of the boundary conditions is best accomplished if the boundaries coincide with some coordinate lines, brought about the development of coordinate transformation of the physical domain i.e. Cartesian coordinates to boundary-fitted curvilinear coordinates such that all the boundaries match the coordinate lines and the need to interpolate the boundary conditions is eliminated^{48-51,56}. The partial differential equations are thus transformed from the Cartesian coordinates into the new coordinate system by appropriate transformation relations. The boundary-conditions are similarly transformed without the need to use interpolation techniques.

The transformed plane is simply a rectangular domain. The transformed-equations and the boundary-conditions are discretized over this plane and the discretized equations are conveniently solved by similar methods in Cartesian space.

It has been shown that the partial differential equations do not change their type i.e. elliptic, parabolic or hyperbolic upon transformation.

3.2 THE ORTHOGONAL AND NON-ORTHOGONAL COORDINATE SYSTEMS

The curvilinear boundary-fitted mesh generated over the physical domain, may be either orthogonal or non-orthogonal. The generation of orthogonal meshes is generally time-consuming^{45,55,65}. In addition, the concentration of the grid lines in certain regions of the domain is not conveniently handled when using orthogonal methods. The use of non-orthogonal systems has the disadvantage that the transformed governing equations become somewhat more complex because of the presence of the non-orthogonal terms; also the finite-difference equations involve 9 discrete-points versus 5 discrete points for orthogonal systems^{45,46}.

The boundary-fitted methods involves the following two tasks for the solution of PDE's:

- (i) method for generating the coordinate systems or grid network,
- (ii) method to model the governing equations in the transformed domain.

The use of non-orthogonal grid may be an optimum alternative for handling arbitrary geometries if the performance of item (ii) above for a non-orthogonal system is comparable to that of an existing orthogonal system and if it functions similarly to the methods used for orthogonal schemes when an orthogonal grid is employed⁴⁵. A number of studies have appeared in the literature on the use of the non-orthogonal numerical solution schemes. For example Hadjisophocleous et. al.⁶⁶ applied a non-orthogonal numerical method for prediction of transient natural convection in enclosures of arbitrary geometry. Shyy, et. al.⁶⁷ and Braaten, et. al.⁶⁸ applied a non-orthogonal numerical scheme using body-fitted coordinates for numerical solution of a recirculating flow problem. Maliska⁴⁶ developed a numerical model using non-orthogonal grids for the solution of the three-dimensional fluid-flow problems in irregular geometries. This method uses a novel grid layout which promotes numerical stability and convergence for the system of equations. Maliska's method is adopted here to be applied to the present analysis considering also any modifications required.

3.3 CURVILINEAR TRANSFORMATION

A transformation is defined between a physical region "D" of any arbitrary shape and a transformed-region of "D*" of rectangular-shape as shown in Figure 3.1. In the physical-region, the Cartesian coordinates x and y are the independent variables and the curvilinear coordinates are the dependent variables. In the transformed region, the coordinates ξ and η are the independent variables and x and y are the dependent variables. There exists a one to one correspondence between the coordinates in the physical-region and the transformed-region.

The general transformation relation from the physical-plane (x,y) to the transformed-plane (ξ, η) are given by⁴⁸⁻⁵¹:

$$\left. \begin{aligned} \xi &= \xi(x, y) \\ \eta &= \eta(x, y) \end{aligned} \right\} \quad (3.1)$$

The Jacobian matrix of this transformation is

$$\underline{J}_1 = \begin{bmatrix} \xi_x & \xi_y \\ \eta_x & \eta_y \end{bmatrix} \quad (3.2)$$

The inverse transformation of Eqn. (3.1) (if exists) is:

$$\left. \begin{aligned} x &= x(\xi, \eta) \\ y &= y(\xi, \eta) \end{aligned} \right\} \quad (3.3)$$

The Jacobian matrix of Eqn. (3.3), denoted by \underline{J}_2 is given by

$$\underline{J}_2 = \begin{bmatrix} x_\xi & x_\eta \\ y_\xi & y_\eta \end{bmatrix} \quad (3.4)$$

The Jacobian determinant or Jacobian simply, is then

$$J = J \left[\begin{array}{c} (x, y) \\ (\xi, \eta) \end{array} \right] = \det[\underline{J}_2] = x_\xi y_\eta - x_\eta y_\xi \neq 0 \quad (3.5)$$

where

$$x_\xi = \frac{\partial x}{\partial \xi}; \quad y_\eta = \frac{\partial y}{\partial \eta}; \quad \text{etc.}$$

The Jacobian matrices, Eqns (3.2) and (3.4) are related by

$$\underline{J}_1 = [\underline{J}_2]^{-1} \quad (3.6)$$

one can readily show that:

$$\left. \begin{aligned} \xi_x &= \frac{y_\eta}{J} & \xi_y &= -\frac{x_\eta}{J} \\ \eta_x &= -\frac{y_\xi}{J} & \eta_y &= \frac{x_\xi}{J} \end{aligned} \right\} \quad (3.7)$$

Refer to Appendix A for derivation.

Partial derivatives are transformed using the following relations:

$$f_x = \frac{1}{J}[y_\eta f_\xi - y_\xi f_\eta] \quad (3.8)$$

$$f_y = \frac{1}{J}[-x_\eta f_\xi + x_\xi f_\eta] \quad (3.9)$$

Refer to Appendix A for derivation.

Higher order derivatives are obtained by repeated application of Eqns. (3.8) and (3.9). The two tasks involved in the transformation are:

- (i) **Coordinate Generation (or Grid Generation)** This is necessary to determine the location of the coordinate lines in the interior of the physical domain. A coordinate line is specified as being coincident with each boundary line segment while the other coordinate varies monotonically along that line. The generation of a coordinate system is thus simply a boundary-value problem.
- (ii) **Transformation of Governing PDE's** This is employed to transform the partial-differential equations under consideration into the new coordinate variables before being discretized. All computations, both to generate the coordinate system and to solve the governing PDE's, can be performed on a rectangular domain in the transformed space.

3.4 NUMERICAL GRID GENERATION

A method of generating the general boundary-fitted coordinate systems is to let the curvilinear coordinates to be the solutions of an elliptic partial differential system in the physical plane, with Dirichlet boundary conditions on all the boundaries^{49-51,54,60}.

An elliptic system is used because the solution of such a system is completely defined in the interior of the region by its values on the boundary. In other words, when the entire closed boundary of the physical region is specified, the partial-differential equations (employed for grid-generation) must be elliptic.

The solution of an elliptic system yields harmonic functions which have continuous derivatives of all orders. Moreover, harmonic-functions obey a maximum principle, which states that the maximum and the minimum values of the function must occur at the boundaries of the region of the physical-domain. Thus, no extrema occur within this region, so that the first derivatives of the function will not simultaneously vanish in this region, and hence the Jacobian will not be zero due to the presence of an extremum. The maximum principle also guarantees the uniqueness of the coordinate functions $\xi(x, y)$ and $\eta(x, y)$.

The physical domain under consideration may be a simply-connected region or a multiply-connected region. The generated coordinate system produces a rectangular domain in the transformed-space (Figure 3.2).

Consider a simply-connected region, the boundary of which is specified at discrete-points (x_b, y_b) . The simplest elliptic system to choose is to use the Laplace equation and to find ξ, η so that a system of Laplace equations is satisfied in the physical plane. that is:

$$\xi_{xx} + \xi_{yy} = 0 \quad (3.10)$$

$$\eta_{xx} + \eta_{yy} = 0 \quad (3.11)$$

or

$$\nabla^2 \xi = 0 \quad (3.12)$$

$$\nabla^2 \eta = 0 \quad (3.13)$$

where

$$\nabla^2 = \frac{\partial^2}{\partial x^2} + \frac{\partial^2}{\partial y^2}$$

with the following Dirichlet boundary-conditions:

$$\left. \begin{array}{l} \xi = \xi_1 \\ \eta = \eta_3(x, y) \end{array} \right\} \quad \text{on } \Gamma_1 \quad (3.14)$$

$$\left. \begin{array}{l} \xi = \xi_3(x, y) \\ \eta = \eta_2 \end{array} \right\} \quad \text{on } \Gamma_2 \quad (3.15)$$

$$\left. \begin{array}{l} \xi = \xi_2 \\ \eta = \eta_4(x, y) \end{array} \right\} \quad \text{on } \Gamma_3 \quad (3.16)$$

$$\left. \begin{array}{l} \xi = \xi_4(x, y) \\ \eta = \eta_1 \end{array} \right\} \quad \text{on } \Gamma_4 \quad (3.17)$$

where ξ_1, ξ_2, η_1 and η_2 are different constants and $\eta_3(x, y), \xi_3(x, y), \eta_4(x, y)$ and $\xi_4(x, y)$ are specified monotonic functions on $\Gamma_1, \Gamma_2, \Gamma_3$ and Γ_4 .

Since it is desired to perform all the numerical computations on the uniform rectangular transformed plane, the dependent and the independent variables in the above

equations must be interchanged. This results in:

$$\alpha x_{\xi\xi} - 2\beta x_{\xi\eta} + \gamma x_{\eta\eta} = 0 \quad (3.18)$$

$$\alpha y_{\xi\xi} - 2\beta y_{\xi\eta} + \gamma y_{\eta\eta} = 0 \quad (3.19)$$

Refer to Appendix A for derivation.

The coupling coefficients in the above-equations are:

$$\alpha = x_{\eta}^2 + y_{\eta}^2 \quad (3.20)$$

$$\beta = x_{\xi}x_{\eta} + y_{\xi}y_{\eta} \quad (3.21)$$

$$\gamma = x_{\xi}^2 + y_{\xi}^2 \quad (3.22)$$

The boundary conditions are:

$$\left. \begin{array}{l} x = f_1(\xi_1, \eta) \\ y = g_1(\xi_1, \eta) \end{array} \right\} \quad \text{on } \Gamma_1^* \quad (3.23)$$

$$\left. \begin{array}{l} x = f_2(\xi, \eta_2) \\ y = g_2(\xi, \eta_2) \end{array} \right\} \quad \text{on } \Gamma_2^* \quad (3.24)$$

$$\left. \begin{array}{l} x = f_3(\xi_2, \eta) \\ y = g_3(\xi_2, \eta) \end{array} \right\} \quad \text{on } \Gamma_3^* \quad (3.25)$$

$$\left. \begin{array}{l} x = f_4(\xi, \eta_1) \\ y = g_4(\xi, \eta_1) \end{array} \right\} \quad \text{on } \Gamma_4^* \quad (3.26)$$

The functions $f_1, g_1, f_2, g_2, f_3, g_3, f_4$ and g_4 are specified by the known shape of the contours $\Gamma_1, \Gamma_2, \Gamma_3$ and Γ_4 and the specified distribution of ξ and η over them.

Equations 3.18 and 3.19 can be solved by A finite-difference method using second-order central difference approximation of derivatives and applying the SOR (successive over-relaxation) method using linearly interpolated initial guess. The discrete values of (x,y) at the corresponding (ξ, η) points are then determined. The finer the mesh, the smaller would be the numerical error.

The grid generation method described in this section is employed to develop a B-type grid generation computer programme required in this work.

3.5 TRANSFORMATION OF THE GOVERNING EQUATIONS

The governing partial-differential equations and the respective boundary-conditions must be transformed to the corresponding curvilinear coordinates using the transformation relations of Section 3.3 in order to be solved in the transformed plane. The problem of solving the governing-equations on a complex physical domain is therefore changed to the solution of the transformed-equations on a uniform grid of rectangular shape in the transformed plane.

In general, the transformation operation generates additional terms in the governing equations so that these equations become more complicated upon transformation.

For the transformation of the governing equations, one has to first decide upon the dependent variables in the transformed-plane for the velocity components which could be either the physical Cartesian velocities or the contravariant velocity components. The concept of contravariant velocities is shown in Figure 3.3. The contravariant velocities are related to the physical Cartesian components by the following relationships:

$$\left. \begin{aligned} U &= y_{\eta}u - x_{\eta}v \\ V &= x_{\xi}v - y_{\xi}u \\ W &= Jw \end{aligned} \right\} \quad (3.27)$$

Use of contravariant velocities as the dependent variables leads to a complex transformation in which the physical interpretation of the transformed equations is also very difficult.

Retaining the physical Cartesian velocities as the dependent variables in the transformation of the equations has the advantage that very complex transformed equations are avoided. Also the equations preserve their conservative form after transformation, which is a desired feature in the physical interpretation of the equations and in the convenience of formulation of discretization equations.

The dependent variables for velocity components selected in this work in the transformation task are the physical-Cartesian velocities, however, both the Cartesian and

the contravariant velocities take part in the structure of the transformed equations and in the solution procedure.

3.6 DISCRETIZATION OF TRANSFORMED EQUATIONS

3.6.1 Grid Configuration

By grid configuration or arrangement one implies a proper choice of storage locations for the dependent variables in the transformed plane for which there are alternative selections. A suitable grid configuration should be chosen for any specific problem. The grid arrangement adopted is largely responsible for obtaining discretization equations which converge fast and exhibit good stability and accuracy. Grid configuration is to be considered only for the variables in the transverse plane and how the variables are located with respect to the axial direction is not of major importance.

3.6.2 Basic Requirements of a Proper Grid Configuration

A favorable grid configuration should be capable of providing the following goals:

- (i) pressure should be located such that the pressure gradient terms in the momentum equations can be accurately evaluated,
- (ii) velocities should be located where they are required for mass conservation,
- (iii) the numerical scheme for non-orthogonal grid should revert to a 5-point equation type when the grid employed is orthogonal¹⁵.

Two of the most important grid arrangements (non-staggered and classical staggered) and the novel grid arrangement⁴⁶ adopted for the current problem are described here.

3.6.3 The Non-Staggered Grid Configuration

In this arrangement (Figure 3.4) all the variables are located at the same grid point location designated by P. There would be a serious drawback in discretization

of pressure gradient terms in the momentum equations using this configuration so that a non-realistic wavy or zigzag pressure-field may lead to a convergent solution. This difficulty, referred to as the checkerboard pressure-field pattern⁶⁹, is avoided if a staggered grid configuration is employed.

3.6.4 The Classical Staggered Grid Configuration

In this arrangement (Figure 3.5) the velocities are located at the middle of the four faces of each cell, while pressure, axial velocity and physical properties are located in the middle of the cell.

The advantages of this layout are as follows:

- (i) the danger of generating wavy pressure-field is eliminated,
- (ii) the velocities are located where they are required for mass balance.

3.6.5 The Grid Configuration Adopted

For a non-orthogonal grid system, the best choice is a classical staggered-grid in which both components of “ u ” and “ v ” velocities are used coincidentally at the same location with the contravariant-velocities normal and parallel to the faces of the cell⁴⁶ (Figures 3.6 and 3.8). This configuration involves one difficulty which can be solved by an interpolation scheme⁴⁶. Due to the fact that one of the contravariant velocities (parallel components) do not enter to satisfy the overall continuity equation, the “ u ” and “ v ” values can depart considerably from their realistic values during the iteration process. The values of these velocities can, however, produce normal components of the contravariant velocities which would satisfy the mass balance equation while the parallel components of the contravariant velocities remain free to assume unrealistic values. The solution to this difficulty is to enforce somehow the continuity equation to also hold for the parallel components of the contravariant velocities. Thus the parallel components of the contravariant velocities are obtained by interpolation from the normal components

of the contravariant velocities which do satisfy the mass conservation (refer to Appendix G for details).

3.6.6 The Discretization Method

The transformed governing equations are discretized using the method known as the "control-volume" finite difference approach^{69,70}. Applying this method, the calculation domain is divided into a number of control volumes such that there is one control-volume surrounding each grid-point. The differential equations are integrated over each control-volume. For 3D problems, triple integrals are involved. In the formulation of the discretization equations, the upwind difference scheme is applied to the convective terms and the central difference approximation to the diffusion terms. A three-dimensional control volume is shown in Figure 3.7.

3.6.7 Location of the Control-Volume Faces

For the proper location of the control-volume faces, the B-type grid or practice-B⁶⁹ is employed here (Figure 3.8). In this arrangement, one first draws the control-volume boundaries and then places a grid-point at the geometric center of each control-volume through which the main grid lines are drawn. If the grid is designed this way; then the entire calculation domain would be covered with regular control-volumes.

3.6.8 The Solution method of the Discretization Equations

The discretization equations are algebraic equations and are solved by a line-by-line tridiagonal matrix (TDMA) algorithm. Introducing a relaxation-factor to the discretization equations one may enhance the convergence of the iterative solution. With the line-by-line method use of overrelaxation is uncommon while underrelaxation is often used to avoid divergence in the iterative solution of the equation⁶⁹.

3.7 SOLUTION PROCEDURE

3.7.1 Use of Primitive Variables Versus Stream Function/Velocity Method

For the two-dimensional fluid-flow problems, one method is to use the stream-function/vorticity formulation, by which the pressure-determination is avoided and the number of equations are reduced from 3 to 2. In three-dimensional fluid-flow problems, however, generalization of the two-dimensional stream-function/vorticity formulation, increases the number of variables from 4 to 6 and hence the method loses its attractive features and what is claimed to be a great advantage. Moreover, by retaining the primitive variables, the equations are solved for the quantities that are of direct interest.

3.7.2 Handling of Pressure-Velocity Coupling in the Parabolic Direction

The method adopted here is that of Raithby Schneider⁷¹. Primarily the momentum equation in the axial-direction is solved with the boundary-condition using a guessed pressure-gradient $\left(\frac{\partial \bar{P}}{\partial \sigma}\right)$ to obtain a tentative axial-velocity w_P^* . The corresponding mass flow rate is

$$M^* = \sum_{\text{all } P} J \rho w^* \quad (3.28)$$

where "all P" denotes all the w -control volumes inside the duct walls. Defining two new variables:

$$Q = -\frac{\partial \bar{P}}{\partial \sigma} \quad \text{and} \quad f_P = \frac{\partial w}{\partial Q} \quad (3.29)$$

The corrected pressure-gradient $\left(\frac{\partial \bar{P}}{\partial \sigma}\right)$ would be related to $\left(\frac{\partial \bar{P}}{\partial \sigma}\right)^*$ by

$$\Delta Q = -\left[\frac{\partial \bar{P}}{\partial \sigma} - \left(\frac{\partial \bar{P}}{\partial \sigma}\right)^* \right] \quad (3.30)$$

And the corrected axial-velocity would be related to w_p^* by

$$w_P = w_p^* + f_P \Delta Q \quad (3.31)$$

where f_P is obtained from the following discretization-equation using appropriate boundary-conditions:

$$A_P^w f_P = A_e^w f_E + A_w^w f_W + A_n^w f_N + A_s^w f_S + J_P \Delta V \quad (3.32)$$

and ΔQ values is chosen to make the total mass flow rate constant, i.e.

$$\Delta Q = \frac{M - M^*}{\sum_{\text{all } P} J_P f_P} \quad (3.33)$$

in which "M" is the exact mass-flow rate known from the inlet conditions.

3.7.3 Pressure-Velocity Coupling in the Transverse Direction

Any assumed pressure distribution is checked by determining whether the velocities obtained from the momentum equations using this pressure field conserves mass or not. Thus, we find the pressure field which drives velocities such that the overall continuity equation is satisfied. Hadjisophocleous et al.⁶⁶, Shyy et al.⁶⁷ and Braaten et al.⁶⁸ employed the SIMPLE algorithm⁶⁹ in their analysis for non-orthogonal systems. Maliska⁴⁶ proposed a mixed scheme comprising of the SIMPLE and the SIMPLER algorithms⁶⁹. In the present work the SIMPLER algorithm modified for non-orthogonal system⁴⁶ is further developed for the solution of the power-law non-Newtonian fluid problems and is employed in the solution procedure. The algorithm is explained briefly in the following paragraph.

The coefficients of the "u" and "v" momentum equations are computed using the best available velocities. A Poisson-like equation for pressure using pseudovelocities is

solved to obtain a tentative pressure-field, P^* , which is used to solve the "u" and "v" momentum equations to obtain the starred-velocities u^* and v^* . These velocities do not, in general, conserve mass. The corresponding values of U^* and V^* are obtained by substituting u^* and v^* in the following relations:

$$U^* = y_\eta u^* - x_\eta v^* \quad (3.34)$$

$$V^* = x_\xi v^* - y_\xi u^* \quad (3.35)$$

These velocities must be corrected by $U - U^*$ and $V - V^*$ respectively, to obtain "U" and "V" velocities which do conserve mass. The above changes are related to the corresponding required changes in the "u" and "v" velocities as follows:

$$U - U^* = y_\eta(u - u^*) - x_\eta(v - v^*) \quad (3.36)$$

$$V - V^* = x_\xi(v - v^*) - y_\xi(u - u^*) \quad (3.37)$$

Estimates of change in "u" and "v" that result from change in "P" are:

$$u_e - u_e^* = -\frac{\Delta V}{A_e^u} \left\{ \frac{P'_E - P'_P}{\Delta \xi} (y_\eta)_e - \frac{P'_N + P'_{NE} - P'_S - P'_{SE}}{4\Delta \eta} (y_\xi)_e \right\} \quad (3.38)$$

$$v_e - v_e^* = -\frac{\Delta V}{A_e^v} \left\{ \frac{P'_N + P'_{NE} - P'_S - P'_{SE}}{4\Delta \eta} (x_\xi)_e - \frac{P'_E - P'_P}{\Delta \xi} (x_\eta)_e \right\} \quad (3.39)$$

in which $P' = P - P^*$. Similar expressions are obtained for $u_n - u_n^*$, $v_n - v_n^*$, $u_w - u_w^*$, $v_w - v_w^*$, $u_s - u_s^*$, and $v_s - v_s^*$. The value of P' is obtained from a Poisson-like pressure-correction equation derived in this work for the power-law non-Newtonian fluid in which the starred-velocities are used (Appendix F). Once the P' is known, the contravariant velocities which enter into the mass-balance (U_e , U_w , V_s , V_n) can be found from the Eqns. (3.36) and (3.37). The other contravariant-velocities (V_e , U_n , V_w , U_s)

are obtained by interpolation (Appendix G). The physical velocities "u" and "v" are readily obtained from the relevant equations.

To obtain an equation for pressure correction, P' , one should substitute the velocity-correction (3.38), (3.39) etc. in Eqns. (3.36) and (3.37) to obtain equations for "U'" and "V'" in terms of U^* , V^* and P' which when substituted in the overall continuity equation:

$$\frac{(\rho U)_e - (\rho U)_w}{\Delta \xi} + \frac{(\rho V)_n - (\rho V)_s}{\Delta \eta} + \frac{(\rho W)_D - (\rho W)_U}{\Delta \sigma} = 0 \quad (3.40)$$

results the following Poisson-like pressure-correction equation:

$$A_P P'_P = A_E P'_E + A_N P'_N + A_S P'_S + A_W P'_W + A_{NE} P'_{NE} + A_{SE} P'_{SE} + A_{NW} P'_{NW} + A_{SW} P'_{SW} + B \quad (3.41)$$

in which

$$A_P = A_E + A_N + A_W + A_S \quad (3.42)$$

also

$$A_{NE} + A_{NW} + A_{SW} + A_{SE} = 0 \quad (3.43)$$

Refer to Appendix F for the values of B and the coefficients. The Poisson-like pressure equations is similar to the equation for pressure-correction equation,

$$A_P P_P = A_E P_E + A_N P_N + A_S P_S + A_W P_W + A_{NE} P_{NE} + A_{SE} P_{SE} + A_{NW} P_{NW} + A_{SW} P_{SW} + B \quad (3.44)$$

with the exception of the B term which is expressed in terms of pseudovelocities for the pressure equation while starred-velocities are used in the relation for pressure-correction.

3.7.4 Outline of the Solution Procedure

In the 3D parabolic solution method, applying marching integration from plane to plane, all the velocity components, pressure, temperature and concentration fields are iterated to convergence over a given plane employing the stored values of these parameters at the upstream plane. The results obtained over the plane under computation is then stored as upstream-plane-data to be employed in the computation at the next downstream plane. This process is followed in the axial direction up to convergence at successive planes.

The method for handling pressure-velocity coupling in the parabolized axial direction and the modified SIMPLER algorithm dealing with the pressure-velocity coupling in the transverse direction are used in the solution procedure for computation over each plane.

Due to the inter-equation coupling and the general interdependence of the physical properties to temperature and mass-fraction, all the equations must be solved simultaneously for each cycle of iteration in the following order:

- axial momentum equation,
- transverse momentum equations,
- energy equation,
- reactant continuity equation.

For the power-law non-Newtonian fluids, the constitutive equation is dependent on the velocity field as well as the temperature and mass-fraction fields for its consistency index. The convergence is further improved by an inner iteration for the axial velocity component in each cycle mentioned above.

The following solution procedure is developed in this study for the solution of 3D parabolized conservation equations in ducts of arbitrary cross-sections for either Newtonian or non-Newtonian fluids:

- (i) compute the coefficients for the axial momentum equation using the best available velocities and using a guessed pressure-gradient solve the axial momentum-equation for a tentative axial-velocity, w^* ,
- (ii) solve for the factor "f" and calculate " ΔQ ",
- (iii) Calculate the corrected axial-velocity field, w , and the corrected pressure-gradient in the axial direction, using the "f" and the " ΔQ " parameters. Proceed to perform an inner iteration for w .
- (iv) using the best available velocities, compute the coefficients for the "u" and "v" momentum equations,
- (v) compute the pseudovelocities, \hat{u} and \hat{v} and the corresponding contravariant components \hat{U} and \hat{V} using the relevant relations,
- (vi) solve the Poisson-like equation for pressure, P , in which \hat{U} and \hat{V} are used,
- (vii) treating this pressure-field as P^* , solve transverse momentum equations for u^* and v^* ,
- (viii) calculate the corresponding U^* and V^* from the relevant equations,
- (ix) solve the Poisson-like equation for pressure-correction, P' , in which U^* and V^* are used,
- (x) correct U^* and V^* velocities using P' solution to obtain "U" and "V" components that conserve mass and obtain the other components of "U" and "V" velocities by interpolation,
- (xi) compute the physical velocities, "u" and "v" from the latter contravariant-velocities using the relevant equations.
- (xii) solve the energy equation,
- (xiii) solve the reactant continuity equation.

With the new velocity field, temperature and mass-fraction values obtained above return to Step (i) and iterate up to convergence.

3.8 CLOSURE

The non-orthogonal boundary-fitted coordinate transformation method is introduced in this chapter for grid generation of the physical domain and transformation of the Cartesian governing equations to the curvilinear coordinate system. The discretization procedure for the transformed equations employing the control volume approach is then explained. A solution procedure, developed in this study, is described briefly.

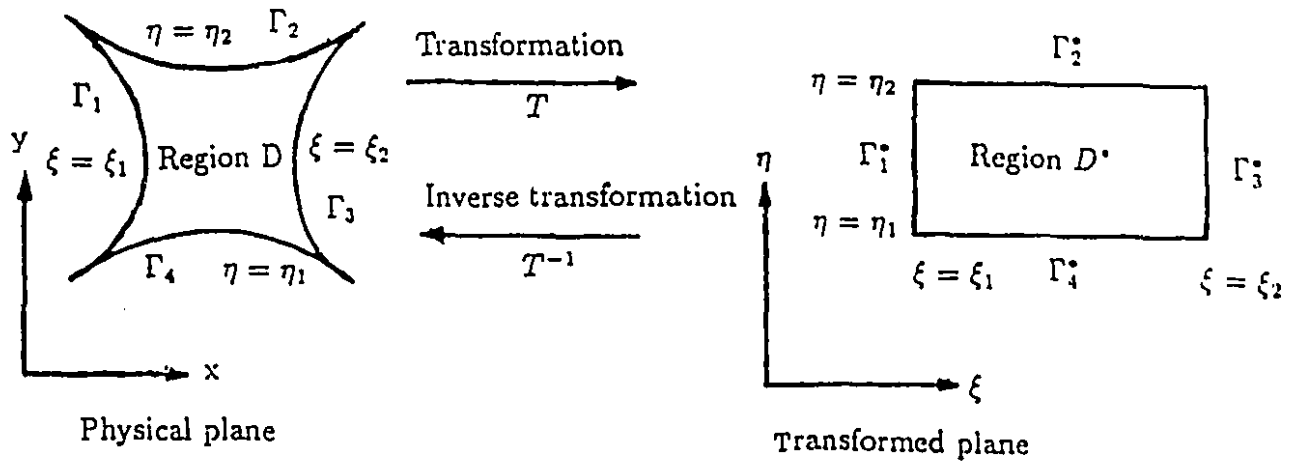
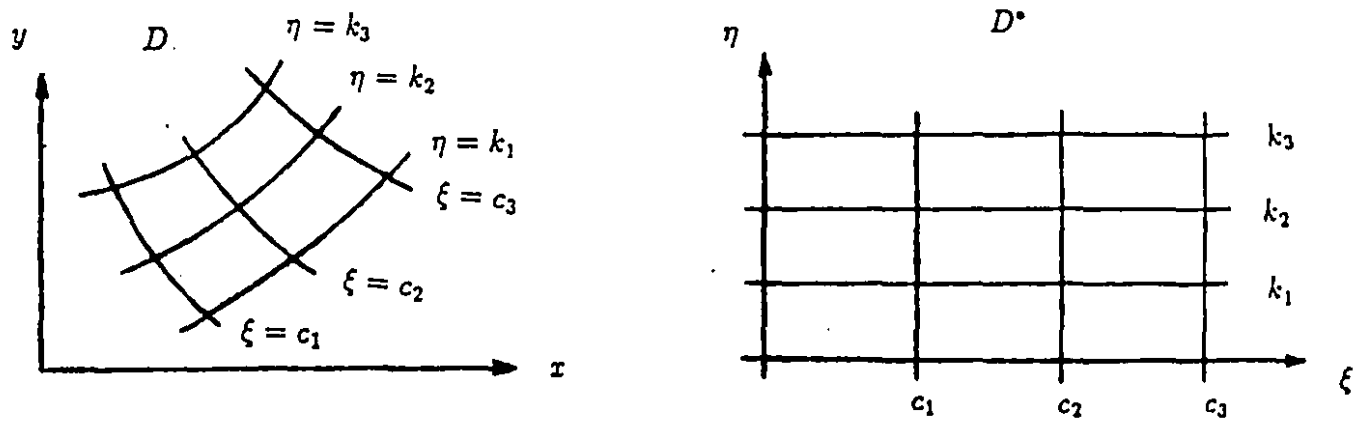


Fig. 3.1 Curvilinear transformation



Curvilinear curves in the physical plane

transformed rectangular domain

Fig. 3.2 Grid generation

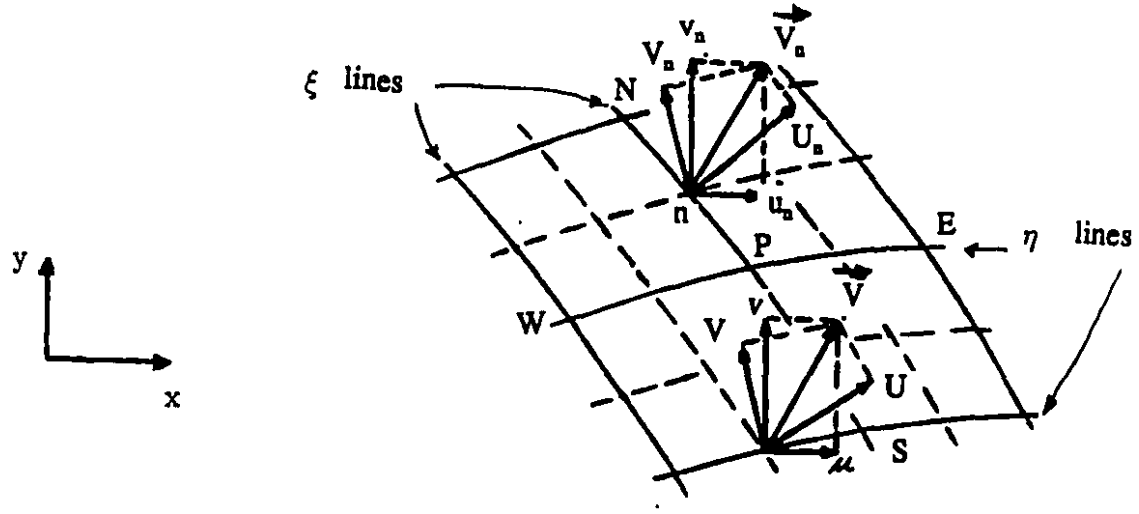


Fig. 3.3 Contravariant velocities

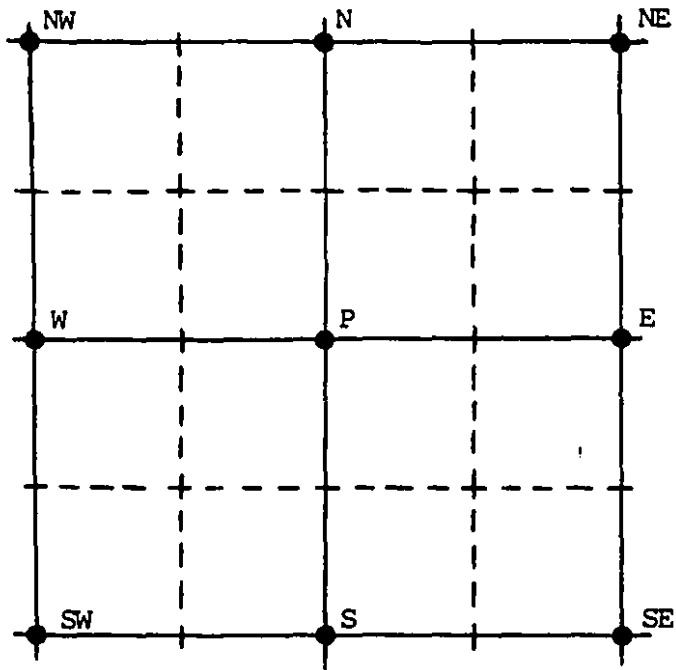


Figure 3.4
Non-staggered Grid Arrangement

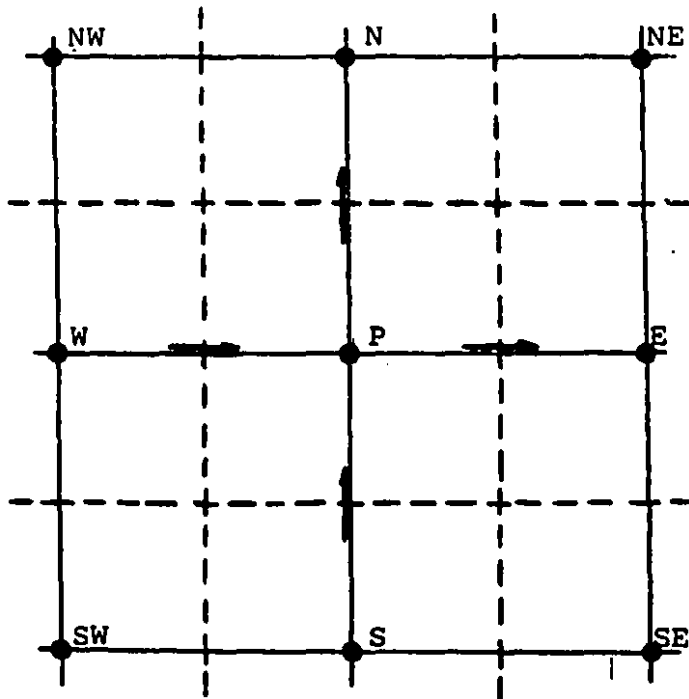


Figure 3.5
Classical Staggered Grid Arrangement

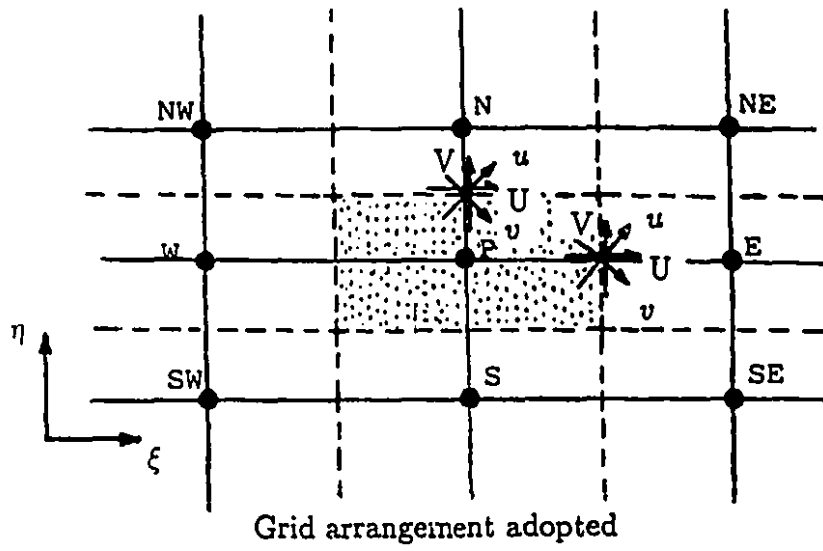


Figure 3.6

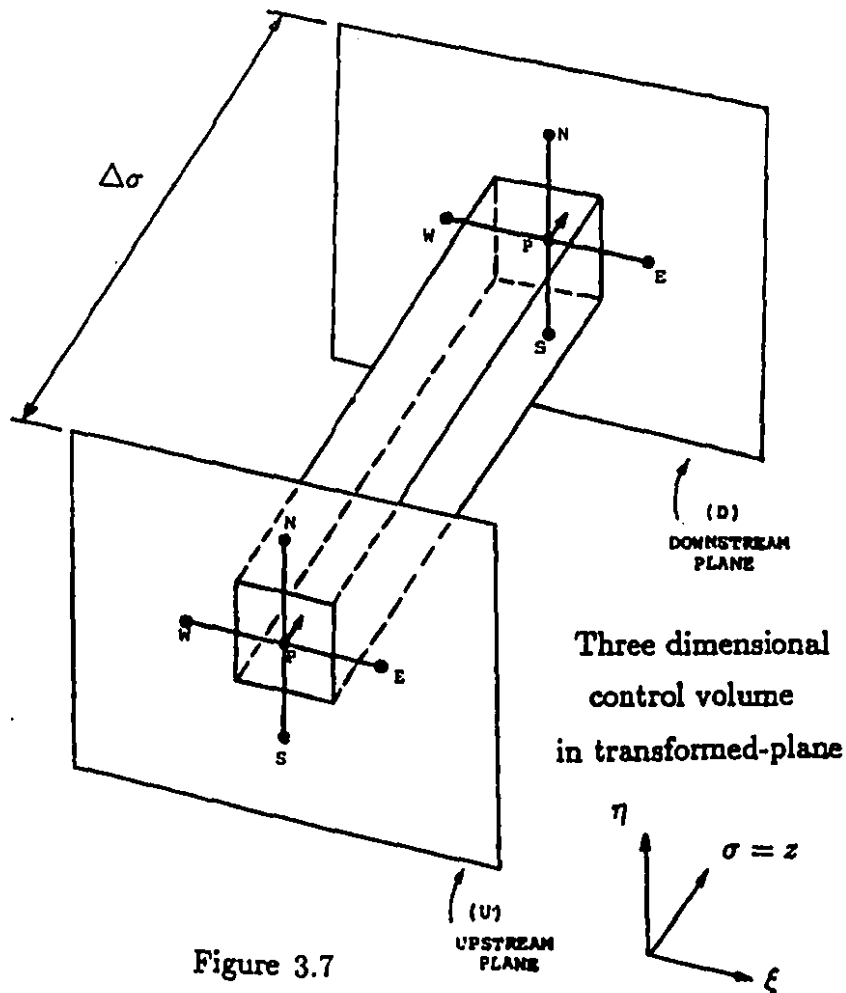


Figure 3.7

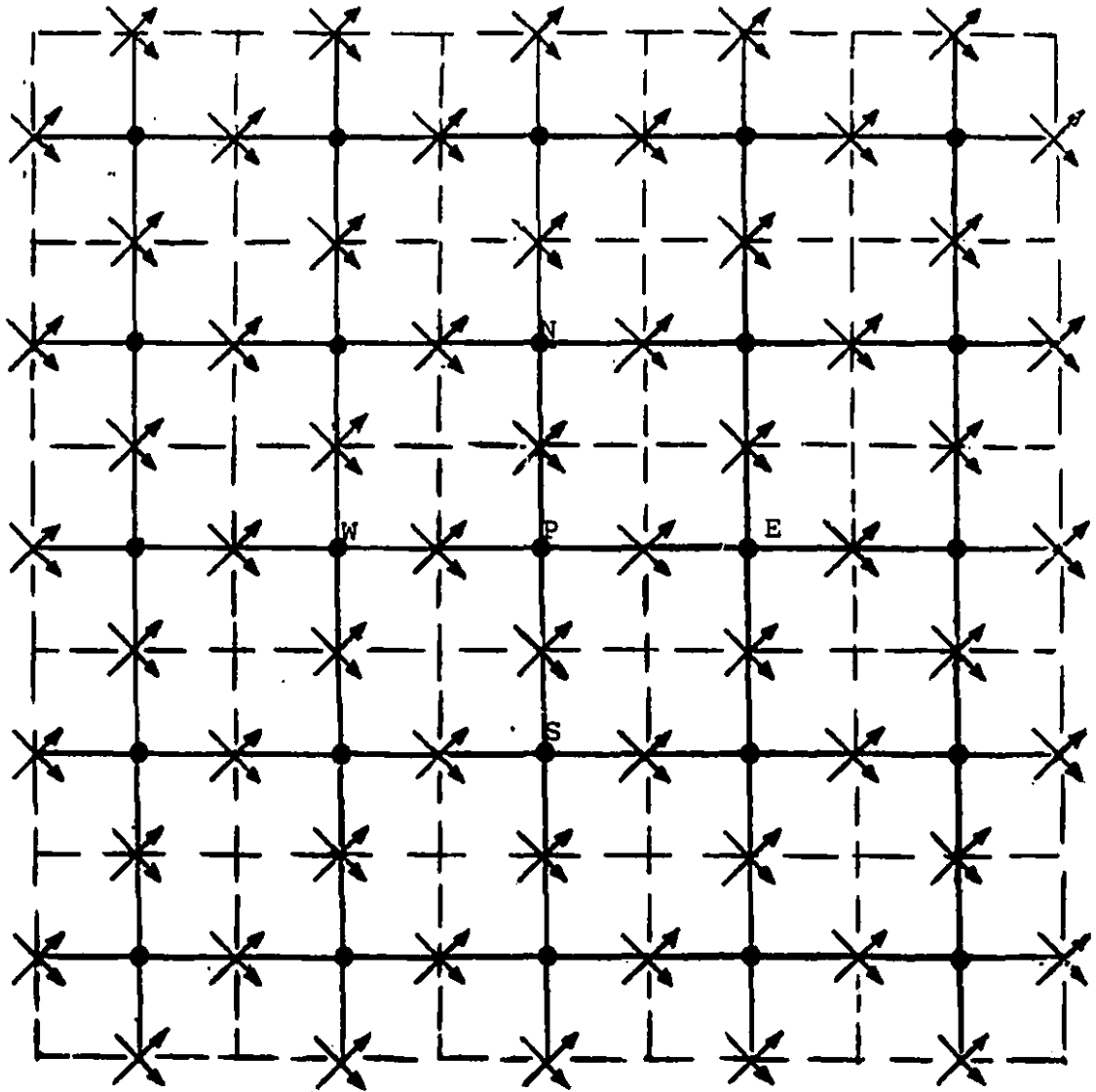


Figure 3.8

Physical Velocities over the Whole Computational Domain

CHAPTER 4

THE TRANSFORMATION AND DISCRETIZATION OF GOVERNING EQUATIONS AND BOUNDARY CONDITIONS

4.1 INTRODUCTION

The final form of the transformed and discretized governing equations followed by the boundary conditions are presented in this chapter. The details of transformation from Cartesian coordinates to the curvilinear coordinates are presented in Appendix B. In this transformation the physical Cartesian velocity components are retained as the dependent variables, while transformation relations of partial derivatives are applied to the parabolized governing PDEs through which the Jacobian of transformation is brought in the manipulated equations. Furthermore, the contravariant velocity components are introduced in the transformed equations substituting their relevant relationships.

It is observed that the conservative form of the governing equations are preserved upon transformation.

The transformed components of the stress tensor, expressed by the power-law constitutive equation, are substituted in the transformed governing equations which are then expanded to their ultimate form before being used for discretization.

It is to be noted that the source term in the transformed energy equation is composed of the viscous dissipation and the heat of reaction terms, while the source term in the transformed reactant continuity equation involves the rate of reactant consumption due to chemical reaction.

A typical derivation of the discretization equations is presented in Appendix C. For each nodal point P, four adjacent control volumes surrounding the interfacial points (e, n, w and s) are considered over which the transformed transverse momentum equations

are integrated and discretized. Thus, four pairs of discretization relations for u and v velocities, namely, (u_e, v_e) , (u_n, v_n) , (u_w, v_w) and (u_s, v_s) are obtained. Meanwhile, the transformed equations for axial momentum, energy and reactant continuity are integrated over the main control volume enclosing the nodal point P from which the discretization equations for w_P , h_P and m_P are obtained.

The discretization of each specific transformed equation, following integration, is accomplished by applying the upwind difference scheme to the convective terms and the central difference scheme to the diffusion terms. Moreover, the fact that the flow field must satisfy the mass conservation equation provides some simplification to the discretized governing equations combined with the discretized overall continuity equation. Finally each equation is cast into the general discretization form, that is, an algebraic relation connecting values of the dependent variable for a group of grid points, bearing their respective coefficients.

Specific derivation is required for the transformation and discretization of the the wall condition for the reactant continuity equation, the details of which are presented in Appendix E.

4.2 THE TRANSFORMED GOVERNING EQUATIONS

4.2.1 The Overall Continuity Equation

$$\frac{\partial}{\partial \xi}(\rho U) + \frac{\partial}{\partial \eta}(\rho V) + \frac{\partial}{\partial \sigma}(\rho W) = 0 \quad (4.1)$$

4.2.2 The Momentum Equations

x-Component

$$\frac{\partial}{\partial \xi}(\rho u U) + \frac{\partial}{\partial \eta}(\rho u V) + \frac{\partial}{\partial \sigma}(\rho u W) = -\frac{\partial}{\partial \xi} [y_{\eta}(\hat{\tau}_{xx}) - x_{\eta}(\hat{\tau}_{yx})] - \frac{\partial}{\partial \eta} [x_{\xi}(\hat{\tau}_{yx}) - y_{\xi}(\hat{\tau}_{xx})] - [y_{\eta} P_{\xi} - y_{\xi} P_{\eta}] \quad (4.2)$$

y-Component

$$\frac{\partial}{\partial \xi}(\rho v U) + \frac{\partial}{\partial \eta}(\rho v V) + \frac{\partial}{\partial \sigma}(\rho v W) = -\frac{\partial}{\partial \xi} [y_{\eta}(\hat{\tau}_{xy}) - x_{\eta}(\hat{\tau}_{yy})] - \frac{\partial}{\partial \eta} [x_{\xi}(\hat{\tau}_{yy}) - y_{\xi}(\hat{\tau}_{xy})] - [x_{\xi} P_{\eta} - x_{\eta} P_{\xi}] - J(\rho - \rho_a)g \quad (4.3)$$

z-Component

$$\frac{\partial}{\partial \xi}(\rho w U) + \frac{\partial}{\partial \eta}(\rho w V) + \frac{\partial}{\partial \sigma}(\rho w W) = -\frac{\partial}{\partial \xi} [y_{\eta}(\hat{\tau}_{xz}) - x_{\eta}(\hat{\tau}_{yz})] - \frac{\partial}{\partial \eta} [x_{\xi}(\hat{\tau}_{yz}) - y_{\xi}(\hat{\tau}_{xz})] - J \frac{d\bar{P}}{d\sigma} \quad (4.4)$$

4.2.3 The Energy Equation

$$\begin{aligned} \frac{\partial}{\partial \xi}(\rho C_p T U) + \frac{\partial}{\partial \eta}(\rho C_p T V) + \frac{\partial}{\partial \sigma}(\rho C_p T W) = \\ \frac{\partial}{\partial \xi} \left[\frac{\alpha}{J} k T_{\xi} - \frac{\beta}{J} k T_{\eta} \right] + \\ \frac{\partial}{\partial \eta} \left[\frac{\gamma}{J} k T_{\eta} - \frac{\beta}{J} k T_{\xi} \right] + J \dot{M} \hat{i} + J(-\Delta H) \dot{R}_A \quad (4.5) \end{aligned}$$

4.2.4 The Reactant Continuity Equation

$$\begin{aligned} \frac{\partial}{\partial \xi}(\rho \omega_A U) + \frac{\partial}{\partial \eta}(\rho \omega_A V) + \frac{\partial}{\partial \sigma}(\rho \omega_A W) = \\ \frac{\partial}{\partial \xi} \left[\frac{\rho D_A}{J} \alpha \omega_\xi - \frac{\rho D_A}{J} \beta \omega_\eta \right] + \\ \frac{\partial}{\partial \eta} \left[\frac{\rho D_A}{J} \gamma \omega_\eta - \frac{\rho D_A}{J} \beta \omega_\xi \right] - J \hat{R}_A \end{aligned} \quad (4.6)$$

where $\omega \equiv \omega_A$ for the derivatives.

4.2.5 The Transformed Forms of Components of Stress-Tensor, "I" and "M"

$$\hat{\tau}_{xx} = -\frac{2}{J} [y_\eta u_\xi - y_\xi u_\eta] \hat{M} \quad (4.7)$$

$$\hat{\tau}_{yy} = -\frac{2}{J} [x_\xi v_\eta - x_\eta v_\xi] \hat{M} \quad (4.8)$$

$$\hat{\tau}_{zz} = -2 \left[\frac{\partial w}{\partial \sigma} \right] \hat{M} \quad (4.9)$$

$$\hat{\tau}_{xy} = \hat{\tau}_{yz} = -\frac{1}{J} [x_\xi u_\eta - x_\eta u_\xi + y_\eta v_\xi - y_\xi v_\eta] \hat{M} \quad (4.10)$$

$$\hat{\tau}_{xz} = \hat{\tau}_{zx} = - \left[\frac{\partial u}{\partial \sigma} + \frac{1}{J} [y_\eta w_\xi - y_\xi w_\eta] \right] \hat{M} \quad (4.11)$$

$$\hat{\tau}_{yz} = \hat{\tau}_{zy} = - \left[\frac{\partial v}{\partial \sigma} + \frac{1}{J} [x_\xi w_\eta - x_\eta w_\xi] \right] \hat{M} \quad (4.12)$$

$$\begin{aligned} \hat{I} = 2 \left[\left(\frac{y_\eta}{J} u_\xi - \frac{y_\xi}{J} u_\eta \right)^2 + \left(\frac{x_\xi}{J} v_\eta - \frac{x_\eta}{J} v_\xi \right)^2 + \left(\frac{\partial w}{\partial \sigma} \right)^2 \right] + \\ \left[\frac{y_\eta}{J} v_\xi - \frac{y_\xi}{J} v_\eta + \frac{x_\xi}{J} u_\eta - \frac{x_\eta}{J} u_\xi \right]^2 + \\ \left[\frac{x_\xi}{J} w_\eta - \frac{x_\eta}{J} w_\xi + \frac{\partial v}{\partial \sigma} \right]^2 + \\ \left[\frac{y_\eta}{J} w_\xi - \frac{y_\xi}{J} w_\eta + \frac{\partial u}{\partial \sigma} \right]^2 \end{aligned} \quad (4.13)$$

$$\hat{M} = \mu \cdot \hat{I}^{\left(\frac{n-1}{2}\right)} \quad (4.14)$$

4.3 THE EXPANDED SET OF TRANSFORMED GOVERNING EQUATIONS

4.3.1 The Overall Continuity Equation

$$\frac{\partial}{\partial \xi}(\rho U) + \frac{\partial}{\partial \eta}(\rho V) + \frac{\partial}{\partial \sigma}(\rho W) = 0 \quad (4.15)$$

4.3.2 The Momentum Equations

x-Component

$$\begin{aligned} \frac{\partial}{\partial \xi}(\rho u U) + \frac{\partial}{\partial \eta}(\rho u V) + \frac{\partial}{\partial \sigma}(\rho u W) = & \frac{\partial}{\partial \xi} \left[C_1^u \frac{\partial u}{\partial \xi} \right] + \frac{\partial}{\partial \xi} \left[C_2^u \frac{\partial u}{\partial \eta} \right] + \\ & \frac{\partial}{\partial \xi} \left[C_3^u \frac{\partial v}{\partial \xi} \right] + \frac{\partial}{\partial \xi} \left[C_4^u \frac{\partial v}{\partial \eta} \right] + \\ & \frac{\partial}{\partial \eta} \left[C_5^u \frac{\partial u}{\partial \eta} \right] + \frac{\partial}{\partial \eta} \left[C_6^u \frac{\partial u}{\partial \xi} \right] + \\ & \frac{\partial}{\partial \eta} \left[C_7^u \frac{\partial v}{\partial \eta} \right] + \frac{\partial}{\partial \eta} \left[C_8^u \frac{\partial v}{\partial \xi} \right] - \hat{P}^u \end{aligned} \quad (4.16)$$

where

$$C_1^u = \frac{\hat{M}}{J} [\alpha + y_\eta^2] \quad (4.17)$$

$$C_2^u = -\frac{\hat{M}}{J} [\beta + y_\xi y_\eta] \quad (4.18)$$

$$C_3^u = -\frac{\hat{M}}{J} x_\eta y_\eta \quad (4.19)$$

$$C_4^u = \frac{\hat{M}}{J} x_\eta y_\xi \quad (4.20)$$

$$C_5^u = \frac{\hat{M}}{J} [\gamma + y_\xi^2] \quad (4.21)$$

$$C_6^u = -\frac{\hat{M}}{J} [\beta + y_\xi y_\eta] \quad (4.22)$$

$$C_7^u = -\frac{\hat{M}}{J} x_\xi y_\xi \quad (4.23)$$

$$C_8^u = \frac{\hat{M}}{J} y_\eta x_\xi \quad (4.24)$$

$$\hat{P}^u = \frac{\partial P}{\partial \xi} y_\eta - \frac{\partial P}{\partial \eta} y_\xi \quad (4.25)$$

y-Component

$$\begin{aligned}
 \frac{\partial}{\partial \xi}(\rho v U) + \frac{\partial}{\partial \eta}(\rho v V) + \frac{\partial}{\partial \sigma}(\rho v W) = & \frac{\partial}{\partial \xi} \left[C_1^v \frac{\partial v}{\partial \xi} \right] + \frac{\partial}{\partial \xi} \left[C_2^v \frac{\partial v}{\partial \eta} \right] + \\
 & \frac{\partial}{\partial \xi} \left[C_3^v \frac{\partial u}{\partial \xi} \right] + \frac{\partial}{\partial \xi} \left[C_4^v \frac{\partial u}{\partial \eta} \right] + \\
 & \frac{\partial}{\partial \eta} \left[C_5^v \frac{\partial v}{\partial \eta} \right] + \frac{\partial}{\partial \eta} \left[C_6^v \frac{\partial v}{\partial \xi} \right] + \\
 & \frac{\partial}{\partial \eta} \left[C_7^v \frac{\partial u}{\partial \eta} \right] + \frac{\partial}{\partial \eta} \left[C_8^v \frac{\partial u}{\partial \xi} \right] - \\
 & \hat{P}^v - \hat{S}^v
 \end{aligned} \tag{4.26}$$

where

$$C_1^v = \frac{\hat{M}}{J}[\alpha + x_\eta^2] \tag{4.27}$$

$$C_2^v = -\frac{\hat{M}}{J}[\beta + x_\xi x_\eta] \tag{4.28}$$

$$C_3^v = -\frac{\hat{M}}{J}x_\eta y_\eta \tag{4.29}$$

$$C_4^v = \frac{\hat{M}}{J}x_\xi y_\eta \tag{4.30}$$

$$C_5^v = \frac{\hat{M}}{J}[\gamma + x_\xi^2] \tag{4.31}$$

$$C_6^v = -\frac{\hat{M}}{J}[\beta + x_\xi x_\eta] \tag{4.32}$$

$$C_7^v = -\frac{\hat{M}}{J}x_\xi y_\xi \tag{4.33}$$

$$C_8^v = \frac{\hat{M}}{J}x_\eta y_\xi \tag{4.34}$$

$$\hat{P}^v = \frac{\partial P}{\partial \eta} x_\xi - \frac{\partial P}{\partial \xi} x_\eta \tag{4.35}$$

$$\hat{S}^v = J(\rho - \rho_a)g \tag{4.36}$$

z-Component

$$\begin{aligned}
 \frac{\partial}{\partial \xi}(\rho w U) + \frac{\partial}{\partial \eta}(\rho w V) + \frac{\partial}{\partial \sigma}(\rho w W) = & \frac{\partial}{\partial \xi} \left[C_1^w \frac{\partial w}{\partial \xi} \right] + \frac{\partial}{\partial \xi} \left[C_2^w \frac{\partial w}{\partial \eta} \right] + \\
 & \frac{\partial}{\partial \xi} \left[C_3^w \frac{\partial u}{\partial \sigma} \right] + \frac{\partial}{\partial \xi} \left[C_4^w \frac{\partial v}{\partial \sigma} \right] + \\
 & \frac{\partial}{\partial \eta} \left[C_5^w \frac{\partial w}{\partial \eta} \right] + \frac{\partial}{\partial \eta} \left[C_6^w \frac{\partial w}{\partial \xi} \right] + \\
 & \frac{\partial}{\partial \eta} \left[C_7^w \frac{\partial u}{\partial \sigma} \right] + \frac{\partial}{\partial \eta} \left[C_8^w \frac{\partial v}{\partial \sigma} \right] - \hat{P}^w \quad (4.37)
 \end{aligned}$$

where

$$C_1^w = \frac{\hat{M}}{J} \alpha \quad (4.38)$$

$$C_2^w = -\frac{\hat{M}}{J} \beta \quad (4.39)$$

$$C_3^w = \hat{M} y_\eta \quad (4.40)$$

$$C_4^w = -\hat{M} x_\eta \quad (4.41)$$

$$C_5^w = \frac{\hat{M}}{J} \gamma \quad (4.42)$$

$$C_6^w = -\frac{\hat{M}}{J} \beta \quad (4.43)$$

$$C_7^w = -\hat{M} y_\xi \quad (4.44)$$

$$C_8^w = \hat{M} x_\xi \quad (4.45)$$

$$\hat{P}^w = J \frac{d\bar{P}}{d\sigma} \quad (4.46)$$

4.3.3 The Energy Equation

$$\begin{aligned} \frac{\partial}{\partial \xi}(\rho h U) + \frac{\partial}{\partial \eta}(\rho h V) + \frac{\partial}{\partial \sigma}(\rho h W) = \frac{\partial}{\partial \xi} \left[C_1^h \frac{\partial h}{\partial \xi} + C_2^h \frac{\partial h}{\partial \eta} \right] + \\ \frac{\partial}{\partial \eta} \left[C_3^h \frac{\partial h}{\partial \eta} + C_4^h \frac{\partial h}{\partial \xi} \right] + \hat{S}^h \end{aligned} \quad (4.47)$$

in which

$$h = C_P T \quad (4.48)$$

$$C_1^h = \frac{\alpha}{J} \frac{k}{C_P} \quad (4.49)$$

$$C_2^h = -\frac{\beta}{J} \frac{k}{C_P} \quad (4.50)$$

$$C_3^h = \frac{\gamma}{J} \frac{k}{C_P} \quad (4.51)$$

$$C_4^h = -\frac{\beta}{J} \frac{k}{C_P} \quad (4.52)$$

$$\hat{S}^h = J \hat{M} \hat{I} + J(-\Delta H) \hat{R}_A \quad (4.53)$$

4.3.4 The Reactant Continuity Equation

$$\begin{aligned} \frac{\partial}{\partial \xi}(\rho m U) + \frac{\partial}{\partial \eta}(\rho m V) + \frac{\partial}{\partial \sigma}(\rho m W) = \frac{\partial}{\partial \xi} \left[C_1^m \frac{\partial m}{\partial \xi} + C_2^m \frac{\partial m}{\partial \eta} \right] + \\ \frac{\partial}{\partial \eta} \left[C_3^m \frac{\partial m}{\partial \eta} + C_4^m \frac{\partial m}{\partial \xi} \right] + \hat{S}^m \end{aligned} \quad (4.54)$$

where

$$m = \omega_A \quad (4.55)$$

$$C_1^m = \frac{\rho D_A}{J} \alpha \quad (4.56)$$

$$C_2^m = -\frac{\rho D_A}{J} \beta \quad (4.57)$$

$$C_3^m = \frac{\rho D_A}{J} \gamma \quad (4.58)$$

$$C_4^m = -\frac{\rho D_A}{J} \beta \quad (4.59)$$

$$\hat{S}^m = -J \hat{R}_A \quad (4.60)$$

4.3.5 The “ \hat{I} ” and “ \hat{M} ” Terms

$$\begin{aligned} \hat{I} = 2 \left\{ \left[\frac{y_\eta}{J} u_\xi - \frac{y_\xi}{J} u_\eta \right]^2 + \left[\frac{x_\xi}{J} v_\eta - \frac{x_\eta}{J} v_\xi \right]^2 + \left[\frac{\partial w}{\partial \sigma} \right]^2 \right\} + \\ \left[\frac{y_\eta}{J} v_\xi - \frac{y_\xi}{J} v_\eta + \frac{x_\xi}{J} u_\eta - \frac{x_\eta}{J} u_\xi \right]^2 + \left[\frac{x_\xi}{J} w_\eta - \frac{x_\eta}{J} w_\xi + \frac{\partial v}{\partial \sigma} \right]^2 + \\ \left[\frac{y_\eta}{J} w_\xi - \frac{y_\xi}{J} w_\eta + \frac{\partial u}{\partial \sigma} \right]^2 \end{aligned} \quad (4.61)$$

$$\hat{M} = \mu \cdot \hat{I}^{\left(\frac{n-1}{2}\right)} \quad (4.62)$$

4.4 THE DISCRETIZATION EQUATIONS

4.4.1 Discretization Equation for “ u_e ”

(Refer to Figure 4.1)

$$\begin{aligned} AP_e^u \cdot u_e = AE_e^u \cdot u_{Ee} + AN_e^u \cdot u_{Ne} + AW_e^u \cdot u_{We} + \\ AS_e^u \cdot u_{Se} + B_e^u - L[\hat{P}_e^u] \Delta V \end{aligned} \quad (4.63)$$

or

$$\begin{aligned} AP_e^u \cdot u_e = \sum A_{(nb)e}^u \cdot u_{(nb)e} + B_e^u - \\ \left\{ \frac{P_E - P_P}{\Delta \xi} y_{\eta e} - \frac{P_N + P_{NE} - P_S - P_{SE}}{4\Delta \eta} y_{\xi e} \right\} \Delta V \end{aligned} \quad (4.64)$$

where

$$AP_e^u = AE_e^u + AN_e^u + AW_e^u + AS_e^u + AU_e \quad (4.65)$$

$$\begin{aligned}
AP_e^u = & \| -(\rho U)_{E,0} \| \Delta \eta \Delta \sigma + \| (\rho U)_{P,0} \| \Delta \eta \Delta \sigma + \| -(\rho V)_{ne,0} \| \Delta \xi \Delta \sigma + \\
& \| (\rho V)_{se,0} \| \Delta \xi \Delta \sigma + (\rho W)_{e,U} \Delta \xi \Delta \eta + \frac{C_{1E}^u \Delta \eta \Delta \sigma}{\Delta \xi} + \frac{C_{1P}^u \Delta \eta \Delta \sigma}{\Delta \xi} + \\
& \frac{C_{5ne}^u \Delta \xi \Delta \sigma}{\Delta \eta} + \frac{C_{5se}^u \Delta \xi \Delta \sigma}{\Delta \eta}
\end{aligned} \quad (4.66)$$

$$AE_e^u = \| -(\rho U)_{E,0} \| \Delta \eta \Delta \sigma + \frac{C_{1E}^u \Delta \eta \Delta \sigma}{\Delta \xi} \quad (4.67)$$

$$AN_e^u = \| -(\rho V)_{ne,0} \| \Delta \xi \Delta \sigma + \frac{C_{5ne}^u \Delta \xi \Delta \sigma}{\Delta \eta} \quad (4.68)$$

$$AW_e^u = \| (\rho U)_{P,0} \| \Delta \eta \Delta \sigma + \frac{C_{1P}^u \Delta \eta \Delta \sigma}{\Delta \xi} \quad (4.69)$$

$$AS_e^u = \| (\rho V)_{se,0} \| \Delta \xi \Delta \sigma + \frac{C_{5se}^u \Delta \xi \Delta \sigma}{\Delta \eta} \quad (4.70)$$

$$AU_e = (\rho W)_{e,U} \Delta \xi \Delta \eta \quad (4.71)$$

$$\begin{aligned}
B_e^u = & AU_e \cdot u_{e,U} + [C_{2E}^u \Delta \sigma + C_{6ne}^u \Delta \sigma] u_1 - [C_{2E}^u \Delta \sigma + C_{6se}^u \Delta \sigma] u_2 - \\
& [C_{2P}^u \Delta \sigma + C_{6ne}^u \Delta \sigma] u_n + [C_{2P}^u \Delta \sigma + C_{6se}^u \Delta \sigma] u_s + \left[\frac{C_{3E}^u \Delta \eta \Delta \sigma}{\Delta \xi} \right] v_{ee} - \\
& \left[\frac{C_{3E}^u \Delta \eta \Delta \sigma}{\Delta \xi} + \frac{C_{3P}^u \Delta \eta \Delta \sigma}{\Delta \xi} + \frac{C_{7ne}^u \Delta \xi \Delta \sigma}{\Delta \eta} + \frac{C_{7se}^u \Delta \xi \Delta \sigma}{\Delta \eta} \right] v_e + \\
& \left[\frac{C_{3P}^u \Delta \eta \Delta \sigma}{\Delta \xi} \right] v_w + [C_{4E}^u \Delta \sigma + C_{8ne}^u \Delta \sigma] v_1 - [C_{4E}^u \Delta \sigma + C_{8se}^u \Delta \sigma] v_2 - \\
& [C_{4P}^u \Delta \sigma + C_{8ne}^u \Delta \sigma] v_n + [C_{4P}^u \Delta \sigma + C_{8se}^u \Delta \sigma] v_s + \\
& \left[\frac{C_{7ne}^u \Delta \xi \Delta \sigma}{\Delta \eta} \right] v_3 + \left[\frac{C_{7se}^u \Delta \xi \Delta \sigma}{\Delta \eta} \right] v_5
\end{aligned} \quad (4.72)$$

$$L[\hat{P}_e^u] \Delta V = \left\{ \frac{P_E - P_P}{\Delta \xi} y_{\eta e} - \frac{P_N + P_{NE} - P_S - P_{SE}}{4 \Delta \eta} y_{\xi e} \right\} \Delta V \quad (4.73)$$

4.4.2 Discretization Equation for "v_e"

(Refer to Figure 4.1)

$$AP_e^v \cdot v_e = AE_e^v \cdot v_{Ee} + AN_e^v \cdot v_{Ne} + AW_e^v \cdot v_{We} + AS_e^v \cdot v_{Se} + B_e^v - L[\hat{P}_e^v] \Delta V \quad (4.74)$$

or

$$AP_e^v \cdot v_e = \sum A_{(nb)e}^v \cdot v_{(nb)e} + B_e^v - \left\{ \frac{P_N + P_{NE} - P_S - P_{SE}}{4\Delta\eta} x_{\xi e} - \frac{P_E - P_P}{\Delta\xi} x_{\eta e} \right\} \Delta V \quad (4.75)$$

where

$$AP_e^v = AE_e^v + AN_e^v + AW_e^v + AS_e^v + AU_e \quad (4.76)$$

$$AP_e^v = \left\| -(\rho U)_{E,o} \right\| \Delta\eta \Delta\sigma + \left\| (\rho U)_{P,o} \right\| \Delta\eta \Delta\sigma + \left\| -(\rho V)_{ne,o} \right\| \Delta\xi \Delta\sigma + \left\| (\rho V)_{se,o} \right\| \Delta\xi \Delta\sigma + (\rho W)_{e,U} \Delta\xi \Delta\eta + \frac{C_{1E}^v \Delta\eta \Delta\sigma}{\Delta\xi} + \frac{C_{1P}^v \Delta\eta \Delta\sigma}{\Delta\xi} + \frac{C_{5ne}^v \Delta\xi \Delta\sigma}{\Delta\eta} + \frac{C_{5se}^v \Delta\xi \Delta\sigma}{\Delta\eta} \quad (4.77)$$

$$AE_e^v = \left\| -(\rho U)_{E,o} \right\| \Delta\eta \Delta\sigma + \frac{C_{1E}^v \Delta\eta \Delta\sigma}{\Delta\xi} \quad (4.78)$$

$$AN_e^v = \left\| -(\rho V)_{ne,o} \right\| \Delta\xi \Delta\sigma + \frac{C_{5ne}^v \Delta\xi \Delta\sigma}{\Delta\eta} \quad (4.79)$$

$$AW_e^v = \left\| (\rho U)_{p,o} \right\| \Delta\eta \Delta\sigma + \frac{C_{1P}^v \Delta\eta \Delta\sigma}{\Delta\xi} \quad (4.80)$$

$$AS_e^v = \left\| (\rho V)_{se,o} \right\| \Delta\xi \Delta\sigma + \frac{C_{5se}^v \Delta\xi \Delta\sigma}{\Delta\eta} \quad (4.81)$$

$$AU_e = (\rho W)_{e,U} \Delta\xi \Delta\eta \quad (4.82)$$

$$\begin{aligned}
B_e^v = & AU_e \cdot v_{e,U} + [C_{2E}^v \Delta \sigma + C_{6ne}^v \Delta \sigma] v_1 - [C_{2E}^v \Delta \sigma + C_{6se}^v \Delta \sigma] v_2 - \\
& [C_{2P}^v \Delta \sigma + C_{6ne}^v \Delta \sigma] v_n + [C_{2P}^v \Delta \sigma + C_{6se}^v \Delta \sigma] v_s + \left[\frac{C_{3E}^v \Delta \eta \Delta \sigma}{\Delta \xi} \right] u_{ee} - \\
& \left[\frac{C_{3E}^v \Delta \eta \Delta \sigma}{\Delta \xi} + \frac{C_{3P}^v \Delta \eta \Delta \sigma}{\Delta \xi} + \frac{C_{7ne}^v \Delta \xi \Delta \sigma}{\Delta \eta} + \frac{C_{7se}^v \Delta \xi \Delta \sigma}{\Delta \eta} \right] u_e + \\
& \left[\frac{C_{3P}^v \Delta \eta \Delta \sigma}{\Delta \xi} \right] u_w + [C_{4E}^v \Delta \sigma + C_{8ne}^v \Delta \sigma] u_1 - [C_{4E}^v \Delta \sigma + C_{8se}^v \Delta \sigma] u_2 - \\
& [C_{4P}^v \Delta \sigma + C_{8ne}^v \Delta \sigma] u_n + [C_{4P}^v \Delta \sigma + C_{8se}^v \Delta \sigma] u_s + \\
& \left[\frac{C_{7ne}^v \Delta \xi \Delta \sigma}{\Delta \eta} \right] u_3 + \left[\frac{C_{7se}^v \Delta \xi \Delta \sigma}{\Delta \eta} \right] u_5 - L[\hat{S}_e^v] \Delta V
\end{aligned} \tag{4.83}$$

$$L[\hat{P}_e^v] \Delta V = \left\{ \frac{P_N + P_{NE} - P_S - P_{SE}}{4\Delta \eta} x_{\xi e} - \frac{P_E - P_P}{\Delta \xi} x_{\eta e} \right\} \Delta V \tag{4.84}$$

$$L[\hat{S}_e^v] \Delta V = J_e (\rho_e - \rho_a) g \cdot \Delta V \tag{4.85}$$

4.4.3 Discretization Equation for "u_n"

(Refer to Figure 4.2)

$$\begin{aligned}
AP_n^u \cdot u_n = & AE_n^u \cdot u_{En} + AN_n^u \cdot u_{Nn} + AW_n^u \cdot u_{Wn} + AS_n^u \cdot u_{Sn} + \\
& B_n^u - L[\hat{P}_n^u] \Delta V
\end{aligned} \tag{4.86}$$

or

$$\begin{aligned}
AP_n^u \cdot u_n = & \sum A_{(nb)n}^u \cdot u_{(nb)n} + B_n^u - \\
& \left\{ \frac{P_{NE} + P_E - P_{NW} - P_W}{4\Delta \xi} y_{\eta n} - \frac{P_N - P_P}{\Delta \eta} y_{\xi n} \right\} \Delta V
\end{aligned} \tag{4.87}$$

where

$$AP_n^u = AE_n^u + AN_n^u + AW_n^u + AS_n^u + AU_n \tag{4.88}$$

$$\begin{aligned}
AP_n^u = & \| -(\rho U)_{ne,0} \| \Delta \eta \Delta \sigma + \| (\rho U)_{nw,0} \| \Delta \eta \Delta \sigma + \\
& \| -(\rho V)_{N,0} \| \Delta \xi \Delta \sigma + \| (\rho V)_{P,0} \| \Delta \xi \Delta \sigma + \\
& (\rho W)_{n,U} \Delta \xi \Delta \eta + \frac{C_{1ne}^u \Delta \eta \Delta \sigma}{\Delta \xi} + \frac{C_{1nw}^u \Delta \eta \Delta \sigma}{\Delta \xi} + \\
& \frac{C_{5N}^u \Delta \xi \Delta \sigma}{\Delta \eta} + \frac{C_{5P}^u \Delta \xi \Delta \sigma}{\Delta \eta}
\end{aligned} \tag{4.89}$$

$$AE_n^u = \| -(\rho U)_{ne,0} \| \Delta \eta \Delta \sigma + \frac{C_{1ne}^u \Delta \eta \Delta \sigma}{\Delta \xi} \tag{4.90}$$

$$AN_n^u = \| -(\rho V)_{N,0} \| \Delta \xi \Delta \sigma + \frac{C_{5N}^u \Delta \xi \Delta \sigma}{\Delta \eta} \tag{4.91}$$

$$AW_n^u = \| (\rho U)_{nw,0} \| \Delta \eta \Delta \sigma + \frac{C_{1nw}^u \Delta \eta \Delta \sigma}{\Delta \xi} \tag{4.92}$$

$$AS_n^u = \| (\rho V)_{P,0} \| \Delta \xi \Delta \sigma + \frac{C_{5P}^u \Delta \xi \Delta \sigma}{\Delta \eta} \tag{4.93}$$

$$AU_n = (\rho W)_{n,U} \Delta \xi \Delta \eta \tag{4.94}$$

$$\begin{aligned}
B_n^u = & AU_n \cdot u_{n,U} + [C_{2ne}^u \Delta \sigma + C_{6N}^u \Delta \sigma] u_3 - [C_{2ne}^u \Delta \sigma + C_{6P}^u \Delta \sigma] u_4 - \\
& [C_{2nw}^u \Delta \sigma + C_{6N}^u \Delta \sigma] u_7 + [C_{2nw}^u \Delta \sigma + C_{6P}^u \Delta \sigma] u_w + \left[\frac{C_{3ne}^u \Delta \eta \Delta \sigma}{\Delta \xi} \right] v_1 - \\
& \left[\frac{C_{3ne}^u \Delta \eta \Delta \sigma}{\Delta \xi} + \frac{C_{3nw}^u \Delta \eta \Delta \sigma}{\Delta \xi} + \frac{C_{7P}^u \Delta \xi \Delta \sigma}{\Delta \eta} + \frac{C_{7N}^u \Delta \xi \Delta \sigma}{\Delta \eta} \right] v_n + \\
& \left[\frac{C_{3nw}^u \Delta \eta \Delta \sigma}{\Delta \xi} \right] v_{11} + [C_{4ne}^u \Delta \sigma + C_{8N}^u \Delta \sigma] v_3 - [C_{4ne}^u \Delta \sigma + C_{8P}^u \Delta \sigma] v_e - \\
& [C_{4nw}^u \Delta \sigma + C_{8N}^u \Delta \sigma] v_7 + [C_{4nw}^u \Delta \sigma + C_{8P}^u \Delta \sigma] v_w + \\
& \left[\frac{C_{7N}^u \Delta \xi \Delta \sigma}{\Delta \eta} \right] v_{nn} + \left[\frac{C_{7P}^u \Delta \xi \Delta \sigma}{\Delta \eta} \right] v_s
\end{aligned} \tag{4.95}$$

$$L[\hat{P}_n^u] \Delta V = \left\{ \frac{P_{NE} + P_E - P_{NW} - P_W}{4 \Delta \xi} y_{\eta n} - \frac{P_N - P_P}{\Delta \eta} y_{\xi n} \right\} \Delta V \tag{4.96}$$

4.4.4 Discretization Equation for “ v_n ”

(Refer to Figure 4.4)

$$AP_n^v \cdot v_n = AE_n^v \cdot v_{E_n} + AN_n^v \cdot v_{N_n} + AW_n^v \cdot v_{W_n} + AS_n^v \cdot v_{S_n} + B_n^v - L[\hat{P}_n^v] \Delta V \quad (4.97)$$

or

$$AP_n^v \cdot v_n = \sum A_{(nb)_n}^v \cdot v_{(nb)_n} + B_n^v - \left\{ \frac{P_N - P_P}{\Delta \eta} x_{\xi n} - \frac{P_{NE} + P_E - P_{NW} - P_W}{4\Delta \xi} x_{\eta n} \right\} \Delta V \quad (4.98)$$

where

$$AP_n^v = AE_n^v + AN_n^v + AW_n^v + AS_n^v + AU_n \quad (4.99)$$

$$AP_n^v = \parallel -(\rho U)_{ne,0} \parallel \Delta \eta \Delta \sigma + \parallel (\rho U)_{nw,0} \parallel \Delta \eta \Delta \sigma + \parallel -(\rho V)_{N,0} \parallel \Delta \xi \Delta \sigma + \parallel (\rho V)_{P,0} \parallel \Delta \xi \Delta \sigma + (\rho W)_{n,U} \Delta \xi \Delta \eta + \frac{C_{1ne}^v \Delta \eta \Delta \sigma}{\Delta \xi} + \frac{C_{1nw}^v \Delta \eta \Delta \sigma}{\Delta \xi} + \frac{C_{5N}^v \Delta \xi \Delta \sigma}{\Delta \eta} + \frac{C_{5P}^v \Delta \xi \Delta \sigma}{\Delta \eta} \quad (4.100)$$

$$AE_n^v = \parallel -(\rho U)_{ne,0} \parallel \Delta \eta \Delta \sigma + \frac{C_{1ne}^v \Delta \eta \Delta \sigma}{\Delta \xi} \quad (4.101)$$

$$AN_n^v = \parallel -(\rho V)_{N,0} \parallel \Delta \xi \Delta \sigma + \frac{C_{5N}^v \Delta \xi \Delta \sigma}{\Delta \eta} \quad (4.102)$$

$$AW_n^v = \parallel (\rho U)_{nw,0} \parallel \Delta \eta \Delta \sigma + \frac{C_{1nw}^v \Delta \eta \Delta \sigma}{\Delta \xi} \quad (4.103)$$

$$AS_n^v = \parallel (\rho V)_{P,0} \parallel \Delta \xi \Delta \sigma + \frac{C_{5P}^v \Delta \xi \Delta \sigma}{\Delta \eta} \quad (4.104)$$

$$AU_n = (\rho W)_{n,U} \Delta \xi \Delta \eta \quad (4.105)$$

$$\begin{aligned}
B_n^v = & AU_n \cdot v_{n,U} + [C_{2ne}^v \Delta \sigma + C_{6N}^v \Delta \sigma] v_3 - [C_{2ne}^v \Delta \sigma + C_{6P}^v \Delta \sigma] v_e - \\
& [C_{2nw}^v \Delta \sigma + C_{6N}^v \Delta \sigma] v_7 + [C_{2nw}^v \Delta \sigma + C_{6P}^v \Delta \sigma] v_w + \left[\frac{C_{3ne}^v \Delta \eta \Delta \sigma}{\Delta \xi} \right] u_1 - \\
& \left[\frac{C_{3ne}^v \Delta \eta \Delta \sigma}{\Delta \xi} + \frac{C_{3nw}^v \Delta \eta \Delta \sigma}{\Delta \xi} + \frac{C_{7N}^v \Delta \xi \Delta \sigma}{\Delta \eta} + \frac{C_{7P}^v \Delta \xi \Delta \sigma}{\Delta \eta} \right] u_n + \\
& \left[\frac{C_{3nw}^v \Delta \eta \Delta \sigma}{\Delta \xi} \right] u_{11} + [C_{4ne}^v \Delta \sigma + C_{8N}^v \Delta \sigma] u_3 - [C_{4ne}^v \Delta \sigma + C_{8P}^v \Delta \sigma] u_e - \\
& [C_{4nw}^v \Delta \sigma + C_{8N}^v \Delta \sigma] u_7 + [C_{4nw}^v \Delta \sigma + C_{8P}^v \Delta \sigma] u_w + \\
& \left[\frac{C_{7N}^v \Delta \xi \Delta \sigma}{\Delta \eta} \right] u_{nn} + \left[\frac{C_{7P}^v \Delta \xi \Delta \sigma}{\Delta \eta} \right] u_s - L[\hat{S}_n^v] \Delta V
\end{aligned} \tag{4.106}$$

$$L[\hat{P}_n^v] \Delta V = \left\{ \frac{P_N - P_P}{\Delta \eta} x_{\xi n} - \frac{P_{NE} + P_E - P_{NW} - P_W}{4 \Delta \xi} x_{\eta n} \right\} \Delta V \tag{4.107}$$

$$L[\hat{S}_n^v] \Delta V = J_n(\rho_n - \rho_a) g \cdot \Delta V \tag{4.108}$$

4.4.5 Discretization Equation for "u_w"

(Refer to Figure 4.3)

$$\begin{aligned}
AP_w^u \cdot u_w = & AE_w^u \cdot u_{Ew} + AN_w^u \cdot u_{Nw} + AW_w^u \cdot u_{Ww} + \\
& AS_w^u \cdot u_{Sw} + B_w^u - L[\hat{P}_w^u] \Delta V
\end{aligned} \tag{4.109}$$

or

$$\begin{aligned}
AP_w^u \cdot u_w = & \sum A_{(nb)w}^u \cdot u_{(nb)w} + B_w^u - \\
& \left\{ \frac{P_P - P_W}{\Delta \xi} y_{\eta w} - \frac{P_N + P_{NW} - P_S - P_{SW}}{4 \Delta \eta} y_{\xi w} \right\} \Delta V
\end{aligned} \tag{4.110}$$

where

$$AP_w^u = AE_w^u + AN_w^u + AW_w^u + AS_w^u + AU_w \tag{4.111}$$

$$\begin{aligned}
AP_w^u = & \| -(\rho U)_{P,0} \|\Delta\eta\Delta\sigma + \|(\rho U)_{W,0} \|\Delta\eta\Delta\sigma + \| -(\rho V)_{nw,0} \|\Delta\xi\Delta\sigma + \\
& \|(\rho V)_{sw,0} \|\Delta\xi\Delta\sigma + (\rho W)_{w,U} \Delta\xi\Delta\eta + \frac{C_{1P}^u \Delta\eta\Delta\sigma}{\Delta\xi} + \frac{C_{1W}^u \Delta\eta\Delta\sigma}{\Delta\xi} + \\
& \frac{C_{5nw}^u \Delta\xi\Delta\sigma}{\Delta\eta} + \frac{C_{5sw}^u \Delta\xi\Delta\sigma}{\Delta\eta}
\end{aligned} \tag{4.112}$$

$$AE_w^u = \| -(\rho U)_{P,0} \|\Delta\eta\Delta\sigma + \frac{C_{1P}^u \Delta\eta\Delta\sigma}{\Delta\xi} \tag{4.113}$$

$$AN_w^u = \| -(\rho V)_{nw,0} \|\Delta\xi\Delta\sigma + \frac{C_{5nw}^u \Delta\xi\Delta\sigma}{\Delta\eta} \tag{4.114}$$

$$AW_w^u = \|(\rho U)_{W,0} \|\Delta\eta\Delta\sigma + \frac{C_{1W}^u \Delta\eta\Delta\sigma}{\Delta\xi} \tag{4.115}$$

$$AS_w^u = \|(\rho V)_{sw,0} \|\Delta\xi\Delta\sigma + \frac{C_{5sw}^u \Delta\xi\Delta\sigma}{\Delta\eta} \tag{4.116}$$

$$AU_w = (\rho W)_{w,U} \Delta\xi\Delta\eta \tag{4.117}$$

$$\begin{aligned}
B_w^u = & AU_w \cdot u_{w,U} + [C_{2P}^u \Delta\sigma + C_{6nw}^u \Delta\sigma]u_n - [C_{2P}^u \Delta\sigma + C_{6sw}^u \Delta\sigma]u_s - \\
& [C_{2W}^u \Delta\sigma + C_{6nw}^u \Delta\sigma]u_{11} + [C_{2W}^u \Delta\sigma + C_{6sw}^u \Delta\sigma]u_{12} + \left[\frac{C_{3P}^u \Delta\eta\Delta\sigma}{\Delta\xi} \right] v_e - \\
& \left[\frac{C_{3P}^u \Delta\eta\Delta\sigma}{\Delta\xi} + \frac{C_{3W}^u \Delta\eta\Delta\sigma}{\Delta\xi} + \frac{C_{7nw}^u \Delta\xi\Delta\sigma}{\Delta\eta} + \frac{C_{7sw}^u \Delta\xi\Delta\sigma}{\Delta\eta} \right] v_w + \\
& \left[\frac{C_{3W}^u \Delta\eta\Delta\sigma}{\Delta\xi} \right] v_{ww} + [C_{4P}^u \Delta\sigma + C_{8nw}^u \Delta\sigma]v_n - [C_{4P}^u \Delta\sigma + C_{8sw}^u \Delta\sigma]v_s - \\
& [C_{4W}^u \Delta\sigma + C_{8nw}^u \Delta\sigma]v_{11} + [C_{4W}^u \Delta\sigma + C_{8sw}^u \Delta\sigma]v_{12} + \\
& \left[\frac{C_{7nw}^u \Delta\xi\Delta\sigma}{\Delta\eta} \right] v_7 + \left[\frac{C_{7sw}^u \Delta\xi\Delta\sigma}{\Delta\eta} \right] v_8
\end{aligned} \tag{4.118}$$

$$L[\hat{P}_w^u] \Delta V = \left\{ \frac{P_P - P_W}{\Delta\xi} y_{\eta w} - \frac{P_N + P_{NW} - P_S - P_{SW}}{4\Delta\eta} y_{\xi w} \right\} \Delta V \tag{4.119}$$

4.4.6 Discretization Equation for “ v_w ”

(Refer to Figure 4.3)

$$AP_w^v \cdot v_w = AE_w^v \cdot v_{Ew} + AN_w^v \cdot v_{Nw} + AW_w^v \cdot v_{Ww} + AS_w^v \cdot v_{Sw} + B_w^v - L[\hat{P}_w^v] \Delta V \quad (4.120)$$

or

$$AP_w^v \cdot v_w = \sum A_{(nb)_w}^v \cdot v_{(nb)_w} + B_w^v - \left\{ \frac{P_{NW} + P_N - P_{SW} - P_S}{4\Delta\eta} x_{\xi w} - \frac{P_P - P_W}{\Delta\xi} x_{\eta w} \right\} \Delta V \quad (4.121)$$

where

$$AP_w^v = AE_w^v + AN_w^v + AW_w^v + AS_w^v + AU_w \quad (4.122)$$

$$AP_w^v = \| -(\rho U)_{P,0} \| \Delta\eta \Delta\sigma + \| (\rho U)_{W,0} \| \Delta\eta \Delta\sigma + \| -(\rho V)_{nw,0} \| \Delta\xi \Delta\sigma + \| (\rho V)_{sw,0} \| \Delta\xi \Delta\sigma + (\rho W)_{w,U} \Delta\xi \Delta\eta + \frac{C_{1P}^v \Delta\eta \Delta\sigma}{\Delta\xi} + \frac{C_{1W}^v \Delta\eta \Delta\sigma}{\Delta\xi} + \frac{C_{5nw}^v \Delta\xi \Delta\sigma}{\Delta\eta} + \frac{C_{5sw}^v \Delta\xi \Delta\sigma}{\Delta\eta} \quad (4.123)$$

$$AE_w^v = \| -(\rho U)_{P,0} \| \Delta\eta \Delta\sigma + \frac{C_{1P}^v \Delta\eta \Delta\sigma}{\Delta\xi} \quad (4.124)$$

$$AN_w^v = \| -(\rho V)_{nw,0} \| \Delta\xi \Delta\sigma + \frac{C_{5nw}^v \Delta\xi \Delta\sigma}{\Delta\eta} \quad (4.125)$$

$$AW_w^v = \| (\rho U)_{W,0} \| \Delta\eta \Delta\sigma + \frac{C_{1W}^v \Delta\eta \Delta\sigma}{\Delta\xi} \quad (4.126)$$

$$AS_w^v = \| (\rho V)_{sw,0} \| \Delta\xi \Delta\sigma + \frac{C_{5sw}^v \Delta\xi \Delta\sigma}{\Delta\eta} \quad (4.127)$$

$$AU_w = (\rho W)_{w,U} \Delta\xi \Delta\eta \quad (4.128)$$

$$\begin{aligned}
B_w^v = & AU_w \cdot v_{w,U} + [C_{2P}^v \Delta \sigma + C_{6nw}^v \Delta \sigma] v_n - [C_{2P}^v \Delta \sigma + C_{6sw}^v \Delta \sigma] v_s - \\
& [C_{2W}^v \Delta \sigma + C_{6nw}^v \Delta \sigma] v_{11} + [C_{2W}^v \Delta \sigma + C_{6sw}^v \Delta \sigma] v_{12} + \left[\frac{C_{3P}^v \Delta \eta \Delta \sigma}{\Delta \xi} \right] u_e - \\
& \left[\frac{C_{3P}^v \Delta \eta \Delta \sigma}{\Delta \xi} + \frac{C_{3W}^v \Delta \eta \Delta \sigma}{\Delta \xi} + \frac{C_{7nw}^v \Delta \xi \Delta \sigma}{\Delta \eta} + \frac{C_{7sw}^v \Delta \xi \Delta \sigma}{\Delta \eta} \right] u_w + \\
& \left[\frac{C_{3W}^v \Delta \eta \Delta \sigma}{\Delta \xi} \right] u_{ww} + [C_{4P}^v \Delta \sigma + C_{8nw}^v \Delta \sigma] u_n - [C_{4P}^v \Delta \sigma + C_{8sw}^v \Delta \sigma] u_s - \\
& [C_{4W}^v \Delta \sigma + C_{8nw}^v \Delta \sigma] u_{11} + [C_{4W}^v \Delta \sigma + C_{8sw}^v \Delta \sigma] u_{12} + \\
& \left[\frac{C_{7nw}^v \Delta \xi \Delta \sigma}{\Delta \eta} \right] u_7 + \left[\frac{C_{7sw}^v \Delta \xi \Delta \sigma}{\Delta \eta} \right] u_8 - L[\hat{S}_w^v] \Delta V
\end{aligned} \tag{4.129}$$

$$L[\hat{P}_w^v] \Delta V = \left\{ \frac{P_N + P_{NW} - P_S - P_{SW}}{4\Delta \eta} x_{\xi w} - \frac{P_P - P_W}{\Delta \xi} x_{\eta w} \right\} \Delta V \tag{4.130}$$

$$L[\hat{S}_w^v] \Delta V = J_w(\rho_w - \rho_a)g \cdot \Delta V \tag{4.131}$$

4.4.7 Discretization Equation for "u,"

(Refer to Figure 4.4)

$$\begin{aligned}
AP_s^u \cdot u_s = & AE_s^u \cdot u_{E_s} + AN_s^u \cdot u_{N_s} + AW_s^u \cdot u_{W_s} + \\
& AS_s^u \cdot u_{S_s} + B_s^u - L[\hat{P}_s^u] \Delta V
\end{aligned} \tag{4.132}$$

or

$$\begin{aligned}
AP_s^u \cdot u_s = & \sum A_{(nb)_s}^u \cdot u_{(nb)_s} + B_s^u - \\
& \left\{ \frac{P_E + P_{SE} - P_W - P_{SW}}{4\Delta \xi} y_{\eta s} \frac{P_P - P_S}{\Delta \eta} y_{\xi s} \right\} \Delta V
\end{aligned} \tag{4.133}$$

where

$$AP_s^u = AE_s^u + AN_s^u + AW_s^u + AS_s^u + AU_s \quad (4.134)$$

$$\begin{aligned} AP_s^u = & \| -(\rho U)_{se,0} \| \Delta \eta \Delta \sigma + \| (\rho U)_{sw,0} \| \Delta \eta \Delta \sigma + \| -(\rho V)_{P,0} \| \Delta \xi \Delta \sigma + \\ & \| (\rho V)_{S,0} \| \Delta \xi \Delta \sigma + (\rho W)_{s,U} \Delta \xi \Delta \eta + \frac{C_{1se}^u \Delta \eta \Delta \sigma}{\Delta \xi} + \frac{C_{1sw}^u \Delta \eta \Delta \sigma}{\Delta \xi} + \\ & \frac{C_{5S}^u \Delta \xi \Delta \sigma}{\Delta \eta} + \frac{C_{5P}^u \Delta \xi \Delta \sigma}{\Delta \eta} \end{aligned} \quad (4.135)$$

$$AE_s^u = \| -(\rho U)_{se,0} \| \Delta \eta \Delta \sigma + \frac{C_{1se}^u \Delta \eta \Delta \sigma}{\Delta \xi} \quad (4.136)$$

$$AN_s^u = \| -(\rho V)_{P,0} \| \Delta \xi \Delta \sigma + \frac{C_{5P}^u \Delta \xi \Delta \sigma}{\Delta \eta} \quad (4.137)$$

$$AW_s^u = \| (\rho U)_{sw,0} \| \Delta \eta \Delta \sigma + \frac{C_{1sw}^u \Delta \eta \Delta \sigma}{\Delta \xi} \quad (4.138)$$

$$AS_s^u = \| (\rho V)_{S,0} \| \Delta \xi \Delta \sigma + \frac{C_{5S}^u \Delta \xi \Delta \sigma}{\Delta \eta} \quad (4.139)$$

$$AU_s = (\rho W)_{s,U} \Delta \xi \Delta \eta \quad (4.140)$$

$$\begin{aligned} B_s^u = & AU_s \cdot u_{s,U} + [C_{2se}^u \Delta \sigma + C_{6P}^u \Delta \sigma] u_e - [C_{2se}^u \Delta \sigma + C_{6S}^u \Delta \sigma] u_s - \\ & [C_{2sw}^u \Delta \sigma + C_{6P}^u \Delta \sigma] u_w + [C_{2sw}^u \Delta \sigma + C_{6S}^u \Delta \sigma] u_8 + \left[\frac{C_{3se}^u \Delta \eta \Delta \sigma}{\Delta \xi} \right] v_2 - \\ & \left[\frac{C_{3se}^u \Delta \eta \Delta \sigma}{\Delta \xi} + \frac{C_{3sw}^u \Delta \eta \Delta \sigma}{\Delta \xi} + \frac{C_{7P}^u \Delta \xi \Delta \sigma}{\Delta \eta} + \frac{C_{7S}^u \Delta \xi \Delta \sigma}{\Delta \eta} \right] v_9 + \\ & \left[\frac{C_{7P}^u \Delta \xi \Delta \sigma}{\Delta \eta} \right] v_n + \left[\frac{C_{3sw}^u \Delta \eta \Delta \sigma}{\Delta \xi} \right] v_{12} + \left[\frac{C_{7S}^u \Delta \xi \Delta \sigma}{\Delta \eta} \right] v_{s3} + \\ & [C_{4se}^u \Delta \sigma + C_{8P}^u \Delta \sigma] v_e - [C_{4se}^u \Delta \sigma + C_{8S}^u \Delta \sigma] v_5 - \\ & [C_{4sw}^u \Delta \sigma + C_{8P}^u \Delta \sigma] v_w + [C_{4sw}^u \Delta \sigma + C_{8S}^u \Delta \sigma] v_8 \end{aligned} \quad (4.141)$$

$$L[\hat{P}_s^u] \Delta V = \left\{ \frac{P_E + P_{SE} - P_W - P_{SW}}{4\Delta \xi} y_{\eta s} - \frac{P_P - P_S}{\Delta \eta} y_{\xi s} \right\} \Delta V \quad (4.142)$$

4.4.8 Discretization Equation for “ v_s ”

(Refer to Figure 4.8)

$$AP_s^v \cdot v_s = AE_s^v \cdot v_{E_s} + AN_s^v \cdot v_{N_s} + AW_s^v \cdot v_{W_s} + AS_s^v \cdot v_{S_s} + B_s^v - L[\dot{P}_s^v] \Delta V \quad (4.143)$$

or

$$AP_s^v \cdot v_s = \sum A_{(nb)_s}^v \cdot v_{(nb)_s} + B_s^v - \left\{ \frac{P_P - P_S}{\Delta \eta} x_{\xi_s} - \frac{P_E + P_{SE} - P_W - P_{SW}}{4\Delta \xi} x_{\eta_s} \right\} \Delta V \quad (4.144)$$

where

$$AP_s^v = AE_s^v + AN_s^v + AW_s^v + AS_s^v + AU_s \quad (4.145)$$

$$AP_s^v = \| -(\rho U)_{se,0} \| \Delta \eta \Delta \sigma + \| (\rho U)_{sw,0} \| \Delta \eta \Delta \sigma + \| -(\rho V)_{P,0} \| \Delta \xi \Delta \sigma + \| (\rho V)_{S,0} \| \Delta \xi \Delta \sigma + (\rho W)_{s,U} \Delta \xi \Delta \eta + \frac{C_{ise}^v \Delta \eta \Delta \sigma}{\Delta \xi} + \frac{C_{isw}^v \Delta \eta \Delta \sigma}{\Delta \xi} + \frac{C_{sp}^v \Delta \xi \Delta \sigma}{\Delta \eta} + \frac{C_{ss}^v \Delta \xi \Delta \sigma}{\Delta \eta} \quad (4.146)$$

$$AE_s^v = \| -(\rho U)_{se,0} \| \Delta \eta \Delta \sigma + \frac{C_{ise}^v \Delta \eta \Delta \sigma}{\Delta \xi} \quad (4.147)$$

$$AN_s^v = \| -(\rho V)_{P,0} \| \Delta \xi \Delta \sigma + \frac{C_{sp}^v \Delta \xi \Delta \sigma}{\Delta \eta} \quad (4.148)$$

$$AW_s^v = \| (\rho U)_{sw,0} \| \Delta \eta \Delta \sigma + \frac{C_{isw}^v \Delta \eta \Delta \sigma}{\Delta \xi} \quad (4.149)$$

$$AS_s^v = \| (\rho V)_{S,0} \| \Delta \xi \Delta \sigma + \frac{C_{ss}^v \Delta \xi \Delta \sigma}{\Delta \eta} \quad (4.150)$$

$$AU_s = (\rho W)_{s,U} \Delta \xi \Delta \eta \quad (4.151)$$

$$\begin{aligned}
B_s^v = & AU_s \cdot v_{s,U} + [C_{2se}^v \Delta\sigma + C_{6P}^v \Delta\sigma] v_e - [C_{2se}^v \Delta\sigma + C_{6S}^v \Delta\sigma] v_s - \\
& [C_{2sw}^v \Delta\sigma + C_{6P}^v \Delta\sigma] v_w + [C_{2sw}^v \Delta\sigma + C_{6S}^v \Delta\sigma] v_8 + \left[\frac{C_{3se}^v \Delta\eta \Delta\sigma}{\Delta\xi} \right] u_2 - \\
& \left[\frac{C_{3se}^v \Delta\eta \Delta\sigma}{\Delta\xi} + \frac{C_{3sw}^v \Delta\eta \Delta\sigma}{\Delta\xi} + \frac{C_{7P}^v \Delta\xi \Delta\sigma}{\Delta\eta} + \frac{C_{7S}^v \Delta\xi \Delta\sigma}{\Delta\eta} \right] u_s + \\
& \left[\frac{C_{3sw}^v \Delta\eta \Delta\sigma}{\Delta\xi} \right] u_{12} + [C_{4se}^v \Delta\sigma + C_{8P}^v \Delta\sigma] u_e - \\
& [C_{4se}^v \Delta\sigma + C_{8S}^v \Delta\sigma] u_s - [C_{4sw}^v \Delta\sigma + C_{8P}^v \Delta\sigma] u_w + \\
& [C_{4sw}^v \Delta\sigma + C_{8S}^v \Delta\sigma] u_8 + \left[\frac{C_{7P}^v \Delta\xi \Delta\sigma}{\Delta\eta} \right] u_n + \\
& \left[\frac{C_{7S}^v \Delta\xi \Delta\sigma}{\Delta\eta} \right] u_{ss} - L[\hat{S}_s^v] \Delta V
\end{aligned} \tag{4.152}$$

$$L[\hat{P}_s^v] \Delta V = \left\{ \frac{P_P - P_S}{\Delta\eta} x_{\xi s} - \frac{P_E + P_{SE} - P_W - P_{SW}}{4\Delta\xi} x_{\eta s} \right\} \Delta V \tag{4.153}$$

$$L[\hat{S}_s^v] \Delta V = J_s(\rho_s - \rho_a)g \cdot \Delta V \tag{4.154}$$

4.4.9 Discretization Equation for "w_P"

(Refer to Figure 4.9)

$$\begin{aligned}
AP_P^w \cdot w_P = & AE_P^w \cdot w_{EP} + AN_P^w \cdot w_{NP} + AW_P^w \cdot w_{WP} + \\
& AS_P^w \cdot w_{SP} + B_P^w - L[\hat{P}_P^w] \Delta V
\end{aligned} \tag{4.155}$$

or

$$AP_P^w \cdot w_P = \sum A_{(nb)P}^w \cdot w_{(nb)P} + B_P^w - J_P \left[\frac{\Delta \bar{P}}{\Delta \sigma} \right] \Delta V \tag{4.156}$$

also

$$AP_P^w = AE_P^w + AN_P^w + AW_P^w + AS_P^w + AU_P \tag{4.157}$$

$$\begin{aligned}
AP_{\bar{P}}^w = & \| -(\rho U)_{e,0} \| \Delta \eta \Delta \sigma + \| (\rho U)_{w,0} \| \Delta \eta \Delta \sigma + \| -(\rho V)_{n,0} \| \Delta \xi \Delta \sigma + \\
& \| (\rho V)_{s,0} \| \Delta \xi \Delta \sigma + (\rho W)_{P,U} \Delta \xi \Delta \eta + \frac{C_{1e}^w \Delta \eta \Delta \sigma}{\Delta \xi} + \frac{C_{1w}^w \Delta \eta \Delta \sigma}{\Delta \xi} + \\
& \frac{C_{5n}^w \Delta \xi \Delta \sigma}{\Delta \eta} + \frac{C_{5s}^w \Delta \xi \Delta \sigma}{\Delta \eta}
\end{aligned} \tag{4.158}$$

$$AE_{\bar{P}}^w = \| -(\rho U)_{e,0} \| \Delta \eta \Delta \sigma + \frac{C_{1e}^w \Delta \eta \Delta \sigma}{\Delta \xi} \tag{4.159}$$

$$AN_{\bar{P}}^w = \| -(\rho V)_{n,0} \| \Delta \xi \Delta \sigma + \frac{C_{5n}^w \Delta \xi \Delta \sigma}{\Delta \eta} \tag{4.160}$$

$$AW_{\bar{P}}^w = \| (\rho U)_{w,0} \| \Delta \eta \Delta \sigma + \frac{C_{1w}^w \Delta \eta \Delta \sigma}{\Delta \xi} \tag{4.161}$$

$$AS_{\bar{P}}^w = \| (\rho V)_{s,0} \| \Delta \xi \Delta \sigma + \frac{C_{5s}^w \Delta \xi \Delta \sigma}{\Delta \eta} \tag{4.162}$$

$$AU_P = (\rho W)_{P,U} \Delta \xi \Delta \eta \tag{4.162}$$

$$\begin{aligned}
B_{\bar{P}}^w = & AU_P \cdot w_{P,U} + [C_{2e}^w \Delta \sigma + C_{6n}^w \Delta \sigma] w_{ne} - [C_{2e}^w \Delta \sigma + C_{6s}^w \Delta \sigma] w_{se} - \\
& [C_{2w}^w \Delta \sigma + C_{6n}^w \Delta \sigma] w_{nw} + [C_{2w}^w \Delta \sigma + C_{6s}^w \Delta \sigma] w_{sw} + \\
& [C_{3e}^w \Delta \eta] u_e - [C_{3e}^{uv} \Delta \eta] u_{e,U} - [C_{3w}^w \Delta \eta] u_w + [C_{3w}^w \Delta \eta] u_{w,U} + \\
& [C_{4e}^w \Delta \eta] v_e - [C_{4e}^w \Delta \eta] v_{e,U} + [C_{4w}^w \Delta \eta] v_w + [C_{4w}^w \Delta \eta] v_{w,U} + \\
& [C_{7n}^w \Delta \xi] u_n - [C_{7n}^w \Delta \xi] u_{n,U} - [C_{7s}^w \Delta \xi] u_s + [C_{7s}^w \Delta \xi] u_{s,U} + \\
& [C_{8n}^w \Delta \xi] v_n - [C_{8n}^w \Delta \xi] v_{n,U} - [C_{8s}^w \Delta \xi] v_s + [C_{8s}^w \Delta \xi] v_{s,U}
\end{aligned} \tag{4.164}$$

$$L[\hat{P}_{\bar{P}}^w] \Delta V = J_P \left[\frac{\Delta \bar{P}}{\Delta \sigma} \right] \Delta V \tag{4.165}$$

4.4.10 Discretization Equation for "h_P"

(Refer to Figure 4.5)

$$\begin{aligned} AP_P^h \cdot h_P &= AE_P^h \cdot h_{EP} + AN_P^h \cdot h_{NP} + AW_P^h \cdot h_{WP} + \\ &AS_P^h \cdot h_{SP} + B_P^h \end{aligned} \quad (4.166)$$

or

$$AP_P^h \cdot h_P = \sum A_{(nb)P}^h \cdot h_{(nb)P} + B_P^h \quad (4.167)$$

also

$$AP_P^h = AE_P^h + AN_P^h + AW_P^h + AS_P^h + AU_P - SP^h \cdot \Delta V \quad (4.168)$$

where

$$SP^h = J_P I_P^{\left(\frac{n+1}{2}\right)} a_1 + J_P a_2 \quad (4.169)$$

$$\begin{aligned} AP_P^h &= \| -(\rho U)_{e,0} \| \Delta \eta \Delta \sigma + \| (\rho U)_{w,0} \| \Delta \eta \Delta \sigma + \| -(\rho V)_{n,0} \| \Delta \xi \Delta \sigma + \\ &\| (\rho V)_{s,0} \| \Delta \xi \Delta \sigma + (\rho W)_{P,U} \Delta \xi \Delta \eta + \frac{C_{1e}^h \Delta \eta \Delta \sigma}{\Delta \xi} + \frac{C_{1w}^h \Delta \eta \Delta \sigma}{\Delta \xi} + \\ &\frac{C_{3n}^h \Delta \xi \Delta \sigma}{\Delta \eta} + \frac{C_{3s}^h \Delta \xi \Delta \sigma}{\Delta \eta} \end{aligned} \quad (4.170)$$

$$AE_P^h = \| -(\rho U)_{e,0} \| \Delta \eta \Delta \sigma + \frac{C_{1e}^h \Delta \eta \Delta \sigma}{\Delta \xi} \quad (4.171)$$

$$AN_P^h = \| -(\rho V)_{n,0} \| \Delta \xi \Delta \sigma + \frac{C_{3n}^h \Delta \xi \Delta \sigma}{\Delta \eta} \quad (4.172)$$

$$AW_P^h = \| (\rho U)_{w,0} \| \Delta \eta \Delta \sigma + \frac{C_{1w}^h \Delta \eta \Delta \sigma}{\Delta \xi} \quad (4.173)$$

$$\Delta S_P^h = \|(\rho V)_{s,0}\| \Delta \xi \Delta \sigma + \frac{C_{3s}^h \Delta \xi \Delta \sigma}{\Delta \eta} \quad (4.174)$$

$$\Delta U_P = (\rho W)_{P,U} \Delta \xi \Delta \eta \quad (4.175)$$

$$\begin{aligned} B_P^h &= \Delta U_P \cdot h_{P,U} + [C_{2e}^h \Delta \sigma + C_{4n}^h \Delta \sigma] h_{ne} - \\ &\quad [C_{2e}^h \Delta \sigma + C_{4s}^h \Delta \sigma] h_{se} + [C_{2w}^h \Delta \sigma + C_{4s}^h \Delta \sigma] h_{sw} - \\ &\quad [C_{2w}^h \Delta \sigma + C_{4n}^h \Delta \sigma] h_{nw} + S_C^h \cdot \Delta V \end{aligned} \quad (4.176)$$

where

$$S_C^h = J_P I_P^{(\frac{n+1}{2})} b_1 + J_P b_2 \quad (4.177)$$

Note: a_1 , b_1 , a_2 and b_2 are obtained from source-term linearization, such that:

$$\mu_P = a_1 h_P + b_1 \quad (4.178)$$

$$(-\Delta H)_P R_{AP} = a_2 h_P + b_2 \quad (4.179)$$

4.4.11 Discretization Equation for “ m_P ”

(Refer to Figure 4.5)

$$\begin{aligned} AP_P^m \cdot m_P &= AE_P^m \cdot m_{EP} + AN_P^m \cdot m_{NP} + AW_P^m \cdot m_{WP} + \\ &\quad AS_P^m \cdot m_{SP} + B_P^m \end{aligned} \quad (4.180)$$

or

$$AP_P^m \cdot m_P = \sum A_{(nb)P}^m \cdot m_{(nb)P} + B_P^m \quad (4.181)$$

also

$$AP_P^m = AE_P^m + AN_P^m + AW_P^m + AS_P^m + \Delta U_P - SP^m \cdot \Delta V \quad (4.182)$$

where

$$SP^m = -J_P \cdot c \quad (4.183)$$

$$\begin{aligned} AP_P^m = & \| -(\rho U)_{e,0} \| \Delta \eta \Delta \sigma + \| (\rho U)_{w,0} \| \Delta \eta \Delta \sigma + \| -(\rho V)_{n,0} \| \Delta \xi \Delta \sigma + \\ & \| (\rho V)_{s,0} \| \Delta \xi \Delta \sigma + (\rho W)_{P,U} \Delta \xi \Delta \eta + \frac{C_{1e}^m \Delta \eta \Delta \sigma}{\Delta \xi} + \frac{C_{1w}^m \Delta \eta \Delta \sigma}{\Delta \xi} + \\ & \frac{C_{3n}^m \Delta \xi \Delta \sigma}{\Delta \eta} + \frac{C_{3s}^m \Delta \xi \Delta \sigma}{\Delta \eta} \end{aligned} \quad (4.184)$$

$$AE_P^m = \| -(\rho U)_{e,0} \| \Delta \eta \Delta \sigma + \frac{C_{1e}^m \Delta \eta \Delta \sigma}{\Delta \xi} \quad (4.185)$$

$$AN_P^m = \| -(\rho V)_{n,0} \| \Delta \xi \Delta \sigma + \frac{C_{3n}^m \Delta \xi \Delta \sigma}{\Delta \eta} \quad (4.186)$$

$$AW_P^m = \| (\rho U)_{w,0} \| \Delta \eta \Delta \sigma + \frac{C_{1w}^m \Delta \eta \Delta \sigma}{\Delta \xi} \quad (4.187)$$

$$AS_P^m = \| (\rho V)_{s,0} \| \Delta \xi \Delta \sigma + \frac{C_{3s}^m \Delta \xi \Delta \sigma}{\Delta \eta} \quad (4.188)$$

$$AU_P = (\rho W)_{P,U} \Delta \xi \Delta \eta \quad (4.189)$$

$$\begin{aligned} B_P^m = & AU_P \cdot m_{P,U} + [C_{2e}^m \Delta \sigma + C_{4n}^m \Delta \sigma] m_{ne} - \\ & [C_{2e}^m \Delta \sigma + C_{4s}^m \Delta \sigma] m_{se} + [C_{2w}^m \Delta \sigma + C_{4s}^m \Delta \sigma] m_{sw} - \\ & [C_{2w}^m \Delta \sigma + C_{4n}^m \Delta \sigma] m_{nw} + S_C^m \cdot \Delta V \end{aligned} \quad (4.190)$$

where

$$S_C^m = -J_P \cdot d \quad (4.191)$$

Note: c and d are obtained from source-term linearization:

$$R_{AP} = c \cdot m_P + d \quad (4.192)$$

4.4.12 Discretization Equation for " \hat{I}_P " and " \hat{M}_P "

$$D_1 = \left[\frac{y_{\eta P}}{J_P} \frac{u_e - u_w}{\Delta \xi} - \frac{y_{\xi P}}{J_P} \frac{u_n - u_s}{\Delta \eta} \right]^2 \quad (4.193)$$

$$D_2 = \left[\frac{x_{\xi P}}{J_P} \frac{v_n - v_s}{\Delta \eta} - \frac{x_{\eta P}}{J_P} \frac{v_e - v_w}{\Delta \xi} \right]^2 \quad (4.194)$$

$$D_3 = \left[\frac{w_P - w_{P,U}}{\Delta \sigma} \right]^2 \quad (4.195)$$

$$D_4 = 2[D_1 + D_2 + D_3] \quad (4.196)$$

$$D_5 = \left[\frac{y_{\eta P}}{J_P} \frac{v_e - v_w}{\Delta \xi} - \frac{y_{\xi P}}{J_P} \frac{v_n - v_s}{\Delta \eta} + \frac{x_{\xi P}}{J_P} \frac{v_n - v_s}{\Delta \eta} - \frac{x_{\eta P}}{J_P} \frac{v_e - v_w}{\Delta \xi} \right]^2 \quad (4.197)$$

$$D_6 = \left[\frac{x_{\xi P}}{J_P} \frac{w_n - w_s}{\Delta \eta} - \frac{x_{\eta P}}{J_P} \frac{w_e - w_w}{\Delta \xi} + \frac{v_P - v_{P,U}}{\Delta \sigma} \right]^2 \quad (4.198)$$

$$D_7 = \left[\frac{u_P - u_{P,U}}{\Delta \sigma} + \frac{y_{\eta P}}{J_P} \frac{w_e - w_w}{\Delta \xi} - \frac{y_{\xi P}}{J_P} \frac{w_n - w_s}{\Delta \eta} \right]^2 \quad (4.199)$$

$$L[\hat{I}_P] = D_4 + D_5 + D_6 + D_7 \quad (4.200)$$

$$L[\hat{M}_P] = \mu_P \cdot [D_4 + D_5 + D_6 + D_7]^{\left(\frac{n-1}{2}\right)} \quad (4.201)$$

4.5 THE DISCRETIZED BOUDBARY-CONDITIONS

Inlet (@ $\sigma = 0$)

(i) Axial Velocity

$$w(\xi, \eta) = w_{inlet} \quad (4.202)$$

(ii) Transverse Velocities

$$u_1(\xi, \eta) = 0. \quad (4.203)$$

$$u_2(\xi, \eta) = 0. \quad (4.204)$$

$$v_1(\xi, \eta) = 0. \quad (4.205)$$

$$v_2(\xi, \eta) = 0. \quad (4.206)$$

(iii) Temperature

$$T(\xi, \eta) = T_{inlet} \quad (4.207)$$

(iv) Reactant Weight-Fraction

$$m(\xi, \eta) = 1.0 \quad (4.208)$$

Walls of the Duct

(i) Axial Velocity

$$\begin{aligned} w(\xi, \eta) = 0. & \quad 1 \leq \xi \leq L1 \quad \text{for } \eta = 1, M1 \\ & \quad 1 \leq \eta \leq M1 \quad \text{for } \xi = 1, L1 \end{aligned} \quad (4.209)$$

(ii) Transverse Velocities

$$u_1(\xi, \eta) = 0. \quad (4.210)$$

$$u_2(\xi, \eta) = 0. \quad 1 \leq \xi \leq L1 \quad \text{for } \eta = 1, M1 \quad (4.211)$$

$$v_1(\xi, \eta) = 0. \quad 1 \leq \eta \leq M1 \quad \text{for } \xi = 1, L1 \quad (4.212)$$

$$v_2(\xi, \eta) = 0. \quad (4.213)$$

(iii) Temperature

$$\begin{aligned} T(\xi, \eta) = T_{wall} & \quad 1 \leq \xi \leq L1 \quad \text{for } \eta = 1, M1 \\ & \quad 1 \leq \eta \leq M1 \quad \text{for } \xi = 1, L1 \end{aligned} \quad (4.214)$$

(iv) Reactant Weight-Fraction

Wall Condition of the Reactant Continuity Equation @ I=1 Boundary

$$AP_P^m \cdot m_P = AE_P^m \cdot m_E + AN_P^m \cdot m_N + AS_P^m \cdot m_S + B_P^m \quad (4.215)$$

or

$$AP_P^m \cdot m_P = \sum A_{(nb)_P}^m \cdot m_{(nb)_P} + B_P^m, \quad (4.216)$$

with

$$AW_P^m = 0.$$

also

$$AP_P^m = AE_P^m + AN_P^m + AS_P^m + AU_P^m - 0.5S_P^m \cdot \Delta V \quad (4.217)$$

$$\begin{aligned} AP_P^m = & \| -(\rho U)_{e,0} \| \Delta \eta \Delta \sigma + \frac{1}{2} \| -(\rho V)_{n,0} \| \Delta \xi \Delta \sigma + \\ & \frac{1}{2} \| (\rho V)_{s,0} \| \Delta \xi \Delta \sigma + \frac{1}{2} (\rho W)_{P,U} \Delta \xi \Delta \eta + \\ & C_{1e}^m \frac{\Delta \eta \Delta \sigma}{\Delta \xi} + \frac{1}{2} C_{3n}^m \frac{\Delta \xi \Delta \sigma}{\Delta \eta} + \frac{1}{2} C_{3s}^m \frac{\Delta \xi \Delta \sigma}{\Delta \eta} + \\ & \frac{1}{2} C_{4n}^m \frac{\Delta \xi \Delta \sigma}{\Delta \eta} \frac{\beta_n}{\alpha_n} + \frac{1}{2} C_{4s}^m \frac{\Delta \xi \Delta \sigma}{\Delta \eta} \frac{\beta_s}{\alpha_s} \end{aligned} \quad (4.218)$$

$$AE_P^m = \| -(\rho U)_{e,0} \| \Delta \eta \Delta \sigma + C_{1e}^m \frac{\Delta \eta \Delta \sigma}{\Delta \xi} \quad (4.219)$$

$$\begin{aligned} AN_P^m = & \frac{1}{2} \| -(\rho V)_{n,0} \| \Delta \xi \Delta \sigma + \frac{1}{2} C_{3n}^m \frac{\Delta \xi \Delta \sigma}{\Delta \eta} + \\ & \frac{1}{2} C_{4n}^m \frac{\Delta \xi \Delta \sigma}{\Delta \eta} \frac{\beta_n}{\alpha_n} \end{aligned} \quad (4.220)$$

$$\begin{aligned} AS_P^m = & \frac{1}{2} \| (\rho V)_{s,0} \| \Delta \xi \Delta \sigma + \frac{1}{2} C_{3s}^m \frac{\Delta \xi \Delta \sigma}{\Delta \eta} + \\ & \frac{1}{2} C_{4s}^m \frac{\Delta \xi \Delta \sigma}{\Delta \eta} \frac{\beta_s}{\alpha_s} \end{aligned} \quad (4.221)$$

$$AU_P = \frac{1}{2} (\rho W)_{P,U} \Delta \xi \Delta \eta \quad (4.222)$$

$$\begin{aligned} B_P^m = & AU_P \cdot m_{P,U} + (C_{1P}^m \Delta \sigma \frac{\beta_P}{\alpha_P} + C_{2P}^m \Delta \sigma) (m_s - m_n) + \\ & C_{2e}^m \Delta \sigma (m_{ne} - m_{se}) + 0.5SC^m \cdot \Delta V \end{aligned} \quad (4.223)$$

Wall Condition of the Reactant Continuity Equation @ I=L1 Boundary

$$AP_P^m \cdot m_P = AN_P^m \cdot m_{NP} + AW_P^m \cdot m_{WP} + AS_P^m \cdot m_{SP} + B_P^m \quad (4.224)$$

or

$$AP_P^m \cdot m_P = \sum A_{(nb)P}^m \cdot m_{(nb)P} + B_P^m, \quad (4.225)$$

with

$$AE_P^m = 0.$$

also

$$AP_P^m = AW_P^m + AN_P^m + AS_P^m + AU_P^m - 0.5S_P^m \cdot \Delta V \quad (4.226)$$

$$AP_P^m = \|(\rho U)_{w,0}\| \Delta \eta \Delta \sigma + \frac{1}{2} \| -(\rho V)_{n,0}\| \Delta \xi \Delta \sigma + \frac{1}{2} \|(\rho V)_{s,0}\| \Delta \xi \Delta \sigma + \frac{1}{2} (\rho W)_{P,U} \Delta \xi \Delta \eta + C_{1w}^m \frac{\Delta \eta \Delta \sigma}{\Delta \xi} + \frac{1}{2} C_{3n}^m \frac{\Delta \xi \Delta \sigma}{\Delta \eta} + \frac{1}{2} C_{3s}^m \frac{\Delta \xi \Delta \sigma}{\Delta \eta} + \frac{1}{2} C_{4n}^m \frac{\Delta \xi \Delta \sigma}{\Delta \eta} \frac{\beta_n}{\alpha_n} + \frac{1}{2} C_{4s}^m \frac{\Delta \xi \Delta \sigma}{\Delta \eta} \frac{\beta_s}{\alpha_s} \quad (4.227)$$

$$AW_P^m = \|(\rho U)_{w,0}\| \Delta \eta \Delta \sigma + C_{1w}^m \frac{\Delta \eta \Delta \sigma}{\Delta \xi} \quad (4.228)$$

$$AN_P^m = \frac{1}{2} \| -(\rho V)_{n,0}\| \Delta \xi \Delta \sigma + \frac{1}{2} C_{3n}^m \frac{\Delta \xi \Delta \sigma}{\Delta \eta} + \frac{1}{2} C_{4n}^m \frac{\Delta \xi \Delta \sigma}{\Delta \eta} \frac{\beta_n}{\alpha_n} \quad (4.229)$$

$$AS_P^m = \frac{1}{2} \|(\rho V)_{s,0}\| \Delta \xi \Delta \sigma + \frac{1}{2} C_{3s}^m \frac{\Delta \xi \Delta \sigma}{\Delta \eta} + \frac{1}{2} C_{4s}^m \frac{\Delta \xi \Delta \sigma}{\Delta \eta} \frac{\beta_s}{\alpha_s} \quad (4.230)$$

$$AU_P^m = \frac{1}{2} (\rho W)_{P,U} \Delta \xi \Delta \eta \quad (4.231)$$

$$B_P^m = AU_P \cdot m_{P,U} + (C_{1P}^m \Delta \sigma \frac{\beta_P}{\alpha_P} + C_{2P}^m \Delta \sigma)(m_n - m_s) + C_{2w}^m \Delta \sigma (m_{sw} - m_{nw}) + 0.5SC^m \cdot \Delta V \quad (4.232)$$

Wall Condition of the Reactant Continuity Equation @ J=1 Boundary

$$\begin{aligned} AP_P^m \cdot m_P &= AE_P^m \cdot m_E + AW_P^m \cdot m_W + \\ &AN_P^m \cdot m_N + B_P^m \end{aligned} \quad (4.233)$$

or

$$AP_P^m \cdot m_P = \sum A_{(nb)_P}^m \cdot m_{(nb)_P} + B_P^m, \quad (4.234)$$

with

$$AS_P^m = 0.$$

also

$$AP_P^m = AE_P^m + AW_P^m + AN_P^m + AU_P^m - 0.5S_P^m \cdot \Delta V \quad (4.235)$$

$$\begin{aligned} AP_P^m &= \frac{1}{2} \| -(\rho U)_{e,0} \| \Delta \eta \Delta \sigma + \frac{1}{2} \| (\rho U)_{w,0} \| \Delta \eta \Delta \sigma + \\ &\| -(\rho V)_{n,0} \| \Delta \xi \Delta \sigma + \frac{1}{2} (\rho W)_{P,U} \Delta \xi \Delta \eta + \\ &\frac{1}{2} C_{1e}^m \frac{\Delta \eta \Delta \sigma}{\Delta \xi} + \frac{1}{2} C_{1w}^m \frac{\Delta \eta \Delta \sigma}{\Delta \xi} + \\ &\frac{1}{2} C_{2e}^m \frac{\Delta \eta \Delta \sigma}{\Delta \xi} \frac{\beta_e}{\gamma_e} + \frac{1}{2} C_{2w}^m \frac{\Delta \eta \Delta \sigma}{\Delta \xi} \frac{\beta_w}{\gamma_w} + \\ &C_{3n}^m \frac{\Delta \xi \Delta \sigma}{\Delta \eta} \end{aligned} \quad (4.236)$$

$$\begin{aligned} AE_P^m &= \frac{1}{2} \| -(\rho U)_{e,0} \| \Delta \eta \Delta \sigma + \frac{1}{2} C_{1e}^m \frac{\Delta \eta \Delta \sigma}{\Delta \xi} \\ &\frac{1}{2} C_{2e}^m \frac{\Delta \eta \Delta \sigma}{\Delta \xi} \frac{\beta_e}{\gamma_e} \end{aligned} \quad (4.237)$$

$$\begin{aligned} AW_P^m &= \frac{1}{2} \| (\rho U)_{w,0} \| \Delta \eta \Delta \sigma + \frac{1}{2} C_{1w}^m \frac{\Delta \eta \Delta \sigma}{\Delta \xi} + \\ &\frac{1}{2} C_{2w}^m \frac{\Delta \eta \Delta \sigma}{\Delta \xi} \frac{\beta_w}{\gamma_w} \end{aligned} \quad (4.238)$$

$$AN_P^m = \| -(\rho V)_{n,0} \| \Delta \xi \Delta \sigma + C_{3n}^m \frac{\Delta \xi \Delta \sigma}{\Delta \eta} \quad (4.239)$$

$$AU_P = \frac{1}{2}(\rho W)_{P,U} \Delta \xi \Delta \eta \quad (4.240)$$

$$B_P^m = AU_P \cdot m_{P,U} + (C_{3P}^m \Delta \sigma \frac{\beta_P}{\gamma_P} + C_{4P}^m \Delta \sigma)(m_w - m_e) + C_{4n}^m \Delta \sigma(m_{ne} - m_{nw}) + 0.5SC^m \cdot \Delta V \quad (4.241)$$

Wall Condition of the Reactant Continuity Equation @ J=M1 Boundary

$$AP_P^m \cdot m_P = AW_P^m \cdot m_P + AS_P^m \cdot m_P + AE_P^m \cdot m_P + B_P^m \quad (4.242)$$

or

$$AP_P^m \cdot m_P = \sum A_{(nb)_P}^m \cdot m_{(nb)_P} + B_P^m, \quad (4.243)$$

with

$$AN_P^m = 0.$$

also

$$AP_P^m = AW_P^m + AS_P^m + AE_P^m + AU_P^m - 0.5S_P^m \cdot \Delta V \quad (4.244)$$

$$\begin{aligned} AP_P^m = & \frac{1}{2} \|(-\rho U)_{e,0}\| \Delta \eta \Delta \sigma + \frac{1}{2} \|(\rho U)_{w,0}\| \Delta \eta \Delta \sigma + \\ & \|(\rho V)_{s,0}\| \Delta \xi \Delta \sigma + \frac{1}{2} (\rho W)_{P,U} \Delta \xi \Delta \eta + \\ & \frac{1}{2} C_{1e}^m \frac{\Delta \eta \Delta \sigma}{\Delta \xi} + \frac{1}{2} C_{1w}^m \frac{\Delta \eta \Delta \sigma}{\Delta \xi} + \\ & \frac{1}{2} C_{2e}^m \frac{\Delta \eta \Delta \sigma}{\Delta \xi} \frac{\beta_e}{\gamma_e} + \frac{1}{2} C_{2w}^m \frac{\Delta \eta \Delta \sigma}{\Delta \xi} \frac{\beta_w}{\gamma_w} + \\ & C_{3s}^m \frac{\Delta \xi \Delta \sigma}{\Delta \eta} \end{aligned} \quad (4.245)$$

$$\begin{aligned}
AE_P^m &= \frac{1}{2} \|(-\rho U)_{e,0}\| \Delta\eta \Delta\sigma + \frac{1}{2} C_{2e}^m \frac{\Delta\eta \Delta\sigma}{\Delta\xi} \frac{\beta_e}{\gamma_e} + \\
&\quad \frac{1}{2} C_{1e}^m \frac{\Delta\eta \Delta\sigma}{\Delta\xi}
\end{aligned} \tag{4.246}$$

$$\begin{aligned}
AW_P^m &= \frac{1}{2} \|(\rho U)_{w,0}\| \Delta\eta \Delta\sigma + \frac{1}{2} C_{2w}^m \frac{\Delta\eta \Delta\sigma}{\Delta\xi} \frac{\beta_w}{\gamma_w} + \\
&\quad \frac{1}{2} C_{1w}^m \frac{\Delta\eta \Delta\sigma}{\Delta\xi}
\end{aligned} \tag{4.247}$$

$$AS_P^m = \|(\rho V)_{s,0}\| \Delta\xi \Delta\sigma + C_{3s}^m \frac{\Delta\xi \Delta\sigma}{\Delta\eta} \tag{4.248}$$

$$AU_P = \frac{1}{2} (\rho W)_{P,U} \Delta\xi \Delta\eta \tag{4.249}$$

$$\begin{aligned}
B_P^m &= AU_P \cdot m_{P,U} + (C_{3P}^m \Delta\sigma \frac{\beta_P}{\gamma_P} + C_{4P}^m \Delta\sigma)(m_e - m_w) + \\
&\quad C_{4s}^m \Delta\sigma (m_{sw} - m_{se}) + 0.5 SC^m \cdot \Delta V
\end{aligned} \tag{4.250}$$

4.6 CLOSURE

This chapter is devoted to the presentation of the transformed and discretized governing equations as well as the boundary conditions.

The coefficients of the discretization equations are alternatively expressed in terms of I and J coordinates in Appendix D to be introduced in the computer programming.

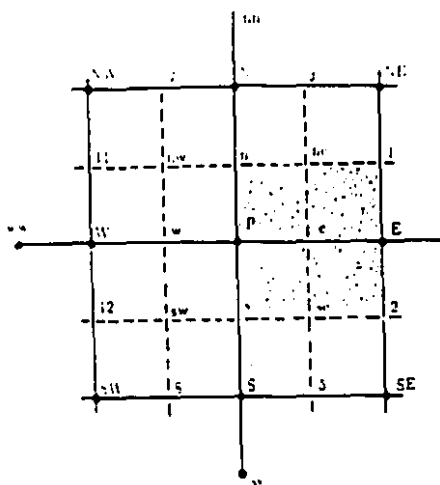


Fig. 4.1 Control volume for u_x and v_x

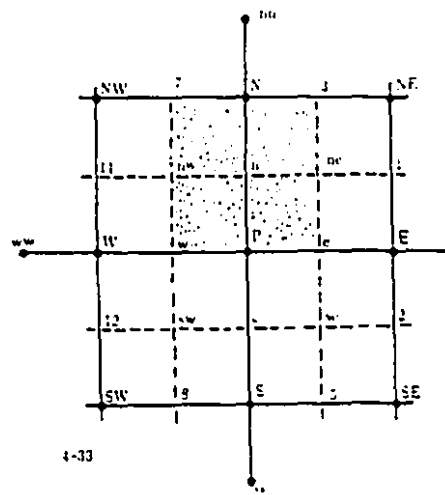


Fig. 4.2 Control volume for u_x and v_x

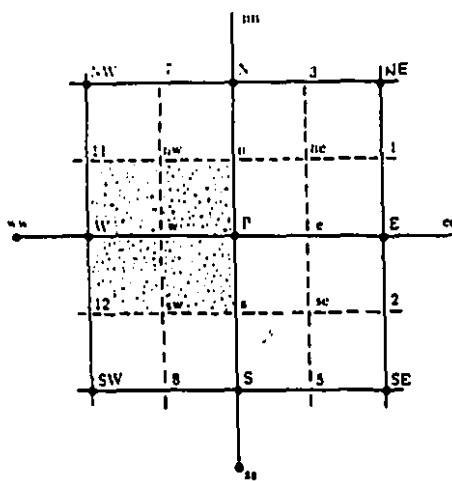


Fig. 4.3 Control volume for u_x and v_x

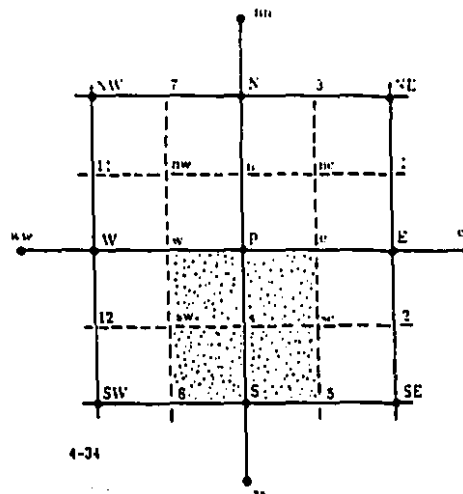


Fig. 4.4 Control volume for u_x and v_x

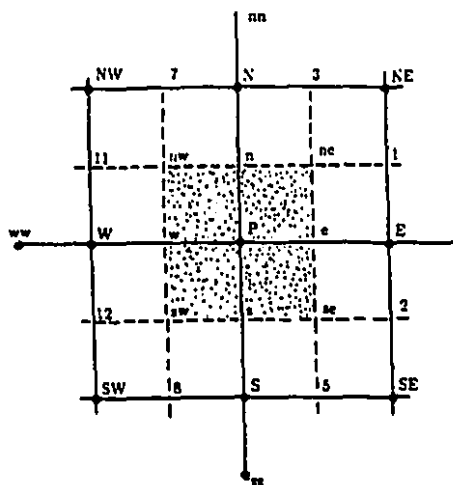


Fig. 4.5 Control volume for w_p , h_p and m_p

CHAPTER 5

POLYMERIZATION OF STYRENE

5.1 INTRODUCTION

The chemical reaction which is selected in the present study for simulation is the thermally initiated polymerization of styrene. This reaction is selected because polystyrene exhibits a power-law non-Newtonian behaviour^{24,29,30} and the reaction is conducted in steady laminar flow tubular reactors. The present work, however, affords a predictive tool for simulation of the manufacturing of polystyrene in ducts of arbitrary cross-sections. Using the model, the following characteristics can be predicted under a specified set of operating conditions:

- (i) velocity and pressure fields,
- (ii) temperature field,
- (iii) concentration field and molecular weight distribution.

Moreover, this reaction is used to examine the validity of the present work comparing the new computational results with the already existing experimental and numerical results in literature.

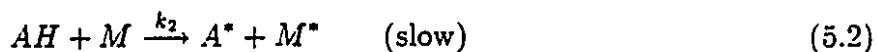
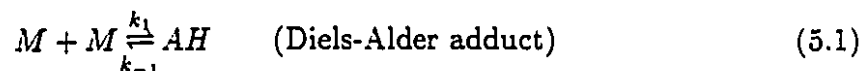
In this chapter the kinetic model for a third order initiation is presented for thermal polymerization of styrene. Also, the correlations of fluid properties of solution mixture, obtained from several sources, are presented. Subsequently a method for estimation of the weight- and number-average molecular weights is outlined. Finally, the thermal stability considerations of polystyrene reactors are discussed.

5.2 KINETICS OF THERMAL POLYMERIZATION OF STYRENE

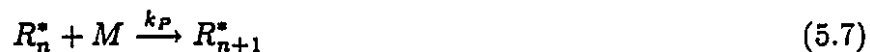
5.2.1 Reaction Mechanism

The reaction mechanism^{72,73} consists of four steps: thermal initiation, propagation, chain transfer to monomer and termination by combination as shown below:

Thermal Initiation:



Propagation:



Chain Transfer to Monomer:



Termination by Combination:



5.2.2 Rate of Reaction

A rate expression^{21,27-30} is obtained by applying the steady-state approximation to the various radical species in the system.

Rate of Thermal Initiation

$$R_i = k_3[A^*][M] + k_4[M^*][M] \quad (5.11)$$

Application of the steady-state assumption to $[A^*]$ and $[M^*]$ results:

$$\frac{d[A^*]}{dt} = k_2[AH][M] - k_3[A^*][M] = 0 \quad (5.12)$$

from which

$$[A^*] = \frac{k_2[AH]}{k_3}, \quad (5.13)$$

and

$$\frac{d[M^*]}{dt} = k_2[AH][M] - k_4[M^*][M] = 0. \quad (5.14)$$

Hence,

$$[M^*] = \frac{k_2[AH]}{k_4}. \quad (5.15)$$

Substituting for $[A^*]$ and $[M^*]$ in Eqn (5.11), one obtains:

$$R_i = 2k_2[M][AH]. \quad (5.16)$$

Application of steady-state assumption to AH results in:

$$\frac{d[AH]}{dt} = k_1[M]^2 - k_{-1}[AH] - k_2[AH][M] - k_5[AH][M] = 0 \quad (5.17)$$

from which

$$[AH] = \frac{k_1[M]^2}{k_{-1} + (k_2 + k_5)[M]}. \quad (5.18)$$

Substituting for $[AH]$ into Eqn (5.16), one obtains:

$$R_i = \frac{2k_1k_2[M]^3}{k_{-1} + (k_2 + k_5)[M]} \quad (5.19)$$

Simplifying Assumptions

Case I: Second-order thermal initiation kinetics

$$\text{if } (k_2 + k_5)[M] \gg k_{-1} \quad (5.20)$$

$$\text{then } R_i = \left(\frac{2k_1k_2}{k_2 + k_5} \right) [M]^2 \quad (5.21)$$

Case II: Third-order thermal initiation kinetics

$$\text{if } k_{-1} \gg (k_2 + k_5)[M], \quad (5.22)$$

$$\text{then } R_i = \left(\frac{2k_1k_2}{k_{-1}} \right) [M]^3 = 2k_i[M]^3. \quad (5.23)$$

Rate of Propagation

$$R_P = k_P[R^*][M]. \quad (5.24)$$

Rate of Termination

$$R_t = k_t[R^*]^2. \quad (5.25)$$

At steady-state the concentration of free radicals is constant and the rate of initiation equals the rate of termination. Then;

$$R_i = k_t[R^*]^2, \quad (5.26)$$

or

$$[R^*] = \left(\frac{R_i}{k_t} \right)^{\frac{1}{2}}. \quad (5.27)$$

Therefore, the rate equation is of the form

$$R_P = k_P[R^*][M], \quad (5.28)$$

or

$$R_P = k_P \left(\frac{R_i}{k_t} \right)^{\frac{1}{2}} [M]. \quad (5.29)$$

Using the simplified third-order thermal initiation kinetics,

$$R_i = 2k_i[M]^3 \quad (5.30)$$

$$R_P = k_P \left(\frac{2k_i[M]^3}{k_t} \right)^{\frac{1}{2}} [M], \quad (5.31)$$

or

$$R_P = k_P \left(\frac{2k_i}{k_t} \right)^{\frac{1}{2}} [M]^{2.5}, \quad (5.32)$$

or

$$R_P = \left(\frac{k_P}{k_t^{\frac{1}{2}}} \right) (2k_i)^{\frac{1}{2}} [M]^{2.5}. \quad (5.33)$$

5.2.3 Kinetic Data^{21,27-30}

$$k_i = 2.019 \times 10^1 e^{(-13810/T)} \frac{m^6}{(kg)^2(s)} \quad (5.34)$$

$$k_P = 1.009 \times 10^5 e^{(-3557/T)} \frac{m^3}{(kg)(s)} \quad (5.35)$$

$$k_{tr,m} = 2.218 \times 10^4 e^{(-6377/T)} \frac{m^3}{(kg)(s)} \quad (5.36)$$

$$k_t = 1.205 \times 10^7 e^{(-844/T)} e^{[-2(A_1 w_P + A_2 w_P^2 + A_3 w_P^3)]} \frac{m^3}{(kg)(s)} \quad (5.37)$$

in which

$$A_1 = 2.57 - 5.05 \times 10^{-3} T \quad (5.38)$$

$$A_2 = 9.56 - 1.76 \times 10^{-2} T \quad (5.39)$$

$$A_3 = -3.03 + 7.85 \times 10^{-3} T \quad (5.40)$$

5.3 DATA FOR SYSTEM PROPERTIES

Table 5.1 lists the thermophysical fluid properties for styrene polymerization:^{24,27-30}

Table 5.1 Fluid properties data

Properties	Correlation	Units
Density	$\rho = 1174.7 - 0.918T + (75.3 + 0.313T)w_P$	$\frac{kg}{m^3}$
Viscosity	$\eta_0 = \exp[-13.04 + 2013/T + MW^{0.16} \times (3.915w_P - 5.437w_P^2 + (0.623 + 1387/T)w_P^3)]$	Pa-s
Thermal Conductivities	$k_m = [2.72 - 2.8 \times 10^{-3}(T - 150) + 1.6 \times 10^{-5}(T - 150)^2](10^{-4})(418.4)$	$\frac{J}{(m)(s)(K)}$
	$k_P = [2.93 + 5.17 \times 10^{-3}(T - 80)](10^{-4})(418.4)$	$\frac{J}{(m)(s)(K)}$
	$k_{mix} = (1 - X_m)k_m + X_mk_P$	$\frac{J}{(m)(s)(K)}$
Specific Heat	$C_P = 1880.0$	$\frac{J}{kg K}$
Mass Diffusivity	$D_m = 2.0 \times 10^{-9}$	$\frac{m^2}{s}$
Heat of Reaction	$\Delta H = -6.7 \times 10^5$	$\frac{J}{kg}$
Power Law Index	$n = 0.2$	

5.4 PREDICTION OF MOLECULAR WEIGHT DISTRIBUTION

The average molecular weight of polymers depend on the temperature and rate of polymerization. In a tubular reactor, the final molecular-weight distribution is the result of continuous blending due to reaction, diffusion and convection. Changes in the molecular weight distribution are caused by continuous blending of increments of new polymer which is assumed to be formed instantaneously due to reaction into

the already existing polymer, and continuous blending of polymer by diffusion and convection^{23,24-30}. The following relations are obtained for cylindrical reactors which are appropriately expressed for non-circular ducts.

5.4.1 Instantaneous Average Molecular Weights

$$\bar{M}_{n,inst} \approx 104.15 \frac{\mu_1}{\mu_0} \quad (5.41)$$

$$\bar{M}_{w,inst} \approx 104.15 \frac{\mu_2}{\mu_1} \quad (5.42)$$

where

$$\mu_0 = R_P \left(C_m + \frac{\beta}{2} \right) \quad (5.43)$$

$$\mu_1 = R_P (C_m + \beta + 1) \approx R_P \quad (5.44)$$

$$\mu_2 = \frac{R_P (2C_m + 3\beta)}{(C_m + \beta)^2} \quad (5.45)$$

in which

$$\beta = \frac{k_t R_P}{k_p^2 [M]^2} \quad (5.46)$$

and

$$C_m = \frac{k_{tr,m}}{k_p} \quad (5.47)$$

5.4.2 Streamline Average Molecular Weight (MNS, MWS)

$$MNS = \frac{\sum w_i}{\sum w_i / M_i} = \frac{\sum_{i=1}^I (\rho_{i+1} w_{P,i+1} - \rho_i w_{P,i})}{\sum_{i=1}^I 2(\rho_{i+1} w_{P,i+1} - \rho_i w_{P,i}) / (M_{n,i} + M_{n,i+1})} \quad (5.48)$$

$$MWS = \frac{\sum w_i M_i}{\sum w_i} = \frac{\sum_{i=1}^I (M_{w,i+1} + M_{w,i})(\rho_{i+1} w_{P,i+1} - \rho_i w_{P,i})}{2 \sum_{i=1}^I (\rho_{i+1} w_{P,i+1} - \rho_i w_{P,i})} \quad (5.49)$$

where w_i is the weight of polymer of molecular weight M_i .

5.4.3 Mixing Cup-Average Molecular Weight (MNA, MWA)

For the polymer leaving the cylindrical reactor:

$$MNA = \frac{2\pi \int_0^R \rho(r)v_z(r)MNS(r)rdr}{2\pi \int_0^R \rho(r)v_z(r)rdr} \quad (5.50)$$

$$MWA = \frac{2\pi \int_0^R \rho(r)v_z(r)MWS(r)rdr}{2\pi \int_0^R \rho(r)v_z(r)rdr} \quad (5.51)$$

5.4.4 Polydispersity of the Polymer

The polydispersity of the polymer is commonly expressed as by taking the ratio of cup-averaged weight average molecular weight to the cup-averaged number average molecular weight (polydispersity = MWA/MNA).

5.5 THERMAL INSTABILITY

Polymerizing solutions are highly viscous liquids with very low thermal conductivities and significant heat-generation due to the exothermic chemical reaction. These properties may lead to hot spots and thermal run away in certain situations^{29,30}. If the heat generated in the reactor is not removed rapidly enough, then a hot spot may occur in the polymerizing mixture due to which the local temperature may rise significantly (thermal runaway). The critical temperature for polystyrene is about 245°C, therefore the hot-spot may lead to a thermal ignition within the reactor above this temperature. For practical reasons, "thermal instability" is defined to occur if $T \geq 200^\circ\text{C}$ anywhere in the reactor. This definition is based on the consideration that setting the maximum operating temperature at 200°C provides a safe limit well below the ignition temperature of polystyrene to insure conservative thermal stability

Ineffective dissipation of heat across tube radius is the main factor leading to the thermally unstable situation in a tubular reactor. It was found that a tube of radius below 2 or 3 cm involves no problems³⁰. In general, depending upon the inlet and the wall temperatures when the tube radius is increased a higher flow rate is required to maintain stable operation. This is due to the fact that a low flow rate and hence a longer residence time leads to very high conversion levels in the center of the tube. The large amount of heat thus generated under these conditions cannot be adequately dissipated because of the poor transfer rate of heat from the center of the tube to the wall. A tube of small radius (1 cm – 2 cm) has been found to be the most desirable in terms of thermal stability even at very low flow rates³⁰.

Styrene polymerization may be practiced in a single tube reactor or in tubes of a shell-and-tube type equipment. In the latter case, assuming that the flow is identical in all tubes, a single tube is representative of the whole system. Husain et. al.²⁴ have observed that polymerization in tubes of a shell-and-tube type vessel can involve unstable flow distribution and recommended a single tube operation in a large diameter tube which on the other hand requires special attention from the thermal stability point of view.

5.6 CLOSURE

This chapter considered the thermal polymerization of styrene in tubular reactors, which is selected as a test case to validate the present work and to obtain new simulation results. The information presented in this chapter regarding the kinetic data, correlations for fluid properties, method of molecular weight predictions and thermal stability aspects of tubular polymerization reactors are employed in the computations in the present study.

CHAPTER 6

THE SELECTED GEOMETRIES AND GRID GENERATION

6.1 INTRODUCTION

The selection of duct geometries of interest and even the angles and side-lengths of some of them is a matter with infinite choices, however, it is logical to try some standard geometries when there is no preference to choose a specific one. It may be imagined, however, to examine the effect of a specific parameter of a geometry such as an angle in a triangle. The requirement to perform such an investigation is not observed at present. The geometries selected in the present study for simulation are listed in table 6.2.

6.2 THE COMPUTER CODES FOR GRID GENERATION

The computer programmes: AGRID.FOR and BGRID.FOR were developed in this study for the generation of A- and B-type grids, respectively. A plotter programme, PLOT.FOR, was developed for grid plots. These programmes were examined under the MUSIC-A operating system on IBM3090 machine. The plots were drawn by the Zeta Plotter available in the Computer Center of McGill University. The computed results of the coordinates of the physical Cartesian domain (x, y) , the coefficients of coordinate transformation (α, β, γ) , the Jacobian of transformation (J) and the difference approximations of the first derivatives $(x_\xi, x_\eta, y_\xi, y_\eta)$ are stored in files for utilization in the main computer code for the solution of the conservation equations in arbitrary cross-sectional ducts. The plotter software also utilizes the stored values of x and y for grid plots. A user's guide to these computer codes is included in Appendix H.

6.3 GRID GENERATION PLOTS

The plotted results of 21×21 B-type grid of the selected geometries are presented in Figures 6.1 through 6.6. The B-type grid is the arrangement used in the solution of conservation equations. The BGRID.FOR and PLOT.FOR programmes were utilized for the generation of these grids. The BGRID.FOR programme contains 435 lines and requires 287, 416 bytes of memory while the execution time is about 0.6 seconds. The optimum relaxation factor for the solution of grid generation equations and the corresponding number of iterations required for the convergence of these equations are listed in Table 6.1. Refer to Appendix A for the method of computation of the optimum relaxation-factor.

Table 6.1 The Optimum Relaxation Factor and Number of Iterations

Geometries	Number of Iterations	Relaxation-Factor
Circular	24	1.71733093
Square	1	1.71733379
Triangular	13	1.71733284
Trapezoidal	13	1.71733284
Pentagonal	21	1.71733379
Hexagonal	20	1.71733284
Rectangular ($AR = 1.5$)	1	1.71733284
Rectangular ($AR = 2.0$)	1	1.71733284

Table 6.2 List of the Selected Geometries

Geometries	
<ul style="list-style-type: none"> • Circular 	
<ul style="list-style-type: none"> • Square 	
<ul style="list-style-type: none"> • Equilateral-triangular 	
<ul style="list-style-type: none"> • Trapezoidal acute angle = 60°, one side twice the other 	
<ul style="list-style-type: none"> • Pentagonal each angle = 108° 	
<ul style="list-style-type: none"> • Hexagonal each angle = 120°, 	
<ul style="list-style-type: none"> • Rectangular aspect-ratio = 1.5 and aspect-ratio = 2.0 	

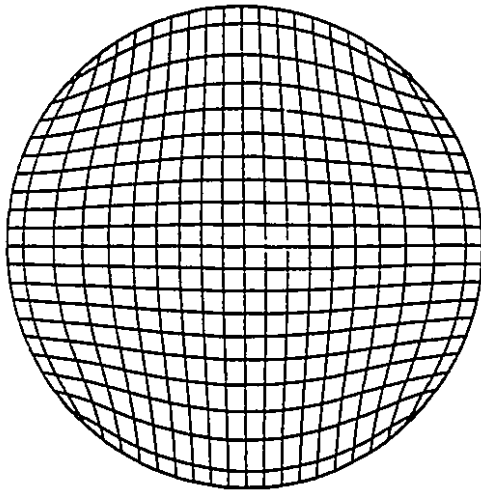


Figure 6.1 21 x 21 B-type grid for circular duct

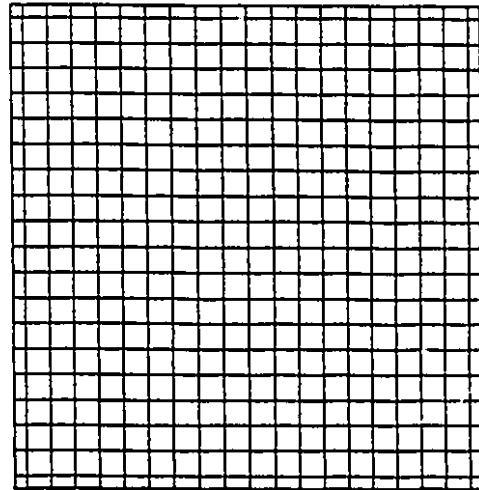


Figure 6.2 21 x 21 B-type grid for square duct

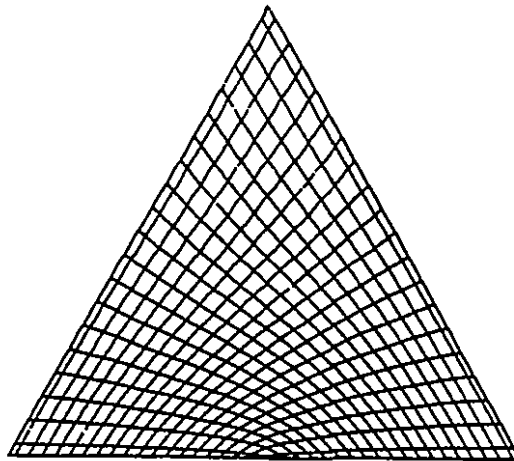


Figure 6.3 21 x 21 B-type grid for triangular duct

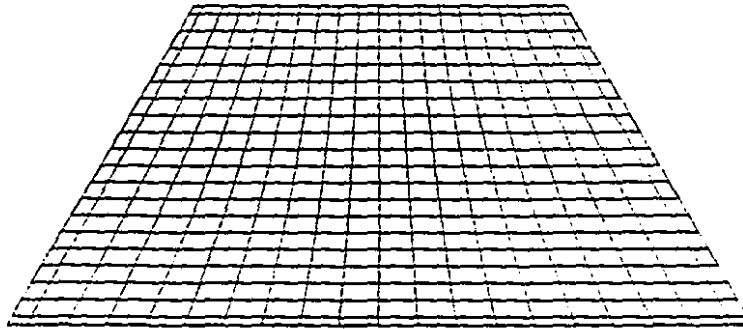


Figure 6.4 21 x 21 B-type grid for trapezoidal duct

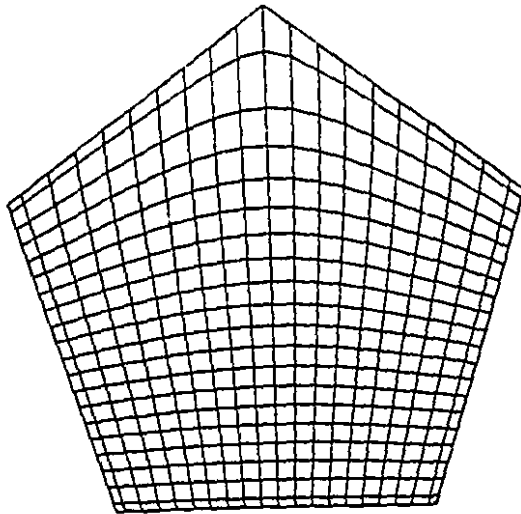


Figure 6.5 21 x 21 B-type grid for pentagonal duct

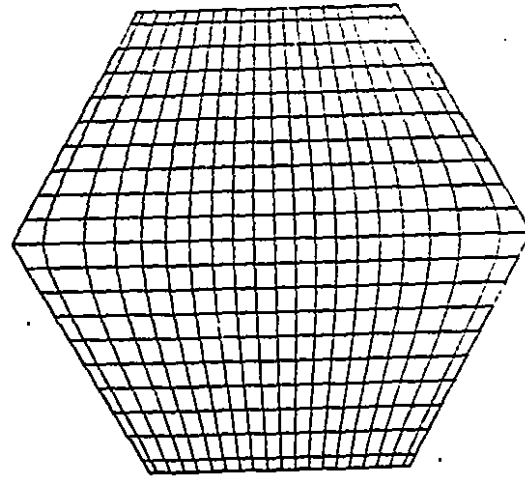


Figure 6.6 21 x 21 B-type grid for hexagonal duct

CHAPTER 7

THE COMPUTER CODE FOR CONSERVATION EQUATIONS

7.1 INTRODUCTION

The equations which model the reacting flow problem examined in this study result in a set of discretization equations, the solution of which required a new computer code to be developed. The solution procedure employed in this code is that explained in Chapter 3. This code has the generality and flexibility to perform computations for combined and individual studies of laminar duct flow transport phenomena: fluid dynamics, heat transfer and mass transfer with chemical reactions in straight ducts of arbitrary cross-sections for Newtonian and for purely viscous non-Newtonian fluids.

Following debugging of the code, numerous computational experiments were required to determine the validity of the algorithms used in the solution procedure in terms of accuracy, convergence and stability. Also determination of the values appropriate relaxation factors for the solution of discretization equations required extensive numerical trials.

This computer code (STAR30.FOR) was run on the MVS operating system of IBM ESA9000 machine. The STAR30.FOR programme contains more than 2500 lines of coding and is composed of a main programme and 32 sub-programmes (subroutines). The memory requirement for this programme is 2720 K and the typical CPU time is about 15 minutes.

The results of computations performed by BGRID.FOR which are stored in files are read by a subroutine and fed to STAR30.FOR to perform iterations for the solution of the discretization equations on planes in the axial parabolized direction marching from station to station.

The major steps followed in the main programme and the functions of the sub-routines are explained in this chapter. A brief user's guide to this computer code is included in Appendix H. Refer to Figures 7.1 and 7.2 for the marching sequence through a duct and a general flow chart of the computer code.

7.2 THE MAIN PROGRAMME

INITIALIZATION

- call GRID,
- call SUPPLY1,
- call INLET,
- call INLETW,
- call FIELDS,
- call BOUND1,
- call CONTVB,
- call CONTV,
- call CONTVW,
- call PROPER,
- call APPVIS,
- * CONTINUE,
- call COEFF,
- ** CONTINUE,
- call FACTW.

SOLVE EQUATIONS OF AXIAL- AND TRANSVERSE-VELOCITIES

- compute B-term and coefficients of w-momentum equations,
- call SOLVE,
- correct "w" and "dp",

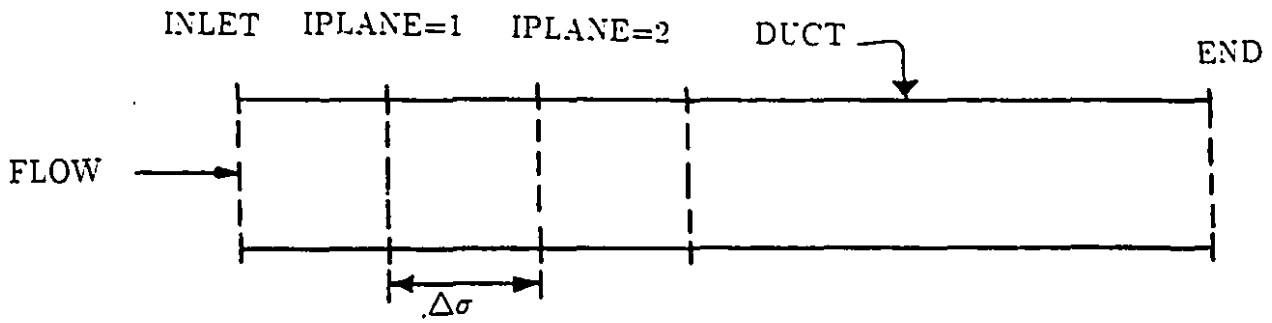


Figure 7.1 Marching Sequence Through a Duct.

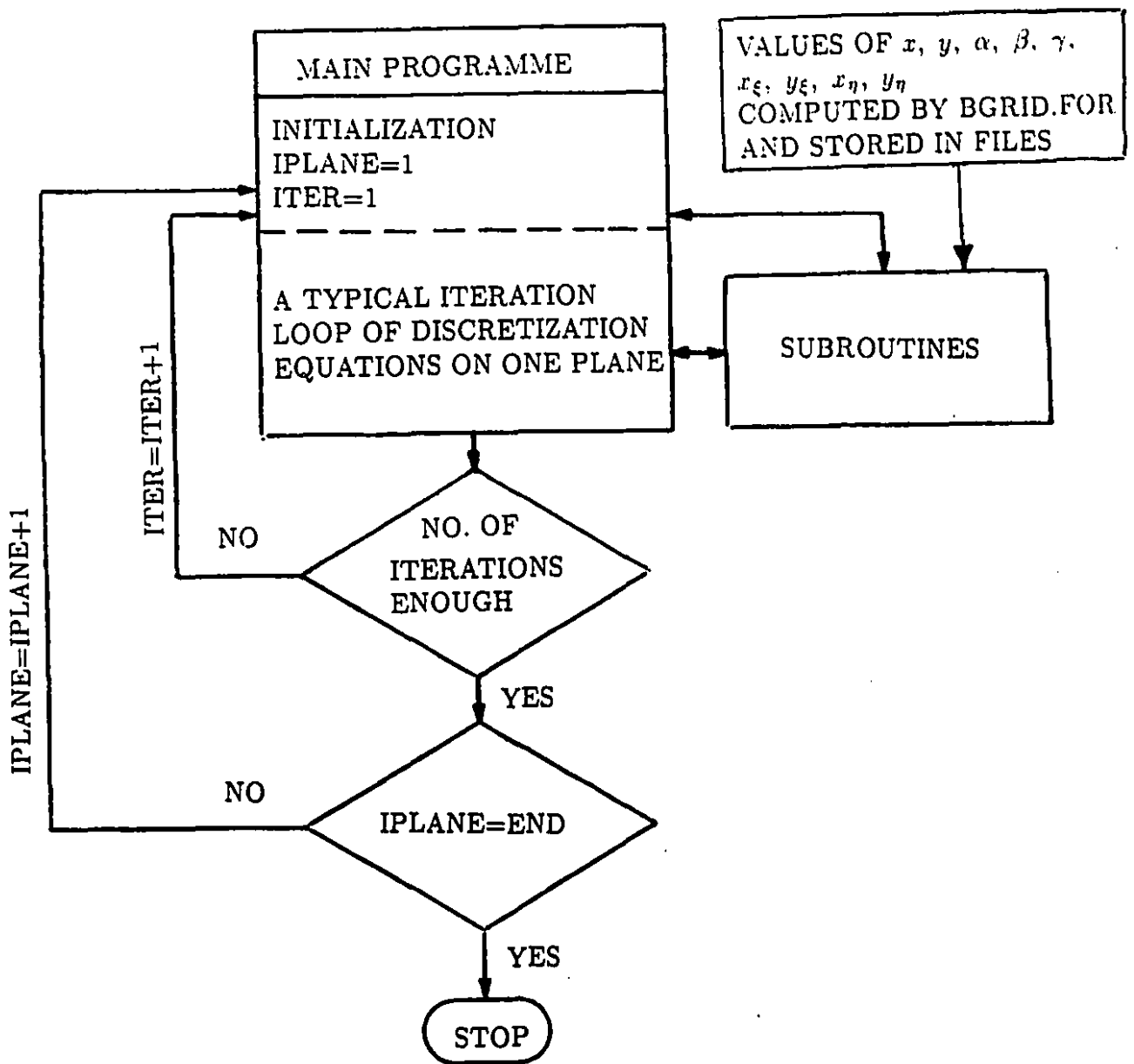


Figure 7.2 Flow Chart of the Computer Programme

- compute residual of axial-velocity equation: call CONVER1,
- compute contravariant velocity "WC": call CONTVW,
- call APPVIS.

COMPUTE B-TERM AND COEFFICIENTS OF TRANSVERSE-VELOCITY EQUATIONS

- call FACTU,
- call FACTV,
- compute BU1 and coefficients for U1 velocity equation,
- compute BV1 and coefficients for V1 velocity equation,
- compute BU2 and coefficients for U2 velocity equation,
- compute BV2 and coefficients for V2 velocity equation.

COMPUTE PRESSURE FIELD ON SIMPLER ALGORITHM

- compute pseudo-contravariant velocities,
- call PRESS,
- compute B-term using pseudo-contravariant velocities,
- call SOLVE,
- compute residual of pressure equation: call CONVER2.

SOLVE TRANSVERSE VELOCITY EQUATIONS FOR TENTATIVE VELOCITY VALUES

- for U1-momentum equation to obtain U1*:
- modify B-term to include pressure gradient,
- call SOLVE,
-
- for V1-momentum equation to obtain V1*:
- modify B-term to include pressure gradient,

- call SOLVE.
-
- for U2-momentum equation to obtain U2*:
- modify B-term to include pressure gradient,
- call SOLVE,
-
- for V2-momentum equation to obtain V2*:
- modify B-term to include pressure gradient,
- call SOLVE,
-
- compute tentative contravariant-velocities (UC1*, VC1*, UC2*, VC2*): call CONTV.

SOLVE PRESSURE CORRECTION EQUATION

- call PRESS,
- compute B-term using starred-contravariant-velocities,
- call SOLVE.

CORRECT TENTATIVE VELOCITY VALUES

- correct contravariant velocities (satisfying mass conservation),
-
- compute contravariant velocities (not satisfying mass conservation),
-
- compute physical velocities: call PHYSICAL,
- compute residuals of cross-stream velocity equations: call CONVER1.

SOLVE ENERGY EQUATION

- call KINET,
- call APPVIS,

- call FACTH,
- compute B-term and coefficients of energy equation,
- call SOLVE,
- compute residual of energy equation: call CONVER1,
- compute "T" values,
- call PROPER,
- call APPVIS,
- compute Nusselt-number.

SOLVE REACTANT CONTINUITY EQUATION

- call KINET,
- call FACTM,
- compute B-term and coefficients of reactant-continuity equation,
- call SOLVE.

UPDATE BOUNDARY VALUES OF REACTANT-CONTINUITY EQUATION

- call PROPER,
- call FACTM,
- call KINET,
- compute B-term and coefficients,
- call SOLVE1 and SOLVE2,
- compute residual of reactant continuity equations: call CONVER1.

UPDATE PHYSICAL PROPERTIES, MOLECULAR WEIGHTS AND APPARENT-VISCOSITY

- call PROPER,
- call KINET,

- call MOLWT,
- call PROPER,
- call APPVIS.

COMPUTE RESIDUALS OF SUCCESSIVE VALUES OF DEPENDENT VARIABLES AND MASS SOURCE — PRINT RESULTS

- call RESIDU,
- write residual values,
- write results of pressure-drop, Nusselt-number, molecular weights, etc.

CHECK NUMBER OF ITERATIONS AND NUMBER OF PLANES

- go to (**) for number of iterations required,
- -----
- if plane-number not equal to end-plane-number go to (***),
- otherwise call OUTPUT to print-out other results at end-plane,

*** continue.

CONTINUE MARCHING SEQUENCE PLANE BY PLANE

- if plane number greater than end-plane-number go to (****) otherwise proceed iterations on the next plane,

- call UPSTR,
- call APPVIS,
- call SUPPLY2 or SUPPLY3,
- GO TO (*),

**** STOP,

- END.

7.3 SUBROUTINES

1. SUBROUTINE GRID

Reads the values of the coefficients of transformation, the Jacobian of transformation and the difference-approximation of first-derivatives already computed by BGRID.FOR and stored in files.

2. SUBROUTINE SUPPLY1

Provides information regarding the geometry, relaxation-factors for the first plane of computation, axial step size, number of stations in the axial direction, etc. This subroutine can be switched to Newtonian, non-Newtonian and styrene polymerization cases to furnish requisite data required to start computations in each case.

3. SUBROUTINE SUPPLY2

Provides the downstream relaxation-factors for computation of hydrodynamics and thermal entrance regions

4. SUBROUTINE SUPPLY3

Provides the downstream relaxation factors for styrene polymerization simulations.

5. SUBROUTINE INLET

Stores duct entrance boundary conditions (except for the axial velocity component) as the upstream plane values for computations over the first plane in marching sequence.

6. SUBROUTINE INLETW

Stores duct entrance boundary condition for the axial velocity component and its contravariant velocity component similar to INLET.

7. SUBROUTINE INLETW1

This subroutine is used to specify parabolic velocity profile at entrance for circular ducts whenever required. Write "CALL INLETW1" after "CALL INLETW" in the main programme for this case.

8. SUBROUTINE COEFF

Computes the AU coefficients in the discretization equations.

9. SUBROUTINE FIELD

Introduces the tentative values of velocity components, pressure, temperature, enthalpy and mass-fraction required to start iterations for the solution of the discretization equations over each plane.

10. SUBROUTINE BOUND

Introduces the boundary conditions required for the iterative solutions mentioned in FIELD.

11. SUBROUTINE CONTV

Computes the contravariant velocities for the field values of the transverse velocity components.

12. SUBROUTINE CONTVW

Computes the contravariant velocities for the field and boundary values of the axial velocity components.

13. SUBROUTINE CONTVB

Computes the contravariant velocities for the boundary values of the transverse velocity components.

14. SUBROUTINE PROPER

Computes the physical-properties: density, viscosity, thermal conductivity, specific heat, mass diffusivity and heat of reaction. This subroutine can be switched to Newtonian, non-Newtonian and styrene polymerization cases.

15. SUBROUTINE UPSTR

Stores the upstream quantities required in marching steps plane by plane.

16. SUBROUTINE PHYSICAL

Computes the transverse physical Cartesian velocities from the contravariant velocity components.

17. SUBROUTINE OUTPUT

Writes the computed results of axial and transverse velocity components, pressure, temperature, mass-fraction, density, viscosity, etc.

18. SUBROUTINE CONVER1

Computes the residuals of discretization equations (except the pressure equation) for convergence criteria.

19. SUBROUTINE CONVER2

Computes the residual of the pressure discretization equation for convergence criteria.

20. SUBROUTINE APPVIS

Computes the apparent viscosity for power-law non-Newtonian fluids.

21. SUBROUTINE FACTU

Computes the transformed diffusion coefficients for u-momentum equation (including u_1 and u_2).

22. SUBROUTINE FACTV

Computes the transformed diffusion coefficients for v-momentum equation (including v_1 and v_2).

23. SUBROUTINE FACTH

Computes the transformed diffusion coefficients for energy equation.

24. SUBROUTINE FACTM

Computes the transformed diffusion coefficients for reactant-continuity equation.

25. SUBROUTINE FACTW

Computes the transformed diffusion coefficients for w-momentum equation.

26. SUBROUTINE PRESS

Computes 9 coefficients of pressure-correction equation.

27. SUBROUTINE SOLVE

Employs a line by line TDMA algorithm for solution of the discretization equation.

28. SUBROUTINE SOLVE1

The same as SOLVE modified for the reactant-continuity boundary condition at $J = 1$ and $J = M1$.

29. SUBROUTINE SOLVE2

The same as SOLVE modified for the reactant-continuity boundary condition at $I = 1$ and $I = L1$.

30. SUBROUTINE RESIDU

Computes the maximum residual values of dependent variables in successive iterations for convergence criteria.

31. SUBROUTINE KINET

Computes the kinetics of the chemical reaction.

32. SUBROUTINE MOLWT

Computes the weight and number average molecular weights, polydispersity and cup-averaged conversion for styrene polymerization.

CHAPTER 8

RESULTS AND DISCUSSIONS

8.1 INTRODUCTION

The present work concerns with the study of simultaneous aspects of duct transport phenomena. Primarily, however, these different aspects: fluid flow, heat transfer and mass transfer with chemical reaction are studied individually for the purpose of validation of system model and computer codes. Some original results are also obtained in these areas. Ultimately the main problem of flow, heat and mass-transfer with chemical reaction is solved in overall and the results are presented and documented. The main purpose of the study was for the non-Newtonian fluids, however, some results were also obtained for Newtonian fluids for validation, wherever required.

8.2 FLUID FLOW

Numerical results are presented in Figs. 8.1-8.19. The specific geometries selected for this analysis are as follows:

- square duct,
- equilateral triangular duct,
- trapezoidal duct (acute-angle = 60° , one side twice the other),
- pentagonal duct (each angle = 108°).

All the above ducts were selected on the basis the same equivalent diameters. Consequently, the same value of the relaxation factor was applied to all the geometries corresponding to each discretization equation. It is believed that this scheme is valid if the geometries selected do not involve oddity. For a pictorial representation of this concept, one may refer to Bejan⁸³ for a scale drawing of the duct sizes for some geometries

having the same equivalent diameter. The inlet Reynolds number values applied for the Newtonian fluid was 900 and that for the non-Newtonian case was 128 respectively. The problem is solved for constant-property fluid and the fluid is considered isothermal in the transversed direction due to which the buoyancy effect is ignored. For the sake of numerical accuracy and computational economy the mesh size selected was 21×21 over the transversed plane. The typical CPU time was about 3 minutes for one run.

The Newtonian case was solved with an axial step size of 0.160 m for which 26 marching stations were required in the axial direction to converge to the fully-developed flow condition. The predicted results for the centerline velocity development, axial pressure gradient and axial velocity profiles on the central plane are presented in Figs. 8.1–8.3. The axial velocity results show an excellent gradual development as expected. Within the numerical accuracy, there is close agreement between the ultimate centerline velocity results and their corresponding theoretical values examined for the square and circular ducts. The computed result for the square duct centerline velocity ($\frac{w_{cl}}{w}$) is 2.110 versus the theoretical value of 2.096 at the fully-developed condition where the relative deviation between two successive values of $\frac{w_{cl}}{w}$ is only 0.24%. The computed result for the circular duct centerline velocity ($\frac{w_{cl}}{w}$) is 1.99 versus the theoretical value of 2.00. Also the results obtained in the present analysis for Newtonian fluids in square ducts exhibit excellent agreement with the experimental measurements of Goldstein et al.⁸⁷ for velocity development and those of Beavers et al.⁸⁸ for pressure-drop values (see Figs. 8.1a and 8.2a). Comparing the fully-developed profile in Fig. 8.3 with Goldstein and Kreid's experimentally measured result, it is observed that the present numerical result over-predicts the Goldstein's profile by only a few percent which seems satisfactory for the fully developed condition obtained at convergence in this work. The Newtonian normalized centerline velocity and dimensionless axial pressure gradient results for different geometries are compared in table 8.1. There exists only slight differences between the results for the selected noncircular ducts. The results obtained by

others in a previous analysis for the normalized axial velocity ($\frac{w_{cl}}{\bar{w}}$) for the triangular and trapezoidal ducts are somewhat different from the results obtained in this analysis. Refer to table 8.2 in this respect.

Table 8. 1 Results for centerline velocity and pressure gradient

Geometries	Newtonian	
	w_{cl}/\bar{w}	$(P_0 - \bar{P})/(\frac{1}{2}\rho w_0^2)$
Square	2.11	9.49
Triangular	2.04	9.63
Trapezoidal	2.06	9.79
Pentagonal	2.03	9.68
Circular (for comparison)	1.99	10.13

Table 8. 2 Results for centerline velocity

Geometries	Newtonian ($\frac{w_{cl}}{\bar{w}}$) at F.D.	
	Previous analysis ¹⁰¹	Present analysis
Triangular	2.222	2.04
Trapezoidal	2.093	2.06

About 5 iterations were required to obtain converged solution over each transversed plane. The convergence criteria was set on the basis of the residual values defined as follows:

- (i) the residual of the momentum equations, that is, the remainder of these equations when the results are substituted for the velocities into these equations. In general $R = \sum a_{nb}\varphi_{nb} + b - a_P\varphi_P$ and R will be zero when the discretization equation is satisfied⁶⁹.
- (ii) the residual of velocities, that is, the difference in velocity values between two successive iterations,

Table 8. 3 shows the residual values of momentum equations and velocities at the fully developed condition.

Table 8. 3 Residual values (fluid-flow)

Geometries	Momentum-equation Residual		Velocity Residual	
	Transverse	Axial	Transverse	Axial
Square	0.12×10^{-6}	0.21×10^{-10}	0.34×10^{-6}	-0.35×10^{-5}
Triangular	0.26×10^{-6}	0.98×10^{-10}	0.60×10^{-6}	-0.44×10^{-5}
Trapezoidal	0.20×10^{-6}	0.36×10^{-10}	0.40×10^{-6}	-0.32×10^{-5}
Pentagonal	0.18×10^{-6}	0.52×10^{-10}	0.44×10^{-6}	-0.35×10^{-5}

It should be noted that the numerical solution procedure which was developed and implemented in this study, did not show any instability or convergence problems.

The development length computed for square duct in this work is $z^* = 0.127$, whereas, the result obtained by Neti et al.⁹⁶ is $z^* = 0.11$ (at F.D. condition). In the analysis of Neti et al.⁹⁶, however, the use of either inlet (or mean) axial velocity in the evaluation of normalized centerline velocity, dimensionless axial pressure gradient and Reynolds number is ambiguous. The Reynolds number in the present analysis is, however, evaluated locally at each of the fixed transversed planes, using the mean axial velocity. The value of development length computed in this analysis for a circular duct is $z^* = 0.136$, whereas the value indicated by Maliska⁴⁵ is $z^* = 0.162$ (at F.D. condition). Note that the development length which is expressed by Langhaar¹⁸ is obtained from the equation $\frac{L_f}{D} = 0.0575(N_{Re})$, that is $\frac{L_f}{D(N_{Re})} = z^* = 0.0575$ at fully developed condition. This value is far from the computed results presented above. There are also other literature values corresponding to triangular and trapezoidal ducts which are far from the results obtained in the present analysis. Table 8. 4 shows the results of development length values obtained in this analysis and some results from literature. The development lengths computed in this work are based on the usual definition of

Table 8. 4 Development length results (n=1)

Geometries	Newtonian Development Length (z^*)	
	Present analysis	Literature Values
Square	0.127	0.09 (ref. 87), 0.110 (ref. 96)
Triangular	0.126	0.0398 (ref. 101)
Trapezoidal	0.124	0.0314 (ref. 101)
Pentagonal	0.129	---
Circular (for comparison)	0.136	0.0575 (ref. 18), 0.162 (ref. 45)

entrance length, which is, the dimensionless length, z^* , corresponding to the centerline velocity to reach 99% of the fully developed condition.

The non-Newtonian analysis is for a polystyrene solution with a power-law index of $n = 0.5$ and Reynolds number value of 128 at inlet. The axial-step size selected was 0.05 m. The axial velocity development shows a plug-flow behavior at all four cross-sectional ducts chosen, although the triangular duct shows a slight delay in the development to a plug flow velocity profile. The results for centerline velocity development, axial pressure gradient and axial velocity profiles on the central plane are presented in Figs. 8.4-8.6. The plug flow behavior observed for the non-Newtonian case was previously predicted by Husain and Hamielec²⁴ in their analytical studies of tubular styrene polymerization. The non-Newtonian case applied to circular ducts in this analysis (not included in the thesis) also showed a plug flow behavior. It is, however, worthwhile to mention that specific non-Newtonian cases should be investigated separately due to the wide range of viscosities involved and the power-law indices.

The solution procedure showed a lower critical limit of axial step size, $\Delta\sigma = 0.01$ m, at which u and v components of velocity field (secondary flow) could not be obtained in conjunction with the w component (primary flow). An upper limit was also observed for the values of $\Delta\sigma$ selected beyond the value mentioned above for both Newtonian

and non-Newtonian cases.

The transverse velocity components, u and v components, supply the fluid that permit axial flow development, the highest value of which occur near the entrance where the most rapid arrangement of the axial velocity takes place⁹⁶. In laminar flow, due to the very small components of transverse velocities, the secondary flow has a small effect on the primary flow and the axial pressure-gradient^{43,46}. The results of secondary flow analysis, obtained in this work, for Newtonian and non-Newtonian cases at one axial location, are presented through Figs. 8.8 to 8.15. Comparing the corresponding z/D_h values, it is observed that the axial location for non-Newtonian case is closer to the entrance than for the Newtonian case. The secondary flow is away from the walls towards the intermediate sections at which it is reversed in direction, for all the geometries. The order of magnitude of the secondary flow velocities for square ducts obtained in this work, conforms with the results illustrated by Briley⁴³. Comparing Newtonian and non-Newtonian secondary-flow results, it is observed that the results of Newtonian case are relatively higher than the results of non-Newtonian case. The reason for this difference is attributed to the primary velocity profile patterns of the two cases, that is, tending to parabolic for Newtonian and plug-flow for non-Newtonian cases. The results of axial-velocity contour plots at F.D. condition, are presented through Figs. 8.16 to 8.19 for Newtonian fluids.

The conventional hydraulic (or equivalent) diameter concept is used in this work for noncircular duct calculations. It is determined such that the ratio of pressure forces acting over the cross-sectional area (A) to frictional forces acting along the wetted perimeter (P) is the same as in a circular pipe, and also such that for the circular pipe $D_h = D$. Therefore, $D_h = 4 \frac{\pi D^2/4}{\pi D} = D = 4 \frac{A}{P}$ for any noncircular ducts. The concept of hydraulic-diameter, when applied to Moody diagram (for circular pipe flow) does not yield favorable results, especially for the laminar region, so that using D_h in laminar flow, the friction factor $f \approx \frac{64}{Re(D_h)}$ would be within $\pm 40\%$ accuracy for

different geometries while in turbulent flow, the friction factor $f \approx f_{Moody}$ is within $\pm 15\%$ accuracy⁹¹. These discrepancies are due to the fact that such an analogy of a noncircular duct with a circular duct does not take into account the effect of nonuniformities or shape factors, such as sides and corners of the noncircular geometry into the correlations already developed for circular tubes. As an example of the effect of the geometric properties in laminar flow is that, in rectangular and triangular ducts, the wall friction varies greatly, being largest near the midpoint of the sides and zero at the corners^{91,92}. In turbulent flow, however, due to the effect of secondary flows, the shear is nearly uniform along the sides, dropping off sharply to zero in the corners^{91,92}. Mathematically the friction factor for circular ducts is usually expressed by a function of the form $f = F(\frac{wD}{\nu}, \frac{\epsilon}{D})$, obtained by dimensional analysis. The use of D_h for noncircular ducts in this form of dependency yields $f = F(\frac{wD_h}{\nu}, \frac{\epsilon}{D_h})$. This introduces error due to the lack of shape-factor effect in this relationship. These effects will, however, be taken into account if one modifies the above functional relationship by $f = F(\frac{wD_h}{\nu}, \frac{\epsilon}{D_h}, \sum \Phi)$ in which Φ stands for any effects due to the geometric nonuniformities. Practically, however, many investigators applied the concept of hydraulic diameter to obtain correlations for laminar friction factor or pressure drop for different geometries, such as isosceles triangular, square and rectangular ducts⁹¹. In this work, the effect of each geometry is introduced through the grid generation parameters into the computations. These parameters are the transformation-coefficients (α, β, γ), the Jacobian of transformation (J) and the difference approximation of the first derivatives ($x_\xi, y_\xi, x_\eta, y_\eta$). The effect of secondary flow, although not significant in laminar flow⁴⁵, is considered in this work. The predicted results are supported by good agreement with the experimental results of square duct and the analytical result of circular duct as shown in Figs. 8.3a and 8.7 respectively. The effect of zero shear rate at the corners of geometries is plainly observed for both Newtonian and non-Newtonian cases. This is shown by centerline axial velocity profiles for triangular and pentagonal ducts (Figs.

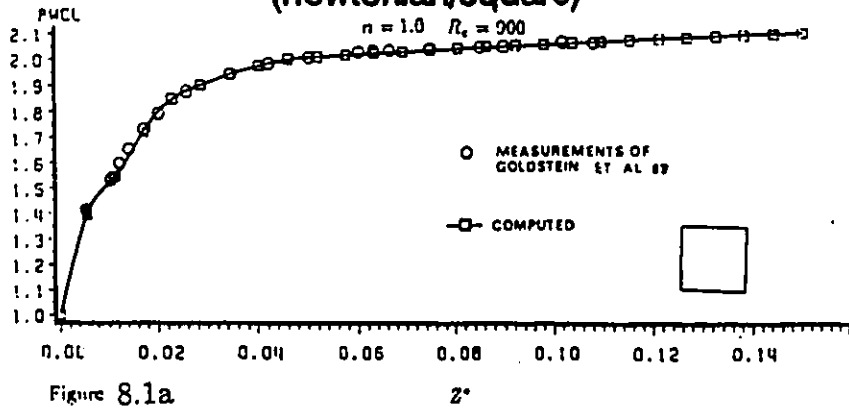
8.3b, 8.3d, 8.6b and 8.6d) in which the axial velocity tend towards its peak value at a location closer to the corners of these ducts rather than the centerline of the ducts.

This work demonstrates the suitability of the numerical model and the solution procedure applied to the 3D parabolized Navier-Stokes equations in straight ducts of arbitrary but constant cross-sections. The favorable agreement obtained between the present numerical solution with the experimental results of Newtonian fluids and the absence of instabilities in the numerical solution procedure, establishes the validity of the numerical modelling and solution procedure employed in the present investigation for fluid flow.

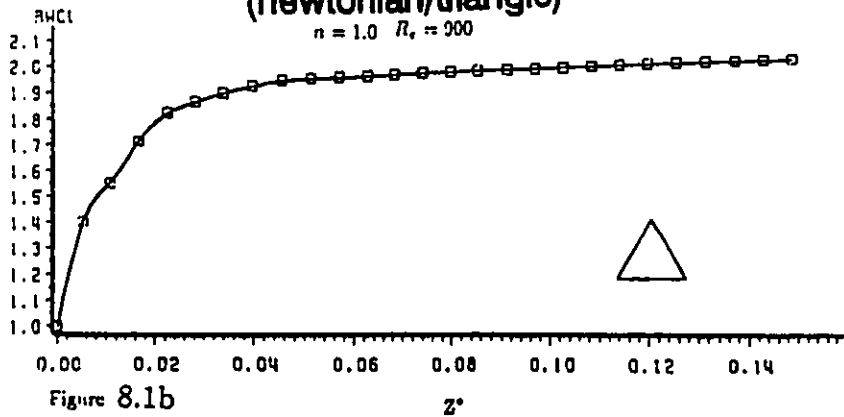
A review of some of the related developments in the numerical methods for the solution of momentum equations reveals the elegant features of the numerical procedure applied to this work. In general, coupling between the momentum and mass conservation equations is often the major cause of the slow convergence of the iterative solution methods. Caretto et al.⁹⁴ applied a numerical method to the solution of the momentum equations which involved an implicit simultaneous solution of coupled nonlinear difference equations without linearization or decoupling. The solution procedure was, however, a point by point iterative method due to which slow convergence is inevitable. The method of Patankar and Spalding⁴², involved linearization and decoupling of the equations. In their method, the non-linear terms (the product terms) of the momentum equations are handled by setting the value of velocities in these terms the same as their values at the previous axial step. The axial momentum equation is treated separately from the transverse momentum equations which are decoupled by assuming a pressure-field in the transverse direction. In the computations of transverse velocities, corrections are made for tentative transverse velocities and pressure field by iteratively solving a Poisson like equation for the pressure-correction. The method proposed by Briley⁴³ requires two Poisson like equations to solve, one for a velocity potential for velocity corrections and the other for the pressure field. The method of Patankar and

Spalding⁴² developed later brought about the SIMPLE and SIMPLER algorithms⁶⁹, in which two Poisson like equations are solved for pressure and pressure corrections. The SIMPLE and SIMPLER algorithms have been already applied to solve problems using the non-orthogonal boundary fitted coordinate transformation system. Some of these works are worthy to mention here. Hadjisophocleous et al.⁶⁶, Shyy et al.⁶⁷ and Braaten et al.⁶⁸ employed the SIMPLE algorithm in their analysis for non-orthogonal systems. Maliska^{45,46} applied a mixed scheme comprising of the SIMPLE and the SIMPLER algorithms. In the present work, the SIMPLER algorithm is further developed for the solution of the power-law non-Newtonian fluid problems. The use of nonorthogonal coordinates versus orthogonal system, has the advantage of getting rid of the generation of orthogonal grids at certain locations which are difficult or impossible to make. The staggered grid employed in this work uses both of the u and v velocity components at each velocity locations. This grid arrangement together with the numerical scheme in which both of the physical Cartesian and contravariant velocities are involved, have led the finite difference equations to converge faster without numerical instabilities. Besides, a combination of upwind difference scheme for the convective terms and central difference scheme for the diffusive terms which is employed in this work, provided satisfactory results.

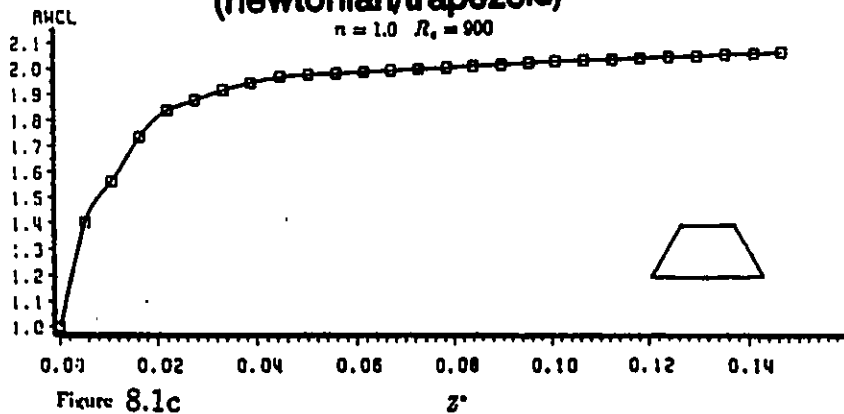
centerline velocity development
(newtonian/square)



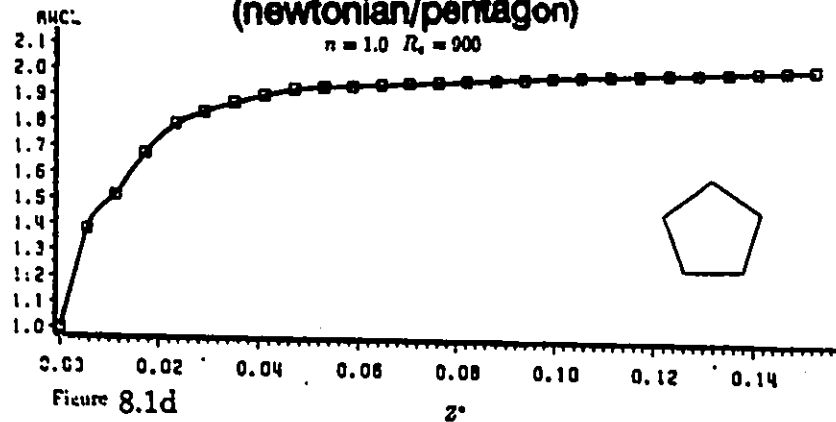
centerline velocity development
(newtonian/triangle)



centerline velocity development
(newtonian/trapezoid)



centerline velocity development
(newtonian/pentagon)



d.l. press. - drop vs d.l. axial - dist.
(newtonian/square)
 $n = 1.0 \quad R_c = 900$

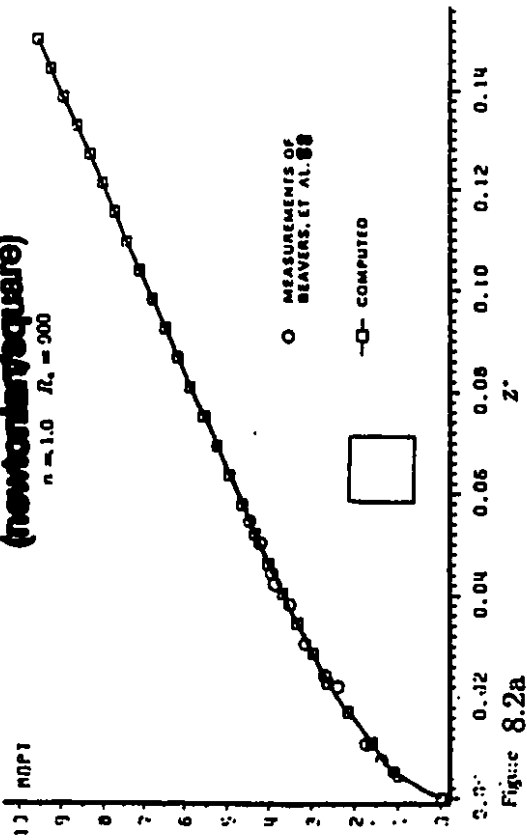


Figure 8.2a

d.l. press. - drop vs d.l. axial - dist.
(newtonian/triangle)
 $n = 1.0 \quad R_c = 900$

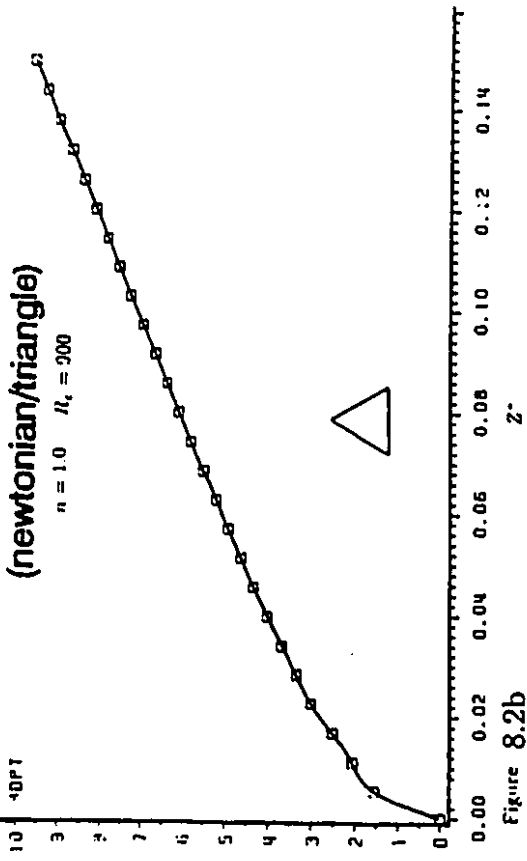


Figure 8.2b

d.l. press. - drop vs d.l. axial - dist.
(newtonian/trapezoid)
 $n = 1.0 \quad R_c = 900$

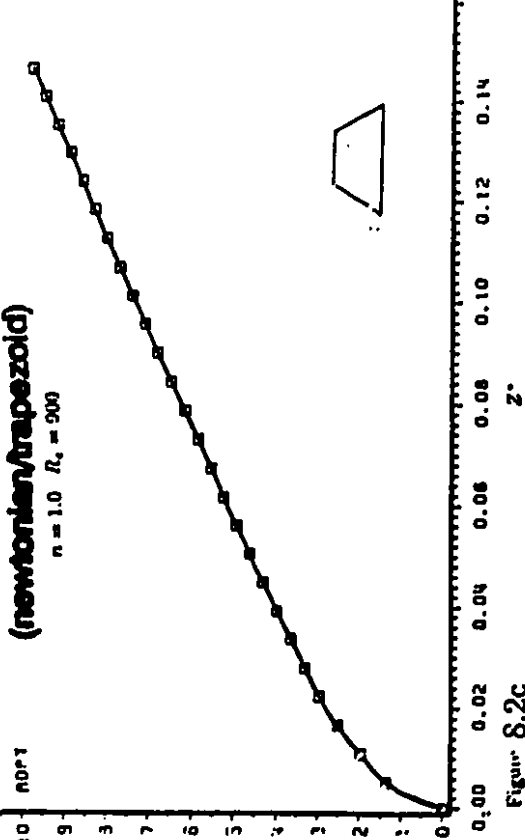


Figure 8.2c

d.l. press. - drop vs d.l. axial - dist.
(newtonian/pentagon)
 $n = 1.0 \quad R_c = 900$

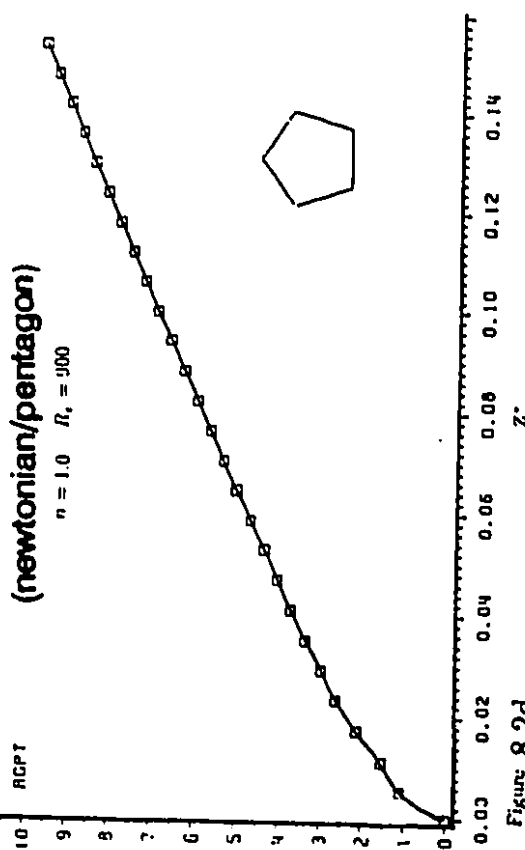
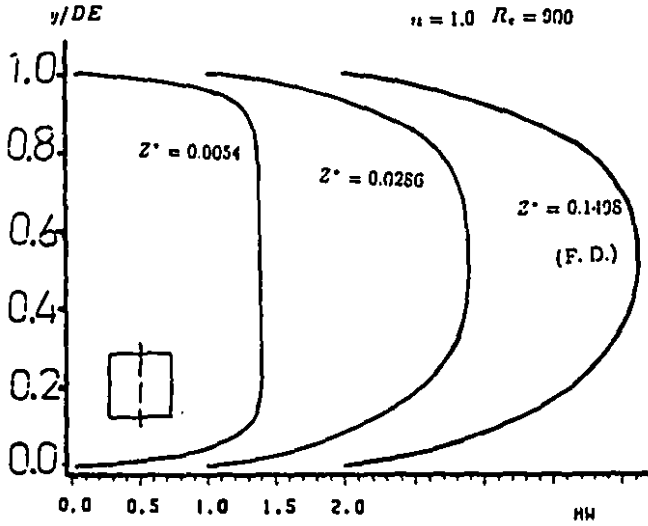


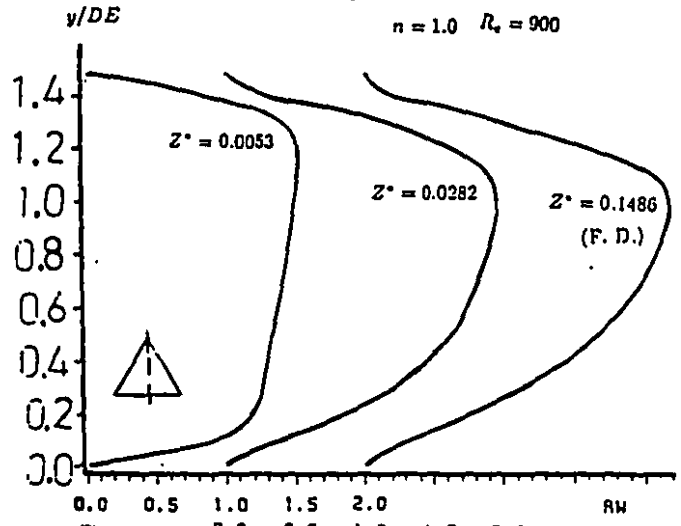
Figure 8.2d

development of axial velocity profile
(newtonian/square)



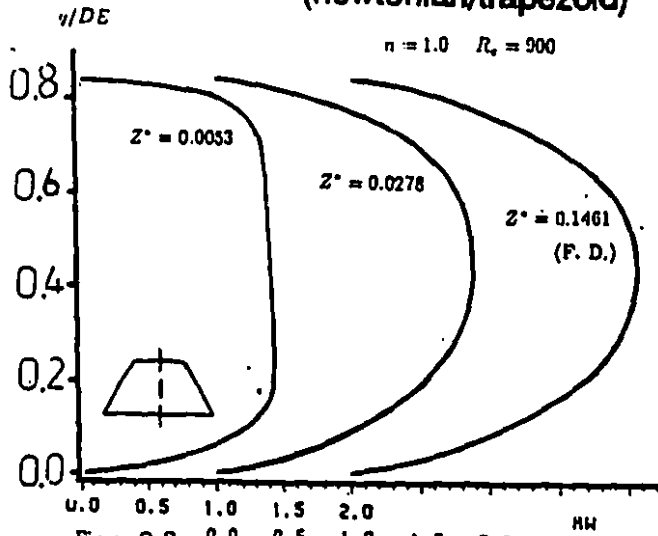
0.0 0.5 1.0 1.5 2.0
0.0 0.5 1.0 1.5 2.0

development of axial velocity profile
(newtonian/triangle)



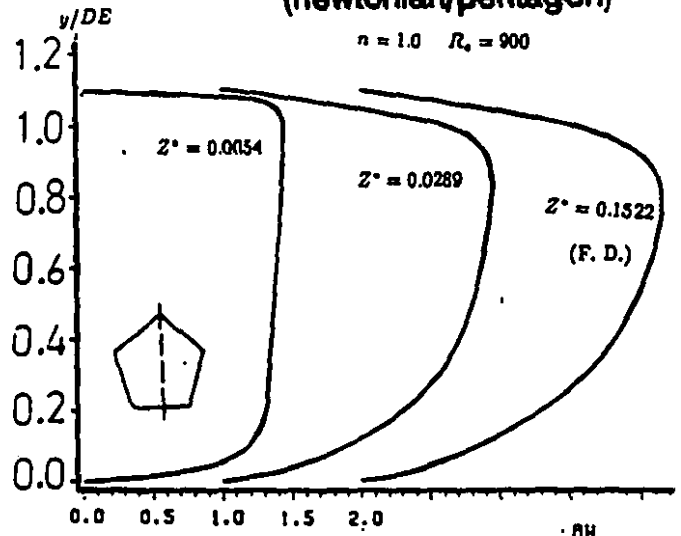
0.0 0.5 1.0 1.5 2.0
0.0 0.5 1.0 1.5 2.0

development of axial velocity profile
(newtonian/trapezoid)

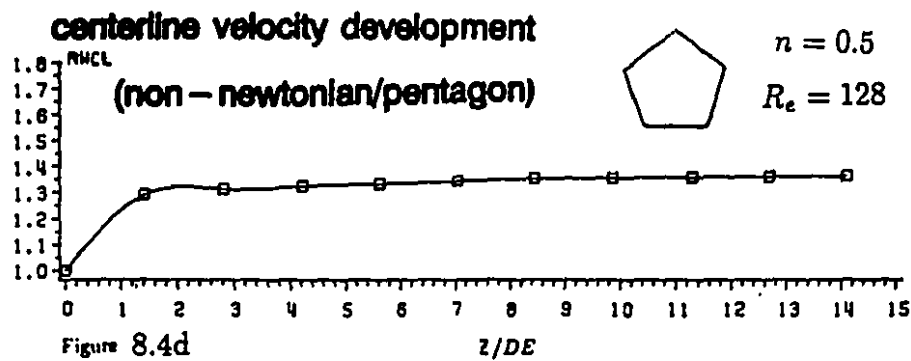
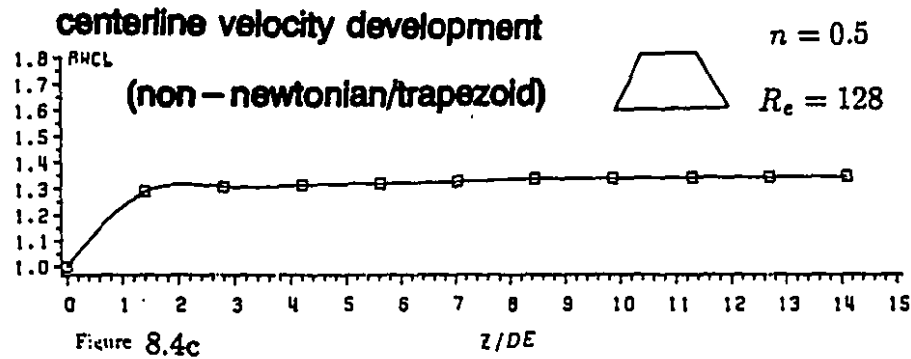
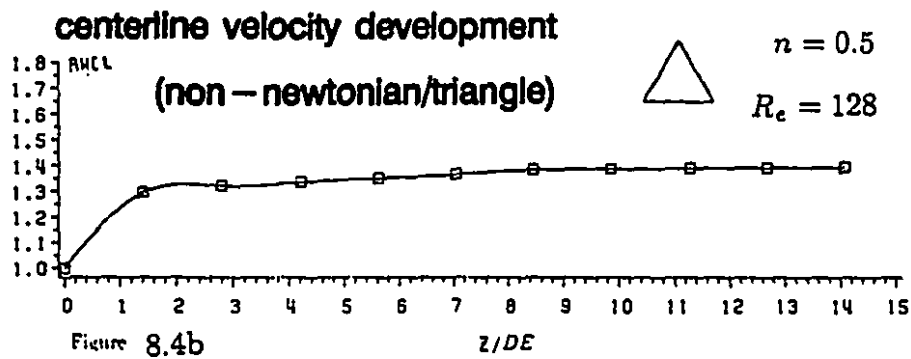
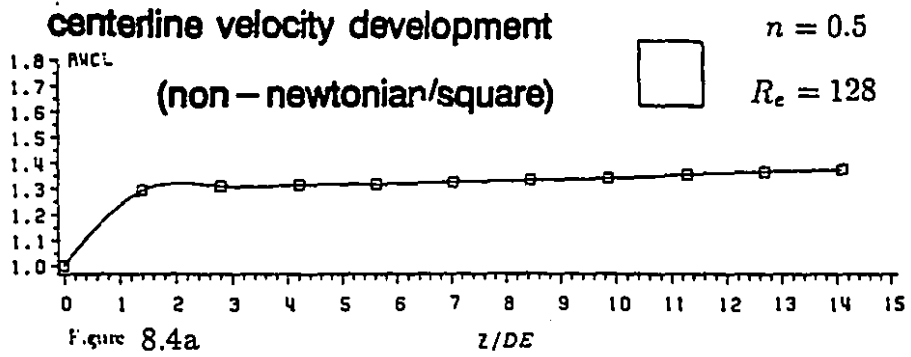


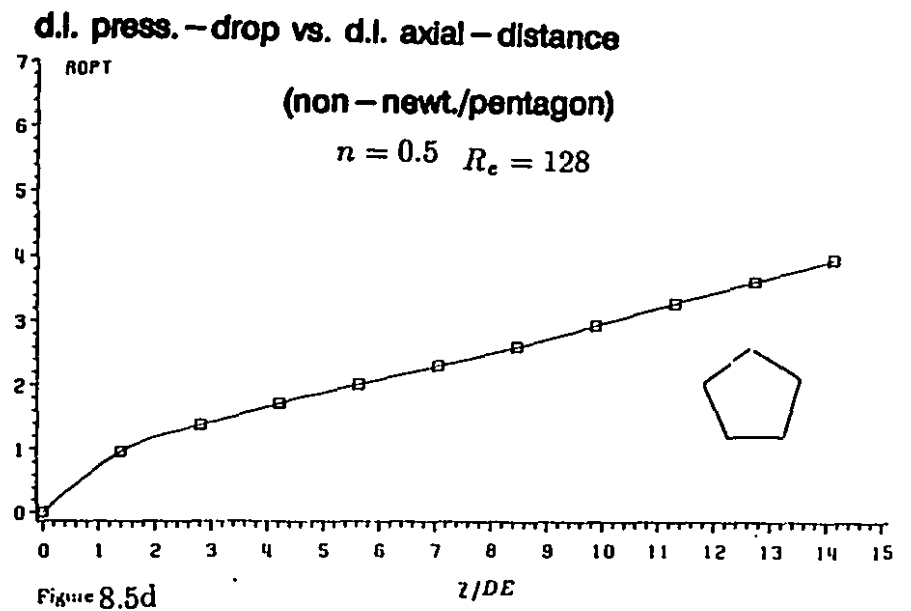
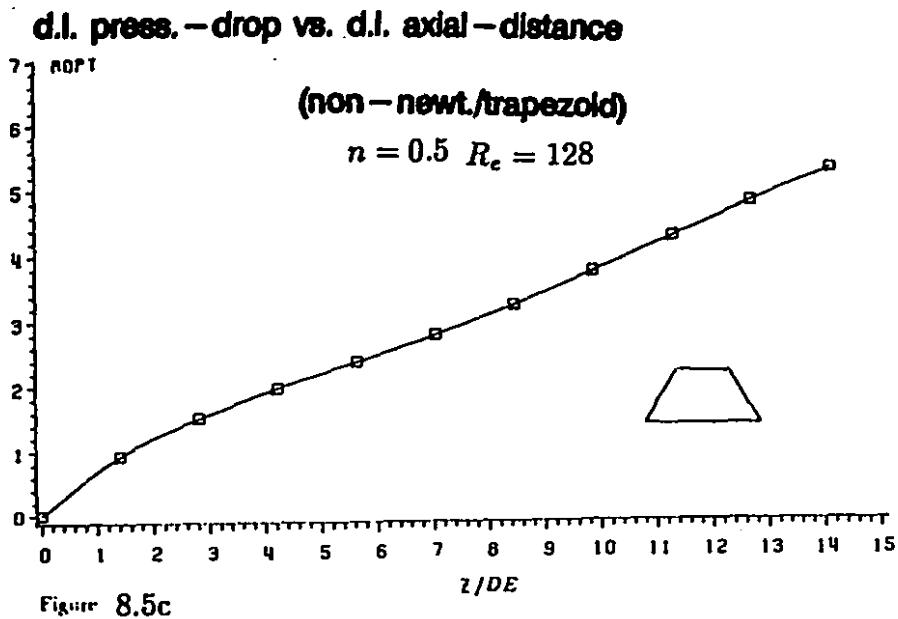
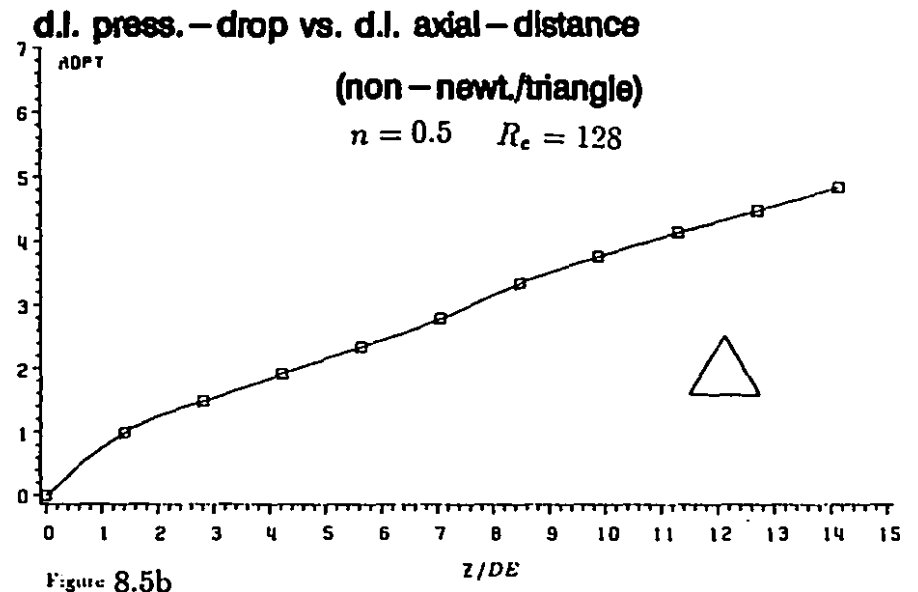
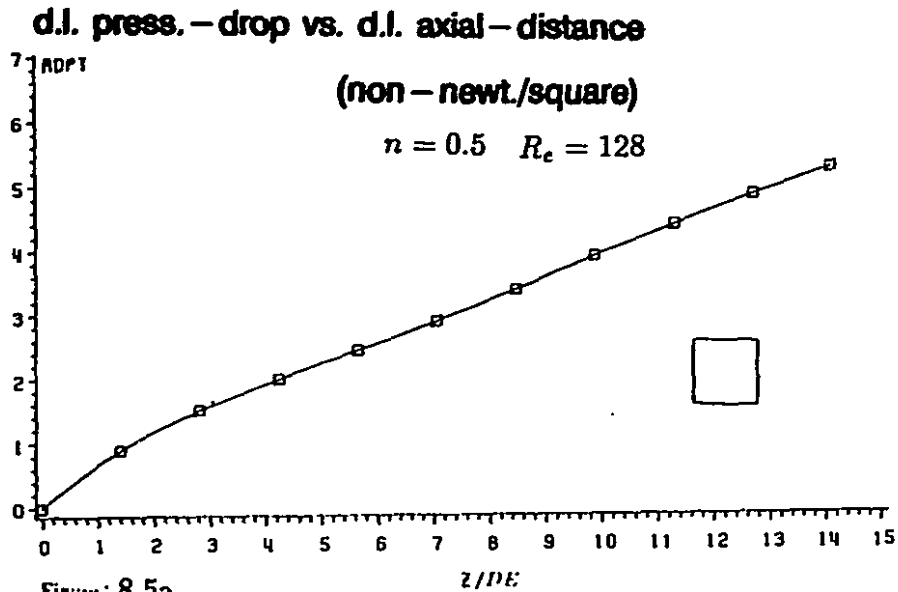
0.0 0.5 1.0 1.5 2.0
0.0 0.5 1.0 1.5 2.0

development of axial velocity profile
(newtonian/pentagon)

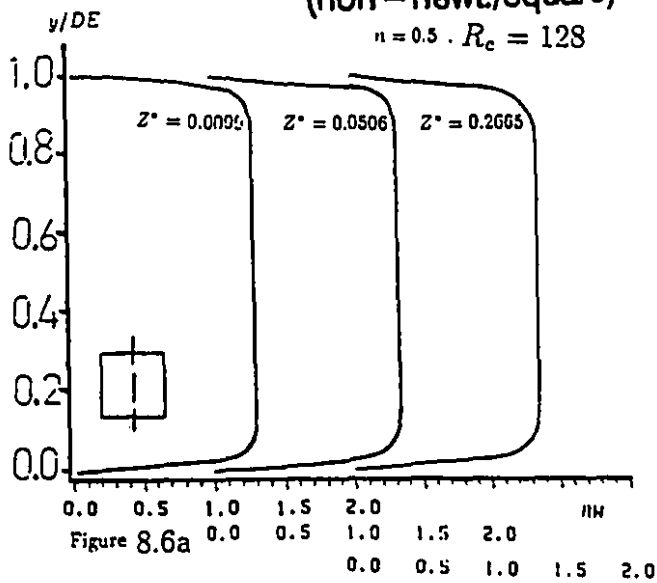


0.0 0.5 1.0 1.5 2.0
0.0 0.5 1.0 1.5 2.0

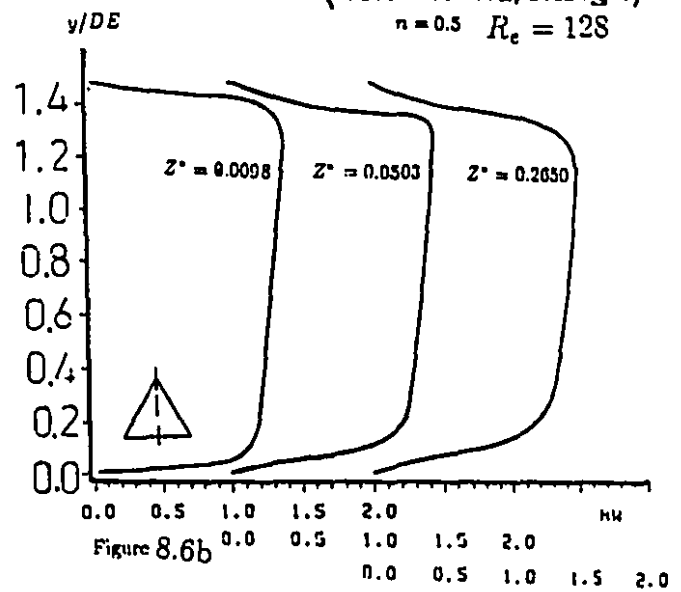




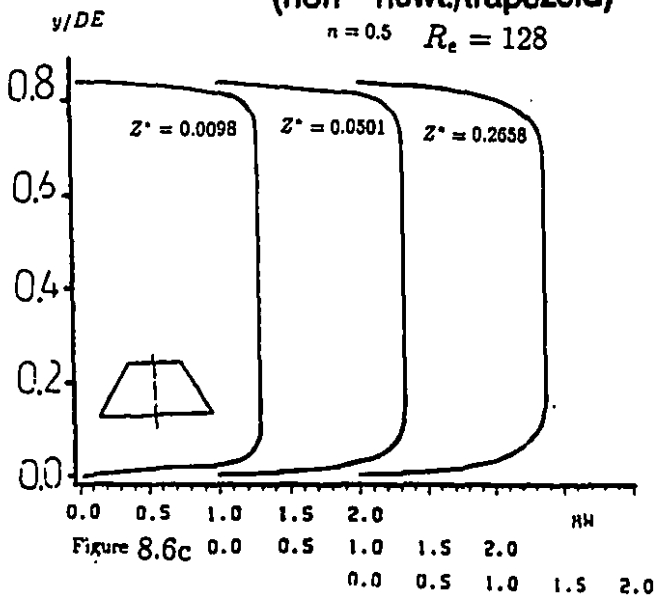
development of axial velocity profile
(non-newt./square)



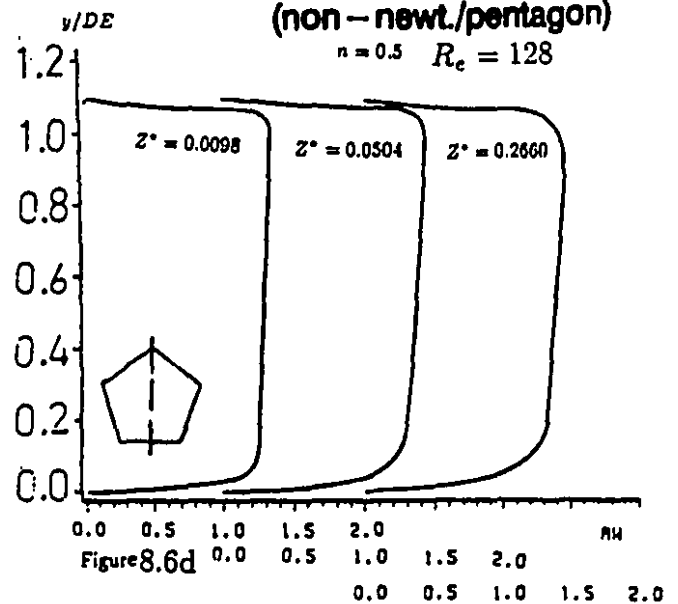
development of axial velocity profile
(non-newt./triangle)



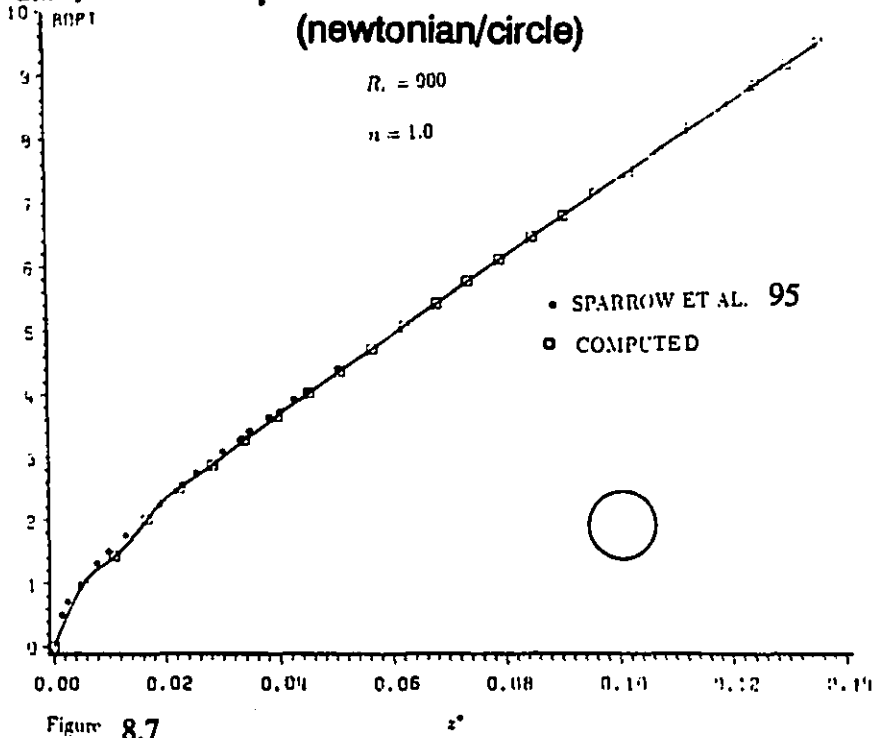
development of axial velocity profile
(non-newt./trapezoid)



development of axial velocity profile
(non-newt./pentagon)



d.l. press-drop vs. d.l. axial-dist.
(newtonian/circle)



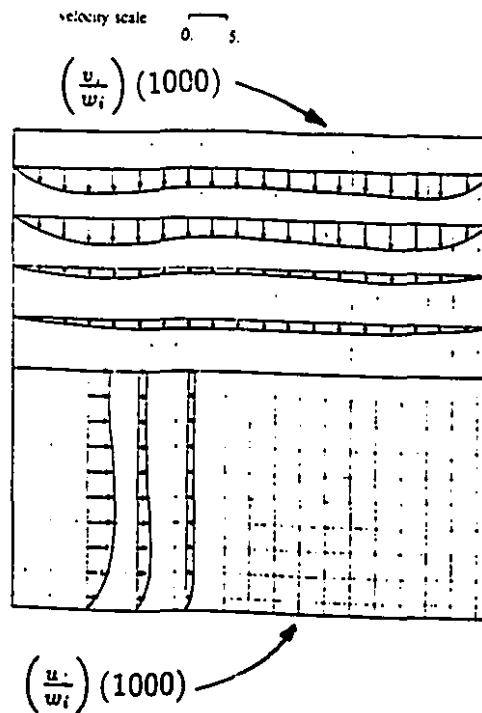


Fig. 8.8 Secondary flow velocity profiles for a square duct, Newtonian fluids, $Re = 900$, $(z/D_h)/Re = 0.0054$

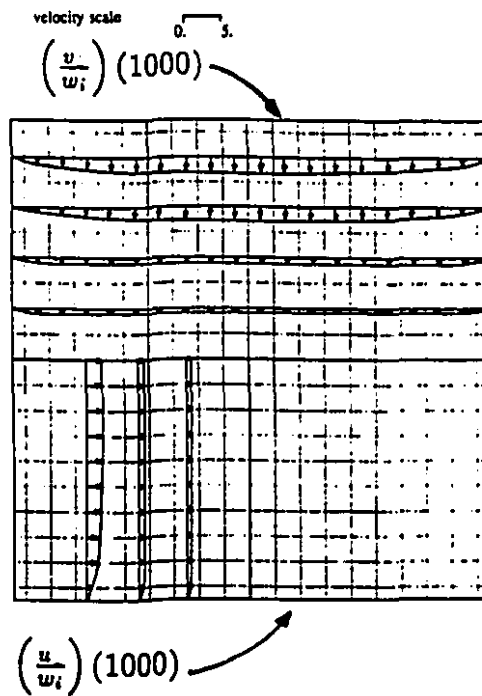


Fig. 8.9 Secondary flow velocity profiles for a square duct, non-Newtonian fluids ($n = 0.5$), $Re = 128$, $(z/D_h)/Re = 0.0115$

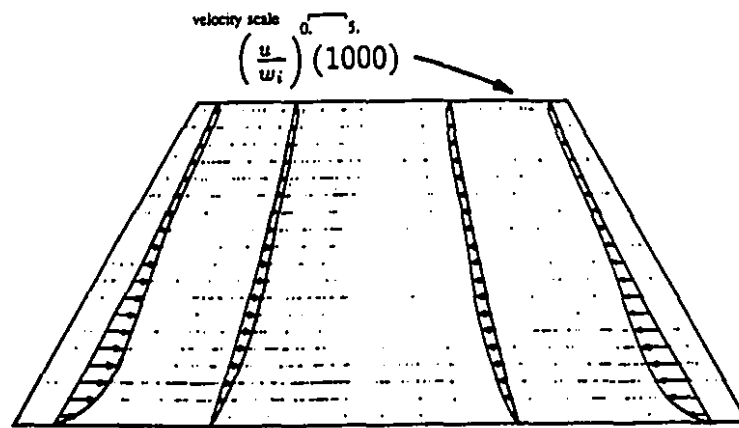
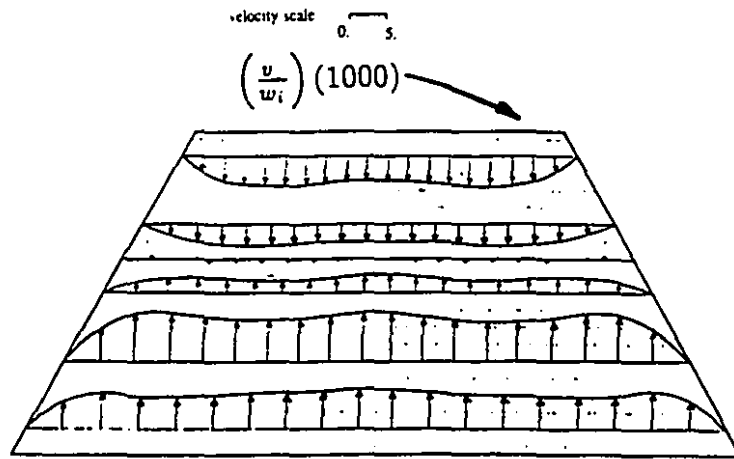


Fig.'s 8.10 a & b Secondary flow velocity profiles for a trapezoidal duct, Newtonian fluids, $Re = 900$, $(z/D_h)/Re = 0.0054$

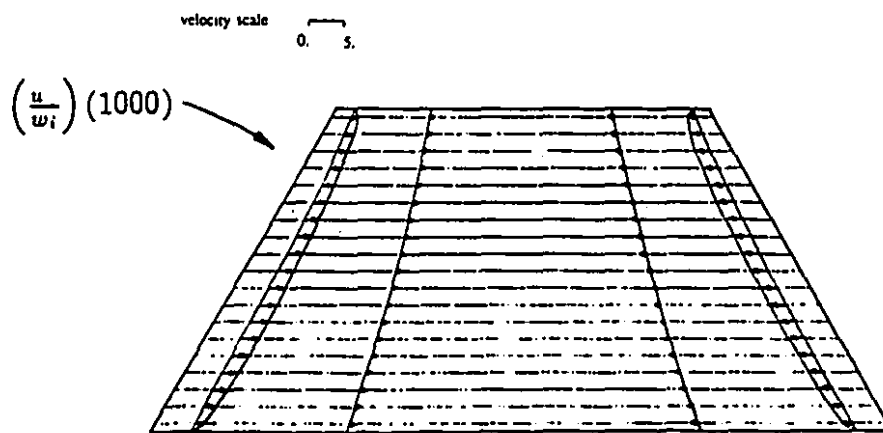
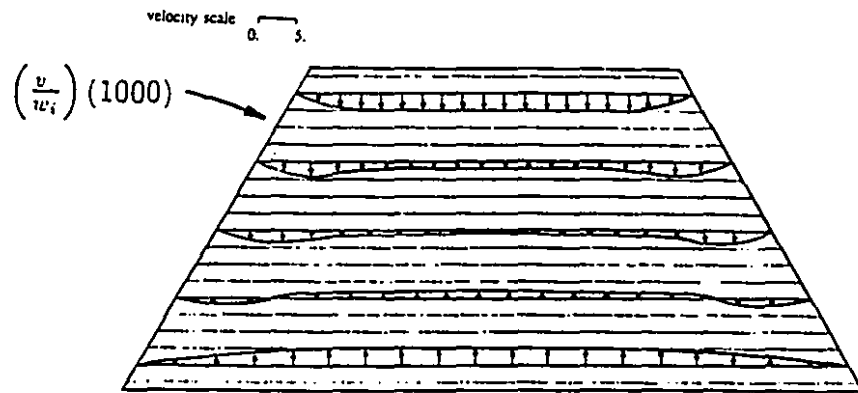


Fig.'s 8.11 a & b Secondary flow velocity profiles for a trapezoidal duct, non-Newtonian fluids ($n = 0.5$), $Re = 128$, $(z/D_0)/Re = 0.0115$

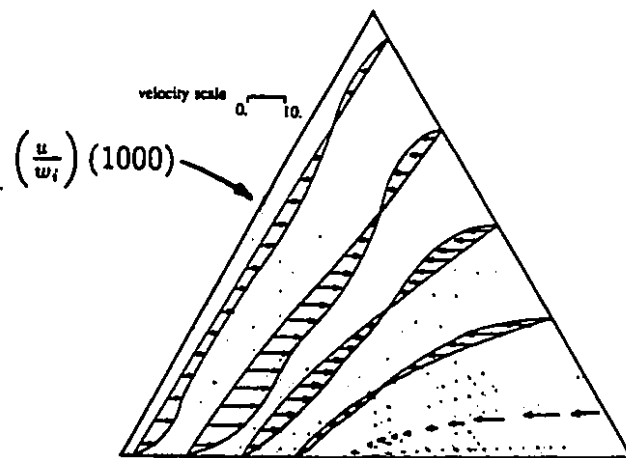
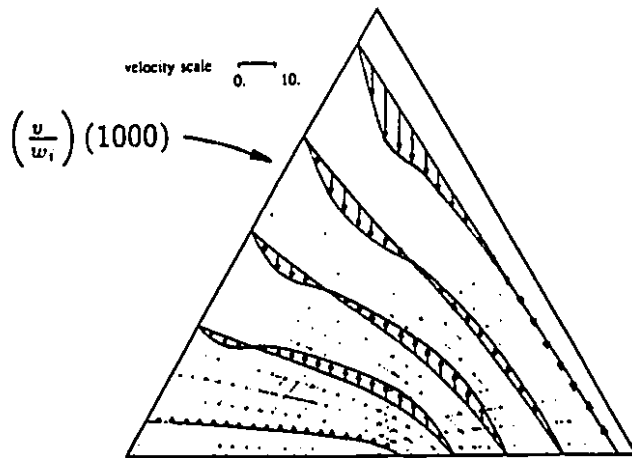


Fig.'s 8.12 a & b Secondary flow velocity profiles for a triangular duct, Newtonian fluids, $Re = 900$, $(z/D_h)/Re = 0.0054$

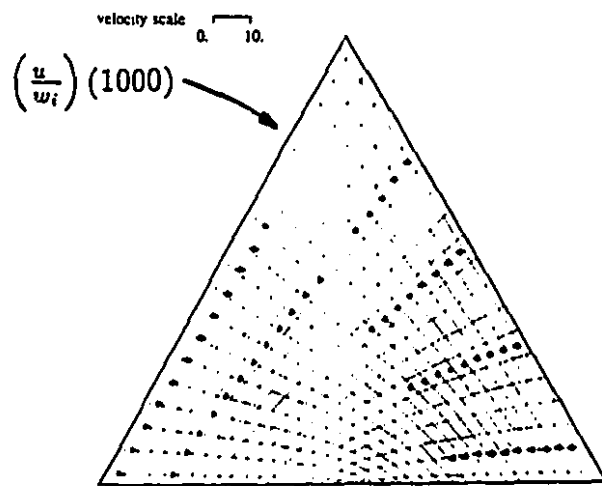
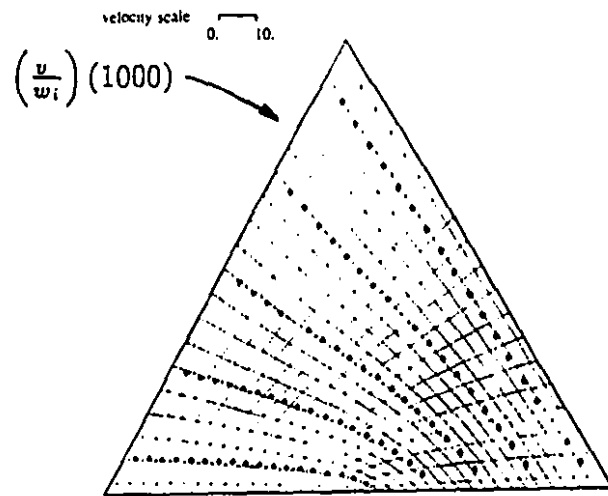


Fig.'s 8.13 a & b Secondary flow velocity profiles for a triangular duct, non-Newtonian fluids ($n = 0.5$), $Re = 128$, $(z/D_h)/Re = 0.0115$

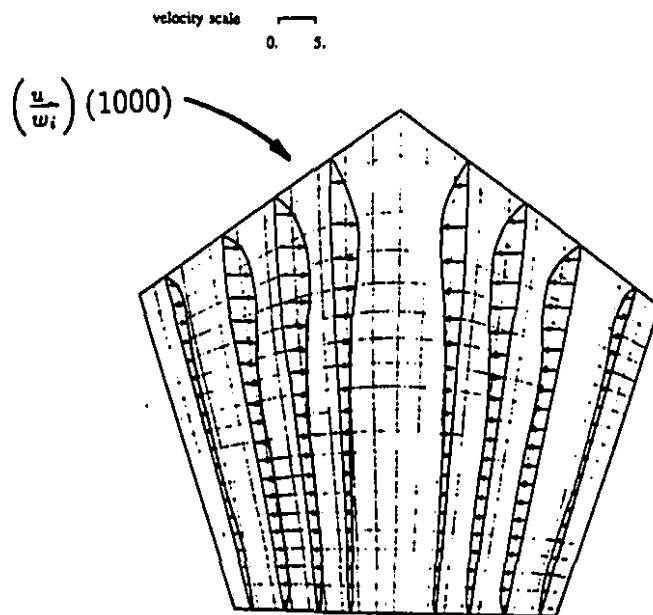
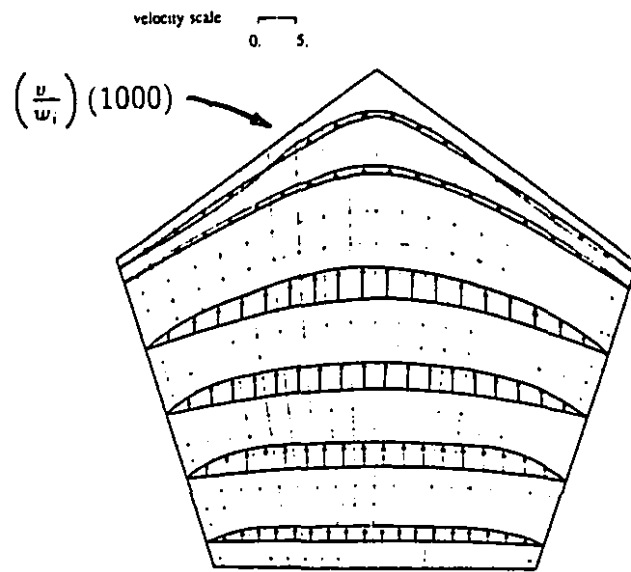


Fig.'s 8.14 a & b Secondary flow velocity profiles for a pentagonal duct, Newtonian fluids, $Re = 900$, $(z/D_h)/Re = 0.0054$

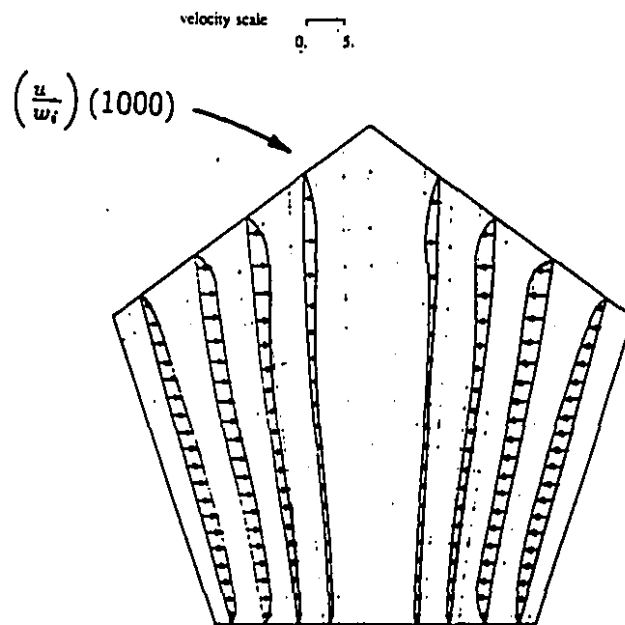
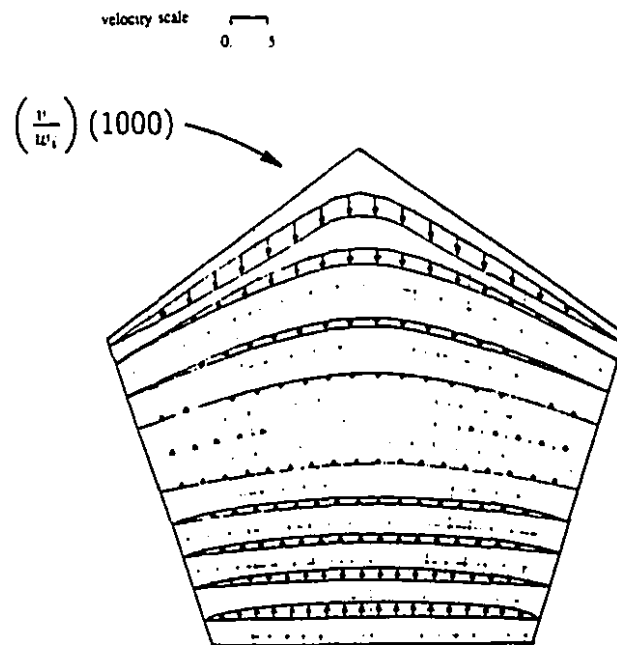


Fig.'s 8.15 a & b Secondary flow velocity profiles for a pentagonal duct, non-Newtonian fluids ($n = 0.5$), $Re = 128$, $(z/D_p)/Re = 0.0115$

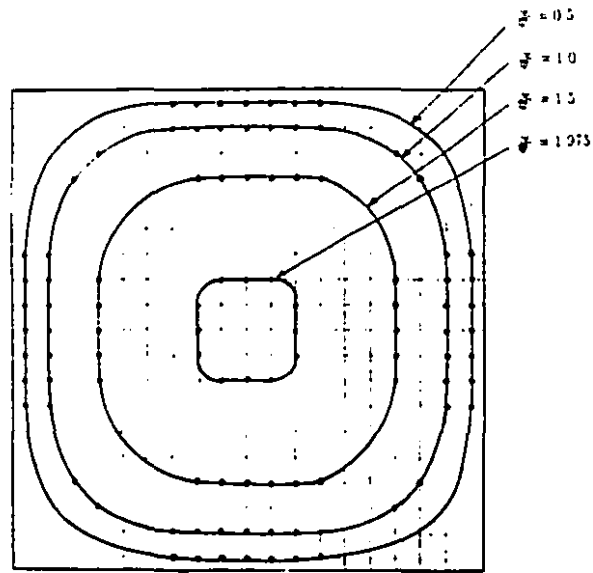


Fig. 8.16 Axial-velocity Contours, Newtonian Fluids, Square Ducts, $Re = 900$
 (@ F.D.)

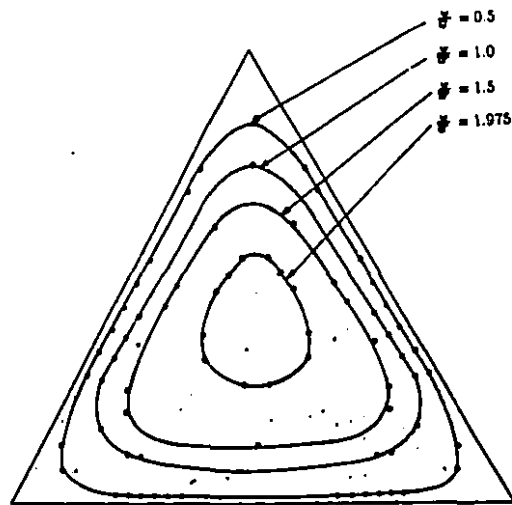


Fig. 8.17 Axial-velocity Contours, Newtonian Fluids, Triangular Ducts, $Re = 900$
 (@ F.D.)

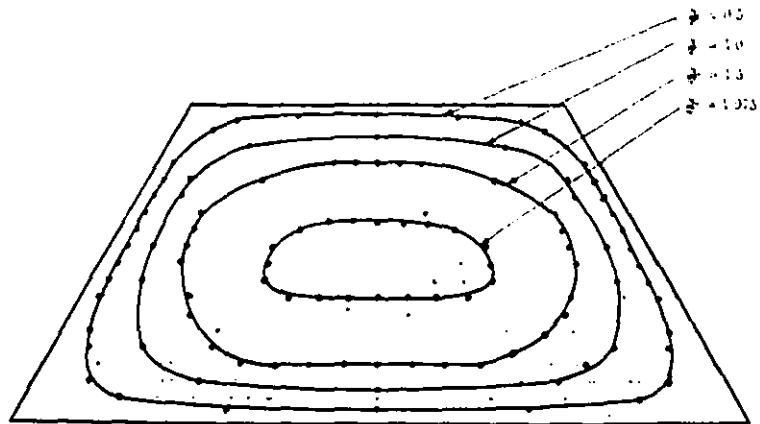


Fig. 8.18 Axial-velocity Contours, Newtonian Fluids, Trapezoidal Ducts, $Re = 900$
 (@ F.D.)

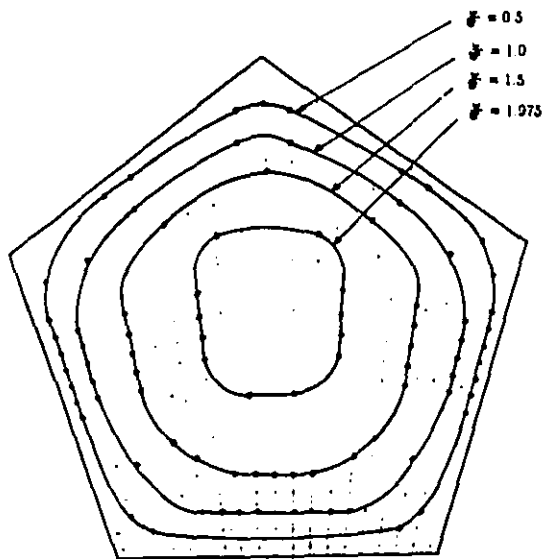


Fig. 8.19 Axial-velocity Contours, Newtonian Fluids, Pentagonal Ducts, $Re = 900$
 (@ F.D.)

8.3 HEAT TRANSFER

The results for heat transfer analysis for constant wall temperature case and for typical $Pr = 6.78$ are shown in Figs. 8.20–8.22, tables 8.6–8.7 and 8.12–8.15. The same geometries are selected in this study as were selected for the fluid-flow study, presented in the previous part of this chapter. Also, circular and rectangular ducts of two different aspect ratio (1/2 and 2/3) were examined for validation of the model and computer code for heat transfer.

Computations were performed on the basis of the same equivalent diameters, so that the same value of the relaxation factors was applied to different geometries corresponding to each discretization equation. As mentioned before, this scheme is valid if the geometries selected do not involve oddity. The Newtonian case was solved for an axial step size of 0.276 m for which 250 marching stations were required in the axial direction to reach to the converged solution. Separate runs were conducted with an axial step size of 0.552 m to confirm the limiting values of Nusselt numbers. The mesh size selected was 21×21 over the transversed-plane as specified before. The memory requirement for computations was 2720 K and the typical CPU time was about 26 minutes for one run. The computations were performed for fully-developed velocity and developing temperature profiles. Referring to Kays et al.⁸¹ the results obtained in this analysis are well suited for the simultaneously developing velocity and temperature profiles for the respective Prandtl number. Viscous dissipation effect was also considered in the present study. The buoyancy effect in this study is negligible due to the close temperatures selected for the fluid at inlet and at wall. Future work, however, is required for mixed-convection studies. About 5 iterations were required to obtain converged solution over each transversed plane. The convergence criteria was set on the residual values similarly defined for the fluid-flow study mentioned before, such that the residuals for this study are as follows:

- (i) the residual of energy equation,

(ii) the residual of enthalpy values between two successive iterations.

Table 3.5 shows the residual values of energy equation and enthalpy values at the converged solution.

Table 8. 5 Residual values (heat-transfer)

Geometry	Energy-equation Residual	Enthalpy Residual
Square	0.303×10^{-7}	-0.275×10^{-4}
Triangular	0.160×10^{-6}	-0.270×10^{-4}
Trapezoidal	0.533×10^{-7}	-0.270×10^{-4}
Pentagonal	0.694×10^{-7}	-0.385×10^{-4}
Rectangular (1/2)	0.224×10^{-7}	-0.357×10^{-4}
Rectangular (2/3)	0.262×10^{-7}	-0.315×10^{-4}
Circular	0.105×10^{-6}	-0.501×10^{-4}

The results of local and mean Nusselt numbers obtained for ducts of different cross-sectional geometries are presented in tables 8.6 and 8.7.

The local Nusselt number for constant temperature wall boundary conditions, $Nu_{loc} = Nu_{z,T}$, is expressed in terms of the fluid bulk-temperature-gradient along the flow path length by

$$Nu_{z,T} = -\frac{1}{4\theta_b} \frac{d\theta_b}{dz^{**}} \quad (8.1)$$

Refer to Appendix G for derivation. The logarithmic mean Nusselt number for constant wall temperature boundary condition is expressed by:

$$Nu_{m,T} = \frac{1}{4Z^{**}} \ln \left(\frac{1}{\theta_b} \right) \quad (8.2)$$

which is obtained from Eqn. (8.1) by integration (Appendix G).

Table 8. 6 $Nu_{z,T}$ variations for different geometries Newtonian Fluids, $Pr = 6.78$

G_z	Square	Triangular	Trapezoidal	Pentagonal
100	4.635	4.373	4.564	4.689
75	4.104	3.871	4.025	4.157
60	3.767	3.576	3.701	3.844
50	3.527	3.377	3.479	3.633
43	3.345	3.234	3.314	3.481
37	3.204	3.126	3.186	3.366
0	2.980	2.598	2.972	3.098

Table 8. 7 $Nu_{m,T}$ variations for different geometries Newtonian Fluids, $Pr = 6.78$

G_z	Square	Triangular	Trapezoidal	Pentagonal
100	7.186	6.841	7.005	7.009
75	6.386	6.072	6.232	6.266
60	5.842	5.555	5.706	5.761
50	5.441	5.178	5.320	5.391
43	5.129	4.889	5.022	5.105
37	4.878	4.659	4.783	4.877
0	2.980	2.598	2.972	3.098

The results for the limiting Nusselt-numbers are indicated in table 8.8 for all geometries under consideration. These values correspond to the dimensionless bulk and centerline temperature values of 0.993 and 0.986 respectively, in which the temperatures are nondimensionalized with the difference between the fluid wall temperature and the fluid temperature at the duct entrance.

The limiting Nusselt numbers (Nu_T) for square, rectangular, triangular and circular ducts obtained in this study are compared with analytical and numerical results of other investigators in table 8.9. These results confirm the validity of the model and computer code for heat transfer in this study.

Table 8. 8 Thermal entry length and limiting Nu_T results

Geometry	G_z	$Z^{**} =$ thermal entry length	Limiting Nu_T	$RT1 =$ $\frac{T_{Bulk} - T_{Inlet}}{T_{Wall} - T_{Inlet}}$	$RT2 =$ $\frac{T_{CL} - T_{Inlet}}{T_{Wall} - T_{Inlet}}$
Square	2.6248	0.381	2.980	0.993	0.986
Triangular	2.5175	0.397	2.598	0.993	0.986
Trapezoidal	2.6200	0.382	2.972	0.993	0.986
Pentagonal	2.9522	0.339	3.098	0.993	0.986
<i>for comparison:</i>					
Rectangular (1/2)	2.9287	0.341	3.363	0.993	0.986
Rectangular (2/3)	2.7346	0.366	3.118	0.993	0.986
Circular	3.1582	0.317	3.603	0.993	0.986

Table 8. 9 Comparison of limiting Nusselt numbers

	Square	Rectangular (1/2)	Rectangular (2/3)	Equilateral Triangular	Circular
Clark and Kays ⁹⁸	2.890	3.390	—	—	—
Dennis et al. ⁹⁷	2.980	3.390	3.120	—	—
Shah and London ⁹⁸	2.976	3.391	3.117	—	—
Schmidt ⁹⁸	2.970	3.383	3.121	—	—
Javeri ⁹⁸	2.981	3.393	—	—	—
Lyczkowski et al. ⁹⁸	2.975	3.395	3.117	—	—
Kays and Crawford ⁸¹	2.980	3.390	—	2.350	3.658
Wibulswas ¹⁰⁰	—	—	—	2.570	—
This Study	2.980	3.363	3.118	2.598	3.603

A comparison of variation of Nusselt number for square duct with some literature data, is presented in Fig. 8.20 which shows a close agreement. The analytical results of Dennis et al.⁹⁷ and numerical results of Lyczkowski et al.⁹⁸ shown in this figure are however, calculated by alternate approaches defined for local Nusselt number. The results obtained in this analysis for $Nu_{z,T}$ and $Nu_{m,T}$ for square ducts for Newtonian

fluids are compared with the numerical solutions of Chandrupatla et al.⁹⁹ in tables 8.10 and 8.11. There is a close agreement between their solutions and the present results for $Nu_{z,T}$ but there are some differences between $Nu_{m,T}$ values. The results obtained by Chandrupatla et al.⁹⁹ are for fully developed velocity profile, with no secondary flow and no viscous dissipation effect. Also, the effect of variation of Prandtl number is ignored in their analysis and no value is mentioned for the Prandtl number corresponding to their results. It is believed that, the differences existing in the results of $Nu_{m,T}$ as observed in table 8.11, are mainly due to the difference in the values of Prandtl numbers. Chandrupatla et al.⁹⁹ ignores the effect of Prandtl number on $Nu_{m,T}$ by the reasoning that it is included in the relevant $\frac{Pr}{(X/4)}$ term⁹⁹. However, Nu_m is affected by Pr through the effect θ_b according to the following relations:

$$Nu_{m,T} = \frac{Pr}{X} \ln \frac{1}{\theta_b} = \frac{1}{4} \frac{Pr}{(X/4)} \ln \left(\frac{1}{\theta_b} \right) \quad (\text{ref. 99}) \quad (8.3)$$

or

$$Nu_{m,T} = \frac{1}{4} G_z \ln \left(\frac{1}{\theta_b} \right) \quad (8.4)$$

but

$$\theta_b = f(Pr) \quad (\text{from energy equation}^{1*}) \quad (8.5)$$

therefore

$$Nu_{m,T} = \frac{1}{4} G_z g(Pr) \quad (8.6)$$

or

$$Nu_{m,T} = h(G_z, Pr) \quad (8.7)$$

The thermal entry length is analyzed in terms of the dimensionless bulk and centerline temperatures in Fig. 8.21 for the selected geometries. The thermal entry length

^{1*} $U \frac{\partial \theta}{\partial x} = \frac{1}{Pr} \left[\frac{\partial^2 \theta}{\partial y^2} + \frac{\partial^2 \theta}{\partial z^2} \right]$ (ref. 99) in which $\theta = \frac{t-t_w}{t_i-t_w}$.

Table 8. 10 Comparison of Nusselt number, $Nu_{z,T}$, variations ($n=1$)

Chandrupatla et al ⁹⁹		Present Analysis	
G_z	$Nu_{z,T}$	G_z	$Nu_{z,T}$
0	2.975	0	2.980
40	3.432	37	3.204
50	3.611	50	3.527
80	4.084	75	4.104
100	4.357	100	4.635
133.3	4.755	127	4.845
200	5.412	190	5.808

Table 8. 11 Comparison of Nusselt number, $Nu_{m,T}$, variations ($n=1$)

Chandrupatla et al ⁹⁹		Present Analysis	
G_z	$Nu_{m,T}$	G_z	$Nu_{m,T}$
0	2.975	0	2.980
40	4.841	37	4.878
50	5.173	50	5.441
80	5.989	75	6.386
100	6.435	100	7.186
133.3	7.068	127	8.084
200	8.084	190	9.612

obtained in this study for square ducts is $Z^{**} = 0.381$ which is close to the value obtained by Neti et al.⁹⁶, $Z^{**} = 0.352$. The value obtained in this study is, however, corresponding to the dimensionless bulk and centerline temperatures of 0.993 and 0.986 respectively while the values obtained by Neti et al.⁹⁶ are that of 0.988 and 0.979 respectively. The results of central plane thermal development are shown in Fig. 8.22 in terms of the dimensionless temperature profiles which are defined differently from that used in table 8.8 and Fig. 8.21. The temperature is nondimensionalized here with the difference between the uniform wall temperature and the bulk fluid temperature. Temperature profiles are shown at three different axial positions.

Table 8. 12 $Nu_{z,T}$ variations for square ducts (for $Re = 900$ & $Pr = 6.78 @ n = 1$)

G_z	$n = 1.25$	$n = 1.0$	$n = 0.75$	$n = 0.50$
100	4.270	4.635	5.855	7.156
75	3.713	4.104	5.410	6.638
60	3.365	3.767	5.076	6.197
50	3.122	3.527	4.786	5.764
43	2.944	3.345	4.527	5.334
37	2.811	3.204	4.294	4.918
0	2.800	2.980	3.169	3.332

Table 8. 13 $Nu_{z,T}$ variations for triangular ducts (for $Re = 900$ & $Pr = 6.78 @ n = 1$)

G_z	$n = 1.25$	$n = 1.0$	$n = 0.75$	$n = 0.50$
100	4.201	4.373	4.860	5.948
75	3.685	3.871	4.383	5.579
60	3.383	3.576	4.092	5.321
50	3.182	3.377	3.883	5.092
43	3.093	3.234	3.722	4.877
37	2.934	3.126	3.593	4.671
0	2.510	2.598	2.738	2.879

Table 8. 14 $Nu_{z,T}$ variations for trapezoidal ducts (for $Re = 900$ & $Pr = 6.78 @ n = 1$)

G_z	$n = 1.25$	$n = 1.0$	$n = 0.75$	$n = 0.50$
100	4.342	4.564	5.535	7.586
75	3.790	4.025	5.068	7.363
60	3.462	3.701	4.754	7.154
50	3.238	3.479	4.503	6.904
43	3.075	3.314	4.291	6.614
37	2.952	3.186	4.105	6.297
0	2.839	2.972	3.141	3.317

Table 8. 15 $Nu_{z,T}$ variations for pentagonal ducts (for $Re = 900$ & $Pr = 6.78 @ n = 1$)

G_z	$n = 1.25$	$n = 1.0$	$n = 0.75$	$n = 0.50$
100	4.500	4.689	5.258	6.502
75	3.956	4.157	4.764	6.163
60	3.641	3.844	4.450	5.886
50	3.436	3.633	4.215	5.610
43	3.292	3.481	4.028	5.331
37	3.189	3.366	3.871	5.058
0	2.962	3.098	3.225	3.388

The results of local Nusselt-number ($Nu_{z,T}$) distribution for power-law non-Newtonian fluids for different geometries are tabulated in tables 8.12 to 8.15 for "n" values of 0.50, 0.75 and 1.25. These results correspond to the Newtonian case of $Re = 900$ and $Pr = 6.78$. The results of Newtonian fluids ($n=1$) are also included in these tables for comparison. These results show that the value of Nusselt number increases by decreasing the power-law exponent (n) at any specific G_z .

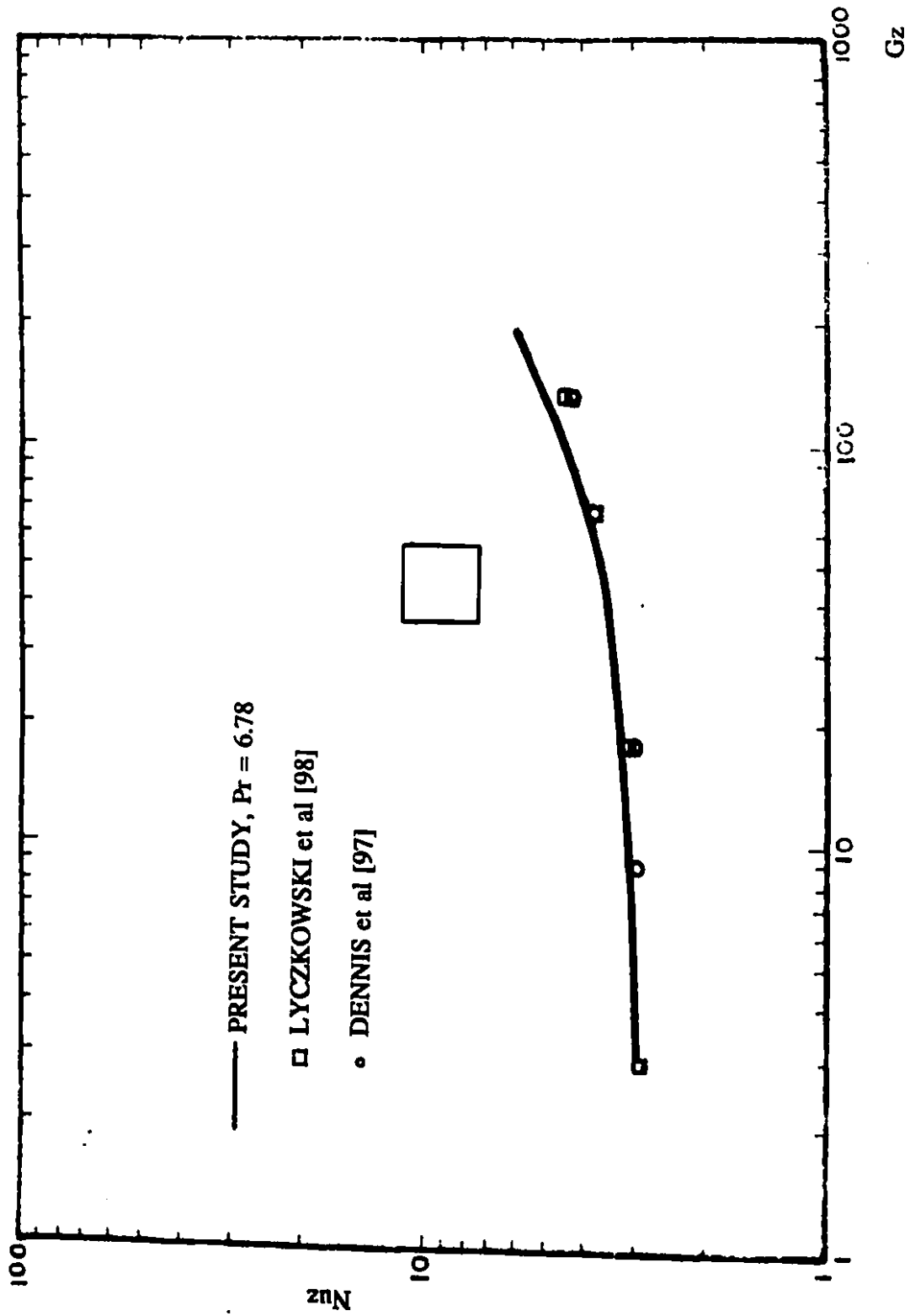


Fig. 8-20 Nusselt number variation along the square duct (Newtonian)

d.l.temperature vs. d.l. axial - dist.(newtonian/square)

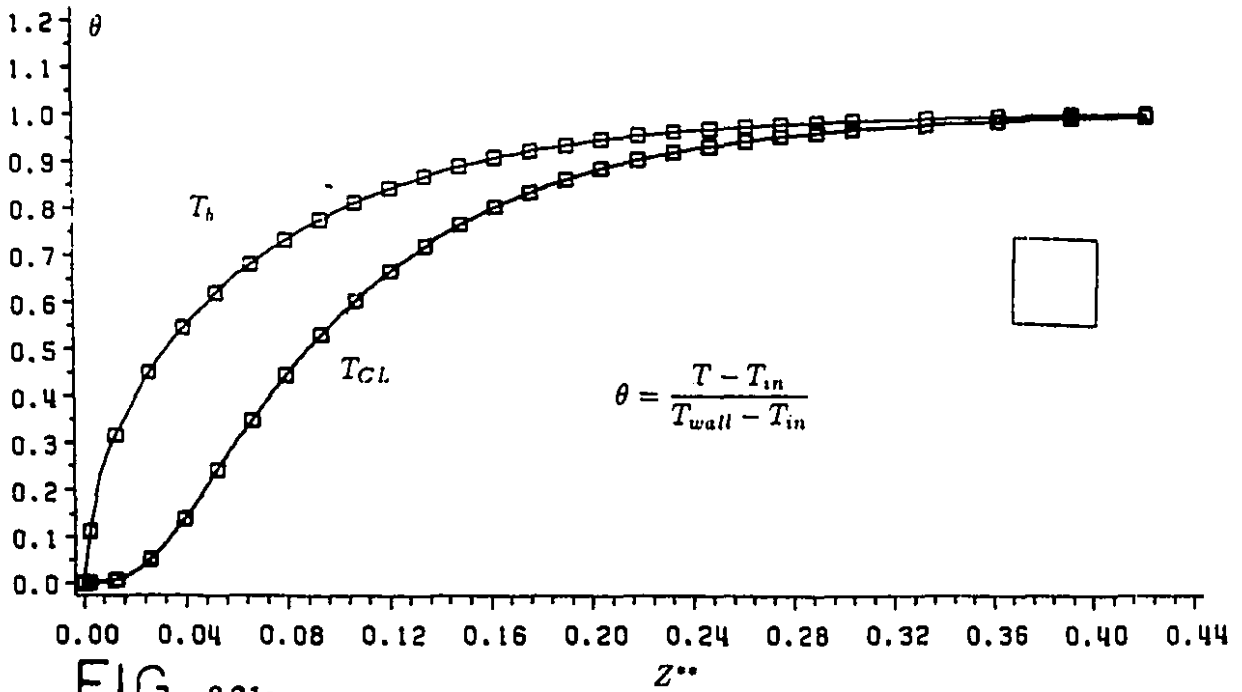


FIG. 8.21a

d.l.temperature vs. d.l. axial - dist.(newtonian/triangle)

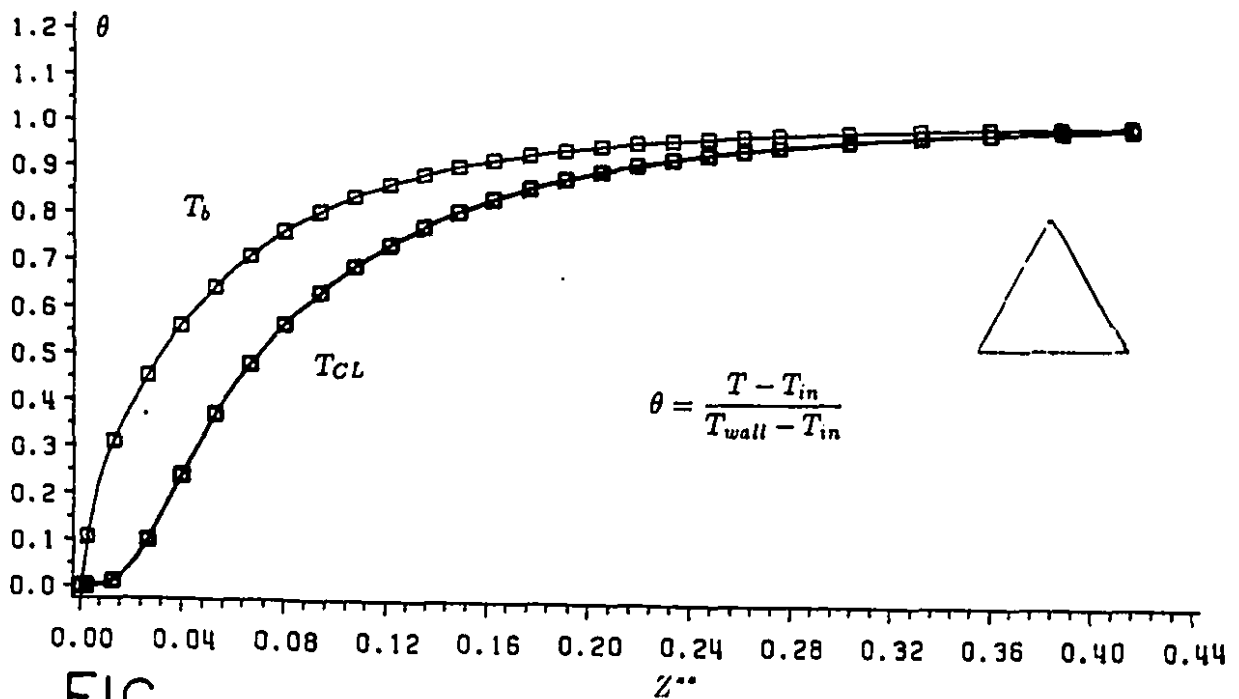
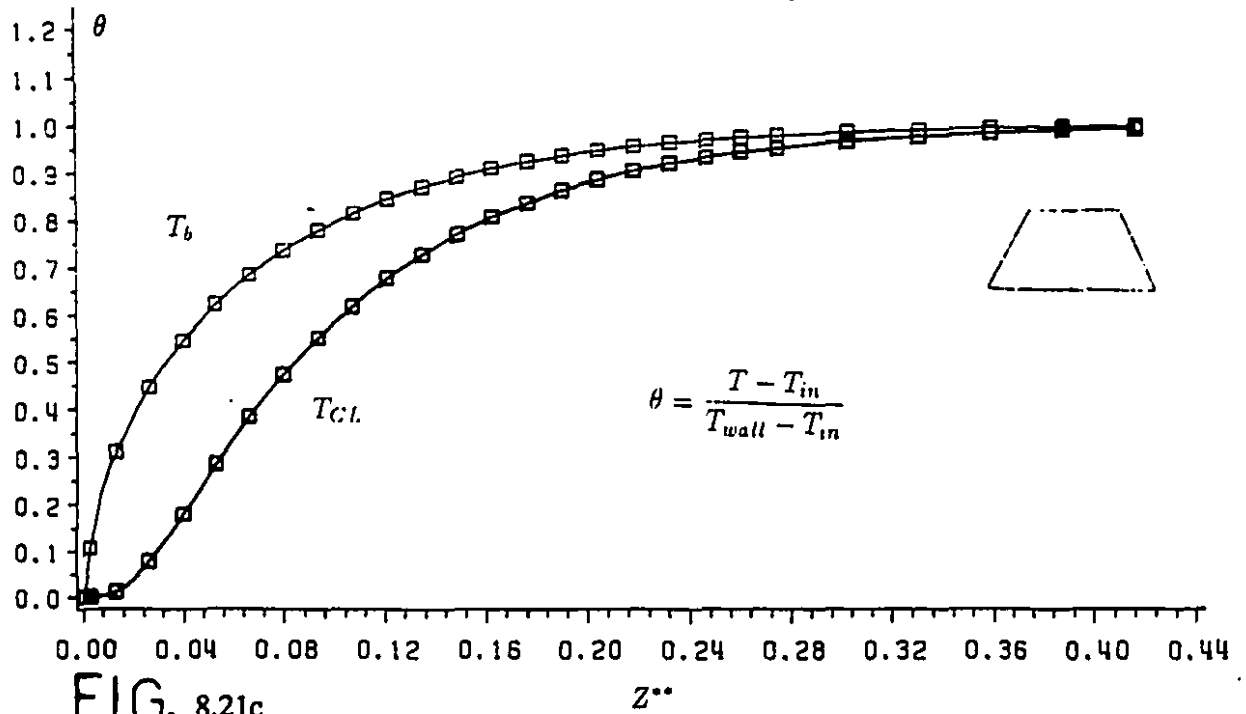
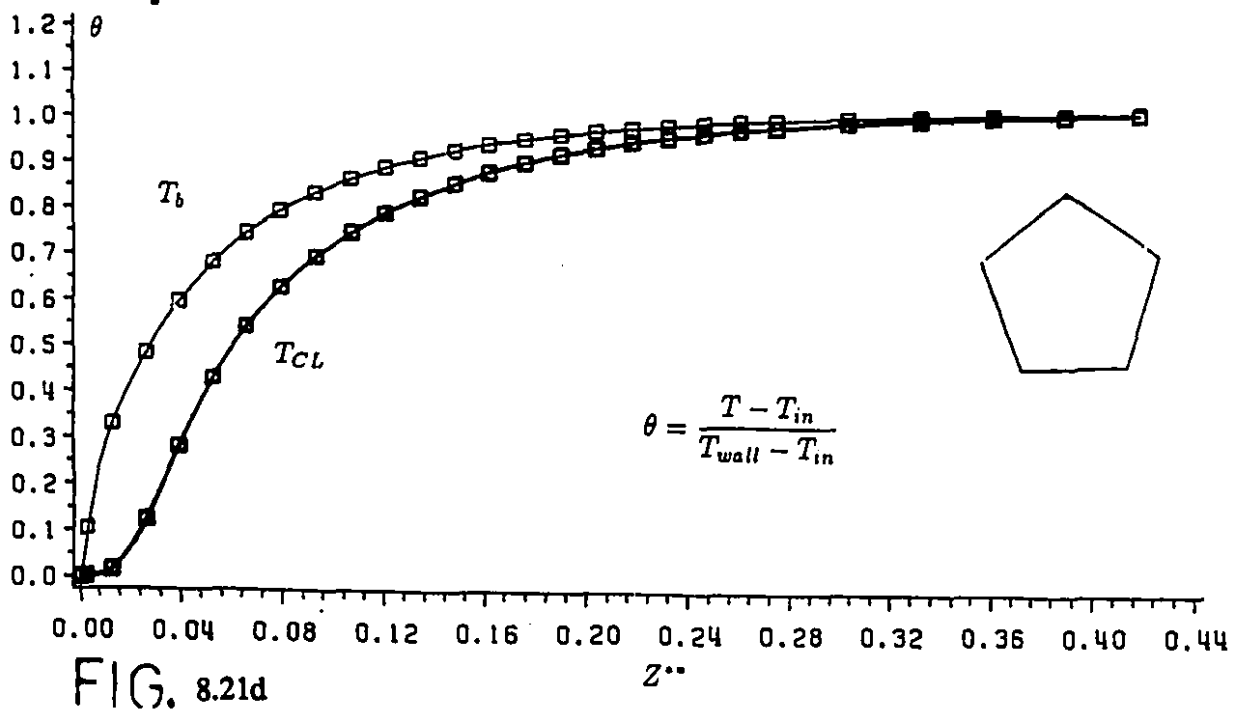


FIG. 8.21b

d.l.temperature vs. d.l. axial – dist. (newtonian/trapezoid)



d.l.temperature vs. d.l. axial – dist. (newtonian/pentagon)



development of temperature profile

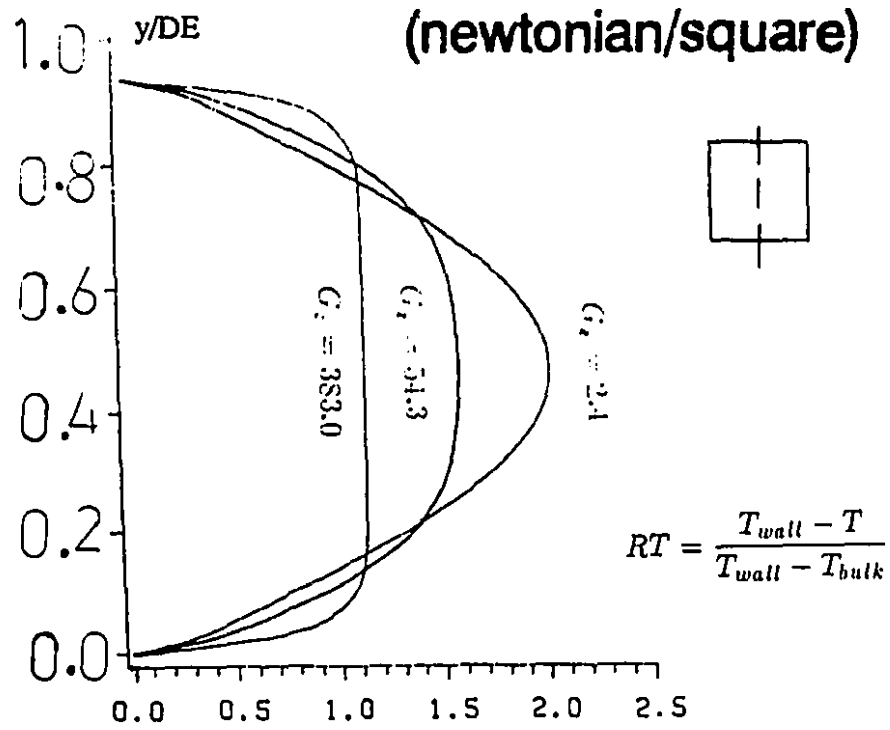


FIG. 8.22a

RT

development of temperature profile

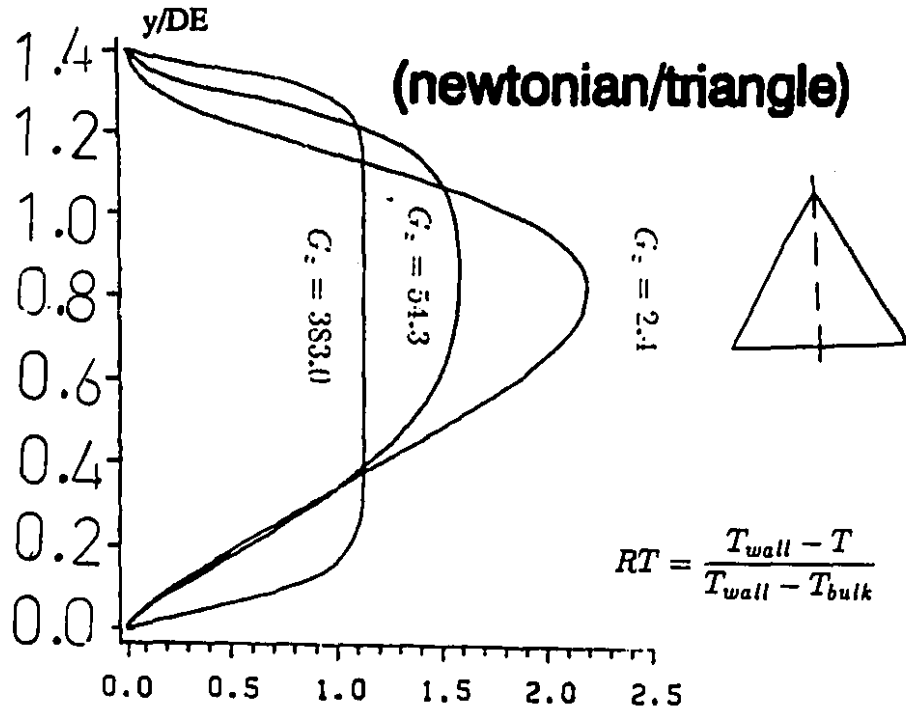


FIG. 8.22b

RT

development of temperature profile

(newtonian/trapezoid)

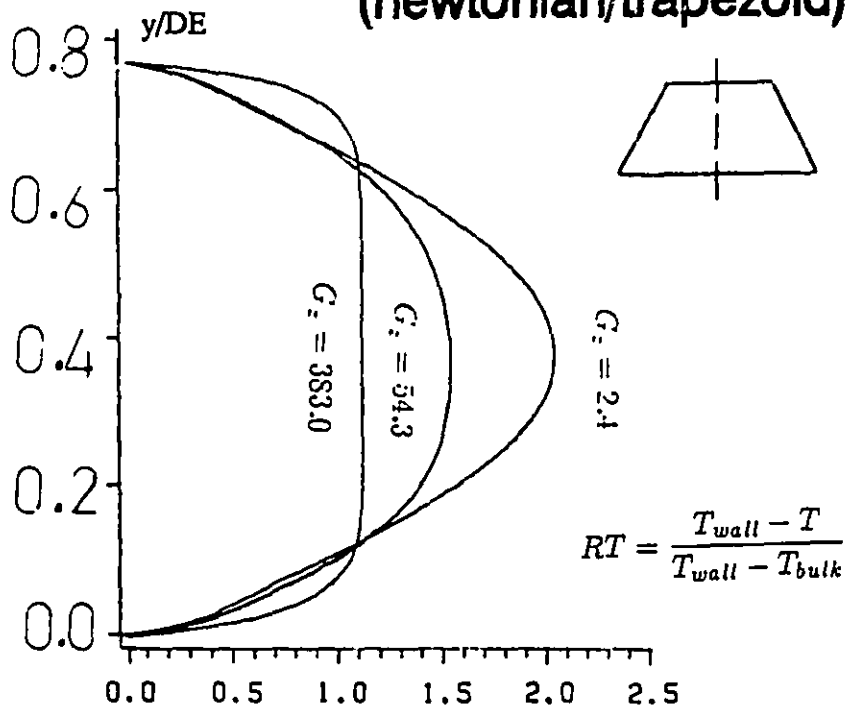


FIG. 8.22c

RT

development of temperature profile

(newtonian/pentagon)

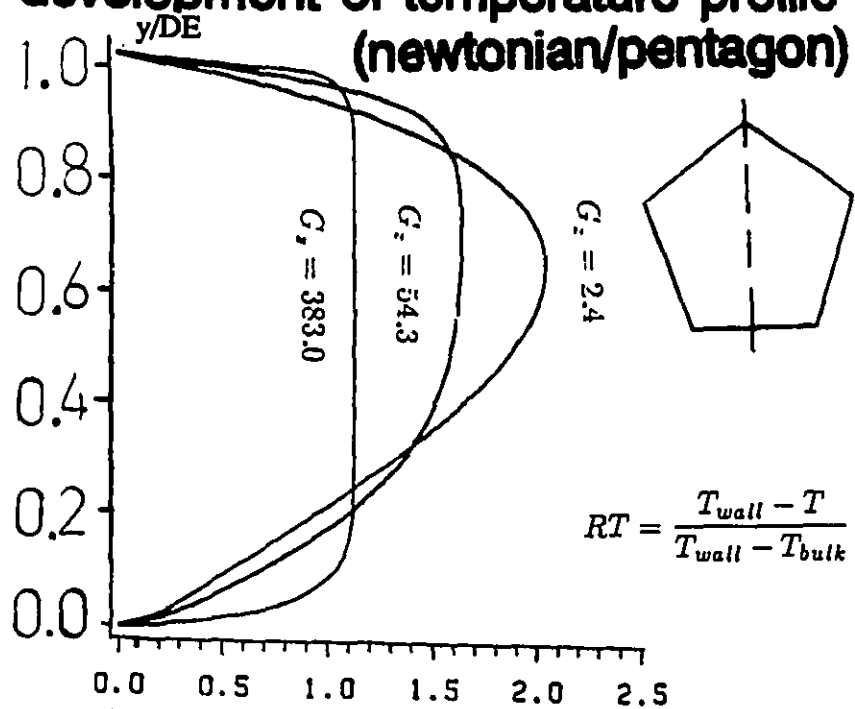


FIG. 8.22d

RT

8.4 MASS TRANSFER WITH CHEMICAL REACTION

In this study the thermal polymerization of styrene is selected for analysis in non-circular cross-sectional duct reactors. The only experimental data available in open literature is that of Valsamis et al.²⁵ for a reaction conversion of 15 wt %. This result is not verified by Chi-Chi Chen²⁷ in his numerical investigation who obtained a value of about 10.0 wt % of conversion for the same set of operating conditions. The result obtained by the present work is close to the value obtained by Chi-Chi Chen²⁷. Refer to tables 8.16a and 8.16b of the following section (i) for details. The validation of system modelling and computer codes for mass-transfer is accomplished through comparison of the numerical results of other investigators with the predicted results obtained by the present computer codes. One may refer to the following sections (ii), (iii) and (iv) for details. The effect of free-convection in this study is ignored for the results to be comparable with literature data in which this effect is not considered. Further investigations which are presented in the following pages show that reaction conversion results are only negligibly affected if free-convection is considered. The effect of variation of number of stations in the axial direction is also observed in tables 8.16b, 8.17b and 8.17c, which indicates a satisfactorily close agreement in the results of conversion for different numbers of stations in the axial direction. The reactor exit results of molecular weights (\bar{M}_w and \bar{M}_n) and total reactor pressure-drop values are also indicated.

Section (i) Valsamis and Biesenberger²⁵, 1976 experimental run:

reactor length	14.6 m
tube diameter	0.0046 m
residence time	5.15 min
inlet/wall temperature	160°C/160°C
conversion	15%

Table 8. 16a Chi-Chi Chen²⁷, 1986, simulation results

Velocity-Profile	Conversion, wt %	Molecular-weights		Polydispersity $\frac{M_w}{M_n}$
		$M_n \times 10^{-5}$	$M_w \times 10^{-5}$	
piston-flow	10.53	1.13	1.99	1.76
parabolic	10.12	1.14	2.00	1.75
$V_z(r, z)$ & $V_r = 0$	9.69	1.14	2.00	1.75
$V_z(r, z)$ & $V_r(r, z)$	9.98	1.14	2.00	1.75

Table 8. 16b Present work simulation results

Number of stations selected in axial-direction	Conversion wt %	Molecular-weights		Polydispersity $\frac{M_w}{M_n}$	Total ΔP (Pa)
		$M_n \times 10^{-5}$	$M_w \times 10^{-5}$		
15	10.13	1.30	2.25	1.73	51.0
30	10.34	1.28	2.22	1.73	58.0

Section (ii) Husain and Hamielec²⁴, 1976:

length of tube	500 cm
tube radius	2.0 cm
inlet velocity	0.0695 cm/sec
inlet feed temperature	100°C
wall temperature	100°C

:

Table 8. 17a Husain and Hamielec²⁴. 1976, simulation results

Length Z (cm)	Conversion, X_m (%)	Molecular-weights		Polydispersity $\frac{M_w}{M_n}$
		$M_n \times 10^{-5}$	$M_w \times 10^{-5}$	
100	1.26	4.16	7.34	1.76
300	3.95	4.04	7.16	1.77
500	6.62	3.96	7.08	1.78

Table 8. 17b Present work simulation results

Number of stations selected in axial direction : 5

Length Z (cm)	Conversion wt %	Molecular-weights		Polydispersity $\frac{M_w}{M_n}$	Total ΔP (Pa)
		$M_n \times 10^{-5}$	$M_w \times 10^{-5}$		
100	1.38	4.22	7.43	1.76	0.037
300	4.14	4.75	8.68	1.83	0.40
500	6.74	4.52	8.20	1.81	1.46

Table 8. 17c Present work simulation results

Number of stations selected in axial direction : 10

Length Z (cm)	Conversion wt %	Molecular-weights		Polydispersity $\frac{M_w}{M_n}$	Total ΔP (Pa)
		$M_n \times 10^{-5}$	$M_w \times 10^{-5}$		
100	1.37	5.09	9.33	1.83	0.06
300	3.95	4.48	8.08	1.80	0.48
500	6.43	4.40	7.87	1.79	1.74

Section (iii) Chi-Chi Chen²⁷, 1986:

length of tube	6.4 m
tube radius	0.55 cm
mass flow	1.345×10^{-4} kg/sec
inlet feed temperature	140°C
wall temperature	135°C

Table 8. 18a Chi-Chi Chen²⁷, 1986, simulation results

Conversion, wt %	Molecular-weights		Polydispersity $\frac{M_w}{M_n}$	Total ΔP (Pa)
	$M_n \times 10^{-5}$	$M_w \times 10^{-5}$		
26.49	1.55	2.87	1.85	758.3

Table 8. 18b Present work simulation results

Number of Stations selected in axial-direction : 10

Conversion, wt %	Molecular-weights		Polydispersity $\frac{M_w}{M_n}$	Total ΔP (Pa)
	$M_n \times 10^{-5}$	$M_w \times 10^{-5}$		
26.60	2.21	3.93	1.78	243.0

Section (iv) C. Kleinstreuer and S. Agarwal²⁹, 1986:

length of tube	5.0 m
tube radius	2 cm
mass flow	0.00002 kg/sec
inlet feed temperature	130°C
wall temperature	100°C

Table 8. 19a C. Kleinstreuer and S. Agarwal²⁹, 1986, simulation result:

Boundary-condition for velocity at entrance	Conversion wt %
Parabolic	54.8

Table 8. 19b Present work simulation results

Number of stations selected in axial direction : 100

Boundary condition for velocity at entrance	Conversion wt %	Molecular-weights		Polydispersity $\frac{M_w}{M_n}$	Total ΔP (Pa)
		$M_n \times 10^{-5}$	$M_w \times 10^{-5}$		
Parabolic	55.35	4.82	9.68	2.01	2792
Uniform	55.22	4.81	9.67	2.01	2617

8.5 SIMULTANEOUS REACTING FLOW, HEAT AND MASS-TRANSFER

Employing the sets of operating data of the previous section, this work is conducted for the analysis of five different cases of thermal polymerization of styrene in arbitrary cross-sectional duct reactors for eight different geometries. The operating conditions for these five cases are reported in table 8.20. Typical CPU time was about 10 minutes for the longest run. About 5 iterations were required on each transversed-plane for convergence. The same convergence indicators were selected here as mentioned previously in Fluid-Flow and Heat-Transfer sections. Refer to Table 8.21 in this respect.

Table 8. 20 Operating conditions

Case	W_{inlet} m/s	T_{inlet} °C	T_{wall} °C	Mass-flow kg/s	Reactor length (m)
# 1	0.000695	100	100	0.7267×10^{-3}	5.0
# 2	0.000695	130	100	0.7027×10^{-3}	5.0
# 3	0.001780	140	135	0.1345×10^{-3}	6.4
# 4	0.000020	130	100	0.2000×10^{-4}	5.0
# 5	0.047250	160	160	0.6095×10^{-3}	14.6

Table 8. 21 Residual values (mass transfer)

Species-continuity equation residual	Mass-fraction residual
0.2×10^{-7}	0.2×10^{-2}

The basis for computations in all the reactors bearing different geometries in their cross-sections and the same length, is the same residence-time in the reactors or the same cross-sectional area, while the same uniform velocity is maintained at inlet of each reactor. The diameter of circular duct corresponding to the cases under study are

Table 8. 22 Diameter of circular-ducts corresponding to non-circular geometries

Cases	# 1	# 2	# 3	# 4	# 5
diameter (m)	0.0400	0.0400	0.01100	0.0400	0.00460

tabulated above. The results obtained in this analysis are indicated in tables 8.23 to 8.27 for the five cases under consideration. In these tables the results of polymer weight fraction (WPA) in wt %, molecular weights (M_n and M_w), polydispersity (\bar{M}_w/\bar{M}_n) and bulk-temperature (°C) are indicated which are corresponding to the conditions at the exit of the reactors. The total pressure-drop results of the reactors are also indicated. Referring to these tables, it is observed that there are only slight differences in the results obtained for different geometries corresponding to each case. Also not a specific geometry is recognized to be generally superior than circular duct reactors from the conversion point of view of the chemical reaction under study, considering the least pressure-drop results also.

The simulation results for molecular-weights distribution, velocity, temperature, concentration, density and viscosity profiles are presented in the attached figures in this section. The plotter subroutine GRAPH1.SAS is utilized to generate these plots.

Referring to tables 8.23-8.27, the following classification is possible from the conversion point of view based on the circular duct (wt%) results:

- Case # 1: 6.74 wt%, low conversion,
- Case # 2: 14.20 wt%, low conversion,
- Case # 3: 26.60 wt%, intermediate conversion,
- Case # 4: 55.20 wt%, high conversion,
- Case # 5: 10.10 wt%, low conversion.

The reason for the low DP results of cases # 1 and # 2 is due to the low level of conversion involved. The relatively higher values of DP of case # 5, which is even at

Table 8. 23 Simulation Results of Styrene Polymerization at Reactor Exit

Case # 1

No.	Geometry	WPA (wt %)	\bar{M}_n ($\frac{kg}{mol}$)	\bar{M}_w ($\frac{kg}{mol}$)	Polydispersity ($\frac{\bar{M}_w}{\bar{M}_n}$)	bulk-temp (°C)	Total DP (Pa)
1	Circular	6.74	452460	819590	1.81	102.3	1.46
2	Square	6.74	452910	820240	1.81	102.2	1.88
3	Triangular	6.38	453450	820660	1.81	101.9	2.70
4	Trapezoidal	6.33	454100	822100	1.81	101.9	2.57
5	Pentagonal	6.63	453810	822110	1.81	102.1	2.28
6	Hexagonal	6.74	452940	820450	1.81	102.3	1.69
7	Rectangular (AR=1.5)	6.70	453784	821697	1.81	102.0	1.91
8	Rectangular (AR=2.0)	6.63	455120	823870	1.81	101.8	1.97

low conversion level, is due to the smaller tube I.D. (0.0046 m) practiced in this case.

An analysis of the attached figures reveals the following major points:

- (i) **Mol. wt. distribution;** All cases except case # 4 (high conversion case) exhibit a peak at a point closer to the reactor inlet. In case # 4, there is a gradual increase in mol. wt. distribution from inlet to the end of the reactor. The results are not conclusive to a generalization.
- (ii) **Axial velocity profile:** All cases exhibit plug flow behavior which is in close agreement with prediction the of Husain and Hamielec²⁴. Some velocity distortion is observed due to the effect of angles as revealed in triangular and pentagonal ducts. This effect is to induce higher rates of generation of polymers at corners rather than at sides due to which viscosity increases around locations closer to angles. The effect on velocity is a retardation of the velocity profile in the vicinity of the angles.

Table 8. 24 Simulation Results of Styrene Polymerization at Reactor Exit

Case # 2

No.	Geometry	WPA (wt %)	\bar{M}_n ($\frac{kg}{kg\ mol}$)	\bar{M}_w ($\frac{kg}{kg\ mol}$)	Polydispersity ($\frac{\bar{M}_w}{\bar{M}_n}$)	bulk-temp (°C)	Total DP (Pa)
1	Circular	14.2	338740	610770	1.8	106.0	1.05
2	Square	12.7	348550	628480	1.8	104.7	2.52
3	Triangular	11.0	351450	634420	1.8	103.7	6.11
4	Trapezoidal	11.3	352080	635670	1.8	103.7	6.36
5	Pentagonal	12.8	347180	625660	1.8	105.0	2.87
6	Hexagonal	13.6	343910	620230	1.8	105.4	2.76
7	Rectangular (AR=1.5)	12.2	351620	634550	1.8	104.1	2.80
8	Rectangular (AR=2.0)	11.5	356170	643600	1.8	103.3	3.26

Table 8. 25 Simulation Results of Styrene Polymerization at Reactor Exit

Case # 3

No.	Geometry	WPA (wt %)	\bar{M}_n ($\frac{kg}{kg\ mol}$)	\bar{M}_w ($\frac{kg}{kg\ mol}$)	Polydispersity ($\frac{\bar{M}_w}{\bar{M}_n}$)	bulk-temp (°C)	Total DP (Pa)
1	Circular	26.6	220716	392673	1.78	136.3	243
2	Square	26.2	221160	393250	1.78	136.1	244
3	Triangular	24.8	220210	391120	1.78	136.0	347
4	Trapezoidal	25.4	220880	392530	1.78	136.0	347
5	Pentagonal	25.8	220420	391860	1.78	136.2	286
6	Hexagonal	26.5	220910	392960	1.78	136.2	254
7	Rectangular (AR=1.5)	25.9	221278	393410	1.78	136.0	242
8	Rectangular (AR=2.0)	25.8	221610	393980	1.78	135.9	261

Table 8. 26 Simulation Results of Styrene Polymerization at Reactor Exit

Case # 4

No.	Geometry	WPA (wt %)	\bar{M}_n ($\frac{kg}{mol}$)	\bar{M}_w ($\frac{kg}{mol}$)	Polydispersity ($\frac{\bar{M}_w}{\bar{M}_n}$)	bulk-temp (°C)	Total DP (Pa)
1	Circular	55.2	481130	966680	2.00	101.4	2617
2	Square	57.2	499470	998160	2.00	101.2	9078
3	Triangular	47.4	486550	940300	1.93	101.1	11540
4	Trapezoidal	50.0	489210	953850	1.95	101.2	3625
5	Pentagonal	54.8	492120	979150	1.99	101.2	41568
6	Hexagonal	55.7	487320	976770	2.00	101.4	7574
7	Rectangular (AR=1.5)	54.1	495730	979780	1.98	101.2	4937
8	Rectangular (AR=2.0)	48.9	488230	947800	1.94	101.1	1910

Table 8. 27 Simulation Results of Styrene Polymerization at Reactor Exit

Case # 5

No.	Geometry	WPA (wt %)	\bar{M}_n ($\frac{kg}{mol}$)	\bar{M}_w ($\frac{kg}{mol}$)	Polydispersity ($\frac{\bar{M}_w}{\bar{M}_n}$)	bulk-temp (°C)	Total DP (Pa)
1	Circular	10.10	129960	225290	1.73	161.0	50.8
2	Square	9.97	130040	225440	1.73	160.9	67.2
3	Triangular	10.56	130330	225810	1.73	160.8	106.1
4	Trapezoidal	10.30	130380	226000	1.73	160.8	117.0
5	Pentagonal	10.20	130132	225600	1.73	160.9	67.8
6	Hexagonal	10.40	130100	225570	1.73	161.0	64.1
7	Rectangular (AR=1.5)	10.20	130250	225810	1.73	160.8	73.9
8	Rectangular (AR=2.0)	10.70	130430	226000	1.73	160.7	106.6

(iii) **Temperature profiles**

Case # 1: Isothermal reactor, exothermic reaction proceeds and the temperature profile is developing to higher values.

Case # 2: Cooled-wall reactor, heat removal is observed from the temperature profile which is developing to lower values.

Case # 3: Mildly cooled-wall reactor, temperature profile is mildly developing to lower values.

Case # 4: cooled-wall reactor, temperature profile is developing to lower values.

Case # 5: Isothermal reactor, temperature profile is developing to higher values.

(iv) **Concentration profile:** The profile is developing. In case of angle effect, such as for triangular and pentagonal ducts, an increase in concentration is observed at these locations.

(v) **Density and viscosity profiles:** The effect of angle, is plainly observed in viscosity profiles such that there is a drastic increase in viscosity close to the angles. This is observed in viscosity profiles for the triangular and pentagonal ducts of all cases. The density profiles are also affected to some extent close to these points.

Effect of Free-Convection Due to the narrow temperature range involved in the transversed direction, the effect of free-convection (buoyancy effect) in this study is found to be negligible. This is observed from the following results which were obtained considering free-convection effect for circular ducts corresponding to the results in tables 8-12.

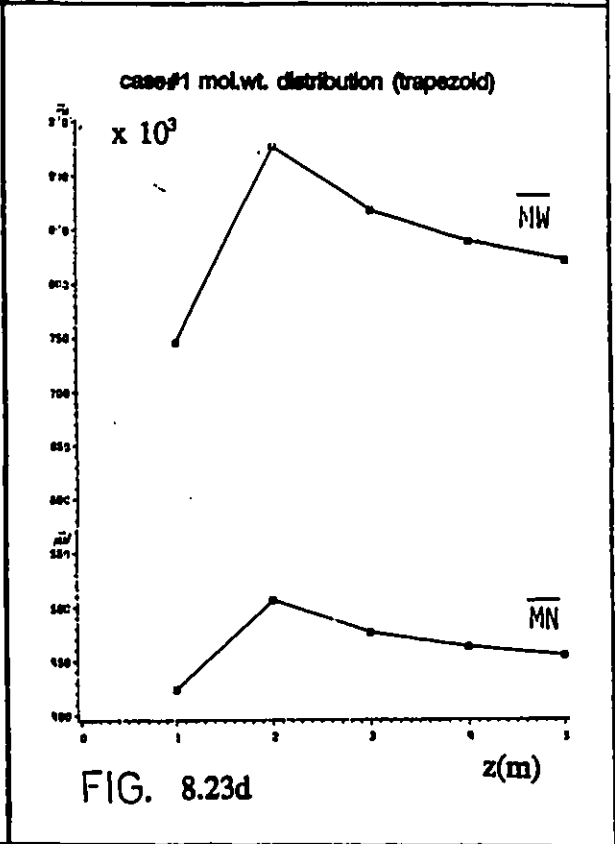
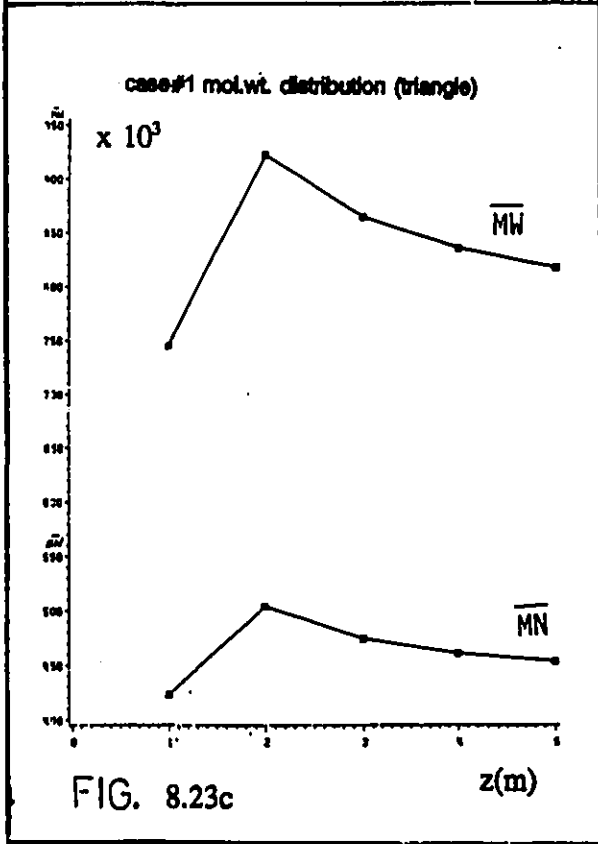
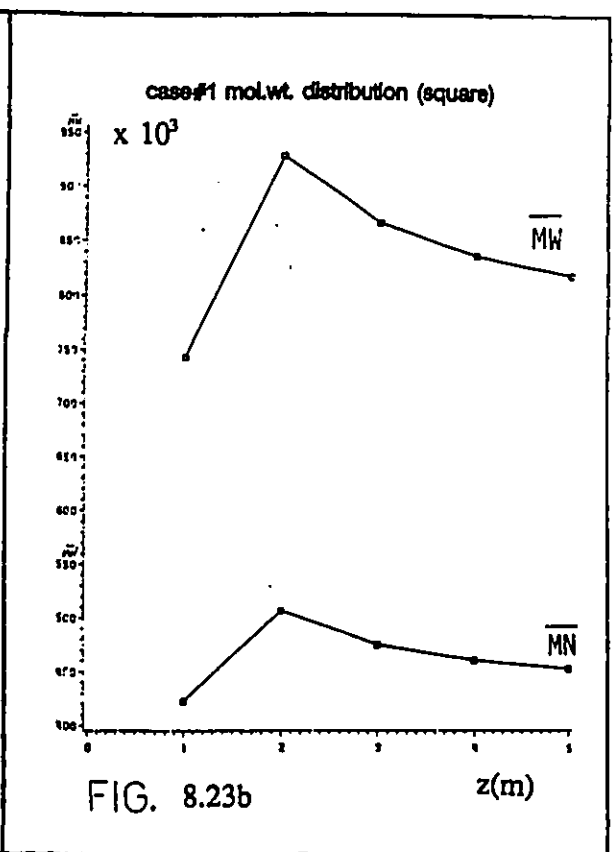
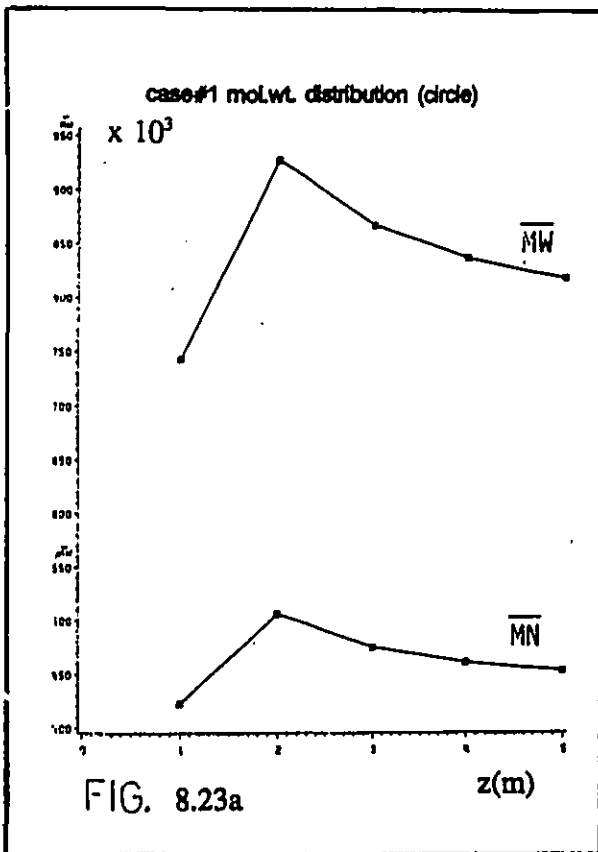
Case # 1: 6.75 wt% conversion,

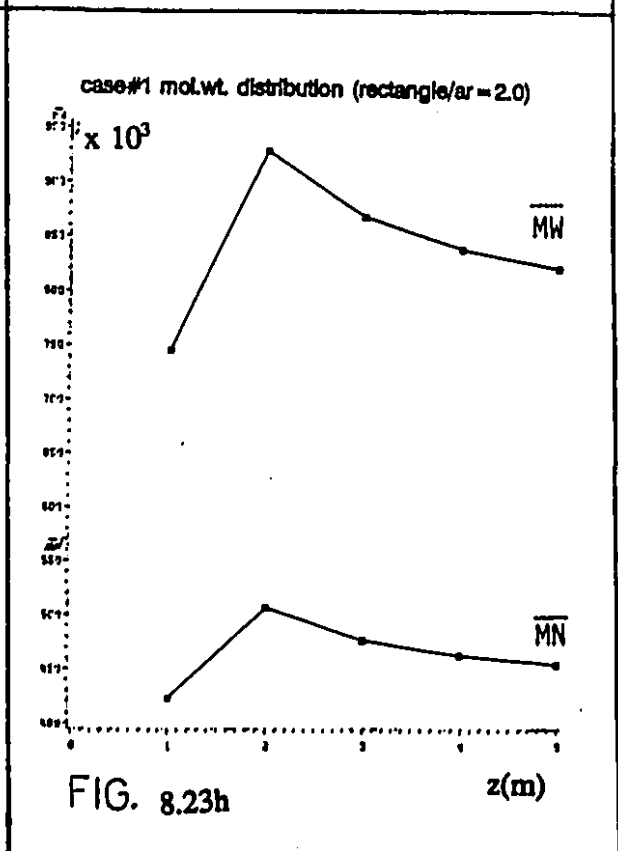
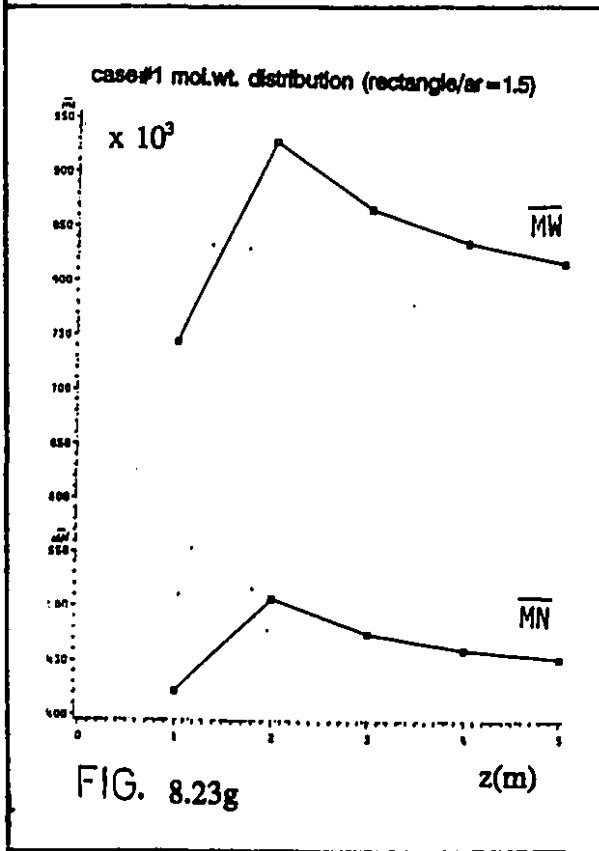
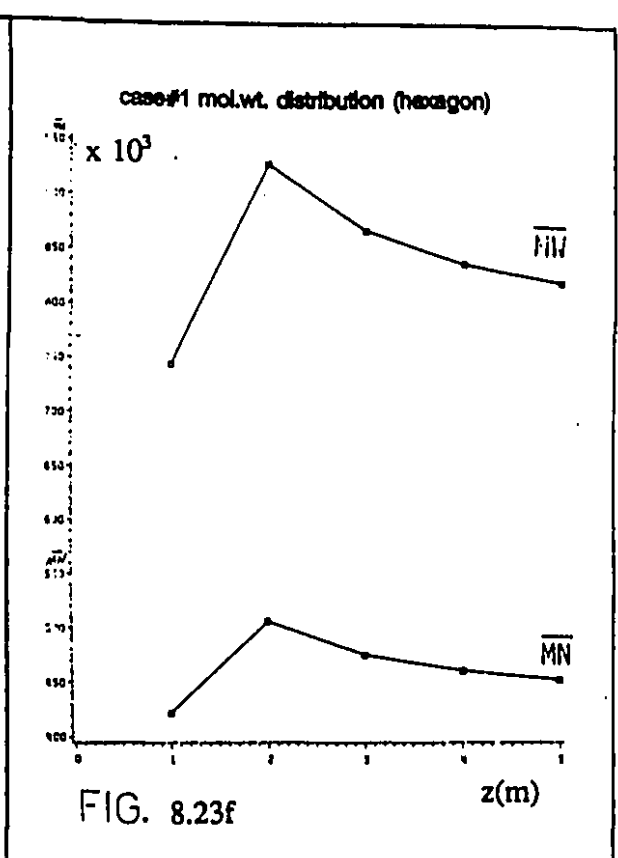
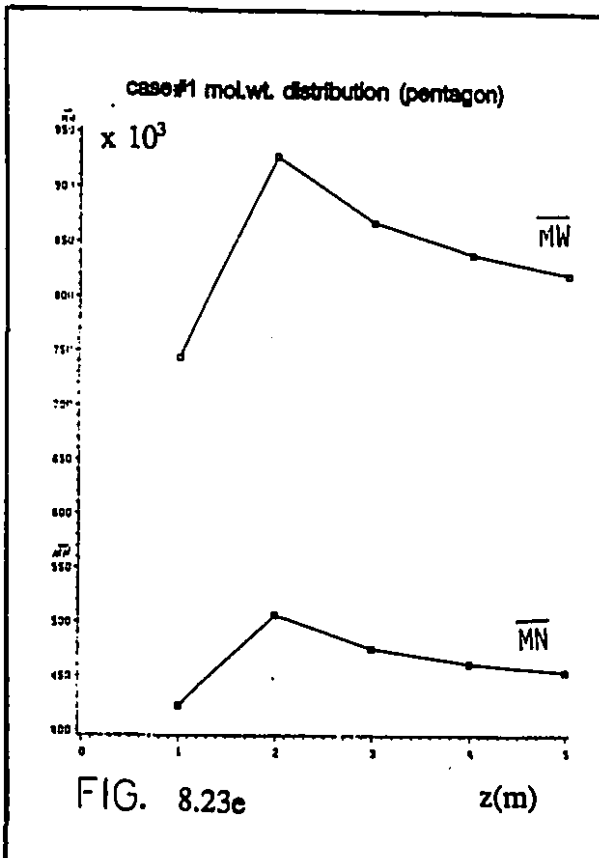
Case # 2: 14.50 wt% conversion,

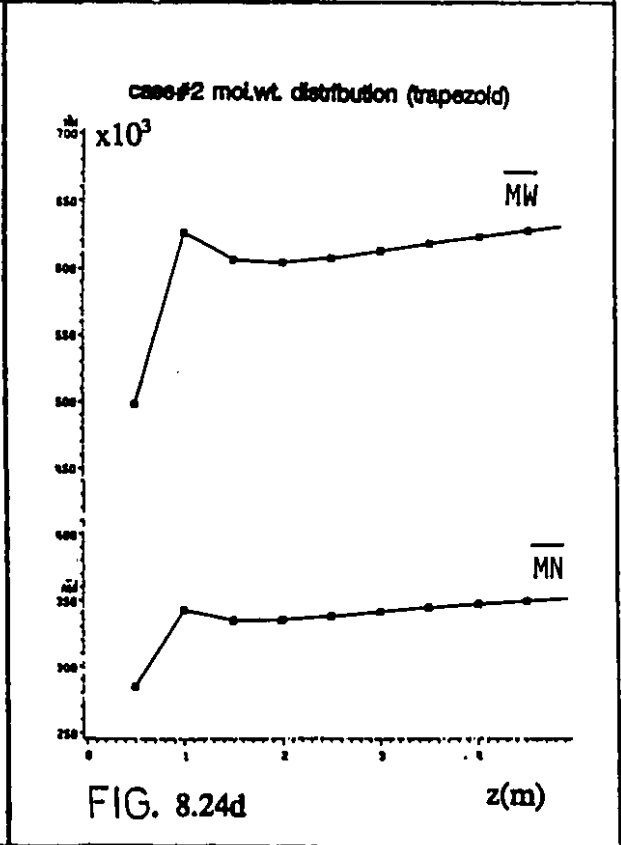
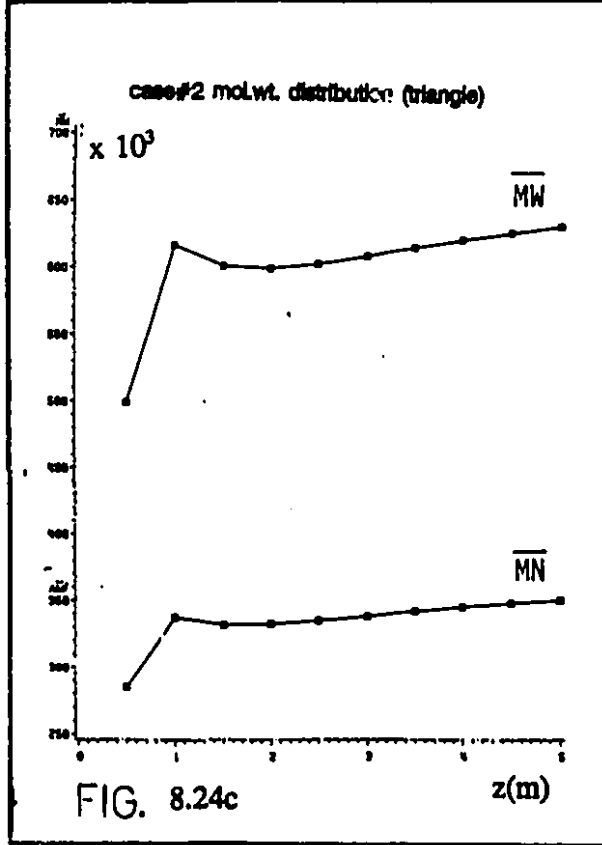
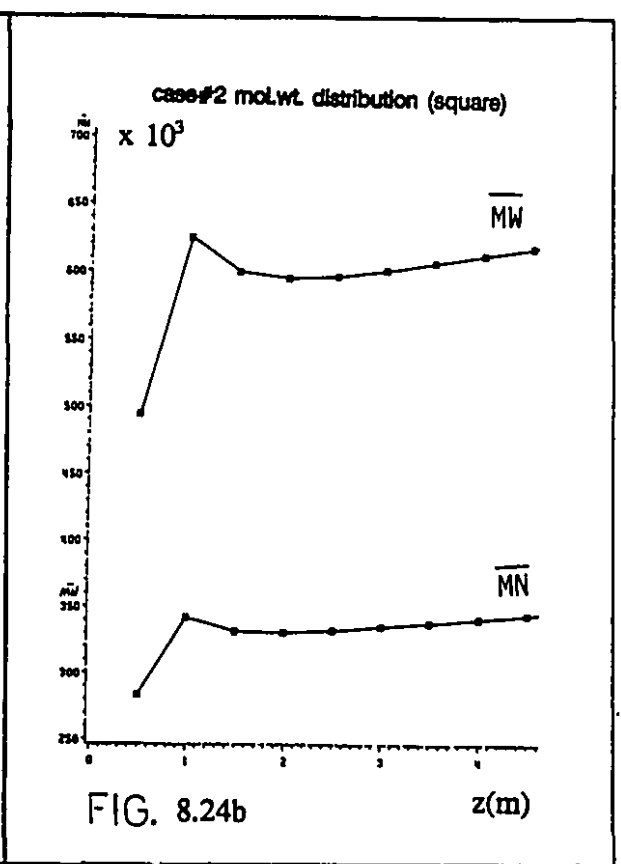
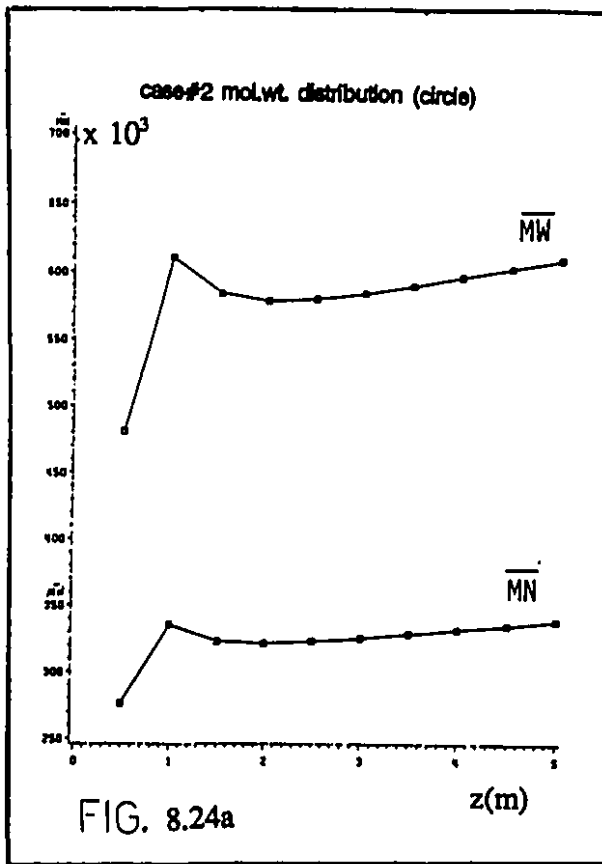
Case # 3: 26.70 wt% conversion,

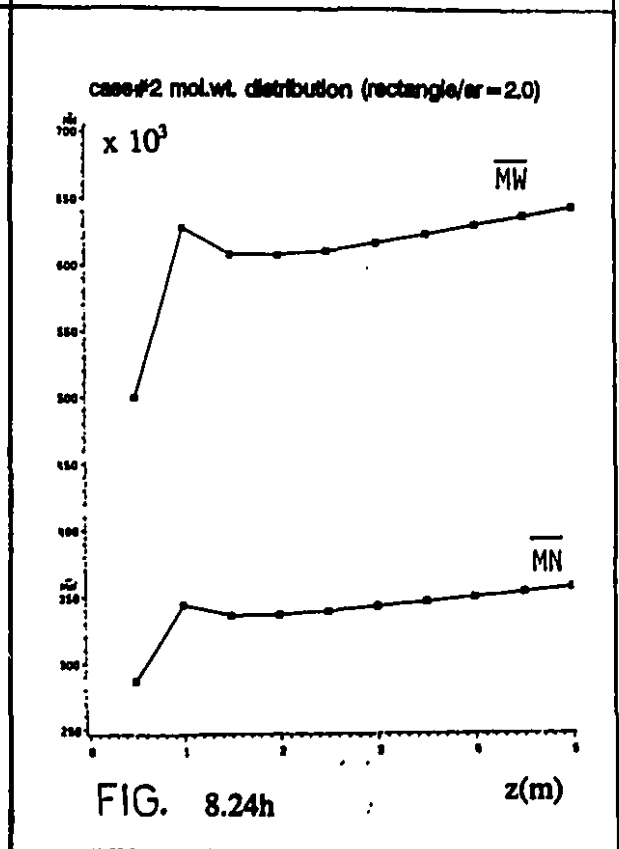
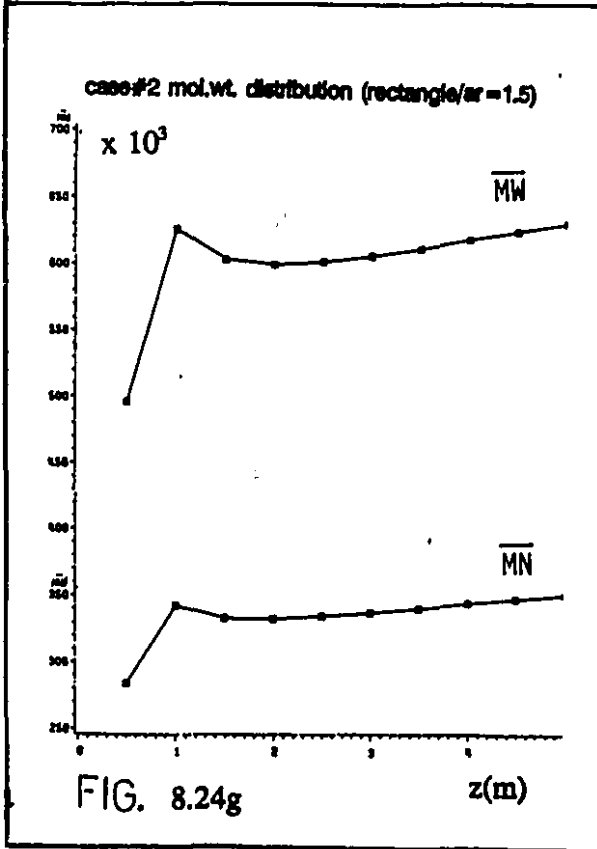
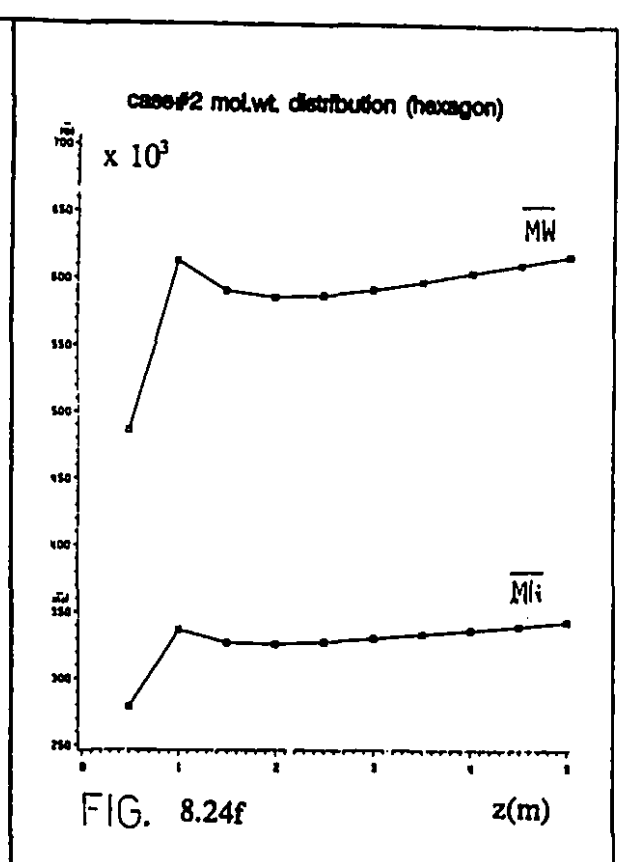
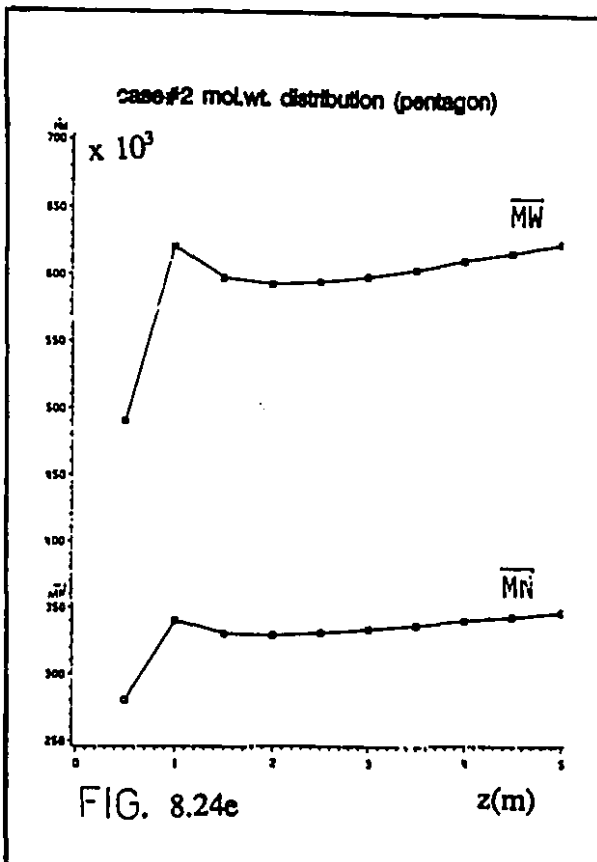
Case # 4: 55.24 wt% conversion,

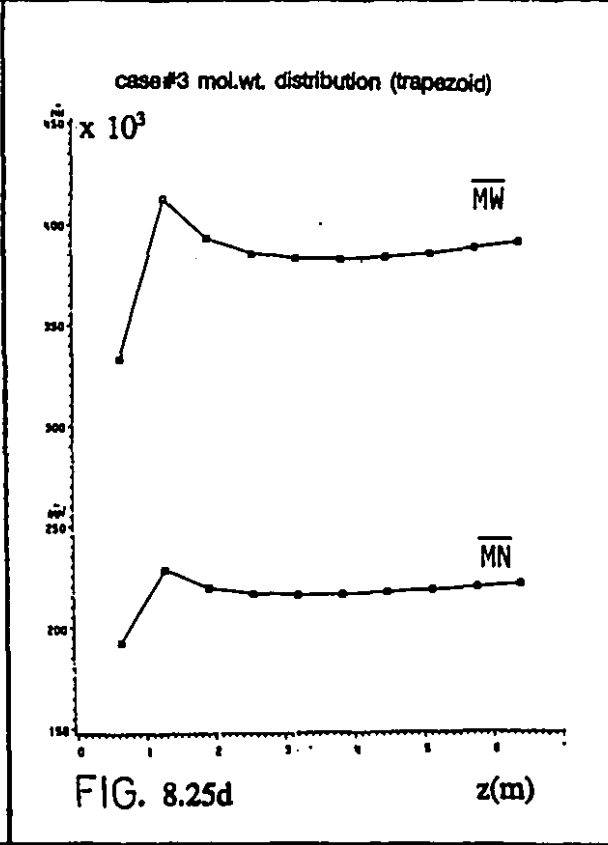
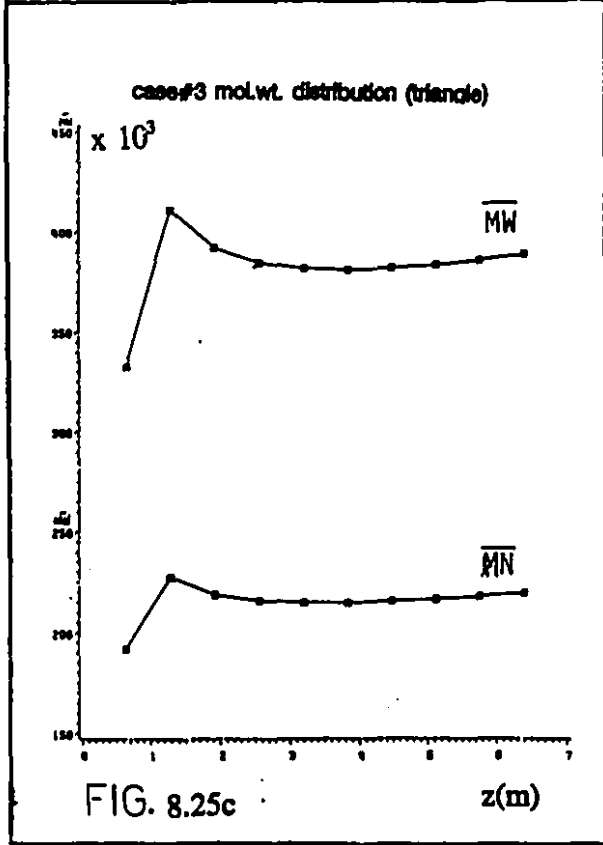
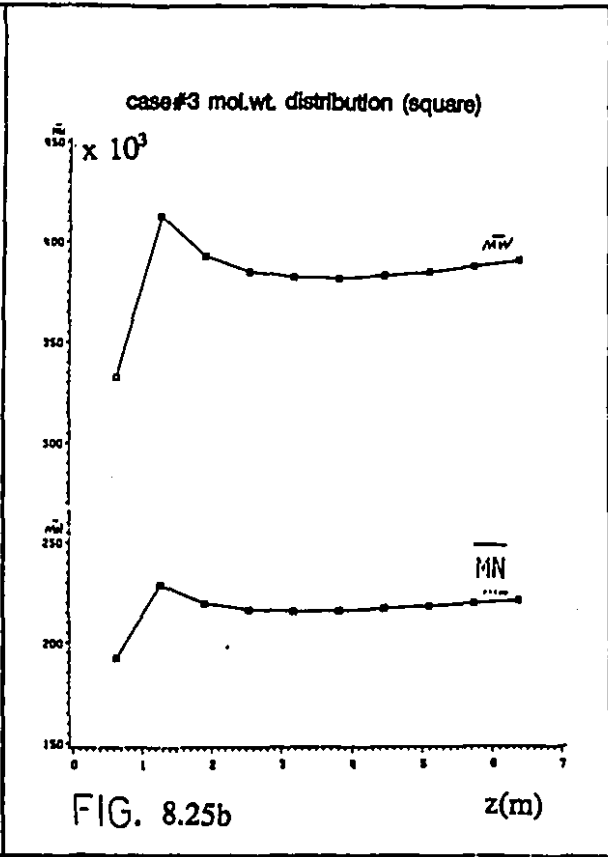
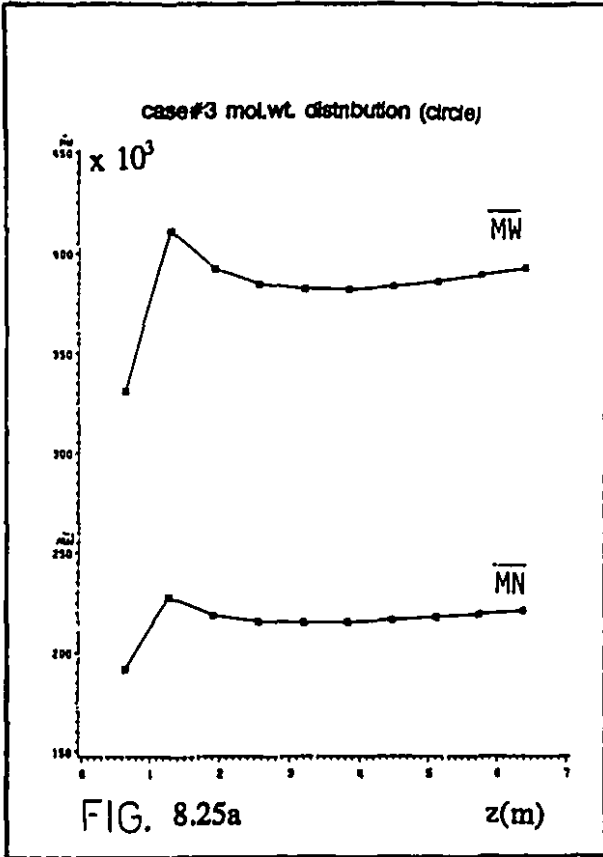
Case # 5: 10.30 wt% conversion.

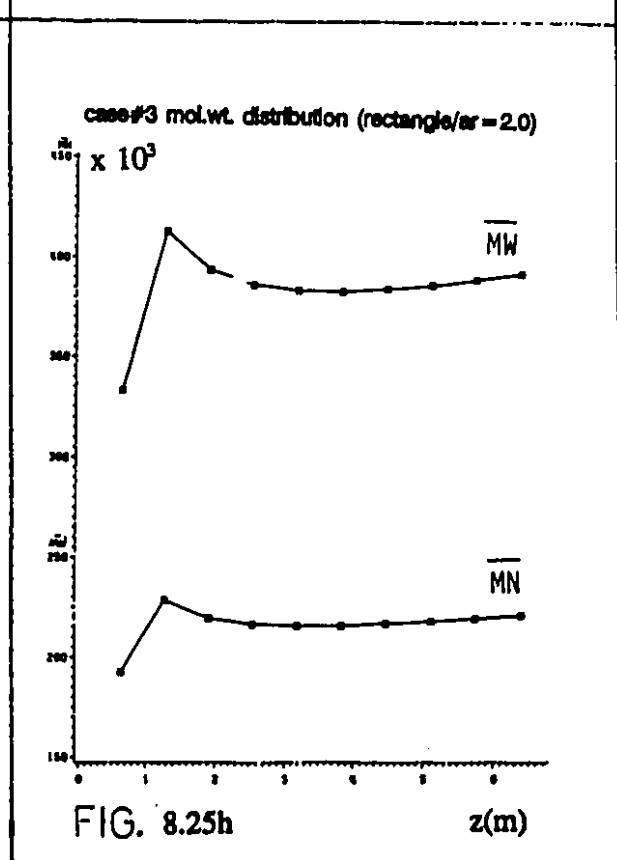
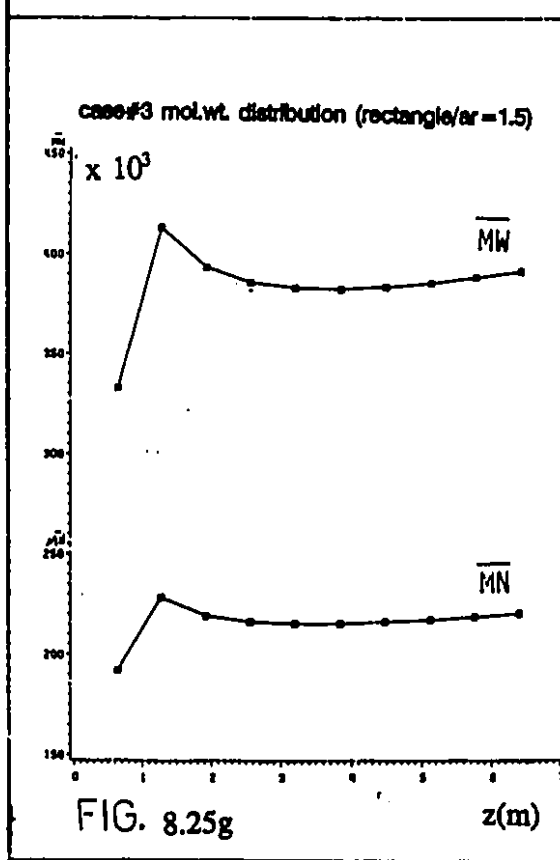
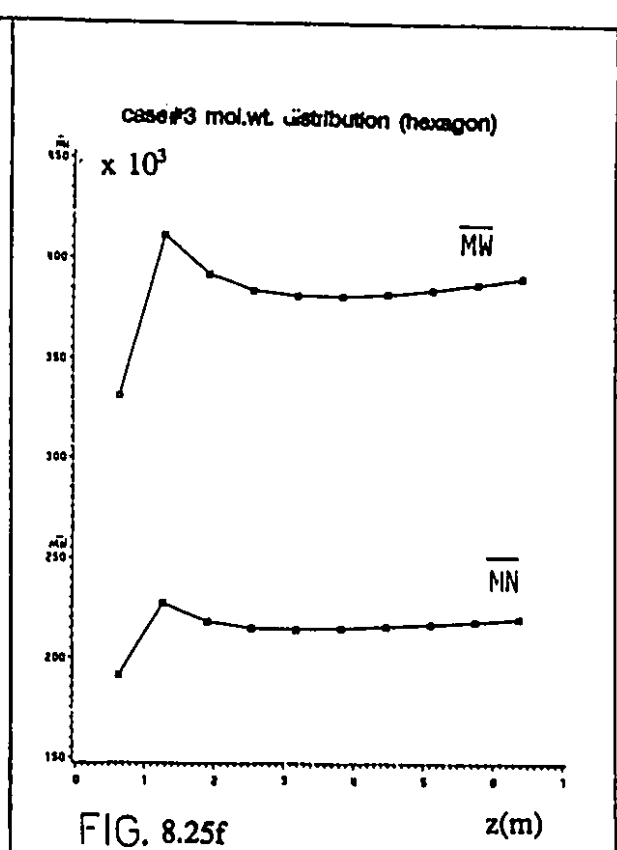
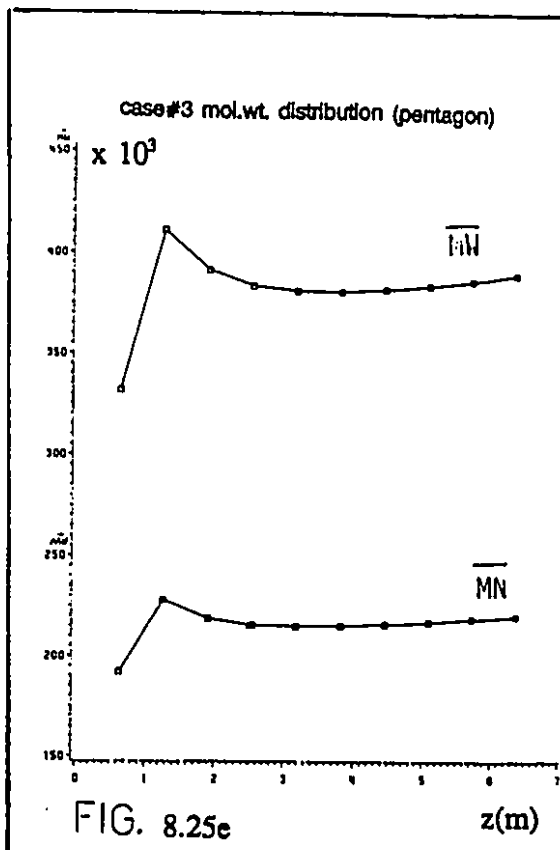


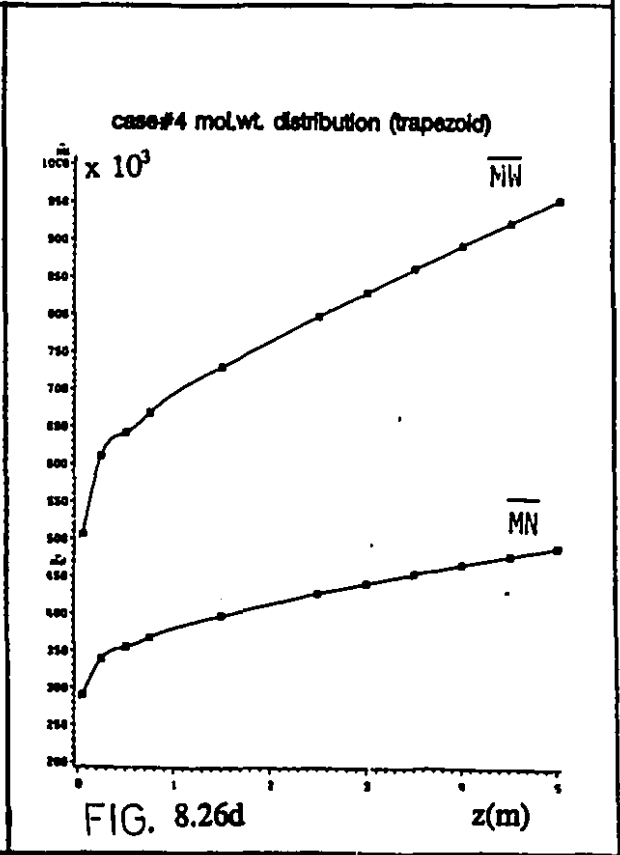
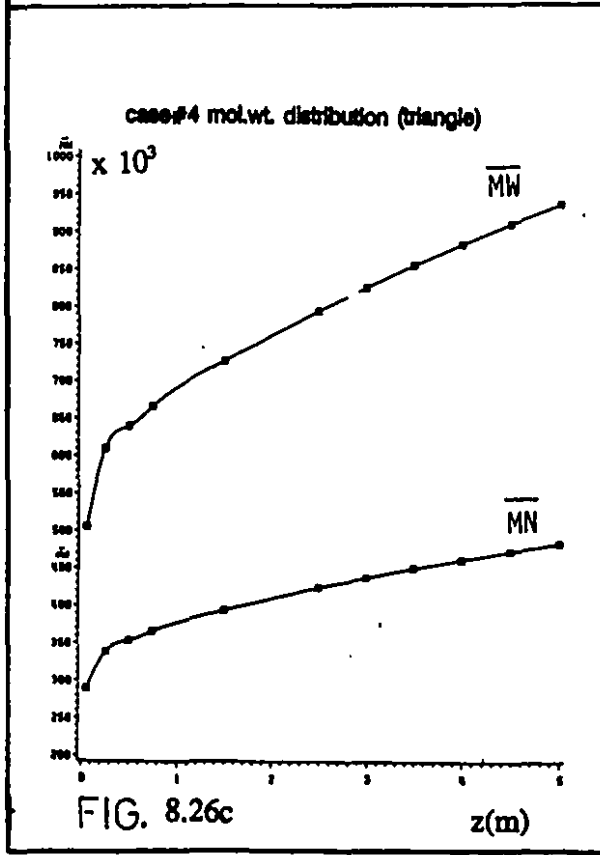
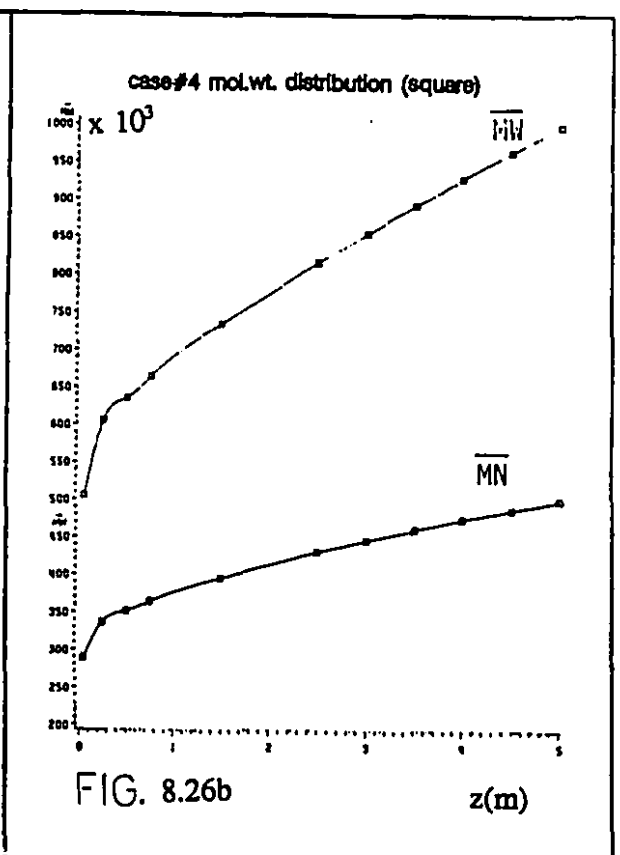
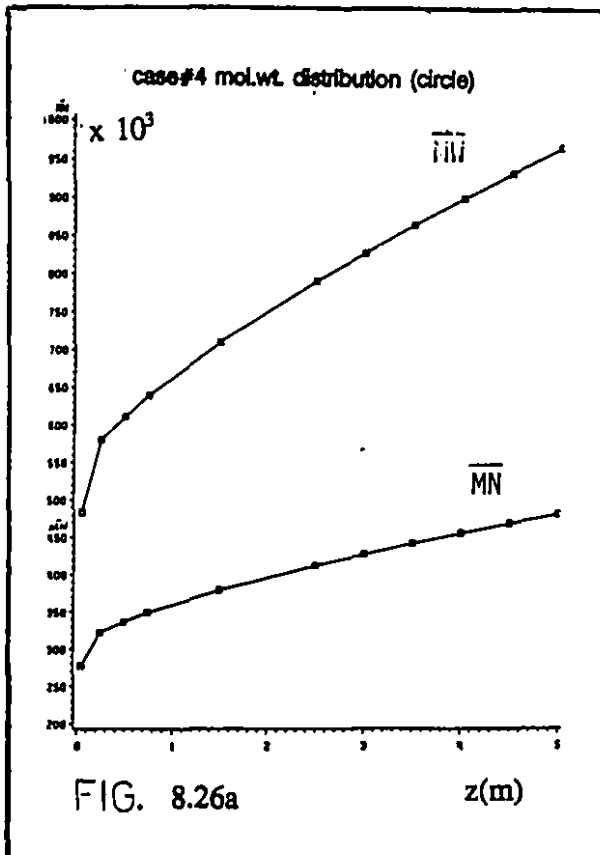


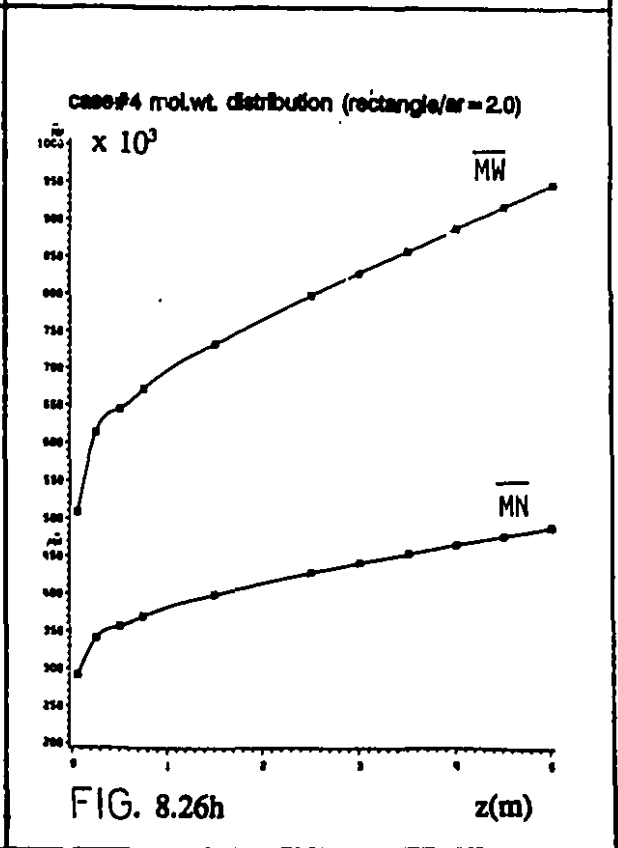
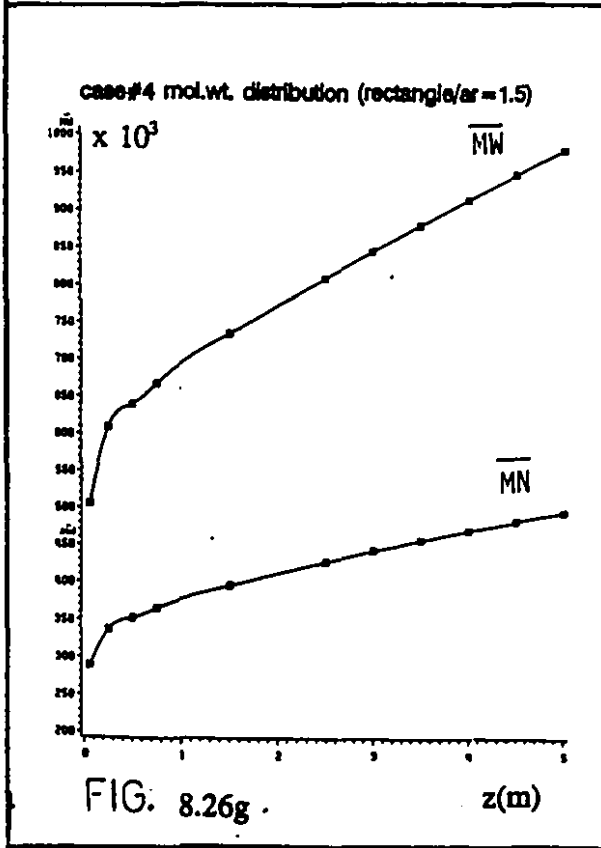
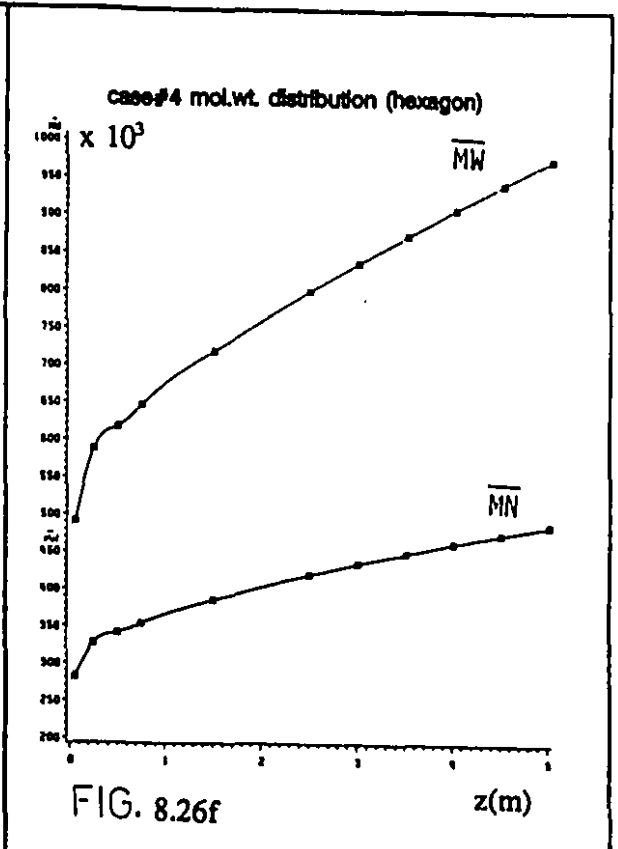
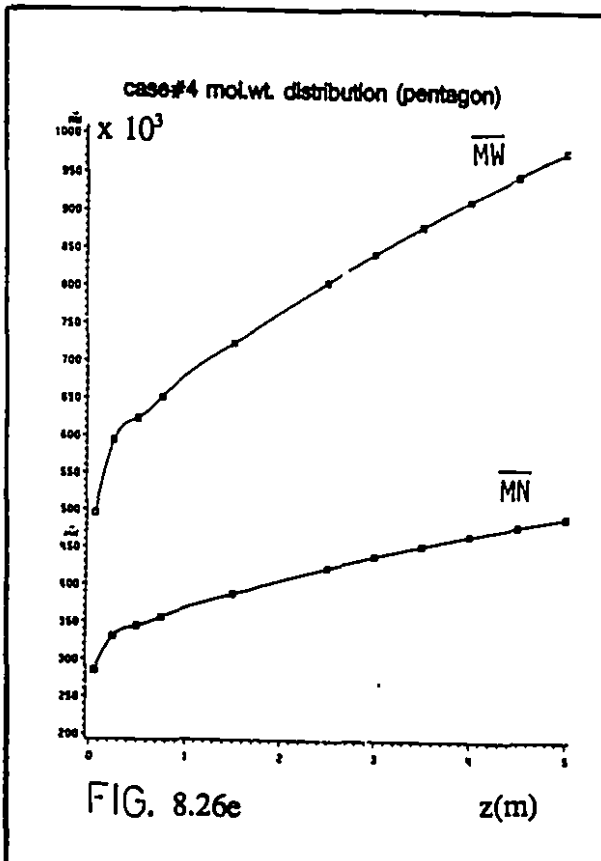


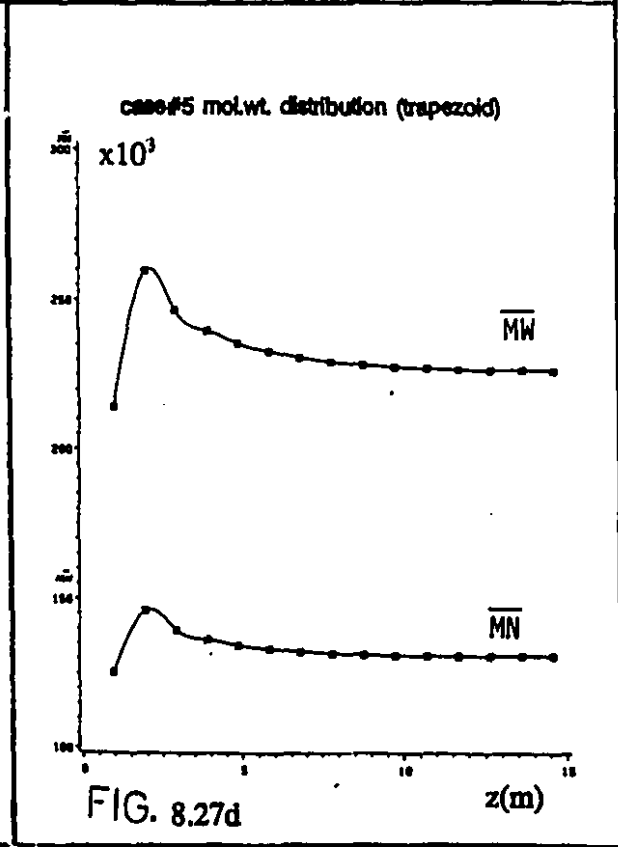
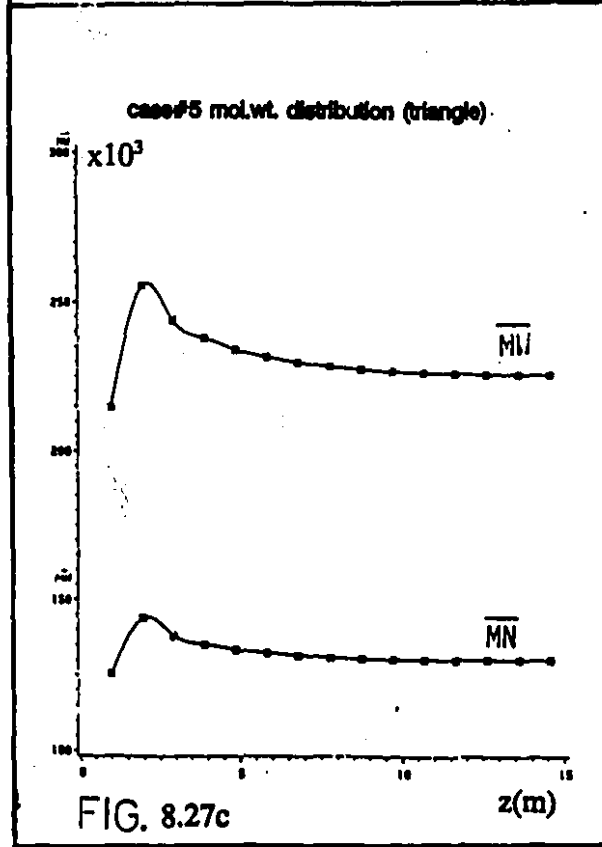
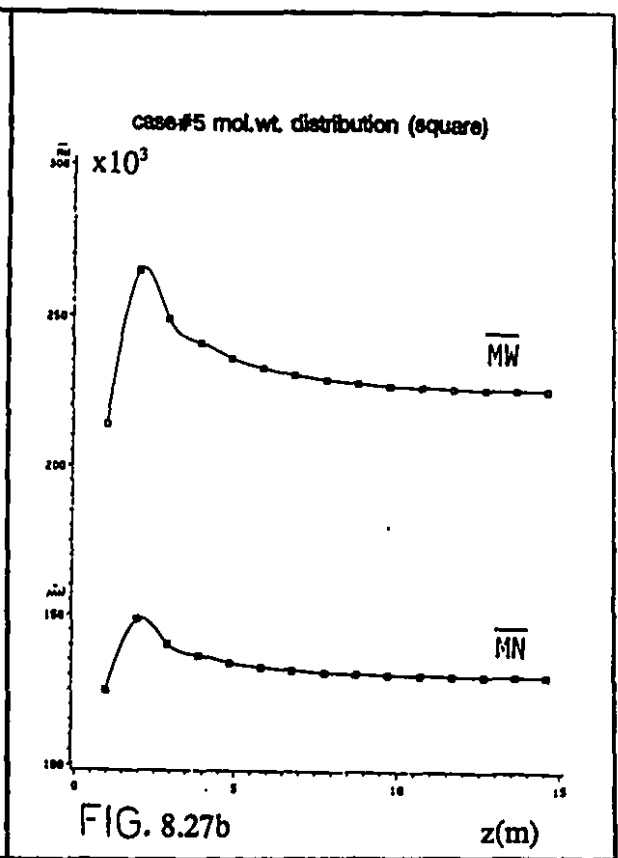
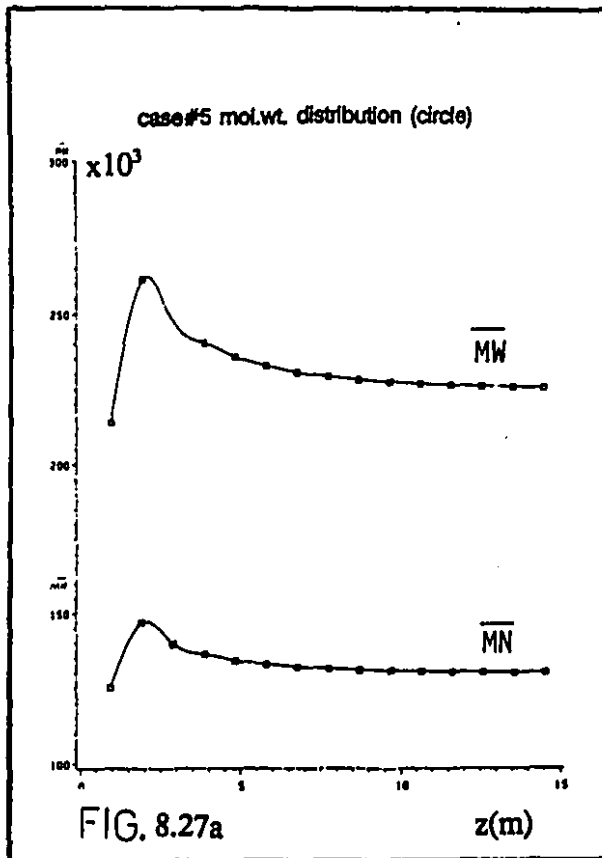












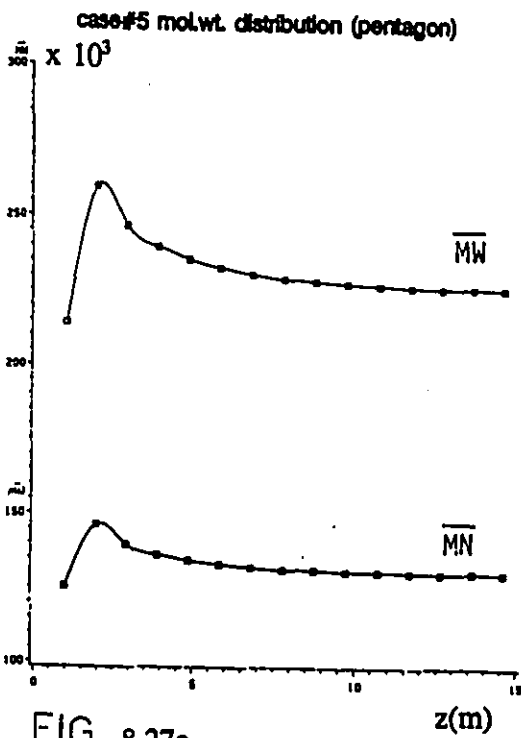


FIG. 8.27e

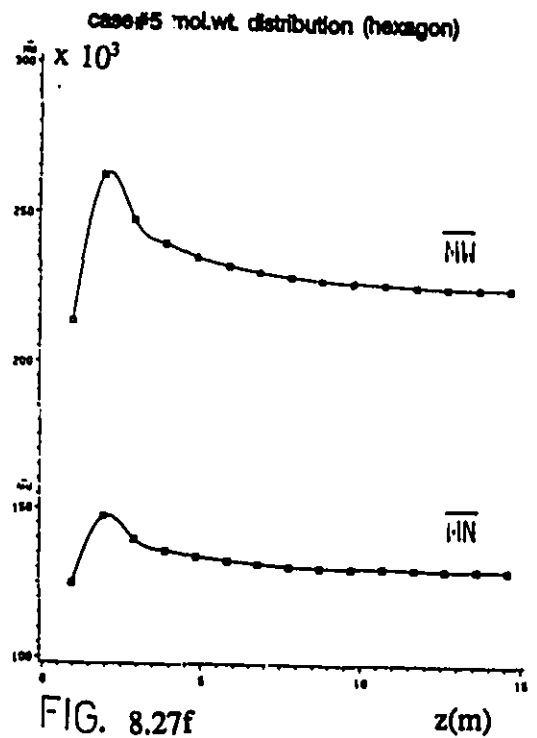


FIG. 8.27f

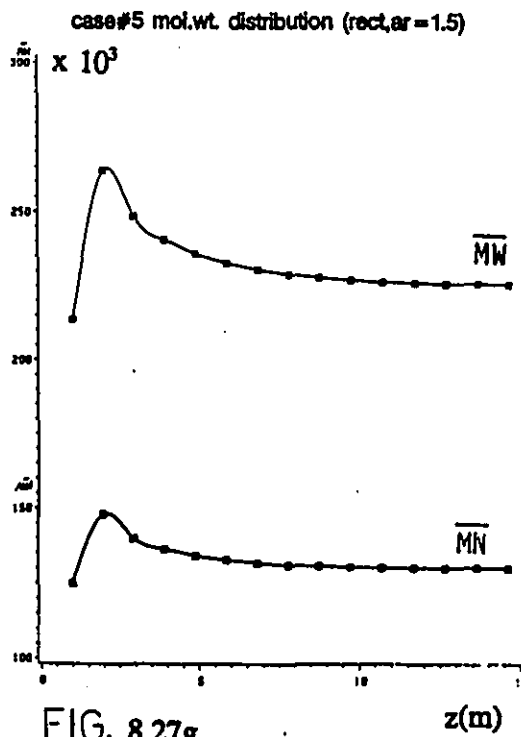


FIG. 8.27g

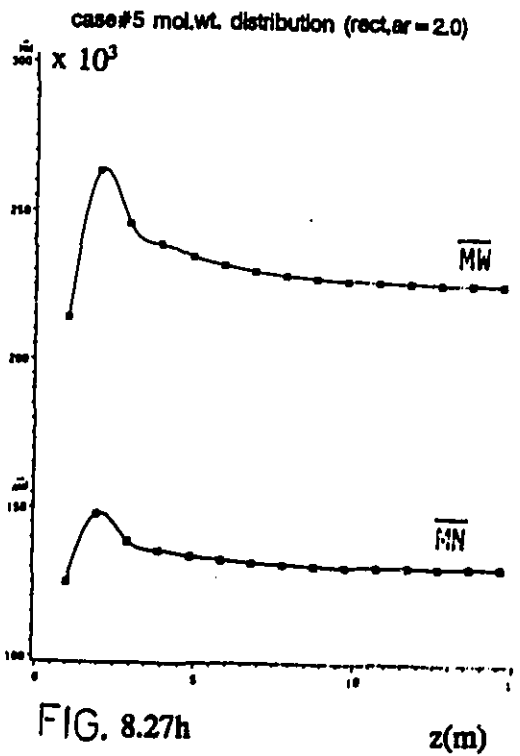


FIG. 8.27h

case#1 axial - velocity profile

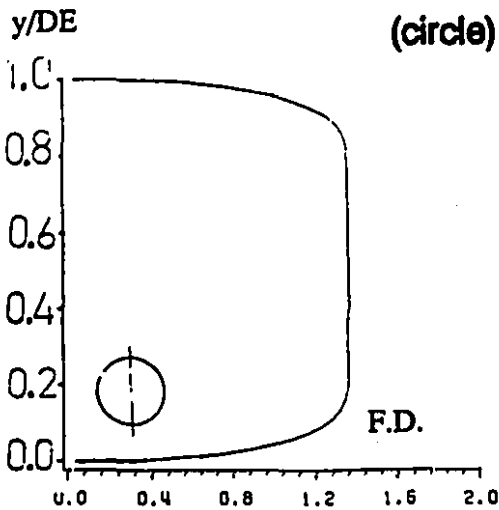


FIG. 8.28a

W/\bar{W}

case#1 axial - velocity profile

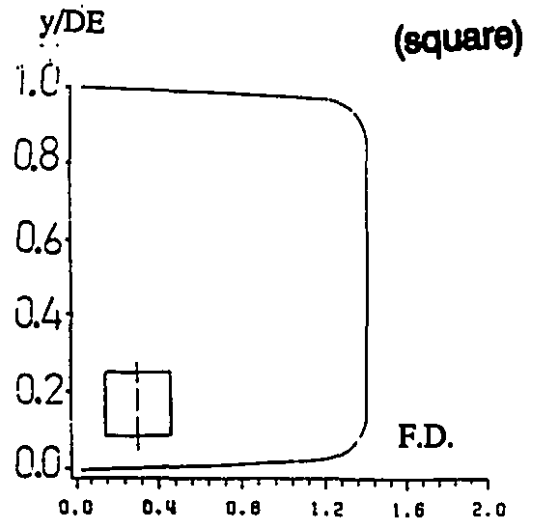


FIG. 8.28b

W/\bar{W}

case#1 axial - velocity profile

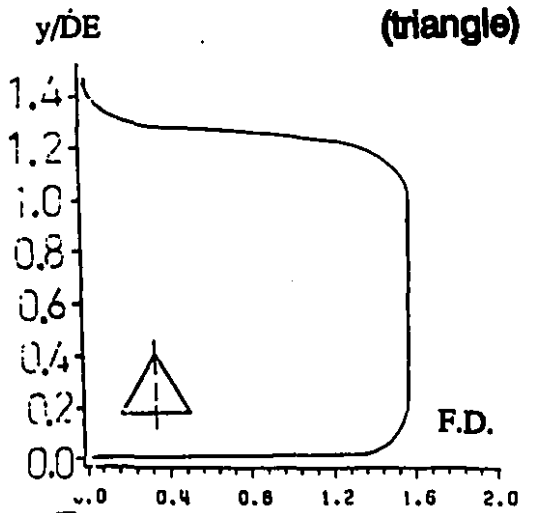


FIG. 8.28c

W/\bar{W}

case#1 axial - velocity profile

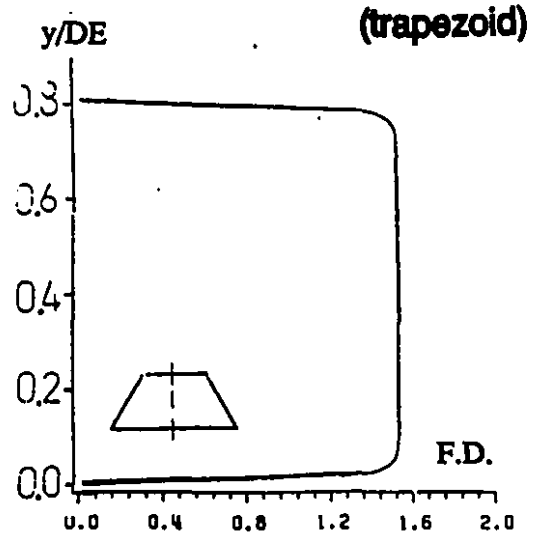
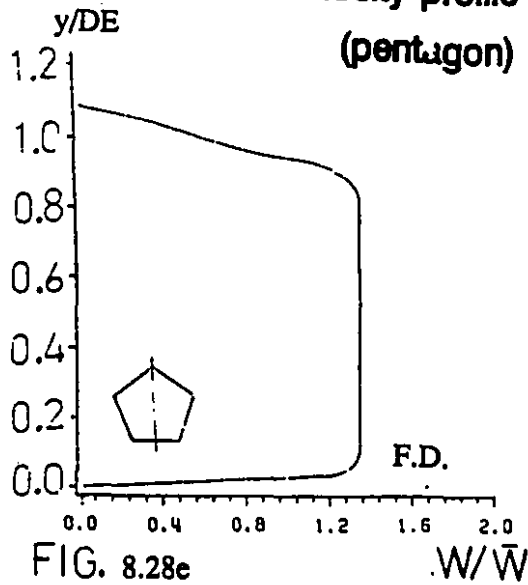


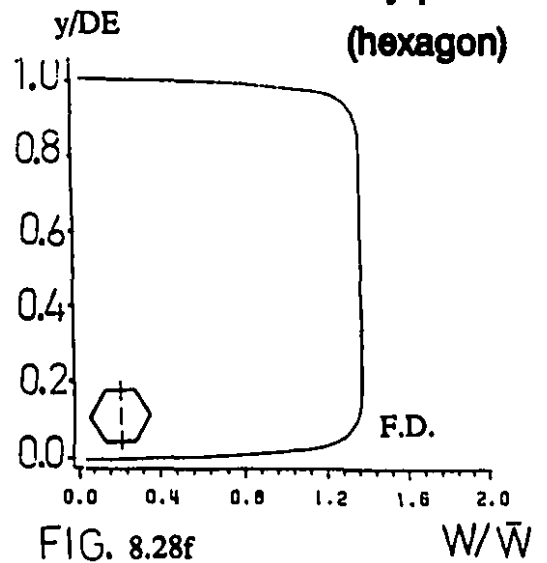
FIG. 8.28d

W/\bar{W}

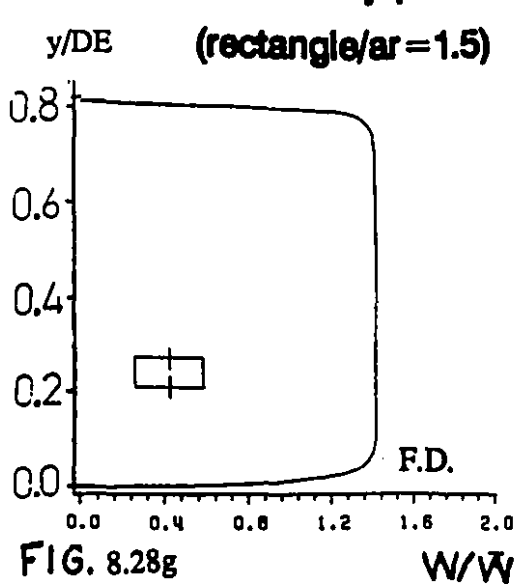
case#1 axial - velocity profile



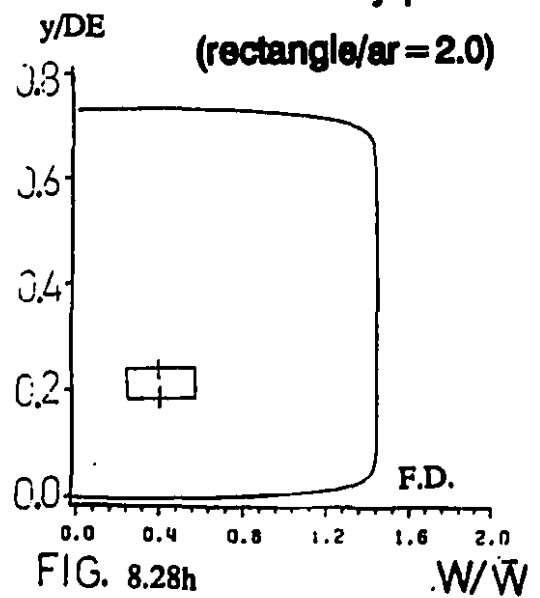
case#1 axial - velocity profile



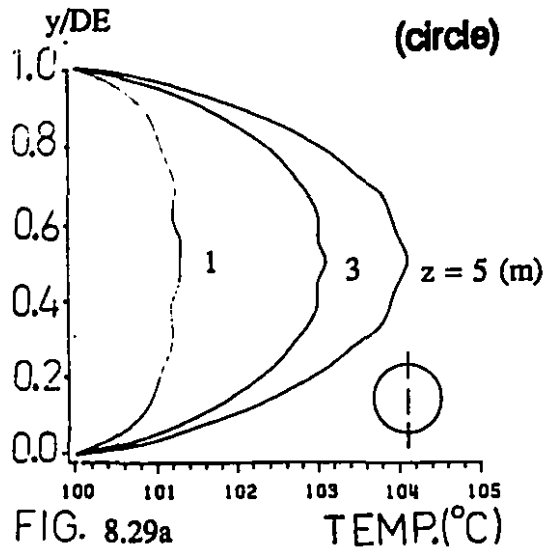
case#1 axial - velocity profile



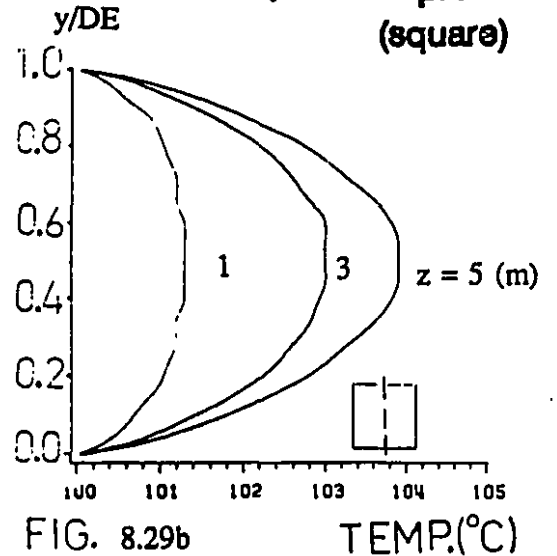
case#1 axial - velocity profile



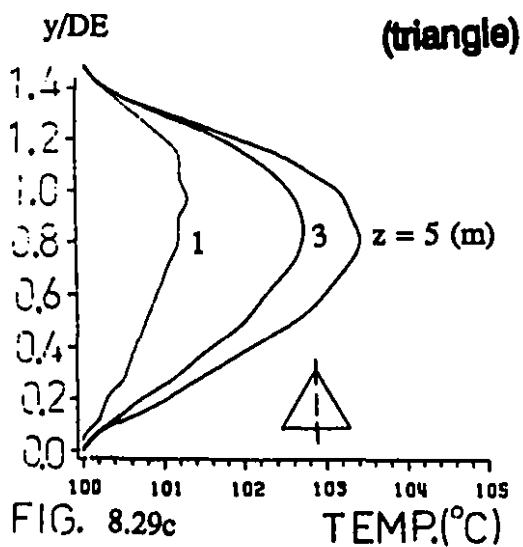
case#1 temperature profile



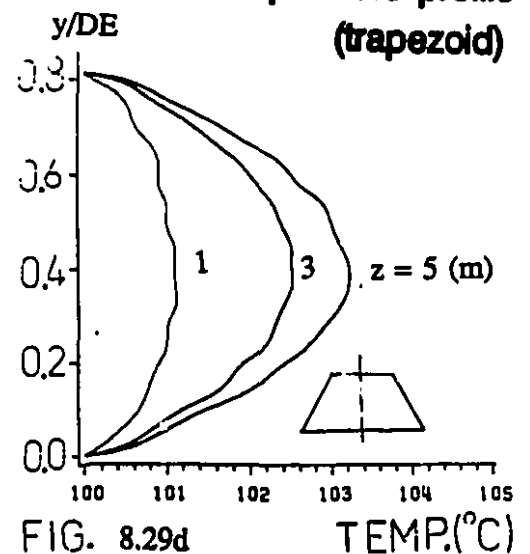
case#1 temperature profile



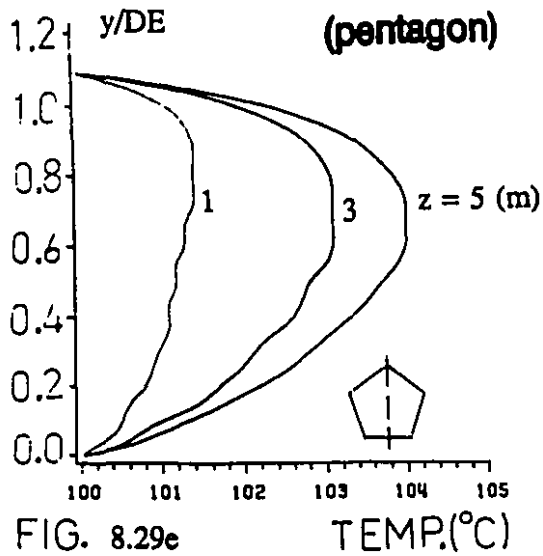
case#1 temperature profile



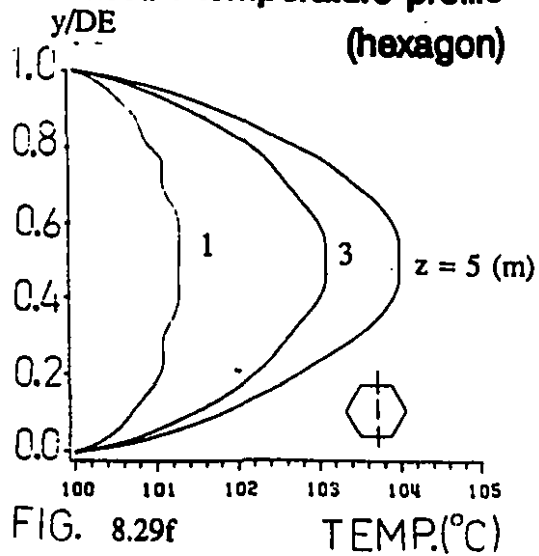
case#1 temperature profile



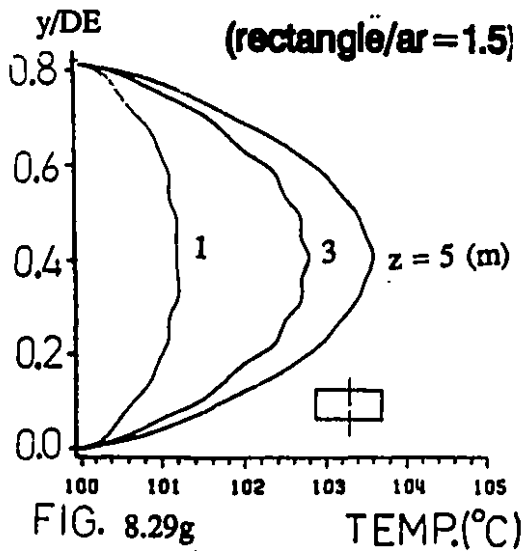
**case#1 temperature profile
(pentagon)**



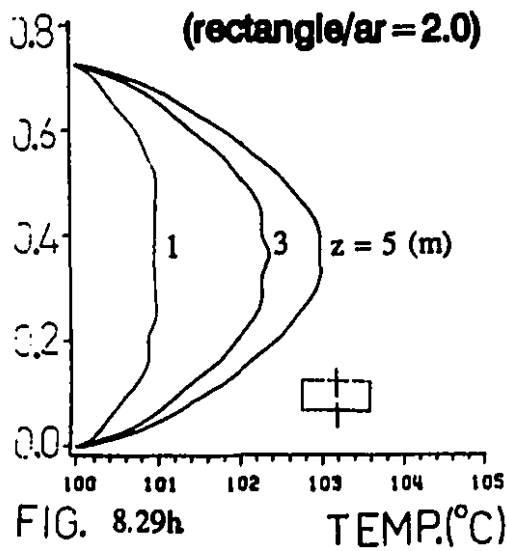
**case#1 temperature profile
(hexagon)**



**case#1 temperature profile
(rectangle/ar = 1.5)**



**case#1 temperature profile
(rectangle/ar = 2.0)**



case#1 polymer - concentration

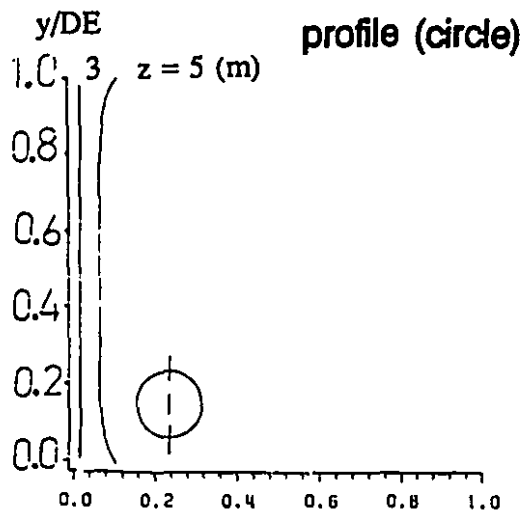


FIG. 8.30a

WP

case#1 concentration profile

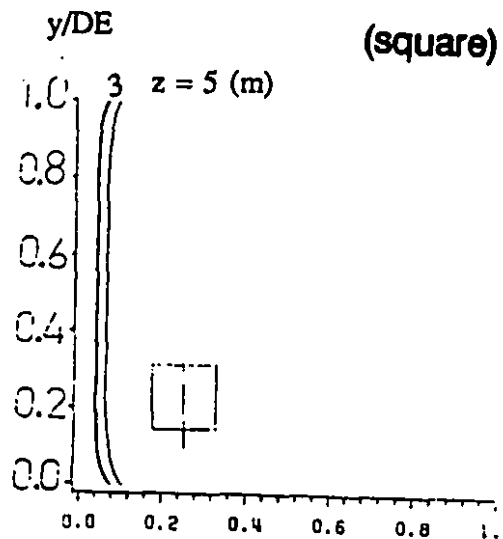


FIG. 8.30b

WP

case#1 polymer - concentration

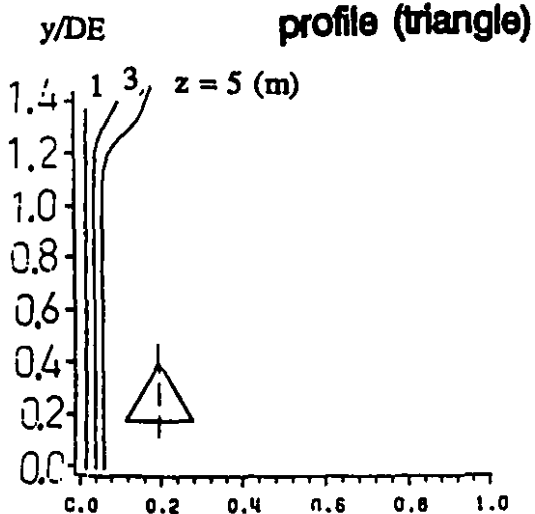


FIG. 8.30c

WP

case#1 polymer - concentration

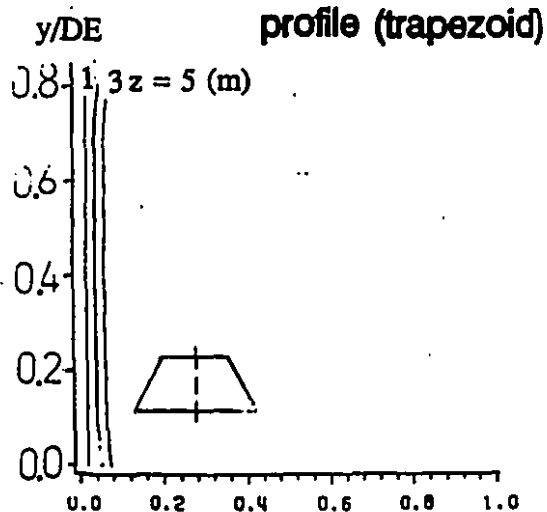


FIG. 8.30d

WP

case#1 polymer - concentration profile (pentagon)

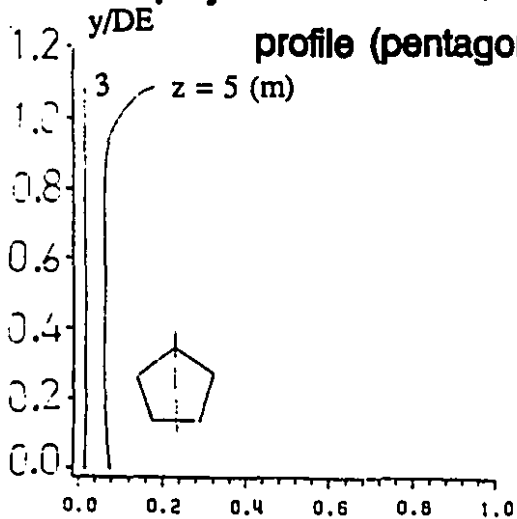


FIG. 8.30e

WP

case#1 polymer - concentration profile (hexagon)

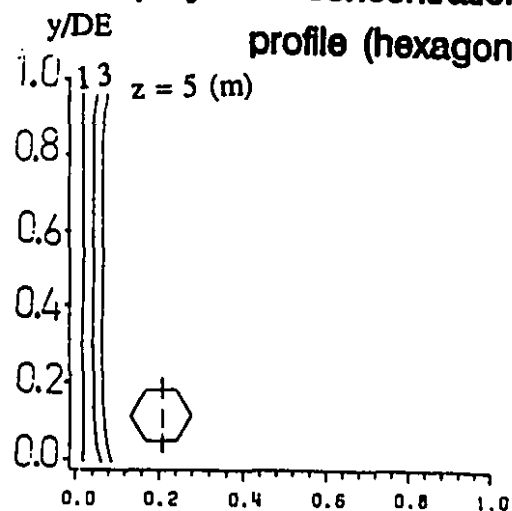


FIG. 8.30f

WP

case#1 polymer - concentration profile (rectangle/ar=1.5)

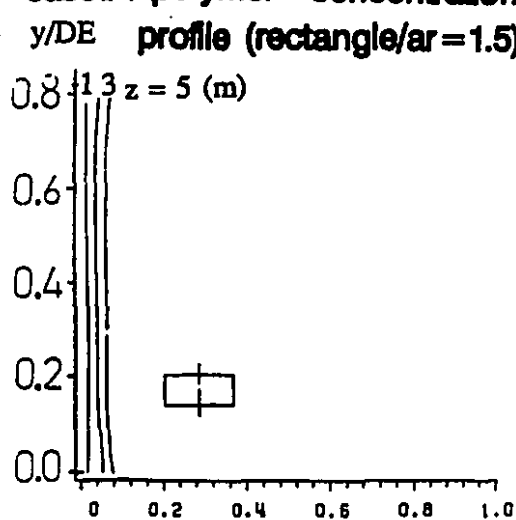


FIG. 8.30g

WP

case#1 polymer - concentration profile (rectangle/ar=2.0)

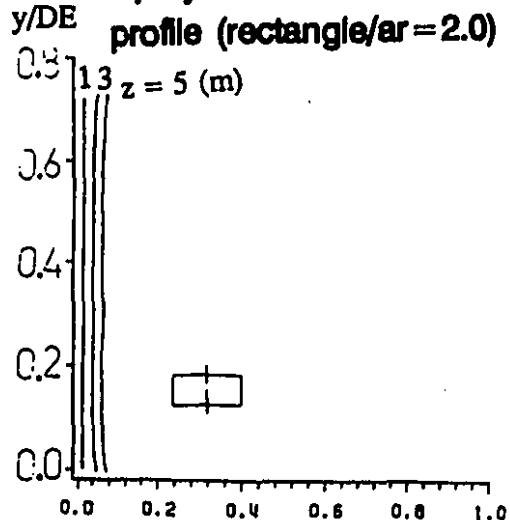
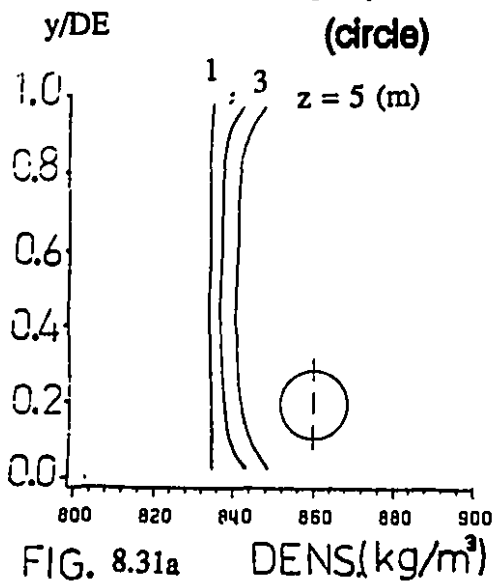


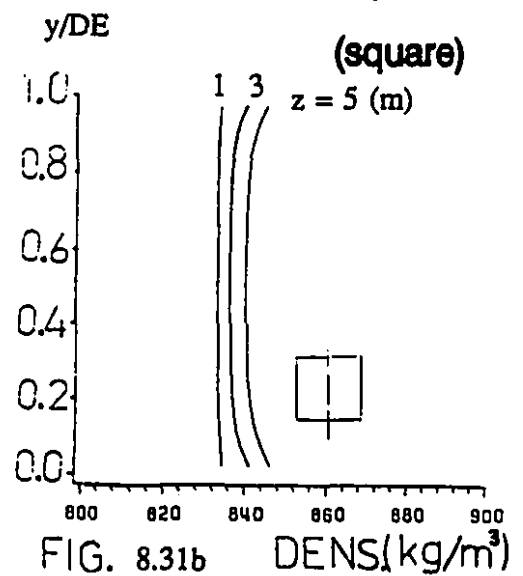
FIG. 8.30h

WP

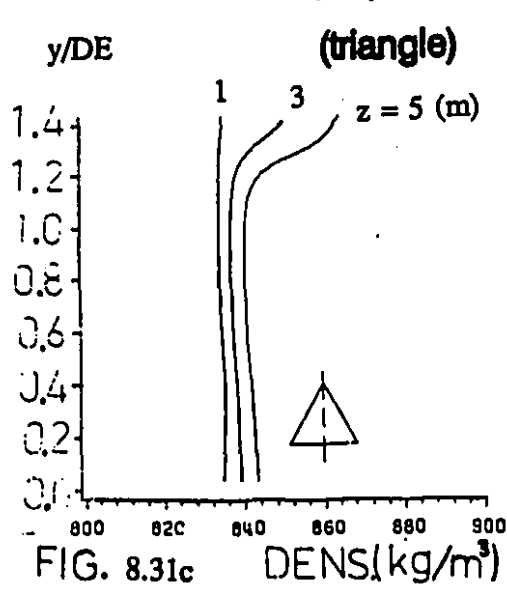
case#1 density - profile



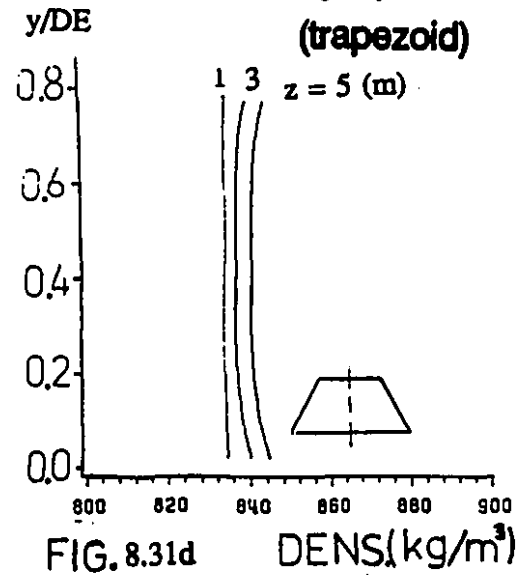
case#1 density - profile

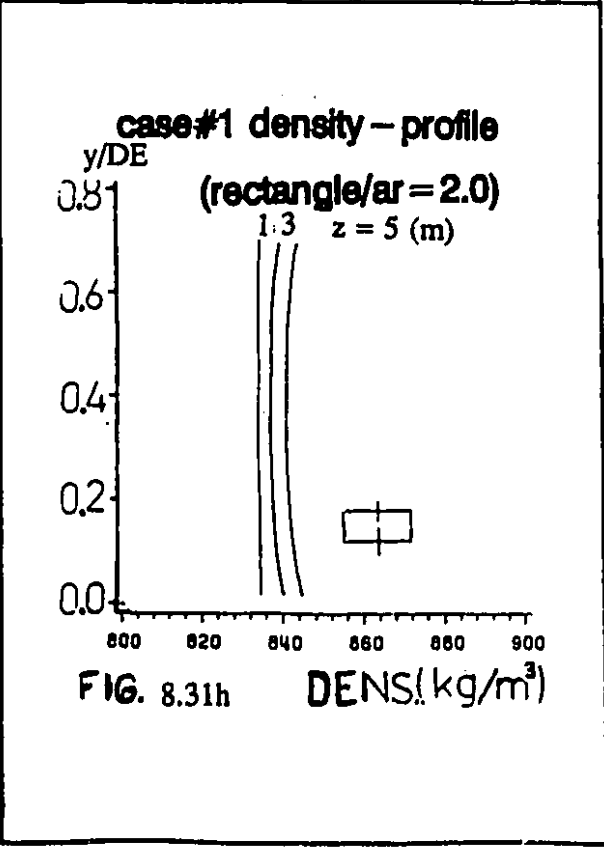
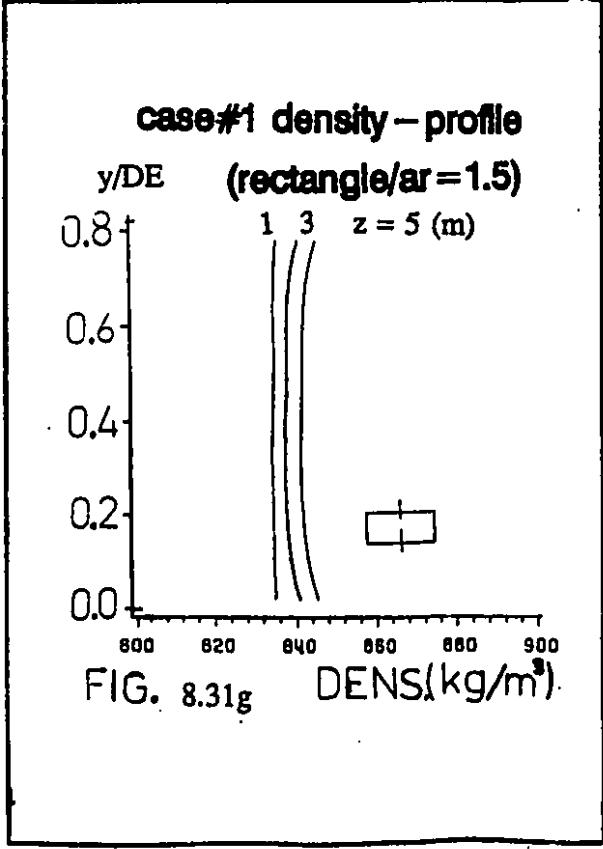
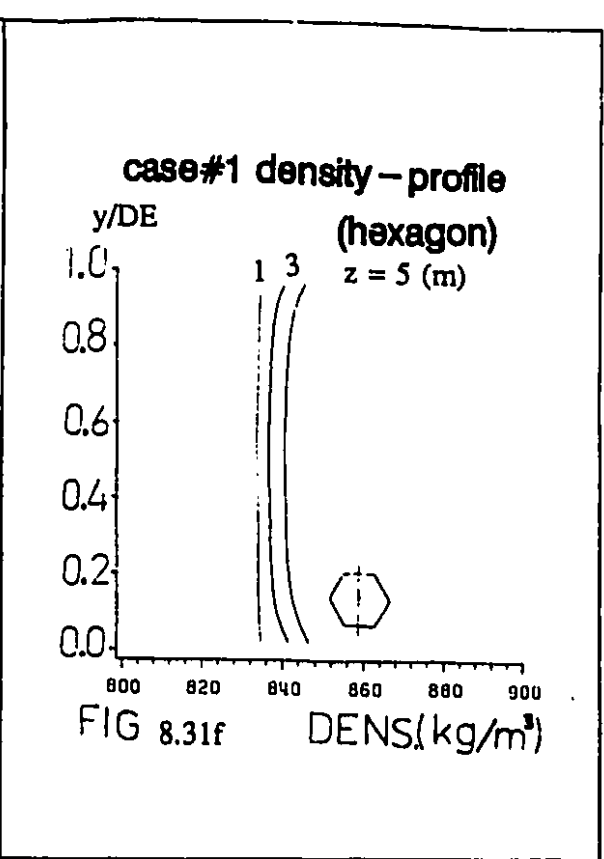
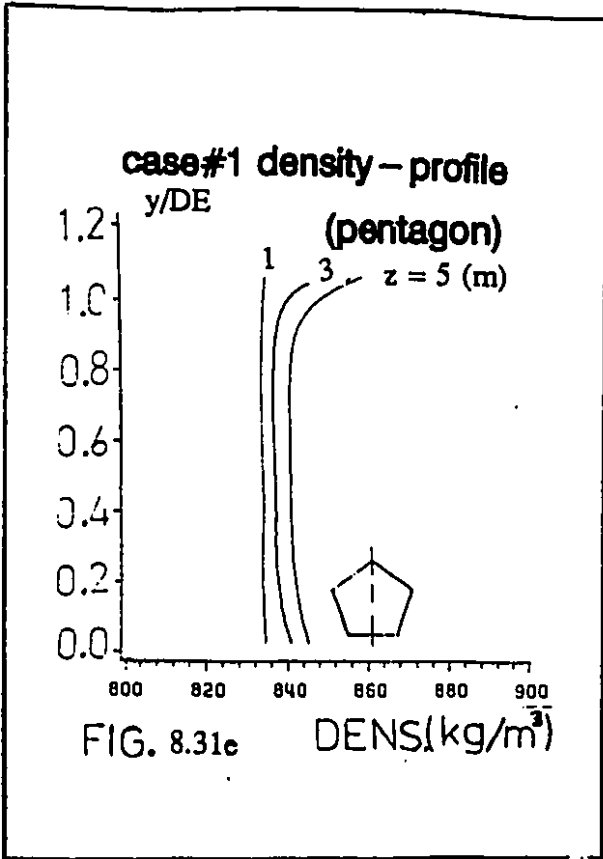


case#1 density - profile



case#1 density - profile





case#1 viscosity - profile

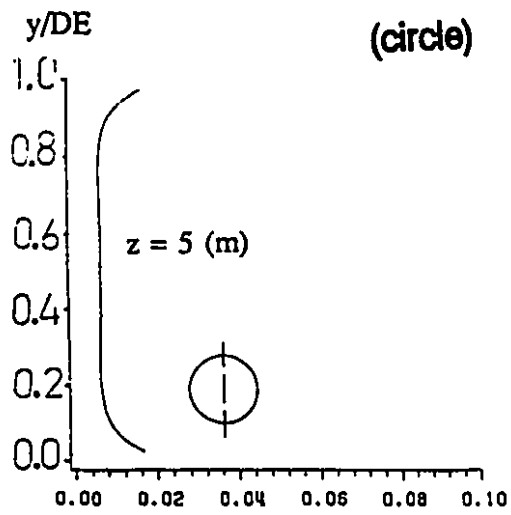


FIG. 8.32a

case#1 viscosity - profile

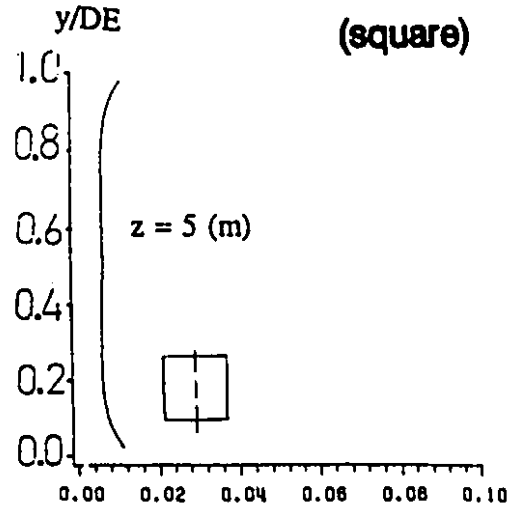


FIG. 8.32b

case#1 viscosity - profile

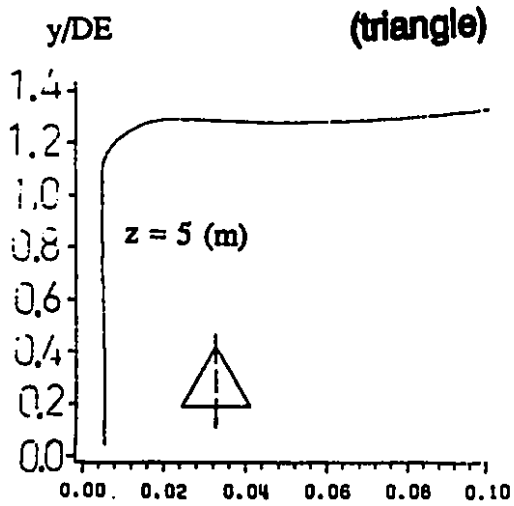


FIG. 8.32c

case#1 viscosity - profile

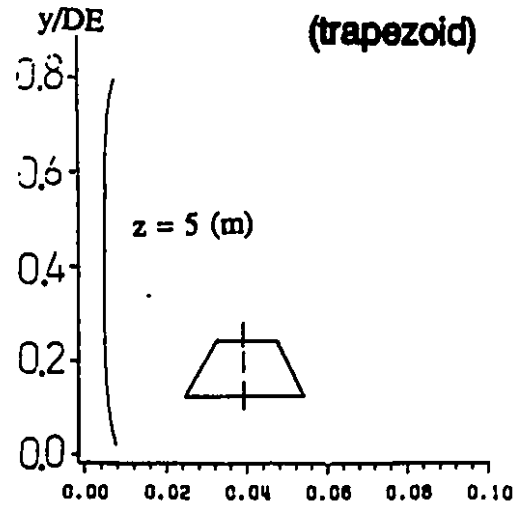
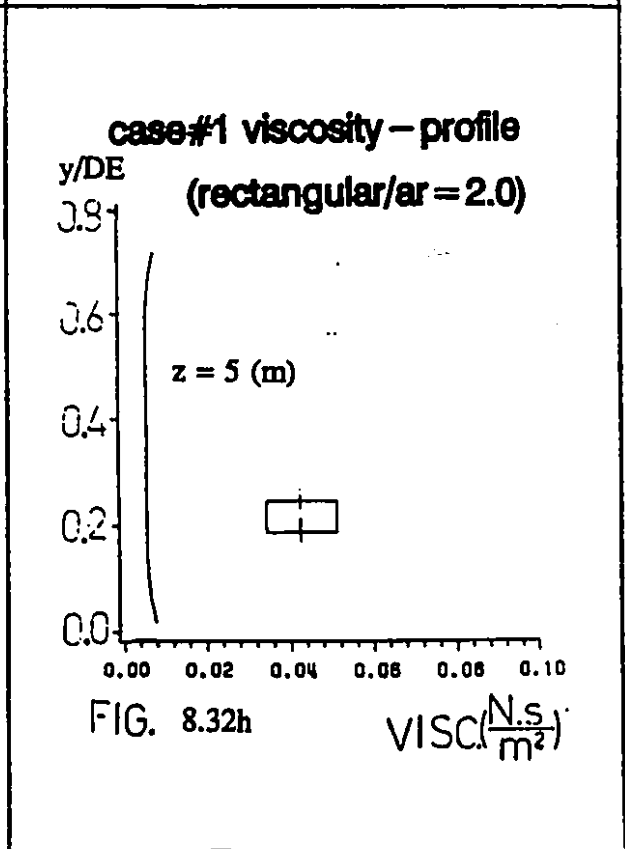
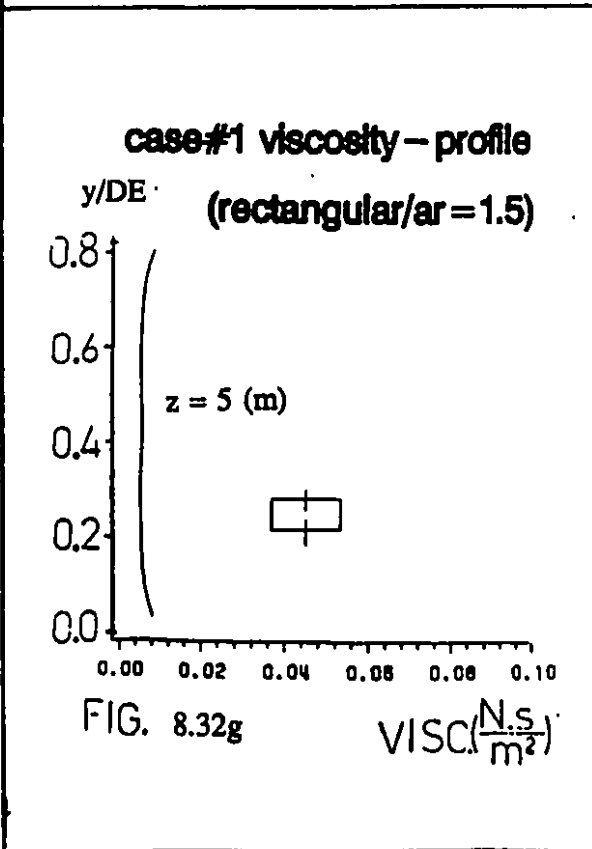
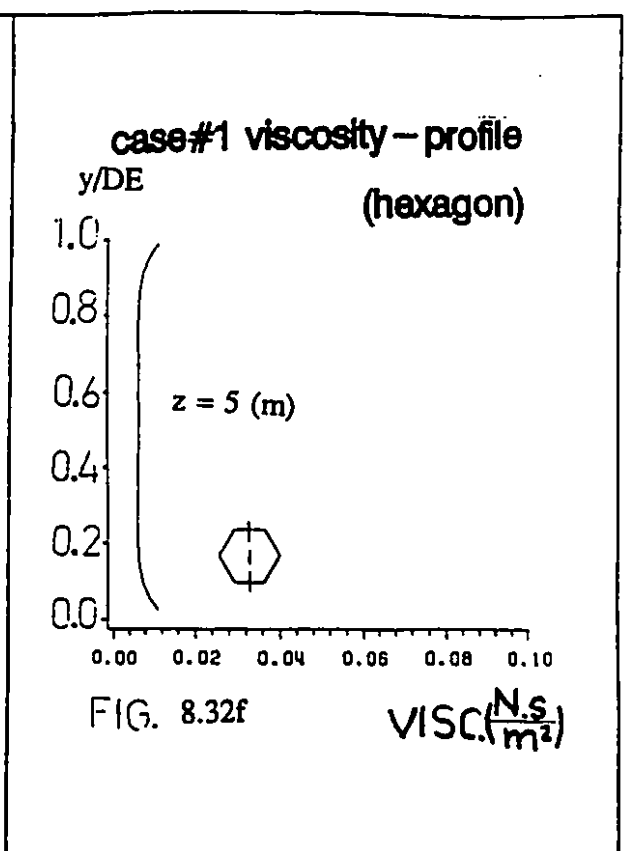
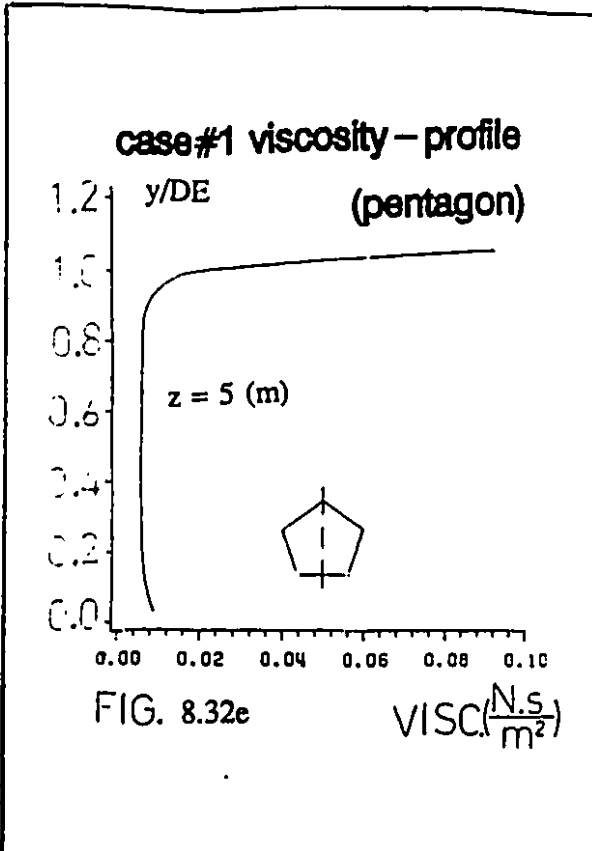
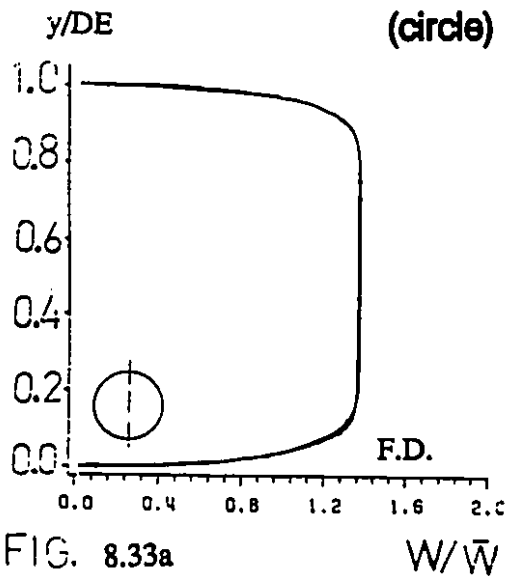


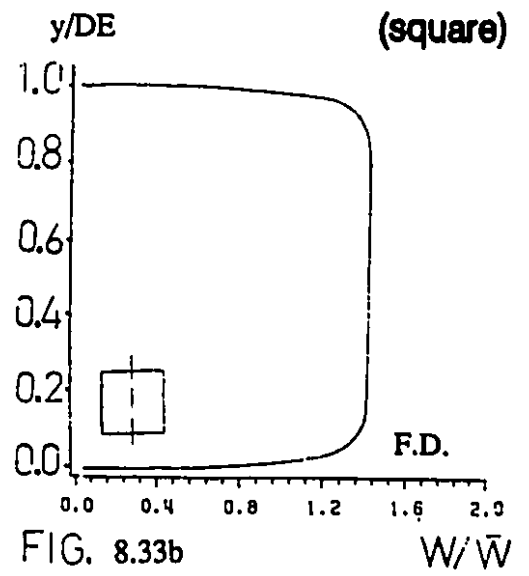
FIG. 8.32d



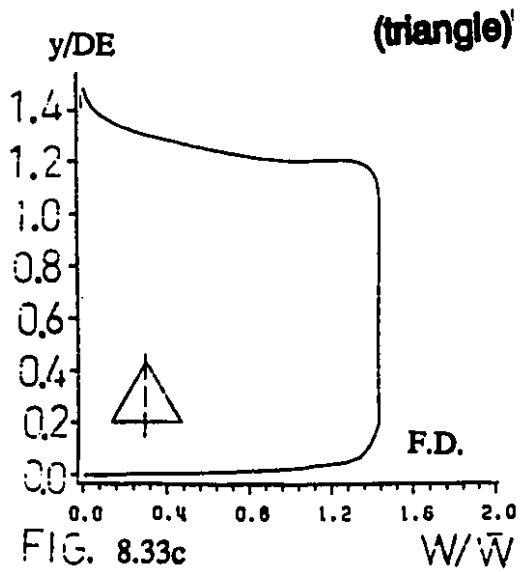
case#2 axial - velocity profile



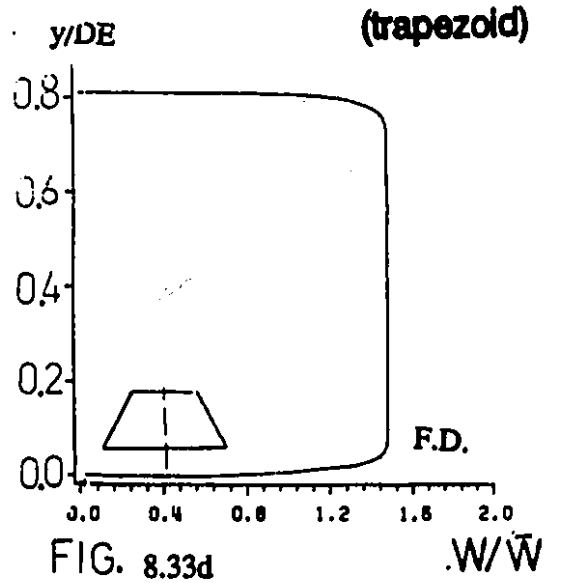
case#2 axial - velocity profile



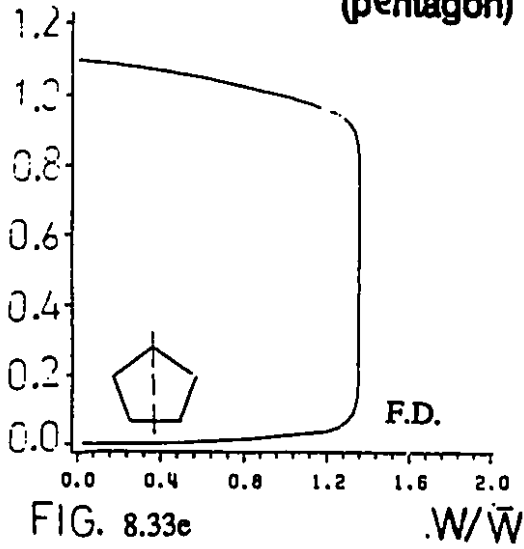
case#2 axial - velocity profile



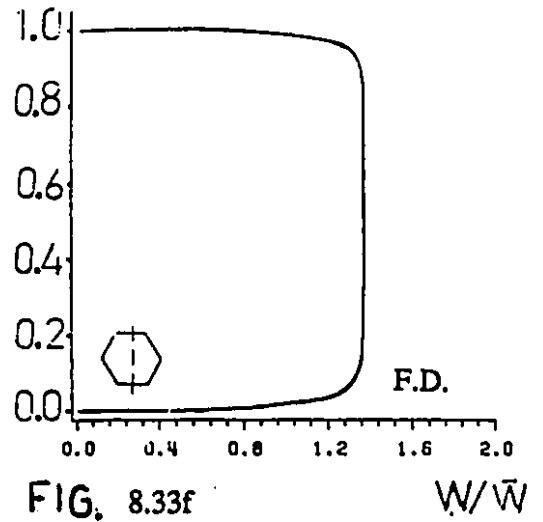
case#2 axial - velocity profile



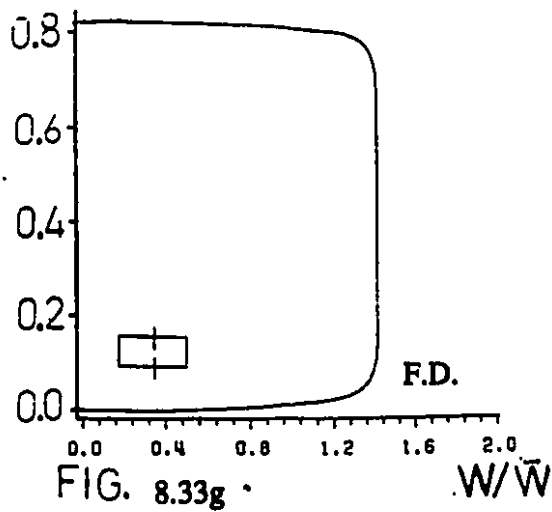
case#2 axial - velocity profile
y/DE (pentagon)



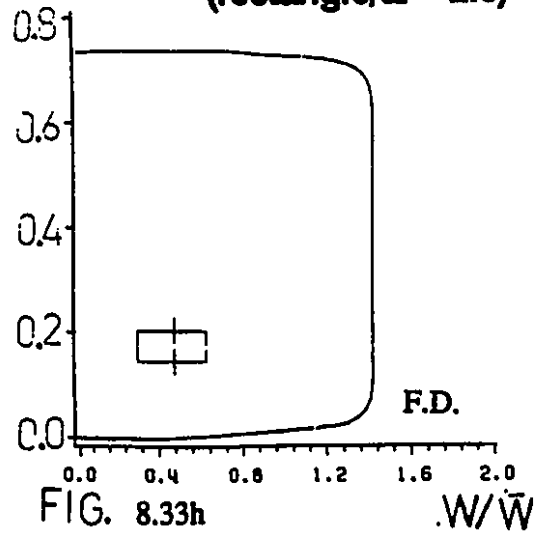
case#2 axial - velocity profile
y/DE (hexagon)



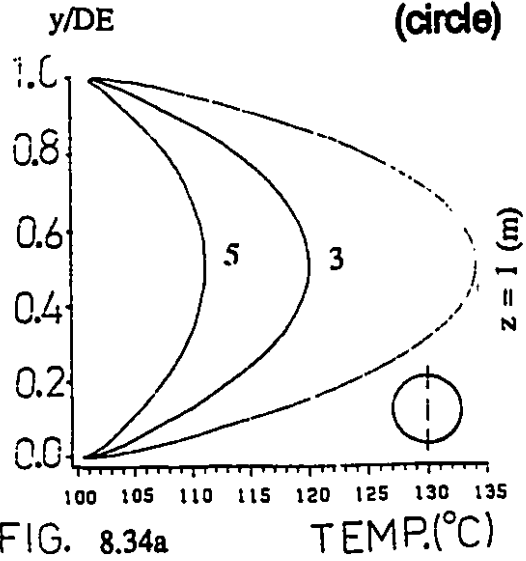
case#2 axial - velocity profile
y/DE (rectangle/ar = 1.5)



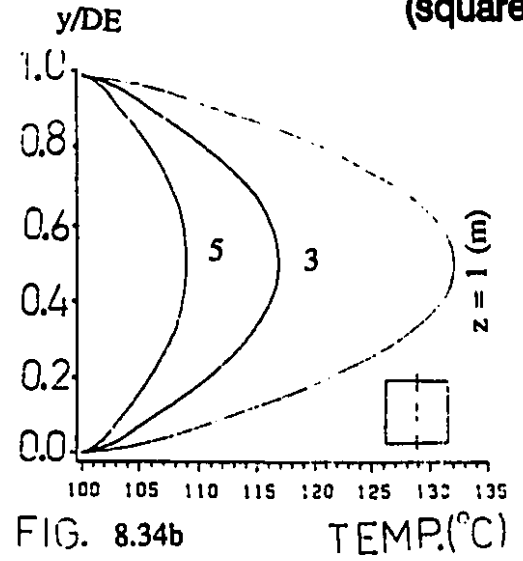
case#2 axial - velocity profile
y/DE (rectangle/ar = 2.0)



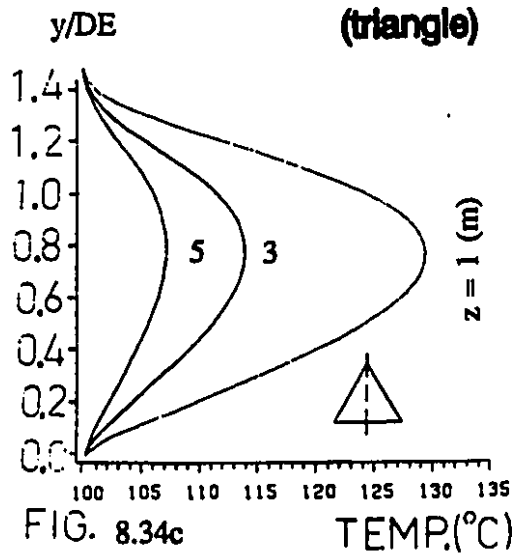
case#2 temperature profile
(circle)



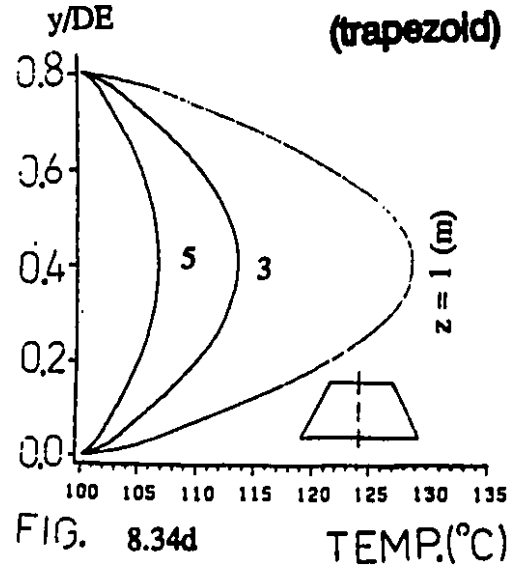
case#2 temperature profile
(square)



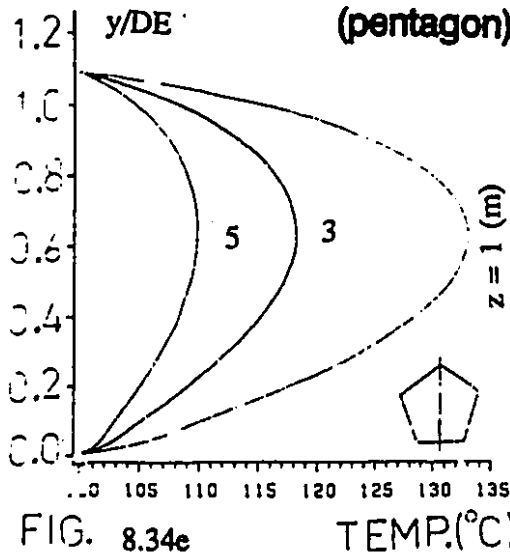
case#2 temperature profile
(triangle)



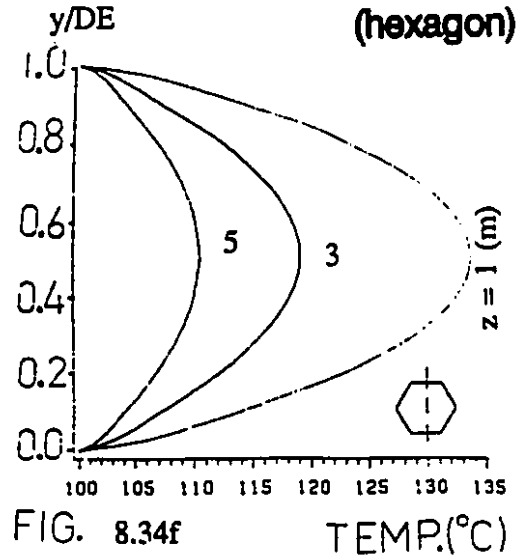
case#2 temperature profile
(trapezoid)



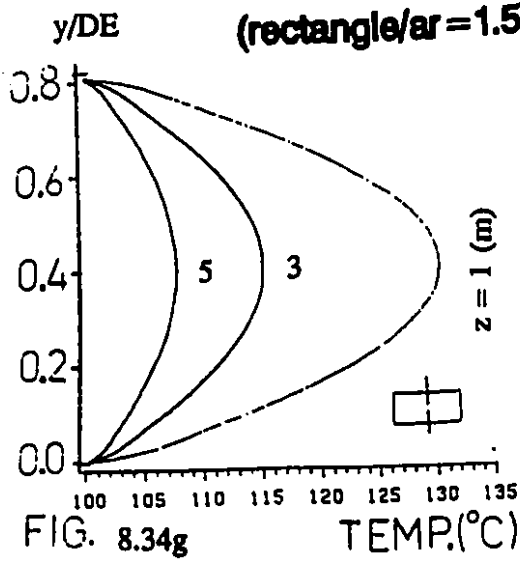
**case#2 temperature profile
(pentagon)**



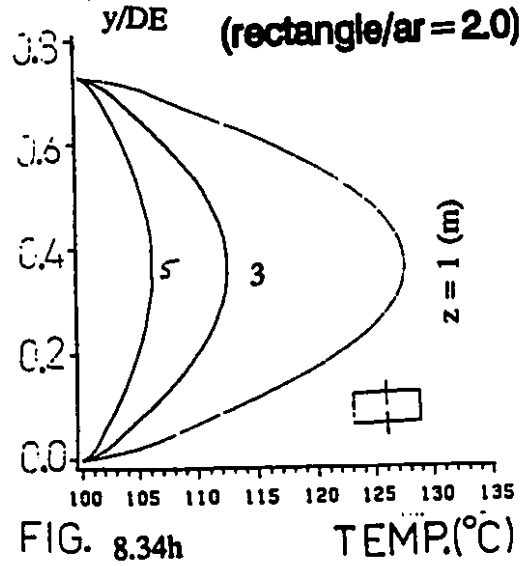
**case#2 temperature profile
(hexagon)**



**case#2 temperature profile
(rectangle/ar = 1.5)**



**case#2 temperature profile
(rectangle/ar = 2.0)**



case#2 polymer - concentration profile (circle)

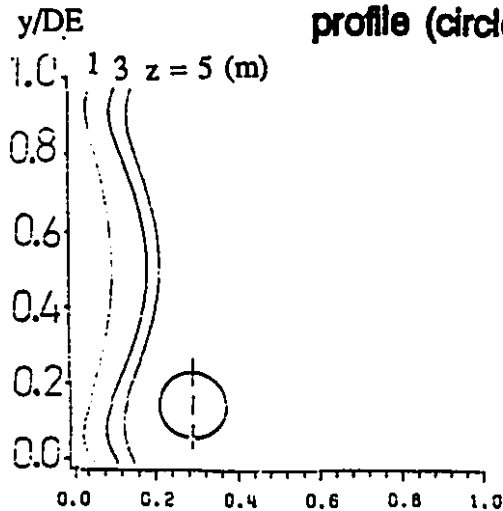


FIG. 8.35a

WP

case#2 polymer - concentration profile (square)

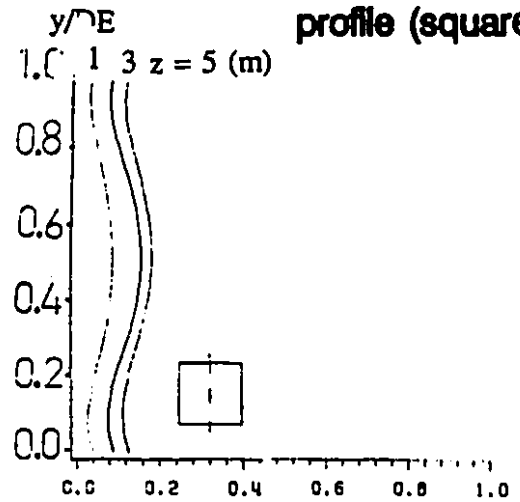


FIG. 8.35b

WP

case#2 polymer - concentration profile (triangle)

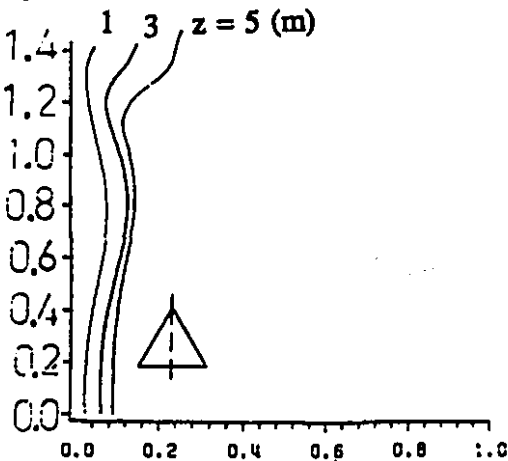


FIG. 8.35c

WP

case#2 polymer - concentration profile (trapezoid)

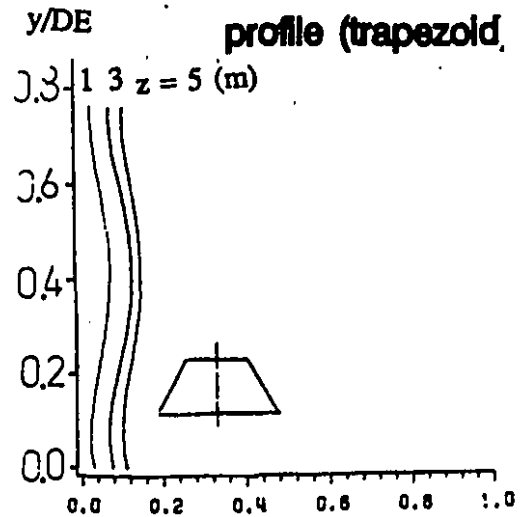


FIG. 8.35d

WP

case#2 polymer - concentration
profile (pentagon)

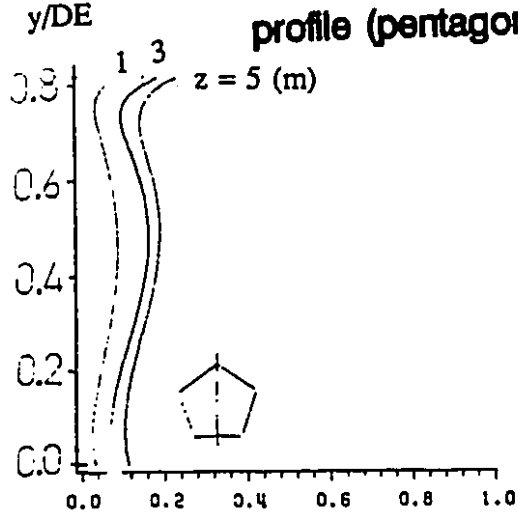


FIG. 8.35e

WP

case#2 polymer - concentration
profile (hexagon)

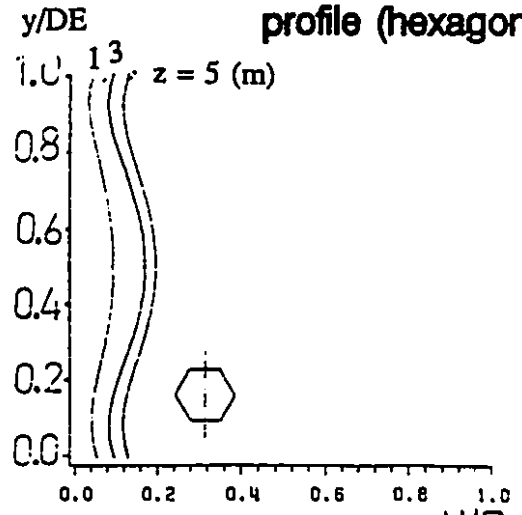


FIG. 8.35f

WP

case#2 polymer - concentration
profile (rectangle/ar=1.5)

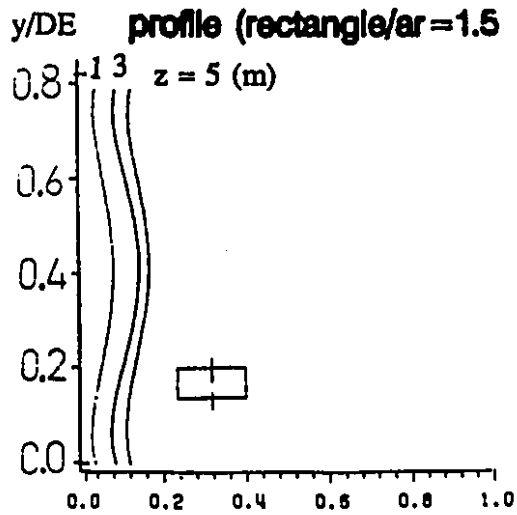


FIG. 8.35g

WP

case#2 polymer - concentration
profile (rectangle/ar=2.0)

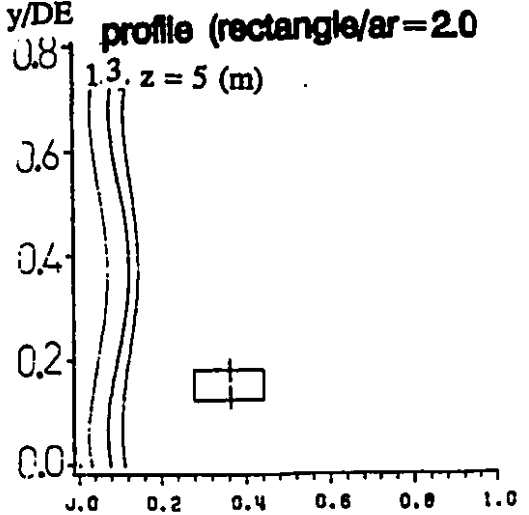


FIG. 8.35h

WP

case#2 density - profile

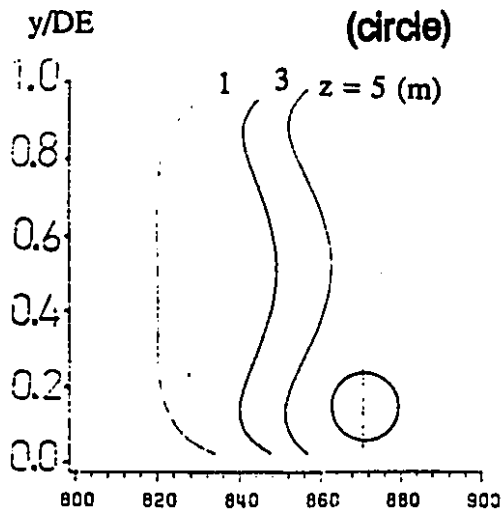


FIG. 8.36a DENS(kg/m³)

case#2 density - profile

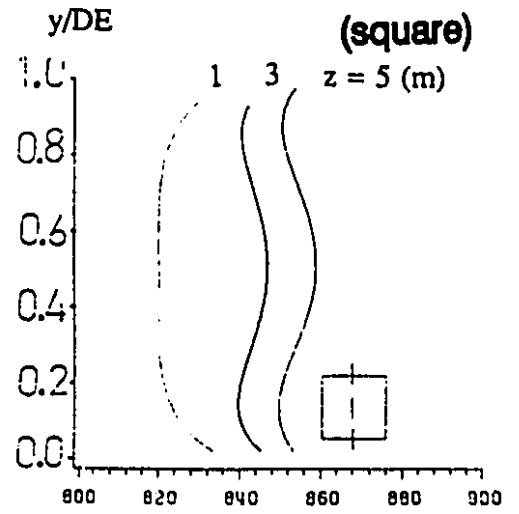


FIG. 8.36b DENS(kg/m³)

case#2 density - profile

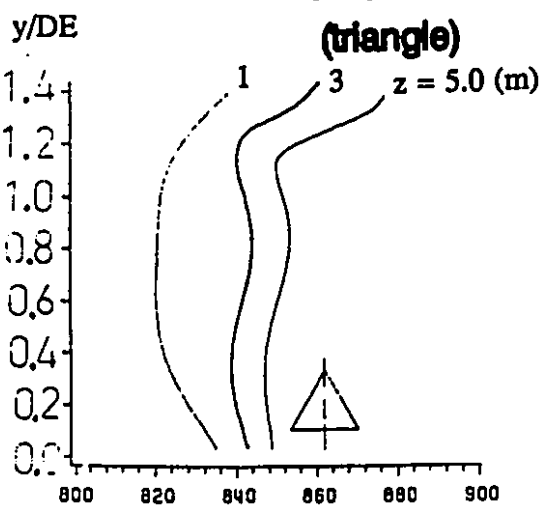


FIG. 8.36c DENS(kg/m³)

case#2 density - profile

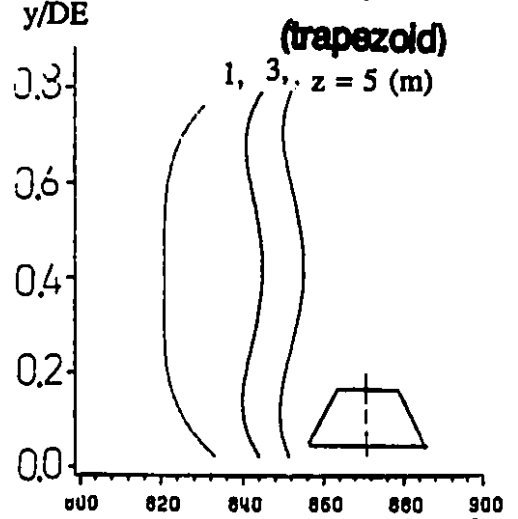
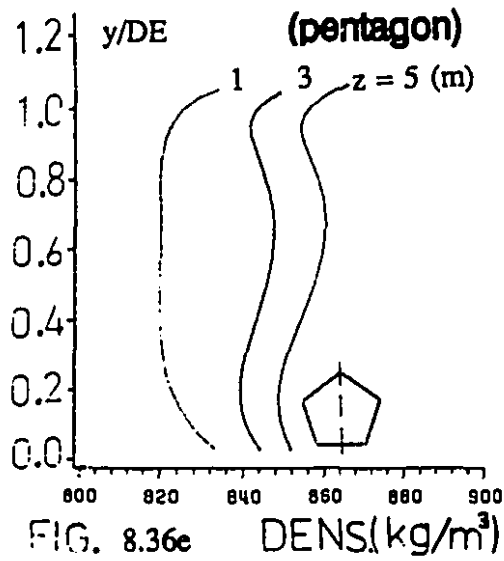
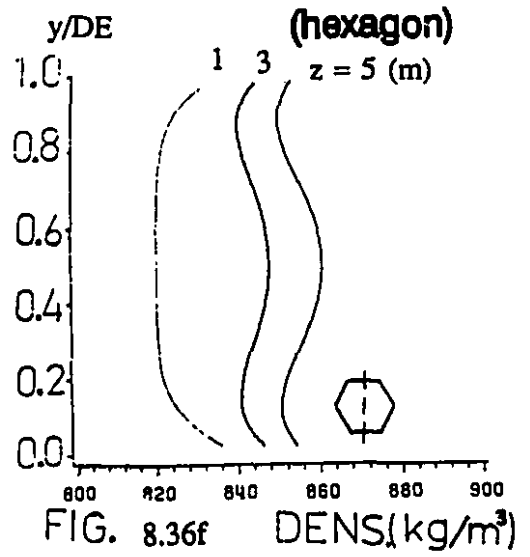


FIG. 8.36d DENS(kg/m³)

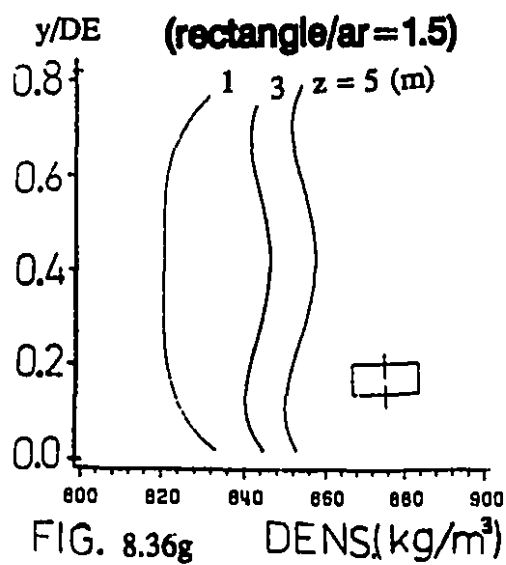
case#2 density - profile



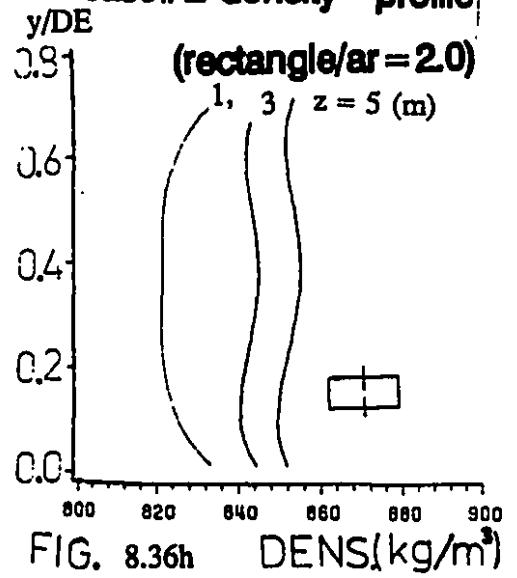
case#2 density - profile



case#2 density - profile



case#2 density - profile



case#2 viscosity - profile

(circle)

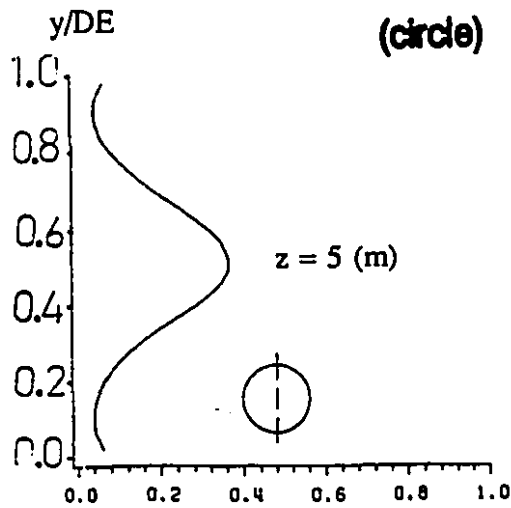


FIG. 8.37a

VISC. ($\frac{N.s}{m^2}$)

case#2 viscosity - profile

(square)

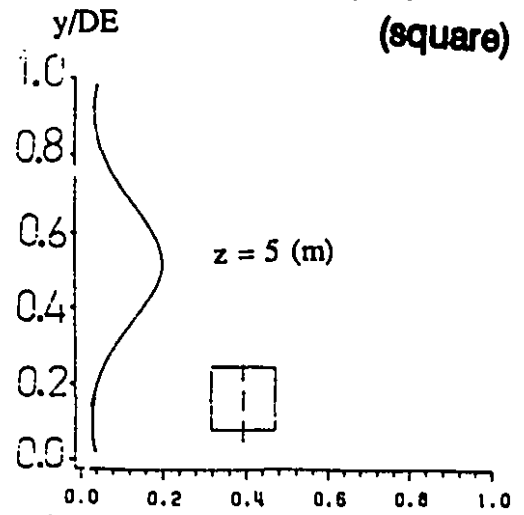


FIG. 8.37b

VISC. ($\frac{N.s}{m^2}$)

case#2 viscosity - profile

(triangle)

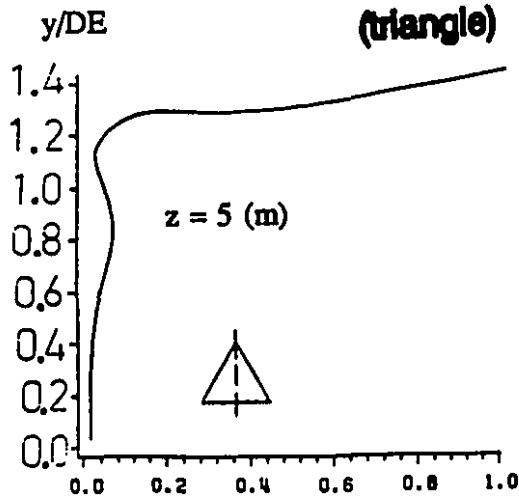


FIG. 8.37c

VISC. ($\frac{N.s}{m^2}$)

case#2 viscosity - profile

(trapezoid)

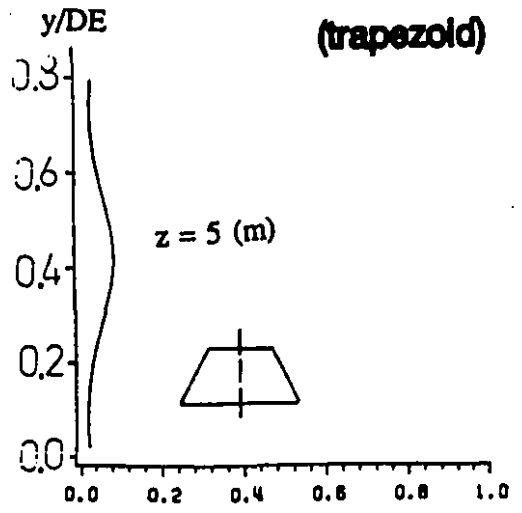
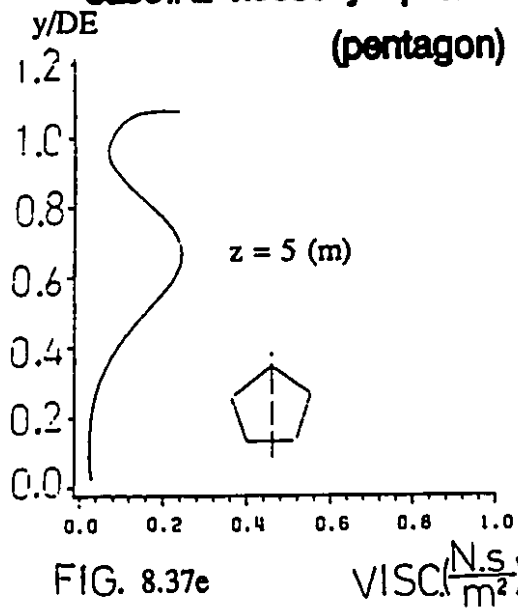


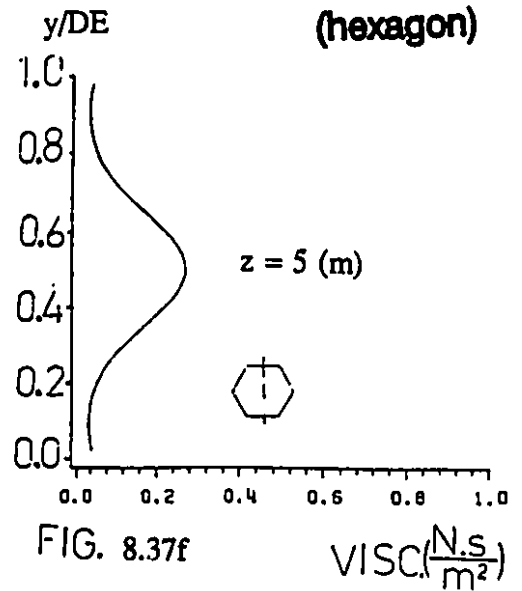
FIG. 8.37d

VISC. ($\frac{N.s}{m^2}$)

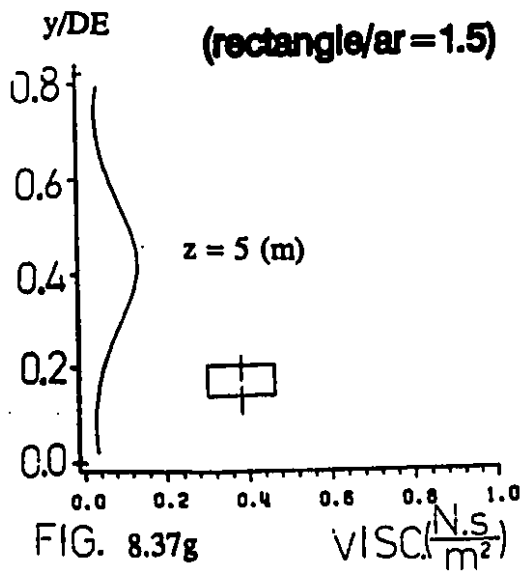
**case#2 viscosity - profile
(pentagon)**



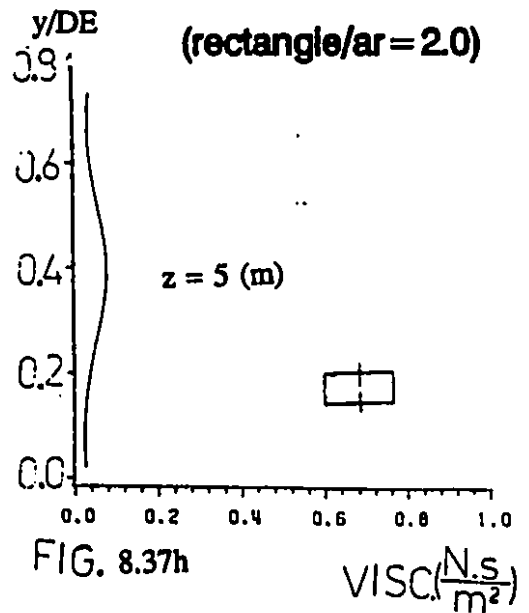
**case#2 viscosity - profile
(hexagon)**



**case#2 viscosity - profile
(rectangle/ar = 1.5)**



**case#2 viscosity profile
(rectangle/ar = 2.0)**



case#3 axial - velocity profile

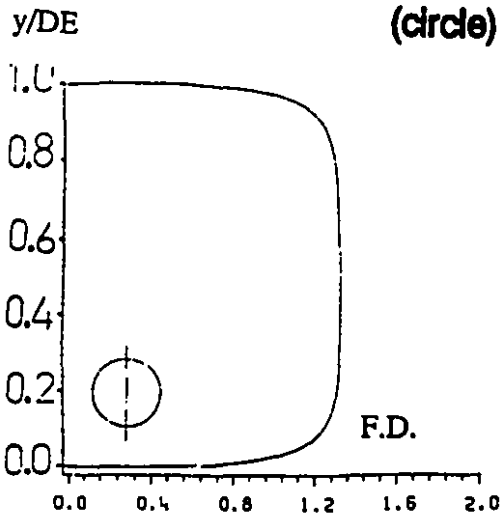


FIG. 8.38a

$VISC. (\frac{N \cdot s}{m^2})$

case#3 axial - velocity profile

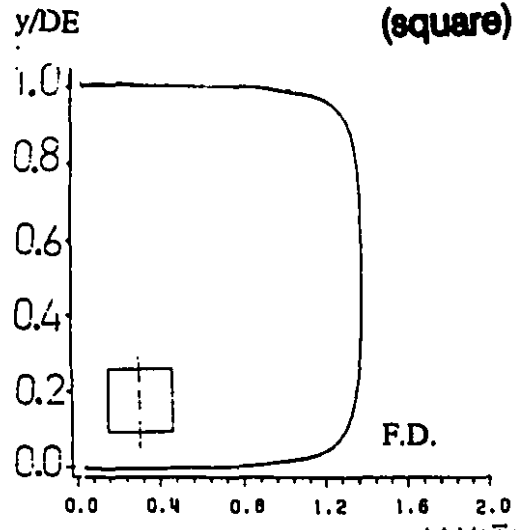


FIG. 8.38b

W/\bar{W}

case#3 axial - velocity profile

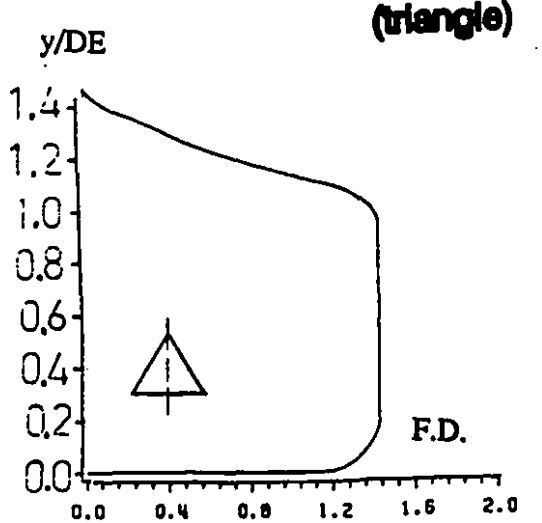


FIG. 8.38c

W/\bar{W}

case#3 axial - velocity profile

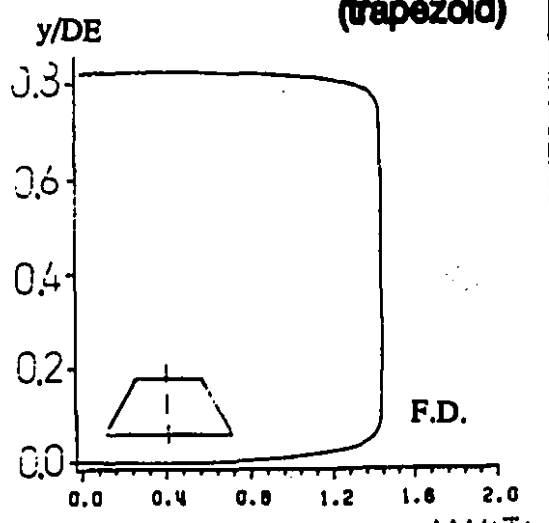
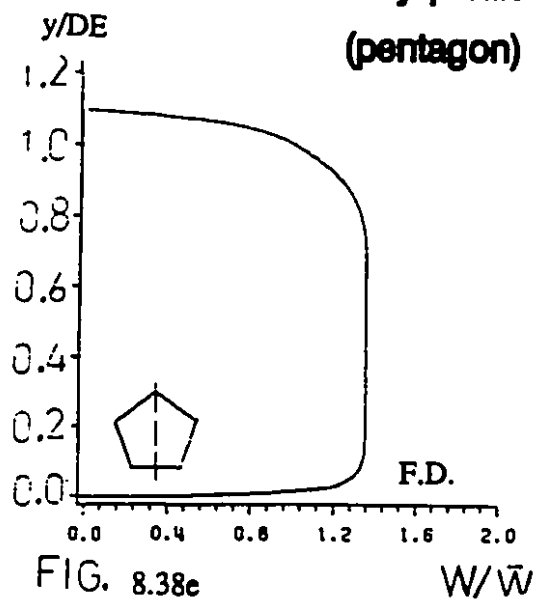


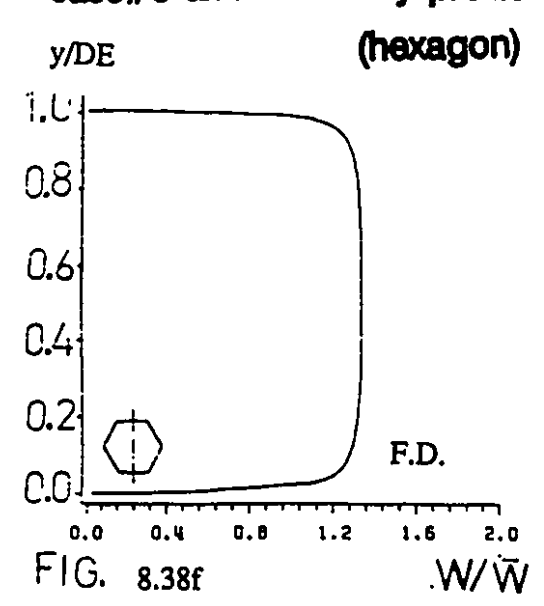
FIG. 8.38d

W/\bar{W}

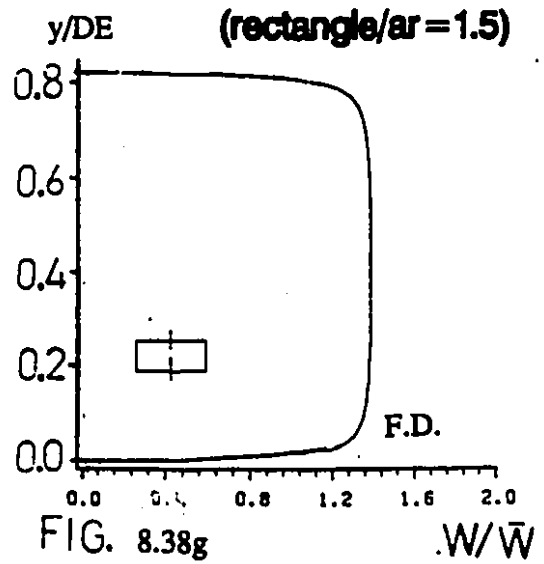
case#3 axial - velocity profile
(pentagon)



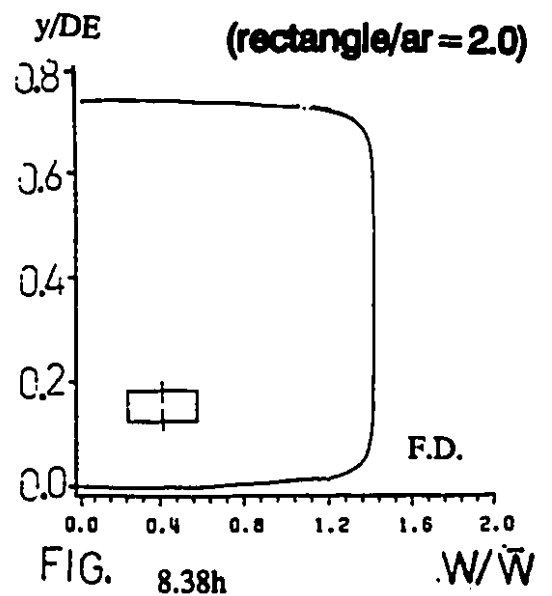
case#3 axial - velocity profile
(hexagon)



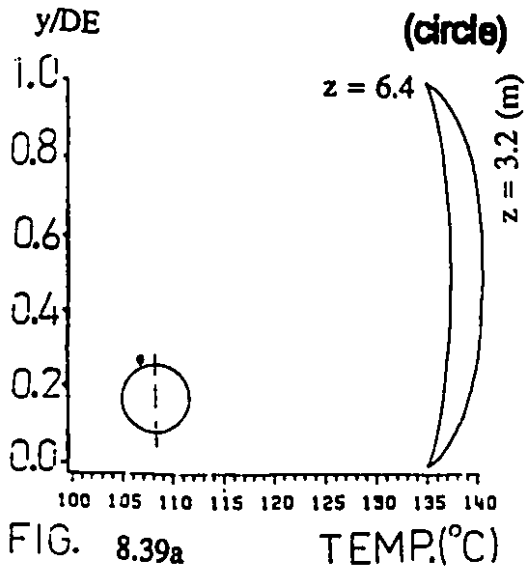
case#3 axial - velocity profile
(rectangle/ar = 1.5)



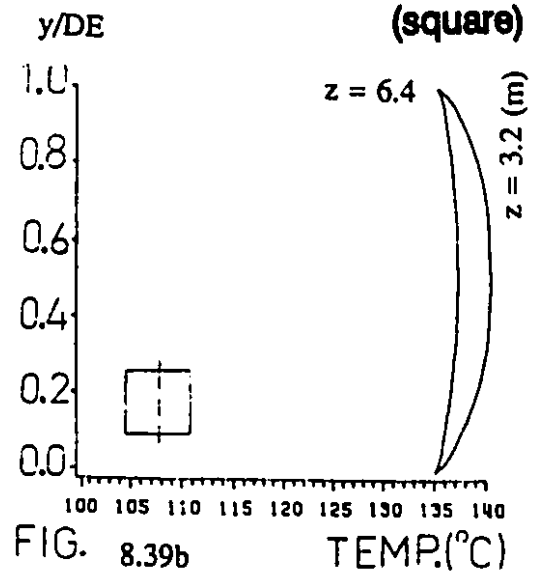
case#3 axial - velocity profile
(rectangle/ar = 2.0)



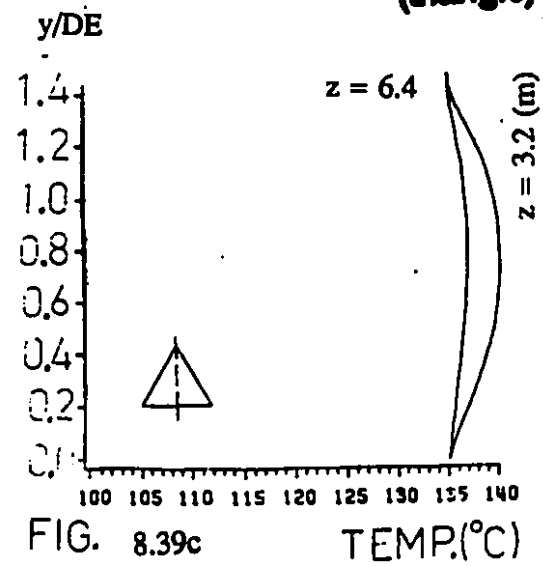
case#3 temperature profile



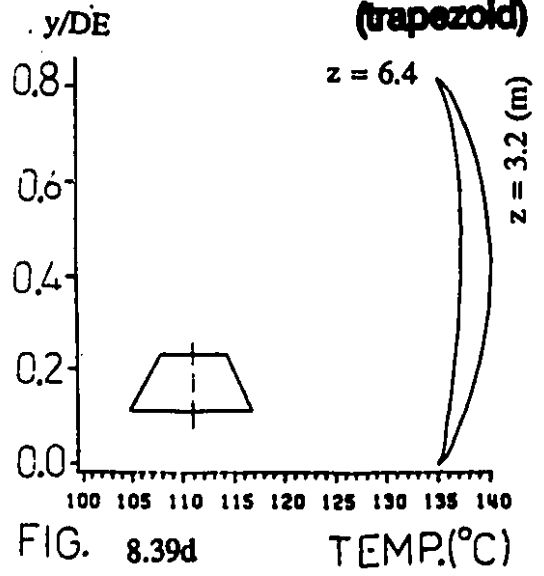
case#3 temperature profile



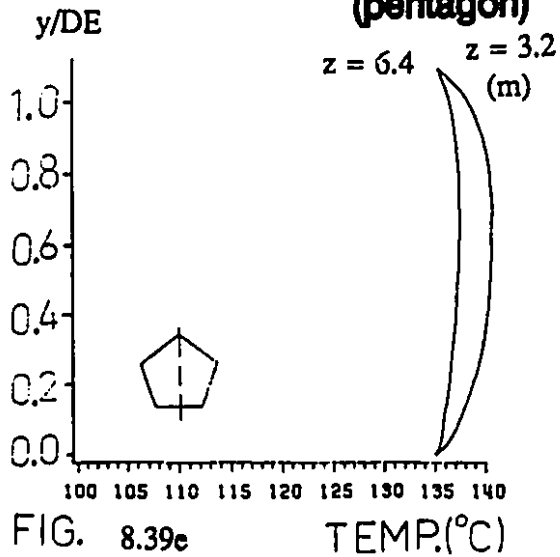
case#3 temperature profile



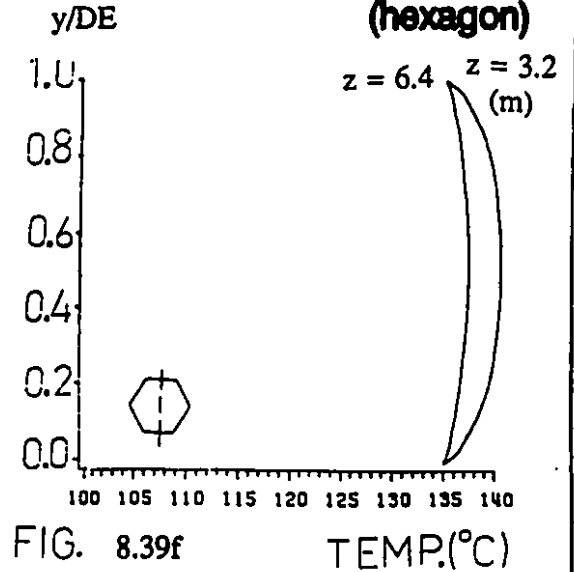
case#3 temperature profile



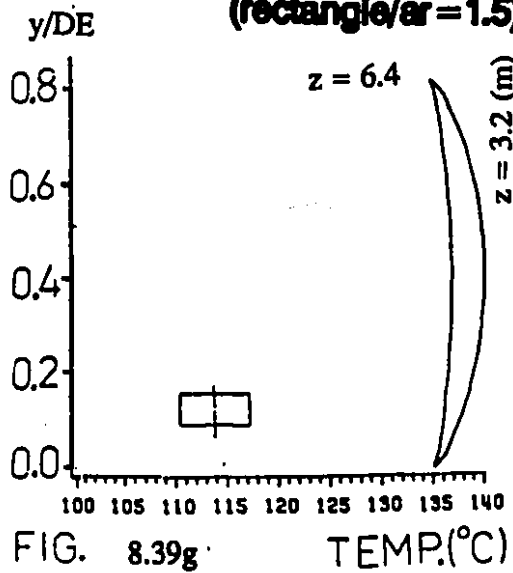
**case #3 temperature profile
(pentagon)**



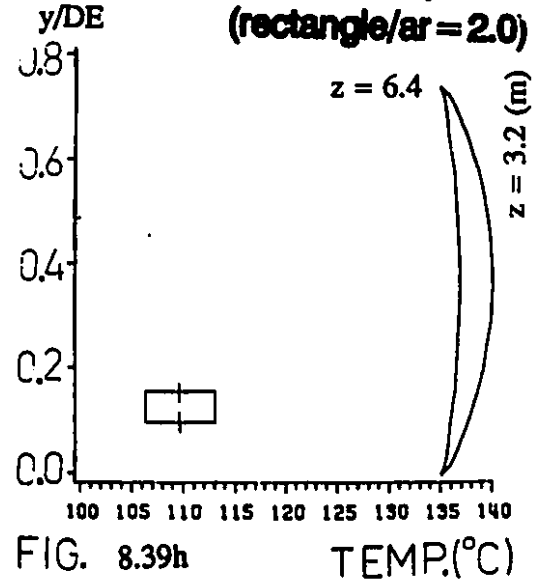
**case #3 temperature profile
(hexagon)**



**case #3 temperature profile
(rectangle/ar = 1.5)**



**case #3 temperature profile
(rectangle/ar = 2.0)**



case#3 polymer concentration profile (circle)

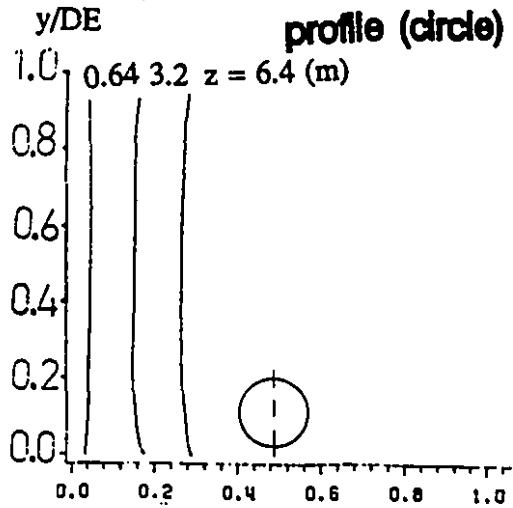


FIG. 8.40a

case#3 polymer concentration profile (square)

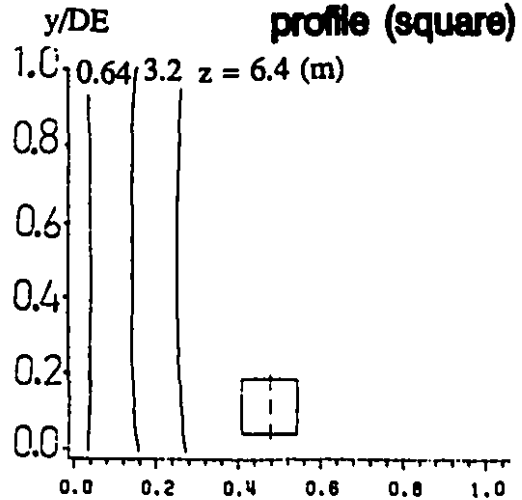


FIG. 8.40b

case#3 polymer concentration profile (triangle)

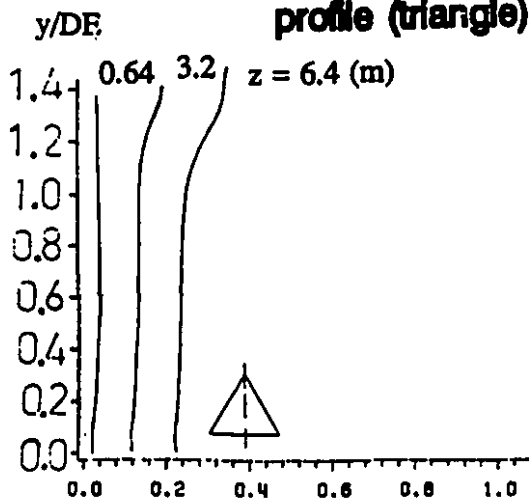


FIG. 8.40c

case#3 polymer concentration profile (trapezoid)

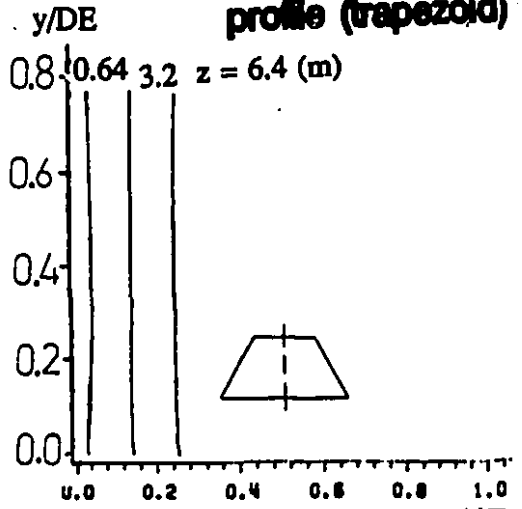


FIG. 8.40d

case #3 polymer concentration profile (pentagon)

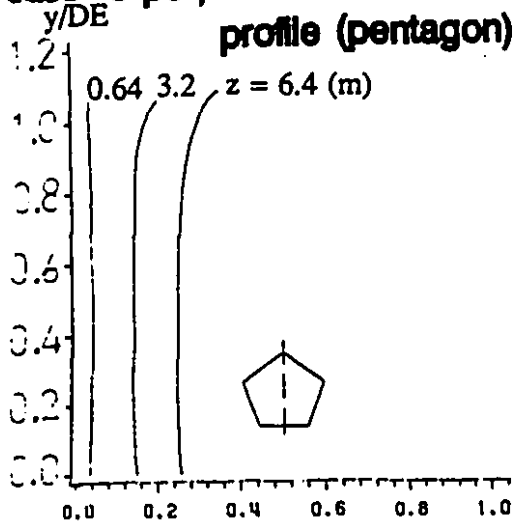


FIG. 8.40e

WP

case #3 polymer concentration profile (hexagon)

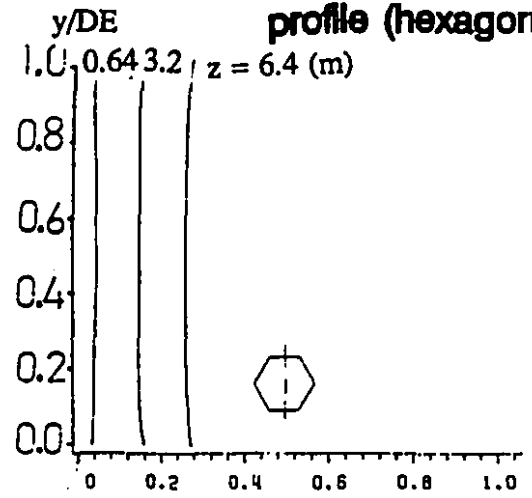


FIG. 8.40f

WP

case #3 polymer concentration profile (rectangle/ar=1.5)

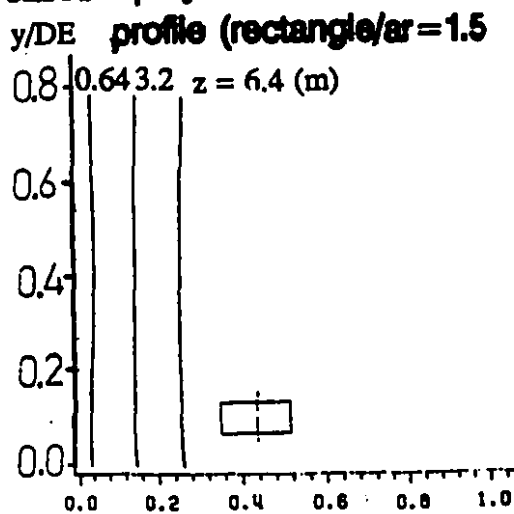


FIG. 8.40g

WP

case #3 polymer concentration profile (rectangle/ar=2.0)

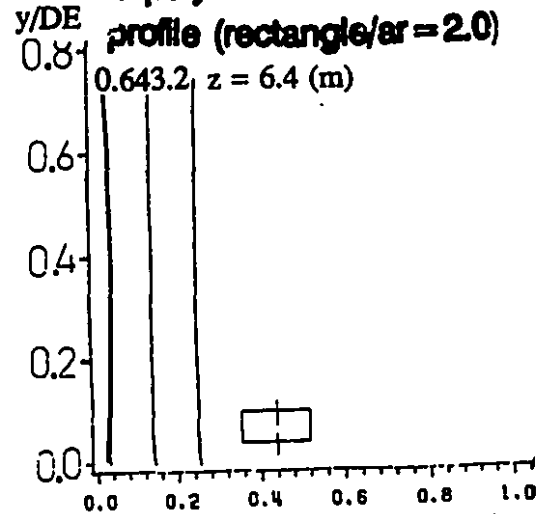


FIG. 8.40h

WP

**case#3 density – profile
(circle)**

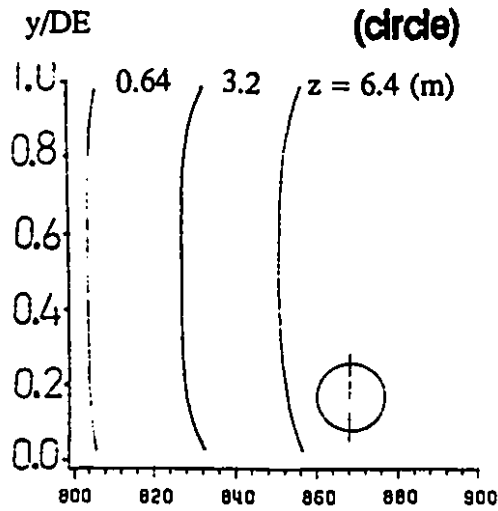


FIG. 8.41a $DENS(kg/m^3)$

**case#3 density – profile
(square)**

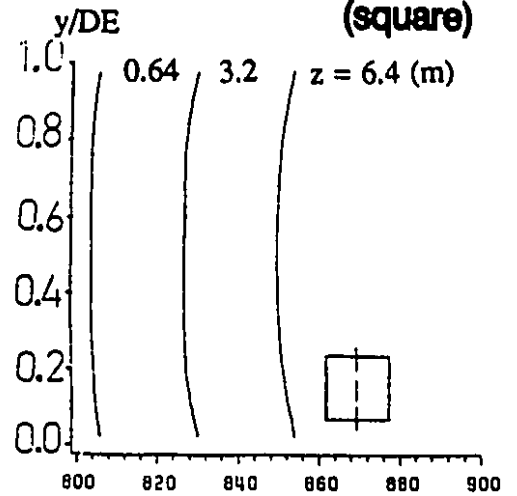


FIG. 8.41b $DENS(kg/m^3)$

**case#3 density – profile
(triangle)**

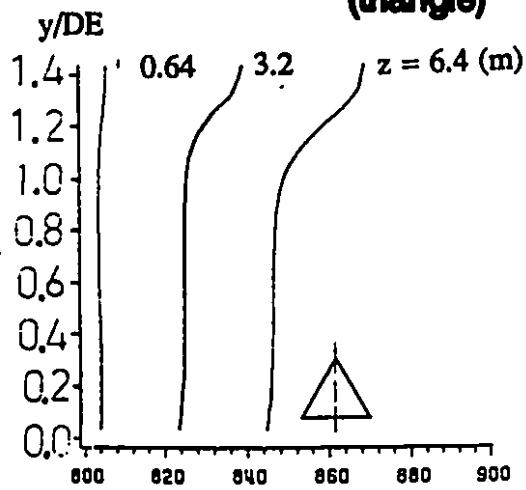


FIG. 8.41c $DENS(kg/m^3)$

**case#3 density – profile
(trapezoid)**

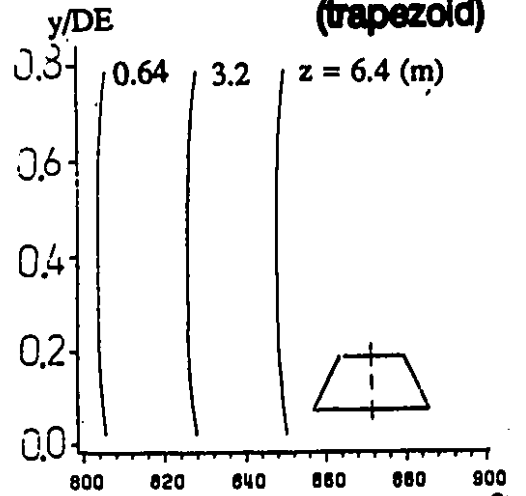
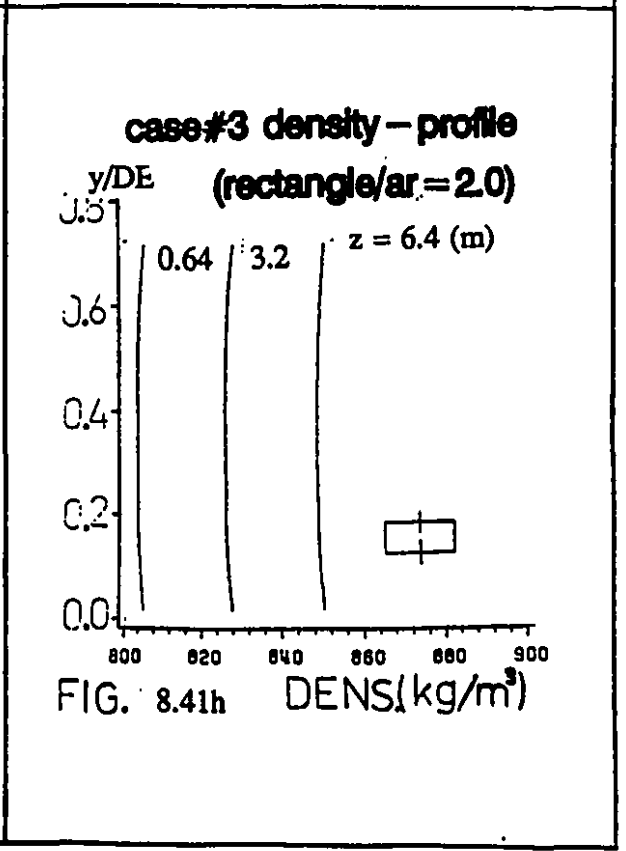
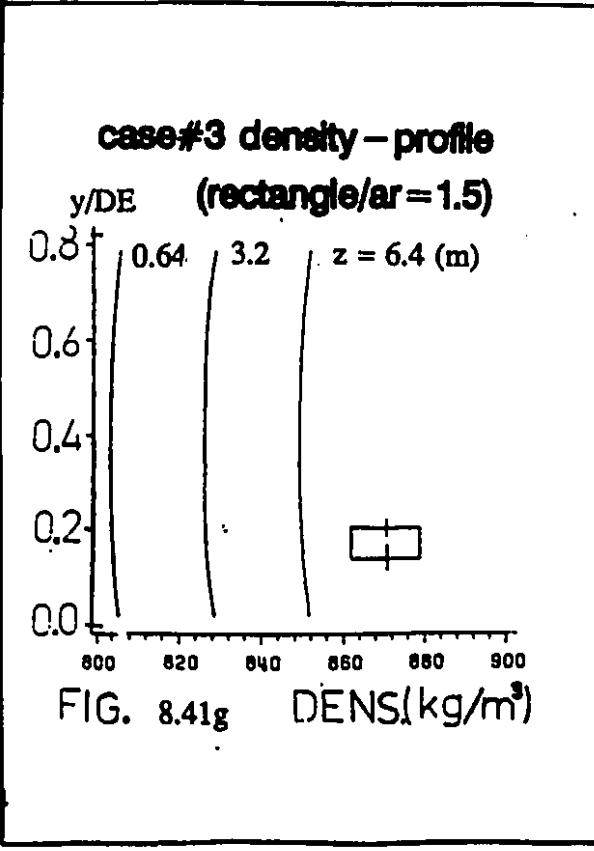
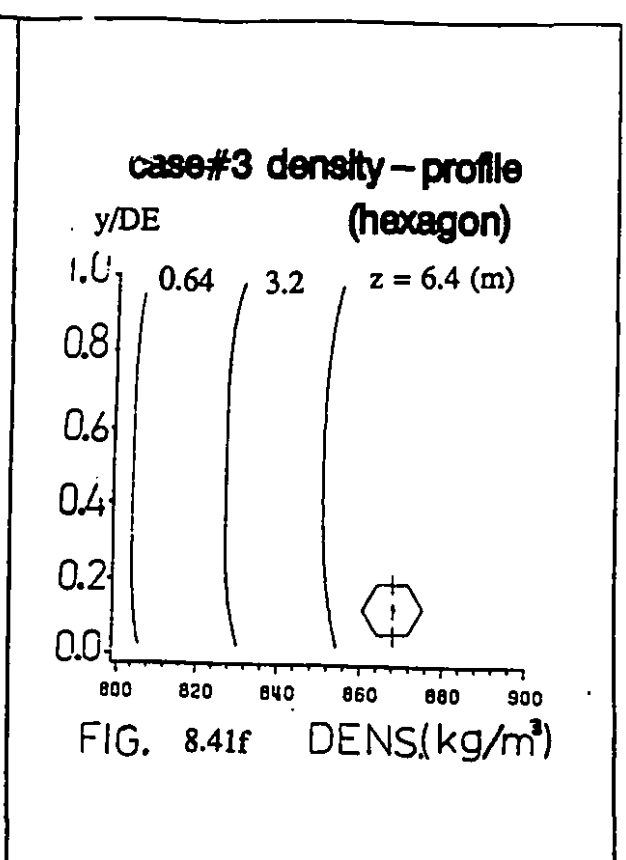
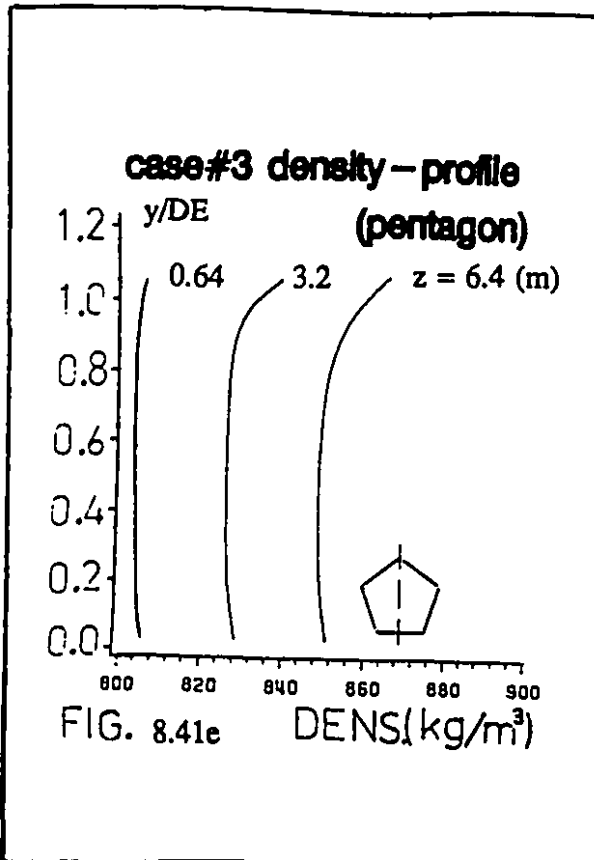
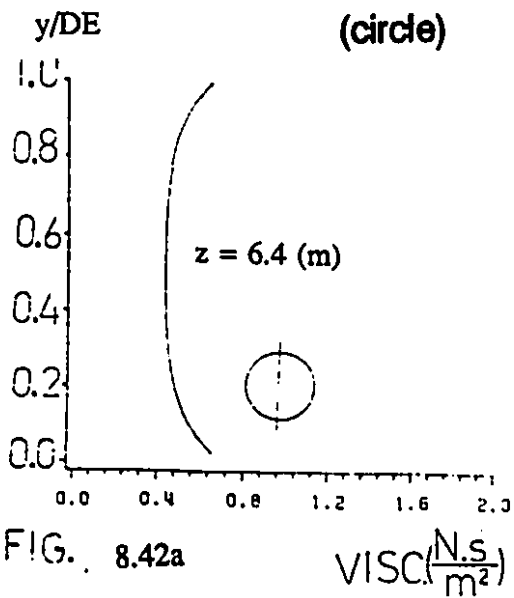


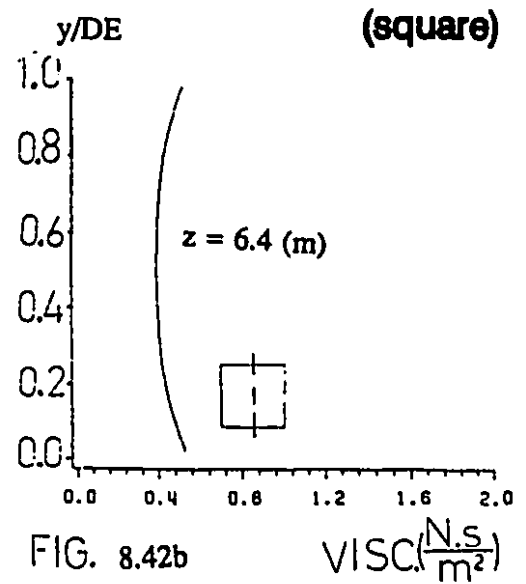
FIG. 8.41d $DENS(kg/m^3)$



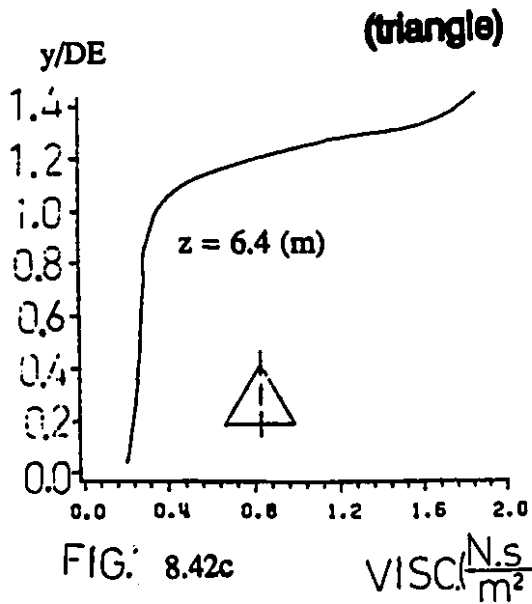
case#3 viscosity profile



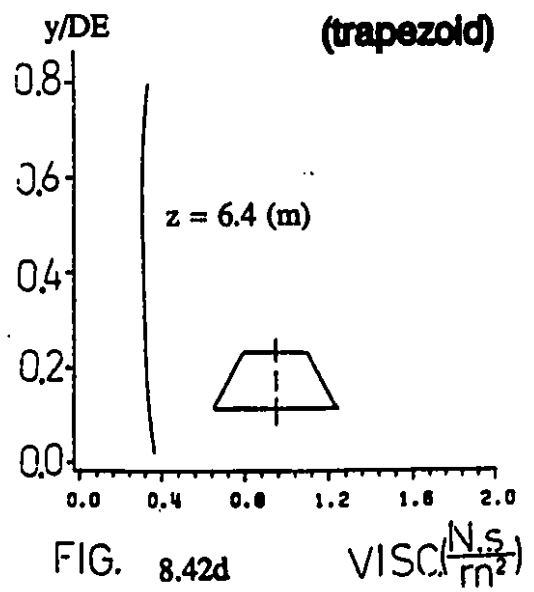
case#3 viscosity - profile



case#3 viscosity - profile



case#3 viscosity - profile



case#3 viscosity - profile
(pentagon)

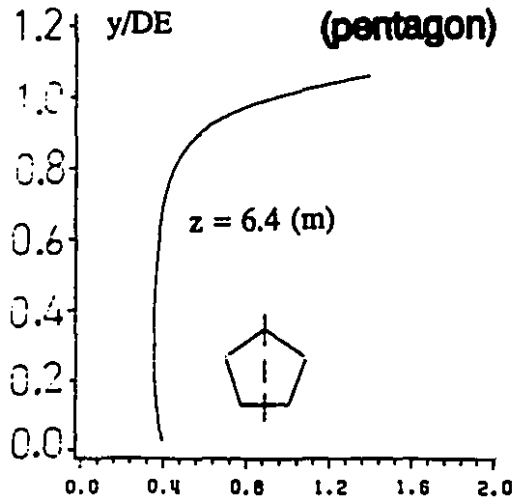


FIG. 8.42c VISC. ($\frac{N \cdot s}{m^2}$)

case#3 viscosity - profile
(hexagon)

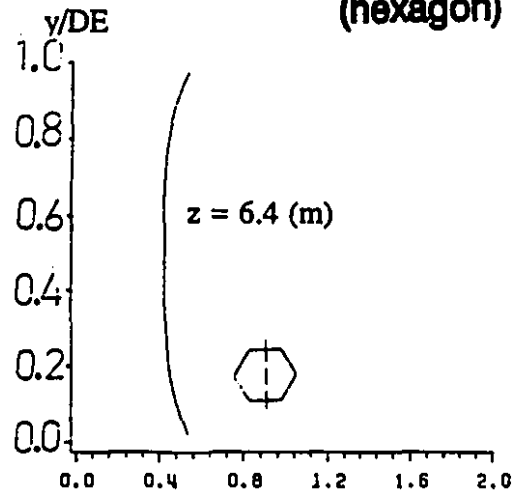


FIG. 8.42f VISC. ($\frac{N \cdot s}{m^2}$)

case#3 viscosity - profile
(rectangle/ar = 1.5)

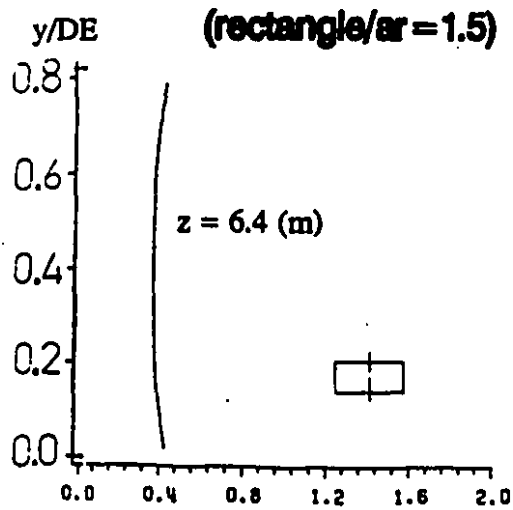


FIG. 8.42g VISC. ($\frac{N \cdot s}{m^2}$)

case#3 viscosity - profile
(rectangle/ar = 2.0)

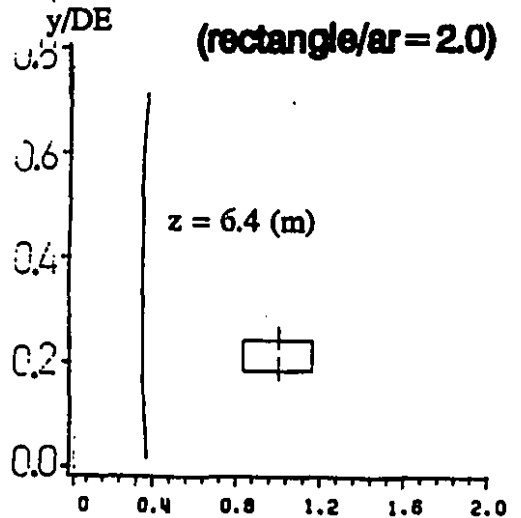
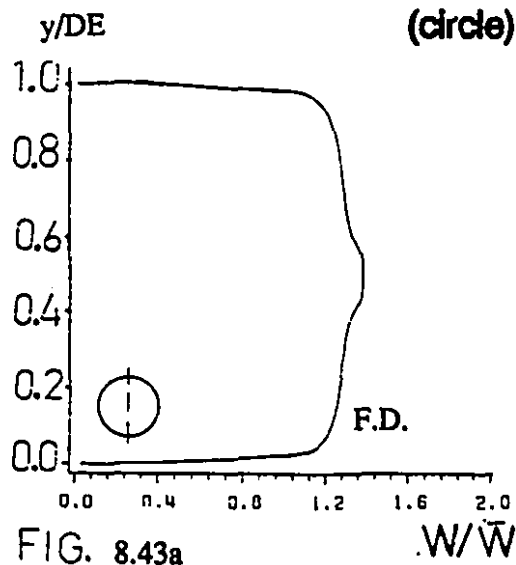
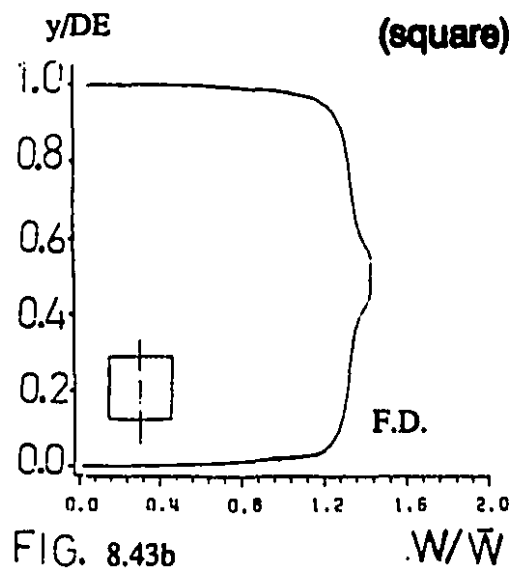


FIG. 8.42h VISC. ($\frac{N \cdot s}{m^2}$)

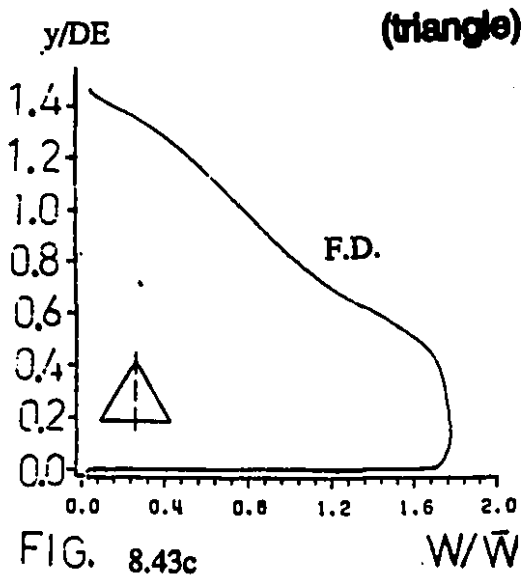
case#4 axial - velocity profile



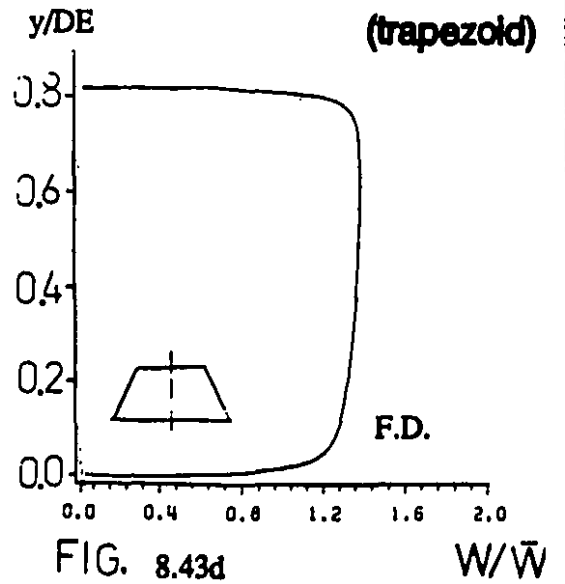
case#4 axial - velocity profile



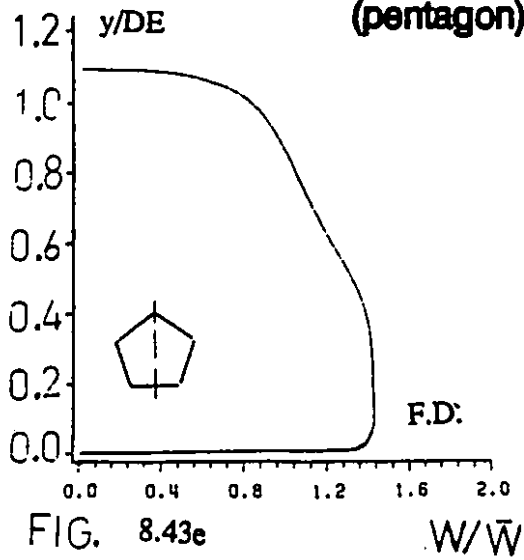
case#4 axial - velocity profile



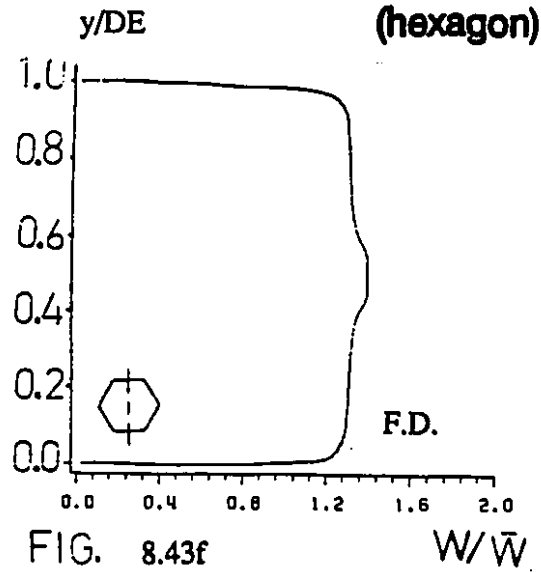
case#4 axial - velocity profile



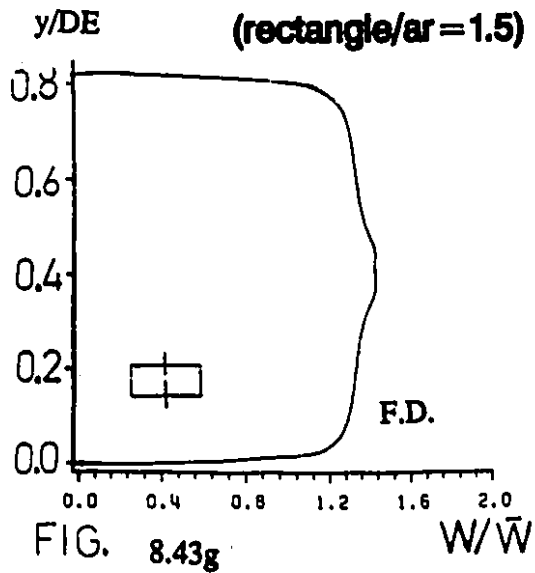
**case#4 axial - velocity profile
(pentagon)**



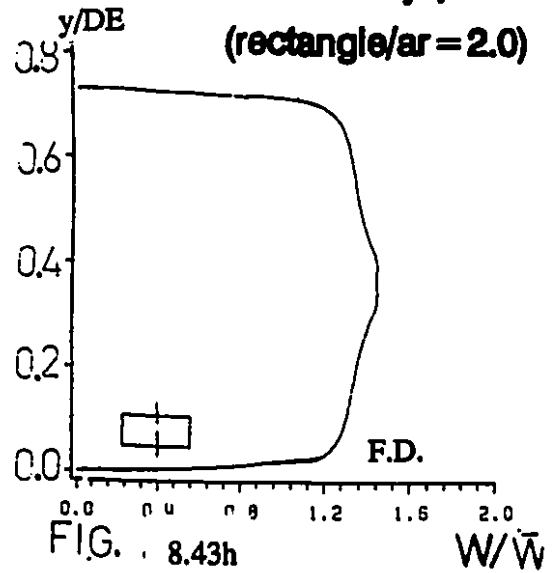
**case#4 axial - velocity profile
(hexagon)**



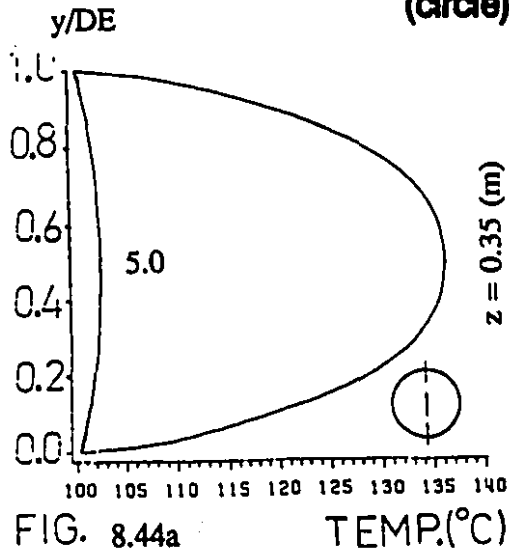
**case#4 axial - velocity profile
(rectangle/ar = 1.5)**



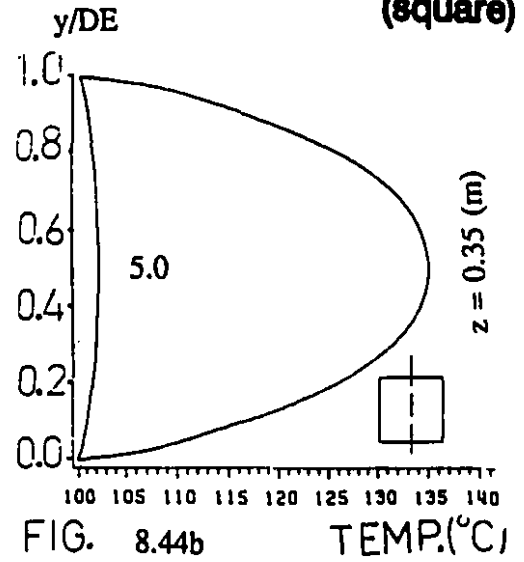
**case#4 axial - velocity profile
(rectangle/ar = 2.0)**



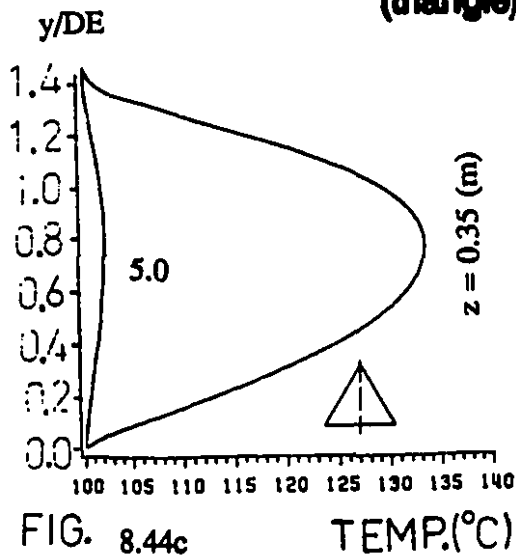
case#4 temperature profile
(circle)



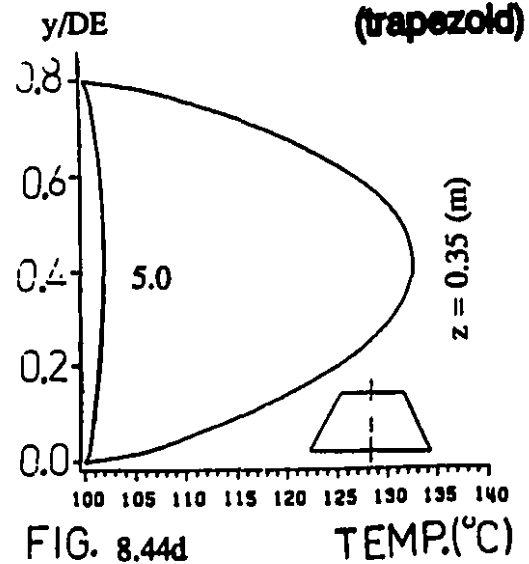
case#4 temperature profile
(square)



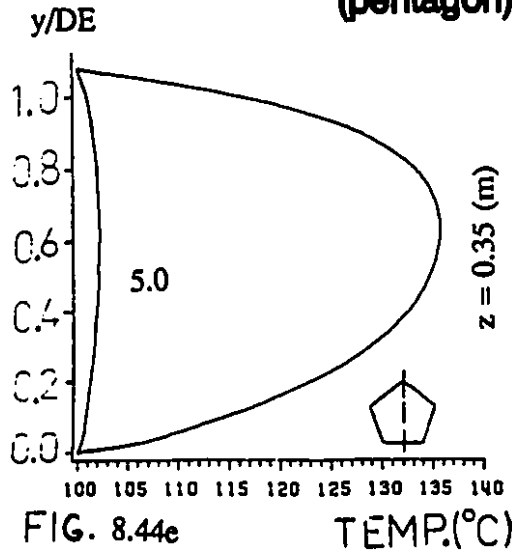
case#4 temperature profile
(triangle)



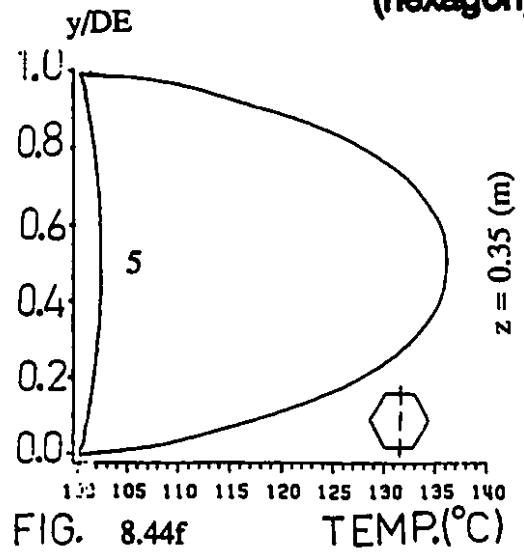
case#4 temperature profile
(trapezoid)



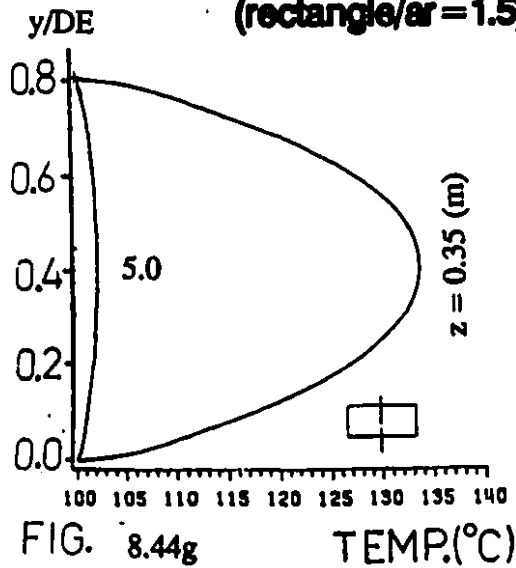
**case#4 temperature profile
(pentagon)**



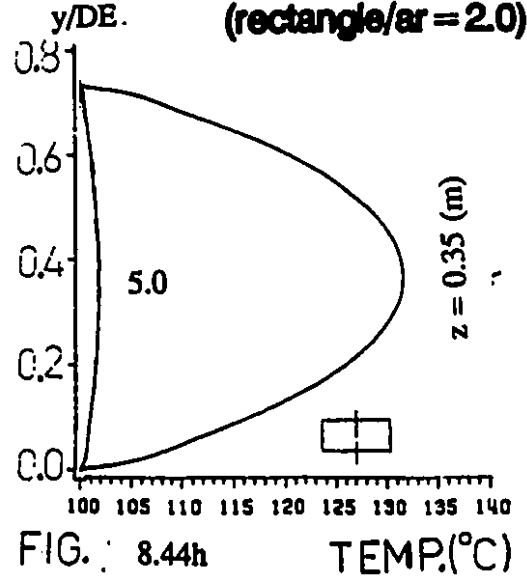
**case#4 temperature profile
(hexagon)**



**case#4 temperature profile
(rectangle/ar = 1.5)**



**case#4 temperature profile
(rectangle/ar = 2.0)**



case#4 polymer concentration profile (circle)

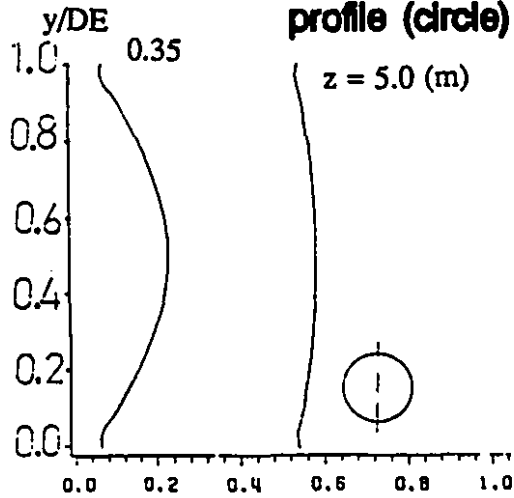


FIG. 8.45a

WP

case#4 polymer concentration profile (square)

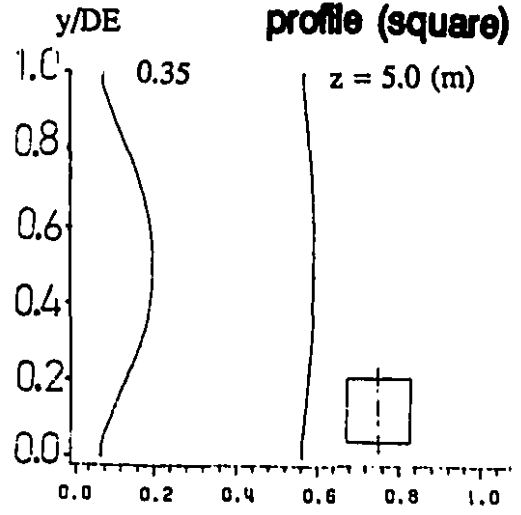


FIG. 8.45b

WP

case#4 polymer concentration profile (triangle)

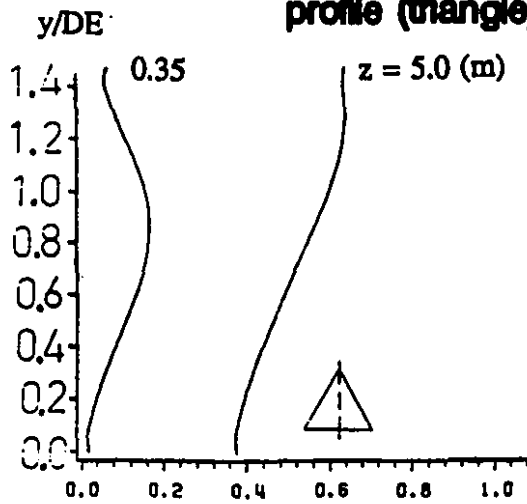


FIG. 8.45c

WP

case#4 polymer concentration profile (trapezoid)

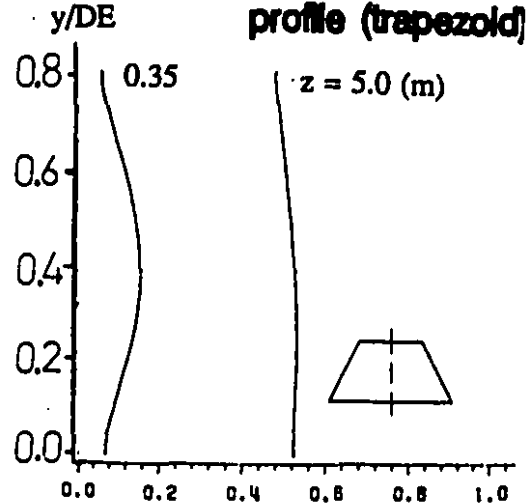


FIG. 8.45d

WP

case#4 polymer concentration profile (pentagon)

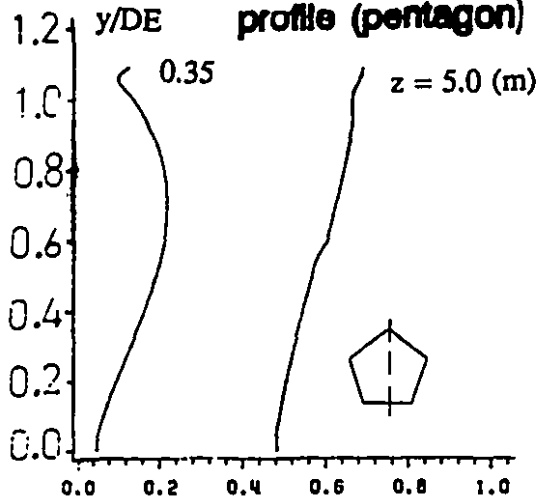


FIG. 8.45e

WP

case#4 polymer concentration profile (hexagon)

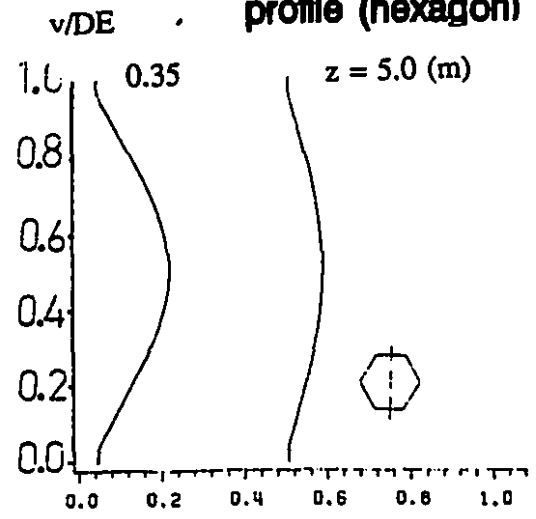


FIG. 8.45f

WP

case#4 polymer concentration profile (rectangle/ar=1.5)

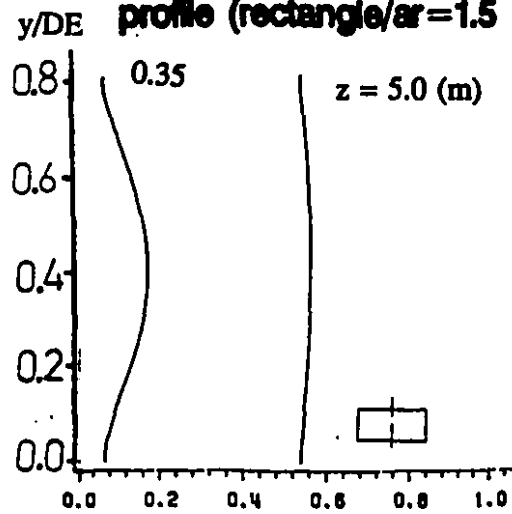


FIG. 8.45g

WP

case#4 polymer concentration profile (rectangle/ar=2.)

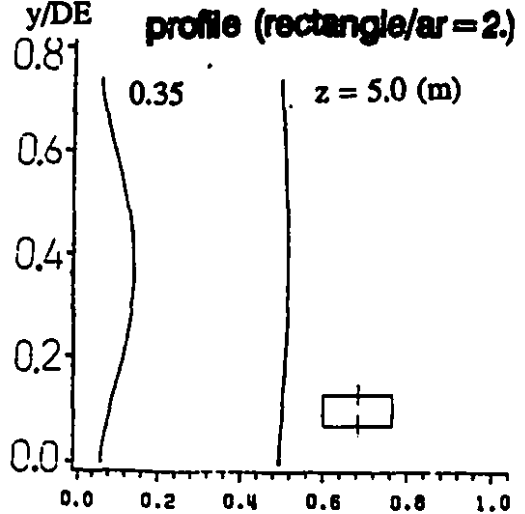


FIG. 8.45h

WP

case#4 density - profile
(circle)

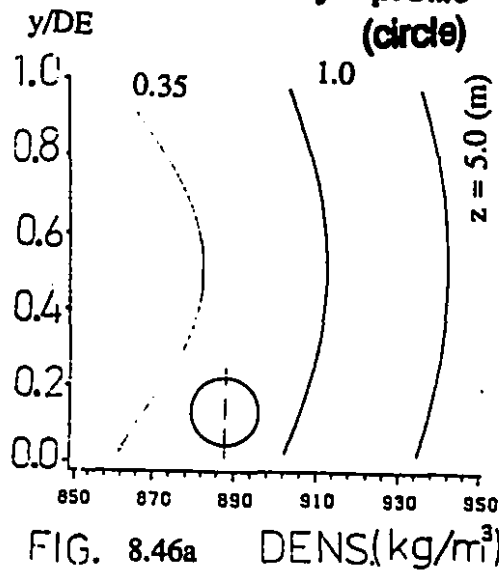


FIG. 8.46a

case#4 density - profile
(square)

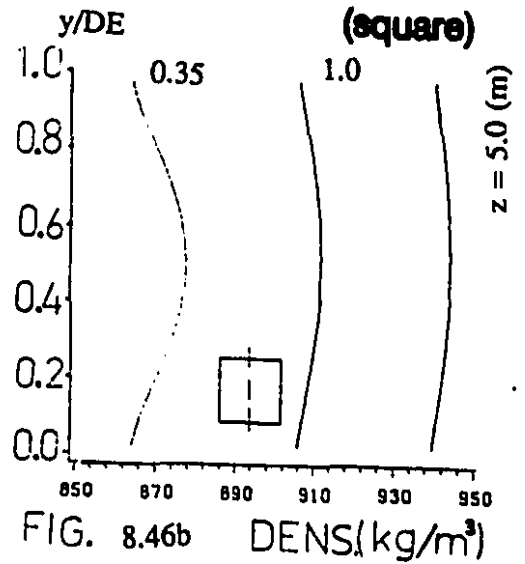


FIG. 8.46b

case#4 density - profile
(triangle)

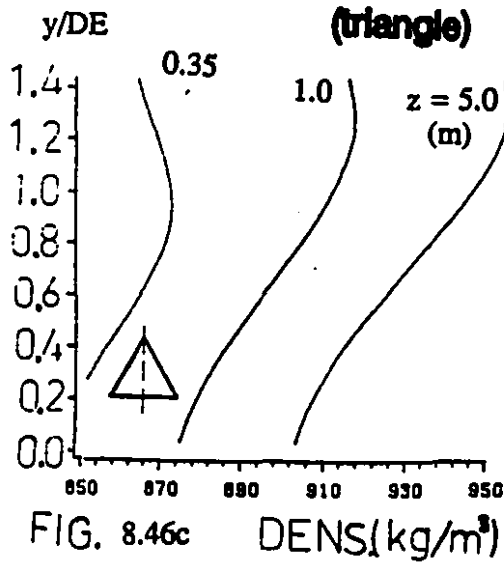


FIG. 8.46c

case#4 density - profile
(trapezoid)

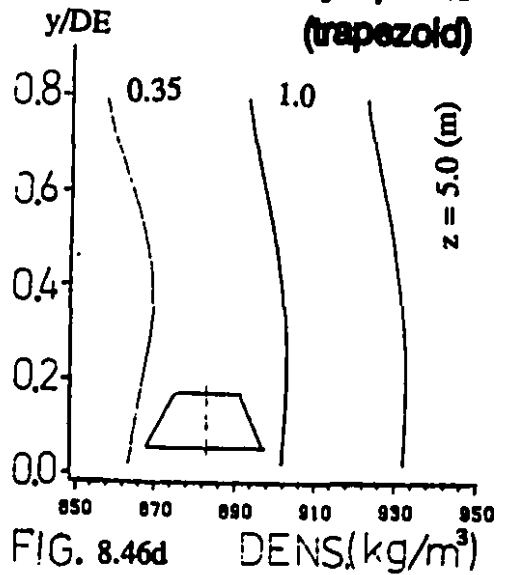
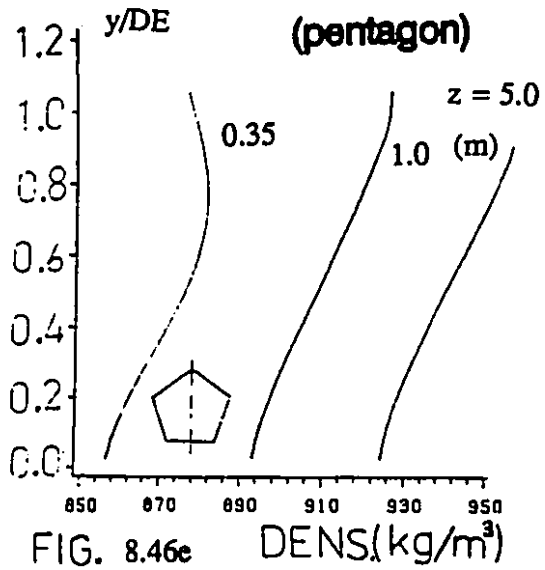
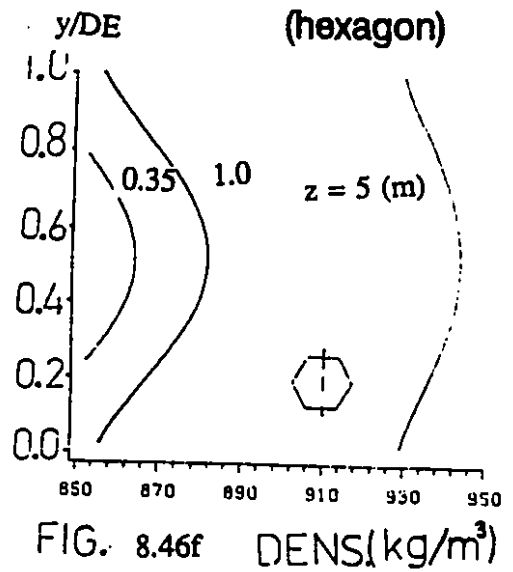


FIG. 8.46d

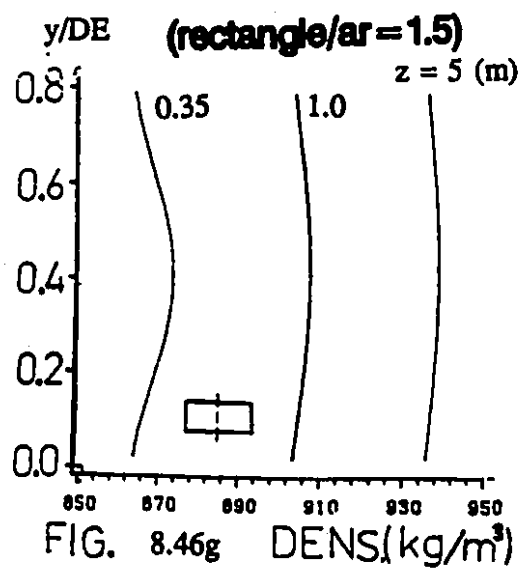
case#4 density - profile



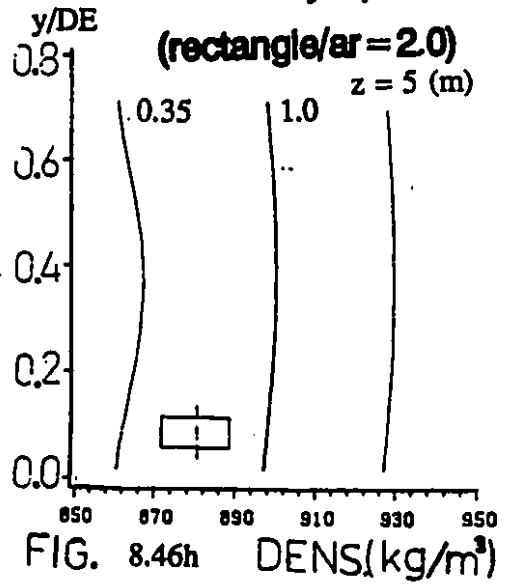
case#4 density - profile



case#4 density - profile



case#4 density - profile



case#4 viscosity - profile

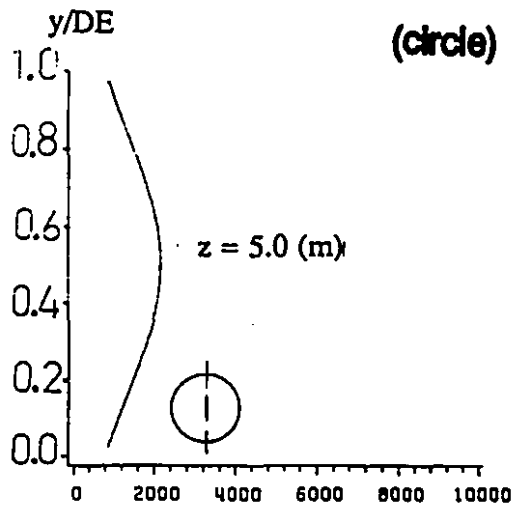


FIG. 8.47a

VISC. ($\frac{N \cdot s}{m^2}$)

case#4 viscosity - profile

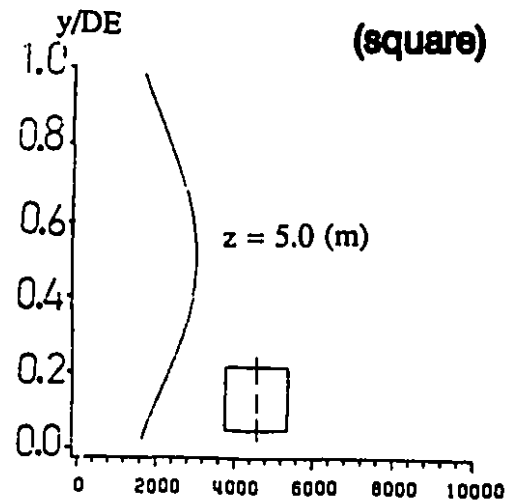


FIG. 8.47b

VISC. ($\frac{N \cdot s}{m^2}$)

case#4 viscosity - profile

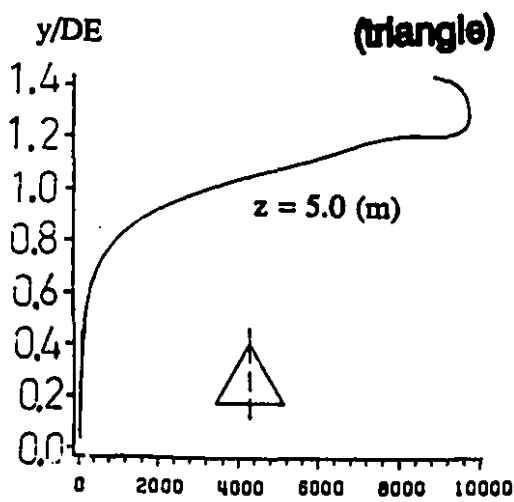


FIG. 8.47c

VISC. ($\frac{N \cdot s}{m^2}$)

case#4 viscosity - profile

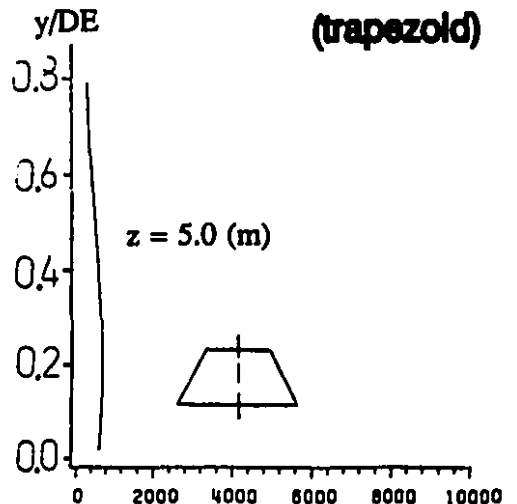


FIG. 8.47d

VISC. ($\frac{N \cdot s}{m^2}$)

case#4 viscosity - profile

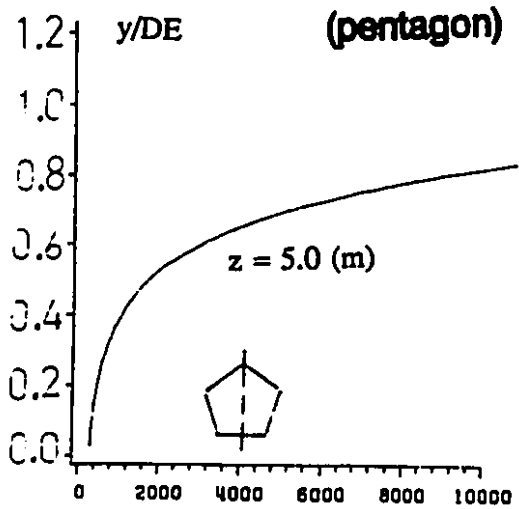


FIG. 8.47e VISC. ($\frac{N.s}{m^2}$)

case#4 viscosity - profile

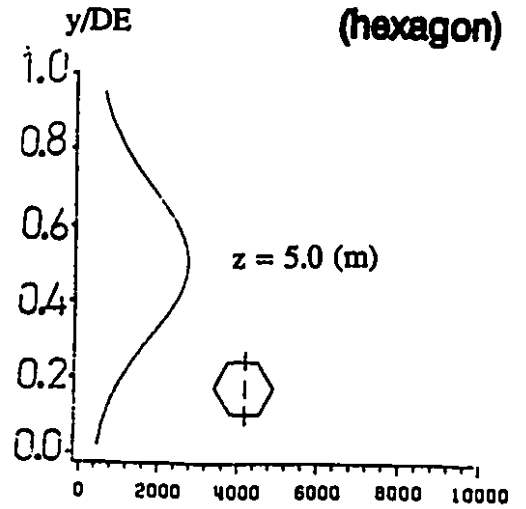


FIG. 8.47f VISC. ($\frac{N.s}{m^2}$)

case#4 viscosity - profile

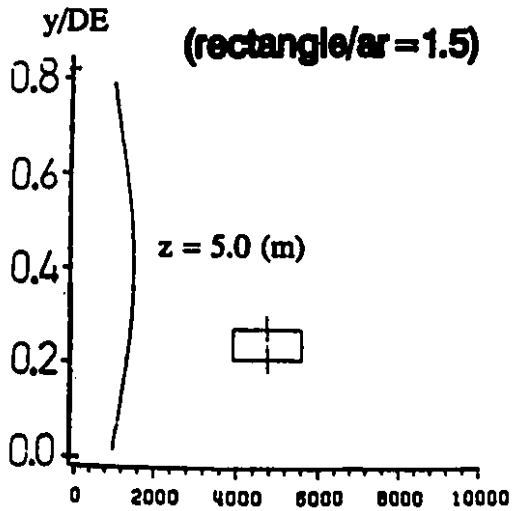


FIG. 8.47g VISC. ($\frac{N.s}{m^2}$)

case#4 viscosity - profile

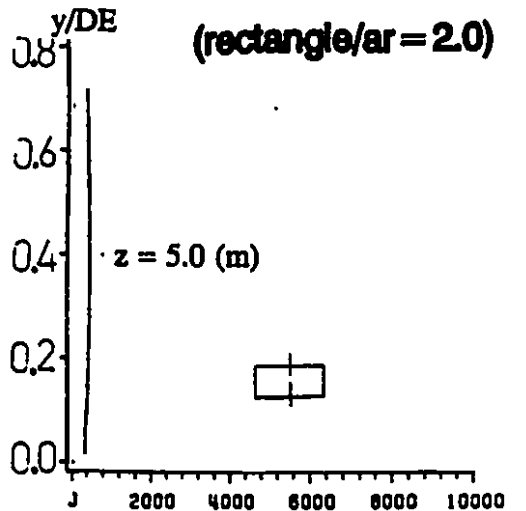
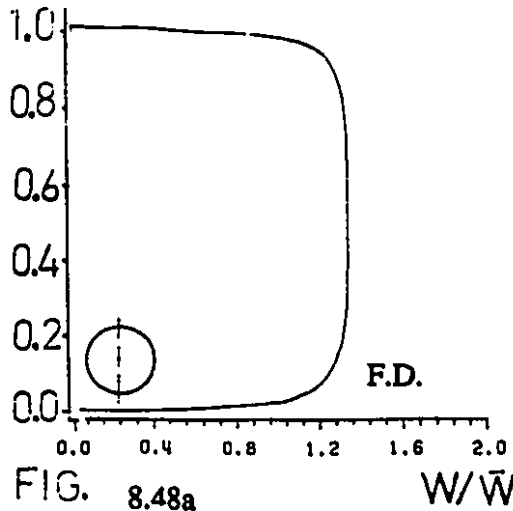


FIG. 8.47h VISC. ($\frac{N.s}{m^2}$)

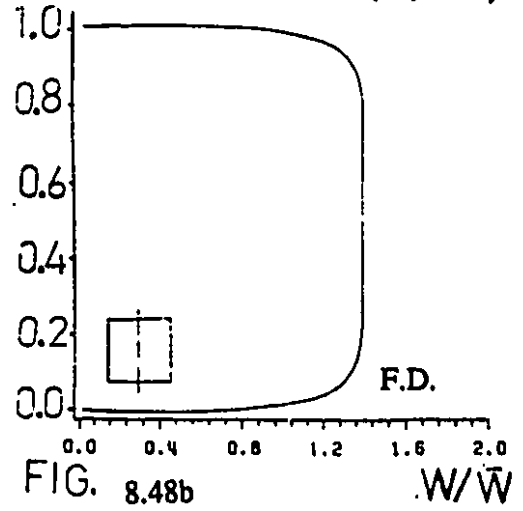
case#5 axial - velocity profile

(circle)



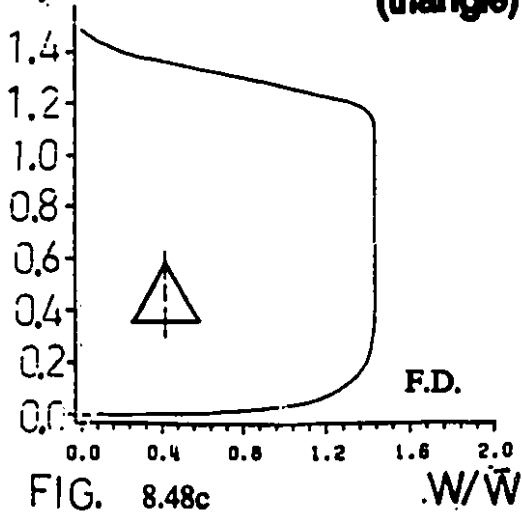
case#5 axial - velocity profile

(square)



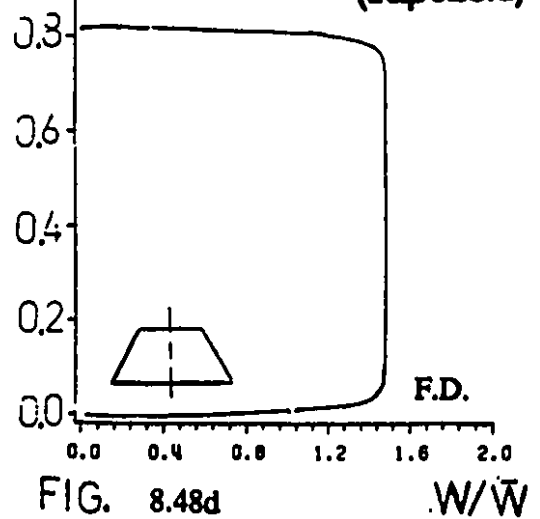
case#5 axial - velocity profile

(triangle)

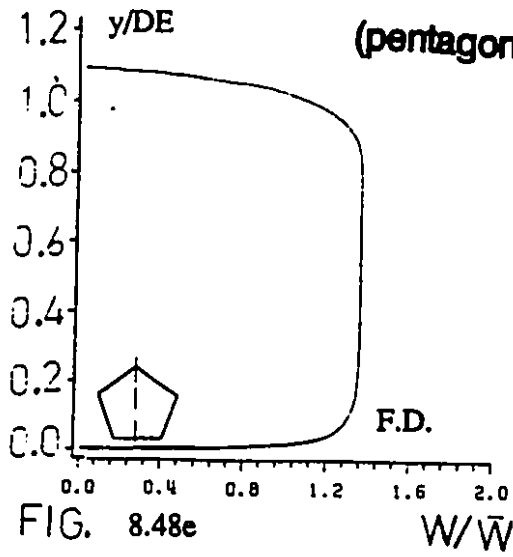


case#5 axial - velocity profile

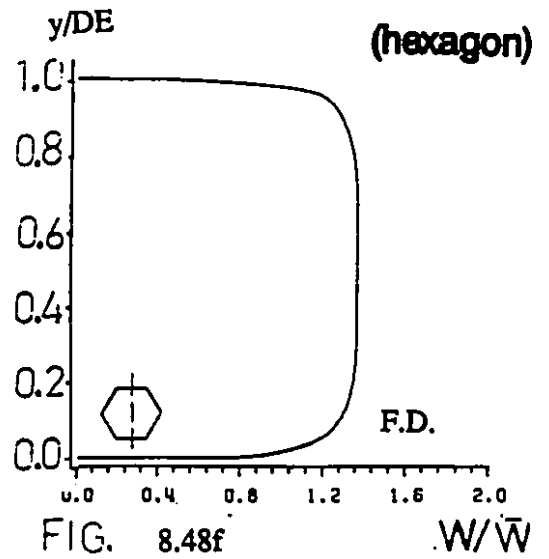
(trapezoid)



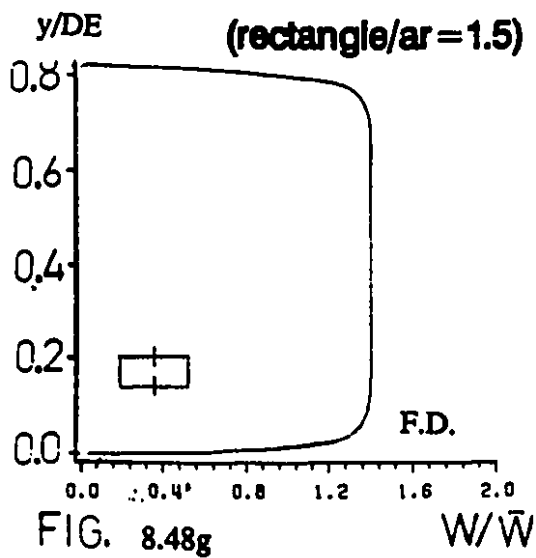
case#5 axial - velocity profile



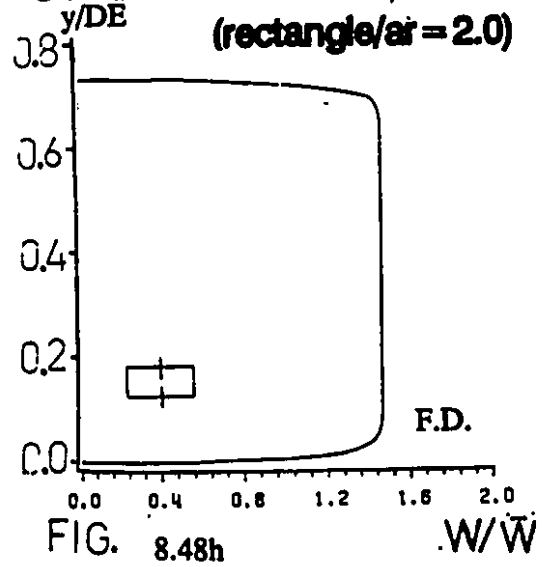
case#5 axial - velocity profile



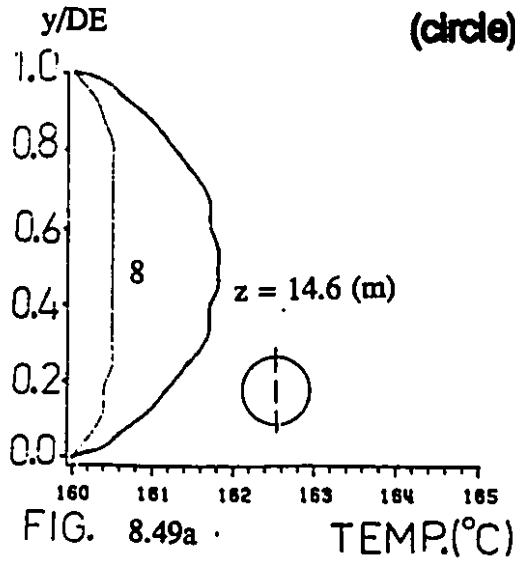
case#5 axial - velocity profile



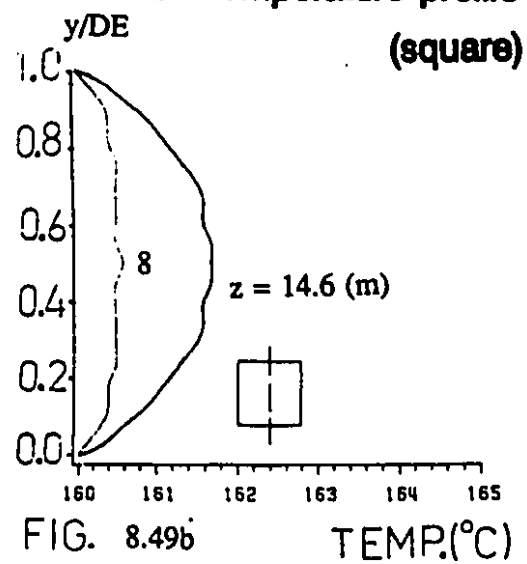
case#5 axial - velocity profile



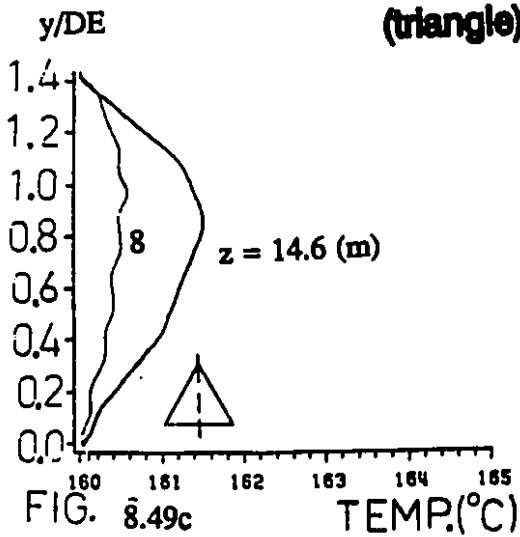
**case #5 temperature profile
(circle)**



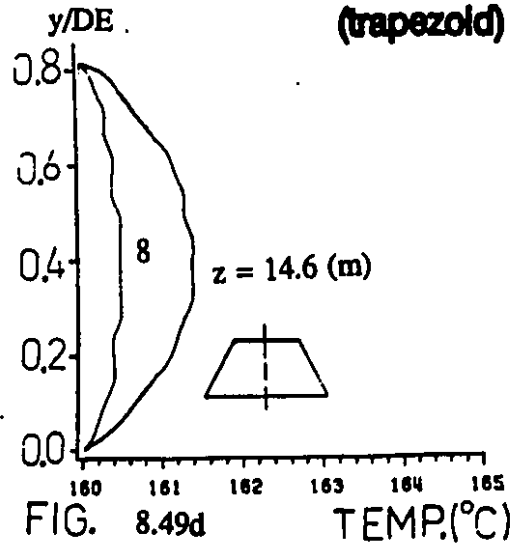
**case #5 temperature profile
(square)**



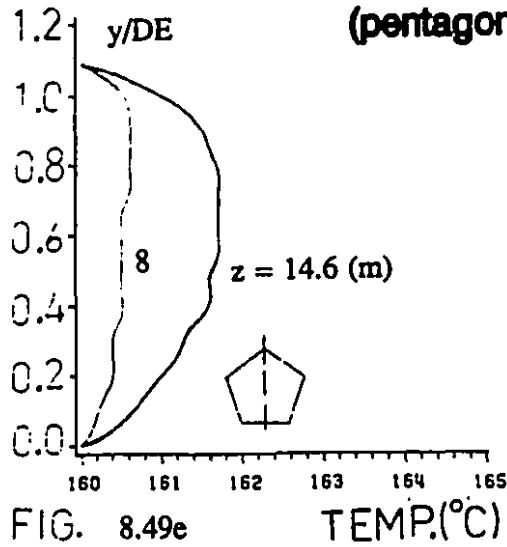
**case #5 temperature profile
(triangle)**



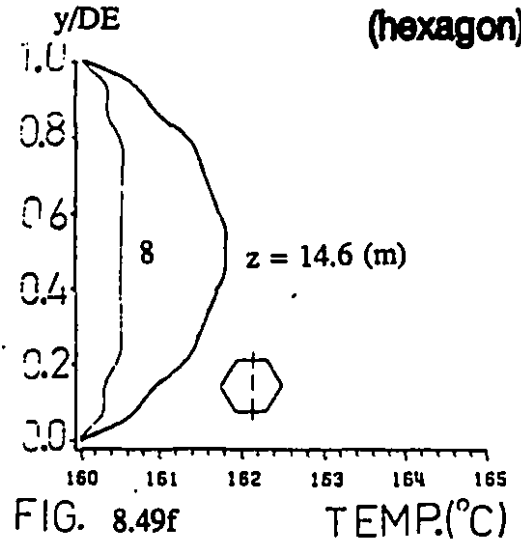
**case #5 temperature profile
(trapezoid)**



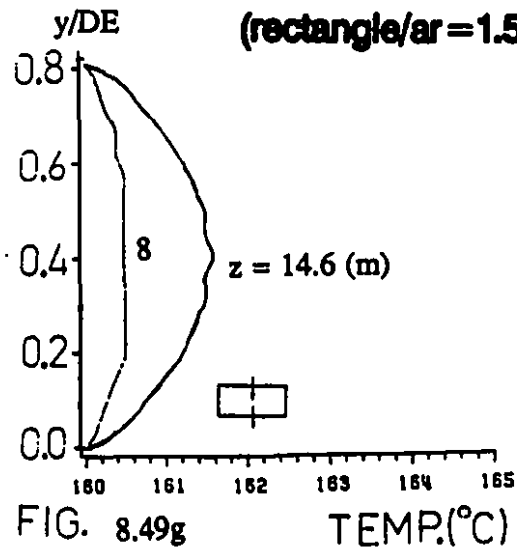
**case#5 temperature profile
(pentagon)**



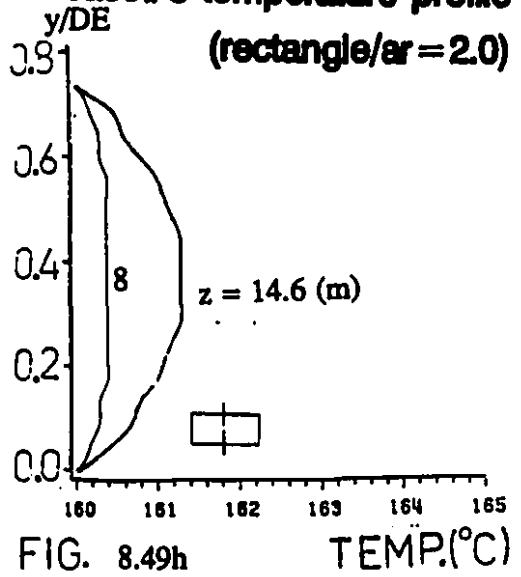
**case#5 temperature profile
(hexagon)**



**case#5 temperature profile
(rectangle/ar = 1.5)**



**case#5 temperature profile
(rectangle/ar = 2.0)**



case#5 polymer - concentration
profile (circle)

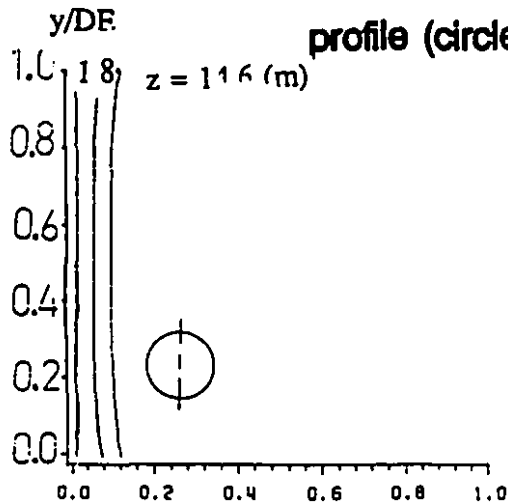


FIG. 8.50a

WP

case#5 polymer - concentration
profile (square)

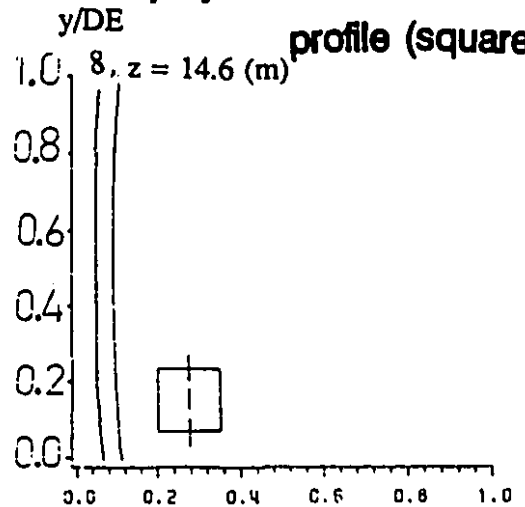


FIG. 8.50b

WP

case#5 polymer - concentration
profile (triangle)

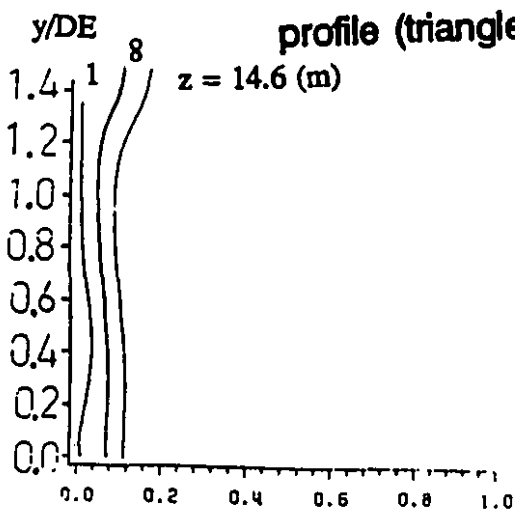


FIG. 8.50c

WP

case#5 polymer - concentration
profile (trapezoid)

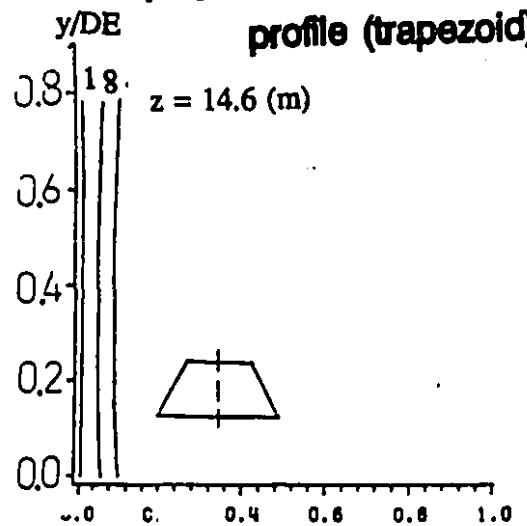


FIG. 8.50d

WP

case#5 polymer - concentration profile (pentagon)

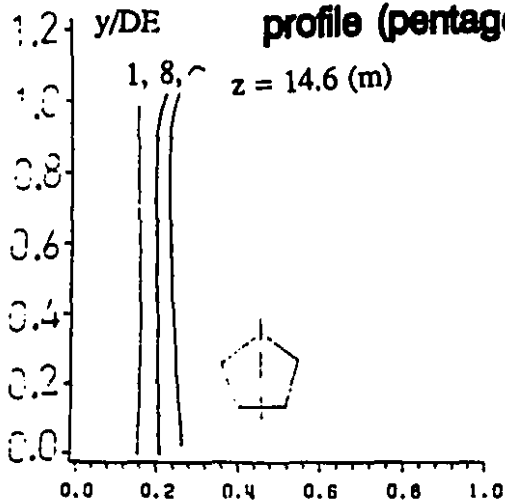


FIG. 8.50e

WP

case#5 polymer - concentration profile (hexagon)

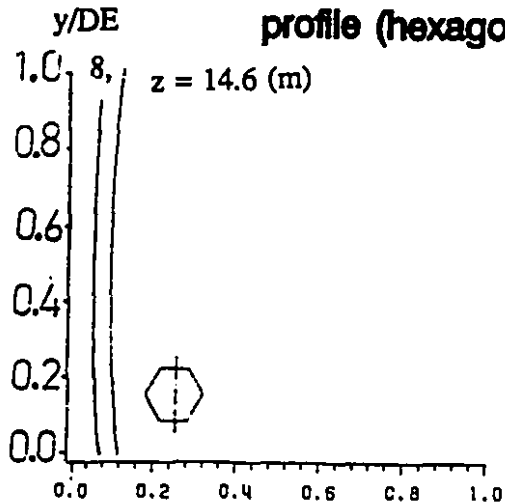


FIG. 8.50f

WP

case#5 polymer - concentration profile (rectangle/ar=1.5)

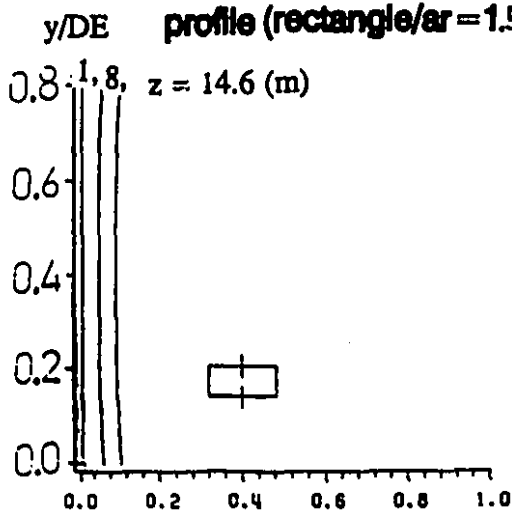


FIG. 8.50g

WP

case#5 polymer - concentration profile (rectangle/ar=2.0)

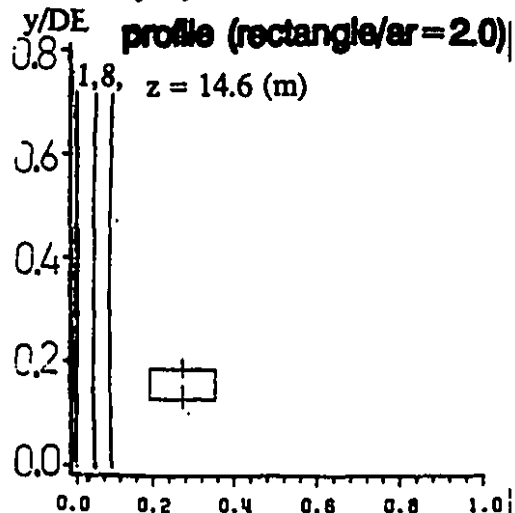
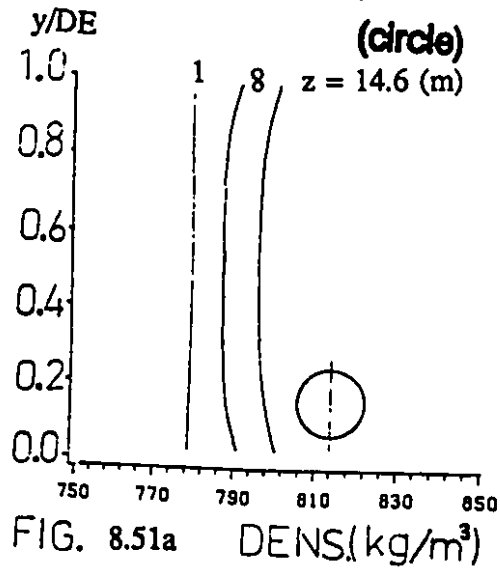


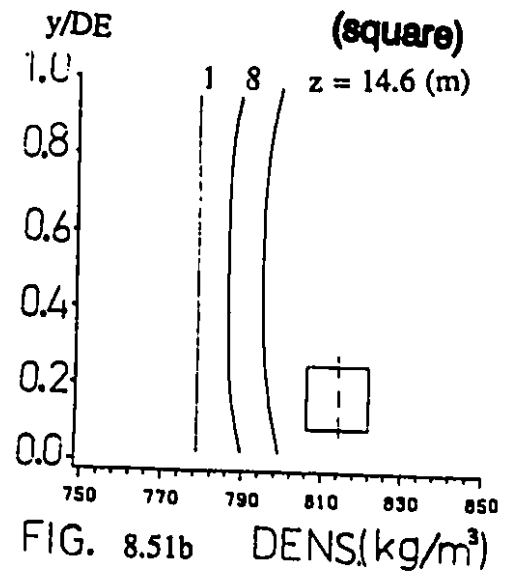
FIG. 8.50h

WP

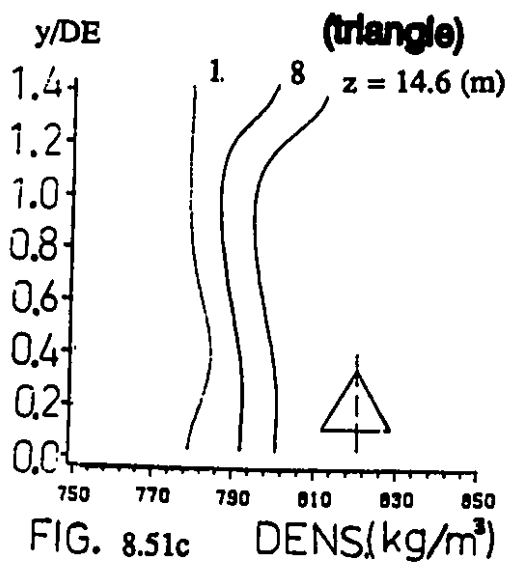
case#5 density – profile



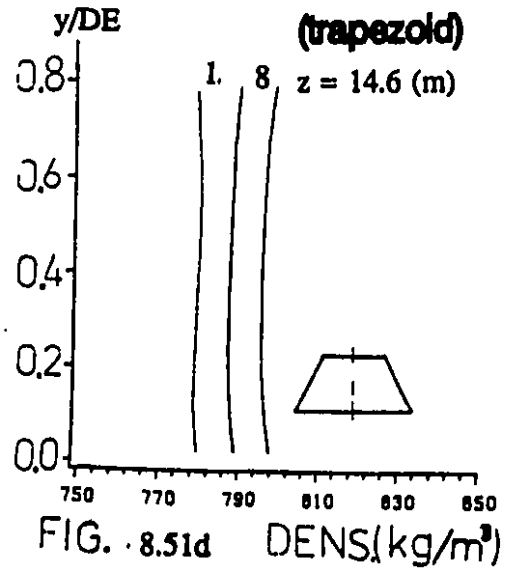
case#5 density – profile

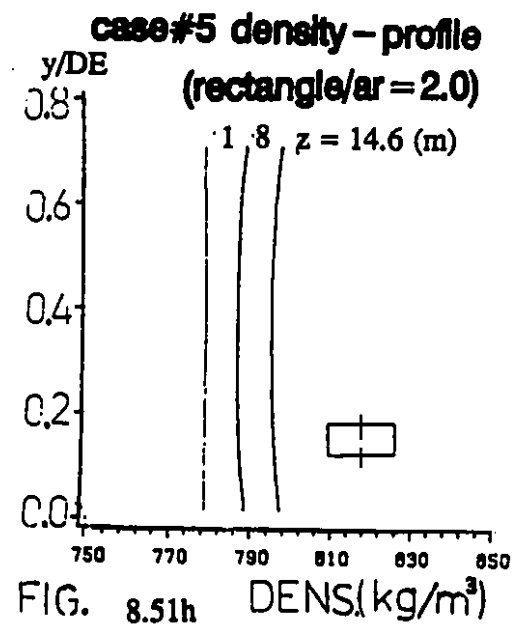
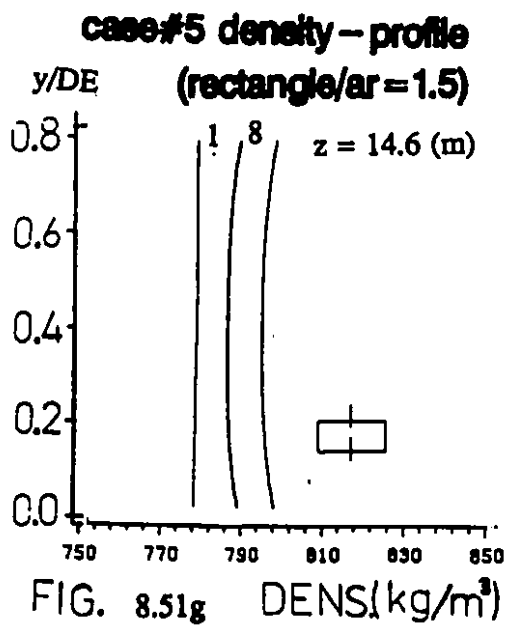
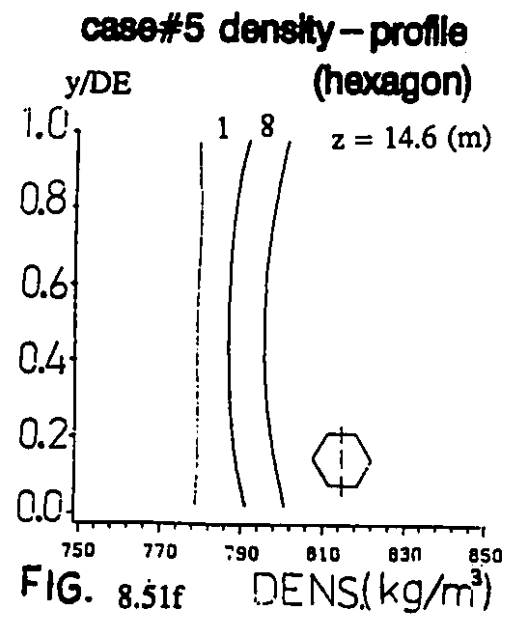
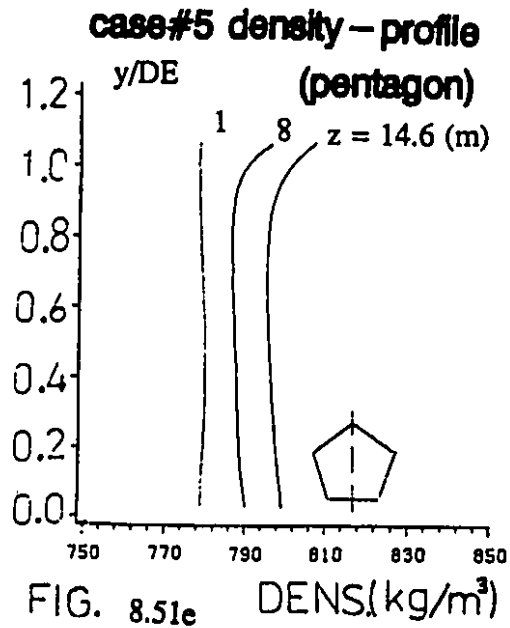


case#5 density – profile

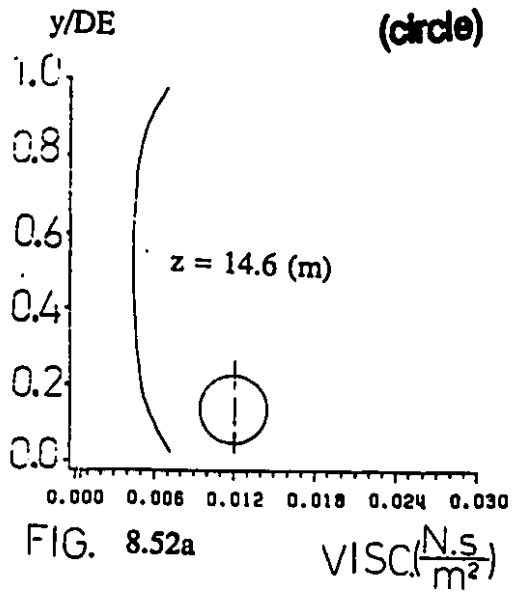


case#5 density – profile

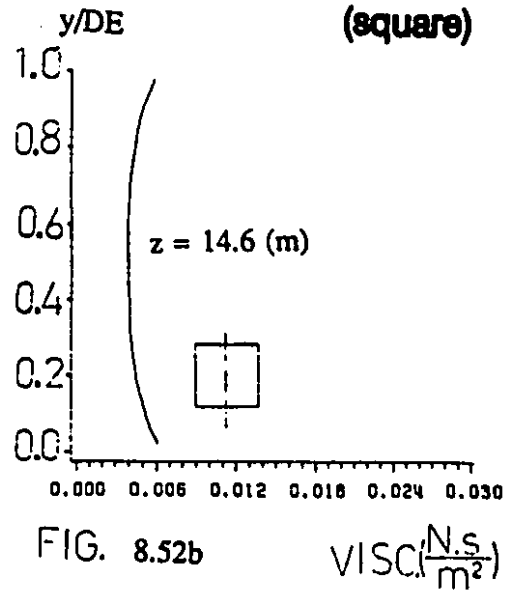




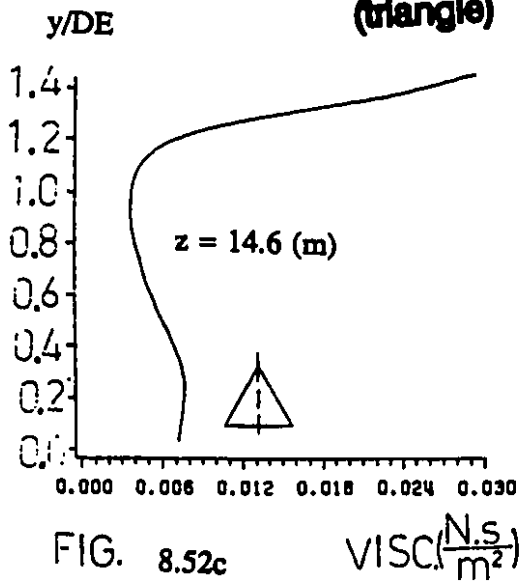
**case#5 viscosity - profile
(circle)**



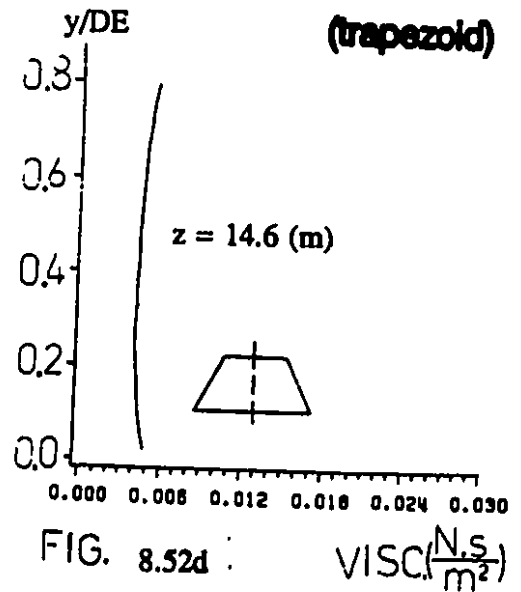
**case#5 viscosity - profile
(square)**



**case#5 viscosity - profile
(triangle)**



**case#5 viscosity - profile
(trapezoid)**



**case#5 viscosity – profile
(pentagon)**

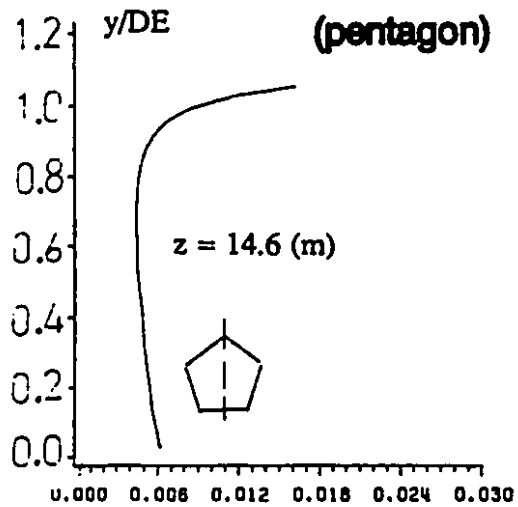


FIG. 8.52e

VISC. ($\frac{N \cdot s}{m^2}$)

**case#5 viscosity – profile
(hexagon)**

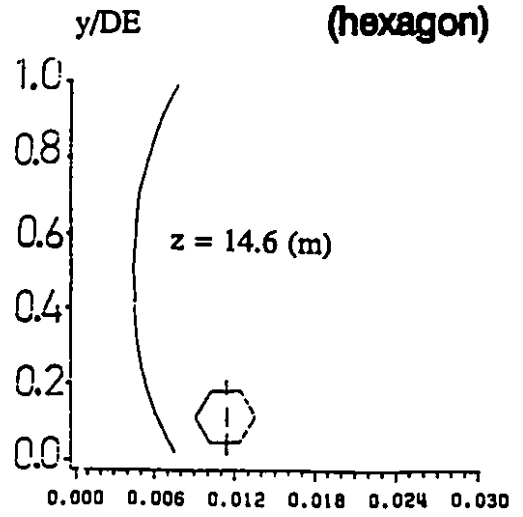


FIG. 8.52f

VISC. ($\frac{N \cdot s}{m^2}$)

**case#5 viscosity – profile
(rectangle/ar = 1.5)**

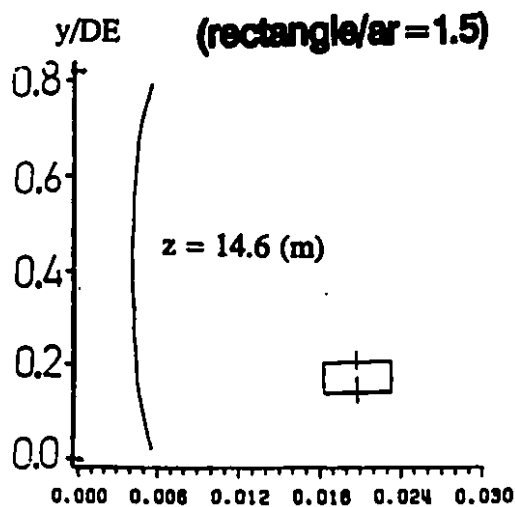


FIG. 8.52g

VISC. ($\frac{N \cdot s}{m^2}$)

**case#5 viscosity – profile
(rectangle/ar = 2.0)**

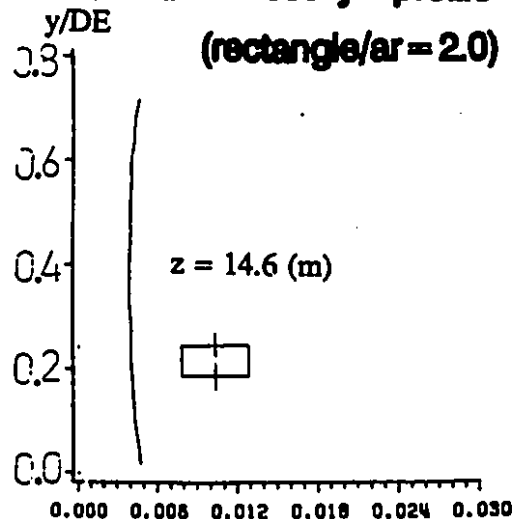


FIG. 8.52h

VISC. ($\frac{N \cdot s}{m^2}$)

CHAPTER 9

CONCLUSIONS AND CONTRIBUTIONS TO KNOWLEDGE

9.1 INTRODUCTION

The fundamental research carried-out in this study to provide a comprehensive solution procedure for steady 3D reacting laminar duct flow, heat and mass transfer in arbitrary cross-sectional ducts, suitable for both Newtonian and non-Newtonian fluids, was consequently accomplished by the development of a computer software for computational studies and simulation purposes. This software was later shown to be a powerful tool for utilization in applied research in the territories of reacting laminar duct flow transport phenomena. An extensive pile of results obtained in this area are presented in the previous chapter. The present chapter summarizes the most outstanding conclusions of this work and the elegant contributions furnished to knowledge in engineering science.

9.2 SUMMARY AND CONCLUSIONS

- (i) The non-orthogonal boundary-fitted coordinate transformation method applied and the numerical solution procedure extended in this work to employ the SIMPLER algorithm for non-Newtonian fluids, is examined successfully without any convergence difficulties and instabilities in computations, for the solution of 3D parabolized conservation equations in straight ducts of arbitrary, but uniform cross-sections.
- (ii) The results obtained for validation of system modelling and computer codes are shown to be in good agreement with the previously obtained results by other investigators for all aspects of the job, viz: fluid-flow, heat-transfer and mass-transfer with chemical reaction considered in this study.

- (iii) The application of non-orthogonal coordinates versus orthogonal systems reveals the advantage of getting rid of the generation of orthogonal grids at certain locations of difficult or impossible to make.
- (iv) The variations in the number of stations in the axial-direction for marching integration, in the parabolized 3D solution procedure, as examined in polystyrene simulation studies, provides satisfactorily close values of results.
- (v) The hydrodynamic center-plane axial-velocity development for the Newtonian fluids ($Re = 900$) shows an excellent gradual development towards parabolic pattern.
- (vi) The hydrodynamic centerline velocity values for noncircular ducts are shown to be not necessarily coincident with the peak value of the axial velocity profile due to the effect of zero shear rate at the corners of the geometries.
- (vii) The hydrodynamic center-plane axial-velocity development for the non-Newtonian case ($Re = 128$), shows a plug-flow behavior for all geometries under consideration. However, some geometries show a slight delay in the development to plug-flow velocity behavior.
- (viii) The hydrodynamic development length values obtained in this work are documented for future references. Some of these results are somewhat far from those declared previously by others.
- (ix) The secondary flow is away from the walls towards the intermediate sections at which it is reversed in direction, for all the geometries. The results of Newtonian case are higher than the results of non-Newtonian case due to the difference in the primary flow velocity profile pattern.
- (x) In the thermal studies of this work, the limiting-value of Nusselt-numbers for several specific geometries conform well with the values previously obtained by other

investigators. The $Nu_{m,T}$ results are different to some extent from the values obtained by Chandrupatla et al⁹⁹. The reason is believed to be due to the difference in the values of Prandtl numbers employed.

- (xi) The thermal entry region development profile ($Pr = 6.78$) shows an excellent gradual development in the axial direction for several geometries.
- (xii) The results for the thermal entry length value of square ducts are close to the result obtained previously by others.
- (xiii) In the simulation of styrene polymerization, only slight differences are observed in the results obtained for different geometries corresponding to each case under consideration.
- (xiv) From the conversion point of the chemical reaction under study, not a specific geometry is recognized to be in general superior than circular duct reactors.
- (xv) The free-convection effect (buoyancy effect) is negligible on the conversion of reaction in the present study.

9.3 CONTRIBUTION TO KNOWLEDGE

The developments listed under items (i)-(v) below are the consequences of the fundamental research carried-out in this work for the numerical solution of reacting laminar duct flow heat and mass transfer in ducts of arbitrary cross-sections for power-law fluids. This job was later followed by an applied research employing the developed computer codes in the potential areas of interest. The originalities obtained in the latter part are listed in items (vi), (vii) and (viii) below.

- (i) Development of the general non-orthogonal boundary-fitted solution procedure to handle non-Newtonian fluids for 3D parabolized conservation equations. This includes the

derivation of the coefficients of the pressure-correction equation to handle power-law fluids to be employed in the SIMPLER algorithm.

- (ii) Contribution to existing knowledge in the area of numerical fluid-flow and heat-transfer by detailed hand-calculations from which appropriate relations are evolved for machine-computations, employing the philosophy of non-orthogonal boundary-fitted coordinate transformation and the control-volume discretization approach.
- (iii) Development of a non-orthogonal grid generation programme in Fortran coding, corresponding to B-type arrangement in the transformed-plane for arbitrary geometries.
- (iv) Development of a general computer programme in Fortran coding for the solution of any 3D laminar duct flow heat and mass transfer problem with chemical reaction in straight ducts of arbitrary cross-sections for Newtonian and non-Newtonian fluids.
- (v) Full testing and validation of system modelling and computer-codes by comparison of the predicted results obtained in this work with the theoretical, experimental and numerical results of other investigators in open literature for the fluid flow, heat transfer and mass transfer aspects of the job.
- (vi) Contribution to existing knowledge in the area of fluid flow by the original results obtained for velocity profile development and pressure-drop analysis of the hydrodynamic entrance region of triangular, trapezoidal and pentagonal ducts for Newtonian and non-Newtonian fluids. Laminar secondary flow analysis is also presented for all geometries mentioned above for both Newtonian and non-Newtonian cases.
- (vii) Contribution to existing knowledge in the area of heat-transfer by the original results obtained for temperature profile development and Nusselt number variations of the

thermal entrance region of the geometries mentioned in item (vi) for Newtonian and non-Newtonian fluids.

- (viii) Contribution to existing knowledge in the area of thermal polymerization of styrene by the original results obtained from simulation of manufacturing of polystyrene in arbitrary cross-sectional duct reactors. In this respect, extensive group of results are documented for five different sets of operating conditions in eight different geometries.

The results in the latter area include molecular weights distribution, pressure-drop analysis, velocity, temperature, concentration, density and viscosity profiles. It is to be mentioned that even for circular duct reactors, there exists only a few results for some of these items in open literature.

REFERENCES

1. R.C.L. Bosworth, Distribution of reaction times for laminar flow in cylindrical reactors, *Phil. Mag.*, 39, No. 7, 847-862, 1948.
2. K.G. Denbigh, The kinetics of continuous reaction process: application to polymerization, *J. Appl. Chem.*, 1, 227-236, 1951.
3. F.A. Cleland, and R.H. Wilhelm, Diffusion and reaction in viscous-flow tubular reactor, *AIChE Journal*, 2, No. 4, 489-497, 1956.
4. H.A. Lauwerier, A diffusion problem with chemical reaction, *Appl. Sci. Res.*, 8, 366-376, 1959.
5. E.H. Wissler, and R.S. Schechter, A further note on a diffusion problem with chemical reaction, *Appl. Sci. Res.*, 10, 198-204, 1961.
6. S. Katz, Chemical reactions catalyzed on a tube wall, *Chem. Eng. Sci.*, 10, 202-211, 1959.
7. R.E. Walker, Chemical reaction and diffusion in a catalytic tubular reactor, *The Physics of Fluids*, 4, 1211-1216, 1961.
8. Chia-Jung Hsu, A method of solution for mass-transfer with chemical reaction under conditions of viscous flow in a tubular reactor, *AIChE Journal*, 11, 938-940, 1965.
9. R.L. Solomon, and J.L. Hudson, Heterogeneous and homogeneous reactions in a tubular reactor, *AIChE Journal*, 13, 545-550, 1967.
10. L.J. Snyder, T.W. Spriggs, and W.E. Stewart, Solution of the equation of change by Galerkin's method, *AIChE Journal*, 10, No. 4, 535-540, 1964.
11. G.M. Brown, Heat or mass transfer in a fluid in laminar flow in a circular or flat conduit, *AIChE Journal*, 6, No. 2, 179-183, 1960.
12. J.R. Sellars, M. Tribus, and J.S. Klein, Heat transfer to laminar flow in a round tube or flat conduit - The Graetz problem extended, *Trans. of the ASME*, 78, 441-448, 1956.
13. R.V. Homsy, and R.D. Strohman, Diffusion and chemical reaction in a tubular reactor with non-Newtonian laminar flow, *AIChE Journal*, 17, 215-219, 1971.
14. F.T. Osborne, Purely convective models for tubular reactors with non-Newtonian flow, *Chem. Eng. Sci.*, 30, 159-166, 1975.
15. O. Levenspiel, *Chemical Reaction Engineering*, John Wiley and Sons, N.Y., 1962.

16. S.Y. Tsay, and H.S. Yu, Diffusion and chemical reaction in the entrance region of a circular tube with non-Newtonian laminar flow, *Journal of The Chinese Institute of Chemical Engineers*, 13, 177-182, 1982.
17. C. Venkatsubramanian, and R. Mashelkar, Convective diffusion with reaction in developing flow of a non-Newtonian fluid, *Ind. Eng. Chem. Process Des. Dev.*, 22, No. 3, 509-514, 1983.
18. H.L. Langhaar, Steady flow in the transition length of a straight tube, *Journal of Applied Mech.*, *Trans. Am. Soc. Mech. Eng.*, 64, (A-55) - (A-58), 1942.
19. O.N. Cavatorta, and R.D. Tonini, Diffusion and chemical reaction in tubular reactor with non-Newtonian fluids, *Int. Comm. Heat Mass Transfer*, 12, 441-449, 1985.
20. J.V. Villadsen, and W.E. Stewart, Solution of boundary-value problems by orthogonal collocation, *Chem. Eng. Sci.*, 22, 1483-1501, 1967.
21. A. Hui, and A.E. Hamielec, Thermal polymerization of styrene at high conversions and temperatures, An experimental study, *J. Appl. Polymer Sci.*, 16, 749-762, 1972.
22. R. Sala, F. Valz-Gris, and L. Zanderighi, A Fluid-dynamic study of a continuous polymerization reactor, *Chem. Eng. Sci.*, 29, 2205-2212, 1974.
23. C.E. Wyman, and L.F. Carter, A numerical model for tubular polymerization reactors, *AIChE Symposium Series*, No. 160, Vol. 72, 1-16, 1976.
24. A Husain, and A.E. Hamielec, Bulk thermal polymerization of styrene in a tubular reactor - a computer study, *AIChE Symposium Series*, No. 160, Vol. 72, 112-127, 1976.
25. L. Valsamis, and J.A. Biesenberger, Continuous bulk polymerization in tubes, *AIChE Symposium Series*, No. 160, Vol. 72, 18-27, 1976.
26. L. Valsamis, and J.A. Biesenberger, Continuous bulk polymerization of styrene in a tubular reactor, *AIChE Annual Meeting*, N.Y., N.Y., 1977.
27. C.C. Chen, Polymerization in a laminar flow tubular reactor, Ph.D. Thesis, Rensselaer Polytechnic Institute, Troy, N.J., 1986.
28. C.C. Chen, and E.B. Nauman, Verification of a complex, variable viscosity model for a tubular polymerization reactor, *Chem. Eng. Sci.*, 44, No. 1, 179-188, 1989.
29. C. Kleinstreuer, and S. Agarwal, Coupled heat and mass transfer in laminar flow, tubular polymerizers, *Int. J. Heat Mass Transfer*, 29, No. 7, 979-986, 1986.
30. S.S. Agarwal, and C. Kleinstreuer, Analysis of styrene polymerization in a continuous flow tubular reactor, *Chem. Eng. Sci.*, 41, No. 12, 3101-3110, 1986.

31. P.V. Shirkov, The salient features of heat and mass-transfer in polymerization processes, USSR Academy of Sciences, 13 - IN - 19, 431-435, 1989.
32. A.Y. Malkin, and P.V. Zhirkov, Flow of polymerizing liquids, Adv. Polymer Sci., 95, 111-147, 1990.
33. R.B. Bird, W.E. Stewart, and E.N. Lightfoot, Transport Phenomena, John Wiley and Sons, N.Y., 1960.
34. A.H.P. Skelland, Non-Newtonian Flow and Heat-Transfer, John Wiley and Sons, N.Y., 1967.
35. A. Lawal, and A.S. Mujumdar, Laminar flow and heat-transfer in power-law fluids flowing in arbitrary cross-sectional ducts, Numerical Heat Transfer, 8, 217-244, 1985.
36. A. Lawal, and A.S. Mujumdar, Forced convection heat transfer to a power-law fluid in arbitrary cross-section ducts, The Canadian Journal of Chem. Eng., 62, 326-333, 1984.
37. A. Lawal, Laminar flow and heat-transfer to variable property power law fluids in ducts of arbitrary but uniform cross-section, Ph.D. Thesis, McGill University, 1985.
38. A. Lawal, and A.S. Mujumdar, Developing flow and heat-transfer to power-law fluids in square, trapezoidal and pentagonal ducts, Int. Comm. in Heat and Mass Transfer, 12, 23-31, 1985.
39. S. Kakac, R.K. Shah, and W. Aung, Handbook of Single-Phase Convective Heat Transfer, John Wiley and Sons, N.Y., 1987.
40. P.H.G. Allen, Heat and mass transfer by combined forced and natural convection, The Institution of Mechanical Engineers, 1972.
41. S. Ostrach, Laminar natural-convection flow and heat transfer of fluids with and without heat sources in channels with constant wall temperatures, NACA Technical Note 2863, 1952.
42. S.V. Patankar, and D.B. Spalding, A calculation procedure for heat, mass and momentum transfer in three-dimensional parabolic flows, Int. J. Heat Mass Transfer, 15, 1787-1806, 1972.
43. W.R. Briley, Numerical method for predicting three-dimensional steady viscous flow in ducts, J. Comp. Physics, 14, 8-28, 1974.
44. D.W. Roberts, and C.K. Forester, Parabolic procedure for flows in ducts with arbitrary cross-sections, AIAA Journal, 17, No. 1, 1979.

45. C.R. Maliska, A solution method for three-dimensional parabolic fluid flow problems in nonorthogonal coordinates, Ph.D. Thesis, University of Waterloo, Canada, 1981.
46. C.R. Maliska, and G.D. Raithby, A method for computing three dimensional flows using non-orthogonal boundary-fitted coordinates, *Int. J. for Numerical Methods in Fluids*, 4, 519-537, 1984.
47. V.S. Prapat, and D.B. Spalding, Fluid flow and heat-transfer in three-dimensional duct flows, *Int. J. Heat Mass Transfer*, 19, 1183-1188, 1976.
48. W.H. Chu, Development of a general finite difference approximation for a general domain, *J. Comp. Physics*, 8, 392-408, 1971.
49. F.C. Thames, J.F. Thompson, C.W. Mastin, and R.L. Walker, Numerical solutions for viscous and potential flow about arbitrary two-dimensional bodies using body-fitted coordinate systems, *J. Comp. Physics*, 24, 245-273, 1977.
50. J.F. Thompson, F.C. Thames, and C.W. Mastin, TOMCAT - A code for numerical generation of boundary-fitted curvilinear coordinate systems on fields containing any number of arbitrary two-dimensional bodies, *J. Comp. Physics*, 24, 274-302, 1977.
51. J.F. Thompson, F.C. Thames, and C.W. Mastin, Boundary-fitted curvilinear coordinate systems for solution of partial differential equations on fields containing any number of arbitrary two-dimensional bodies, Report CR-2729, NASA Langley Research Centre, 1977.
52. C.W. Mastin, and J.F. Thompson, Three-dimensional body-fitted coordinate systems for numerical solution of the Navier-Stokes equations, AIAA 78-1147, 1978.
53. P.D. Thomas, and J.F. Middlecoff, Direct control of the grid point distribution in meshes generated by elliptic equations, *AIAA Journal*, 18, No. 6, 1980.
54. Numerical Grid Generation Techniques, NASA Conference Publication 2166, NASA Langley Research Center, 1980.
55. C.D. Mobley, and R.J. Stewart, On the numerical generation of boundary fitted orthogonal curvilinear coordinate systems, *J. Comp. Physics*, 34, 124-135, 1980.
56. J.F. Thompson, U.A. Warsi, and C.W. Mastin, Boundary-fitted coordinate systems for numerical solution of partial differential equations - A Review, *J. Comp. Physics*, 47, 1-108, 1982.
57. J.F. Thompson, Grid generation techniques in computational fluid dynamics, *AIAA Journal*, 22, No. 11, 1505-1523, 1984.

58. C.F. Shieh, Three-dimensional grid generation using elliptic equations with direct grid distribution control, *AIAA Journal*, 22, No. 3, 361-364, 1984.
59. K. Miki, and T. Takagi, A domain decomposition and overlapping method for the generation of three-dimensional boundary-fitted coordinate systems, *J. Comp. Physics*, 53, 319-330, 1984.
60. J.F. Thompson, U.A. Warsi, and C.W. Mastin, *Numerical Grid Generation*, North-Holland, 1985.
61. J. Hauser, H.G. Paap, D. Eppel, and S. Sengupta, Boundary conformed coordinate systems for selected two-dimensional fluid flow selected two-dimensional fluid flow problems. Part I: Generation of BFCs, *Int. Journal for Num. Methods in Fluids*, 6, 507-527, 1986.
62. G.A. Jenkins, and R.J. Keller, A boundary fitted coordinate system for the prediction of flooding in natural river systems, *Computational Techniques and Applications: CTAC-87*, Elsevier Science Publishers B.V. (North-Holland), 301-311, 1988.
63. J.F. Thompson, Three-dimensional grid generation for complex configurations - recent progress, *AGARD 309*, North Atlantic Treaty Organization, 1988.
64. S. Ramanathan, and R. Kumar, Comparison of boundary-fitted coordinates with finite-element approach for solution of conduction problems, *Numerical Heat Transfer*, 14, 187-211, 1988.
65. J.F. Gabitto, and R.J. Aguerre, A method for generation of discrete orthogonal coordinates, *Latin American Research*, 20, 95-101, 1990.
66. G.V. Hadjisophocleous, A.C.M. Sousa, and J.E.S. Venart, Prediction of transient natural convection in enclosures of arbitrary geometry using a nonorthogonal numerical model, *Numerical Heat Transfer*, 13, 373-392, 1988.
67. W. Shyy, S.S. Tong, and S.M. Correa, Numerical recirculating flow calculation using a body-fitted coordinate system, *Numerical Heat Transfer*, 8, 99-113, 1985.
68. M. Braaten, and W. Shyy, A study of recirculating flow computation using body-fitted coordinates: consistency aspects and mesh skewness, *Numerical Heat Transfer*, 9, 559-574, 1988.
69. S.V. Patankar, *Numerical Heat Transfer and Fluid Flow*, Hemisphere Publishing Corporation, N.Y., 1980.
70. S.V. Patankar, *Computation of Conduction and Duct Flow Heat Transfer*, Innovative Research Inc., Maple Grove, MN, 1991.

71. G.D. Raithby, and G.E. Schneider, Numerical solution of problems in incompressible fluid flow: treatment of the velocity - pressure coupling, *Numerical Heat Transfer*, 2, 417-440, 1979.
72. F.R. Mayo, The dimerization of styrene, *J. Amer. Chem. Soc.*, 90, 1289-1295, 1968.
73. Y.K. Chong, E. Rizzardo, and D.H. Solomon, Confirmation of the Mayo mechanism for the initiation of the thermal polymerization of styrene, *J. Amer. Chem. Soc.*, 105, 7761-7762, 1983.
74. R. Courant, and F. John, *Calculus and Analysis*, Vol. 2, John Wiley and Sons, N.Y. 1974.
75. L. Lapidus, and G.F. Pinder, *Numerical Solution of Partial Differential Equations in Science and Engineering*, John Wiley and Sons, N.Y., 1982.
76. P.J. Roache, *Computational Fluid Dynamics*, Hermosa Publishers, Albuquerque, N.M., 1972.
77. D.A. Anderson, J.C. Tannehill, and R.H. Pletcher, *Computational Fluid Mechanics and Heat Transfer*, McGraw-Hill, N.Y., 1984.
78. K.A. Hoffmann, *Computational Fluid Dynamics for Engineers*, Engineering Education System, TX, 1989.
79. B.A. Finlayson, *The Method of Weighted Residuals and Variational Principles*, Academic Press, N.Y., 1972.
80. R. Aris, *Vectors, Tensors, and the Basic Equations of Fluid Mechanics*, Prentice-Hall, Englewood Cliffs, N.J., 1962.
81. W.M. Kays, and M.E. Crawford, *Convective Heat and Mass Transfer*, 2nd Ed., McGraw-Hill, N.Y., 1980.
82. V.S. Arpaci, and P.S. Larsen, *Convective Heat Transfer*, Prentice Hall, N.J., 1984.
83. A. Bejan, *Convection Heat Transfer*, John Wiley and Sons, N.Y., 1984.
84. E.R.G. Eckert, and R.M. Drake, *Analysis of Heat and Mass Transfer*, McGraw-Hill, N.Y., 1972.
85. D.E. Rosner, *Transport Processes in Chemically Reacting Flow Systems*, Butterworths, Stoneham, MA, 1986.
86. W.J. Minkowycz, E.M. Sparrow, G.E. Schneider, and R.H. Pletcher, *Handbook of Numerical Heat Transfer*, John Wiley and Sons, N.Y., 1988.

87. R.G. Goldstein, and D.K. Kreid, Measurement of laminar flow development in a square duct using a Laser-Doppler flowmeter, *J. Appl. Mech.*, 34, 813-818, 1967.
88. G.S. Beavers, E.M. Sparrow, and Magnuson, Experiments on hydrodynamically developing flow in rectangular ducts of arbitrary aspect ratio, *Int. J. Heat Mass Transfer*, 13, 689-702, 1970.
89. E.M. Sparrow, and S.H. Lin, Flow development in the hydrodynamic entrance region of tubes and ducts, *The Physics of Fluids*, 7, No. 3, 338-347, 1964.
90. E. Reshotko, Experimental study of the stability of pipe flow, Report No. 20-364, Jet Propulsion Laboratory, California Institute of Technology, 1958.
91. F.M. White, *Fluid Mechanics*, 2nd edition, McGraw Hill, N.Y., 1986.
92. W.R. Debler, *Fluid Mechanics Fundamentals*, Prentice Hall, N.J., 1990.
93. R.B. Bird, *Dynamics of Polymeric Liquids*, Vol. 1, John Wiley and Sons, N.Y., 1977.
94. L.S. Caretto, R.M. Curr, and D.B. Spalding, *Compt. Meth. Appl. Mech. and Engr.*, 1, 39, 1973.
95. E.M. Sparrow, S.H. Lin, and T.S. Lundgren, Flow development in the hydrodynamic entrance region of tubes and ducts, *The Physics of Fluids*, 7, 338-347, 1964.
96. S. Netti, and R. Eichhorn, Combined hydrodynamic and thermal development in a square duct, *Numerical Heat Transfer*, 6, 497-510, 1983.
97. S.C.R. Dennis, A.M. Mercer, and G. Poots, Forced heat convection in laminar flow through rectangular ducts, *Q. Appl. Math.*, 17, 285-297, 1959.
98. R.W. Lyczkowski, C.W. Solbrig, and D. Gidaspow, Forced convection heat transfer in rectangular duct, *Nucl. Eng. Design*, 67, 357-378, 1981.
99. A.R. Chandrupatla, and V.M.K. Sastri, Laminar forced convection heat transfer of a non-Newtonian fluid in a square duct, *Int. J. Heat Mass Transfer*, 20, 1315-1324, 1977.
100. P. Wibulswas, Laminar flow heat transfer in non-circular ducts, Ph.D. thesis, London University, London, 1966.
101. R.K. Shah, Laminar flow friction and forced convection heat transfer in ducts of arbitrary geometry, *Int. J. Heat Mass Transfer*, 18, 849-862, 1975

NOMENCLATURE

a	coefficient in the discretization equation
A	cross sectional area
AH	Diels-Alder dimer
AR, ar	aspect ratio
a_1, a_2	constants
B, b	constant term in discretization equation
b	constant
b	constant term in discretization equation
b_1, b_2	constants
c	a constant
C_m	chain transfer constant for monomer
C_P	specific heat
C_1^ϕ, C_2^ϕ , etc.	transformed diffusion coefficient for dependent variable ϕ
D	pipe diameter
D	domain in Cartesian coordinates
D	coefficients in transformed equations
D, D_m	mass diffusivity
DP	pressure drop
DE, D_h	equivalent or hydraulic diameter
D_A	mass diffusivity of A
D^*	domain in transformed coordinates
d.l.	dimensionless
f	friction factor
f	a function
f	defined by Eqn. (3.29)

NOMENCLATURE (*Continue*)

F. D.	fully-developed
g	a function
g	acceleration due to gravity
G_z	Graetz number ($G_z = \frac{1}{z^{0.5}}$)
h	a function
h	enthalpy ($h = C_p T$)
I	viscous dissipation function
I	index of "ξ" axis in transformed plane
J	index of "η" axis in transformed plane
J	Jacobian of transformation
k	a constant
k	thermal conductivity
k_i	rate constant for thermal initiation
k_p	rate constant for propagation
k_t	rate constant for termination
$k_{tr,m}$	rate constant for chain transfer to monomer
L	duct length
L_e	entrance length
$L1$	maximum value of "I" index
$M1$	maximum value of "J" index
m	mass fraction
M	monomer
M	apparent viscosity for a power-law fluid
M	mass flow rate
$[M]$	monomer concentration

NOMENCLATURE (Continue)

$\bar{M}_{n,inst}$	instantaneous number average molecular weight
$\bar{M}_{w,inst}$	instantaneous weight average molecular weight
$M_{w,i}$	weight average molecular weight at axial position i at any streamline
$\bar{M}_{n,i}$	number average molecular weight at axial position i at any streamline n
MWS	weight average molecular weight for a streamline at the reactant exit
MNS	number average molecular weight for a streamline at the reactant exit
MWA, \bar{M}_w	cup-averaged weight average molecular-weight
MNA, \bar{M}_n	cup-averaged number average molecular-weight
n	power-law index
\mathbf{n}	unit normal vector
Nu	Nusselt number
Nu_T	limiting Nusselt number
$Nu_{z,T}$	local Nusselt number
$Nu_{m,T}$	mean Nusselt number
P	wetted perimeter
P	nodal point
P	total pressure (dynamic + hydrostatic), (refer to page 2-13)
P	dynamic-pressure (refer to page 2-13)
Pr	Prandtl number ($Pr = \frac{C_P \mu \bar{w}^{n-1}}{k D_h^{n-1}}$)
P'	pressure correction
P_0	static pressure at inlet
\bar{P}	mean viscous pressure
Pe	Peclet number ($Pe = Re \cdot Pr = \left(\frac{\rho \bar{w}^{2-n} D_h^n}{\mu} \right) \left(\frac{C_P \mu \bar{w}^{n-1}}{k D_h^{n-1}} \right) = \frac{\rho C_P D_h \bar{w}}{k}$)
P_{n+m}	dead polymers of chain length $(n + m)$
q	heat flux

NOMENCLATURE (*Continue*)

Q	heat flow
Q	defined by Eqn. (3.29)
Q_m	mass flow rate
Q_R	heat of reaction
RDPT	$(P_0 - \bar{P})/(\frac{1}{2}\rho w_0^2)$
R	residual of discretization equation
R_A	mass rate of consumption of reactant "A" due to chemical reaction
Re	Reynolds number ($Re = \frac{\rho D_h^n \bar{w}^{2-n}}{\mu}$), general, for power-law fluids and Newtonian fluid at n=1.0
Re, N_{Re}	Reynolds number ($Re = \frac{\rho(D_h)\bar{w}}{\mu}$), for Newtonian fluids
R_i	rate of thermal initiation
R_p	rate of polymerization
R_t	rate of termination
R_n^*, R_m^*	radical chains of length n and m
RW	axial velocity ratio ($\frac{w}{\bar{w}}$)
RWCL	centerline velocity ratio ($\frac{w_{cl}}{\bar{w}}$)
S	source-term
SC	constant part of linearized source term
SP	coefficient of the dependent variable in the linearized source term
\bar{w}	mean axial velocity
w_{cl}	centerline velocity
w_0	inlet velocity
WPA	polymer average weight fraction
w_p	polymer weight fraction
w_i	inlet velocity

NOMENCLATURE (*Continue*)

t	time coordinate
t_l	inlet temperature
T	temperature
T_w	wall temperature
T_b	bulk temperature
T_{CL}	centerline temperature
T_i	inlet temperature
V	volume
\mathbf{v}	velocity vector
$[\mathbf{v}]$	average velocity
u, v, w	velocity components in the Cartesian system
$\hat{u}, \hat{v}, \hat{w}$	pseudovelocity components
$\hat{U}, \hat{V}, \hat{W}$	pseudovelocity components
u^*, v^*, w^*	tentative velocity field
U^*, V^*, W^*	tentative contravariant velocity field
x, y, z	Cartesian coordinate system
X	dimensionless axial distance, defined in ref. 99
X_m	monomer conversion
E, W, N, S	nodes neighbouring to P
$NE, NW,$	nodes neighbouring to P
SE, SW	nodes neighbouring to P
z	duct length
Z^*	dimensionless axial-distance, $Z^* = \frac{z}{D_h \cdot Re_{(local)}}$, for Newtonian fluids
Z^{**}	dimensionless axial distance, $Z^{**} = (z/D_h)/P_e$

Greek Letters

α	relaxation factor
β	defined parameter
α, β, γ	coordinate transformation coefficients
ξ, η, σ	axes of curvilinear coordinate
μ	consistency index (for power-law fluids) and viscosity (for Newtonian fluids)
ρ	density
ρ_a	arithmetic mean density for duct cross-section
η_0	viscosity
Γ	bounding surface
τ_{ij}	stress-tensor
ΔH	heat of reaction
Δ_{ij}	rate of deformation tensor
ΔP	pressure-drop in the duct
ϵ	roughness
ν	kinematic viscosity
φ	general dependent variable
Φ	dimensionless variable standing for geometric nonuniformity effect
ω	mass-fraction
ω_A	mass-fraction of "A"
μ_0	zeroth moment of polymer chain distribution
μ_1	1 st moment of polymer chain distribution
μ_2	2 nd moment of polymer chain distribution
ϕ	a general dependent variable
θ_b	dimensionless bulk temperature, $\theta_b = (t_b - t_w)/(t_l - t_w)$

Superscripts

- ^ refers to transformed quantities, except for velocities
- * a tentative value
- * transformed plane

Subscripts

- m monomer
- nb general neighbour grid point
- P polymer
- P central grid point under consideration
- U upstream plane
- D downstream plane

Special Symbols

- $L[]$ finite-difference approximation of the quantity in brackets
- $\|A, B, \dots\|$ largest of A, B, ...

APPENDIX A
DERIVATION OF TRANSFORMATION RELATIONS

A. 1 BASIC RELATIONS

$$J = x_{\xi}y_{\eta} - x_{\eta}y_{\xi} \quad (A.1)$$

$$\alpha = x_{\eta}^2 + y_{\eta}^2 \quad (A.2)$$

$$\beta = x_{\xi}x_{\eta} + y_{\xi}y_{\eta} \quad (A.3)$$

$$\gamma = x_{\xi}^2 + y_{\xi}^2 \quad (A.4)$$

A. 2 DERIVATION OF DERIVATIVE-TRANSFORMATIONS

$$\xi_x = \frac{y_{\eta}}{J} \quad (A.5)$$

$$\eta_x = -\frac{y_{\xi}}{J} \quad (A.6)$$

$$\xi_y = -\frac{x_{\eta}}{J} \quad (A.7)$$

$$\eta_y = \frac{x_{\xi}}{J} \quad (A.8)$$

let

$$x = x(\xi, \eta) \quad \& \quad y = y(\xi, \eta) \quad (A.9)$$

$$dx = \frac{\partial x}{\partial \xi} d\xi + \frac{\partial x}{\partial \eta} d\eta \quad \& \quad dy = \frac{\partial y}{\partial \xi} d\xi + \frac{\partial y}{\partial \eta} d\eta \quad (A.10)$$

(I)

$$\frac{dx}{dx} = \frac{\partial x}{\partial \xi} \frac{d\xi}{dx} + \frac{\partial x}{\partial \eta} \frac{d\eta}{dx} \quad \& \quad \frac{dy}{dx} = \frac{\partial y}{\partial \xi} \frac{d\xi}{dx} + \frac{\partial y}{\partial \eta} \frac{d\eta}{dx} \quad (A.11)$$

$$x_{\xi}\xi_x + x_{\eta}\eta_x = 1 \quad \& \quad y_{\xi}\xi_x + y_{\eta}\eta_x = 0 \quad (A.12)$$

(I-a)

$$\xi_x = \frac{\begin{vmatrix} 1 & x_\eta \\ 0 & y_\eta \end{vmatrix}}{\begin{vmatrix} x_\xi & x_\eta \\ y_\xi & y_\eta \end{vmatrix}} = \frac{y_\eta}{x_\xi y_\eta - x_\eta y_\xi} = \frac{y_\eta}{J} \quad (\text{A.13})$$

(I-b)

$$\eta_x = \frac{\begin{vmatrix} x_\xi & 1 \\ y_\xi & 0 \end{vmatrix}}{\begin{vmatrix} x_\xi & x_\eta \\ y_\xi & y_\eta \end{vmatrix}} = \frac{-y_\xi}{x_\xi y_\eta - x_\eta y_\xi} = \frac{-y_\xi}{J} \quad (\text{A.14})$$

(II)

$$\frac{dx}{dy} = \frac{\partial x}{\partial \xi} \frac{d\xi}{dy} + \frac{\partial x}{\partial \eta} \frac{d\eta}{dy} \quad \& \quad \frac{dy}{dy} = \frac{\partial y}{\partial \xi} \frac{d\xi}{dy} + \frac{\partial y}{\partial \eta} \frac{d\eta}{dy} \quad (\text{A.15})$$

$$x_\xi \xi_y + x_\eta \eta_y = 0 \quad \& \quad y_\xi \xi_y + y_\eta \eta_y = 1 \quad (\text{A.16})$$

(II-a)

$$\xi_y = \frac{\begin{vmatrix} 0 & x_\eta \\ 1 & y_\eta \end{vmatrix}}{\begin{vmatrix} x_\xi & x_\eta \\ y_\xi & y_\eta \end{vmatrix}} = \frac{-x_\eta}{x_\xi y_\eta - x_\eta y_\xi} = \frac{-x_\eta}{J} \quad (\text{A.17})$$

(II-b)

$$\eta_y = \frac{\begin{vmatrix} x_\xi & 0 \\ y_\xi & 1 \end{vmatrix}}{\begin{vmatrix} x_\xi & x_\eta \\ y_\xi & y_\eta \end{vmatrix}} = \frac{x_\xi}{x_\xi y_\eta - x_\eta y_\xi} = \frac{x_\xi}{J} \quad (\text{A.18})$$

A. 3 DERIVATION OF RELATIONS $\frac{\partial f}{\partial x}$ & $\frac{\partial f}{\partial y}$

$$\frac{\partial}{\partial x} = \frac{y_{\eta}}{J} \frac{\partial}{\partial \xi} - \frac{y_{\xi}}{J} \frac{\partial}{\partial \eta} \quad \& \quad \frac{\partial}{\partial y} = -\frac{x_{\eta}}{J} \frac{\partial}{\partial \xi} + \frac{x_{\xi}}{J} \frac{\partial}{\partial \eta} \quad (A.19)$$

let $f = f(x, y)$

$$df = \frac{\partial f}{\partial x} dx + \frac{\partial f}{\partial y} dy \quad (A.20)$$

as $x = x(\xi, \eta)$ and $y = y(\xi, \eta)$, then

$$f = f(\xi, \eta) \quad (A.21)$$

$$\frac{\partial f}{\partial \xi} = \left(\frac{\partial f}{\partial x} \right) \left(\frac{\partial x}{\partial \xi} \right) + \left(\frac{\partial f}{\partial y} \right) \left(\frac{\partial y}{\partial \xi} \right) \quad \&$$

$$\frac{\partial f}{\partial \eta} = \left(\frac{\partial f}{\partial x} \right) \left(\frac{\partial x}{\partial \eta} \right) + \left(\frac{\partial f}{\partial y} \right) \left(\frac{\partial y}{\partial \eta} \right) \quad (A.22)$$

or alternatively:

$$\frac{\partial f}{\partial \xi} = \left(\frac{\partial f}{\partial x} \right) x_{\xi} + \left(\frac{\partial f}{\partial y} \right) y_{\xi} \quad \& \quad \frac{\partial f}{\partial \eta} = \left(\frac{\partial f}{\partial x} \right) x_{\eta} + \left(\frac{\partial f}{\partial y} \right) y_{\eta} \quad (A.23)$$

$$\frac{\partial f}{\partial x} = \frac{\begin{vmatrix} \frac{\partial f}{\partial \xi} & y_{\xi} \\ \frac{\partial f}{\partial \eta} & y_{\eta} \end{vmatrix}}{\begin{vmatrix} x_{\xi} & y_{\xi} \\ x_{\eta} & y_{\eta} \end{vmatrix}} = \frac{\left(\frac{\partial f}{\partial \xi} \right) y_{\eta} - \left(\frac{\partial f}{\partial \eta} \right) y_{\xi}}{x_{\xi} y_{\eta} - x_{\eta} y_{\xi}} = \frac{\left(\frac{\partial f}{\partial \xi} \right) y_{\eta} - \left(\frac{\partial f}{\partial \eta} \right) y_{\xi}}{J} \quad (A.24)$$

$$\frac{\partial f}{\partial y} = \frac{\begin{vmatrix} x_{\xi} & \frac{\partial f}{\partial \xi} \\ x_{\eta} & \frac{\partial f}{\partial \eta} \end{vmatrix}}{\begin{vmatrix} x_{\xi} & y_{\xi} \\ x_{\eta} & y_{\eta} \end{vmatrix}} = \frac{\left(\frac{\partial f}{\partial \eta} \right) x_{\xi} - \left(\frac{\partial f}{\partial \xi} \right) x_{\eta}}{x_{\xi} y_{\eta} - x_{\eta} y_{\xi}} = \frac{\left(\frac{\partial f}{\partial \eta} \right) x_{\xi} - \left(\frac{\partial f}{\partial \xi} \right) x_{\eta}}{J} \quad (A.25)$$

Summary

$$\frac{\partial f}{\partial x} = \frac{\left(\frac{\partial f}{\partial \xi}\right) y_{\eta} - \left(\frac{\partial f}{\partial \eta}\right) y_{\xi}}{J} \quad \& \quad \frac{\partial f}{\partial y} = \frac{\left(\frac{\partial f}{\partial \eta}\right) x_{\xi} - \left(\frac{\partial f}{\partial \xi}\right) x_{\eta}}{J} \quad (A.26)$$

$$f_x = \frac{(f_{\xi} y_{\eta} - f_{\eta} y_{\xi})}{J} \quad \& \quad f_y = \frac{(f_{\eta} x_{\xi} - f_{\xi} x_{\eta})}{J} \quad (A.27)$$

$$\frac{\partial}{\partial x} = \frac{\left(\frac{\partial}{\partial \xi}\right) y_{\eta} - \left(\frac{\partial}{\partial \eta}\right) y_{\xi}}{J} \quad \& \quad \frac{\partial}{\partial y} = \frac{\left(\frac{\partial}{\partial \eta}\right) x_{\xi} - \left(\frac{\partial}{\partial \xi}\right) x_{\eta}}{J} \quad (A.28)$$

or alternatively

$$\frac{\partial}{\partial x} = \frac{y_{\eta}}{J} \frac{\partial}{\partial \xi} - \frac{y_{\xi}}{J} \frac{\partial}{\partial \eta} \quad \& \quad \frac{\partial}{\partial y} = -\frac{x_{\eta}}{J} \frac{\partial}{\partial \xi} + \frac{x_{\xi}}{J} \frac{\partial}{\partial \eta} \quad (A.29)$$

A. 4 TRANSFORMATION OF POISSON EQUATIONS

$$f = f(\xi, \eta) \quad \xi = \xi(x, y), \quad \eta = \eta(x, y)$$
$$df = \frac{\partial f}{\partial \xi} d\xi + \frac{\partial f}{\partial \eta} d\eta \quad (A.30)$$

(i) Evaluate the First Derivative

$$\frac{\partial f}{\partial x} = \frac{\partial f}{\partial \xi} \frac{\partial \xi}{\partial x} + \frac{\partial f}{\partial \eta} \frac{\partial \eta}{\partial x} \quad \& \quad \frac{\partial f}{\partial y} = \frac{\partial f}{\partial \xi} \frac{\partial \xi}{\partial y} + \frac{\partial f}{\partial \eta} \frac{\partial \eta}{\partial y} \quad (A.31)$$

or alternatively:

$$f_x = f_\xi \xi_x + f_\eta \eta_x \quad \& \quad f_y = f_\xi \xi_y + f_\eta \eta_y \quad (A.32)$$

(ii) Evaluate the Second Derivatives:

$$\frac{\partial}{\partial x} \frac{\partial f}{\partial x} = \frac{\partial f}{\partial \xi} \frac{\partial^2 \xi}{\partial x^2} + \frac{\partial}{\partial x} \left(\frac{\partial f}{\partial \xi} \right) \frac{\partial \xi}{\partial x} + \frac{\partial f}{\partial \eta} \frac{\partial^2 \eta}{\partial x^2} + \frac{\partial}{\partial x} \left(\frac{\partial f}{\partial \eta} \right) \frac{\partial \eta}{\partial x} \quad (A.33)$$

$$\frac{\partial}{\partial y} \frac{\partial f}{\partial y} = \frac{\partial f}{\partial \xi} \frac{\partial^2 \xi}{\partial y^2} + \frac{\partial}{\partial y} \left(\frac{\partial f}{\partial \xi} \right) \frac{\partial \xi}{\partial y} + \frac{\partial f}{\partial \eta} \frac{\partial^2 \eta}{\partial y^2} + \frac{\partial}{\partial y} \left(\frac{\partial f}{\partial \eta} \right) \frac{\partial \eta}{\partial y} \quad (A.34)$$

or alternatively

$$\begin{aligned} f_{xx} &= f_\xi \xi_{xx} + (f_\xi)_x \xi_x + f_\eta \eta_{xx} + (f_\eta)_x \eta_x \quad \& \\ f_{yy} &= f_\xi \xi_{yy} + (f_\xi)_y \xi_y + f_\eta \eta_{yy} + (f_\eta)_y \eta_y \end{aligned} \quad (A.35)$$

Now evaluate $(f_\xi)_x$, $(f_\eta)_x$, $(f_\xi)_y$ & $(f_\eta)_y$:

$$\begin{aligned} d \left(\frac{\partial f}{\partial \xi} \right) &= \frac{\partial}{\partial \xi} \left(\frac{\partial f}{\partial \xi} \right) d\xi + \frac{\partial}{\partial \eta} \left(\frac{\partial f}{\partial \xi} \right) d\eta \quad \& \\ d \left(\frac{\partial f}{\partial \eta} \right) &= \frac{\partial}{\partial \xi} \left(\frac{\partial f}{\partial \eta} \right) d\xi + \frac{\partial}{\partial \eta} \left(\frac{\partial f}{\partial \eta} \right) d\eta \end{aligned} \quad (A.36)$$

Therefore:

$$\frac{\partial}{\partial x} \left(\frac{\partial f}{\partial \xi} \right) = \frac{\partial}{\partial \xi} \left(\frac{\partial f}{\partial \xi} \right) \frac{\partial \xi}{\partial x} + \frac{\partial}{\partial \eta} \left(\frac{\partial f}{\partial \xi} \right) \frac{\partial \eta}{\partial x} \quad (A.37)$$

$$\frac{\partial}{\partial x} \left(\frac{\partial f}{\partial \eta} \right) = \frac{\partial}{\partial \xi} \left(\frac{\partial f}{\partial \eta} \right) \frac{\partial \xi}{\partial x} + \frac{\partial}{\partial \eta} \left(\frac{\partial f}{\partial \eta} \right) \frac{\partial \eta}{\partial x} \quad (A.38)$$

$$\frac{\partial}{\partial y} \left(\frac{\partial f}{\partial \xi} \right) = \frac{\partial}{\partial \xi} \left(\frac{\partial f}{\partial \xi} \right) \frac{\partial \xi}{\partial y} + \frac{\partial}{\partial \eta} \left(\frac{\partial f}{\partial \xi} \right) \frac{\partial \eta}{\partial y} \quad (A.39)$$

$$\frac{\partial}{\partial y} \left(\frac{\partial f}{\partial \eta} \right) = \frac{\partial}{\partial \xi} \left(\frac{\partial f}{\partial \eta} \right) \frac{\partial \xi}{\partial y} + \frac{\partial}{\partial \eta} \left(\frac{\partial f}{\partial \eta} \right) \frac{\partial \eta}{\partial y} \quad (A.40)$$

or alternatively:

$$(f_{\xi})_x = f_{\xi\xi}\xi_x + f_{\xi\eta}\eta_x \quad (A.41)$$

$$(f_{\eta})_x = f_{\xi\eta}\xi_x + f_{\eta\eta}\eta_x \quad (A.42)$$

$$(f_{\xi})_y = f_{\xi\xi}\xi_y + f_{\xi\eta}\eta_y \quad (A.43)$$

$$(f_{\eta})_y = f_{\xi\eta}\xi_y + f_{\eta\eta}\eta_y \quad (A.44)$$

Now substitute in f_{xx} & f_{yy} :

$$f_{xx} = f_{\xi\xi}\xi_{xx} + f_{\xi\xi}\xi_x^2 + f_{\xi\eta}\xi_x\eta_x + f_{\eta\eta}\eta_{xx} + f_{\xi\eta}\xi_x\eta_x + f_{\eta\eta}\eta_x^2 \quad (A.45)$$

$$f_{yy} = f_{\xi\xi}\xi_{yy} + f_{\xi\xi}\xi_y^2 + f_{\xi\eta}\xi_y\eta_y + f_{\eta\eta}\eta_{yy} + f_{\xi\eta}\xi_y\eta_y + f_{\eta\eta}\eta_y^2 \quad (A.46)$$

or

$$f_{xx} = f_{\xi\xi}\xi_{xx} + f_{\xi\xi}\xi_x^2 + 2f_{\xi\eta}\xi_x\eta_x + f_{\eta\eta}\eta_{xx} + f_{\eta\eta}\eta_x^2 \quad (A.47)$$

$$f_{yy} = f_{\xi\xi}\xi_{yy} + f_{\xi\xi}\xi_y^2 + 2f_{\xi\eta}\xi_y\eta_y + f_{\eta\eta}\eta_{yy} + f_{\eta\eta}\eta_y^2 \quad (A.48)$$

let $f = x$ in f_{xx} :

$$\xi_{xx}x_{\xi} + \xi_x^2x_{\xi\xi} + 2\xi_x\eta_x x_{\xi\eta} + \eta_{xx}x_{\eta} + \eta_x^2x_{\eta\eta} = 0 \quad (A.49)$$

and $f = y$ in f_{xx} :

$$\xi_{xx}y_{\xi} + \xi_x^2y_{\xi\xi} + 2\xi_x\eta_x y_{\xi\eta} + \eta_{xx}y_{\eta} + \eta_x^2y_{\eta\eta} = 0 \quad (A.50)$$

or alternatively:

$$\xi_{xx}x_\xi + \eta_{xx}x_\eta = -(\xi_x^2 x_{\xi\xi} + 2\xi_x \eta_x x_{\xi\eta} + \eta_x^2 x_{\eta\eta}) \quad (A.51)$$

$$\xi_{xx}y_\xi + \eta_{xx}y_\eta = -(\xi_x^2 y_{\xi\xi} + 2\xi_x \eta_x y_{\xi\eta} + \eta_x^2 y_{\eta\eta}) \quad (A.52)$$

let

$$\xi_x^2 x_{\xi\xi} + 2\xi_x \eta_x x_{\xi\eta} + \eta_x^2 x_{\eta\eta} = E_1 \quad (A.53)$$

and

$$\xi_x^2 y_{\xi\xi} + 2\xi_x \eta_x y_{\xi\eta} + \eta_x^2 y_{\eta\eta} = F_1 \quad (A.54)$$

Then

$$\xi_{xx}x_\xi + \eta_{xx}x_\eta = -E_1 \quad (A.55)$$

$$\xi_{xx}y_\xi + \eta_{xx}y_\eta = -F_1 \quad (A.56)$$

$$\xi_{xx} = \frac{\begin{vmatrix} -E_1 & x_\eta \\ -F_1 & y_\eta \end{vmatrix}}{\begin{vmatrix} x_\xi & x_\eta \\ y_\xi & y_\eta \end{vmatrix}} = \frac{-E_1 y_\eta + F_1 x_\eta}{J} \quad (A.57)$$

$$\eta_{xx} = \frac{\begin{vmatrix} x_\xi & -E_1 \\ y_\xi & -F_1 \end{vmatrix}}{\begin{vmatrix} x_\xi & x_\eta \\ y_\xi & y_\eta \end{vmatrix}} = \frac{-F_1 x_\xi + E_1 y_\xi}{J} \quad (A.58)$$

$$\xi_{xx} = \frac{-E_1(J\xi_x) + F_1(-J\xi_y)}{J} \quad (A.59)$$

$$\eta_{xx} = \frac{-F_1(J\eta_y) + E_1(-J\eta_x)}{J} \quad (A.60)$$

$$\xi_{xx} = -(E_1 \xi_x + F_1 \xi_y) \quad (A.61)$$

$$\eta_{xx} = -(E_1 \eta_x + F_1 \eta_y) \quad (A.62)$$

let $f = x$ in f_{yy} :

$$\xi_{yy} x_\xi + \xi_y^2 x_{\xi\xi} + 2\xi_y \eta_y x_{\xi\eta} + \eta_{yy} x_\eta + \eta_y^2 x_{\eta\eta} = 0 \quad (A.63)$$

and $f = y$ in f_{yy} :

$$\xi_{yy} y_\xi + \xi_y^2 y_{\xi\xi} + 2\xi_y \eta_y y_{\xi\eta} + \eta_{yy} y_\eta + \eta_y^2 y_{\eta\eta} = 0 \quad (A.64)$$

or alternatively:

$$\xi_{yy} x_\xi + \eta_{yy} x_\eta = -(\xi_y^2 x_{\xi\xi} + 2\xi_y \eta_y x_{\xi\eta} + \eta_y^2 x_{\eta\eta}) \quad (A.65)$$

$$\xi_{yy} y_\xi + \eta_{yy} y_\eta = -(\xi_y^2 y_{\xi\xi} + 2\xi_y \eta_y y_{\xi\eta} + \eta_y^2 y_{\eta\eta}) \quad (A.66)$$

or

$$\xi_{yy} x_\xi + \eta_{yy} x_\eta = -E_2 \quad (A.67)$$

$$\xi_{yy} y_\xi + \eta_{yy} y_\eta = -F_2 \quad (A.68)$$

in which

$$E_2 = \xi_y^2 x_{\xi\xi} + 2\xi_y \eta_y x_{\xi\eta} + \eta_y^2 x_{\eta\eta} \quad (A.69)$$

$$F_2 = \xi_y^2 y_{\xi\xi} + 2\xi_y \eta_y y_{\xi\eta} + \eta_y^2 y_{\eta\eta} \quad (A.70)$$

$$\xi_{yy} = \frac{\begin{vmatrix} -E_2 & x_\eta \\ -F_2 & y_\eta \end{vmatrix}}{\begin{vmatrix} x_\xi & x_\eta \\ y_\xi & y_\eta \end{vmatrix}} = \frac{-E_2 y_\eta + F_2 x_\eta}{x_\xi y_\eta - x_\eta y_\xi} \quad (A.71)$$

$$\eta_{yy} = \frac{\begin{vmatrix} x_\xi & -E_2 \\ y_\xi & -F_2 \end{vmatrix}}{\begin{vmatrix} x_\xi & x_\eta \\ y_\xi & y_\eta \end{vmatrix}} = \frac{-F_2 x_\xi + E_2 y_\xi}{x_\xi y_\eta - x_\eta y_\xi} \quad (A.72)$$

$$\xi_{yy} = \frac{-E_2(J\xi_x) + F_2(-J\xi_y)}{J} \quad (A.73)$$

$$\eta_{yy} = \frac{-F_2(J\eta_y) + E_2(-J\eta_x)}{J} \quad (A.74)$$

or

$$\xi_{yy} = -(E_2\xi_x + F_2\xi_y) \quad (A.75)$$

$$\eta_{yy} = -(E_2\eta_x + F_2\eta_y) \quad (A.76)$$

Using

$$\xi_{xx} = -(E_1\xi_x + F_1\xi_y) \quad (A.77)$$

$$\eta_{xx} = -(E_1\eta_x + F_1\eta_y) \quad (A.78)$$

and

$$\xi_{yy} = -(E_2\xi_x + F_2\xi_y) \quad (A.79)$$

$$\eta_{yy} = -(E_2\eta_x + F_2\eta_y) \quad (A.80)$$

Substitute into Poisson equations:

$$\xi_{xx} + \xi_{yy} = P(\xi, \eta) \quad (A.81)$$

$$\eta_{xx} + \eta_{yy} = Q(\xi, \eta) \quad (A.82)$$

$$-(E_1\xi_x + F_1\xi_y) - (E_2\xi_x + F_2\xi_y) = P \quad (A.83)$$

$$-(E_1\eta_x + F_1\eta_y) - (E_2\eta_x + F_2\eta_y) = Q \quad (A.84)$$

$$-(E_1 + E_2)\xi_x - (F_1 + F_2)\xi_y = P \quad (A.85)$$

$$-(E_1 + E_2)\eta_x - (F_1 + F_2)\eta_y = Q \quad (A.86)$$

let

$$E_1 + E_2 = E \quad \& \quad F_1 + F_2 = F \quad (A.87)$$

then

$$E\xi_x + F\xi_y = -P \quad (A.88)$$

$$E\eta_x + F\eta_y = -Q \quad (A.89)$$

$$\frac{Ey_\eta}{J} - \frac{Fx_\eta}{J} = -P \quad (A.90)$$

$$-\frac{Ey_\xi}{J} + \frac{Fx_\xi}{J} = -Q \quad (A.91)$$

$$-E \left(\frac{y_\eta}{J} \right) + F \left(\frac{x_\eta}{J} \right) = P \quad (A.92)$$

$$E \left(\frac{y_\xi}{J} \right) - F \left(\frac{x_\xi}{J} \right) = Q \quad (A.93)$$

$$-y_\eta E + x_\eta F = JP \quad (A.94)$$

$$y_\xi E - x_\xi F = JQ \quad (A.95)$$

$$E = \frac{\begin{vmatrix} JP & x_\eta \\ JQ & -x_\xi \end{vmatrix}}{\begin{vmatrix} -y_\eta & x_\eta \\ y_\xi & -x_\xi \end{vmatrix}} = \frac{-JPx_\xi - JQx_\eta}{y_\eta x_\xi - y_\xi x_\eta} \quad (A.96)$$

$$F = \frac{\begin{vmatrix} -y_\eta & JP \\ y_\xi & JQ \end{vmatrix}}{\begin{vmatrix} -y_\eta & x_\eta \\ y_\xi & -x_\xi \end{vmatrix}} = \frac{-JQy_\eta - Jpy_\xi}{y_\eta x_\xi - y_\xi x_\eta} \quad (A.97)$$

$$E = \frac{-J(Px_\xi + Qx_\eta)}{J} \quad (A.98)$$

$$F = \frac{-J(Qy_\eta + Py_\xi)}{J} \quad (A.99)$$

$$E = -(Px_\xi + Qx_\eta) \quad (A.100)$$

$$F = -(Py_\xi + Qy_\eta) \quad (A.101)$$

Now let

$$E_1 + E_2 = E \quad (A.102)$$

$$\begin{aligned} \xi_x^2 x_{\xi\xi} + 2\xi_x \eta_x x_{\xi\eta} + \eta_x^2 x_{\eta\eta} + \xi_y^2 x_{\xi\xi} + 2\xi_y \eta_y x_{\xi\eta} + \\ \eta_y^2 x_{\eta\eta} = -(Px_\xi + Qx_\eta) \end{aligned} \quad (A.103)$$

and

$$F_1 + F_2 = F \quad (A.104)$$

$$\begin{aligned} \xi_x^2 y_{\xi\xi} + 2\xi_x \eta_x y_{\xi\eta} + \eta_x^2 y_{\eta\eta} + \xi_y^2 y_{\xi\xi} + 2\xi_y \eta_y y_{\xi\eta} + \\ \eta_y^2 y_{\eta\eta} = -(Py_\xi + Qy_\eta) \end{aligned} \quad (A.105)$$

from Eqn. (A.103)

$$\begin{aligned} x_{\xi\xi} \left(\frac{y_\eta}{J}\right)^2 + 2x_{\xi\eta} \left(\frac{y_\eta}{J}\right) \left(-\frac{y_\xi}{J}\right) + x_{\eta\eta} \left(-\frac{y_\xi}{J}\right)^2 + x_{\xi\xi} \left(-\frac{x_\eta}{J}\right)^2 + \\ 2x_{\xi\eta} \left(-\frac{x_\eta}{J}\right) \left(\frac{x_\xi}{J}\right) + x_{\eta\eta} \left(\frac{x_\xi}{J}\right)^2 = -(Px_\xi + Qx_\eta) \end{aligned} \quad (A.106)$$

$$x_{\xi\xi} \frac{(x_{\eta}^2 + y_{\eta}^2)}{J^2} + x_{\eta\eta} \frac{(x_{\xi}^2 + y_{\xi}^2)}{J^2} - 2x_{\xi\eta} \frac{(x_{\xi}x_{\eta} + y_{\xi}y_{\eta})}{J^2} = -(Px_{\xi} + Qx_{\eta}) \quad (A.107)$$

$$\frac{\alpha}{J^2} x_{\xi\xi} + \frac{\gamma}{J^2} x_{\eta\eta} - \frac{2\beta x_{\xi\eta}}{J^2} = -(Px_{\xi} + Qx_{\eta}) \quad (A.108)$$

or

$$\frac{\alpha x_{\xi\xi}}{J^2} + \frac{\gamma x_{\eta\eta}}{J^2} - \frac{2\beta x_{\xi\eta}}{J^2} = -(Px_{\xi} + Qx_{\eta}) \quad (A.109)$$

from Eqn. (A.105)

$$y_{\xi\xi}(\xi_x^2 + \xi_y^2) + y_{\eta\eta}(\eta_x^2 + \eta_y^2) + 2y_{\xi\eta}(\xi_x\eta_x + \xi_y\eta_y) = -(Py_{\xi} + Qy_{\eta}) \quad (A.110)$$

$$y_{\xi\xi} \left[\left(\frac{y_{\eta}}{J} \right)^2 + \left(\frac{-x_{\eta}}{J} \right)^2 \right] + y_{\eta\eta} \left[\left(\frac{-y_{\xi}}{J} \right)^2 + \left(\frac{x_{\xi}}{J} \right)^2 \right] + 2y_{\xi\eta} \left[\left(\frac{y_{\eta}}{J} \right) \left(\frac{-y_{\xi}}{J} \right) + \left(\frac{-x_{\eta}}{J} \right) \left(\frac{x_{\xi}}{J} \right) \right] = -(Py_{\xi} + Qy_{\eta}) \quad (A.111)$$

$$y_{\xi\xi} \frac{(y_{\eta}^2 + x_{\eta}^2)}{J^2} + y_{\eta\eta} \frac{(y_{\xi}^2 + x_{\xi}^2)}{J^2} - 2y_{\xi\eta} \frac{(x_{\xi}x_{\eta} + y_{\xi}y_{\eta})}{J^2} = -(Py_{\xi} + Qy_{\eta}) \quad (A.112)$$

$$\frac{\alpha y_{\xi\xi}}{J^2} + \frac{\gamma y_{\eta\eta}}{J^2} - \frac{2\beta y_{\xi\eta}}{J^2} = -(Py_{\xi} + Qy_{\eta}) \quad (A.113)$$

Summary

$$\alpha x_{\xi\xi} + \gamma x_{\eta\eta} - 2\beta x_{\xi\eta} = -J^2(Px_{\xi} + Qx_{\eta}) \quad (A.114)$$

$$\alpha y_{\xi\xi} + \gamma y_{\eta\eta} - 2\beta y_{\xi\eta} = -J^2(Py_{\xi} + Qy_{\eta}) \quad (A.115)$$

or

$$\alpha x_{\xi\xi} + \gamma x_{\eta\eta} - 2\beta x_{\xi\eta} + J^2(Px_{\xi} + Qx_{\eta}) = 0 \quad (A.116)$$

$$\alpha y_{\xi\xi} + \gamma y_{\eta\eta} - 2\beta y_{\xi\eta} + J^2(Py_{\xi} + Qy_{\eta}) = 0 \quad (A.117)$$

Note: An alternate method of derivation of the above equations is to apply the concepts of differential-geometry⁶¹.

A. 5 DERIVATION OF DISCRETIZATION-EQUATION FOR GRID-GENERATION EQUATIONS

A. 5.1 Second-Order Central-Differential Approximation of Derivatives

$$x_{\xi} = \frac{(x_{i+1,j} - x_{i-1,j})}{2h} \quad (A.118)$$

$$x_{\eta} = \frac{(x_{i,j+1} - x_{i,j-1})}{2h} \quad (A.119)$$

$$x_{\xi\xi} = \frac{(x_{i-1,j} - 2x_{i,j} + x_{i+1,j})}{h^2} \quad (A.120)$$

$$x_{\eta\eta} = \frac{(x_{i,j-1} - 2x_{i,j} + x_{i,j+1})}{h^2} \quad (A.121)$$

$$x_{\xi\eta} = \frac{(x_{i+1,j+1} - x_{i-1,j+1} + x_{i-1,j-1} - x_{i+1,j-1})}{4h^2} \quad (A.122)$$

A. 5.2 Discretization of Grid-Generation Equations

Consider the transformed Laplace Equation:

$$\alpha x_{\xi\xi} - 2\beta x_{\xi\eta} + \gamma x_{\eta\eta} = 0 \quad (A.123)$$

Using the above relationships for the approximation of derivatives:

$$\alpha_{i,j}(x_{i-1,j} - 2x_{i,j} + x_{i+1,j}) + \gamma_{i,j}(x_{i,j-1} - 2x_{i,j} + x_{i,j+1}) - 2\beta_{i,j}(x_{i+1,j+1} - x_{i-1,j+1} + x_{i-1,j-1} - x_{i+1,j-1})/4 = 0 \quad (A.124)$$

in which

$$h = \Delta\xi = \Delta\eta = 1 \quad (A.125)$$

and

$$\alpha_{i,j} = (x_{\eta}^2 + y_{\eta}^2)_{i,j} \quad (A.126)$$

$$\beta_{i,j} = (x_{\xi}x_{\eta} + y_{\xi}y_{\eta})_{i,j} \quad (A.127)$$

$$\gamma_{i,j} = (x_{\xi}^2 + y_{\xi}^2)_{i,j} \quad (\text{A.128})$$

$$J_{i,j} = (x_{\xi}y_{\eta} - x_{\eta}y_{\xi})_{i,j} \quad (\text{A.129})$$

taking

$$T1 = \frac{\alpha_{i,j}}{2(\alpha_{i,j} + \gamma_{i,j})} \quad (\text{A.130})$$

$$T2 = \frac{\gamma_{i,j}}{2(\alpha_{i,j} + \gamma_{i,j})} \quad (\text{A.131})$$

$$T3 = \frac{\beta_{i,j}}{4(\alpha_{i,j} + \gamma_{i,j})} \quad (\text{A.132})$$

$$x_{i,j} - (x_{i-1,j} + x_{i+1,j})T1 - (x_{i,j-1} + x_{i,j+1})T2 + \\ (x_{i+1,j+1} - x_{i-1,j+1} + x_{i-1,j-1} - x_{i+1,j-1})T3 = 0 \quad (\text{A.133})$$

or alternatively

$$x(I, J) = [x(I1, J) + x(I2, J)]T1 + [x(I, J1) + x(I, J2)]T2 - \\ [x(I2, J2) - x(I1, J2) + x(I1, J1) - x(I2, J1)]T3 \quad (\text{A.134})$$

in which $I1 = I - 1$, $I2 = I + 1$, $J1 = J - 1$ and $J2 = J + 1$. Introducing the relaxation-factor " ω " one can write:

$$x(I, J) = \omega\{[x(I1, j) + x(I2, J)]T1 + [x(I, J1) + x(I, J2)]T2 - \\ [x(I2, J2) - x(I1, J2) + x(I1, J1) - x(I2, J1)]T3\} - \\ (\omega - 1)x(I, J) \quad (\text{A.135})$$

or alternatively

$$x(I, J) = (1 - \omega)x(I, J) + \omega\{[x(I1, J) + x(I2, J)]T1 + \\ [x(I, J1) + x(I, J2)]T2 - [x(I2, J2) - x(I1, J2) + \\ x(I1, J1) - x(I2, J1)]T3\} \quad (\text{A.136})$$

Similarly

$$y(I, J) = (1 - \omega)y(I, J) + \omega\{[y(I1, J) + y(I2, J)]T1 + \\ [y(I, J1) + y(I, J2)]T2 - [y(I2, J2) - y(I1, J2) + \\ y(I1, J1) - y(I2, J1)]T3\} \quad (\text{A.137})$$

Optimum Relaxation Factors

$$\omega_{ij} = \frac{2}{1 + \sqrt{1 \pm \rho_{ij}^2}} \quad \begin{array}{l} + \text{ (underrelaxation)} \quad 0 < \omega \leq 1 \\ - \text{ (overrelaxation)} \quad 1 \leq \omega < 2 \end{array}$$

in which ρ_{ij} is expressed⁵¹ as

$$\rho_{ij} = \frac{1}{\alpha_{ij} + \gamma_{ij}} \left[\sqrt{\left| \alpha_{ij}^2 - \frac{J_{ij}^4 P_{ij}^2}{4} \right| \cos \left(\frac{\pi}{IMAX - 1} \right)} + \sqrt{\left| \gamma_{ij}^2 - \frac{J_{ij}^4 Q_{ij}^2}{4} \right| \cos \left(\frac{\pi}{JMAX - 1} \right)} \right]$$

Note: Overrelaxation is often used in conjunction with the Gauss-Seidel method⁶⁹, the resulting scheme being known as Successive Overrelaxation (SOR) method.

Linearly-Interpolated Initial Guess for the Iterative Solution of the Equations⁵¹

The values of "x" and "y" at each point in the field are set equal to the average of the four boundary-points having either the same ξ index or the same η index, the average being weighted by the distance to the boundary in the transformed plane.

Thus:

$$2x_{ij} = \left(\frac{JMAX - i}{JMAX - 1} \right) x_{i,1} + \left(\frac{j - 1}{JMAX - 1} \right) x_{i,JMAX} + \left(\frac{IMAX - i}{IMAX - 1} \right) x_{1,j} + \left(\frac{i - 1}{IMAX - 1} \right) x_{IMAX,j}$$

for

$$i = 2, 3, \dots, IMAX - 1 \quad \text{and}$$

$$j = 2, 3, \dots, JMAX - 1$$

An analogous equation is used for y.

APPENDIX B

DERIVATION OF TRANSFORMED GOVERNING EQUATIONS

B.1 The Overall Continuity Equation

$$\frac{\partial}{\partial x}(\rho u) + \frac{\partial}{\partial y}(\rho v) + \frac{\partial}{\partial z}(\rho w) = 0 \quad (\text{B.1})$$

$$\frac{1}{J} [y_{\eta}(\rho u)_{\xi} - y_{\xi}(\rho u)_{\eta}] + \frac{1}{J} [x_{\xi}(\rho v)_{\eta} - x_{\eta}(\rho v)_{\xi}] + \frac{\partial}{\partial \sigma}(\rho w) = 0 \quad (\text{B.2})$$

$$y_{\eta}(\rho u)_{\xi} - y_{\xi}(\rho u)_{\eta} + x_{\xi}(\rho v)_{\eta} - x_{\eta}(\rho v)_{\xi} + J \frac{\partial}{\partial \sigma}(\rho w) = 0 \quad (\text{B.3})$$

$$\frac{\partial}{\partial \xi} [y_{\eta}(\rho u) - x_{\eta}(\rho v)] + \frac{\partial}{\partial \eta} [x_{\xi}(\rho v) - y_{\xi}(\rho u)] + J \frac{\partial}{\partial \sigma}(\rho w) = 0 \quad (\text{B.4})$$

$$\frac{\partial}{\partial \xi} [\rho (y_{\eta} u - x_{\eta} v)] + \frac{\partial}{\partial \eta} [\rho (x_{\xi} v - y_{\xi} u)] + \frac{\partial}{\partial \sigma}(\rho w) = 0 \quad (\text{B.5})$$

but

$$y_{\eta} u - x_{\eta} v = U$$

$$x_{\xi} v - y_{\xi} u = V \quad (\text{B.6})$$

$$Jw = W$$

therefore

$$\frac{\partial}{\partial \xi}(\rho U) + \frac{\partial}{\partial \eta}(\rho V) + \frac{\partial}{\partial \sigma}(\rho W) = 0 \quad (\text{B.7})$$

B.2 The Momentum Equation

B.2.1 x-component

$$\frac{\partial}{\partial x} (\rho u^2) + \frac{\partial}{\partial y} (\rho vu) + \frac{\partial}{\partial z} (\rho wu) = -\frac{\partial p}{\partial x} - \left(\frac{\partial \tau_{xx}}{\partial x} + \frac{\partial \tau_{yx}}{\partial y} \right) \quad (\text{B.8})$$

let

$$\omega = \frac{\partial}{\partial x} (\rho u^2) + \frac{\partial}{\partial y} (\rho vu) \quad (\text{B.9})$$

$$\omega = \frac{y_\eta (\rho u^2)_\xi - y_\xi (\rho u^2)_\eta}{J} + \frac{x_\xi (\rho vu)_\eta - x_\eta (\rho vu)_\xi}{J} \quad (\text{B.10})$$

$$\omega = \frac{1}{J} [y_\eta (\rho u^2)_\xi - y_\xi (\rho u^2)_\eta] + \frac{1}{J} [x_\xi (\rho vu)_\eta - x_\eta (\rho vu)_\xi] \quad (\text{B.11})$$

$$\omega = \frac{1}{J} \frac{\partial}{\partial \xi} [y_\eta (\rho u^2) - x_\eta (\rho vu)] + \frac{1}{J} \frac{\partial}{\partial \eta} [x_\xi (\rho vu) - y_\xi (\rho u^2)] \quad (\text{B.12})$$

$$\omega = \frac{1}{J} \frac{\partial}{\partial \xi} [(\rho u) (y_\eta u - x_\eta v)] + \frac{1}{J} \frac{\partial}{\partial \eta} [(\rho u) (x_\xi v - y_\xi u)] \quad (\text{B.13})$$

but

$$\begin{aligned} y_\eta u - x_\eta v &= U \\ x_\xi v - y_\xi u &= V \end{aligned} \quad (\text{B.14})$$

therefore

$$\omega = \frac{1}{J} \frac{\partial}{\partial \xi} [\rho u U] + \frac{1}{J} \frac{\partial}{\partial \eta} [\rho u V] \quad (\text{B.15})$$

$$LHS = \frac{1}{J} \frac{\partial}{\partial \xi} (\rho u U) + \frac{1}{J} \frac{\partial}{\partial \eta} (\rho u V) + \frac{\partial}{\partial \sigma} (\rho u W) \quad (B.16)$$

$$RHS = -\frac{\partial p}{\partial x} \left(\frac{\partial \tau_{xx}}{\partial x} + \frac{\partial \tau_{yx}}{\partial y} \right) \quad (B.17)$$

$$RHS = -\frac{1}{J} [y_{\eta} p_{\xi} - y_{\xi} p_{\eta}] - \frac{1}{J} [y_{\eta} (\hat{\tau}_{xx})_{\xi} - y_{\xi} (\hat{\tau}_{xx})_{\eta}] \\ - \frac{1}{J} [x_{\xi} (\hat{\tau}_{yx})_{\eta} - x_{\eta} (\hat{\tau}_{yx})_{\xi}] \quad (B.18)$$

$$RHS = -\frac{1}{J} [y_{\eta} p_{\xi} - y_{\xi} p_{\eta}] - \frac{1}{J} [y_{\eta} (\hat{\tau}_{xx})_{\xi} - x_{\eta} (\hat{\tau}_{yx})_{\xi}] \\ - \frac{1}{J} [x_{\xi} (\hat{\tau}_{yx})_{\eta} - y_{\xi} (\hat{\tau}_{xx})_{\eta}] \quad (B.19)$$

$$RHS = -\frac{1}{J} \frac{\partial}{\partial \xi} [y_{\eta} (\hat{\tau}_{xx}) - x_{\eta} (\hat{\tau}_{yx})] - \frac{1}{J} \frac{\partial}{\partial \eta} [x_{\xi} (\hat{\tau}_{yx}) - y_{\xi} (\hat{\tau}_{xx})] \\ - \frac{1}{J} [y_{\eta} p_{\xi} - y_{\xi} p_{\eta}] \quad (B.20)$$

Therefore, x-component:

$$\frac{1}{J} \frac{\partial}{\partial \xi} (\rho u U) + \frac{1}{J} \frac{\partial}{\partial \eta} (\rho u V) + \frac{\partial}{\partial \sigma} (\rho u W) = -\frac{1}{J} \frac{\partial}{\partial \xi} [y_{\eta} (\hat{\tau}_{xx}) - x_{\eta} (\hat{\tau}_{yx})] \\ - \frac{1}{J} \frac{\partial}{\partial \eta} [x_{\xi} (\hat{\tau}_{yx}) - y_{\xi} (\hat{\tau}_{xx})] - \frac{1}{J} [y_{\eta} p_{\xi} - y_{\xi} p_{\eta}] \quad (B.21)$$

or

$$\frac{\partial}{\partial \xi} (\rho u U) + \frac{\partial}{\partial \eta} (\rho u V) + \frac{\partial}{\partial \sigma} (\rho u W) = -\frac{\partial}{\partial \xi} [y_{\eta} (\hat{\tau}_{xx}) - x_{\eta} (\hat{\tau}_{yx})] \\ - \frac{\partial}{\partial \eta} [x_{\xi} (\hat{\tau}_{yx}) - y_{\xi} (\hat{\tau}_{xx})] - [y_{\eta} p_{\xi} - y_{\xi} p_{\eta}] \quad (B.22)$$

2.2.2 y-component

$$\frac{\partial}{\partial x} (\rho uv) + \frac{\partial}{\partial y} (\rho v^2) + \frac{\partial}{\partial z} (\rho wv) - \frac{\partial p}{\partial y} - \left(\frac{\partial \tau_{xy}}{\partial x} + \frac{\partial \tau_{yy}}{\partial y} \right) - (\rho - \rho_a) g \quad (\text{B.23})$$

$$(\omega) - \frac{1}{J} [y_\eta (\rho uv)_\xi - y_\xi (\rho uv)_\eta] + \frac{1}{J} [x_\xi (\rho v^2)_\eta - x_\eta (\rho v^2)_\xi] \quad (\text{B.24})$$

$$(\omega) - \frac{1}{J} \frac{\partial}{\partial \xi} [y_\eta (\rho uv) - x_\eta (\rho v^2)] + \frac{1}{J} \frac{\partial}{\partial \eta} [x_\xi (\rho v^2) - y_\xi (\rho uv)] \quad (\text{B.25})$$

$$(\omega) - \frac{1}{J} \frac{\partial}{\partial \xi} [\rho v (y_\eta u - x_\eta v)] + \frac{1}{J} \frac{\partial}{\partial \eta} [\rho v (x_\xi v - y_\xi u)] \quad (\text{B.26})$$

but

$$\begin{aligned} y_\eta u - x_\eta v &= U \\ x_\xi v - y_\xi u &= V \end{aligned} \quad (\text{B.27})$$

$$(\omega) - \frac{1}{J} \frac{\partial}{\partial \xi} [\rho v U] + \frac{1}{J} \frac{\partial}{\partial \eta} [\rho v V]$$

$$LHS = \frac{1}{J} \frac{\partial}{\partial \xi} (\rho v U) + \frac{1}{J} \frac{\partial}{\partial \eta} (\rho v V) + \frac{\partial}{\partial z} (\rho wv) \quad (\text{B.28})$$

$$RHS = -\frac{\partial p}{\partial y} - \left(\frac{\partial \tau_{xy}}{\partial x} + \frac{\partial \tau_{yy}}{\partial y} \right) - (\rho - \rho_a) g \quad (\text{B.29})$$

$$\begin{aligned}
 RHS = & -\frac{1}{J} (x_{\xi} p_{\eta} - x_{\eta} p_{\xi}) - \frac{1}{J} [y_{\eta} (\widehat{\tau}_{xy})_{\xi} - y_{\xi} (\widehat{\tau}_{xy})_{\eta}] \\
 & - \frac{1}{J} [x_{\xi} (\widehat{\tau}_{yy})_{\eta} - x_{\eta} (\widehat{\tau}_{yy})_{\xi}] - (\rho - \rho_a) g
 \end{aligned} \tag{B.30}$$

$$\begin{aligned}
 RHS = & -\frac{1}{J} (x_{\xi} p_{\eta} - x_{\eta} p_{\xi}) - \frac{1}{J} [y_{\eta} (\widehat{\tau}_{xy})_{\xi} - x_{\eta} (\widehat{\tau}_{yy})_{\xi}] \\
 & - \frac{1}{J} [x_{\xi} (\widehat{\tau}_{yy})_{\eta} - y_{\xi} (\widehat{\tau}_{xy})_{\eta}] - (\rho - \rho_a) g
 \end{aligned} \tag{B.31}$$

$$\begin{aligned}
 RHS = & -\frac{1}{J} \frac{\partial}{\partial \xi} [y_{\eta} (\widehat{\tau}_{xy}) - x_{\eta} (\widehat{\tau}_{yy})] - \frac{1}{J} \frac{\partial}{\partial \eta} [x_{\xi} (\widehat{\tau}_{yy}) - y_{\xi} (\widehat{\tau}_{xy})] \\
 & - \frac{1}{J} (x_{\xi} p_{\eta} - x_{\eta} p_{\xi}) - (\rho - \rho_a) g
 \end{aligned} \tag{B.32}$$

therefore y-component:

$$\begin{aligned}
 \frac{1}{J} \frac{\partial}{\partial \xi} (\rho v U) + \frac{1}{J} \frac{\partial}{\partial \eta} (\rho v V) + \frac{\partial}{\partial \sigma} (\rho w v) = & -\frac{1}{J} \frac{\partial}{\partial \xi} [y_{\eta} (\widehat{\tau}_{xy}) - x_{\eta} (\widehat{\tau}_{yy})] \\
 - \frac{1}{J} \frac{\partial}{\partial \eta} [x_{\xi} (\widehat{\tau}_{yy}) - y_{\xi} (\widehat{\tau}_{xy})] - \frac{1}{J} (x_{\xi} p_{\eta} - x_{\eta} p_{\xi}) - & (\rho - \rho_a) g
 \end{aligned} \tag{B.33}$$

$$\begin{aligned}
 \frac{\partial}{\partial \xi} (\rho v U) + \frac{\partial}{\partial \eta} (\rho v V) + \frac{\partial}{\partial \sigma} (\rho w v) = & -\frac{\partial}{\partial \xi} [y_{\eta} (\widehat{\tau}_{xy}) - x_{\eta} (\widehat{\tau}_{yy})] \\
 - \frac{\partial}{\partial \eta} [x_{\xi} (\widehat{\tau}_{yy}) - y_{\xi} (\widehat{\tau}_{xy})] - (x_{\xi} p_{\eta} - x_{\eta} p_{\xi}) - & J(\rho - \rho_a) g
 \end{aligned} \tag{B.34}$$

2.3 z-component

$$\frac{\partial}{\partial x} (\rho uw) + \frac{\partial}{\partial y} (\rho vw) + \frac{\partial}{\partial z} (\rho w^2) - \frac{d\bar{\phi}}{dz} - \left(\frac{\partial \tau_{xz}}{\partial x} + \frac{\partial \tau_{yz}}{\partial y} \right) \quad (\text{B.35})$$

$$\omega = \frac{\partial}{\partial x} (\rho uw) + \frac{\partial}{\partial y} (\rho vw) \quad (\text{B.36})$$

$$\omega = \frac{1}{J} [y_\eta (\rho uw)_\xi - y_\xi (\rho uw)_\eta] + \frac{1}{J} [x_\xi (\rho vw)_\eta - x_\eta (\rho vw)_\xi] \quad (\text{B.37})$$

$$\omega = \frac{1}{J} \frac{\partial}{\partial \xi} [y_\eta (\rho uw) - x_\eta (\rho vw)] + \frac{1}{J} \frac{\partial}{\partial \eta} [x_\xi (\rho vw) - y_\xi (\rho uw)] \quad (\text{B.38})$$

$$\omega = \frac{1}{J} \frac{\partial}{\partial \xi} [(\rho w) (y_\eta u - x_\eta v)] + \frac{1}{J} \frac{\partial}{\partial \eta} [(\rho w) (x_\xi v - y_\xi u)] \quad (\text{B.39})$$

but

$$\begin{aligned} y_\eta u - x_\eta v &= U \\ x_\xi v - y_\xi u &= V \end{aligned} \quad (\text{B.40})$$

therefore

$$\omega = \frac{1}{J} \frac{\partial}{\partial \xi} [(\rho w) U] + \frac{1}{J} \frac{\partial}{\partial \eta} [(\rho w) V] \quad (\text{B.41})$$

$$(2) - \frac{1}{J} \frac{\partial}{\partial \xi} (\rho w U) + \frac{1}{J} \frac{\partial}{\partial \eta} (\rho w V) \quad (\text{B.42})$$

$$LHS = \frac{1}{J} \frac{\partial}{\partial \xi} (\rho w U) + \frac{1}{J} \frac{\partial}{\partial \eta} (\rho w V) + \frac{\partial}{\partial \sigma} (\rho w^2) \quad (\text{B.43})$$

$$RHS = - \frac{d\bar{p}}{d\sigma} - \left(\frac{\partial \tau_{xz}}{\partial x} + \frac{\partial \tau_{yz}}{\partial y} \right) \quad (\text{B.44})$$

$$RHS = - \frac{d\bar{p}}{d\sigma} - \frac{1}{J} [y_{\eta} (\hat{\tau}_{xz})_{\xi} - y_{\xi} (\hat{\tau}_{xz})_{\eta}] \\ - \frac{1}{J} [x_{\xi} (\hat{\tau}_{yz})_{\eta} - x_{\eta} (\hat{\tau}_{yz})_{\xi}] \quad (\text{B.45})$$

$$RHS = - \frac{d\bar{p}}{d\sigma} - \frac{1}{J} [y_{\eta} (\hat{\tau}_{xz})_{\xi} - x_{\eta} (\hat{\tau}_{yz})_{\xi}] \\ - \frac{1}{J} [x_{\xi} (\hat{\tau}_{yz})_{\eta} - x_{\xi} (\hat{\tau}_{xz})_{\eta}] \quad (\text{B.46})$$

$$RHS = - \frac{1}{J} \frac{\partial}{\partial \xi} [y_{\eta} (\hat{\tau}_{xz}) - x_{\eta} (\hat{\tau}_{yz})] \\ - \frac{1}{J} \frac{\partial}{\partial \eta} [x_{\xi} (\hat{\tau}_{yz}) - y_{\xi} (\hat{\tau}_{xz})] - \frac{d\bar{p}}{d\sigma} \quad (\text{B.47})$$

Therefore z-component:

$$\begin{aligned}
 & \frac{1}{J} \frac{\partial}{\partial \xi} (\rho w U) + \frac{1}{J} \frac{\partial}{\partial \eta} (\rho w V) + \frac{\partial}{\partial \sigma} (\rho w^2) - \\
 & - \frac{1}{J} \frac{\partial}{\partial \xi} [y_{\eta} (\hat{\tau}_{xz}) - x_{\eta} (\hat{\tau}_{yz})] \\
 & - \frac{1}{J} \frac{\partial}{\partial \eta} [x_{\xi} (\hat{\tau}_{yz}) - y_{\xi} (\hat{\tau}_{xz})] - \frac{d\bar{p}}{d\sigma}
 \end{aligned} \tag{B.48}$$

or

$$\begin{aligned}
 & \frac{\partial}{\partial \xi} (\rho w U) + \frac{\partial}{\partial \eta} (\rho w V) + \frac{\partial}{\partial \sigma} (\rho w W) - \\
 & - \frac{\partial}{\partial \xi} [y_{\eta} (\hat{\tau}_{xz}) - x_{\eta} (\hat{\tau}_{yz})] \\
 & - \frac{\partial}{\partial \eta} [x_{\xi} (\hat{\tau}_{yz}) - y_{\xi} (\hat{\tau}_{xz})] - J \frac{d\bar{p}}{d\sigma}
 \end{aligned} \tag{B.49}$$

B.3 The Energy Equation

$$\begin{aligned} \frac{\partial}{\partial x} (\rho C_p T u) + \frac{\partial}{\partial y} (\rho C_p T v) + \frac{\partial}{\partial z} (\rho C_p T w) - \\ \frac{\partial}{\partial x} \left(k \frac{\partial T}{\partial x} \right) + \frac{\partial}{\partial y} \left(k \frac{\partial T}{\partial y} \right) + MI + (-\Delta H) R_A \end{aligned} \quad (B.50)$$

$$LHS = \frac{\partial}{\partial x} (\rho C_p T u) + \frac{\partial}{\partial y} (\rho C_p T v) + \frac{\partial}{\partial z} (\rho C_p T w)$$

$$\begin{aligned} LHS = \frac{1}{J} [y_\eta (\rho C_p T u)_\xi - y_\xi (\rho C_p T u)_\eta] \\ + \frac{1}{J} [x_\xi (\rho C_p T v)_\eta - x_\eta (\rho C_p T v)_\xi] \\ + \frac{\partial}{\partial \sigma} (\rho C_p T w) \end{aligned} \quad (B.51)$$

$$\begin{aligned} LHS = \frac{1}{J} \frac{\partial}{\partial \xi} [y_\eta (\rho C_p T u) - x_\eta (\rho C_p T v)] \\ + \frac{1}{J} \frac{\partial}{\partial \eta} [x_\xi (\rho C_p T v) - y_\xi (\rho C_p T u)] \\ + \frac{\partial}{\partial \sigma} (\rho C_p T w) \end{aligned} \quad (B.52)$$

$$\begin{aligned} LHS = \frac{1}{J} \frac{\partial}{\partial \xi} [\rho C_p T (y_\eta u - x_\eta v)] \\ + \frac{1}{J} \frac{\partial}{\partial \eta} [\rho C_p T (x_\xi v - y_\xi u)] \\ + \frac{\partial}{\partial \sigma} (\rho C_p T w) \end{aligned} \quad (B.53)$$

but

$$\begin{aligned} y_{\eta} u - x_{\eta} v &= U \\ x_{\xi} v - y_{\xi} u &= V \end{aligned} \quad (\text{B.54})$$

$$\text{LHS} = \frac{1}{J} \frac{\partial}{\partial \xi} (\rho C_p T U) + \frac{1}{J} \frac{\partial}{\partial \eta} (\rho C_p T V) + \frac{\partial}{\partial \sigma} (\rho C_p T W) \quad (\text{B.55})$$

$$(\omega) = \frac{\partial}{\partial x} \left(k \frac{\partial T}{\partial x} \right) + \frac{\partial}{\partial y} \left(k \frac{\partial T}{\partial y} \right) \quad (\text{B.56a})$$

$$(\omega) = \frac{1}{J} \left[y_{\eta} \left(k \frac{\partial T}{\partial x} \right)_{\xi} - y_{\xi} \left(k \frac{\partial T}{\partial x} \right)_{\eta} \right] + \frac{1}{J} \left[x_{\xi} \left(k \frac{\partial T}{\partial y} \right)_{\eta} - x_{\eta} \left(k \frac{\partial T}{\partial y} \right)_{\xi} \right] \quad (\text{B.56b})$$

$$(\omega) = \frac{1}{J} \left[y_{\eta} \left(k \frac{\partial T}{\partial x} \right)_{\xi} - x_{\eta} \left(k \frac{\partial T}{\partial y} \right)_{\xi} \right] + \frac{1}{J} \left[x_{\xi} \left(k \frac{\partial T}{\partial y} \right)_{\eta} - y_{\xi} \left(k \frac{\partial T}{\partial x} \right)_{\eta} \right] \quad (\text{B.57})$$

$$(\omega) = \frac{1}{J} \frac{\partial}{\partial \xi} \left[y_{\eta} \left(k \frac{\partial T}{\partial x} \right) - x_{\eta} \left(k \frac{\partial T}{\partial y} \right) \right] + \frac{1}{J} \frac{\partial}{\partial \eta} \left[x_{\xi} \left(k \frac{\partial T}{\partial y} \right) - y_{\xi} \left(k \frac{\partial T}{\partial x} \right) \right] \quad (\text{B.58})$$

$$\begin{aligned} (\omega) &= \frac{1}{J} \frac{\partial}{\partial \xi} \left[\left(y_{\eta} k \frac{y_{\eta} T_{\xi} - y_{\xi} T_{\eta}}{J} \right) - \left(x_{\eta} k \frac{x_{\xi} T_{\eta} - x_{\eta} T_{\xi}}{J} \right) \right] \\ &+ \frac{1}{J} \frac{\partial}{\partial \eta} \left[\left(x_{\xi} k \frac{x_{\xi} T_{\eta} - x_{\eta} T_{\xi}}{J} \right) - \left(y_{\xi} k \frac{y_{\eta} T_{\xi} - y_{\xi} T_{\eta}}{J} \right) \right] \end{aligned} \quad (\text{B.59})$$

$$\begin{aligned}
(\omega) &= \frac{1}{J} \frac{\partial}{\partial \xi} \left[\frac{1}{J} (y_{\eta}^2 k T_{\xi} - y_{\eta} y_{\xi} k T_{\eta} - k x_{\eta} x_{\xi} T_{\eta} + k x_{\eta}^2 T_{\xi}) \right] \\
&+ \frac{1}{J} \frac{\partial}{\partial \eta} \left[\frac{1}{J} (x_{\xi}^2 k T_{\eta} - x_{\xi} x_{\eta} k T_{\xi} - k y_{\xi} y_{\eta} T_{\xi} + k y_{\xi}^2 T_{\eta}) \right]
\end{aligned} \tag{B.60}$$

$$\begin{aligned}
(\omega) &= \frac{1}{J} \frac{\partial}{\partial \xi} \left[\frac{k}{J} T_{\xi} (y_{\eta}^2 + x_{\eta}^2) - \frac{k T_{\eta}}{J} (y_{\eta} y_{\xi} + x_{\eta} x_{\xi}) \right] \\
&+ \frac{1}{J} \frac{\partial}{\partial \eta} \left[\frac{k}{J} T_{\eta} (x_{\xi}^2 + y_{\xi}^2) - \frac{k T_{\xi}}{J} (x_{\xi} x_{\eta} + y_{\xi} y_{\eta}) \right]
\end{aligned} \tag{B.61}$$

but

$$\begin{aligned}
x_{\eta}^2 + y_{\eta}^2 &= \alpha \\
x_{\eta} x_{\xi} + y_{\eta} y_{\xi} &= \beta \\
x_{\xi}^2 + y_{\xi}^2 &= \gamma
\end{aligned} \tag{B.62}$$

$$(\omega) = \frac{1}{J} \frac{\partial}{\partial \xi} \left(\frac{\alpha k T_{\xi}}{J} - \frac{\beta k T_{\eta}}{J} \right) + \frac{1}{J} \frac{\partial}{\partial \eta} \left(\frac{\gamma k T_{\eta}}{J} - \frac{\beta k T_{\xi}}{J} \right) \tag{B.63}$$

$$(\omega) = \frac{1}{J} \frac{\partial}{\partial \xi} \left(\frac{\alpha}{J} k T_{\xi} - \frac{\beta}{J} k T_{\eta} \right) + \frac{1}{J} \frac{\partial}{\partial \eta} \left(\frac{\gamma}{J} k T_{\eta} - \frac{\beta}{J} k T_{\xi} \right) \tag{B.64}$$

$$RHS = \frac{1}{J} \frac{\partial}{\partial \xi} \left(\frac{\alpha}{J} k T_{\xi} - \frac{\beta}{J} k T_{\eta} \right) + \frac{1}{J} \frac{\partial}{\partial \eta} \left(\frac{\gamma}{J} k T_{\eta} - \frac{\beta}{J} k T_{\xi} \right) + \hat{M} \hat{I} + (-\Delta H) \hat{R}_A \tag{B.65}$$

Therefore the energy equation:

$$\begin{aligned} & \frac{1}{J} \frac{\partial}{\partial \xi} (\rho C_p T U) + \frac{1}{J} \frac{\partial}{\partial \eta} (\rho C_p T V) + \frac{\partial}{\partial \sigma} (\rho C_p T W) - \\ & \frac{1}{J} \frac{\partial}{\partial \xi} \left(\frac{\alpha}{J} k T_\xi - \frac{\beta}{J} k T_\eta \right) + \frac{1}{J} \frac{\partial}{\partial \eta} \left(\frac{\gamma}{J} k T_\eta - \frac{\beta}{J} k T_\xi \right) \\ & + \hat{M} \hat{I} + (-\Delta H) \hat{R}_A \end{aligned} \quad (\text{B.66})$$

$$\begin{aligned} & \frac{\partial}{\partial \xi} (\rho C_p T U) + \frac{\partial}{\partial \eta} (\rho C_p T V) + \frac{\partial}{\partial \sigma} (\rho C_p T W) - \\ & \frac{\partial}{\partial \xi} \left(\frac{\alpha}{J} k T_\xi - \frac{\beta}{J} k T_\eta \right) + \frac{\partial}{\partial \eta} \left(\frac{\gamma}{J} k T_\eta - \frac{\beta}{J} k T_\xi \right) \\ & + J \hat{M} \hat{I} + J (-\Delta H) \hat{R}_A \end{aligned} \quad (\text{B.67})$$

B.4 The Reactant Continuity Equation

$$\begin{aligned} & \frac{\partial}{\partial x} (\rho \omega_A u) + \frac{\partial}{\partial y} (\rho \omega_A v) + \frac{\partial}{\partial z} (\rho \omega_A w) - \\ & \frac{\partial}{\partial x} \left(\rho D_A \frac{\partial \omega_A}{\partial x} \right) + \frac{\partial}{\partial y} \left(\rho D_A \frac{\partial \omega_A}{\partial y} \right) - \hat{R}_A \end{aligned} \quad (\text{B.68})$$

$$LHS = \frac{\partial}{\partial x} (\rho \omega_A u) + \frac{\partial}{\partial y} (\rho \omega_A v) + \frac{\partial}{\partial z} (\rho \omega_A w) \quad (\text{B.69})$$

$$\begin{aligned} LHS = & \frac{y_\eta}{J} (\rho \omega_A u)_\xi - \frac{y_\xi}{J} (\rho \omega_A u)_\eta + \frac{x_\xi}{J} (\rho \omega_A v)_\eta \\ & - \frac{x_\eta}{J} (\rho \omega_A v)_\xi + \frac{\partial}{\partial \sigma} (\rho \omega_A w) \end{aligned} \quad (\text{B.70})$$

$$LHS = \frac{1}{J} \frac{\partial}{\partial \xi} [y_\eta (\rho \omega_A u) - x_\eta (\rho \omega_A v)] + \frac{1}{J} \frac{\partial}{\partial \eta} [x_\xi (\rho \omega_A v) - y_\xi (\rho \omega_A u)] + \frac{\partial}{\partial \sigma} (\rho \omega_A w) \quad (\text{B.71})$$

$$LHS = \frac{1}{J} \frac{\partial}{\partial \xi} [\rho \omega_A (uy_\eta - vx_\eta)] + \frac{1}{J} \frac{\partial}{\partial \eta} [\rho \omega_A (vx_\xi - uy_\xi)] + \frac{\partial}{\partial \sigma} (\rho \omega_A w) \quad (\text{B.72})$$

but

$$\begin{aligned} uy_\eta - vx_\eta &= U \\ vx_\xi - uy_\xi &= V \end{aligned} \quad (\text{B.73})$$

therefore

$$LHS = \frac{1}{J} \frac{\partial}{\partial \xi} (\rho \omega_A U) + \frac{1}{J} \frac{\partial}{\partial \eta} (\rho \omega_A V) + \frac{\partial}{\partial \sigma} (\rho \omega_A w) \quad (\text{B.74})$$

$$(i) - \frac{\partial}{\partial x} \left(\rho D_A \frac{\partial \omega_A}{\partial x} \right) + \frac{\partial}{\partial y} \left(\rho D_A \frac{\partial \omega_A}{\partial y} \right) \quad (\text{B.75})$$

$$(ii) - \frac{y_\eta}{J} \frac{\partial}{\partial \xi} \left(\rho D_A \frac{\partial \omega_A}{\partial x} \right) - \frac{y_\xi}{J} \frac{\partial}{\partial \eta} \left(\rho D_A \frac{\partial \omega_A}{\partial x} \right) \\ + \frac{x_\xi}{J} \frac{\partial}{\partial \eta} \left(\rho D_A \frac{\partial \omega_A}{\partial y} \right) - \frac{x_\eta}{J} \frac{\partial}{\partial \xi} \left(\rho D_A \frac{\partial \omega_A}{\partial y} \right) \quad (\text{B.76})$$

$$(i) - \frac{1}{J} \frac{\partial}{\partial \xi} \left[y_\eta \rho D_A \frac{\partial \omega_A}{\partial x} - x_\eta \rho D_A \frac{\partial \omega_A}{\partial y} \right] \\ + \frac{1}{J} \frac{\partial}{\partial \eta} \left[x_\xi \rho D_A \frac{\partial \omega_A}{\partial y} - y_\xi \rho D_A \frac{\partial \omega_A}{\partial x} \right] \quad (\text{B.77})$$

$$(i) - \frac{1}{J} \frac{\partial}{\partial \xi} \left[y_\eta \rho D_A \frac{y_\eta \omega_\xi - y_\xi \omega_\eta}{J} - x_\eta \rho D_A \frac{x_\xi \omega_\eta - x_\eta \omega_\xi}{J} \right] \\ + \frac{1}{J} \frac{\partial}{\partial \eta} \left[x_\xi \rho D_A \frac{x_\xi \omega_\eta - x_\eta \omega_\xi}{J} - y_\xi \rho D_A \frac{y_\eta \omega_\xi - y_\xi \omega_\eta}{J} \right] \quad (\text{B.78})$$

$$(i) - \frac{1}{J} \frac{\partial}{\partial \xi} \left[y_\eta \rho D_A \left(\frac{y_\eta}{J} \omega_\xi - \frac{y_\xi}{J} \omega_\eta \right) - x_\eta \rho D_A \left(\frac{x_\xi}{J} \omega_\eta - \frac{x_\eta}{J} \omega_\xi \right) \right] \\ + \frac{1}{J} \frac{\partial}{\partial \eta} \left[x_\xi \rho D_A \left(\frac{x_\xi}{J} \omega_\eta - \frac{x_\eta}{J} \omega_\xi \right) - y_\xi \rho D_A \left(\frac{y_\eta}{J} \omega_\xi - \frac{y_\xi}{J} \omega_\eta \right) \right] \quad (\text{B.79})$$

$$(i) - \frac{1}{J} \frac{\partial}{\partial \xi} \left[\rho D_A \left(\frac{y_\eta^2}{J} \omega_\xi - \frac{y_\xi y_\eta}{J} \omega_\eta \right) - \rho D_A \left(\frac{x_\eta x_\xi}{J} \omega_\eta - \frac{x_\eta^2}{J} \omega_\xi \right) \right] \\ + \frac{1}{J} \frac{\partial}{\partial \eta} \left[\rho D_A \left(\frac{x_\xi^2}{J} \omega_\eta - \frac{x_\xi x_\eta}{J} \omega_\xi \right) - \rho D_A \left(\frac{y_\xi y_\eta}{J} \omega_\xi - \frac{y_\xi^2}{J} \omega_\eta \right) \right] \quad (\text{B.80})$$

$$\begin{aligned} \dot{\omega} = & \frac{1}{J} \frac{\partial}{\partial \xi} \left[\rho D_A \frac{(y_\eta^2 + x_\xi^2)}{J} \omega_\xi - \rho D_A \frac{(y_\xi y_\eta + x_\eta x_\xi)}{J} \omega_\eta \right] \\ & + \frac{1}{J} \frac{\partial}{\partial \eta} \left[\rho D_A \frac{(x_\xi^2 + y_\xi^2)}{J} \omega_\eta - \rho D_A \frac{(x_\xi x_\eta + y_\xi y_\eta)}{J} \omega_\xi \right] \end{aligned} \quad (\text{B.81})$$

but

$$\begin{aligned} y_\eta^2 + x_\eta^2 &= \alpha \\ y_\xi y_\eta + x_\eta x_\xi &= \beta \\ x_\xi^2 + y_\xi^2 &= \gamma \end{aligned} \quad (\text{B.82})$$

$$\dot{\omega} = \frac{1}{J} \frac{\partial}{\partial \xi} \left[\rho D_A \frac{\alpha}{J} \omega_\xi - \rho D_A \frac{\beta}{J} \omega_\eta \right] + \frac{1}{J} \frac{\partial}{\partial \eta} \left[\rho D_A \frac{\gamma}{J} \omega_\eta - \rho D_A \frac{\beta}{J} \omega_\xi \right] \quad (\text{B.83})$$

$$RHS = \frac{1}{J} \frac{\partial}{\partial \xi} \left[\frac{\rho D_A}{J} \alpha \omega_\xi - \frac{\rho D_A}{J} \beta \omega_\eta \right] + \frac{1}{J} \frac{\partial}{\partial \eta} \left[\frac{\rho D_A}{J} \gamma \omega_\eta - \frac{\rho D_A}{J} \beta \omega_\xi \right] - \hat{R}_A \quad (\text{B.84})$$

Therefore, the reactant continuity equation:

$$\begin{aligned} \frac{1}{J} \frac{\partial}{\partial \xi} (\rho \omega_A U) + \frac{1}{J} \frac{\partial}{\partial \eta} (\rho \omega_A V) + \frac{\partial}{\partial \sigma} (\rho \omega_A W) - \frac{1}{J} \frac{\partial}{\partial \xi} \left[\frac{\rho D_A}{J} \alpha \omega_\xi - \frac{\rho D_A}{J} \beta \omega_\eta \right] \\ + \frac{1}{J} \frac{\partial}{\partial \eta} \left[\frac{\rho D_A}{J} \gamma \omega_\eta - \frac{\rho D_A}{J} \beta \omega_\xi \right] - \hat{R}_A \end{aligned} \quad (\text{B.85})$$

The reactant continuity equation:

$$\begin{aligned} \frac{\partial}{\partial \xi} (\rho \omega_A U) + \frac{\partial}{\partial \eta} (\rho \omega_A V) + \frac{\partial}{\partial \sigma} (\rho \omega_A W) - \frac{\partial}{\partial \xi} \left[\frac{\rho D_A}{J} \alpha \omega_\xi - \frac{\rho D_A}{J} \beta \omega_\eta \right] \\ + \frac{\partial}{\partial \eta} \left[\frac{\rho D_A}{J} \gamma \omega_\eta - \frac{\rho D_A}{J} \beta \omega_\xi \right] - J \hat{R}_A \end{aligned} \quad (\text{B.86})$$

B5. The Transformed Form of the Components of Stress-Tensor

$$\hat{\tau}_{xx} = L \left[-2\mu \left(\frac{\partial u}{\partial x} \right) I^{\frac{n-1}{2}} \right] - L \left[2 \left(\frac{\partial u}{\partial x} \right) \right] \hat{M} - \frac{2}{J} [y_{\eta} u_{\xi} - y_{\xi} u_{\eta}] \hat{M} \quad (\text{B.87})$$

$$\hat{\tau}_{yy} = L \left[-2\mu \left(\frac{\partial v}{\partial y} \right) I^{\frac{n-1}{2}} \right] - L \left[2 \left(\frac{\partial v}{\partial y} \right) \right] \hat{M} - \frac{2}{J} [x_{\xi} v_{\eta} - x_{\eta} v_{\xi}] \hat{M} \quad (\text{B.88})$$

$$\hat{\tau}_{zz} = L \left[-2\mu \left(\frac{\partial w}{\partial z} \right) I^{\frac{n-1}{2}} \right] - L \left[2 \left(\frac{\partial w}{\partial z} \right) \right] \hat{M} \quad (\text{B.89})$$

$$\hat{\tau}_{xy} = \hat{\tau}_{yx} = L \left[-\mu \left(\frac{\partial u}{\partial y} + \frac{\partial v}{\partial x} \right) I^{\frac{n-1}{2}} \right] - L \left[\left(\frac{\partial u}{\partial y} + \frac{\partial v}{\partial x} \right) \right] \hat{M} \quad (\text{B.90})$$

$$\hat{\tau}_{xy} = \hat{\tau}_{yx} = -\frac{1}{J} [x_{\xi} u_{\eta} - x_{\eta} u_{\xi} + y_{\eta} v_{\xi} - y_{\xi} v_{\eta}] \hat{M} \quad (\text{B.91})$$

$$\hat{\tau}_{xz} = \hat{\tau}_{zx} = L \left[\mu \left(\frac{\partial u}{\partial z} + \frac{\partial w}{\partial x} \right) I^{\frac{n-1}{2}} \right] - L \left[\left(\frac{\partial u}{\partial z} + \frac{\partial w}{\partial x} \right) \right] \hat{M} \quad (\text{B.92})$$

$$\hat{\tau}_{xz} = \hat{\tau}_{zx} = -\left[\frac{\partial u}{\partial z} + \frac{1}{J} (y_{\eta} w_{\xi} - y_{\xi} w_{\eta}) \right] \hat{M} \quad (\text{B.93})$$

$$\hat{\tau}_{yz} = \hat{\tau}_{zy} = -L \left[\mu \left(\frac{\partial w}{\partial y} + \frac{\partial v}{\partial z} \right) I^{\frac{n-1}{2}} \right] = -L \left[\left(\frac{\partial w}{\partial y} + \frac{\partial v}{\partial z} \right) \right] \hat{M} \quad (\text{B.94})$$

$$\hat{\tau}_{yz} = \hat{\tau}_{zy} = - \left[\frac{1}{J} (x_{\xi} w_{\eta} - x_{\eta} w_{\xi}) + \frac{\partial v}{\partial \sigma} \right] \hat{M} \quad (\text{B.95})$$

B.6 The Transformed Form of I and M

$$I = 2 \left[\left(\frac{\partial u}{\partial x} \right)^2 + \left(\frac{\partial v}{\partial y} \right)^2 + \left(\frac{\partial w}{\partial z} \right)^2 \right] + \left(\frac{\partial v}{\partial x} + \frac{\partial u}{\partial y} \right)^2 + \left(\frac{\partial w}{\partial y} + \frac{\partial v}{\partial z} \right)^2 + \left(\frac{\partial u}{\partial z} + \frac{\partial w}{\partial x} \right)^2 \quad (\text{B.96})$$

$$\hat{I} = 2 \left[\left(\frac{y_{\eta}}{J} u_{\xi} - \frac{y_{\xi}}{J} u_{\eta} \right)^2 + \left(\frac{x_{\xi}}{J} v_{\eta} - \frac{x_{\eta}}{J} v_{\xi} \right)^2 + \left(\frac{\partial w}{\partial \sigma} \right)^2 \right] + \left(\frac{y_{\eta}}{J} v_{\xi} - \frac{y_{\xi}}{J} v_{\eta} + \frac{x_{\xi}}{J} u_{\eta} - \frac{x_{\eta}}{J} u_{\xi} \right)^2 + \left(\frac{x_{\xi}}{J} w_{\eta} - \frac{x_{\eta}}{J} w_{\xi} + \frac{\partial v}{\partial \sigma} \right)^2 + \left(\frac{\partial u}{\partial \sigma} + \frac{y_{\eta}}{J} w_{\xi} - \frac{y_{\xi}}{J} w_{\eta} \right)^2 \quad (\text{B.97})$$

$$\hat{M} = \mu \hat{I}^{\frac{n-1}{2}} \quad (\text{B.98})$$

APPENDIX C
DERIVATION OF DISCRETIZATION EQUATIONS

Typical derivation for u_e (refer to Fig. C.1)

$$\begin{aligned}
& \int_U^D \int_{se}^{ne} \int_P^E \frac{\partial}{\partial \xi} (\rho u U) d\xi d\eta d\sigma + \int_U^D \int_P^E \int_{se}^{ne} \frac{\partial}{\partial \eta} (\rho u V) d\eta d\xi d\sigma + \\
& \int_{se}^{ne} \int_P^E \int_U^D \frac{\partial}{\partial \sigma} (\rho u W) d\sigma d\xi d\eta = \int_U^D \int_{se}^{ne} \int_P^E \frac{\partial}{\partial \xi} (C_1^u \frac{\partial u}{\partial \xi}) d\xi d\eta d\sigma + \\
& \int_U^D \int_{se}^{ne} \int_P^E \frac{\partial}{\partial \xi} (C_2^u \frac{\partial u}{\partial \eta}) d\xi d\eta d\sigma + \int_U^D \int_{se}^{ne} \int_P^E \frac{\partial}{\partial \xi} (C_3^u \frac{\partial v}{\partial \xi}) d\xi d\eta d\sigma + \\
& \int_U^D \int_{se}^{ne} \int_P^E \frac{\partial}{\partial \xi} (C_4^u \frac{\partial v}{\partial \eta}) d\xi d\eta d\sigma + \int_U^D \int_P^E \int_{se}^{ne} \frac{\partial}{\partial \eta} (C_5^u \frac{\partial u}{\partial \eta}) d\eta d\xi d\sigma + \\
& \int_U^D \int_P^E \int_{se}^{ne} \frac{\partial}{\partial \eta} (C_6^u \frac{\partial u}{\partial \xi}) d\eta d\xi d\sigma + \int_U^D \int_P^E \int_{se}^{ne} \frac{\partial}{\partial \eta} (C_7^u \frac{\partial v}{\partial \eta}) d\eta d\xi d\sigma + \\
& \int_U^D \int_P^E \int_{se}^{ne} \frac{\partial}{\partial \eta} (C_8^u \frac{\partial v}{\partial \xi}) d\eta d\xi d\sigma - \int_U^D \int_{se}^{ne} \int_P^E \hat{P}^u d\xi d\eta d\sigma \quad (C.1)
\end{aligned}$$

$$\begin{aligned}
& (\rho u U)_E \Delta \eta \Delta \sigma - (\rho u U)_P \Delta \eta \Delta \sigma + (\rho u V)_{ne} \Delta \xi \Delta \sigma - (\rho u V)_{se} \Delta \xi \Delta \sigma + \\
& (\rho u W)_{e,D} \Delta \xi \Delta \eta - (\rho u W)_{e,U} \Delta \xi \Delta \eta = \left(C_1^u \frac{\partial u}{\partial \xi} \right)_E \Delta \eta \Delta \sigma - \left(C_1^u \frac{\partial u}{\partial \xi} \right)_P \Delta \eta \Delta \sigma + \\
& \left(C_2^u \frac{\partial u}{\partial \eta} \right)_E \Delta \eta \Delta \sigma - \left(C_2^u \frac{\partial u}{\partial \eta} \right)_P \Delta \eta \Delta \sigma + \left(C_3^u \frac{\partial v}{\partial \xi} \right)_E \Delta \eta \Delta \sigma - \left(C_3^u \frac{\partial v}{\partial \xi} \right)_P \Delta \eta \Delta \sigma + \\
& \left(C_4^u \frac{\partial v}{\partial \eta} \right)_E \Delta \eta \Delta \sigma - \left(C_4^u \frac{\partial v}{\partial \eta} \right)_P \Delta \eta \Delta \sigma + \left(C_5^u \frac{\partial u}{\partial \eta} \right)_{ne} \Delta \xi \Delta \sigma - \left(C_5^u \frac{\partial u}{\partial \eta} \right)_{se} \Delta \xi \Delta \sigma + \\
& \left(C_6^u \frac{\partial u}{\partial \xi} \right)_{ne} \Delta \xi \Delta \sigma - \left(C_6^u \frac{\partial u}{\partial \xi} \right)_{se} \Delta \xi \Delta \sigma + \left(C_7^u \frac{\partial v}{\partial \eta} \right)_{ne} \Delta \xi \Delta \sigma - \left(C_7^u \frac{\partial v}{\partial \eta} \right)_{se} \Delta \xi \Delta \sigma + \\
& \left(C_8^u \frac{\partial v}{\partial \xi} \right)_{ne} \Delta \xi \Delta \sigma - \left(C_8^u \frac{\partial v}{\partial \xi} \right)_{se} \Delta \xi \Delta \sigma - \hat{P}_e^u \Delta V \quad (C.2)
\end{aligned}$$

$$\begin{aligned}
LHS &= (\rho U)_E \Delta \eta \Delta \sigma u_E - (\rho U)_P \Delta \eta \Delta \sigma u_P + (\rho V)_{ne} \Delta \xi \Delta \sigma u_{ne} - \\
& (\rho V)_{se} \Delta \xi \Delta \sigma u_{se} + (\rho W)_{e,D} \Delta \xi \Delta \eta u_e - (\rho W)_{e,U} \Delta \xi \Delta \eta u_{e,U} \quad (C.3)
\end{aligned}$$

$$\begin{aligned}
LHS = & \|(\rho U)_{E,0}\|\Delta\eta\Delta\sigma u_e - \| -(\rho U)_{E,0}\|\Delta\eta\Delta\sigma u_{ee} - \\
& \{ \|(\rho U)_{P,0}\|\Delta\eta\Delta\sigma u_w - \| -(\rho U)_{P,0}\|\Delta\eta\Delta\sigma u_e \} + \\
& \|(\rho V)_{ne,0}\|\Delta\xi\Delta\sigma u_e - \| -(\rho V)_{ne,0}\|\Delta\xi\Delta\sigma u_3 - \\
& \{ \|(\rho V)_{se,0}\|\Delta\xi\Delta\sigma u_5 - \| -(\rho V)_{se,0}\|\Delta\xi\Delta\sigma u_e \} + \\
& (\rho W)_{e,D}\Delta\xi\Delta\eta u_e - (\rho W)_{e,U}\Delta\xi\Delta\eta u_{e,U}
\end{aligned} \tag{C.4}$$

$$\begin{aligned}
LHS = & \|(\rho U)_{E,0}\|\Delta\eta\Delta\sigma u_e - \| -(\rho U)_{E,0}\|\Delta\eta\Delta\sigma u_{ee} - \\
& \|(\rho U)_{P,0}\|\Delta\eta\Delta\sigma u_w + \| -(\rho U)_{P,0}\|\Delta\eta\Delta\sigma u_e + \\
& \|(\rho V)_{ne,0}\|\Delta\xi\Delta\sigma u_e - \| -(\rho V)_{ne,0}\|\Delta\xi\Delta\sigma u_3 - \\
& \|(\rho V)_{se,0}\|\Delta\xi\Delta\sigma u_5 + \| -(\rho V)_{se,0}\|\Delta\xi\Delta\sigma u_e + \\
& (\rho W)_{e,D}\Delta\xi\Delta\eta u_e - (\rho W)_{e,U}\Delta\xi\Delta\eta u_{e,U}
\end{aligned} \tag{C.5}$$

write the continuity equation:

$$\frac{\partial}{\partial\xi}(\rho U) + \frac{\partial}{\partial\eta}(\rho V) + \frac{\partial}{\partial\sigma}(\rho W) = 0 \tag{C.6}$$

$$\begin{aligned}
& \int_U^D \int_{se}^{ne} \int_P^E \frac{\partial}{\partial\xi}(\rho U) d\xi d\eta d\sigma + \int_U^D \int_P^E \int_{se}^{ne} \frac{\partial}{\partial\eta}(\rho V) d\eta d\xi d\sigma + \\
& \int_{se}^{ne} \int_P^E \int_U^D \frac{\partial}{\partial\sigma}(\rho W) d\sigma d\xi d\eta = 0
\end{aligned} \tag{C.7}$$

$$\begin{aligned}
& (\rho U)_E \Delta\eta \Delta\sigma - (\rho U)_P \Delta\eta \Delta\sigma + (\rho V)_{ne} \Delta\xi \Delta\sigma - \\
& (\rho V)_{se} \Delta\xi \Delta\sigma + (\rho W)_{e,D} \Delta\xi \Delta\eta - (\rho W)_{e,U} \Delta\xi \Delta\eta = 0
\end{aligned} \tag{C.8}$$

multiply by $-u_e$

$$\begin{aligned}
& -(\rho U)_E \Delta\eta \Delta\sigma u_e + (\rho U)_P \Delta\eta \Delta\sigma u_e - (\rho V)_{ne} \Delta\xi \Delta\sigma u_e + \\
& (\rho V)_{se} \Delta\xi \Delta\sigma u_e - (\rho W)_{e,D} \Delta\xi \Delta\eta u_e + (\rho W)_{e,U} \Delta\xi \Delta\eta u_e = 0
\end{aligned} \tag{C.9}$$

add Eqn. (C.5) to Eqn. (C.9)

$$\begin{aligned}
LHS = & \|(\rho U)_{E,0}\|\Delta\eta\Delta\sigma u_e - \| -(\rho U)_{E,0}\|\Delta\eta\Delta\sigma u_{ee} - \\
& \|(\rho U)_{P,0}\|\Delta\eta\Delta\sigma u_w + \| -(\rho U)_{P,0}\|\Delta\eta\Delta\sigma u_e + \\
& \|(\rho V)_{ne,0}\|\Delta\xi\Delta\sigma u_e - \| -(\rho V)_{ne,0}\|\Delta\xi\Delta\sigma u_3 - \\
& \|(\rho V)_{se,0}\|\Delta\xi\Delta\sigma u_5 + \| -(\rho V)_{se,0}\|\Delta\xi\Delta\sigma u_e + \\
& (\rho W)_{e,D}\Delta\xi\Delta\eta u_e - (\rho W)_{e,U}\Delta\xi\Delta\eta u_{e,U} - \\
& (\rho U)_E\Delta\eta\Delta\sigma u_e + (\rho U)_P\Delta\eta\Delta\sigma u_e - (\rho V)_{ne}\Delta\xi\Delta\sigma u_e + \\
& (\rho V)_{se}\Delta\xi\Delta\sigma u_e - (\rho W)_{e,D}\Delta\xi\Delta\eta u_e + (\rho W)_{e,U}\Delta\xi\Delta\eta u_e \quad (C.10)
\end{aligned}$$

$$\begin{aligned}
LHS = & \| -(\rho U)_{E,0}\|\Delta\eta\Delta\sigma u_e - \| -(\rho U)_{E,0}\|\Delta\eta\Delta\sigma u_{ee} - \\
& \|(\rho U)_{P,0}\|\Delta\eta\Delta\sigma u_w + \|(\rho U)_{P,0}\|\Delta\eta\Delta\sigma u_e + \\
& \| -(\rho V)_{ne,0}\|\Delta\xi\Delta\sigma u_e - \| -(\rho V)_{ne,0}\|\Delta\xi\Delta\sigma u_3 - \\
& \|(\rho V)_{se,0}\|\Delta\xi\Delta\sigma u_5 + \| (\rho V)_{se,0}\|\Delta\xi\Delta\sigma u_e + \\
& (\rho W)_{e,U}\Delta\xi\Delta\eta u_e - (\rho W)_{e,U}\Delta\xi\Delta\eta u_{e,U} \quad (C.11)
\end{aligned}$$

$$\begin{aligned}
RHS = & C_{1E}^u\Delta\eta\Delta\sigma\left(\frac{\partial u}{\partial\xi}\right)_E - C_{1P}^u\Delta\eta\Delta\sigma\left(\frac{\partial u}{\partial\xi}\right)_P + C_{2E}^u\Delta\eta\Delta\sigma\left(\frac{\partial u}{\partial\eta}\right)_E - \\
& C_{2P}^u\Delta\eta\Delta\sigma\left(\frac{\partial u}{\partial\eta}\right)_P + C_{3E}^u\Delta\eta\Delta\sigma\left(\frac{\partial v}{\partial\xi}\right)_E - C_{3P}^u\Delta\eta\Delta\sigma\left(\frac{\partial v}{\partial\xi}\right)_P + \\
& C_{4E}^u\Delta\eta\Delta\sigma\left(\frac{\partial v}{\partial\eta}\right)_E - C_{4P}^u\Delta\eta\Delta\sigma\left(\frac{\partial v}{\partial\eta}\right)_P + C_{5ne}^u\Delta\xi\Delta\sigma\left(\frac{\partial u}{\partial\eta}\right)_{ne} - \\
& C_{5se}^u\Delta\xi\Delta\sigma\left(\frac{\partial u}{\partial\eta}\right)_{se} + C_{6ne}^u\Delta\xi\Delta\sigma\left(\frac{\partial u}{\partial\xi}\right)_{ne} - C_{6se}^u\Delta\xi\Delta\sigma\left(\frac{\partial u}{\partial\xi}\right)_{se} + \\
& C_{7ne}^u\Delta\xi\Delta\sigma\left(\frac{\partial v}{\partial\eta}\right)_{ne} - C_{7se}^u\Delta\xi\Delta\sigma\left(\frac{\partial v}{\partial\eta}\right)_{se} + C_{8ne}^u\Delta\xi\Delta\sigma\left(\frac{\partial v}{\partial\xi}\right)_{ne} - \\
& C_{8se}^u\Delta\xi\Delta\sigma\left(\frac{\partial v}{\partial\xi}\right)_{se} - \hat{P}_e^u\Delta V \quad (C.12)
\end{aligned}$$

$$\begin{aligned}
RHS = & C_{1E}^u \Delta \eta \Delta \sigma \frac{u_{ee} - u_e}{\Delta \xi} - C_{1P}^u \Delta \eta \Delta \sigma \frac{u_e - u_w}{\Delta \xi} + C_{2E}^u \Delta \eta \Delta \sigma \frac{u_1 - u_2}{\Delta \eta} - \\
& C_{2P}^u \Delta \eta \Delta \sigma \frac{u_n - u_s}{\Delta \eta} + C_{3E}^u \Delta \eta \Delta \sigma \frac{v_{ee} - v_e}{\Delta \xi} - C_{3P}^u \Delta \eta \Delta \sigma \frac{v_e - v_w}{\Delta \xi} + \\
& C_{4E}^u \Delta \eta \Delta \sigma \frac{v_1 - v_2}{\Delta \eta} - C_{4P}^u \Delta \eta \Delta \sigma \frac{v_n - v_s}{\Delta \eta} + C_{5ne}^u \Delta \xi \Delta \sigma \frac{u_3 - u_e}{\Delta \eta} - \\
& C_{5se}^u \Delta \xi \Delta \sigma \frac{u_e - u_s}{\Delta \eta} + C_{6ne}^u \Delta \xi \Delta \sigma \frac{u_1 - u_n}{\Delta \xi} - C_{6se}^u \Delta \xi \Delta \sigma \frac{u_2 - u_s}{\Delta \xi} + \\
& C_{7ne}^u \Delta \xi \Delta \sigma \frac{v_3 - v_e}{\Delta \eta} - C_{7se}^u \Delta \xi \Delta \sigma \frac{v_e - v_s}{\Delta \eta} + C_{8ne}^u \Delta \xi \Delta \sigma \frac{v_1 - v_n}{\Delta \xi} - \\
& C_{8se}^u \Delta \xi \Delta \sigma \frac{v_2 - v_s}{\Delta \xi} - L[\hat{P}_e^u] \Delta V
\end{aligned} \tag{C.13}$$

$$\begin{aligned}
RHS = & \frac{C_{1E}^u \Delta \eta \Delta \sigma}{\Delta \xi} u_{ee} - \frac{C_{1E}^u \Delta \eta \Delta \sigma}{\Delta \xi} u_e - \frac{C_{1P}^u \Delta \eta \Delta \sigma}{\Delta \xi} u_e + \\
& \frac{C_{1P}^u \Delta \eta \Delta \sigma}{\Delta \xi} u_w + C_{2E}^u \Delta \sigma u_1 - C_{2E}^u \Delta \sigma u_2 - C_{2P}^u \Delta \sigma u_n + \\
& C_{2P}^u \Delta \sigma u_s + \frac{C_{3E}^u \Delta \eta \Delta \sigma}{\Delta \xi} v_{ee} - \frac{C_{3E}^u \Delta \eta \Delta \sigma}{\Delta \xi} v_e - \\
& \frac{C_{3P}^u \Delta \eta \Delta \sigma}{\Delta \xi} v_e + \frac{C_{3P}^u \Delta \eta \Delta \sigma}{\Delta \xi} v_w + C_{4E}^u \Delta \sigma v_1 - C_{4E}^u \Delta \sigma v_2 - \\
& C_{4P}^u \Delta \sigma v_n + C_{4P}^u \Delta \sigma v_s + \frac{C_{5ne}^u \Delta \xi \Delta \sigma}{\Delta \eta} u_3 - \frac{C_{5ne}^u \Delta \xi \Delta \sigma}{\Delta \eta} u_e - \\
& \frac{C_{5se}^u \Delta \xi \Delta \sigma}{\Delta \eta} u_e + \frac{C_{5se}^u \Delta \xi \Delta \sigma}{\Delta \eta} u_s + C_{6ne}^u \Delta \sigma u_1 - C_{6ne}^u \Delta \sigma u_n - \\
& C_{6se}^u \Delta \sigma u_2 + C_{6se}^u \Delta \sigma u_s + \frac{C_{7ne}^u \Delta \xi \Delta \sigma}{\Delta \eta} v_3 - \frac{C_{7ne}^u \Delta \xi \Delta \sigma}{\Delta \eta} v_e - \\
& \frac{C_{7se}^u \Delta \xi \Delta \sigma}{\Delta \eta} v_e + \frac{C_{7se}^u \Delta \xi \Delta \sigma}{\Delta \eta} v_s + C_{8ne}^u \Delta \sigma v_1 - C_{8ne}^u \Delta \sigma v_n - \\
& C_{8se}^u \Delta \sigma v_2 + C_{8se}^u \Delta \sigma v_s - L[\hat{P}_e^u] \Delta V
\end{aligned} \tag{C.14}$$

$$\begin{aligned}
& \{ \| -(\rho U)_{E,0} \| \Delta \eta \Delta \sigma + \| (\rho U)_{P,0} \| \Delta \eta \Delta \sigma + \| -(\rho V)_{ne,0} \| \Delta \xi \Delta \sigma + \| (\rho V)_{se,0} \| \Delta \xi \Delta \sigma + \\
& (\rho W)_{e,U} \Delta \xi \Delta \eta + \frac{C_{1E}^u \Delta \eta \Delta \sigma}{\Delta \xi} + \frac{C_{1P}^u \Delta \eta \Delta \sigma}{\Delta \xi} + \frac{C_{5ne}^u \Delta \xi \Delta \sigma}{\Delta \eta} + \frac{C_{5se}^u \Delta \xi \Delta \sigma}{\Delta \eta} \} u_e = \\
& \{ \| -(\rho U)_{E,0} \| \Delta \eta \Delta \sigma + \frac{C_{1E}^u \Delta \eta \Delta \sigma}{\Delta \xi} \} u_{ee} + \{ \| (\rho U)_{P,0} \| \Delta \eta \Delta \sigma + \frac{C_{1P}^u \Delta \eta \Delta \sigma}{\Delta \xi} \} u_w + \\
& \{ \| -(\rho V)_{ne,0} \| \Delta \xi \Delta \sigma + \frac{C_{5ne}^u \Delta \xi \Delta \sigma}{\Delta \eta} \} u_3 + \{ \| (\rho V)_{se,0} \| \Delta \xi \Delta \sigma + \frac{C_{5se}^u \Delta \xi \Delta \sigma}{\Delta \eta} \} u_5 + \\
& (\rho W)_{e,U} \Delta \xi \Delta \eta u_{e,U} + [C_{2E}^u \Delta \sigma + C_{6ne}^u \Delta \sigma] u_1 + [-C_{2E}^u \Delta \sigma - C_{6se}^u \Delta \sigma] u_2 + \\
& [-C_{2P}^u \Delta \sigma - C_{6ne}^u \Delta \sigma] u_n + [C_{2P}^u \Delta \sigma + C_{6se}^u \Delta \sigma] u_s + \left[\frac{C_{3E}^u \Delta \eta \Delta \sigma}{\Delta \xi} \right] v_{ee} + \\
& \left[-\frac{C_{3E}^u \Delta \eta \Delta \sigma}{\Delta \xi} - \frac{C_{3P}^u \Delta \eta \Delta \sigma}{\Delta \xi} - \frac{C_{7ne}^u \Delta \xi \Delta \sigma}{\Delta \eta} - \frac{C_{7se}^u \Delta \xi \Delta \sigma}{\Delta \eta} \right] v_e + \left[\frac{C_{3P}^u \Delta \eta \Delta \sigma}{\Delta \xi} \right] v_w + \\
& [C_{4E}^u \Delta \sigma + C_{8ne}^u \Delta \sigma] v_1 + [-C_{4E}^u \Delta \sigma - C_{8se}^u \Delta \sigma] v_2 + [-C_{4P}^u \Delta \sigma - C_{8ne}^u \Delta \sigma] v_n + \\
& [C_{4P}^u \Delta \sigma + C_{8se}^u \Delta \sigma] v_s + \left[\frac{C_{7ne}^u \Delta \xi \Delta \sigma}{\Delta \eta} \right] v_3 + \left[\frac{C_{7se}^u \Delta \xi \Delta \sigma}{\Delta \eta} \right] v_5 - L[\hat{P}_e^u] \Delta V \quad (C.15)
\end{aligned}$$

$$L[\hat{P}_e^u] = L \left[\frac{\partial P}{\partial \xi} y_\eta - \frac{\partial P}{\partial \eta} y_\xi \right]_e \quad (C.16)$$

$$L[\hat{P}_e^u] = L \left[\left(\frac{\partial P}{\partial \xi} \right)_e y_{\eta e} - \left(\frac{\partial P}{\partial \eta} \right)_e y_{\xi e} \right] \quad (C.17)$$

$$L[\hat{P}_e^u] = \left(\frac{P_E - P_P}{\Delta \xi} \right) y_{\eta e} - \left(\frac{P_{ne} - P_{se}}{\Delta \eta} \right) y_{\xi e} \quad (C.18)$$

$$L[\hat{P}_e^u] = \left[\frac{P_E - P_P}{\Delta \xi} \right] y_{\eta e} - \left[\frac{P_N + P_{NE} - P_S - P_{SE}}{4\Delta \eta} \right] y_{\xi e} \quad (C.19)$$

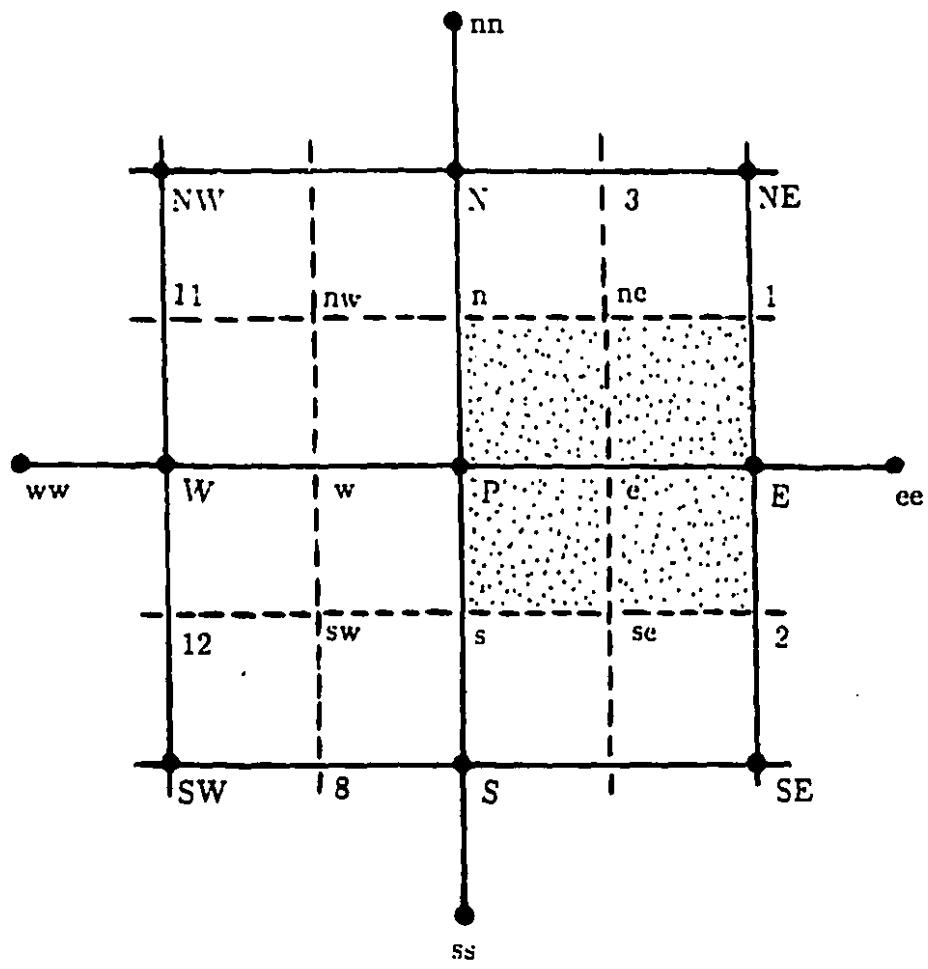


Figure C.1
 Typical derivation for u_e

APPENDIX D
MODELLING OF COEFFICIENTS OF DISCRETIZATION
EQUATIONS IN I-J COORDINATES

D. 1 COEFFICIENTS FOR THE "U1" MOMENTUM EQUATION

(Refer to Figs. D.1 and D.2)

"AE" and "AW" Inter-Relationship

$$\left. \begin{aligned} AE_w^u &= \| -(\rho U)_{P,0} \Delta\eta\Delta\sigma + \frac{C_{1P}^u \Delta\eta\Delta\sigma}{\Delta\xi} \| \\ AW_w^u &= \| (\rho U)_{W,0} \Delta\eta\Delta\sigma + \frac{C_{1W}^u \Delta\eta\Delta\sigma}{\Delta\xi} \| \end{aligned} \right\} \quad (D.1)$$

In terms of I & J

$$\left. \begin{aligned} AE(I, J) &= \| -(\rho U)(I, J), 0 \| \Delta\eta\Delta\sigma + \frac{CU1(I, J) \Delta\eta\Delta\sigma}{\Delta\xi} \| \\ AW(I, J) &= \| (\rho U)(I-1, J), 0 \| \Delta\eta\Delta\sigma + \frac{CU1(I-1, J) \Delta\eta\Delta\sigma}{\Delta\xi} \| \end{aligned} \right\} \quad (D.2)$$

from Eqn. (D.2) changing $I, J \rightarrow I+1, J$

$$AW(I+1, J) = \| (\rho U)(I, J), 0 \| \Delta\eta\Delta\sigma + \frac{CU1(I, J) \Delta\eta\Delta\sigma}{\Delta\xi} \quad (D.3)$$

Subtract $(\rho U)(I, J)$ from Eqn. (D.3)

$$\begin{aligned} AW(I+1, J) - (\rho U)(I, J) &= \| (\rho U)(I, J), 0 \| \Delta\eta\Delta\sigma - \\ &(\rho U)(I, J) + \frac{CU1(I, J) \Delta\eta\Delta\sigma}{\Delta\xi} \end{aligned} \quad (D.4)$$

or

$$\begin{aligned} AW(I+1, J) - (\rho U)(I, J) &= \| -(\rho U)(I, J), 0 \| \Delta\eta\Delta\sigma + \\ &\frac{CU1(I, J) \Delta\eta\Delta\sigma}{\Delta\xi} \end{aligned} \quad (D.5)$$

The terms on the right hand side of Eqn. (D.5) is equal to $AE(I, J)$ according to Eqn. (D.2). Therefore

$$AW(I+1, J) - (\rho U)(I, J) = AE(I, J) \quad (D.6)$$

or alternatively

$$AE(I, J) = AW(I+1, J) - FLOW \quad (D.7)$$

$$AW(I+1, J) = AMAX1(0., FLOW) \Delta\eta\Delta\sigma + DIFF \quad (D.8)$$

in which

$$FLOW = (\rho U)(I, J) \quad (D.9)$$

$$DIFF = \frac{CU1(I, J) \Delta\eta\Delta\sigma}{\Delta\xi} \quad (D.10)$$

from Figure D.3:

$$FLOW = \frac{RHO1 \cdot UC1(I, J) + RHO2 \cdot UC1(I + 1, J)}{2} \quad (D.11)$$

in which

$$\left. \begin{aligned} RHO1 &= 0.5(RHO(I, J) + RHO(I - 1, J)) \\ RHO2 &= 0.5(RHO(I, J) + RHO(I + 1, J)) \end{aligned} \right\} \quad (D.12)$$

$$DIFF = \frac{CU1(I, J)\Delta\eta\Delta\sigma}{\Delta\xi} \quad (D.13)$$

“AN” and “AS” Inter-Relationship

$$\left. \begin{aligned} AN_w^u &= \| -(\rho V)_{nw}, 0 \| \Delta\xi\Delta\sigma + \frac{C_{3nw}^u \Delta\xi\Delta\sigma}{\Delta\eta} \\ AS_w^u &= \| (\rho V)_{sw}, 0 \| \Delta\xi\Delta\sigma + \frac{C_{3sw}^u \Delta\xi\Delta\sigma}{\Delta\eta} \end{aligned} \right\} \quad (D.14)$$

In terms of I & J

$$\left. \begin{aligned} AN(I, J) &= \| -(\rho V)A, 0 \| \Delta\xi\Delta\sigma + \frac{CU5A\Delta\xi\Delta\sigma}{\Delta\eta} \\ AS(I, J) &= \| (\rho V)B, 0 \| \Delta\xi\Delta\sigma + \frac{CU5B\Delta\xi\Delta\sigma}{\Delta\eta} \end{aligned} \right\} \quad (D.15)$$

from Eqn. (D.15) changing $I, J \rightarrow I, J + 1$

$$AS(I, J + 1) = \| (\rho V)A, 0 \| \Delta\xi\Delta\sigma + \frac{CU5A\Delta\xi\Delta\sigma}{\Delta\eta} \quad (D.16)$$

Using $B \rightarrow A$ due to the transformation $I, J \rightarrow I, J + 1$:

Proof:

designate “B”:

$$“B” \rightarrow \begin{bmatrix} I-1, J & I, J \\ I-1, J-1 & B & I, J-1 \end{bmatrix}$$

change “B”:

$$\begin{aligned} I, J \rightarrow I, J + 1 &\Rightarrow \begin{bmatrix} I-1, J & I, J \\ I-1, J-1 & B & I, J-1 \end{bmatrix} \\ &\rightarrow \begin{bmatrix} I-1, J+1 & I, J+1 \\ I-1, J & I, J \end{bmatrix} \end{aligned}$$

the latter shows the location of “A” in the middle, that is

$$\begin{bmatrix} I-1, J+1 & I, J+1 \\ I-1, J & I, J \end{bmatrix} A$$

Subtract $(\rho V)A$ from Eqn. (D.16)

$$AS(I, J+1) - (\rho V)A = \|(\rho V)A, 0\| \Delta\xi \Delta\sigma - (\rho V)A + \frac{CU5A \Delta\xi \Delta\sigma}{\Delta\eta} \quad (D.17)$$

or

$$AS(I, J+1) - (\rho V)A = \| -(\rho V)A, 0\| \Delta\xi \Delta\sigma + \frac{CU5A \Delta\xi \Delta\sigma}{\Delta\eta} \quad (D.18)$$

The terms on the right hand side of Eqn. (D.18) is equal to $AN(I, J)$ according to Eqn. (D.15). Therefore

$$AS(I, J+1) - (\rho V)A = AN(I, J) \quad (D.19)$$

or alternatively

$$AN(I, J) = AS(I, J+1) - FLOW \quad (D.20)$$

$$AS(I, J+1) = AMAX1(0., FLOW) \Delta\xi \Delta\sigma + DIFF \quad (D.21)$$

in which

$$FLOW = (\rho V)A \quad (D.22)$$

$$DIFF = \frac{CU5A \Delta\xi \Delta\sigma}{\Delta\eta} \quad (D.23)$$

from Figure D.4:

$$FLOW = \frac{RHO1 \cdot VC2(I-1, J+1) + RHO2 \cdot VC2(I, J+1)}{2} * \quad (D.24)$$

in which

$$\left. \begin{aligned} RHO1 &= 0.5(RHO(I-1, J) + RHO(I-1, J+1)) \\ RHO2 &= 0.5(RHO(I, J) + RHO(I, J+1)) \end{aligned} \right\} \quad (D.25)$$

$$DIFF = \frac{[CU5(I, J) + CU5(I, J+1) + CU5(I-1, J+1) + CU5(I-1, J)] \Delta\xi \Delta\sigma}{4\Delta\eta} \quad (D.26)$$

* *Proof:*

$$\rho : \frac{M}{V}$$

$$V : \frac{L}{t}$$

$$FLOW = \rho \cdot V : \left(\frac{M}{V}\right) \left(\frac{L}{t}\right) = \left(\frac{M}{L^3}\right) \left(\frac{L}{t}\right) = \frac{M}{L^2 t} \quad (\text{mass flux})$$

$$FLOW \text{ AREA} : \left(\frac{M}{L^2 t}\right) (L^2) = \frac{M}{t} \quad (\text{mass flow rate})$$

To evaluate "FLOW" at point "A":

from Figure D.5:

$$\begin{aligned} (FLOW)_A(\Delta\xi)(\Delta\sigma) &= RHO1 \cdot VC2(I-1, J+1) \cdot \left(\frac{\Delta\xi}{2}\right)(\Delta\sigma) + \\ &\quad RHO2 \cdot VC2(I, J+1) \cdot \left(\frac{\Delta\xi}{2}\right)(\Delta\sigma) \end{aligned} \quad (D.27)$$

$$(FLOW)_A = \frac{RHO1 \cdot VC2(I-1, J+1) + RHO2 \cdot VC2(I, J+1)}{2} \quad (D.28)$$

NOTE 1

Consider the following relationships:

$$AE(I, J) = AW(I+1, J) - FLOW$$

$$AW(I+1, J) = AMAX1(0., FLOW)\Delta\eta\Delta\sigma + DIFF$$

- (i) as "AW" is calculated for the c.v.'s designated by $(I+1, J)$, therefore in the process of changing I from 3 to $L2$, "AW" would not be calculated for the c.v.'s designated by $(3, J)$, that is, the far-west c.v.'s. $AW(3, J)$ is to be calculated in a separate process.
- (ii) as "AE" is obtained from $AW(I+1, J)$, therefore to calculate "AE" for the far-east c.v.'s, $AE(L2, J)$, it is necessary to calculate $AW(L1, J)$ which needs a separate treatment.

NOTE 2

Consider the following relationships:

$$AN(I, J) = AS(I, J + 1) - FLOW$$

$$AS(I, J + 1) = AMAX1(0., FLOW)\Delta\xi\Delta\sigma + DIFF$$

- (i) as "AS" is calculated for the c.v.'s designated by (I, J + 1), therefore in the process of changing J from 2 to M2, "AS" would not be calculated for the c.v.'s designated by (I, 2), that is, the far-south c.v.'s. AS(I, 2) is to be calculated in a separate process.
- (ii) as "AN" is obtained from AS(I, J + 1), therefore to calculate "AN" for the far-north c.v.'s, AN(I, M2), it is necessary to calculate AS(I, M1) which needs a separate treatment.

To Obtain AW(3, J)

Using

$$AW(I + 1, J) = AMAX1(0., FLOW)\Delta\eta\Delta\sigma + DIFF \quad (D.29)$$

let $I = 2$

$$AW(3, J) = AMAX1(0., FLOW)\Delta\eta\Delta\sigma + DIFF \quad (D.30)$$

in which

$$FLOW = (\rho U)(I, J) = (\rho U)(2, J) \quad (D.31)$$

$$DIFF = \frac{CU1(I, J)\Delta\eta\Delta\sigma}{\Delta\xi} = \frac{CU1(2, J)\Delta\eta\Delta\sigma}{\Delta\xi} \quad (D.32)$$

from Figure D.6:

$$FLOW = \frac{RHO(1, J) \cdot UC1(2, J) + RHO1 \cdot UC1(3, J)}{2} \quad (D.33)$$

in which

$$RHO1 = \frac{RHO(2, J) + RHO(3, J)}{2} \quad (D.34)$$

$$DIFF = \frac{CU1(2, J)\Delta\eta\Delta\sigma}{\Delta\xi} \quad (D.35)$$

To Obtain $AE(L2, J)$

Using

$$AE(I, J) = AW(I + 1, J) - FLOW \quad (D.36)$$

$$AW(I + 1, J) = AMAX1(0., FLOW)\Delta\eta\Delta\sigma + DIFF \quad (D.37)$$

let $I = L2$

$$AE(I, L2) = AW(L1, J) - FLOW \quad (D.38)$$

$$AW(L1, J) = AMAX1(0., FLOW)\Delta\eta\Delta\sigma + DIFF \quad (D.39)$$

in which

$$FLOW = (\rho U)(I, J) = (\rho U)(L2, J) \quad (D.40)$$

$$DIFF = \frac{CU1(I, J)\Delta\eta\Delta\sigma}{\Delta\xi} = \frac{CU1(L2, J)\Delta\eta\Delta\sigma}{\Delta\xi} \quad (D.41)$$

from Figure D.7:

$$FLOW = \frac{RHO(L1, J) \cdot UC1(L1, J) + RHO1 \cdot UC1(L2, J)}{2} \quad (D.42)$$

in which

$$RHO1 = \frac{RHO(L2, J) + RHO(L3, J)}{2} \quad (D.42)$$

$$DIFF = \frac{CU1(L2, J)\Delta\eta\Delta\sigma}{\Delta\xi} \quad (D.43)$$

To Obtain $AS(I, 2)$

Using

$$AS(I, J + 1) = AMAX1(0., FLOW)\Delta\xi\Delta\sigma + DIFF \quad (D.45)$$

let $J = 1$

$$AS(I, 2) = AMAX1(0., FLOW)\Delta\xi\Delta\sigma + DIFF \quad (D.46)$$

in which

$$FLOW = (\rho V)A \quad (D.47)$$

$$DIFF = \frac{CU5A\Delta\xi\Delta\sigma}{\Delta\eta} \quad (D.48)$$

from Figure D.8:

$$FLOW = \frac{RHO(I,1) \cdot VC2(I,2) + RHO(I-1,1) \cdot VC2(I-1,2)}{2} \quad (D.49)$$

in which

$$DIFF = \frac{[CU5(I,1) + CU5(I-1,1)]\Delta\xi\Delta\sigma}{\Delta\eta} \quad (D.50)$$

To Obtain $AN(I, M2)$

Using

$$AN(I, J) = AS(I, J+1) - FLOW \quad (D.51)$$

$$AS(I, J+1) = AMAX1(0., FLOW)\Delta\xi\Delta\sigma + DIFF \quad (D.52)$$

let $J = M2$

$$AN(I, M2) = AS(I, M1) - FLOW \quad (D.53)$$

$$AS(I, M1) = AMAX1(0., FLOW)\Delta\xi\Delta\sigma + DIFF \quad (D.54)$$

in which

$$FLOW = (\rho V)A \quad (D.55)$$

$$DIFF = \frac{CU5A\Delta\xi\Delta\sigma}{\Delta\eta} \quad (D.56)$$

from Figure D.9:

$$FLOW = \frac{RHO(I, M1) \cdot VC2(I, M1) + RHO(I-1, M1) \cdot VC2(I-1, M1)}{2} \quad (D.57)$$

$$DIFF = \frac{[CU5(I-1, M1) + CU5(I, M1)]\Delta\xi\Delta\sigma}{\Delta\eta} \quad (D.58)$$

D. 2 COEFFICIENTS FOR THE "U2" MOMENTUM EQUATION

(Refer to Figs. D.10 and D.11)

"AW" and "AE" Inter-Relationship

$$\left. \begin{aligned} AE_s^u &= \| -(\rho U)_{se}, 0 \| \Delta\eta \Delta\sigma + \frac{C_{i,se}^u \Delta\eta \Delta\sigma}{\Delta\xi} \\ AW_s^u &= \| (\rho U)_{sw}, 0 \| \Delta\eta \Delta\sigma + \frac{C_{i,sw}^u \Delta\eta \Delta\sigma}{\Delta\xi} \end{aligned} \right\} \quad (D.59)$$

In terms of I & J

$$\left. \begin{aligned} AE(I, J) &= \| -(\rho U)_{C}, 0 \| \Delta\eta \Delta\sigma + \frac{CU1C \Delta\eta \Delta\sigma}{\Delta\xi} \\ AW(I, J) &= \| (\rho U)_{B}, 0 \| \Delta\eta \Delta\sigma + \frac{CU1B \Delta\eta \Delta\sigma}{\Delta\xi} \end{aligned} \right\} \quad (D.60)$$

from Eqn. (D.60) changing $I, J \rightarrow I+1, J$

$$AW(I+1, J) = \| (\rho U)_{C}, 0 \| \Delta\eta \Delta\sigma + \frac{CU1C \Delta\eta \Delta\sigma}{\Delta\xi} \quad (D.61)$$

Using $B \rightarrow C$ due to the transformation $I, J \rightarrow I+1, J$:

Proof:

designate "B":

$$\text{"B"} \rightarrow \begin{bmatrix} I-1, J & & I, J \\ & B & \\ I-1, J-1 & & I, J-1 \end{bmatrix}$$

change "B":

$$\begin{aligned} I, J \rightarrow I+1, J &\Rightarrow \begin{bmatrix} I-1, J & & I, J \\ & B & \\ I-1, J-1 & & I, J-1 \end{bmatrix} \\ &\rightarrow \begin{bmatrix} & & I+1, J \\ I, J & & \\ & & I+1, J-1 \end{bmatrix} \end{aligned}$$

the latter shows the location of "C" in the middle, that is

$$\begin{bmatrix} & & I+1, J \\ I, J & C & \\ & & I+1, J-1 \end{bmatrix}$$

Subtract $(\rho U)C$ from both sides of Eqn. (D.61)

$$AW(I+1, J) - (\rho U)C = \|(\rho U)C, 0\| \Delta\eta \Delta\sigma - (\rho U)C + \frac{CU1C \Delta\eta \Delta\sigma}{\Delta\xi} \quad (D.62)$$

or

$$AW(I+1, J) - (\rho U)C = \| -(\rho U)C, 0\| \Delta\eta \Delta\sigma + \frac{CU1C \Delta\eta \Delta\sigma}{\Delta\xi} \quad (D.63)$$

The terms on the right hand side of Eqn. (D.63) is equal to $AE(I, J)$ according to Eqn. (D.60). Therefore

$$AW(I+1, J) - (\rho U)C = AE(I, J) \quad (D.64)$$

or alternatively

$$AE(I, J) = AW(I+1, J) - FLOW \quad (D.65)$$

$$AW(I+1, J) = AMAX1(0., FLOW) \Delta\eta \Delta\sigma + DIFF \quad (D.66)$$

in which

$$FLOW = (\rho U)C \quad (D.67)$$

$$DIFF = \frac{CU1C \Delta\eta \Delta\sigma}{\Delta\xi} \quad (D.68)$$

from Figure D.12:

$$FLOW = \frac{RHO1 \cdot UC1(I+1, J-1) + RHO2 \cdot UC1(I+1, J)}{2} * \quad (D.69)$$

in which

$$\left. \begin{aligned} RHO1 &= 0.5(RHO(I, J-1) + RHO(I+1, J-1)) \\ RHO2 &= 0.5(RHO(I, J) + RHO(I+1, J)) \end{aligned} \right\} \quad (D.70)$$

$$DIFF = \frac{[CU1(I+1, J) + CU1(I+1, J-1) + CU1(I, J-1) + CU1(I, J)] \Delta\eta \Delta\sigma}{4\Delta\xi} \quad (D.71)$$

* Proof:

$$FLOW = \rho U : \frac{M}{L^2 t} \quad (\text{mass flux})$$

$$(FLOW)(AREA) : \frac{M}{t} \quad (\text{mass flow-rate})$$

To evaluate "FLOW" at point "C"

from Figure D.13:

$$(FLOW)_C(\Delta\eta)(\Delta\sigma) = RHO1 \cdot UC1(I+1, J-1) \left(\frac{\Delta\eta}{2} \right) (\Delta\sigma) +$$

$$RHO2 \cdot UC1(I+1, J) \left(\frac{\Delta\eta}{2} \right) (\Delta\sigma) \quad (D.72)$$

$$(FLOW)_C = \frac{RHO1 \cdot UC1(I+1, J-1) + RHO2 \cdot UC1(I+1, J)}{2} \quad (D.73)$$

"AN" and "AS" Inter-Relationship

$$\left. \begin{aligned} AN_s^u &= \| -(\rho V)_P, 0 \| \Delta\xi \Delta\sigma + \frac{C_{5P}^u \Delta\xi \Delta\sigma}{\Delta\eta} \\ AS_s^u &= \| (\rho V)_S, 0 \| \Delta\xi \Delta\sigma + \frac{C_{5S}^u \Delta\xi \Delta\sigma}{\Delta\eta} \end{aligned} \right\} \quad (D.74)$$

In terms of I & J

$$\left. \begin{aligned} AN(I, J) &= \| -(\rho V)(I, J), 0 \| \Delta\xi \Delta\sigma + \frac{CU5(I, J) \Delta\xi \Delta\sigma}{\Delta\eta} \\ AS(I, J) &= \| (\rho V)(I, J-1), 0 \| \Delta\xi \Delta\sigma + \frac{CU5(I, J-1) \Delta\xi \Delta\sigma}{\Delta\eta} \end{aligned} \right\} \quad (D.75)$$

from Eqn. (D.75) changing $I, J \rightarrow I, J+1$:

$$AS(I, J+1) = \| (\rho V)(I, J), 0 \| \Delta\xi \Delta\sigma + \frac{CU5(I, J) \Delta\xi \Delta\sigma}{\Delta\eta} \quad (D.76)$$

Subtract $(\rho V)(I, J)$ from Eqn. (D.76)

$$AS(I, J+1) - (\rho V)(I, J) = \| (\rho V)(I, J), 0 \| \Delta\xi \Delta\sigma - (\rho V)(I, J) +$$

$$\frac{CU5(I, J) \Delta\xi \Delta\sigma}{\Delta\eta} \quad (D.77)$$

or

$$AS(I, J+1) - (\rho V)(I, J) = \| -(\rho V)(I, J), 0 \| \Delta\xi \Delta\sigma +$$

$$\frac{CU5(I, J) \Delta\xi \Delta\sigma}{\Delta\eta} \quad (D.78)$$

The terms on the right hand side of Eqn. (D.78) is equal to $AN(I, J)$ according to Eqn. (D.75). Therefore

$$AS(I, J + 1) - (\rho V)(I, J) = AN(I, J) \quad (D.79)$$

or alternatively

$$AN(I, J) = AS(I, J + 1) - FLOW \quad (D.80)$$

$$AS(I, J + 1) = AMAX1(0., FLOW)\Delta\xi\Delta\sigma + DIFF \quad (D.81)$$

in which

$$FLOW = (\rho V)(I, J) \quad (D.82)$$

$$DIFF = \frac{CU5(I, J)\Delta\xi\Delta\sigma}{\Delta\eta} \quad (D.83)$$

from Figure D.14:

$$FLOW = \frac{RHO2 \cdot VC2(I, J) + RHO1 \cdot VC2(I, J + 1)}{2} \quad (D.74)$$

in which

$$\left. \begin{aligned} RHO1 &= 0.5(RHO(I, J) + RHO(I, J + 1)) \\ RHO2 &= 0.5(RHO(I, J - 1) + RHO(I, J)) \end{aligned} \right\} \quad (D.85)$$

$$DIFF = \frac{CU5(I, J)\Delta\xi\Delta\sigma}{\Delta\eta} \quad (D.86)$$

To Obtain $AW(2, J)$

Using

$$AW(I + 1, J) = AMAX1(0., FLOW)\Delta\eta\Delta\sigma + DIFF \quad (D.87)$$

let $I = 1$

$$AW(2, J) = AMAX1(0., FLOW)\Delta\eta\Delta\sigma + DIFF \quad (D.88)$$

in which

$$FLOW = (\rho U)C \quad (D.89)$$

$$DIFF = \frac{CU1C\Delta\eta\Delta\sigma}{\Delta\xi} \quad (D.89)$$

from Figure D.15:

$$FLOW = \frac{RHO(1, J) \cdot UC1(2, J) + RHO(1, J - 1) \cdot UC1(2, J - 1)}{2} \quad (D.91)$$

$$DIFF = \frac{CU1(1, J - 1) + CU1(1, J) \Delta \eta \Delta \sigma}{2 \Delta \xi} \quad (D.92)$$

To Obtain $AE(L2, J)$

Using

$$AE(I, J) = AW(I + 1, J) - FLOW \quad (D.93)$$

$$AW(I + 1, J) = AMAX1(0., FLOW) \Delta \eta \Delta \sigma + DIFF \quad (D.94)$$

let $I = L2$

$$AE(L2, J) = AW(L1, J) - FLOW \quad (D.95)$$

$$AW(L1, J) = AMAX1(0., FLOW) \Delta \eta \Delta \sigma + DIFF \quad (D.96)$$

in which

$$FLOW = (\rho U) C \quad (D.97)$$

$$DIFF = \frac{CU1C \Delta \eta \Delta \sigma}{\Delta \xi} \quad (D.98)$$

from Figure D.16:

$$FLOW = \frac{RHO(L1, J) \cdot UC1(L1, J) + RHO(L1, J - 1) \cdot UC1(L1, J - 1)}{2} \quad (D.99)$$

$$DIFF = \frac{[CU1(L1, J) + CU1(L1, J - 1)] \Delta \eta \Delta \sigma}{2 \Delta \xi} \quad (D.100)$$

To Obtain $AS(I, 3)$

Using

$$AS(I, J + 1) = AMAX1(0., FLOW) \Delta \xi \Delta \sigma + DIFF \quad (D.101)$$

let $J = 2$

$$AS(I, 3) = AMAX1(0., FLOW) \Delta \xi \Delta \sigma + DIFF \quad (D.102)$$

in which

$$FLOW = (\rho V)(I, J) = (\rho V)(I, 2) \quad (D.103)$$

$$DIFF = \frac{CU5(I, J)\Delta\xi\Delta\sigma}{\Delta\eta} = \frac{CU5(I, 2)\Delta\xi\Delta\sigma}{\Delta\eta} \quad (D.104)$$

from Figure D.17:

$$FLOW = \frac{RHO1 \cdot VC2(I, 3) + RHO(I, 1) \cdot VC2(I, 2)}{2} \quad (D.105)$$

in which

$$RHO1 = \frac{RHO(I, 2) + RHO(I, 3)}{2} \quad (D.106)$$

$$DIFF = \frac{CU5(I, 2)\Delta\xi\Delta\sigma}{\Delta\eta} \quad (D.107)$$

To Obtain $AN(I, M2)$

Using

$$AN(I, J) = AS(I, J + 1) - FLOW \quad (D.108)$$

$$AS(I, J + 1) = AMAX1(0., FLOW)\Delta\xi\Delta\sigma + DIFF \quad (D.109)$$

let $J = M2$

$$AN(I, M2) = AS(I, M1) - FLOW \quad (D.110)$$

$$AS(I, M1) = AMAX1(0., FLOW)\Delta\xi\Delta\sigma + DIFF \quad (D.111)$$

in which

$$FLOW = (\rho V)(I, J) = (\rho V)(I, M2) \quad (D.112)$$

$$DIFF = \frac{CU5(I, J)\Delta\xi\Delta\sigma}{\Delta\eta} = \frac{CU5(I, M2)\Delta\xi\Delta\sigma}{\Delta\eta} \quad (D.113)$$

from Figure D.18:

$$FLOW = \frac{RHO1 \cdot VC2(I, M2) + RHO(I, M1) \cdot VC2(I, M1)}{2} \quad (D.114)$$

in which

$$RHO1 = \frac{RHO(I, M3) + RHO(I, M2)}{2} \quad (D.115)$$

$$DIFF = \frac{CU5(I, M2)\Delta\xi\Delta\sigma}{\Delta\eta} \quad (D.116)$$

D. 3 COEFFICIENTS FOR THE "W" MOMENTUM EQUATION

(Refer to Figs. D.19 and D.20)

"AE" and "AW" Inter-Relationship

$$\left. \begin{aligned} AE_p^w &= \| -(\rho U)_e, 0 \| \Delta\eta \Delta\sigma + \frac{C_{1e}^w \Delta\eta \Delta\sigma}{\Delta\xi} \\ AW_p^w &= \| (\rho U)_w, 0 \| \Delta\eta \Delta\sigma + \frac{C_{1w}^w \Delta\eta \Delta\sigma}{\Delta\xi} \end{aligned} \right\} \quad (D.117)$$

In terms of I & J

$$\left. \begin{aligned} AE(I, J) &= \| -(\rho U)(\overline{I+1}, J), 0 \| \Delta\eta \Delta\sigma + \frac{CW1(\overline{I+1}, J) \Delta\eta \Delta\sigma}{\Delta\xi} \\ AW(I, J) &= \| (\rho U)(\overline{I}, J), 0 \| \Delta\eta \Delta\sigma + \frac{CW1(\overline{I}, J) \Delta\eta \Delta\sigma}{\Delta\xi} \end{aligned} \right\} \quad (D.118)$$

from Eqn. (D.118) changing $I, J \rightarrow I+1, J$:

$$AW(I+1, J) = \| (\rho U)(\overline{I+1}, J), 0 \| \Delta\eta \Delta\sigma + \frac{CW1(\overline{I+1}, J) \Delta\eta \Delta\sigma}{\Delta\xi} \quad (D.119)$$

Subtract $(\rho U)(\overline{I+1}, J)$ from both sides of Eqn. (D.119)

$$\begin{aligned} AW(I+1, J) - (\rho U)(\overline{I+1}, J) &= \| (\rho U)(\overline{I+1}, J), 0 \| \Delta\eta \Delta\sigma - \\ &(\rho U)(\overline{I+1}, J) + \frac{CW1(\overline{I+1}, J) \Delta\eta \Delta\sigma}{\Delta\xi} \end{aligned} \quad (D.120)$$

or

$$\begin{aligned} AW(I+1, J) - (\rho U)(\overline{I+1}, J) &= \| -(\rho U)(\overline{I+1}, J), 0 \| \Delta\eta \Delta\sigma + \\ &\frac{CW1(\overline{I+1}, J) \Delta\eta \Delta\sigma}{\Delta\xi} \end{aligned} \quad (D.121)$$

The terms on the right hand side of Eqn. (D.121) is equal to $AE(I, J)$ according to Eqn. (D.118). Therefore

$$AW(I+1, J) - (\rho U)(\overline{I+1}, J) = AE(I, J) \quad (D.122)$$

or alternatively

$$AE(I, J) = AW(I+1, J) - FLOW \quad (D.123)$$

$$AW(I+1, J) = AMAX1(0., FLOW) \Delta\eta \Delta\sigma + DIFF \quad (D.124)$$

in which

$$FLOW = (\rho U)(\overline{I+1}, J) \quad (D.125)$$

$$DIFF = \frac{CW1(\overline{I+1}, J)\Delta\eta\Delta\sigma}{\Delta\xi} \quad (D.126)$$

from Figure D.21:

$$FLOW = RHO1 \cdot UC1(I+1, J) \quad (D.127)$$

in which

$$RHO1 = \frac{RHO(I, J) + RHO(I+1, J)}{2} \quad (D.128)$$

$$DIFF = \frac{(CW1(I, J) + CW1(I+1, J))\Delta\eta\Delta\sigma}{2\Delta\xi} \quad (D.129)$$

“AN_p” and “AS_p” Inter-Relationship

$$\left. \begin{aligned} AN_p &= \| -(\rho V)_n, 0 \| \Delta\xi\Delta\sigma + \frac{C_{3n}^w \Delta\xi\Delta\sigma}{\Delta\eta} \\ AS_p &= \| (\rho V)_s, 0 \| \Delta\xi\Delta\sigma + \frac{C_{3s}^w \Delta\xi\Delta\sigma}{\Delta\eta} \end{aligned} \right\} \quad (D.130)$$

In terms of I & J

$$\left. \begin{aligned} AN(I, J) &= \| -(\rho V)(I, \overline{J+1}), 0 \| \Delta\xi\Delta\sigma + \frac{CW5(I, \overline{J+1})\Delta\xi\Delta\sigma}{\Delta\eta} \\ AS(I, J) &= \| (\rho V)(I, \overline{J}), 0 \| \Delta\xi\Delta\sigma + \frac{CW5(I, \overline{J})\Delta\xi\Delta\sigma}{\Delta\eta} \end{aligned} \right\} \quad (D.131)$$

from Eqn. (D.131) changing $I, J \rightarrow I, J+1$:

$$AS(I, J+1) = \| (\rho V)(I, \overline{J+1}), 0 \| \Delta\xi\Delta\sigma + \frac{CW5(I, \overline{J+1})\Delta\xi\Delta\sigma}{\Delta\eta} \quad (D.132)$$

Subtract $(\rho V)(I, \overline{J+1})$ from both sides of Eqn. (D.132)

$$AS(I, J+1) - (\rho V)(I, \overline{J+1}) = \| (\rho V)(I, \overline{J+1}), 0 \| \Delta\xi\Delta\sigma - (\rho V)(I, \overline{J+1}) + \frac{CW5(I, \overline{J+1})\Delta\xi\Delta\sigma}{\Delta\eta} \quad (D.133)$$

or

$$AS(I, J+1) - (\rho V)(I, \overline{J+1}) = \| -(\rho V)(I, \overline{J+1}), 0 \| \Delta\xi\Delta\sigma + \frac{CW5(I, \overline{J+1})\Delta\xi\Delta\sigma}{\Delta\eta} \quad (D.134)$$

The terms on the right hand side of Eqn. (D.134) is equal to $AN(I, J)$ according to Eqn. (D.131). Therefore

$$AS(I, J+1) - (\rho V)(I, \overline{J+1}) = AN(I, J) \quad (D.135)$$

or alternatively

$$AN(I, J) = AS(I, J + 1) - FLOW \quad (D.136)$$

$$AS(I, J + 1) = AMAX1(0., FLOW)\Delta\xi\Delta\sigma + DIFF \quad (D.137)$$

in which

$$FLOW = (\rho V)(I, \overline{J+1}) \quad (D.138)$$

$$DIFF = \frac{CW5(I, \overline{J+1})\Delta\xi\Delta\sigma}{\Delta\eta} \quad (D.139)$$

from Figure D.22:

$$FLOW = RHO1 \cdot VC2(I, J + 1) \quad (D.140)$$

in which

$$RHO1 = \frac{RHO(I, J) + RHO(I, J + 1)}{2} \quad (D.141)$$

$$DIFF = \frac{[CW5(I, J) + CW5(I, J + 1)]\Delta\xi\Delta\sigma}{2\Delta\eta} \quad (D.142)$$

To Obtain $AW(2, J)$

Using

$$AW(I + 1, J) = AMAX1(0., FLOW)\Delta\eta\Delta\sigma + DIFF \quad (D.143)$$

let $I = 1$

$$AW(2, J) = AMAX1(0., FLOW)\Delta\eta\Delta\sigma + DIFF \quad (D.144)$$

in which

$$FLOW = (\rho U)(\overline{I+1}, J) = (\rho U)(\overline{2}, J) = (\rho U)(1, J) \quad (D.145)$$

$$\begin{aligned} DIFF &= \frac{CW1(\overline{I+1}, J)\Delta\eta\Delta\sigma}{\Delta\xi} = \frac{CW1(\overline{2}, J)\Delta\eta\Delta\sigma}{\Delta\xi} \\ &= \frac{CW1(1, J)\Delta\eta\Delta\sigma}{\Delta\xi} \end{aligned} \quad (D.146)$$

from Figure D.23:

$$FLOW = RHO(1, J) \cdot UC1(2, J) \quad (D.147)$$

$$DIFF = \frac{CW1(1, J)\Delta\eta\Delta\sigma}{\Delta\xi} \quad (D.148)$$

To Obtain $AE(L2, J)$

Using

$$AE(I, J) = AW(I + 1, J) - FLOW \quad (D.149)$$

$$AW(I + 1, J) = AMAX1(0., FLOW)\Delta\eta\Delta\sigma + DIFF \quad (D.150)$$

let $I = L2$

$$AE(L2, J) = AW(L1, J) - FLOW \quad (D.151)$$

$$AW(L1, J) = AMAX1(0., FLOW)\Delta\eta\Delta\sigma + DIFF \quad (D.152)$$

in which

$$FLOW = (\rho U)(\overline{I+1}, J) = (\rho U)(\overline{L1}, J) = (\rho U)(L1, J) \quad (D.153)$$

$$\begin{aligned} DIFF &= \frac{CW1(\overline{I+1}, J)\Delta\eta\Delta\sigma}{\Delta\xi} = \frac{CW1(\overline{L1}, J)\Delta\eta\Delta\sigma}{\Delta\xi} \\ &= \frac{CW1(L1, J)\Delta\eta\Delta\sigma}{\Delta\xi} \end{aligned} \quad (D.154)$$

from Figure D.24:

$$FLOW = RHO(L1, J) \cdot UC1(L1, J) \quad (D.155)$$

$$DIFF = \frac{CW1(L1, J)\Delta\eta\Delta\sigma}{\Delta\xi} \quad (D.156)$$

To Obtain $AS(I, 2)$

Using

$$AS(I, J + 1) = AMAX1(0., FLOW)\Delta\xi\Delta\sigma + DIFF \quad (D.157)$$

let $J = 1$

$$AS(I, 2) = AMAX1(0., FLOW)\Delta\xi\Delta\sigma + DIFF \quad (D.158)$$

in which

$$FLOW = (\rho V)(I, \overline{J+1}) = (\rho V)(I, \overline{2}) = (\rho V)(I, 1) \quad (D.159)$$

$$\begin{aligned} DIFF &= \frac{CW5(I, \overline{J+1})\Delta\xi\Delta\sigma}{\Delta\eta} = \frac{CW5(I, \overline{2})\Delta\xi\Delta\sigma}{\Delta\eta} \\ &= \frac{CW5(I, 1)\Delta\xi\Delta\sigma}{\Delta\eta} \end{aligned} \quad (D.160)$$

from Figure D.25:

$$FLOW = RHO(I, 1) \cdot VC2(I, 2) \quad (D.161)$$

$$DIFF = \frac{CW5(I, 1)\Delta\xi\Delta\sigma}{\Delta\eta} \quad (D.162)$$

To Obtain $AN(I, M2)$

Using

$$AN(I, J) = AS(I, J+1) - FLOW \quad (D.163)$$

$$AS(I, J+1) = AMAX1(0., FLOW)\Delta\xi\Delta\sigma + DIFF \quad (D.164)$$

let $J = M2$

$$AN(I, M2) = AS(I, M1) - FLOW \quad (D.165)$$

$$AS(I, M1) = AMAX1(0., FLOW)\Delta\xi\Delta\sigma + DIFF \quad (D.166)$$

in which

$$FLOW = (\rho V)(I, \overline{J+1}) = (\rho V)(I, \overline{M1}) = (\rho V)(I, M1) \quad (D.167)$$

$$\begin{aligned} DIFF &= \frac{CW5(I, \overline{J+1})\Delta\xi\Delta\sigma}{\Delta\eta} = \frac{CW5(I, \overline{M1})\Delta\xi\Delta\sigma}{\Delta\eta} \\ &= \frac{CW5(I, M1)\Delta\xi\Delta\sigma}{\Delta\eta} \end{aligned} \quad (D.168)$$

from Figure D.26:

$$FLOW = RHO(I, M1) \cdot VC2(I, M1) \quad (D.169)$$

$$DIFF = \frac{CW5(I, M1)\Delta\xi\Delta\sigma}{\Delta\eta} \quad (D.170)$$

D. 4 COEFFICIENTS FOR THE ENERGY EQUATION

(Refer to Figs. D.27 and D.28)

“AE” and “AW” Inter-Relationship

$$\left. \begin{aligned} AE_p^h &= \left\| -(\rho U)_e, 0 \right\| \Delta \eta \Delta \sigma + \frac{C_{1e}^h \Delta \eta \Delta \sigma}{\Delta \xi} \\ AW_p^h &= \left\| (\rho U)_w, 0 \right\| \Delta \eta \Delta \sigma + \frac{C_{1w}^h \Delta \eta \Delta \sigma}{\Delta \xi} \end{aligned} \right\} \quad (D.171)$$

In terms of I & J

$$\left. \begin{aligned} AE(I, J) &= \left\| -(\rho U)(\overline{I+1}, J), 0 \right\| \Delta \eta \Delta \sigma + \frac{CH1(\overline{I+1}, J) \Delta \eta \Delta \sigma}{\Delta \xi} \\ AW(I, J) &= \left\| (\rho U)(\overline{I}, J), 0 \right\| \Delta \eta \Delta \sigma + \frac{CH1(\overline{I}, J) \Delta \eta \Delta \sigma}{\Delta \xi} \end{aligned} \right\} \quad (D.172)$$

from Eqn. (D.172) changing $I, J \rightarrow I+1, J$, one can write:

$$AW(I+1, J) = \left\| (\rho U)(\overline{I+1}, J), 0 \right\| \Delta \eta \Delta \sigma + \frac{CH1(\overline{I+1}, J) \Delta \eta \Delta \sigma}{\Delta \xi} \quad (D.173)$$

Subtract $(\rho U)(\overline{I+1}, J)$ from both sides of Eqn. (D.173)

$$\begin{aligned} AW(I+1, J) - (\rho U)(\overline{I+1}, J) &= \left\| (\rho U)(\overline{I+1}, J), 0 \right\| \Delta \eta \Delta \sigma - \\ &\quad (\rho U)(\overline{I+1}, J) + \frac{CH1(\overline{I+1}, J) \Delta \eta \Delta \sigma}{\Delta \xi} \end{aligned} \quad (D.174)$$

or

$$\begin{aligned} AW(I+1, J) - (\rho U)(\overline{I+1}, J) &= \left\| -(\rho U)(\overline{I+1}, J), 0 \right\| \Delta \eta \Delta \sigma + \\ &\quad \frac{CH1(\overline{I+1}, J) \Delta \eta \Delta \sigma}{\Delta \xi} \end{aligned} \quad (D.175)$$

The terms on the right hand side of Eqn. (D.175) is equal to $AE(I, J)$ according to Eqn. (D.172). Therefore

$$AW(I+1, J) - (\rho U)(\overline{I+1}, J) = AE(I, J) \quad (D.176)$$

or

$$AE(I, J) = AW(I+1, J) - (\rho U)(\overline{I+1}, J) \quad (D.177)$$

or alternatively

$$AE(I, J) = AW(I+1, J) - FLOW \quad (D.178)$$

$$AW(I+1, J) = AMAX1(0., FLOW) \Delta \eta \Delta \sigma + DIFF \quad (D.179)$$

in which

$$FLOW = (\rho U)(\overline{I+1}, J) \quad (D.180)$$

$$DIFF = \frac{CH1(\overline{I+1}, J)\Delta\eta\Delta\sigma}{\Delta\xi} \quad (D.181)$$

from Figure D.29:

$$FLOW = RHO1 \cdot UC1(I+1, J) \quad (D.182)$$

in which

$$RHO1 = \frac{RHO(I, J) + RHO(I+1, J)}{2} \quad (D.183)$$

$$DIFF = \frac{(CH1(I, J) + CH1(I+1, J))\Delta\eta\Delta\sigma}{2\Delta\xi} \quad (D.184)$$

“AN” and “AS” Inter-Relationship

$$\left. \begin{aligned} AN_p^h &= \| -(\rho V)_n, 0 \| \Delta\xi\Delta\sigma + \frac{C_{3n}^h \Delta\xi\Delta\sigma}{\Delta\eta} \\ AS_p^h &= \| (\rho V)_s, 0 \| \Delta\xi\Delta\sigma + \frac{C_{3s}^h \Delta\xi\Delta\sigma}{\Delta\eta} \end{aligned} \right\} \quad (D.185)$$

In terms of I & J

$$\left. \begin{aligned} AN(I, J) &= \| -(\rho V)(I, \overline{J+1}), 0 \| \Delta\xi\Delta\sigma + \frac{CH3(I, \overline{J+1})\Delta\xi\Delta\sigma}{\Delta\eta} \\ AS(I, J) &= \| (\rho V)(I, \overline{J}), 0 \| \Delta\xi\Delta\sigma + \frac{CH3(I, \overline{J})\Delta\xi\Delta\sigma}{\Delta\eta} \end{aligned} \right\} \quad (D.186)$$

from Eqn. (D.186) changing $I, J \rightarrow I, J+1$:

$$AS(I, J+1) = \| (\rho V)(I, \overline{J+1}), 0 \| \Delta\xi\Delta\sigma + \frac{CH3(I, \overline{J+1})\Delta\xi\Delta\sigma}{\Delta\eta} \quad (D.187)$$

Subtract $(\rho V)(I, \overline{J+1})$ from both sides of Eqn. (D.187)

$$AS(I, J+1) - (\rho V)(I, \overline{J+1}) = \| (\rho V)(I, \overline{J+1}), 0 \| \Delta\xi\Delta\sigma - (\rho V)(I, \overline{J+1}) + \frac{CH3(I, \overline{J+1})\Delta\xi\Delta\sigma}{\Delta\eta} \quad (D.188)$$

or

$$AS(I, J+1) - (\rho V)(I, \overline{J+1}) = \| -(\rho V)(I, \overline{J+1}), 0 \| \Delta\xi\Delta\sigma + \frac{CH3(I, \overline{J+1})\Delta\xi\Delta\sigma}{\Delta\eta} \quad (D.189)$$

The terms on the right hand side of Eqn. (D.189) is equal to $AN(I, J)$ according to

Eqn. (D.186). Therefore

$$AS(I, J + 1) - (\rho V)(I, \overline{J + 1}) = AN(I, J) \quad (D.190)$$

or alternatively

$$AN(I, J) = AS(I, J + 1) - FLOW \quad (D.191)$$

$$AS(I, J + 1) = AMAX1(0., FLOW)\Delta\xi\Delta\sigma + DIFF \quad (D.192)$$

in which

$$FLOW = (\rho V)(I, \overline{J + 1}) \quad (D.193)$$

$$DIFF = \frac{CH3(I, \overline{J + 1})\Delta\xi\Delta\sigma}{\Delta\eta} \quad (D.194)$$

from Figure D.30:

$$FLOW = RHO1 \cdot VC2(I, J + 1) \quad (D.195)$$

in which

$$RHO1 = \frac{RHO(I, J) + RHO(I, J + 1)}{2} \quad (D.196)$$

$$DIFF = \frac{[CH3(I, J) + CH3(I, J + 1)]\Delta\xi\Delta\sigma}{2\Delta\eta} \quad (D.197)$$

To Obtain AW(2, J)

Using

$$AW(I + 1, J) = AMAX1(0., FLOW)\Delta\eta\Delta\sigma + DIFF \quad (D.198)$$

let $I = 1$

$$AW(2, J) = AMAX1(0., FLOW)\Delta\eta\Delta\sigma + DIFF \quad (D.199)$$

in which

$$FLOW = (\rho U)(\overline{I + 1}, J) = (\rho U)(\overline{2}, J) = (\rho U)(1, J) \quad (D.200)$$

$$\begin{aligned} DIFF &= \frac{CH1(\overline{I + 1}, J)\Delta\eta\Delta\sigma}{\Delta\xi} = \frac{CH1(\overline{2}, J)\Delta\eta\Delta\sigma}{\Delta\xi} \\ &= \frac{CH1(1, J)\Delta\eta\Delta\sigma}{\Delta\xi} \end{aligned} \quad (D.201)$$

from Figure D.31:

$$FLOW = RHO(1, J) \cdot UC1(2, J) \quad (D.202)$$

$$DIFF = \frac{CH1(1, J)\Delta\eta\Delta\sigma}{\Delta\xi} \quad (D.203)$$

To Obtain $AE(L2, J)$

Using

$$AE(I, J) = AW(I + 1, J) - FLOW \quad (D.204)$$

$$AW(I + 1, J) = AMAX1(0., FLOW)\Delta\eta\Delta\sigma + DIFF \quad (D.205)$$

let $I = L2$

$$AE(L2, J) = AW(L1, J) - FLOW \quad (D.206)$$

$$AW(L1, J) = AMAX1(0., FLOW)\Delta\eta\Delta\sigma + DIFF \quad (D.207)$$

in which

$$FLOW = (\rho U)(\overline{I+1}, J) = (\rho U)(\overline{L1}, J) = (\rho U)(L1, J) \quad (D.208)$$

$$\begin{aligned} DIFF &= \frac{CH1(\overline{I+1}, J)\Delta\eta\Delta\sigma}{\Delta\xi} = \frac{CH1(\overline{L1}, J)\Delta\eta\Delta\sigma}{\Delta\xi} \\ &= \frac{CH1(L1, J)\Delta\eta\Delta\sigma}{\Delta\xi} \end{aligned} \quad (D.209)$$

from Figure D.32:

$$FLOW = RHO(L1, J) \cdot UC1(L1, J) \quad (D.210)$$

$$DIFF = \frac{CH1(L1, J)\Delta\eta\Delta\sigma}{\Delta\xi} \quad (D.211)$$

To Obtain $AS(I, 2)$

Using

$$AS(I, J + 1) = AMAX1(0., FLOW)\Delta\xi\Delta\sigma + DIFF \quad (D.212)$$

let $J = 1$

$$AS(I, 2) = AMAX1(0., FLOW)\Delta\xi\Delta\sigma + DIFF \quad (D.213)$$

in which

$$FLOW = (\rho V)(I, \overline{J+1}) = (\rho V)(I, \overline{2}) = (\rho V)(I, 1) \quad (D.214)$$

$$\begin{aligned} DIFF &= \frac{CH3(I, \overline{J+1})\Delta\xi\Delta\sigma}{\Delta\eta} = \frac{CH3(I, \overline{2})\Delta\xi\Delta\sigma}{\Delta\eta} \\ &= \frac{CH3(I, 1)\Delta\xi\Delta\sigma}{\Delta\eta} \end{aligned} \quad (D.215)$$

from Figure D.33:

$$FLOW = RHO(I, 1) \cdot VC2(I, 2) \quad (D.216)$$

$$DIFF = \frac{CH3(I, 1)\Delta\xi\Delta\sigma}{\Delta\eta} \quad (D.217)$$

To Obtain $AN(I, M2)$

Using

$$AN(I, J) = AS(I, J+1) - FLOW \quad (D.218)$$

let $J = M2$

$$AN(I, M2) = AS(I, M1) - FLOW \quad (D.219)$$

in which

$$FLOW = (\rho V)(I, \overline{J+1}) = (\rho V)(I, \overline{M1}) = (\rho V)(I, M1) \quad (D.220)$$

$$\begin{aligned} DIFF &= \frac{CH3(I, \overline{J+1})\Delta\xi\Delta\sigma}{\Delta\eta} = \frac{CH3(I, \overline{M1})\Delta\xi\Delta\sigma}{\Delta\eta} \\ &= \frac{CH3(I, M1)\Delta\xi\Delta\sigma}{\Delta\eta} \end{aligned} \quad (D.221)$$

from Figure D.34:

$$FLOW = RHO(I, M1) \cdot VC2(I, M1) \quad (D.222)$$

$$DIFF = \frac{CH3(I, M1)\Delta\xi\Delta\sigma}{\Delta\eta} \quad (D.223)$$

Range of variations of I and J

I = 3 to L2

J = 2 to M2

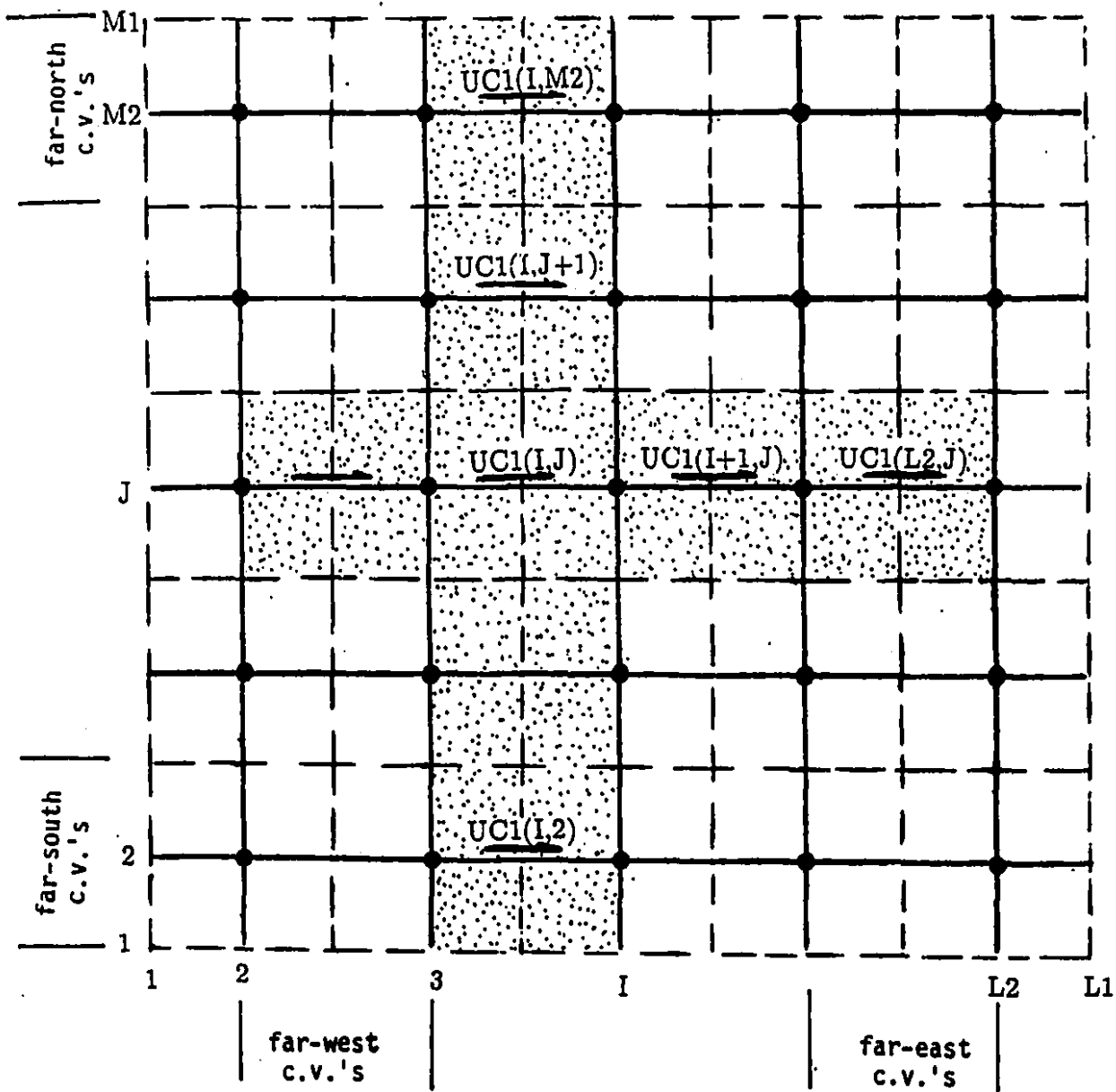


Figure D.1

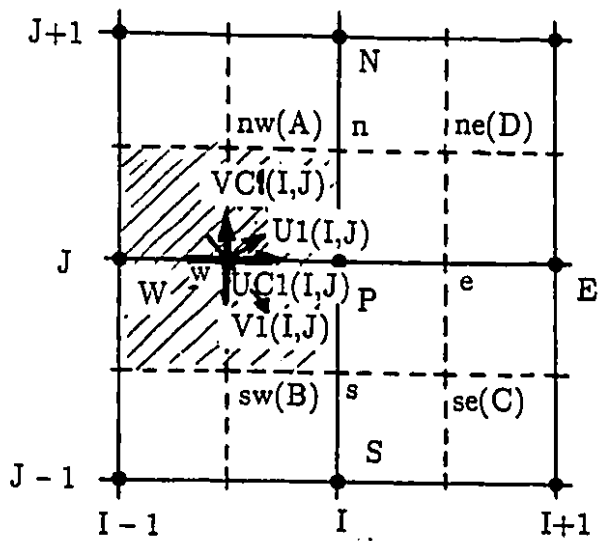


Figure D.2

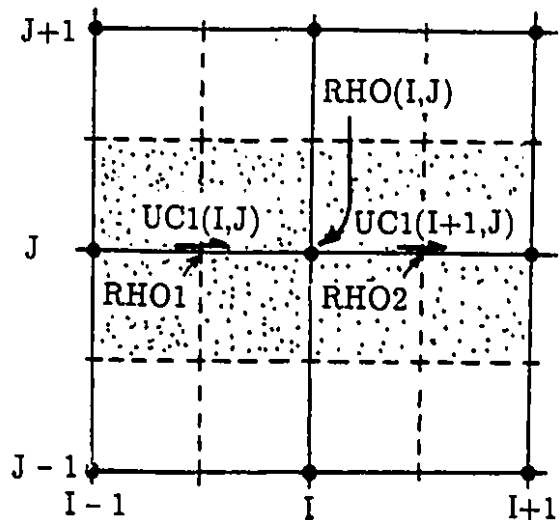


Figure D.3

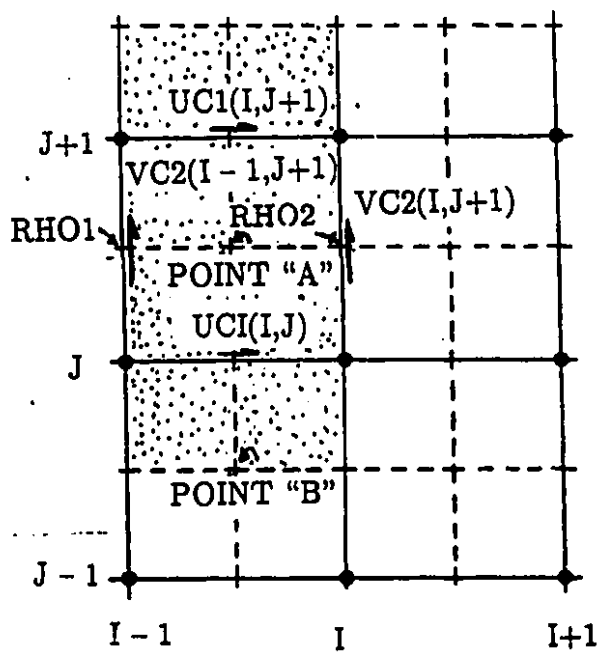


Figure D.4

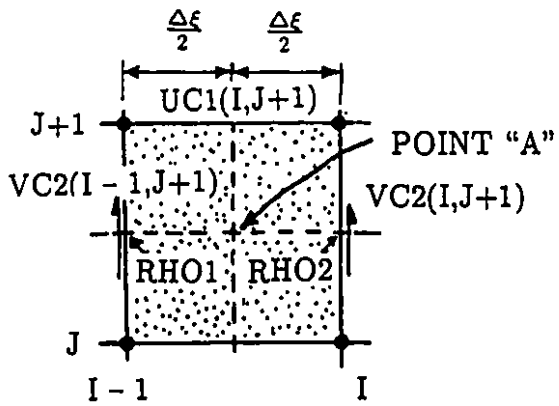


Figure D.5

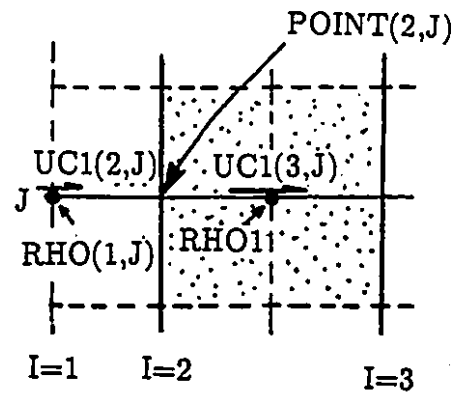


Figure D.6

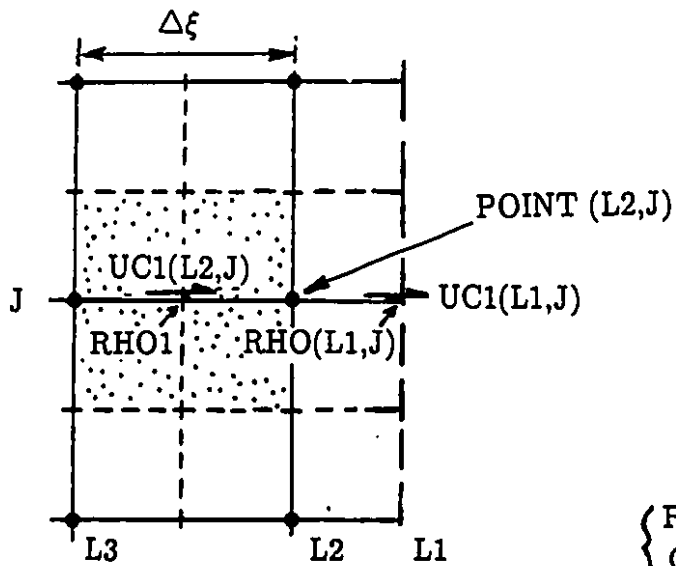


Figure D.7

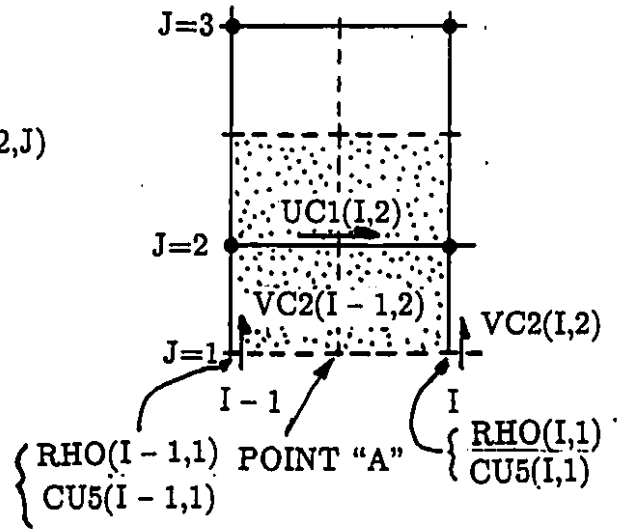


Figure D.8

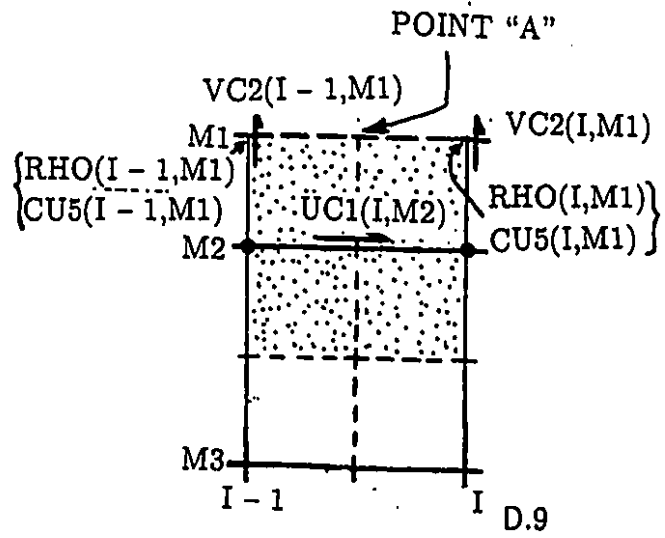


Figure D.9

Range of variations of I and J

I = 2 to L2

J = 3 to M2

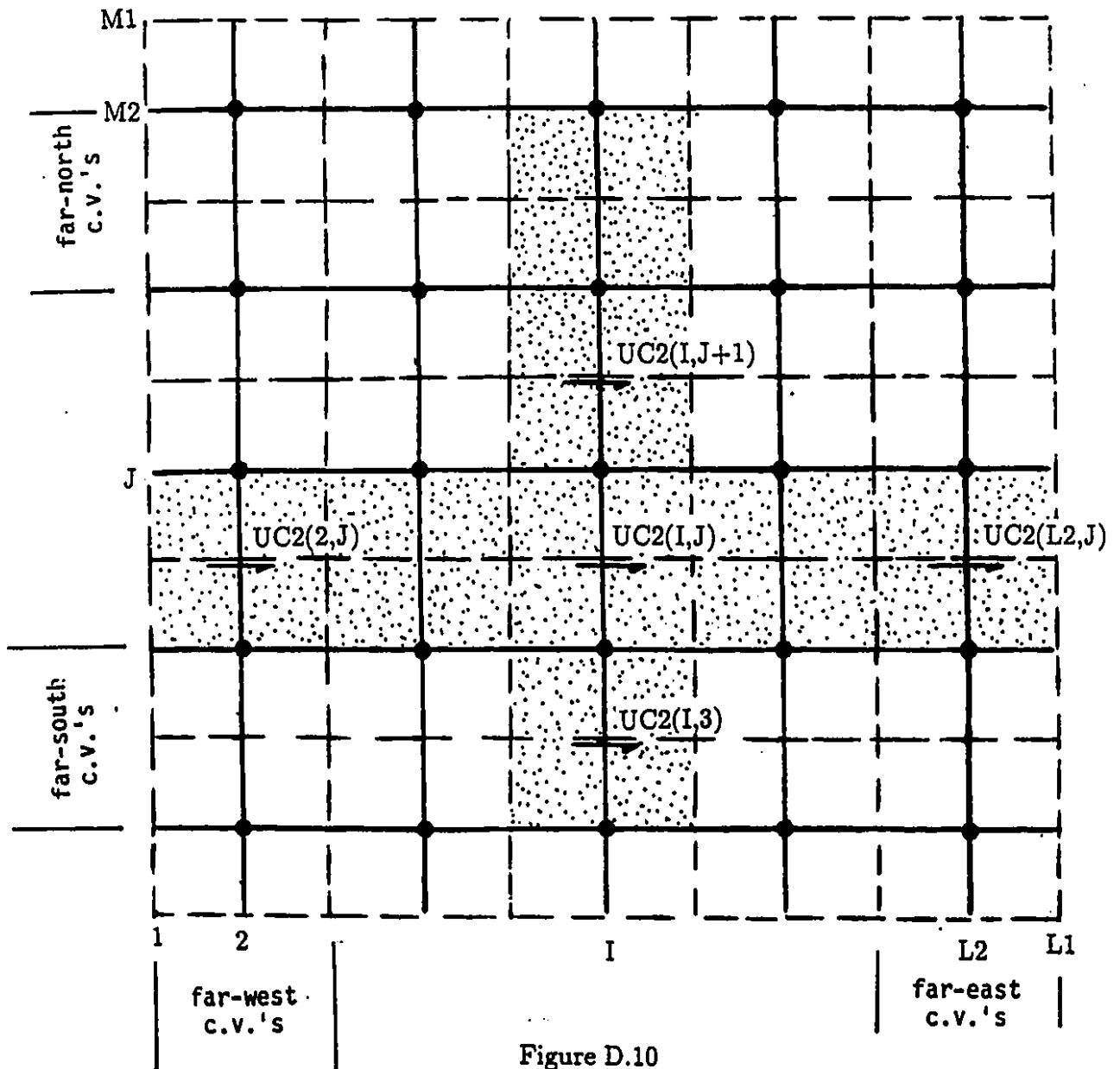


Figure D.10

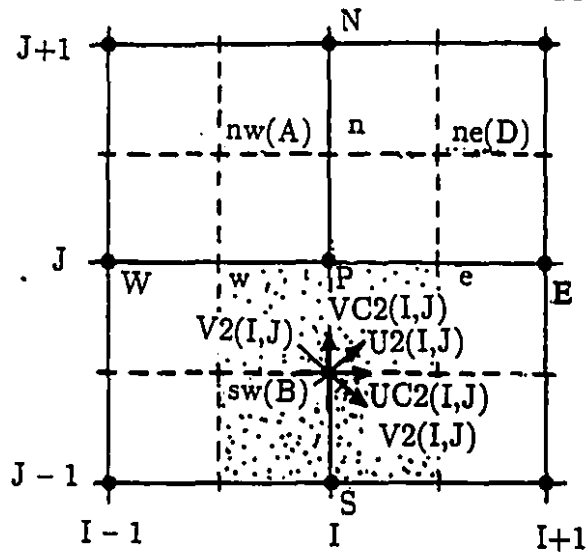


Figure D.11

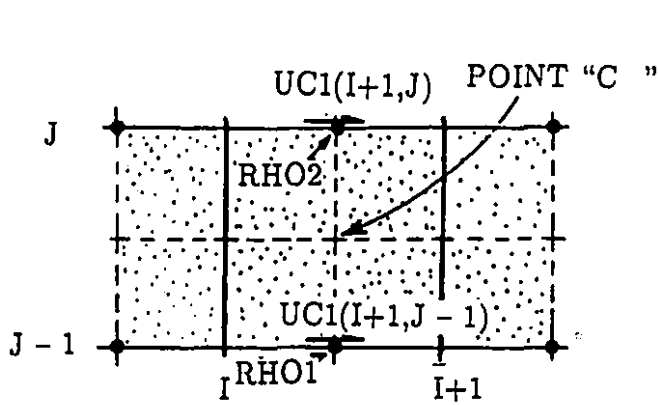


Figure D.12

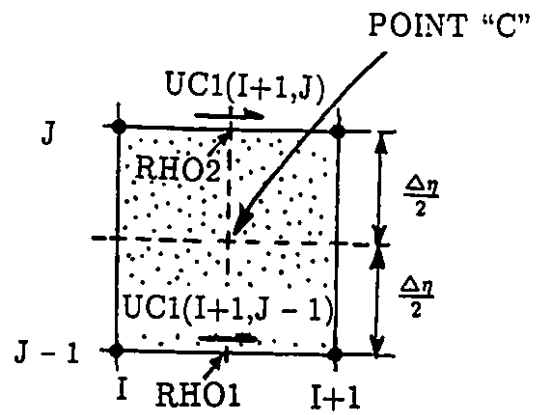


Figure D.13

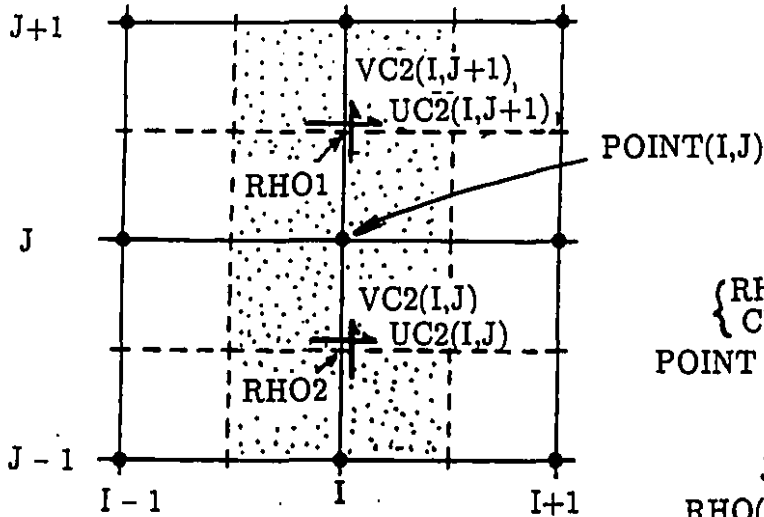


Figure D.14

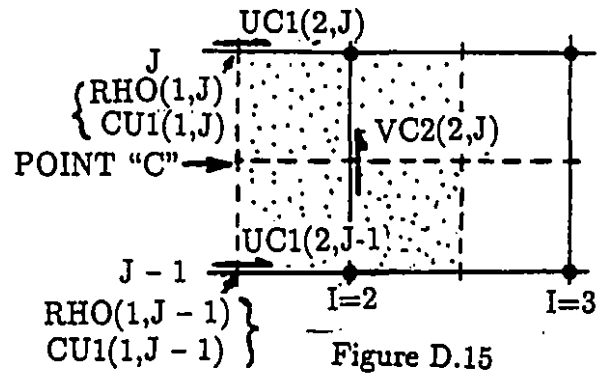


Figure D.15

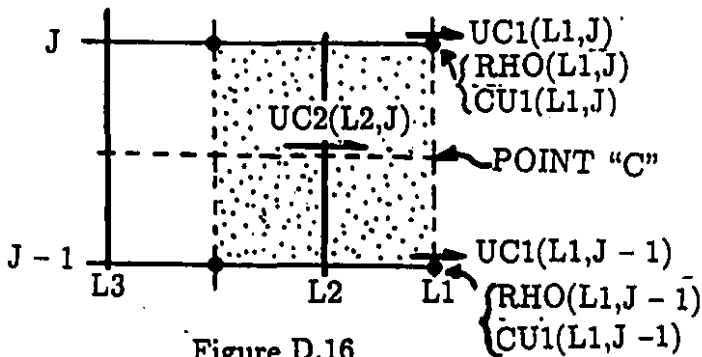


Figure D.16

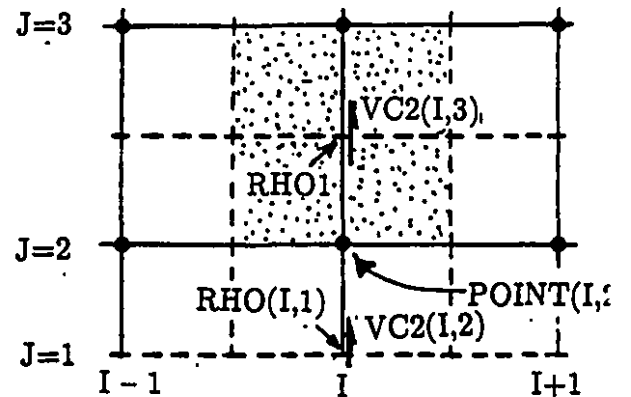


Figure D.17

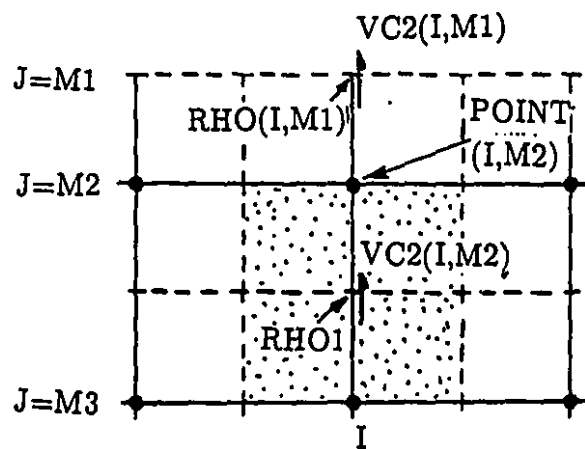


Figure D.18

Range of variations of I and J

I = 2 to L2

J = 2 to M2

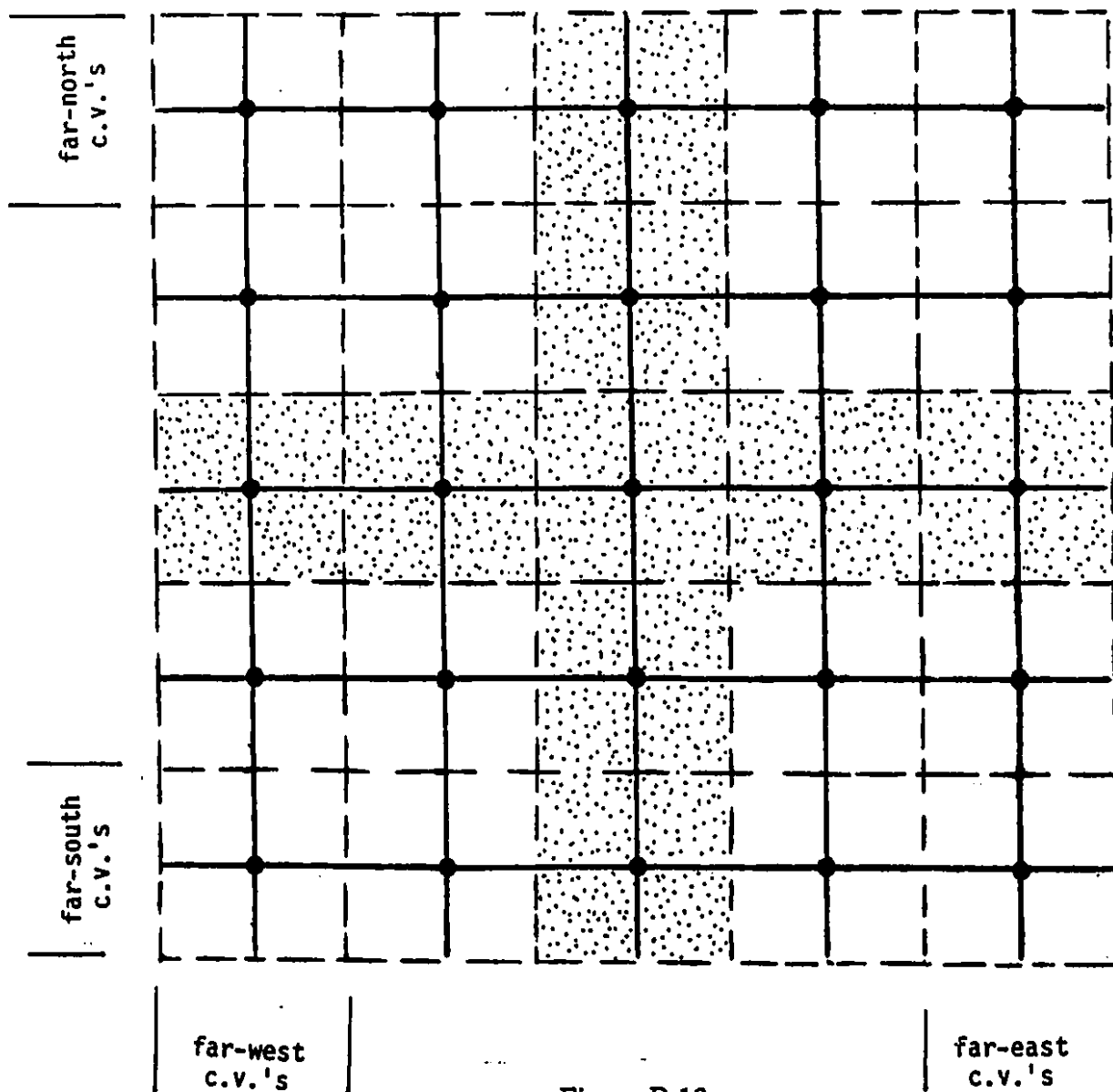


Figure D.19

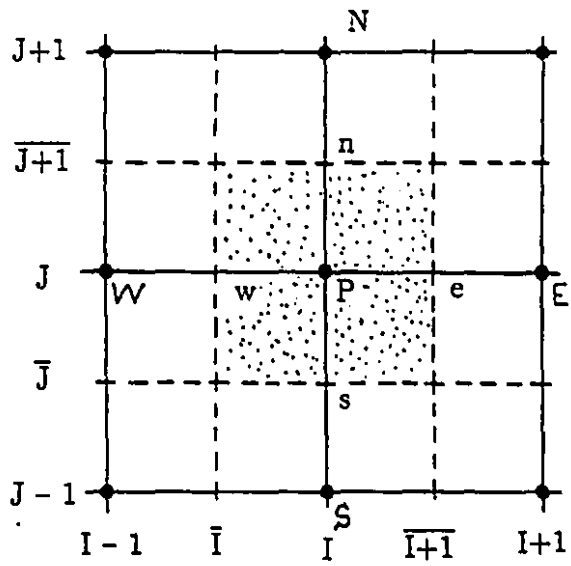


Figure D.20

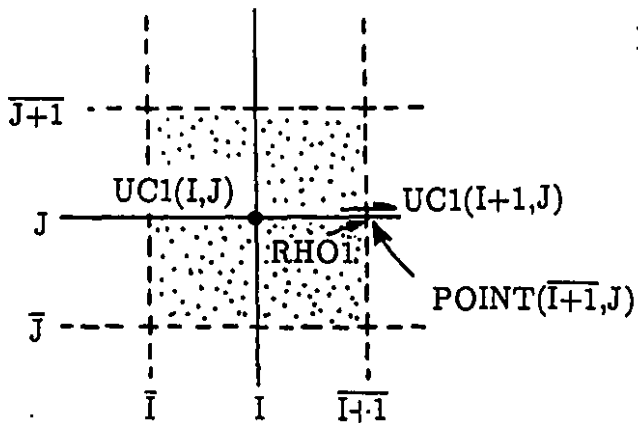


Figure D.21

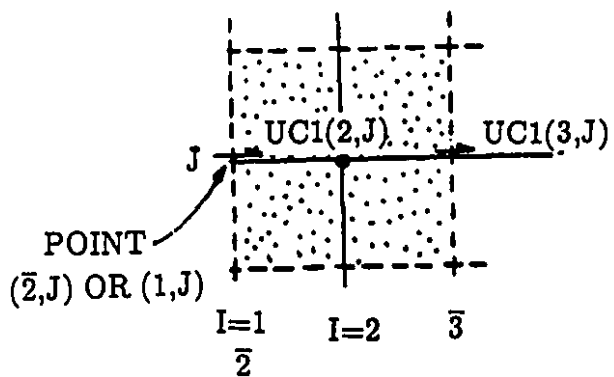


Figure D.23

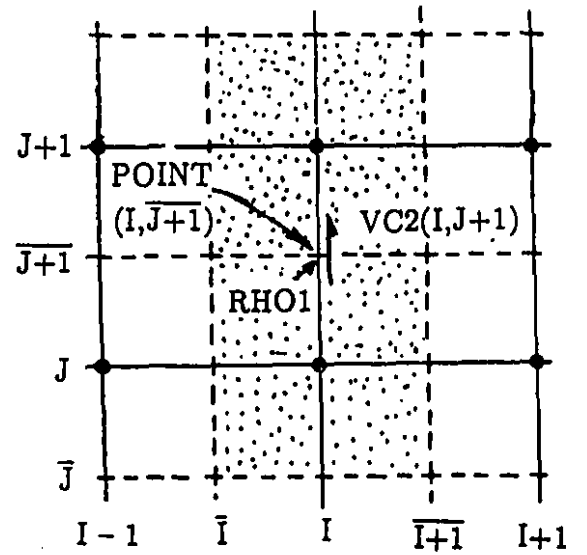


Figure D.22

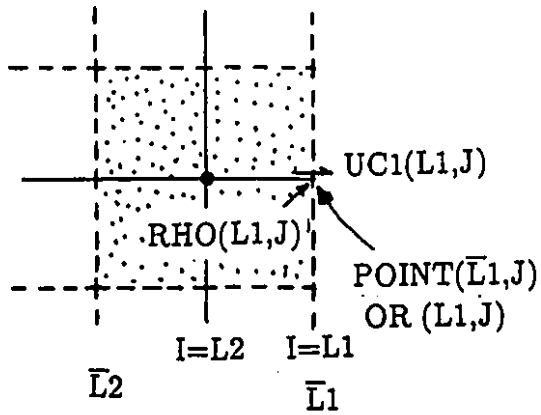


Figure D.24

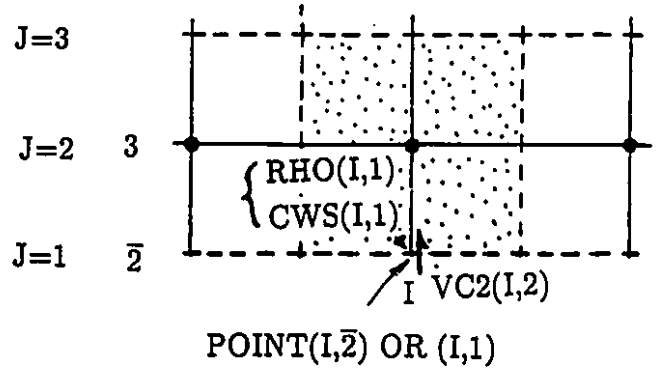


Figure D.25

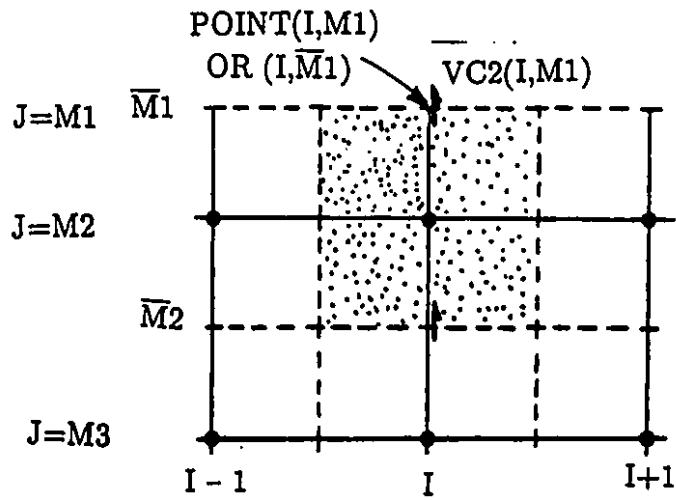
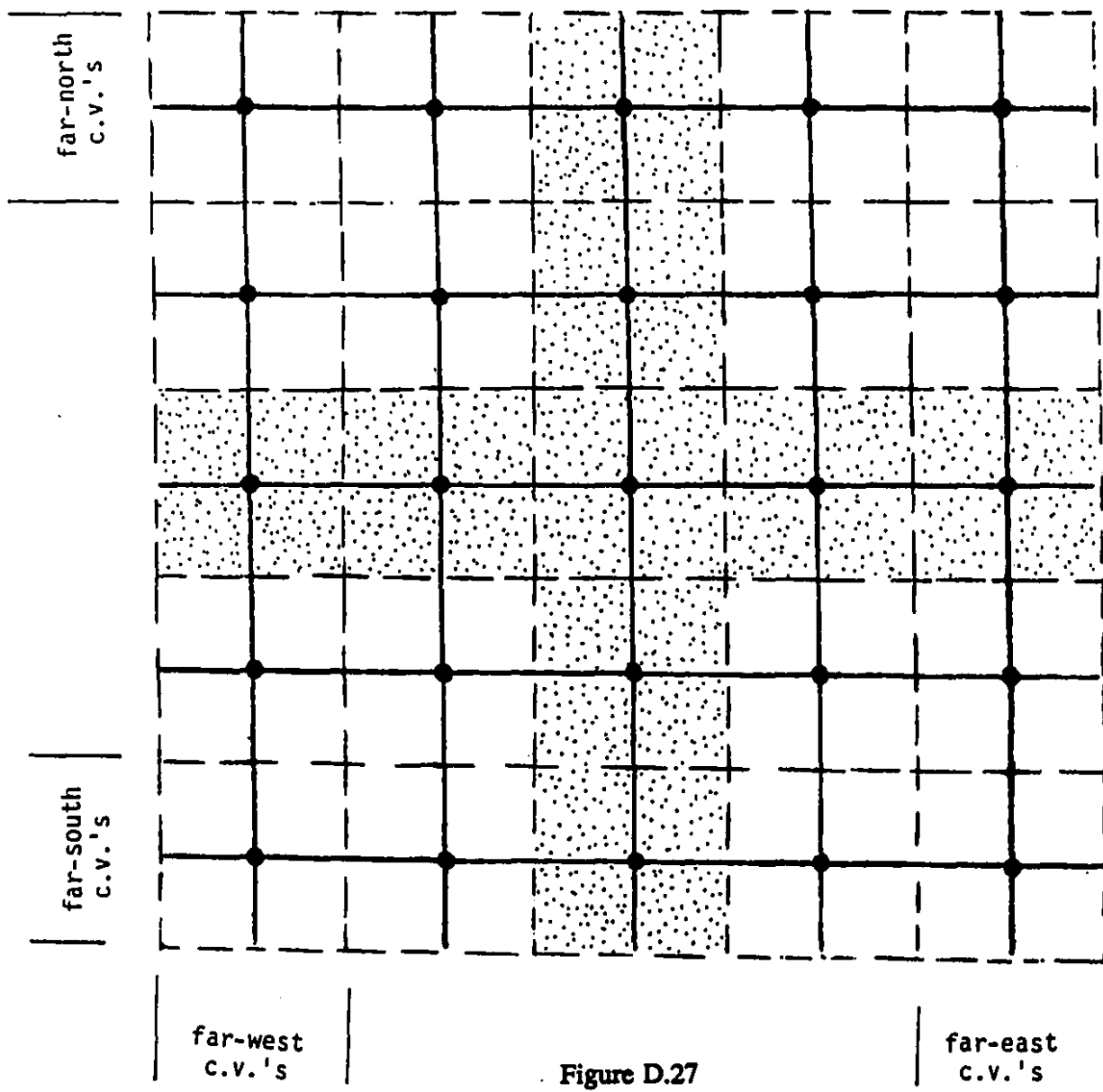


Figure D.26

Range of variations of I and J

I = 2 to L2

J = 2 to M2



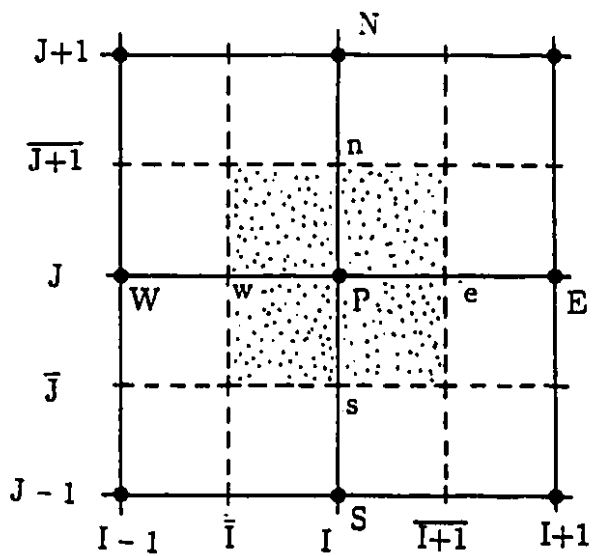


Figure D.28

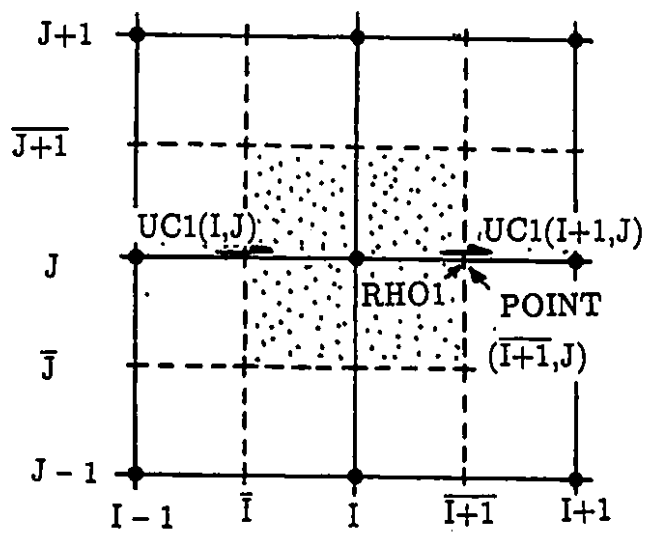


Figure D.29

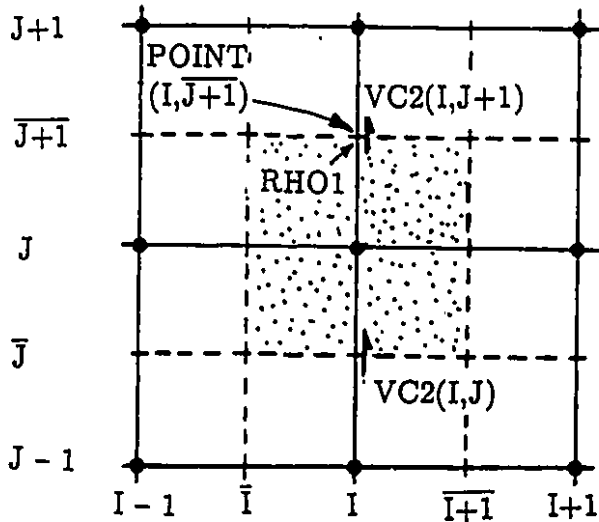


Figure D.30

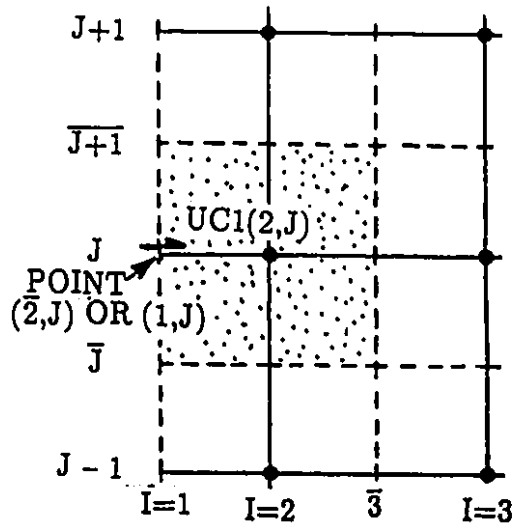


Figure D.31

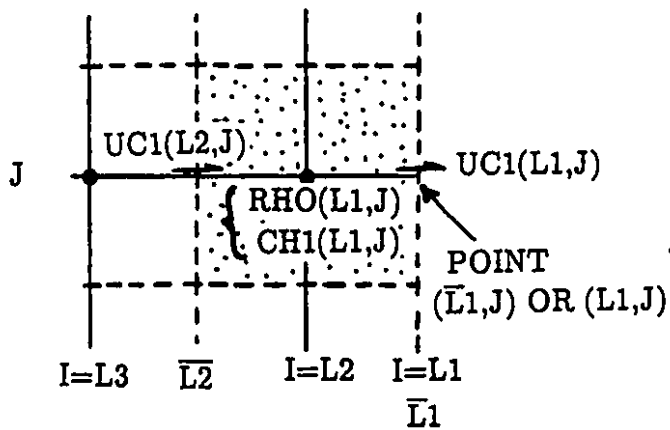


Figure D.32

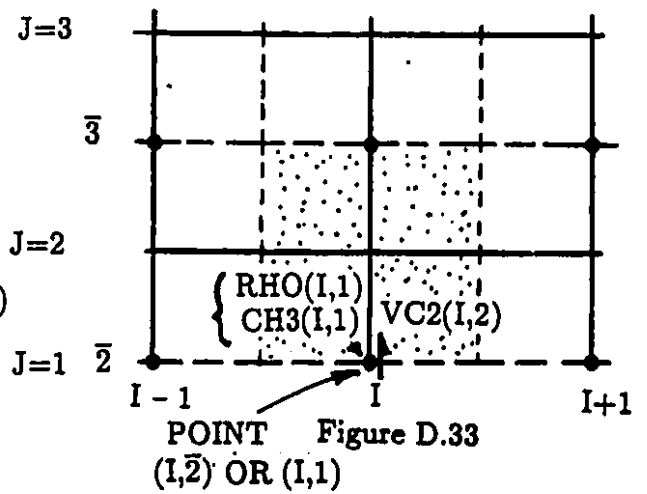


Figure D.33
POINT (I, 2) OR (I, 1)

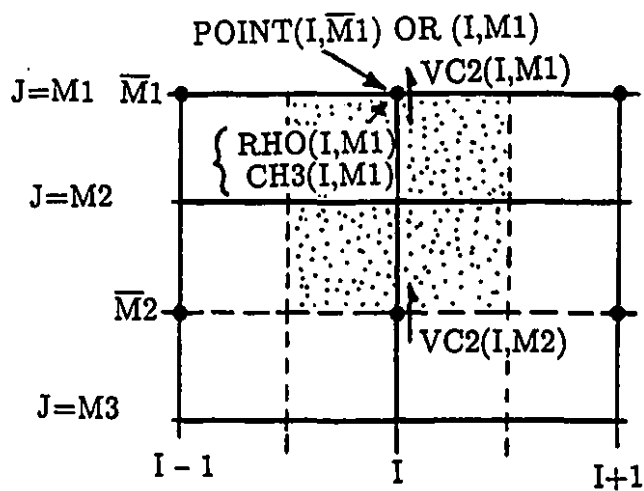


Figure D.34

APPENDIX E
DERIVATION OF DISCRETIZED
BOUNDARY CONDITIONS FOR
REACTANT CONTINUITY EQUATION

TRANSFORMATION RELATIONS FOR DIRECTIONAL DERIVATIVES

$$\left. \frac{\partial f}{\partial n} \right|_{\eta} = \frac{(\gamma f_{\eta} - \beta f_{\xi})}{J\sqrt{\gamma}} \quad (E.1)$$

$$\left. \frac{\partial f}{\partial n} \right|_{\xi} = \frac{(\alpha f_{\xi} - \beta f_{\eta})}{J\sqrt{\alpha}} \quad (E.2)$$

or

$$\left. \frac{\partial f}{\partial n} \right|_{\eta} = \frac{1}{J\sqrt{\gamma}} \left[\gamma \frac{\partial f}{\partial \eta} - \beta \frac{\partial f}{\partial \xi} \right] \quad (E.3)$$

$$\left. \frac{\partial f}{\partial n} \right|_{\xi} = \frac{1}{J\sqrt{\alpha}} \left[\alpha \frac{\partial f}{\partial \xi} - \beta \frac{\partial f}{\partial \eta} \right] \quad (E.4)$$

TRANSFORMATION OF BOUNDARY-CONDITIONS

$$\left. \frac{\partial m}{\partial n} \right|_{\eta=\text{wall}} = \frac{1}{J_{\text{wall}}\sqrt{\gamma_{\text{wall}}}} \left[\gamma_{\text{wall}} \left. \frac{\partial m}{\partial \eta} \right|_{\text{wall}} - \beta_{\text{wall}} \left. \frac{\partial m}{\partial \xi} \right|_{\text{wall}} \right] \quad (E.5)$$

but

$$\left. \frac{\partial m}{\partial n} \right|_{\eta=\text{wall}} = 0 \quad (E.6)$$

therefore

$$\frac{1}{J_{\text{wall}}\sqrt{\gamma_{\text{wall}}}} \left[\gamma_{\text{wall}} \left. \frac{\partial m}{\partial \eta} \right|_{\text{wall}} - \beta_{\text{wall}} \left. \frac{\partial m}{\partial \xi} \right|_{\text{wall}} \right] = 0 \quad (E.7)$$

or

$$\gamma_{\text{wall}} \left. \frac{\partial m}{\partial \eta} \right|_{\text{wall}} - \beta_{\text{wall}} \left. \frac{\partial m}{\partial \xi} \right|_{\text{wall}} = 0 \quad (E.8)$$

from which

$$\left. \frac{\partial m}{\partial \eta} \right|_{\text{wall}} = \frac{\beta_{\text{wall}}}{\gamma_{\text{wall}}} \left. \frac{\partial m}{\partial \xi} \right|_{\text{wall}} \quad (E.9)$$

and

$$\left. \frac{\partial m}{\partial n} \right|_{\xi=\text{wall}} = \frac{1}{J_{\text{wall}}\sqrt{\alpha_{\text{wall}}}} \left[\alpha_{\text{wall}} \left. \frac{\partial m}{\partial \xi} \right|_{\text{wall}} - \beta_{\text{wall}} \left. \frac{\partial m}{\partial \eta} \right|_{\text{wall}} \right] \quad (E.10)$$

but

$$\left. \frac{\partial m}{\partial n} \right|_{\xi=\text{wall}} = 0 \quad (E.11)$$

therefore

$$\frac{1}{J_{\text{wall}} \sqrt{\alpha_{\text{wall}}}} \left[\alpha_{\text{wall}} \left. \frac{\partial m}{\partial \xi} \right|_{\text{wall}} - \beta_{\text{wall}} \left. \frac{\partial m}{\partial \eta} \right|_{\text{wall}} \right] = 0 \quad (E.12)$$

or

$$\alpha_{\text{wall}} \left. \frac{\partial m}{\partial \xi} \right|_{\text{wall}} - \beta_{\text{wall}} \left. \frac{\partial m}{\partial \eta} \right|_{\text{wall}} = 0 \quad (E.13)$$

from which

$$\left. \frac{\partial m}{\partial \xi} \right|_{\text{wall}} = \frac{\beta_{\text{wall}}}{\alpha_{\text{wall}}} \left. \frac{\partial m}{\partial \eta} \right|_{\text{wall}} \quad (E.14)$$

(Refer to Figs. E.1 and E.2)

**DERIVATION OF DISCRETIZATION EQUATION
FOR m_P
@ $J = M1$ BOUNDARY
(Typical Derivation)**

(Refer to Fig. E.3)

$$\begin{aligned} & \int_U^D \int_s^P \int_w^e \frac{\partial}{\partial \xi} (\rho U m) d\xi d\eta d\sigma + \int_U^D \int_w^e \int_s^P \frac{\partial}{\partial \eta} (\rho V m) d\eta d\xi d\sigma + \\ & \int_s^P \int_w^e \int_U^D \frac{\partial}{\partial \sigma} (\rho W m) d\sigma d\xi d\eta = \int_U^D \int_s^P \int_w^e \frac{\partial}{\partial \xi} (C_1^m \frac{\partial m}{\partial \xi}) d\xi d\eta d\sigma + \\ & \int_U^D \int_s^P \int_w^e \frac{\partial}{\partial \xi} (C_2^m \frac{\partial m}{\partial \eta}) d\xi d\eta d\sigma + \int_U^D \int_w^e \int_s^P \frac{\partial}{\partial \eta} (C_3^m \frac{\partial m}{\partial \eta}) d\eta d\xi d\sigma + \\ & \int_U^D \int_w^e \int_s^P \frac{\partial}{\partial \eta} (C_4^m \frac{\partial m}{\partial \xi}) d\eta d\xi d\sigma + \int_U^D \int_s^P \int_w^e \hat{S}^m d\xi d\eta d\sigma \end{aligned} \quad (E.15)$$

$$\begin{aligned}
& \frac{1}{2}(\rho U m)_e \Delta \eta \Delta \sigma - \frac{1}{2}(\rho U m)_w \Delta \eta \Delta \sigma + (\rho V m)_P \Delta \xi \Delta \sigma - \\
& (\rho V m)_s \Delta \xi \Delta \sigma + \frac{1}{2}(\rho W m)_{P,D} \Delta \xi \Delta \eta - \frac{1}{2}(\rho W m)_{P,U} \Delta \xi \Delta \eta = \\
& \frac{1}{2} \left(C_1^m \frac{\partial m}{\partial \xi} \right)_e \Delta \eta \Delta \sigma - \frac{1}{2} \left(C_1^m \frac{\partial m}{\partial \xi} \right)_w \Delta \eta \Delta \sigma + \frac{1}{2} \left(C_2^m \frac{\partial m}{\partial \eta} \right)_e \Delta \eta \Delta \sigma - \\
& \frac{1}{2} \left(C_2^m \frac{\partial m}{\partial \eta} \right)_w \Delta \eta \Delta \sigma + \left(C_3^m \frac{\partial m}{\partial \eta} \right)_P \Delta \xi \Delta \sigma - \left(C_3^m \frac{\partial m}{\partial \eta} \right)_s \Delta \xi \Delta \sigma + \\
& \left(C_4^m \frac{\partial m}{\partial \xi} \right)_P \Delta \xi \Delta \sigma - \left(C_4^m \frac{\partial m}{\partial \xi} \right)_s \Delta \xi \Delta \sigma + \frac{1}{2} \hat{S}_P^m \Delta \xi \Delta \eta \Delta \sigma \quad (E.16)
\end{aligned}$$

$$\begin{aligned}
LHS = & \frac{1}{2}(\rho U m)_e \Delta \eta \Delta \sigma - \frac{1}{2}(\rho U m)_w \Delta \eta \Delta \sigma + (\rho V m)_P \Delta \xi \Delta \sigma - \\
& (\rho V m)_s \Delta \xi \Delta \sigma + \frac{1}{2}(\rho W m)_{P,D} \Delta \xi \Delta \eta - \frac{1}{2}(\rho W m)_{P,U} \Delta \xi \Delta \eta \quad (E.17)
\end{aligned}$$

$$\begin{aligned}
LHS = & \frac{1}{2}(\rho U)_e \Delta \eta \Delta \sigma m_e - \frac{1}{2}(\rho U)_w \Delta \eta \Delta \sigma m_w + (\rho V)_P \Delta \xi \Delta \sigma m_P - \\
& (\rho V)_s \Delta \xi \Delta \sigma m_s + \frac{1}{2}(\rho W)_{P,D} \Delta \xi \Delta \eta m_P - \frac{1}{2}(\rho W)_{P,U} \Delta \xi \Delta \eta m_{P,U} \quad (E.18)
\end{aligned}$$

$$\begin{aligned}
LHS = & \frac{1}{2} \{ \|(\rho U)_{e,0}\| \Delta \eta \Delta \sigma m_P - \| -(\rho U)_{e,0}\| \Delta \eta \Delta \sigma m_E \} - \\
& \frac{1}{2} \{ \|(\rho U)_{w,0}\| \Delta \eta \Delta \sigma m_W - \| -(\rho U)_{w,0}\| \Delta \eta \Delta \sigma m_P \} + \\
& (\rho V)_P \Delta \xi \Delta \sigma m_P - \{ \|(\rho V)_{s,0}\| \Delta \xi \Delta \sigma m_S - \\
& \| -(\rho V)_{s,0}\| \Delta \xi \Delta \sigma m_P \} + \frac{1}{2}(\rho W)_{P,D} \Delta \xi \Delta \eta m_P - \\
& \frac{1}{2}(\rho W)_{P,U} \Delta \xi \Delta \eta m_{P,U} \quad (E.19)
\end{aligned}$$

$$\begin{aligned}
LHS = & \frac{1}{2} \|(\rho U)_{e,0}\| \Delta\eta \Delta\sigma m_P - \frac{1}{2} \| -(\rho U)_{e,0}\| \Delta\eta \Delta\sigma m_E - \\
& \frac{1}{2} \|(\rho U)_{w,0}\| \Delta\eta \Delta\sigma m_W + \frac{1}{2} \| -(\rho U)_{w,0}\| \Delta\eta \Delta\sigma m_P + \\
& (\rho V)_P \Delta\xi \Delta\sigma m_P - \|(\rho V)_{s,0}\| \Delta\xi \Delta\sigma m_S + \\
& \| -(\rho V)_{s,0}\| \Delta\xi \Delta\sigma m_P + \frac{1}{2} (\rho W)_{P,D} \Delta\xi \Delta\eta m_P - \\
& \frac{1}{2} (\rho W)_{P,U} \Delta\xi \Delta\eta m_{P,U}
\end{aligned} \tag{E.20}$$

Write the continuity equation:

$$\frac{\partial}{\partial\xi}(\rho U) + \frac{\partial}{\partial\eta}(\rho V) + \frac{\partial}{\partial\sigma}(\rho W) = 0 \tag{E.21}$$

$$\begin{aligned}
& \int_U^D \int_s^P \int_w^e \frac{\partial}{\partial\xi}(\rho U) d\xi d\eta d\sigma + \int_U^D \int_w^e \int_s^P \frac{\partial}{\partial\eta}(\rho V) d\eta d\xi d\sigma + \\
& \int_s^P \int_w^e \int_U^D \frac{\partial}{\partial\sigma}(\rho W) d\sigma d\xi d\eta = 0
\end{aligned} \tag{E.22}$$

$$\begin{aligned}
& \frac{1}{2} [(\rho U)_e - (\rho U)_w] \Delta\eta \Delta\sigma + [(\rho V)_P - (\rho V)_s] \Delta\xi \Delta\sigma + \\
& \frac{1}{2} [(\rho W)_{P,D} - (\rho W)_{P,U}] \Delta\xi \Delta\eta = 0
\end{aligned} \tag{E.23}$$

$$\begin{aligned}
& \frac{1}{2} (\rho U)_e \Delta\eta \Delta\sigma - \frac{1}{2} (\rho U)_w \Delta\eta \Delta\sigma + (\rho V)_P \Delta\xi \Delta\sigma - \\
& (\rho V)_s \Delta\xi \Delta\sigma + \frac{1}{2} (\rho W)_{P,D} \Delta\xi \Delta\eta - \frac{1}{2} (\rho W)_{P,U} \Delta\xi \Delta\eta = 0
\end{aligned} \tag{E.24}$$

Multiply by $-m_P$

$$\begin{aligned}
& -\frac{1}{2} (\rho U)_e \Delta\eta \Delta\sigma m_P + \frac{1}{2} (\rho U)_w \Delta\eta \Delta\sigma m_P - (\rho V)_P \Delta\xi \Delta\sigma m_P + \\
& (\rho V)_s \Delta\xi \Delta\sigma m_P - \frac{1}{2} (\rho W)_{P,D} \Delta\xi \Delta\eta m_P + \frac{1}{2} (\rho W)_{P,U} \Delta\xi \Delta\eta m_P = 0
\end{aligned} \tag{E.25}$$

$$\begin{aligned}
LHS = & \frac{1}{2} \|(\rho U)_{e,0}\| \Delta\eta \Delta\sigma m_P - \frac{1}{2} \| -(\rho U)_{e,0}\| \Delta\eta \Delta\sigma m_E - \\
& \frac{1}{2} \|(\rho U)_{w,0}\| \Delta\eta \Delta\sigma m_W + \frac{1}{2} \| -(\rho U)_{w,0}\| \Delta\eta \Delta\sigma m_P + \\
& (\rho V)_P \Delta\xi \Delta\sigma m_P - \|(\rho V)_{s,0}\| \Delta\xi \Delta\sigma m_S + \\
& \| -(\rho V)_{s,0}\| \Delta\xi \Delta\sigma m_P + \frac{1}{2} (\rho W)_{P,D} \Delta\xi \Delta\eta m_P - \\
& \frac{1}{2} (\rho W)_{P,U} \Delta\xi \Delta\eta m_{P,U} - \frac{1}{2} (\rho U)_e \Delta\eta \Delta\sigma m_P + \frac{1}{2} (\rho U)_w \Delta\eta \Delta\sigma m_P - \\
& (\rho V)_P \Delta\xi \Delta\sigma m_P + (\rho V)_s \Delta\xi \Delta\sigma m_P - \frac{1}{2} (\rho W)_{P,D} \Delta\xi \Delta\eta m_P + \\
& \frac{1}{2} (\rho W)_{P,U} \Delta\xi \Delta\eta m_P
\end{aligned} \tag{E.26}$$

$$\begin{aligned}
LHS = & \frac{1}{2} \| -(\rho U)_{e,0}\| \Delta\eta \Delta\sigma m_P - \frac{1}{2} \| -(\rho U)_{e,0}\| \Delta\eta \Delta\sigma m_E - \\
& \frac{1}{2} \|(\rho U)_{w,0}\| \Delta\eta \Delta\sigma m_W + \frac{1}{2} \|(\rho U)_{w,0}\| \Delta\eta \Delta\sigma m_P - \\
& \|(\rho V)_{s,0}\| \Delta\xi \Delta\sigma m_S + \|(\rho V)_{s,0}\| \Delta\xi \Delta\sigma m_P + \\
& \frac{1}{2} (\rho W)_{P,U} \Delta\xi \Delta\eta m_P - \frac{1}{2} (\rho W)_{P,U} \Delta\xi \Delta\eta m_{P,U}
\end{aligned} \tag{E.27}$$

$$\begin{aligned}
RHS = & \frac{1}{2} C_{1e}^m \Delta\eta \Delta\sigma \left(\frac{\partial m}{\partial \xi} \right)_e - \frac{1}{2} C_{1w}^m \Delta\eta \Delta\sigma \left(\frac{\partial m}{\partial \xi} \right)_w + \\
& \frac{1}{2} C_{2e}^m \Delta\eta \Delta\sigma \left(\frac{\partial m}{\partial \eta} \right)_e - \frac{1}{2} C_{2w}^m \Delta\eta \Delta\sigma \left(\frac{\partial m}{\partial \eta} \right)_w + \\
& C_{3P}^m \Delta\xi \Delta\sigma \left(\frac{\partial m}{\partial \eta} \right)_P - C_{3s}^m \Delta\xi \Delta\sigma \left(\frac{\partial m}{\partial \eta} \right)_s + \\
& C_{4P}^m \Delta\xi \Delta\sigma \left(\frac{\partial m}{\partial \xi} \right)_P - C_{4s}^m \Delta\xi \Delta\sigma \left(\frac{\partial m}{\partial \xi} \right)_s + \\
& \frac{1}{2} \hat{S}_P^m \Delta\xi \Delta\eta \Delta\sigma
\end{aligned} \tag{E.28}$$

$$\left(\frac{\partial m}{\partial \eta}\right)_P = \frac{\beta_P}{\gamma_P} \left(\frac{\partial m}{\partial \xi}\right)_P \quad (E.29)$$

$$\left(\frac{\partial m}{\partial \eta}\right)_e = \frac{\beta_e}{\gamma_e} \left(\frac{\partial m}{\partial \xi}\right)_e \quad (E.30)$$

$$\left(\frac{\partial m}{\partial \eta}\right)_w = \frac{\beta_w}{\gamma_w} \left(\frac{\partial m}{\partial \xi}\right)_w \quad (E.31)$$

$$\begin{aligned} RHS = & \frac{1}{2} C_{1e}^m \Delta \eta \Delta \sigma \left(\frac{\partial m}{\partial \xi}\right)_e - \frac{1}{2} C_{1w}^m \Delta \eta \Delta \sigma \left(\frac{\partial m}{\partial \xi}\right)_w + \\ & \frac{1}{2} C_{2e}^m \Delta \eta \Delta \sigma \frac{\beta_e}{\gamma_e} \left(\frac{\partial m}{\partial \xi}\right)_e - \frac{1}{2} C_{2w}^m \Delta \eta \Delta \sigma \frac{\beta_w}{\gamma_w} \left(\frac{\partial m}{\partial \xi}\right)_w + \\ & C_{3P}^m \Delta \xi \Delta \sigma \frac{\beta_P}{\gamma_P} \left(\frac{\partial m}{\partial \xi}\right)_P - C_{3s}^m \Delta \xi \Delta \sigma \left(\frac{\partial m}{\partial \eta}\right)_s + \\ & C_{4P}^m \Delta \xi \Delta \sigma \left(\frac{\partial m}{\partial \xi}\right)_P - C_{4s}^m \Delta \xi \Delta \sigma \left(\frac{\partial m}{\partial \xi}\right)_s + \\ & \frac{1}{2} \hat{S}_P^m \Delta V \end{aligned} \quad (E.32)$$

$$\begin{aligned} RHS = & \frac{1}{2} C_{1e}^m \Delta \eta \Delta \sigma \frac{m_E - m_P}{\Delta \xi} - \frac{1}{2} C_{1w}^m \Delta \eta \Delta \sigma \frac{m_P - m_W}{\Delta \xi} + \\ & \frac{1}{2} C_{2e}^m \Delta \eta \Delta \sigma \frac{\beta_e}{\gamma_e} \frac{m_E - m_P}{\Delta \xi} - \frac{1}{2} C_{2w}^m \Delta \eta \Delta \sigma \frac{\beta_w}{\gamma_w} \frac{m_P - m_W}{\Delta \xi} + \\ & C_{3P}^m \Delta \xi \Delta \sigma \frac{\beta_P}{\gamma_P} \frac{m_e - m_w}{\Delta \xi} - C_{3s}^m \Delta \xi \Delta \sigma \frac{m_P - m_S}{\Delta \eta} + \\ & C_{4P}^m \Delta \xi \Delta \sigma \frac{m_e - m_w}{\Delta \xi} - C_{4s}^m \Delta \xi \Delta \sigma \frac{m_{se} - m_{sw}}{\Delta \xi} + \\ & \frac{1}{2} L[\hat{S}_P^m] \Delta V \end{aligned} \quad (E.33)$$

$$\begin{aligned}
RHS = & \frac{1}{2}C_{1e}^m \frac{\Delta\eta\Delta\sigma}{\Delta\xi} m_E - \frac{1}{2}C_{1e}^m \frac{\Delta\eta\Delta\sigma}{\Delta\xi} m_P - \frac{1}{2}C_{1w}^m \frac{\Delta\eta\Delta\sigma}{\Delta\xi} m_P + \\
& \frac{1}{2}C_{1w}^m \frac{\Delta\eta\Delta\sigma}{\Delta\xi} m_W + \frac{1}{2}C_{2e}^m \frac{\Delta\eta\Delta\sigma}{\Delta\xi} \frac{\beta_e}{\gamma_e} m_E - \frac{1}{2}C_{2e}^m \frac{\Delta\eta\Delta\sigma}{\Delta\xi} \frac{\beta_e}{\gamma_e} m_P - \\
& \frac{1}{2}C_{2w}^m \frac{\Delta\eta\Delta\sigma}{\Delta\xi} \frac{\beta_w}{\gamma_w} m_P + \frac{1}{2}C_{2w}^m \frac{\Delta\eta\Delta\sigma}{\Delta\xi} \frac{\beta_w}{\gamma_w} m_W + C_{3P}^m \Delta\sigma \frac{\beta_P}{\gamma_P} m_e - \\
& C_{3P}^m \Delta\sigma \frac{\beta_P}{\gamma_P} m_w - C_{3s}^m \frac{\Delta\xi\Delta\sigma}{\Delta\eta} m_P + C_{3s}^m \frac{\Delta\xi\Delta\sigma}{\Delta\eta} m_S + \\
& C_{4P}^m \Delta\sigma m_e - C_{4P}^m \Delta\sigma m_w - C_{4s}^m \Delta\sigma m_{se} + \\
& C_{4s}^m \Delta\sigma m_{sw} + \frac{1}{2}L[\hat{S}_P^m]\Delta V \tag{E.34}
\end{aligned}$$

$$\begin{aligned}
& \left\{ \frac{1}{2} \| -(\rho U)_{e,0} \| \Delta\eta\Delta\sigma + \frac{1}{2} \| (\rho U)_{w,0} \| \Delta\eta\Delta\sigma + \| (\rho V)_{s,0} \| \Delta\xi\Delta\sigma + \right. \\
& \left. \frac{1}{2}(\rho W)_{P,U} \Delta\xi\Delta\eta + \frac{1}{2}C_{1e}^m \frac{\Delta\eta\Delta\sigma}{\Delta\xi} + \frac{1}{2}C_{1w}^m \frac{\Delta\eta\Delta\sigma}{\Delta\xi} + \right. \\
& \left. \frac{1}{2}C_{2e}^m \frac{\Delta\eta\Delta\sigma}{\Delta\xi} \frac{\beta_e}{\gamma_e} + \frac{1}{2}C_{2w}^m \frac{\Delta\eta\Delta\sigma}{\Delta\xi} \frac{\beta_w}{\gamma_w} + C_{3s}^m \frac{\Delta\xi\Delta\sigma}{\Delta\eta} \right\} m_P = \\
& \left\{ \frac{1}{2} \| -(\rho U)_{e,0} \| \Delta\eta\Delta\sigma + \frac{1}{2}C_{2e}^m \frac{\Delta\eta\Delta\sigma}{\Delta\xi} \frac{\beta_e}{\gamma_e} + \frac{1}{2}C_{1e}^m \frac{\Delta\eta\Delta\sigma}{\Delta\xi} \right\} m_E + \\
& \left\{ \frac{1}{2} \| (\rho U)_{w,0} \| \Delta\eta\Delta\sigma + \frac{1}{2}C_{2w}^m \frac{\Delta\eta\Delta\sigma}{\Delta\xi} \frac{\beta_w}{\gamma_w} + \frac{1}{2}C_{1w}^m \frac{\Delta\eta\Delta\sigma}{\Delta\xi} \right\} m_W + \\
& \left\{ \| (\rho V)_{s,0} \| \Delta\xi\Delta\sigma + C_{3s}^m \frac{\Delta\xi\Delta\sigma}{\Delta\eta} \right\} m_S + \frac{1}{2}(\rho W)_{P,U} \Delta\xi\Delta\eta m_{P,U} + \\
& (C_{3P}^m \Delta\sigma \frac{\beta_P}{\gamma_P} + C_{4P}^m \Delta\sigma)(m_e - m_w) + C_{4s}^m \Delta\sigma(m_{sw} - m_{se}) + \frac{1}{2}L[\hat{S}_P^m]\Delta V \tag{E.35}
\end{aligned}$$

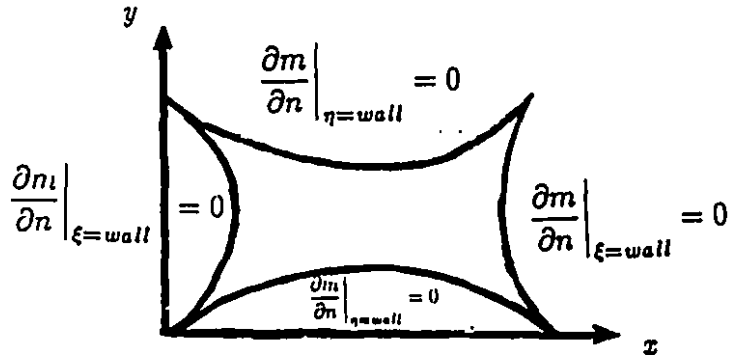


Fig. E.1 Boundary condition on the physical plane

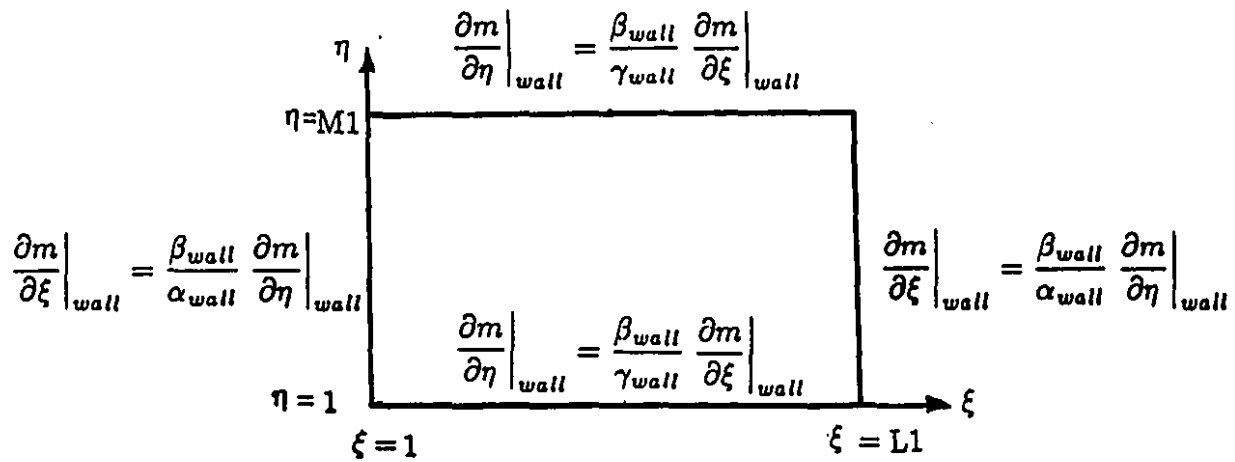
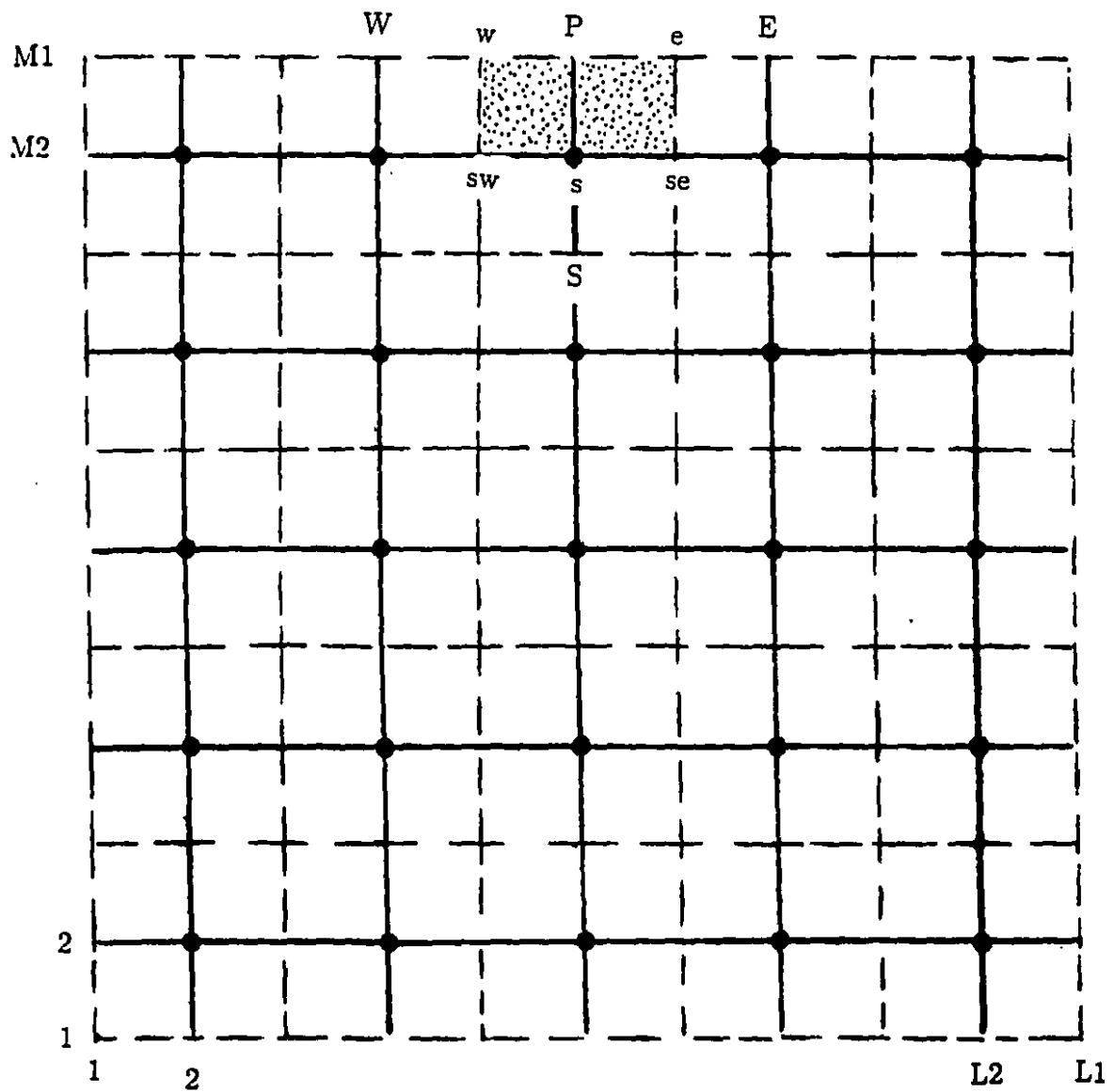


Fig. E.2 Boundary condition on the computational plane

Figure E.3 control-volume @ J = M1 boundary



APPENDIX F
DERIVATION OF RELATIONS OF PRESSURE-VELOCITY
COUPLING IN TRANSVERSE DIRECTION

F. 1 DERIVATION OF PRESSURE-CORRECTION EQUATIONS

Consider the continuity equation in transformed plane:

$$\frac{\partial(\rho U)}{\partial \xi} + \frac{\partial(\rho V)}{\partial \eta} + \frac{\partial(\rho W)}{\partial \sigma} = 0 \quad (F.1)$$

integrate this equation over an interior control-volume:

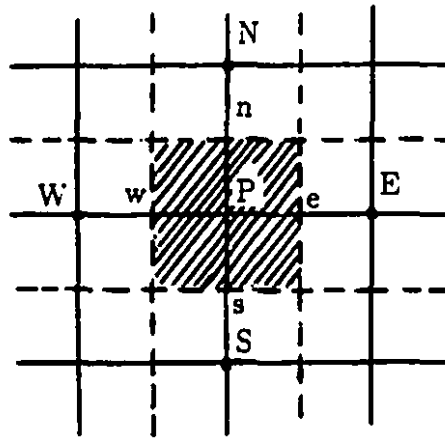


Fig. F1

$$\int_U^D \int_s^n \int_w^e \frac{\partial(\rho U)}{\partial \xi} d\xi d\eta d\sigma + \int_U^D \int_w^e \int_s^n \frac{\partial(\rho V)}{\partial \eta} d\eta d\xi d\sigma + \int_s^n \int_w^e \int_U^D \frac{\partial(\rho W)}{\partial \sigma} d\sigma d\xi d\eta = 0 \quad (F.2)$$

which is thereby discretized:

$$[(\rho U)_e - (\rho U)_w] \Delta \eta \Delta \sigma + [(\rho V)_n - (\rho V)_s] \Delta \xi \Delta \sigma + [(\rho W)_D - (\rho W)_U] \Delta \xi \Delta \eta = 0 \quad (F.3)$$

dividing by $\Delta V = \Delta\xi\Delta\eta\Delta\sigma$ one obtains:

$$\frac{(\rho U)_e - (\rho U)_w}{\Delta\xi} + \frac{(\rho V)_n - (\rho V)_s}{\Delta\eta} + \frac{(\rho W)_D - (\rho W)_U}{\Delta\sigma} = 0 \quad (F.4)$$

or alternatively:

$$\frac{\rho_e U_e - \rho_w U_w}{\Delta\xi} + \frac{\rho_n V_n - \rho_s V_s}{\Delta\eta} + \frac{\rho_D W_D - \rho_U W_U}{\Delta\sigma} = 0 \quad (F.5)$$

Now consider the contravariant velocities relations

$$\left. \begin{aligned} U &= uy_\eta - vx_\eta \\ V &= vx_\xi - uy_\xi \end{aligned} \right\} \quad (F.6)$$

for which the starred-velocities:

$$\left. \begin{aligned} U^* &= u^*y_\eta - v^*x_\eta \\ V^* &= v^*x_\xi - u^*y_\xi \end{aligned} \right\} \quad (F.7)$$

or by difference

$$\left. \begin{aligned} U - U^* &= (u - u^*)y_\eta - (v - v^*)x_\eta \\ V - V^* &= (v - v^*)x_\xi - (u - u^*)y_\xi \end{aligned} \right\} \quad (F.8)$$

or

$$\left. \begin{aligned} U &= U^* + (u - u^*)y_\eta - (v - v^*)x_\eta \\ V &= V^* + (v - v^*)x_\xi - (u - u^*)y_\xi \end{aligned} \right\} \quad (F.9)$$

but

$$\left. \begin{aligned} u - u^* &= u' \\ v - v^* &= v' \end{aligned} \right\} \quad (F.10)$$

Eqn. (F.10) is for the velocity corrections of u and v . Then

$$\left. \begin{aligned} U &= U^* + u'y_\eta - v'x_\eta \\ V &= V^* + v'x_\xi - u'y_\xi \end{aligned} \right\} \quad (F.11)$$

Eqn. (F.11) is the contravariant-velocities in terms of starred-quantities and velocity-corrections, from which

$$\left. \begin{aligned} U_e &= U_e^* + u'_e y_{\eta e} - v'_e x_{\eta e} \\ U_w &= U_w^* + u'_w y_{\eta w} - v'_w x_{\eta w} \end{aligned} \right\} \quad (F.12)$$

and

$$\left. \begin{aligned} V_n &= V_n^* + v'_n x_{\xi n} - u'_n y_{\xi n} \\ V_s &= V_s^* + v'_s x_{\xi s} - u'_s y_{\xi s} \end{aligned} \right\} \quad (F.13)$$

Substituting the latter discrete values of contravariant-velocities in Eqn. (F.5):

$$\begin{aligned} & (\rho_e U_e^* + \rho_e u'_e y_{\eta e} - \rho_e v'_e x_{\eta e} - \rho_w U_w^* - \rho_w u'_w y_{\eta w} + \rho_w v'_w x_{\eta w}) \frac{1}{\Delta \xi} + \\ & (\rho_n V_n^* + \rho_n v'_n x_{\xi n} - \rho_n u'_n y_{\xi n} - \rho_s V_s^* - \rho_s v'_s x_{\xi s} + \rho_s u'_s y_{\xi s}) \frac{1}{\Delta \eta} + \\ & (\rho_D W_D - \rho_U W_U) \frac{1}{\Delta \sigma} = 0 \end{aligned} \quad (F.14)$$

or alternatively

$$\begin{aligned} & \frac{\rho_e u'_e y_{\eta e}}{\Delta \xi} - \frac{\rho_e v'_e x_{\eta e}}{\Delta \xi} - \frac{\rho_w u'_w y_{\eta w}}{\Delta \xi} + \frac{\rho_w v'_w x_{\eta w}}{\Delta \xi} + \\ & \frac{\rho_n v'_n x_{\xi n}}{\Delta \eta} - \frac{\rho_n u'_n y_{\xi n}}{\Delta \eta} - \frac{\rho_s v'_s x_{\xi s}}{\Delta \eta} + \frac{\rho_s u'_s y_{\xi s}}{\Delta \eta} + \\ & \frac{\rho_e U_e^* - \rho_w U_w^*}{\Delta \xi} + \frac{\rho_n V_n^* - \rho_s V_s^*}{\Delta \eta} + \frac{\rho_D W_D - \rho_U W_U}{\Delta \sigma} = 0 \end{aligned} \quad (F.15)$$

let

$$\frac{\rho_e U_e^* - \rho_w U_w^*}{\Delta \xi} + \frac{\rho_n V_n^* - \rho_s V_s^*}{\Delta \eta} + \frac{\rho_D W_D - \rho_U W_U}{\Delta \sigma} = S \quad (F.16)$$

then

$$\begin{aligned} & \frac{\rho_e u'_e y_{\eta e}}{\Delta \xi} - \frac{\rho_e v'_e x_{\eta e}}{\Delta \xi} - \frac{\rho_w u'_w y_{\eta w}}{\Delta \xi} + \frac{\rho_w v'_w x_{\eta w}}{\Delta \xi} + \\ & \frac{\rho_n v'_n x_{\xi n}}{\Delta \eta} - \frac{\rho_n u'_n y_{\xi n}}{\Delta \eta} - \frac{\rho_s v'_s x_{\xi s}}{\Delta \eta} + \frac{\rho_s u'_s y_{\xi s}}{\Delta \eta} + S = 0 \end{aligned} \quad (F.17)$$

One should obtain the relations for the velocity-corrections (i. e., u'_e , v'_e , u'_w , v'_w , u'_n , v'_n , u'_s , v'_s) to substitute in Eqn. (F.17).

F. 1. 1 List of Discretization Equations for Transverse Velocity
Components ($u_e, v_e, u_n, v_n, u_w, v_w, u_s, v_s$)

$$AP_e^u u_e = \sum A_{(nb)_e}^u u_{(nb)_e} + B_e^u - \left\{ \frac{P_E - P_P}{\Delta \xi} y_{\eta e} - \frac{P_N + P_{NE} - P_S - P_{SE}}{4\Delta \eta} y_{\xi e} \right\} \Delta V \quad (F.18)$$

$$AP_e^v v_e = \sum A_{(nb)_e}^v v_{(nb)_e} + B_e^v - \left\{ \frac{P_N + P_{NE} - P_S - P_{SE}}{4\Delta \eta} x_{\xi e} - \frac{P_E - P_P}{\Delta \xi} x_{\eta e} \right\} \Delta V \quad (F.19)$$

$$AP_n^u u_n = \sum A_{(nb)_n}^u u_{(nb)_n} + B_n^u - \left\{ \frac{P_{NE} + P_E - P_W - P_{NW}}{4\Delta \xi} y_{\eta n} - \frac{P_N - P_P}{\Delta \eta} y_{\xi n} \right\} \Delta V \quad (F.20)$$

$$AP_n^v v_n = \sum A_{(nb)_n}^v v_{(nb)_n} + B_n^v - \left\{ \frac{P_N - P_P}{\Delta \eta} x_{\xi n} - \frac{P_{NE} + P_E - P_W - P_{NW}}{4\Delta \xi} x_{\eta n} \right\} \Delta V \quad (F.21)$$

$$AP_w^u u_w = \sum A_{(nb)_w}^u u_{(nb)_w} + B_w^u - \left\{ \frac{P_P - P_W}{\Delta \xi} y_{\eta w} - \frac{P_N + P_{NW} - P_S - P_{SW}}{4\Delta \eta} y_{\xi w} \right\} \Delta V \quad (F.22)$$

$$AP_w^v v_w = \sum A_{(nb)_w}^v v_{(nb)_w} + B_w^v - \left\{ \frac{P_N + P_{NW} - P_S - P_{SW}}{4\Delta \eta} x_{\xi w} - \frac{P_P - P_W}{\Delta \xi} x_{\eta w} \right\} \Delta V \quad (F.23)$$

$$AP_s^u u_s = \sum A_{(nb)_s}^u u_{(nb)_s} + B_s^u - \left\{ \frac{P_E + P_{SE} - P_W - P_{SW}}{4\Delta \xi} y_{\eta s} - \frac{P_P - P_S}{\Delta \eta} y_{\xi s} \right\} \Delta V \quad (F.24)$$

$$AP_s^v v_s = \sum A_{(nb)_s}^v v_{(nb)_s} + B_s^v - \left\{ \frac{P_P - P_S}{\Delta \eta} x_{\xi s} - \frac{P_E + P_{SE} - P_W - P_{SW}}{4\Delta \xi} x_{\eta s} \right\} \Delta V \quad (F.25)$$

F. 1. 2 Derivation of Relations for Velocity-Corrections

Velocity-Correction u'_e

$$AP_e^u u_e = \sum A_{(nb)_e}^u u_{(nb)_e} + B_e^u - \left\{ \frac{P_E - P_P}{\Delta \xi} y_{\eta e} - \frac{P_N + P_{NE} - P_S - P_{SE}}{4\Delta \eta} y_{\xi e} \right\} \Delta V \quad (F.26)$$

$$AP_e^u u_e^* = \sum A_{(nb)_e}^u u_{(nb)_e}^* + B_e^u - \left\{ \frac{P_E^* - P_P^*}{\Delta \xi} y_{\eta e} - \frac{P_N^* + P_{NE}^* - P_S^* - P_{SE}^*}{4\Delta \eta} y_{\xi e} \right\} \Delta V \quad (F.27)$$

Subtract: Eqn. (F.26) - Eqn (F.27)

$$AP_e^u [u_e - u_e^*] = \sum A_{(nb)_e}^u u_{(nb)_e} - \sum A_{(nb)_e}^u u_{(nb)_e}^* - \left\{ \frac{(P_E - P_E^*) - (P_P - P_P^*)}{\Delta \xi} y_{\eta e} - \frac{(P_N - P_N^*) + (P_{NE} - P_{NE}^*) - (P_S - P_S^*) - (P_{SE} - P_{SE}^*)}{4\Delta \eta} y_{\xi e} \right\} \Delta V \quad (F.28)$$

let

$$\sum A_{(nb)_e}^u u_{(nb)_e} - \sum A_{(nb)_e}^u u_{(nb)_e}^* \approx 0 \quad (F.29)$$

then

$$AP_e^u u'_e = -\Delta V \left\{ \frac{P'_E - P'_P}{\Delta \xi} y_{\eta e} - \frac{P'_N + P'_{NE} - P'_S - P'_{SE}}{4\Delta \eta} y_{\xi e} \right\} \quad (F.30)$$

$$u'_e = -\frac{\Delta V}{AP_e^u} \left\{ \frac{P'_E - P'_P}{\Delta \xi} y_{\eta e} - \frac{P'_N + P'_{NE} - P'_S - P'_{SE}}{4\Delta \eta} y_{\xi e} \right\} \quad (F.31)$$

Velocity-Correction v'_e

$$AP_e^v v_e = \sum A_{(nb)_e}^v v_{(nb)_e} + B_e^v - \left\{ \frac{P_N + P_{NE} - P_S - P_{SE}}{4\Delta\eta} x_{\xi e} - \frac{P_E - P_P}{\Delta\xi} x_{\eta e} \right\} \Delta V \quad (F.32)$$

$$AP_e^v v_e^* = \sum A_{(nb)_e}^v v_{(nb)_e}^* + B_e^v - \left\{ \frac{P_N^* + P_{NE}^* - P_S^* - P_{SE}^*}{4\Delta\eta} x_{\xi e} - \frac{P_E^* - P_P^*}{\Delta\xi} x_{\eta e} \right\} \Delta V \quad (F.33)$$

Subtract: Eqn. (F.32) - Eqn (F.33)

$$AP_e^v [v_e - v_e^*] = \sum A_{(nb)_e}^v v_{(nb)_e} - \sum A_{(nb)_e}^v v_{(nb)_e}^* - \left\{ \frac{(P_N - P_N^*) + (P_{NE} - P_{NE}^*) - (P_S - P_S^*) - (P_{SE} - P_{SE}^*)}{4\Delta\eta} x_{\xi e} - \frac{(P_E - P_E^*) - (P_P - P_P^*)}{\Delta\xi} x_{\eta e} \right\} \Delta V \quad (F.34)$$

let

$$\sum A_{(nb)_e}^v v_{(nb)_e} - \sum A_{(nb)_e}^v v_{(nb)_e}^* \approx 0 \quad (F.35)$$

then

$$AP_e^v v'_e = -\Delta V \left\{ \frac{P'_N + P'_{NE} - P'_S - P'_{SE}}{4\Delta\eta} x_{\xi e} - \frac{P'_E - P'_P}{\Delta\xi} x_{\eta e} \right\} \quad (F.36)$$

$$v'_e = -\frac{\Delta V}{AP_e^v} \left\{ \frac{P'_N + P'_{NE} - P'_S - P'_{SE}}{4\Delta\eta} x_{\xi e} - \frac{P'_E - P'_P}{\Delta\xi} x_{\eta e} \right\} \quad (F.37)$$

Velocity-Correction u'_w

$$AP_w^u u_w = \sum A_{(nb)_w}^u u_{(nb)_w} + B_w^u - \left\{ \frac{P_P - P_W}{\Delta\xi} y_{\eta w} - \frac{P_N + P_{NW} - P_S - P_{SW}}{4\Delta\eta} y_{\xi w} \right\} \Delta V \quad (F.38)$$

$$AP_w^u u_w^* = \sum A_{(nb)_w}^u u_{(nb)_w}^* + B_w^u - \left\{ \frac{P_P^* - P_W^*}{\Delta\xi} y_{\eta w} - \frac{P_N^* + P_{NW}^* - P_S^* - P_{SW}^*}{4\Delta\eta} y_{\xi w} \right\} \Delta V \quad (F.39)$$

Subtract: Eqn. (F.38) - Eqn (F.39)

$$AP_w^u [u_w - u_w^*] = \sum A_{(nb)_w}^u u_{(nb)_w} - \sum A_{(nb)_w}^u u_{(nb)_w}^* - \left\{ \frac{(P_P - P_P^*) - (P_W - P_W^*)}{\Delta\xi} y_{\eta w} - \frac{(P_N - P_N^*) + (P_{NW} - P_{NW}^*) - (P_S - P_S^*) - (P_{SW} - P_{SW}^*)}{4\Delta\eta} y_{\xi w} \right\} \Delta V \quad (F.40)$$

let

$$\sum A_{(nb)_w}^u u_{(nb)_w} - \sum A_{(nb)_w}^u u_{(nb)_w}^* \approx 0 \quad (F.41)$$

then

$$AP_w^u u'_w = -\Delta V \left\{ \frac{P'_P - P'_W}{\Delta\xi} y_{\eta w} - \frac{P'_N + P'_{NW} - P'_S - P'_{SW}}{4\Delta\eta} y_{\xi w} \right\} \quad (F.42)$$

$$u'_w = -\frac{\Delta V}{AP_w^u} \left\{ \frac{P'_P - P'_W}{\Delta\xi} y_{\eta w} - \frac{P'_N + P'_{NW} - P'_S - P'_{SW}}{4\Delta\eta} y_{\xi w} \right\} \quad (F.43)$$

Velocity-Correction v'_w

$$AP_w^v v_w = \sum A_{(nb)_w}^v v_{(nb)_w} + B_w^v - \left\{ \frac{P_N + P_{NW} - P_S - P_{SW}}{4\Delta\eta} x_{\xi w} - \frac{P_P - P_W}{\Delta\xi} x_{\eta w} \right\} \Delta V \quad (F.44)$$

$$AP_w^v v_w^* = \sum A_{(nb)_w}^v v_{(nb)_w}^* + B_w^v - \left\{ \frac{P_N^* + P_{NW}^* - P_S^* - P_{SW}^*}{4\Delta\eta} x_{\xi w} - \frac{P_P^* - P_W^*}{\Delta\xi} x_{\eta w} \right\} \Delta V \quad (F.45)$$

Subtract: Eqn. (F.44) – Eqn (F.45)

$$AP_w^v [v_w - v_w^*] = \sum A_{(nb)_w}^v v_{(nb)_w} - \sum A_{(nb)_w}^v v_{(nb)_w}^* - \left\{ \frac{(P_N - P_N^*) + (P_{NW} - P_{NW}^*) - (P_S - P_S^*) - (P_{SW} - P_{SW}^*)}{4\Delta\eta} x_{\xi w} - \frac{(P_P - P_P^*) - (P_W - P_W^*)}{\Delta\xi} x_{\eta w} \right\} \Delta V \quad (F.46)$$

let

$$\sum A_{(nb)_w}^v v_{(nb)_w} - \sum A_{(nb)_w}^v v_{(nb)_w}^* \approx 0 \quad (F.46a)$$

then

$$AP_w^v v'_w = -\Delta V \left\{ \frac{P'_N + P'_{NW} - P'_S - P'_{SW}}{4\Delta\eta} x_{\xi w} - \frac{P'_P - P'_W}{\Delta\xi} x_{\eta w} \right\} \quad (F.47)$$

$$v'_w = -\frac{\Delta V}{AP_w^v} \left\{ \frac{P'_N + P'_{NW} - P'_S - P'_{SW}}{4\Delta\eta} x_{\xi w} - \frac{P'_P - P'_W}{\Delta\xi} x_{\eta w} \right\} \quad (F.48)$$

Velocity-Correction u'_n

$$AP_n^u u_n = \sum A_{(nb)_n}^u u_{(nb)_n} + B_n^u - \left\{ \frac{P_E + P_{NE} - P_W - P_{NW}}{4\Delta\xi} y_{\eta n} - \frac{P_N - P_P}{\Delta\eta} y_{\xi n} \right\} \Delta V \quad (F.49)$$

$$AP_n^u u_n^* = \sum A_{(nb)_n}^u u_{(nb)_n}^* + B_n^u - \left\{ \frac{P_E^* + P_{NE}^* - P_W^* - P_{NW}^*}{4\Delta\xi} y_{\eta n} - \frac{P_N^* - P_P^*}{\Delta\eta} y_{\xi n} \right\} \Delta V \quad (F.50)$$

Subtract: Eqn. (F.49) - Eqn (F.50)

$$AP_n^u [u_n - u_n^*] = \sum A_{(nb)_n}^u u_{(nb)_n} - \sum A_{(nb)_n}^u u_{(nb)_n}^* - \left\{ \frac{(P_E - P_E^*) + (P_{NE} - P_{NE}^*) - (P_W - P_W^*) - (P_{NW} - P_{NW}^*)}{4\Delta\xi} y_{\eta n} - \frac{(P_N - P_N^*) - (P_P - P_P^*)}{\Delta\eta} y_{\xi n} \right\} \Delta V \quad (F.51)$$

let

$$\sum A_{(nb)_n}^u u_{(nb)_n} - \sum A_{(nb)_n}^u u_{(nb)_n}^* \approx 0 \quad (F.52)$$

then

$$AP_n^u u'_n = -\Delta V \left\{ \frac{P'_E + P'_{NE} - P'_W - P'_{NW}}{4\Delta\xi} y_{\eta n} - \frac{P'_N - P'_P}{\Delta\eta} y_{\xi n} \right\} \quad (F.53)$$

$$u'_n = -\frac{\Delta V}{AP_n^u} \left\{ \frac{P'_E + P'_{NE} - P'_W - P'_{NW}}{4\Delta\xi} y_{\eta n} - \frac{P'_N - P'_P}{\Delta\eta} y_{\xi n} \right\} \quad (F.54)$$

Velocity-Correction v'_n

$$AP_n^v v_n = \sum A_{(nb)_n}^v v_{(nb)_n} + B_n^v - \left\{ \frac{P_N - P_P}{\Delta\eta} x_{\xi n} - \frac{P_E + P_{NE} - P_W - P_{NW}}{4\Delta\xi} x_{\eta n} \right\} \Delta V \quad (F.55)$$

$$AP_n^v v_n^* = \sum A_{(nb)_n}^v v_{(nb)_n}^* + B_n^v - \left\{ \frac{P_N^* - P_P^*}{\Delta\eta} x_{\xi n} - \frac{P_E^* + P_{NE}^* - P_W^* - P_{NW}^*}{4\Delta\xi} x_{\eta n} \right\} \Delta V \quad (F.56)$$

Subtract: Eqn. (F.55) - Eqn (F.56)

$$AP_n^v [v_n - v_n^*] = \sum A_{(nb)_n}^v v_{(nb)_n} - \sum A_{(nb)_n}^v v_{(nb)_n}^* - \left\{ \frac{(P_N - P_N^*) - (P_P - P_P^*)}{\Delta\eta} x_{\xi n} - \frac{(P_E - P_E^*) + (P_{NE} - P_{NE}^*) - (P_W - P_W^*) - (P_{NW} - P_{NW}^*)}{4\Delta\xi} x_{\eta n} \right\} \Delta V \quad (F.57)$$

let

$$\sum A_{(nb)_n}^v v_{(nb)_n} - \sum A_{(nb)_n}^v v_{(nb)_n}^* \approx 0 \quad (F.58)$$

then

$$AP_n^v v'_n = -\Delta V \left\{ \frac{P'_N - P'_P}{\Delta\eta} x_{\xi n} - \frac{P'_E + P'_{NE} - P'_W - P'_{NW}}{4\Delta\xi} x_{\eta n} \right\} \quad (F.59)$$

$$v'_n = -\frac{\Delta V}{AP_n^v} \left\{ \frac{P'_N - P'_P}{\Delta\eta} x_{\xi n} - \frac{P'_E + P'_{NE} - P'_W - P'_{NW}}{4\Delta\xi} x_{\eta n} \right\} \quad (F.60)$$

Velocity-Correction u'_s

$$AP_s^u u_s = \sum A_{(nb),s}^u u_{(nb),s} + B_s^u - \left\{ \frac{P_E + P_{SE} - P_W - P_{SW}}{4\Delta\xi} y_{\eta s} - \frac{P_P - P_S}{\Delta\eta} y_{\xi s} \right\} \Delta V \quad (F.61)$$

$$AP_s^u u_s^* = \sum A_{(nb),s}^u u_{(nb),s}^* + B_s^u - \left\{ \frac{P_E^* + P_{SE}^* - P_W^* - P_{SW}^*}{4\Delta\xi} y_{\eta s} - \frac{P_P^* - P_S^*}{\Delta\eta} y_{\xi s} \right\} \Delta V \quad (F.62)$$

Subtract: Eqn. (F.61) - Eqn (F.62)

$$AP_s^u [u_s - u_s^*] = \sum A_{(nb),s}^u u_{(nb),s} - \sum A_{(nb),s}^u u_{(nb),s}^* - \left\{ \frac{(P_E - P_E^*) + (P_{SE} - P_{SE}^*) - (P_W - P_W^*) - (P_{SW} - P_{SW}^*)}{4\Delta\xi} y_{\eta s} - \frac{(P_P - P_P^*) - (P_S - P_S^*)}{\Delta\eta} y_{\xi s} \right\} \Delta V \quad (F.63)$$

let

$$\sum A_{(nb),s}^u u_{(nb),s} - \sum A_{(nb),s}^u u_{(nb),s}^* \approx 0 \quad (F.64)$$

then

$$AP_s^u u'_s = -\Delta V \left\{ \frac{P'_E + P'_{SE} - P'_W - P'_{SW}}{4\Delta\xi} y_{\eta s} - \frac{P'_P - P'_S}{\Delta\eta} y_{\xi s} \right\} \quad (F.65)$$

$$u'_s = -\frac{\Delta V}{AP_s^u} \left\{ \frac{P'_E + P'_{SE} - P'_W - P'_{SW}}{4\Delta\xi} y_{\eta s} - \frac{P'_P - P'_S}{\Delta\eta} y_{\xi s} \right\} \quad (F.66)$$

Velocity-Correction v'_s

$$AP_s^v v_s = \sum A_{(nb),s}^v v_{(nb),s} + B_s^v - \left\{ \frac{P_P - P_S}{\Delta\eta} x_{\xi s} - \frac{P_E + P_{SE} - P_W - P_{SW}}{4\Delta\xi} x_{\eta s} \right\} \Delta V \quad (F.67)$$

$$AP_s^v v_s^* = \sum A_{(nb),s}^v v_{(nb),s}^* + B_s^v - \left\{ \frac{P_P^* - P_S^*}{\Delta\eta} x_{\xi s} - \frac{P_E^* + P_{SE}^* - P_W^* - P_{SW}^*}{4\Delta\xi} x_{\eta s} \right\} \Delta V \quad (F.68)$$

Subtract: Eqn. (F.67) - Eqn (F.68)

$$AP_s^v [v_s - v_s^*] = \sum A_{(nb),s}^v v_{(nb),s} - \sum A_{(nb),s}^v v_{(nb),s}^* - \left\{ \frac{(P_P - P_P^*) - (P_S - P_S^*)}{\Delta\eta} x_{\xi s} - \frac{(P_E - P_E^*) + (P_{SE} - P_{SE}^*) - (P_W - P_W^*) - (P_{SW} - P_{SW}^*)}{4\Delta\xi} x_{\eta s} \right\} \Delta V \quad (F.69)$$

let

$$\sum A_{(nb),s}^v v_{(nb),s} - \sum A_{(nb),s}^v v_{(nb),s}^* \approx 0 \quad (F.70)$$

then

$$AP_s^v v'_s = -\Delta V \left\{ \frac{P_P - P_S}{\Delta\eta} x_{\xi s} - \frac{P_E + P_{SE} - P_W - P_{SW}}{4\Delta\xi} x_{\eta s} \right\} \quad (F.71)$$

$$v'_s = -\frac{\Delta V}{AP_s^v} \left\{ \frac{P_P - P_S}{\Delta\eta} x_{\xi s} - \frac{P_E + P_{SE} - P_W - P_{SW}}{4\Delta\xi} x_{\eta s} \right\} \quad (F.72)$$

F. 1. 3 Summary of Relations for Velocity Corrections

$$u'_e = -\frac{\Delta V}{AP_e^u} \left\{ \frac{P'_E - P'_P}{\Delta \xi} y_{\eta e} - \frac{P'_N + P'_{NE} - P'_S - P'_{SE}}{4\Delta \eta} y_{\xi e} \right\} \quad (F.73)$$

$$v'_e = -\frac{\Delta V}{AP_e^v} \left\{ \frac{P'_N + P'_{NE} - P'_S - P'_{SE}}{4\Delta \eta} x_{\xi e} - \frac{P'_E - P'_P}{\Delta \xi} x_{\eta e} \right\} \quad (F.74)$$

$$u'_w = -\frac{\Delta V}{AP_w^u} \left\{ \frac{P'_P - P'_W}{\Delta \xi} y_{\eta w} - \frac{P'_N + P'_{NW} - P'_S - P'_{SW}}{4\Delta \eta} y_{\xi w} \right\} \quad (F.75)$$

$$v'_w = -\frac{\Delta V}{AP_w^v} \left\{ \frac{P'_N + P'_{NW} - P'_S - P'_{SW}}{4\Delta \eta} x_{\xi w} - \frac{P'_P - P'_W}{\Delta \xi} x_{\eta w} \right\} \quad (F.76)$$

$$v'_n = -\frac{\Delta V}{AP_n^v} \left\{ \frac{P'_N - P'_P}{\Delta \eta} x_{\xi n} - \frac{P'_E + P'_{NE} - P'_W - P'_{NW}}{4\Delta \xi} x_{\eta n} \right\} \quad (F.77)$$

$$u'_n = -\frac{\Delta V}{AP_n^u} \left\{ \frac{P'_E + P'_{NE} - P'_W - P'_{NW}}{4\Delta \xi} y_{\eta n} - \frac{P'_N - P'_P}{\Delta \eta} y_{\xi n} \right\} \quad (F.78)$$

$$v'_s = -\frac{\Delta V}{AP_s^v} \left\{ \frac{P'_P - P'_S}{\Delta \eta} x_{\xi s} - \frac{P'_E + P'_{SE} - P'_W - P'_{SW}}{4\Delta \xi} x_{\eta s} \right\} \quad (F.79)$$

$$u'_s = -\frac{\Delta V}{AP_s^u} \left\{ \frac{P'_E + P'_{SE} - P'_W - P'_{SW}}{4\Delta \xi} y_{\eta s} - \frac{P'_P - P'_S}{\Delta \eta} y_{\xi s} \right\} \quad (F.80)$$

F. 1. 4 Substitution of Velocity-Corrections in Eqn. (F.17)

$$\begin{aligned} & -\frac{\rho_e \Delta \xi \Delta \eta \Delta \sigma y_{\eta e}}{AP_e^u \Delta \xi} \left\{ \frac{P'_E - P'_P}{\Delta \xi} y_{\eta e} - \frac{P'_N + P'_{NE} - P'_S - P'_{SE}}{4\Delta \eta} y_{\eta e} \right\} + \\ & \frac{\rho_e \Delta \xi \Delta \eta \Delta \sigma x_{\eta e}}{AP_e^v \Delta \xi} \left\{ \frac{P'_N + P'_{NE} - P'_S - P'_{SE}}{4\Delta \eta} x_{\xi e} - \frac{P'_E - P'_P}{\Delta \xi} x_{\eta e} \right\} + \\ & \frac{\rho_w \Delta \xi \Delta \eta \Delta \sigma y_{\eta w}}{AP_w^u \Delta \xi} \left\{ \frac{P'_P - P'_W}{\Delta \xi} y_{\eta w} - \frac{P'_N + P'_{NW} - P'_S - P'_{SW}}{4\Delta \eta} y_{\xi w} \right\} - \\ & \frac{\rho_w \Delta \xi \Delta \eta \Delta \sigma x_{\eta w}}{AP_w^v \Delta \xi} \left\{ \frac{P'_N + P'_{NW} - P'_S - P'_{SW}}{4\Delta \eta} x_{\xi w} - \frac{P'_P - P'_W}{\Delta \xi} x_{\eta w} \right\} - \\ & \frac{\rho_n \Delta \xi \Delta \eta \Delta \sigma x_{\xi n}}{AP_n^v \Delta \eta} \left\{ \frac{P'_N - P'_P}{\Delta \eta} x_{\xi n} - \frac{P'_E + P'_{NE} - P'_W - P'_{NW}}{4\Delta \xi} x_{\eta n} \right\} + \\ & \frac{\rho_n \Delta \xi \Delta \eta \Delta \sigma y_{\xi n}}{AP_n^u \Delta \eta} \left\{ \frac{P'_E + P'_{NE} - P'_W - P'_{NW}}{4\Delta \xi} y_{\eta n} - \frac{P'_N - P'_P}{\Delta \eta} y_{\xi n} \right\} + \\ & \frac{\rho_s \Delta \xi \Delta \eta \Delta \sigma x_{\xi s}}{AP_s^v \Delta \eta} \left\{ \frac{P'_P - P'_S}{\Delta \eta} x_{\xi s} - \frac{P'_E + P'_{SE} - P'_W - P'_{SW}}{4\Delta \xi} x_{\eta s} \right\} - \\ & \frac{\rho_s \Delta \xi \Delta \eta \Delta \sigma y_{\xi s}}{AP_s^u \Delta \eta} \left\{ \frac{P'_E + P'_{SE} - P'_W - P'_{SW}}{4\Delta \xi} y_{\eta s} - \frac{P'_P - P'_S}{\Delta \eta} y_{\xi s} \right\} + S = 0 \quad (F.81) \end{aligned}$$

which can be simplified:

$$\begin{aligned}
& -\frac{\rho_e \Delta \eta \Delta \sigma y_{\eta e}^2}{AP_e^u \Delta \xi} [P'_E - P'_P] + \frac{\rho_e \Delta \sigma y_{\eta e} y_{\xi e}}{4AP_e^u} [P'_N + P'_{NE} - P'_S - P'_{SE}] + \\
& \frac{\rho_e \Delta \sigma x_{\eta e} x_{\xi e}}{4AP_e^v} [P'_N + P'_{NE} - P'_S - P'_{SE}] - \frac{\rho_e \Delta \eta \Delta \sigma x_{\eta e}^2}{AP_e^v \Delta \xi} [P'_E - P'_P] + \\
& \frac{\rho_w \Delta \eta \Delta \sigma y_{\eta w}^2}{AP_w^u \Delta \xi} [P'_P - P'_W] - \frac{\rho_w \Delta \sigma y_{\eta w} y_{\xi w}}{4AP_w^u} [P'_N + P'_{NW} - P'_S - P'_{SW}] - \\
& \frac{\rho_w \Delta \sigma x_{\eta w} x_{\xi w}}{4AP_w^v} [P'_N + P'_{NW} - P'_S - P'_{SW}] + \frac{\rho_w \Delta \eta \Delta \sigma x_{\eta w}^2}{AP_w^v \Delta \xi} [P'_P - P'_W] - \\
& \frac{\rho_n \Delta \xi \Delta \sigma x_{\xi n}^2}{AP_n^v \Delta \eta} [P'_N - P'_P] + \frac{\rho_n \Delta \sigma x_{\eta n} x_{\xi n}}{4AP_n^v} [P'_E + P'_{NE} - P'_W - P'_{NW}] + \\
& \frac{\rho_n \Delta \sigma y_{\eta n} y_{\xi n}}{4AP_n^u} [P'_E + P'_{NE} - P'_W - P'_{NW}] - \frac{\rho_n \Delta \xi \Delta \sigma y_{\xi n}^2}{AP_n^u \Delta \eta} [P'_N - P'_P] + \\
& \frac{\rho_s \Delta \xi \Delta \sigma x_{\xi s}^2}{AP_s^v \Delta \eta} [P'_P - P'_S] - \frac{\rho_s \Delta \sigma x_{\eta s} x_{\xi s}}{4AP_s^v} [P'_E + P'_{SE} - P'_W - P'_{SW}] - \\
& \frac{\rho_s \Delta \sigma y_{\eta s} y_{\xi s}}{4AP_s^u} [P'_E + P'_{SE} - P'_W - P'_{SW}] + \frac{\rho_s \Delta \xi \Delta \sigma y_{\xi s}^2}{AP_s^u \Delta \eta} [P'_P - P'_S] + S = 0 \quad (F.82)
\end{aligned}$$

and more simplification:

$$\begin{aligned}
& P'_P \left[\frac{\rho_e \Delta \eta \Delta \sigma y_{\eta e}^2}{AP_e^u \Delta \xi} + \frac{\rho_e \Delta \eta \Delta \sigma x_{\eta e}^2}{AP_e^v \Delta \xi} + \frac{\rho_w \Delta \eta \Delta \sigma y_{\eta w}^2}{AP_w^u \Delta \xi} + \frac{\rho_w \Delta \eta \Delta \sigma x_{\eta w}^2}{AP_w^v \Delta \xi} + \right. \\
& \quad \left. \frac{\rho_n \Delta \xi \Delta \sigma x_{\xi n}^2}{AP_n^v \Delta \eta} + \frac{\rho_n \Delta \xi \Delta \sigma y_{\xi n}^2}{AP_n^u \Delta \eta} + \frac{\rho_s \Delta \xi \Delta \sigma x_{\xi s}^2}{AP_s^v \Delta \eta} + \frac{\rho_s \Delta \xi \Delta \sigma y_{\xi s}^2}{AP_s^u \Delta \eta} \right] = \\
& P'_E \left[\frac{\rho_e \Delta \eta \Delta \sigma y_{\eta e}^2}{AP_e^u \Delta \xi} + \frac{\rho_e \Delta \eta \Delta \sigma x_{\eta e}^2}{AP_e^v \Delta \xi} - \frac{\rho_n \Delta \sigma x_{\eta n} x_{\xi n}}{4AP_n^v} - \frac{\rho_n \Delta \sigma y_{\eta n} y_{\xi n}}{4AP_n^u} + \right. \\
& \quad \left. \frac{\rho_s \Delta \sigma x_{\eta s} x_{\xi s}}{4AP_s^v} + \frac{\rho_s \Delta \sigma y_{\eta s} y_{\xi s}}{4AP_s^u} \right] + P'_N \left[-\frac{\rho_e \Delta \sigma y_{\eta e} y_{\xi e}}{4AP_e^u} - \frac{\rho_e \Delta \sigma x_{\eta e} x_{\xi e}}{4AP_e^v} + \right. \\
& \quad \left. \frac{\rho_w \Delta \sigma y_{\eta w} y_{\xi w}}{4AP_w^u} + \frac{\rho_w \Delta \sigma x_{\eta w} x_{\xi w}}{4AP_w^v} + \frac{\rho_n \Delta \xi \Delta \sigma x_{\xi n}^2}{AP_n^u \Delta \eta} + \frac{\rho_n \Delta \xi \Delta \sigma y_{\xi n}^2}{AP_n^v \Delta \eta} \right] + \\
& P'_S \left[\frac{\rho_e \Delta \sigma y_{\eta e} y_{\xi e}}{4AP_e^u} + \frac{\rho_e \Delta \sigma x_{\eta e} x_{\xi e}}{4AP_e^v} - \frac{\rho_w \Delta \sigma y_{\eta w} y_{\xi w}}{4AP_w^u} - \frac{\rho_w \Delta \sigma x_{\eta w} x_{\xi w}}{4AP_w^v} + \right. \\
& \quad \left. \frac{\rho_s \Delta \xi \Delta \sigma x_{\xi s}^2}{AP_s^v \Delta \eta} + \frac{\rho_s \Delta \xi \Delta \sigma y_{\xi s}^2}{AP_s^u \Delta \eta} \right] + P'_W \left[\frac{\rho_w \Delta \eta \Delta \sigma y_{\eta w}^2}{AP_w^u \Delta \xi} + \frac{\rho_w \Delta \eta \Delta \sigma x_{\eta w}^2}{AP_w^v \Delta \xi} + \right. \\
& \quad \left. \frac{\rho_n \Delta \sigma x_{\xi n} x_{\eta n}}{4AP_n^v} + \frac{\rho_n \Delta \sigma y_{\xi n} y_{\eta n}}{4AP_n^u} - \frac{\rho_s \Delta \sigma x_{\eta s} x_{\xi s}}{4AP_s^v} - \frac{\rho_s \Delta \sigma y_{\eta s} y_{\xi s}}{4AP_s^u} \right] + \\
& P'_{NE} \left[-\frac{\rho_e \Delta \sigma y_{\xi e} y_{\eta e}}{4AP_e^u} - \frac{\rho_e \Delta \sigma x_{\xi e} x_{\eta e}}{4AP_e^v} - \frac{\rho_n \Delta \sigma x_{\eta n} x_{\xi n}}{4AP_n^v} - \frac{\rho_n \Delta \sigma y_{\eta n} y_{\xi n}}{4AP_n^u} \right] + \\
& P'_{SE} \left[\frac{\rho_e \Delta \sigma y_{\xi e} y_{\eta e}}{4AP_e^u} + \frac{\rho_e \Delta \sigma x_{\xi e} x_{\eta e}}{4AP_e^v} + \frac{\rho_s \Delta \sigma x_{\eta s} x_{\xi s}}{4AP_s^v} + \frac{\rho_s \Delta \sigma y_{\eta s} y_{\xi s}}{4AP_s^u} \right] + \\
& P'_{NW} \left[\frac{\rho_w \Delta \sigma y_{\xi w} y_{\eta w}}{4AP_w^u} + \frac{\rho_w \Delta \sigma x_{\xi w} x_{\eta w}}{4AP_w^v} + \frac{\rho_n \Delta \sigma x_{\eta n} x_{\xi n}}{4AP_n^v} + \frac{\rho_n \Delta \sigma y_{\eta n} y_{\xi n}}{4AP_n^u} \right] + \\
& P'_{SW} \left[-\frac{\rho_w \Delta \sigma y_{\xi w} y_{\eta w}}{4AP_w^u} - \frac{\rho_w \Delta \sigma x_{\xi w} x_{\eta w}}{4AP_w^v} - \frac{\rho_s \Delta \sigma x_{\eta s} x_{\xi s}}{4AP_s^v} - \frac{\rho_s \Delta \sigma y_{\eta s} y_{\xi s}}{4AP_s^u} \right] + \\
& \quad \frac{\rho_w U_w^* - \rho_e U_e^*}{\Delta \xi} + \frac{\rho_s V_s^* - \rho_n V_n^*}{\Delta \eta} + \frac{\rho_U W_U - \rho_D W_D}{\Delta \sigma} \tag{F.83}
\end{aligned}$$

F. 1. 5 Final Results

$$A_P = \frac{\rho_e \Delta \eta \Delta \sigma y_{\eta e}^2}{AP_e^u \Delta \xi} + \frac{\rho_e \Delta \eta \Delta \sigma x_{\eta e}^2}{AP_e^v \Delta \xi} + \frac{\rho_w \Delta \eta \Delta \sigma y_{\eta w}^2}{AP_w^u \Delta \xi} + \frac{\rho_w \Delta \eta \Delta \sigma x_{\eta w}^2}{AP_w^v \Delta \xi} +$$

$$\frac{\rho_n \Delta \xi \Delta \sigma y_{\xi n}^2}{AP_n^u \Delta \eta} + \frac{\rho_n \Delta \xi \Delta \sigma x_{\xi n}^2}{AP_n^v \Delta \eta} + \frac{\rho_s \Delta \xi \Delta \sigma x_{\xi s}^2}{AP_s^v \Delta \eta} + \frac{\rho_s \Delta \xi \Delta \sigma y_{\xi s}^2}{AP_s^u \Delta \eta} \quad (F.84)$$

$$A_E = \frac{\rho_e \Delta \eta \Delta \sigma y_{\eta e}^2}{AP_e^u \Delta \xi} + \frac{\rho_e \Delta \eta \Delta \sigma x_{\eta e}^2}{AP_e^v \Delta \xi} - \frac{\rho_n \Delta \sigma x_{\xi n} x_{\eta n}}{4AP_n^v} - \frac{\rho_n \Delta \sigma y_{\xi n} y_{\eta n}}{4AP_n^u} +$$

$$\frac{\rho_s \Delta \sigma x_{\xi s} x_{\eta s}}{4AP_s^v} + \frac{\rho_s \Delta \sigma y_{\xi s} y_{\eta s}}{4AP_s^u} \quad (F.85)$$

$$A_N = -\frac{\rho_e \Delta \sigma y_{\xi e} y_{\eta e}}{4AP_e^u} - \frac{\rho_e \Delta \sigma x_{\xi e} x_{\eta e}}{4AP_e^v} + \frac{\rho_w \Delta \sigma y_{\xi w} y_{\eta w}}{4AP_w^u} + \frac{\rho_w \Delta \sigma x_{\xi w} x_{\eta w}}{4AP_w^v} +$$

$$\frac{\rho_n \Delta \xi \Delta \sigma x_{\xi n}^2}{AP_n^v \Delta \eta} + \frac{\rho_n \Delta \xi \Delta \sigma y_{\xi n}^2}{AP_n^u \Delta \eta} \quad (F.86)$$

$$A_S = \frac{\rho_e \Delta \sigma y_{\xi e} y_{\eta e}}{4AP_e^u} + \frac{\rho_e \Delta \sigma x_{\xi e} x_{\eta e}}{4AP_e^v} - \frac{\rho_w \Delta \sigma y_{\xi w} y_{\eta w}}{4AP_w^u} - \frac{\rho_w \Delta \sigma x_{\xi w} x_{\eta w}}{4AP_w^v} +$$

$$\frac{\rho_s \Delta \xi \Delta \sigma x_{\xi s}^2}{AP_s^v \Delta \eta} + \frac{\rho_s \Delta \xi \Delta \sigma y_{\xi s}^2}{AP_s^u \Delta \eta} \quad (F.87)$$

$$A_W = \frac{\rho_w \Delta \eta \Delta \sigma y_{\eta w}^2}{AP_w^u \Delta \xi} + \frac{\rho_w \Delta \eta \Delta \sigma x_{\eta w}^2}{AP_w^v \Delta \xi} + \frac{\rho_n \Delta \sigma x_{\xi n} x_{\eta n}}{4AP_n^v} + \frac{\rho_n \Delta \sigma y_{\xi n} y_{\eta n}}{4AP_n^u} -$$

$$\frac{\rho_s \Delta \sigma x_{\xi s} x_{\eta s}}{4AP_s^v} - \frac{\rho_s \Delta \sigma y_{\xi s} y_{\eta s}}{4AP_s^u} \quad (F.88)$$

$$A_{NE} = -\frac{\rho_e \Delta \sigma x_{\xi e} x_{\eta e}}{4AP_e^v} - \frac{\rho_e \Delta \sigma y_{\xi e} y_{\eta e}}{4AP_e^u} - \frac{\rho_n \Delta \sigma x_{\xi n} x_{\eta n}}{4AP_n^v} - \frac{\rho_n \Delta \sigma y_{\xi n} y_{\eta n}}{4AP_n^u} \quad (F.89)$$

$$A_{SE} = \frac{\rho_e \Delta \sigma x_{\xi e} x_{\eta e}}{4AP_e^v} + \frac{\rho_e \Delta \sigma y_{\xi e} y_{\eta e}}{4AP_e^u} + \frac{\rho_s \Delta \sigma x_{\xi s} x_{\eta s}}{4AP_s^v} + \frac{\rho_s \Delta \sigma y_{\xi s} y_{\eta s}}{4AP_s^u} \quad (F.90)$$

$$A_{NW} = \frac{\rho_w \Delta \sigma x_{\xi w} x_{\eta w}}{4AP_w^v} + \frac{\rho_w \Delta \sigma y_{\xi w} y_{\eta w}}{4AP_w^u} + \frac{\rho_n \Delta \sigma x_{\xi n} x_{\eta n}}{4AP_n^v} + \frac{\rho_n \Delta \sigma y_{\xi n} y_{\eta n}}{4AP_n^u} \quad (F.91)$$

$$A_{SW} = -\frac{\rho_w \Delta \sigma x_{\xi w} x_{\eta w}}{4AP_w^v} - \frac{\rho_w \Delta \sigma y_{\xi w} y_{\eta w}}{4AP_w^u} - \frac{\rho_s \Delta \sigma x_{\xi s} x_{\eta s}}{4AP_s^v} - \frac{\rho_s \Delta \sigma y_{\xi s} y_{\eta s}}{4AP_s^u} \quad (F.92)$$

$$A_P P'_P = A_E P'_E + A_N P'_N + A_W P'_W + A_S P'_S + A_{NE} P'_{NE} + A_{SE} P'_{SE} +$$

$$A_{NW} P'_{NW} + A_{SW} P'_{SW} + B \quad (F.93)$$

in which

$$B = \frac{\rho_w U_w^* - \rho_e U_e^*}{\Delta \xi} + \frac{\rho_s V_s^* - \rho_n V_n^*}{\Delta \eta} + \frac{\rho_U W_U - \rho_D W_D}{\Delta \sigma} \quad (F.94)$$

also

$$A_P = A_E + A_N + A_W + A_S \quad (F.95)$$

and

$$A_{NE} + A_{SE} + A_{NW} + A_{SW} = 0 \quad (F.96)$$

Notes

1. Taking " ρ " = constant in the above formulations (which can be consequently dropped from the coefficients and the "B" term) showed to be effective in the convergence of the problem.
2. The values of $\Delta\xi = \Delta\eta = 1$ for simplicity.

$$A_P = \frac{\Delta\sigma y_{\eta e}^2}{AP_e^u} + \frac{\Delta\sigma x_{\eta e}^2}{AP_e^v} + \frac{\Delta\sigma y_{\eta w}^2}{AP_w^u} + \frac{\Delta\sigma x_{\eta w}^2}{AP_w^v} + \frac{\Delta\sigma y_{\xi n}^2}{AP_n^u} + \frac{\Delta\sigma x_{\xi n}^2}{AP_n^v} + \frac{\Delta\sigma x_{\xi s}^2}{AP_s^v} + \frac{\Delta\sigma y_{\xi s}^2}{AP_s^u} \quad (F.97)$$

$$A_E = \frac{\Delta\sigma y_{\eta e}^2}{AP_e^u} + \frac{\Delta\sigma x_{\eta e}^2}{AP_e^v} - \frac{\Delta\sigma x_{\xi n} x_{\eta n}}{4AP_n^v} - \frac{\Delta\sigma y_{\xi n} y_{\eta n}}{4AP_n^u} + \frac{\Delta\sigma x_{\xi s} x_{\eta s}}{4AP_s^v} + \frac{\Delta\sigma y_{\xi s} y_{\eta s}}{4AP_s^u} \quad (F.98)$$

$$A_N = -\frac{\Delta\sigma y_{\xi e} y_{\eta e}}{4AP_e^u} - \frac{\Delta\sigma x_{\xi e} x_{\eta e}}{4AP_e^v} + \frac{\Delta\sigma y_{\xi w} y_{\eta w}}{4AP_w^u} + \frac{\Delta\sigma x_{\xi w} x_{\eta w}}{4AP_w^v} + \frac{\Delta\sigma x_{\xi n}^2}{AP_n^v} + \frac{\Delta\sigma y_{\xi n}^2}{AP_n^u} \quad (F.99)$$

$$A_S = \frac{\Delta\sigma y_{\xi e} y_{\eta e}}{4AP_e^u} + \frac{\Delta\sigma x_{\xi e} x_{\eta e}}{4AP_e^v} - \frac{\Delta\sigma y_{\xi w} y_{\eta w}}{4AP_w^u} - \frac{\Delta\sigma x_{\xi w} x_{\eta w}}{4AP_w^v} + \frac{\Delta\sigma x_{\xi s}^2}{AP_s^v} + \frac{\Delta\sigma y_{\xi s}^2}{AP_s^u} \quad (F.100)$$

$$A_W = \frac{\Delta\sigma y_{\eta w}^2}{AP_w^u} + \frac{\Delta\sigma x_{\eta w}^2}{AP_w^v} + \frac{\Delta\sigma x_{\xi n} x_{\eta n}}{4AP_n^v} + \frac{\Delta\sigma y_{\xi n} y_{\eta n}}{4AP_n^u} - \frac{\Delta\sigma x_{\xi s} x_{\eta s}}{4AP_s^v} - \frac{\Delta\sigma y_{\xi s} y_{\eta s}}{4AP_s^u} \quad (F.101)$$

$$A_{NE} = -\frac{\Delta\sigma x_{\xi e} x_{\eta e}}{4AP_e^v} - \frac{\Delta\sigma y_{\xi e} y_{\eta e}}{4AP_e^u} - \frac{\Delta\sigma x_{\xi n} x_{\eta n}}{4AP_n^v} - \frac{\Delta\sigma y_{\xi n} y_{\eta n}}{4AP_n^u} \quad (F.102)$$

$$A_{SE} = \frac{\Delta\sigma x_{\xi e} x_{\eta e}}{4AP_e^v} + \frac{\Delta\sigma y_{\xi e} y_{\eta e}}{4AP_e^u} + \frac{\Delta\sigma x_{\xi s} x_{\eta s}}{4AP_s^v} + \frac{\Delta\sigma y_{\xi s} y_{\eta s}}{4AP_s^u} \quad (F.103)$$

$$A_{NW} = \frac{\Delta\sigma x_{\xi w} x_{\eta w}}{4AP_w^v} + \frac{\Delta\sigma y_{\xi w} y_{\eta w}}{4AP_w^u} + \frac{\Delta\sigma x_{\xi n} x_{\eta n}}{4AP_n^v} + \frac{\Delta\sigma y_{\xi n} y_{\eta n}}{4AP_n^u} \quad (F.104)$$

$$A_{SW} = -\frac{\Delta\sigma x_{\xi w} x_{\eta w}}{4AP_w^v} - \frac{\Delta\sigma y_{\xi w} y_{\eta w}}{4AP_w^u} - \frac{\Delta\sigma x_{\xi s} x_{\eta s}}{4AP_s^v} - \frac{\Delta\sigma y_{\xi s} y_{\eta s}}{4AP_s^u} \quad (F.105)$$

$$A_P P'_P = A_E P'_E + A_N P'_N + A_W P'_W + A_S P'_S + A_{NE} P'_{NE} + A_{SE} P'_{SE} + A_{NW} P'_{NW} + A_{SW} P'_{SW} + B \quad (F.106)$$

in which

$$B = (U_w^* - U_e^*) + (V_s^* - V_n^*) + \frac{(W_U - W_D)}{\Delta\sigma} \quad (F.107)$$

also

$$A_P = A_E + A_N + A_W + A_S \quad (F.108)$$

and

$$A_{NE} + A_{SE} + A_{NW} + A_{SW} = 0 \quad (F.109)$$

F. 1. 6 Special case: Maliska et. al.⁴⁶

This case is valid for Newtonian fluids.

Assumptions:

1) Constant “ ρ ”

2) $\Delta\xi = \Delta\eta = 1$ (F.110)

3)

$$\left. \begin{aligned} AP_e^u &= AP_e^v = A_e \\ AP_w^u &= AP_w^v = A_w \\ AP_n^u &= AP_n^v = A_n \\ AP_s^u &= AP_s^v = A_s \end{aligned} \right\} \quad (F.111)$$

$$\begin{aligned} & P'_P \left[\frac{\Delta\sigma y_{\eta e}^2}{A_e} + \frac{\Delta\sigma x_{\eta e}^2}{A_e} + \frac{\Delta\sigma y_{\eta w}^2}{A_w} + \frac{\Delta\sigma x_{\eta w}^2}{A_w} + \frac{\Delta\sigma x_{\xi n}^2}{A_n} + \right. \\ & \quad \left. \frac{\Delta\sigma y_{\xi n}^2}{A_n} + \frac{\Delta\sigma x_{\xi s}^2}{A_s} + \frac{\Delta\sigma y_{\xi s}^2}{A_s} \right] = P'_E \left[\frac{\Delta\sigma y_{\eta e}^2}{A_e} + \frac{\Delta\sigma x_{\eta e}^2}{A_e} - \right. \\ & \quad \left. \frac{\Delta\sigma x_{\eta n} x_{\xi n}}{4A_n} - \frac{\Delta\sigma y_{\eta n} y_{\xi n}}{4A_n} + \frac{\Delta\sigma x_{\eta s} x_{\xi s}}{4A_s} + \frac{\Delta\sigma y_{\eta s} y_{\xi s}}{4A_s} \right] + P'_N \left[-\frac{\Delta\sigma y_{\eta e} y_{\xi e}}{4A_e} - \right. \\ & \quad \left. \frac{\Delta\sigma x_{\eta e} x_{\xi e}}{4A_e} + \frac{\Delta\sigma y_{\eta w} y_{\xi w}}{4A_w} + \frac{\Delta\sigma x_{\eta w} x_{\xi w}}{4A_w} + \frac{\Delta\sigma x_{\xi n}^2}{A_n} + \frac{\Delta\sigma y_{\xi n}^2}{A_n} \right] + \\ & P'_S \left[\frac{\Delta\sigma y_{\eta e} y_{\xi e}}{4A_e} + \frac{\Delta\sigma x_{\eta e} x_{\xi e}}{4A_e} - \frac{\Delta\sigma y_{\eta w} y_{\xi w}}{4A_w} - \frac{\Delta\sigma x_{\eta w} x_{\xi w}}{4A_w} + \frac{\Delta\sigma x_{\xi s}^2}{A_s} + \right. \\ & \quad \left. \frac{\Delta\sigma y_{\xi s}^2}{A_s} \right] + P'_W \left[\frac{\Delta\sigma x_{\xi n} x_{\eta n}}{4A_n} + \frac{\Delta\sigma y_{\xi n} y_{\eta n}}{4A_n} - \frac{\Delta\sigma y_{\eta s} y_{\xi s}}{4A_s} - \frac{\Delta\sigma x_{\eta s} x_{\xi s}}{4A_s} + \right. \\ & \quad \left. \frac{\Delta\sigma y_{\eta w}^2}{A_w} + \frac{\Delta\sigma x_{\eta w}^2}{A_w} \right] + P'_{NE} \left[-\frac{\Delta\sigma y_{\xi e} y_{\eta e}}{4A_e} - \frac{\Delta\sigma x_{\xi e} x_{\eta e}}{4A_e} - \frac{\Delta\sigma x_{\eta n} x_{\xi n}}{4A_n} - \right. \\ & \quad \left. \frac{\Delta\sigma y_{\eta n} y_{\xi n}}{4A_n} \right] + P'_{SE} \left[\frac{\Delta\sigma y_{\xi e} y_{\eta e}}{4A_e} + \frac{\Delta\sigma x_{\xi e} x_{\eta e}}{4A_e} + \frac{\Delta\sigma x_{\eta s} x_{\xi s}}{4A_s} + \frac{\Delta\sigma y_{\eta s} y_{\xi s}}{4A_s} \right] + \\ & P'_{NW} \left[\frac{\Delta\sigma y_{\xi w} y_{\eta w}}{4A_w} + \frac{\Delta\sigma x_{\xi w} x_{\eta w}}{4A_w} + \frac{\Delta\sigma x_{\eta n} x_{\xi n}}{4A_n} + \frac{\Delta\sigma y_{\eta n} y_{\xi n}}{4A_n} \right] + \\ & P'_{SE} \left[-\frac{\Delta\sigma y_{\xi w} y_{\eta w}}{4A_w} - \frac{\Delta\sigma x_{\xi w} x_{\eta w}}{4A_w} - \frac{\Delta\sigma x_{\eta s} x_{\xi s}}{4A_s} - \frac{\Delta\sigma y_{\eta s} y_{\xi s}}{4A_s} \right] + \\ & \quad (U_w^* - U_e^*) + (V_s^* - V_n^*) + \frac{(W_U - W_D)}{\Delta\sigma} \quad (F.112) \end{aligned}$$

Using

$$\begin{aligned}
& P'_P \left[\frac{\Delta\sigma(y_{\eta e}^2 + x_{\eta e}^2)}{A_e} + \frac{\Delta\sigma(y_{\eta w}^2 + x_{\eta w}^2)}{A_w} + \frac{\Delta\sigma(x_{\xi n}^2 + y_{\xi n}^2)}{A_n} + \frac{\Delta\sigma(x_{\xi s}^2 + y_{\xi s}^2)}{A_s} \right] = \\
& P'_E \left[\frac{\Delta\sigma(y_{\eta e}^2 + x_{\eta e}^2)}{A_e} - \frac{\Delta\sigma(x_{\eta n}x_{\xi n} + y_{\eta n}y_{\xi n})}{4A_n} + \frac{\Delta\sigma(x_{\eta s}x_{\xi s} + y_{\eta s}y_{\xi s})}{4A_s} \right] + \\
& P'_N \left[-\frac{\Delta\sigma(y_{\eta e}y_{\xi e} + x_{\eta e}x_{\xi e})}{4A_e} + \frac{\Delta\sigma(y_{\eta w}y_{\xi w} + x_{\eta w}x_{\xi w})}{4A_w} + \frac{\Delta\sigma(x_{\xi n}^2 + y_{\xi n}^2)}{A_n} \right] + \\
& P'_S \left[\frac{\Delta\sigma(y_{\eta e}y_{\xi e} + x_{\eta e}x_{\xi e})}{4A_e} - \frac{\Delta\sigma(y_{\eta w}y_{\xi w} + x_{\eta w}x_{\xi w})}{4A_w} + \frac{\Delta\sigma(x_{\xi s}^2 + y_{\xi s}^2)}{A_s} \right] + \\
& P'_W \left[\frac{\Delta\sigma(x_{\eta w}^2 + y_{\eta w}^2)}{A_w} + \frac{\Delta\sigma(x_{\xi n}x_{\eta n} + y_{\xi n}y_{\eta n})}{4A_n} - \frac{\Delta\sigma(x_{\eta s}x_{\xi s} + y_{\eta s}y_{\xi s})}{4A_s} \right] + \\
& P'_{NE} \left[-\frac{\Delta\sigma(x_{\xi e}x_{\eta e} + y_{\xi e}y_{\eta e})}{4A_e} - \frac{\Delta\sigma(x_{\eta n}x_{\xi n} + y_{\eta n}y_{\xi n})}{4A_n} \right] + \\
& P'_{SE} \left[\frac{\Delta\sigma(x_{\xi e}x_{\eta e} + y_{\xi e}y_{\eta e})}{4A_e} + \frac{\Delta\sigma(x_{\eta s}x_{\xi s} + y_{\eta s}y_{\xi s})}{4A_s} \right] + \\
& P'_{NW} \left[\frac{\Delta\sigma(x_{\xi w}x_{\eta w} + y_{\xi w}y_{\eta w})}{4A_w} + \frac{\Delta\sigma(x_{\eta n}x_{\xi n} + y_{\eta n}y_{\xi n})}{4A_n} \right] + \\
& P'_{SE} \left[-\frac{\Delta\sigma(x_{\xi w}x_{\eta w} + y_{\xi w}y_{\eta w})}{4A_w} - \frac{\Delta\sigma(x_{\eta s}x_{\xi s} + y_{\eta s}y_{\xi s})}{4A_s} \right] + \\
& (U_w^* - U_e^*) + (V_s^* - V_n^*) + \frac{(W_U - W_D)}{\Delta\sigma} \tag{F.113}
\end{aligned}$$

Using

$$x_{\eta}^2 + y_{\eta}^2 = \alpha \tag{F.114}$$

$$x_{\xi}x_{\eta} + y_{\xi}y_{\eta} = \beta \tag{F.115}$$

$$x_{\xi}^2 + y_{\xi}^2 = \gamma \tag{F.116}$$

$$\begin{aligned}
& \left[\frac{\Delta\sigma}{A_e} \alpha_e + \frac{\Delta\sigma}{A_w} \alpha_w + \frac{\Delta\sigma}{A_n} \gamma_n + \frac{\Delta\sigma}{A_s} \gamma_s \right] P'_P = \\
& \left[\frac{\Delta\sigma}{A_e} \alpha_e - \frac{\Delta\sigma}{4A_n} \beta_n + \frac{\Delta\sigma}{4A_s} \beta_s \right] P'_E + \left[-\frac{\Delta\sigma}{4A_e} \beta_e + \frac{\Delta\sigma}{4A_w} \beta_w + \frac{\Delta\sigma}{A_n} \gamma_n \right] P'_N + \\
& \left[\frac{\Delta\sigma}{4A_e} \beta_e - \frac{\Delta\sigma}{4A_w} \beta_w + \frac{\Delta\sigma}{A_s} \gamma_s \right] P'_S + \left[\frac{\Delta\sigma}{A_w} \alpha_w + \frac{\Delta\sigma}{4A_n} \beta_n - \frac{\Delta\sigma}{4A_s} \beta_s \right] P'_W + \\
& \left[-\frac{\Delta\sigma}{4A_e} \beta_e - \frac{\Delta\sigma}{4A_n} \beta_n \right] P'_{NE} + \left[\frac{\Delta\sigma}{4A_e} \beta_e + \frac{\Delta\sigma}{4A_s} \beta_s \right] P'_{SE} + \\
& \left[\frac{\Delta\sigma}{4A_w} \beta_w + \frac{\Delta\sigma}{4A_n} \beta_n \right] P'_{NW} + \left[-\frac{\Delta\sigma}{4A_w} \beta_w - \frac{\Delta\sigma}{4A_s} \beta_s \right] P'_{SW} + \\
& (U_w^* - U_e^*) + (V_s^* - V_n^*) + \frac{(W_U - W_D)}{\Delta\sigma}
\end{aligned} \tag{F.117}$$

F. 1. 7 Final Results of Special Case

$$A_P = \frac{\Delta\sigma}{A_e} \alpha_e + \frac{\Delta\sigma}{A_w} \alpha_w + \frac{\Delta\sigma}{A_n} \gamma_n + \frac{\Delta\sigma}{A_s} \gamma_s \tag{F.118}$$

$$A_E = \frac{\Delta\sigma}{A_e} \alpha_e - \frac{\Delta\sigma}{4A_n} \beta_n + \frac{\Delta\sigma}{4A_s} \beta_s \tag{F.119}$$

$$A_N = -\frac{\Delta\sigma}{4A_e} \beta_e + \frac{\Delta\sigma}{4A_w} \beta_w + \frac{\Delta\sigma}{A_n} \gamma_n \tag{F.120}$$

$$A_S = \frac{\Delta\sigma}{4A_e} \beta_e - \frac{\Delta\sigma}{4A_w} \beta_w + \frac{\Delta\sigma}{A_s} \gamma_s \tag{F.121}$$

$$A_W = \frac{\Delta\sigma}{A_w} \alpha_w + \frac{\Delta\sigma}{4A_n} \beta_n - \frac{\Delta\sigma}{4A_s} \beta_s \tag{F.122}$$

$$A_{NE} = -\frac{\Delta\sigma}{4A_e} \beta_e - \frac{\Delta\sigma}{4A_n} \beta_n \tag{F.123}$$

$$A_{SE} = \frac{\Delta\sigma}{4A_e} \beta_e + \frac{\Delta\sigma}{4A_s} \beta_s \tag{F.124}$$

$$A_{NW} = \frac{\Delta\sigma}{4A_w} \beta_w + \frac{\Delta\sigma}{4A_n} \beta_n \tag{F.125}$$

$$A_{SW} = -\frac{\Delta\sigma}{4A_w} \beta_w - \frac{\Delta\sigma}{4A_s} \beta_s \tag{F.126}$$

$$\begin{aligned}
A_P P'_P &= A_E P'_E + A_N P'_N + A_W P'_W + A_S P'_S + A_{NE} P'_{NE} + \\
& A_{SE} P'_{SE} + A_{NW} P'_{NW} + A_{SW} P'_{SW} + B
\end{aligned} \tag{F.127}$$

in which

$$B = (U_w^* - U_e^*) + (V_s^* - V_n^*) + \frac{W_U - W_D}{\Delta\sigma} \quad (F.128)$$

and

$$A_P = A_E + A_N + A_W + A_S \quad (F.129)$$

also

$$A_{NE} + A_{SE} + A_{NW} + A_{SW} = 0 \quad (F.130)$$

F. 2 DERIVATION OF THE PRESSURE-EQUATION FOR SIMPLER ALGORITHM

Momentum Equation:

$$A_P^u u_e = \sum A_{(nb)_e}^u u_{(nb)_e} + B_e^u - \left\{ \frac{P_E - P_P}{\Delta\xi} y_{\eta e} - \frac{P_N + P_{NE} - P_S - P_{SE}}{4\Delta\eta} y_{\xi e} \right\} \Delta V \quad (F.131)$$

is written as:

$$u_e = \frac{\sum A_{(nb)_e}^u u_{(nb)_e}}{A_P^u} - \frac{\Delta V}{A_P^u} \left\{ \frac{P_E - P_P}{\Delta\xi} y_{\eta e} - \frac{P_N + P_{NE} - P_S - P_{SE}}{4\Delta\eta} y_{\xi e} \right\} \quad (F.132)$$

Let us define pseudovelocity \hat{u}_e as

$$\hat{u}_e = \frac{\sum A_{(nb)_e}^u u_{(nb)_e} + B_e^u}{A_P^u} \quad (F.133)$$

The momentum equation is then written:

$$u_e = \hat{u}_e - \frac{\Delta V}{A_P^u} \left\{ \frac{P_E - P_P}{\Delta\xi} y_{\eta e} - \frac{P_N + P_{NE} - P_S - P_{SE}}{4\Delta\eta} y_{\xi e} \right\} \quad (F.134)$$

F. 2. 1 Summary of Relations for Velocity Components

$$u_e = \hat{u}_e - \frac{\Delta V}{AP_e^u} \left\{ \frac{P_E - P_P}{\Delta \xi} y_{\eta e} - \frac{P_N + P_{NE} - P_S - P_{SE}}{4\Delta \eta} y_{\xi e} \right\} \quad (F.135)$$

$$v_e = \hat{v}_e - \frac{\Delta V}{AP_e^v} \left\{ \frac{P_N + P_{NE} - P_S - P_{SE}}{4\Delta \eta} x_{\xi e} - \frac{P_E - P_P}{\Delta \xi} x_{\eta e} \right\} \quad (F.136)$$

$$u_n = \hat{u}_n - \frac{\Delta V}{AP_n^u} \left\{ \frac{P_E + P_{NE} - P_W - P_{NW}}{4\Delta \xi} y_{\eta n} - \frac{P_N - P_P}{\Delta \eta} y_{\xi n} \right\} \quad (F.137)$$

$$v_n = \hat{v}_n - \frac{\Delta V}{AP_n^v} \left\{ \frac{P_N - P_P}{\Delta \eta} x_{\xi n} - \frac{P_E + P_{NE} - P_W - P_{NW}}{4\Delta \xi} x_{\eta n} \right\} \quad (F.138)$$

$$u_w = \hat{u}_w - \frac{\Delta V}{AP_w^u} \left\{ \frac{P_P - P_W}{\Delta \xi} y_{\eta w} - \frac{P_N + P_{NW} - P_S - P_{SW}}{4\Delta \eta} y_{\xi w} \right\} \quad (F.139)$$

$$v_w = \hat{v}_w - \frac{\Delta V}{AP_w^v} \left\{ \frac{P_N + P_{NW} - P_S - P_{SW}}{4\Delta \eta} x_{\xi w} - \frac{P_P - P_W}{\Delta \xi} x_{\eta w} \right\} \quad (F.140)$$

$$u_s = \hat{u}_s - \frac{\Delta V}{AP_s^u} \left\{ \frac{P_E + P_{SE} - P_W - P_{SW}}{4\Delta \xi} y_{\eta s} - \frac{P_P - P_S}{\Delta \eta} y_{\xi s} \right\} \quad (F.141)$$

$$v_s = \hat{v}_s - \frac{\Delta V}{AP_s^v} \left\{ \frac{P_P - P_S}{\Delta \eta} x_{\xi s} - \frac{P_E + P_{SE} - P_W - P_{SW}}{4\Delta \xi} x_{\eta s} \right\} \quad (F.142)$$

Comparing these results with the Eqns (F.73) to (F.80):

$$\begin{Bmatrix} \hat{u} \\ \hat{v} \end{Bmatrix} \quad \text{stand in place of} \quad \begin{Bmatrix} u^* \\ v^* \end{Bmatrix}$$

and "P" stands in place of "P'". Then

$$\begin{aligned} A_P P_P = & A_E P_E + A_N P_N + A_W P_W + A_S P_S + A_{NE} P_{NE} + \\ & A_{SE} P_{SE} + A_{NW} P_{NW} + A_{SW} P_{SW} + B \end{aligned} \quad (F.143)$$

where

$$B = \frac{\rho_w \hat{U}_w - \rho_e \hat{U}_e}{\Delta \xi} + \frac{\rho_s \hat{V}_s - \rho_n \hat{V}_n}{\Delta \eta} + \frac{\rho_U W_U - \rho_D W_D}{\Delta \sigma} \quad (F.144)$$

Note that a constant " ρ " in the above formulation showed an effective convergence in practice.

F. 2. 2 Relations for Pseudovelocities in I and J Coordinates

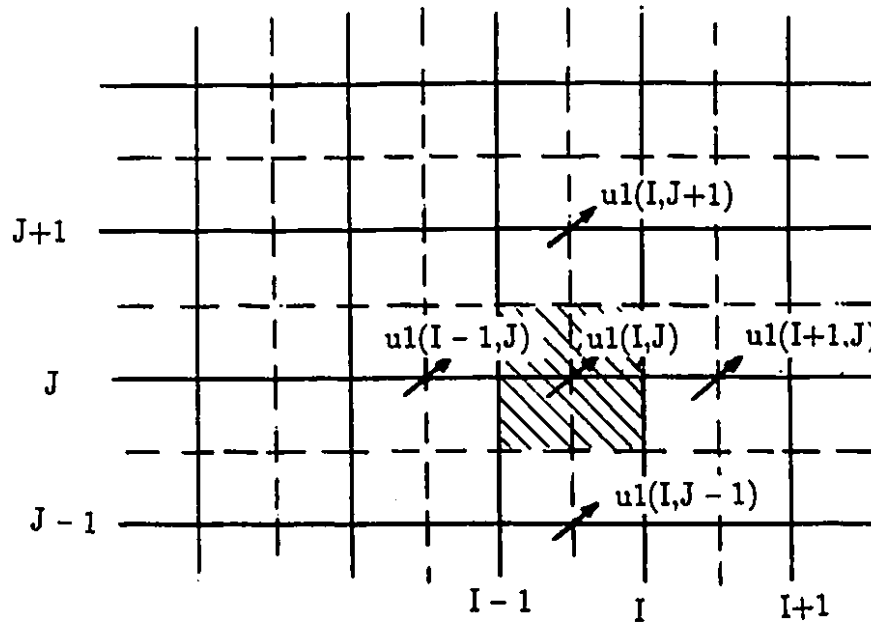


Fig. F2

$$\begin{aligned}
 U1P(I, J) = & (AE(I, J) \times U1(I + 1, J) + AN(I, J) \times U1(I, J + 1) + \\
 & AW(I, J) \times U1(I - 1, J) + AS(I, J) \times U1(I, J - 1) + \\
 & CON(I, J)) / AP(I, J)
 \end{aligned}
 \tag{F.145}$$

$$\begin{aligned}
 V1P(I, J) = & (AE(I, J) \times V1(I + 1, J) + AN(I, J) \times V1(I, J + 1) + \\
 & AW(I, J) \times V1(I - 1, J) + AS(I, J) \times V1(I, J - 1) + \\
 & CON(I, J)) / AP(I, J)
 \end{aligned}
 \tag{F.146}$$

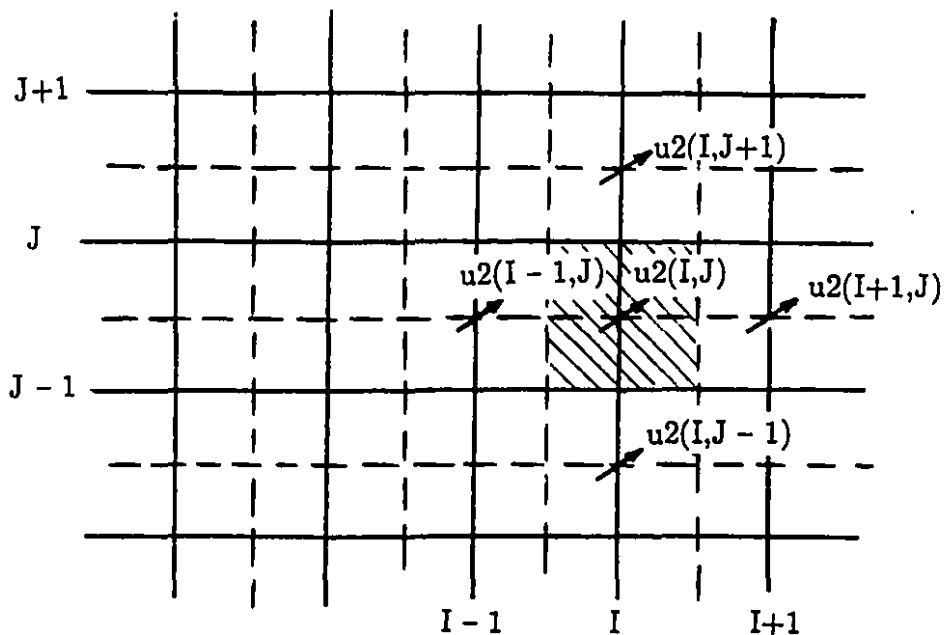


Fig. F3

$$\begin{aligned}
 V_2P(I, J) = & (AE(I, J) \times V_2(I+1, J) + AN(I, J) \times V_2(I, J+1) + \\
 & AW(I, J) \times V_2(I-1, J) + AS(I, J) \times V_2(I, J-1) + \\
 & CON(I, J)) / AP(I, J)
 \end{aligned} \tag{F.147}$$

$$\begin{aligned}
 U_2P(I, J) = & (AE(I, J) \times U_2(I+1, J) + AN(I, J) \times U_2(I, J+1) + \\
 & AW(I, J) \times U_2(I-1, J) + AS(I, J) \times U_2(I, J-1) + \\
 & CON(I, J)) / AP(I, J)
 \end{aligned} \tag{F.148}$$

APPENDIX G
DERIVATION OF MISCELLANEOUS RELATIONS

G.1 CONTRAVARIANT VELOCITIES

UC1 and VC1 (Figure G.1)

$$U1 = u_1 y_{\eta 1} - v_1 x_{\eta 1} \quad (G.1)$$

$$V1 = v_1 x_{\xi 1} - u_1 y_{\xi 1} \quad (G.2)$$

$$UC1(I, J) = U1(I, J) y_{\eta 1} - V1(I, J) x_{\eta 1} \quad (G.3)$$

$$VC1(I, J) = V1(I, J) x_{\xi 1} - U1(I, J) y_{\xi 1} \quad (G.4)$$

$$I = 3 \text{ to } L2 \quad \text{and} \quad J = 2 \text{ to } M2$$

UC2 and VC2 (Figure G.2)

$$U2 = u_2 y_{\eta 2} - v_2 x_{\eta 2} \quad (G.5)$$

$$V2 = v_2 x_{\xi 2} - u_2 y_{\xi 2} \quad (G.6)$$

$$UC2(I, J) = U2(I, J) y_{\eta 2} - V2(I, J) x_{\eta 2} \quad (G.7)$$

$$VC2(I, J) = V2(I, J) x_{\xi 2} - U2(I, J) y_{\xi 2} \quad (G.8)$$

$$I = 2 \text{ to } L2 \quad \text{and} \quad J = 3 \text{ to } M2$$

WC (Figure G.3)

$$WC(I, J) = JAC(I, J) \cdot W(I, J) \quad (G.9)$$

$$I = 2 \text{ to } L2 \quad \text{and} \quad J = 2 \text{ to } M2$$

UC1 and VC1 at the Boundaries

J = 2 to M2

$$UC1(2, J) = U1(2, J) y_{\eta}(1, J) - V1(2, J) x_{\eta}(1, J) \quad (G.10)$$

$$VC1(2, J) = V1(2, J) x_{\xi}(1, J) - U1(2, J) y_{\xi}(1, J) \quad (G.11)$$

J = 2 to M2

$$UC1(L1, J) = U1(L1, J)y_{\eta}(L1, J) - V1(L1, J)x_{\eta}(L1, J) \quad (G.12)$$

$$VC1(L1, J) = V1(L1, J)x_{\xi}(L1, J) - U1(L1, J)y_{\xi}(L1, J) \quad (G.13)$$

UC2 and VC2 at the Boundaries

I = 2 to L2

$$UC2(I, 2) = U2(I, 2)y_{\eta}(I, 1) - V2(I, 2)x_{\eta}(I, 1) \quad (G.14)$$

$$VC2(I, 2) = V2(I, 2)x_{\xi}(I, 1) - U2(I, 2)y_{\xi}(I, 1) \quad (G.15)$$

I = 2 to L2

$$UC2(I, M1) = U2(I, M1)y_{\eta}(I, M1) - V2(I, M1)x_{\eta}(I, M1) \quad (G.16)$$

$$VC2(I, M1) = V2(I, M1)x_{\xi}(I, M1) - U2(I, M1)y_{\xi}(I, M1) \quad (G.17)$$

WC at the Boundaries

I = 2 to L2

$$WC(I, 1) = JAC(I, 1) \cdot W(I, 1) \quad (G.18)$$

I = 2 to L2

$$WC(I, M1) = JAC(I, M1) \cdot W(I, M1) \quad (G.19)$$

I = 2 to M2

$$WC(1, J) = JAC(1, J) \cdot W(1, J) \quad (G.20)$$

J = 2 to M2

$$WC(L1, J) = JAC(L1, J) \cdot W(L1, J) \quad (G.21)$$

G.2 CONTRAVARIANT VELOCITIES SATISFYING MASS-CONSERVATION

(Figure G.4)

$$U1 = u_1 y_\eta - v_1 x_\eta \quad (G.22)$$

$$V2 = v_2 x_\xi - u_2 y_\xi \quad (G.23)$$

$$U1^* = u_1^* y_\eta - v_1^* x_\eta \quad (G.24)$$

$$V2^* = v_2^* x_\xi - u_2^* y_\xi \quad (G.25)$$

$$(U1 - U1^*) = (u_1 - u_1^*) y_\eta - (v_1 - v_1^*) x_\eta \quad (G.26)$$

$$(V2 - V2^*) = (v_2 - v_2^*) x_\xi - (u_2 - u_2^*) y_\xi \quad (G.27)$$

let

$$\left. \begin{array}{l} u_1 - u_1^* = u'_1 \\ v_1 - v_1^* = v'_1 \end{array} \right\} \quad (G.28)$$

and

$$\left. \begin{array}{l} u_2 - u_2^* = u'_2 \\ v_2 - v_2^* = v'_2 \end{array} \right\} \quad (G.29)$$

$$U1 = U1^* + u'_1 y_\eta - v'_1 x_\eta \quad (G.30)$$

$$V2 = V2^* + v'_2 x_\xi - u'_2 y_\xi \quad (G.31)$$

in alternate form let

$$\left. \begin{array}{l} u'_1 = DU1 \\ v'_1 = DV1 \end{array} \right\} \quad (G.32)$$

$$\left. \begin{array}{l} u'_2 = DU2 \\ v'_2 = DV2 \end{array} \right\} \quad (G.33)$$

then

$$U1 = U1^* + DU1 y_\eta - DV1 x_\eta \quad (G.34)$$

$$V2 = V2^* + DV2 x_\xi - DU2 y_\xi \quad (G.35)$$

@ points "w" and "s":

$$U1_w = U1_w^* + DU1_w \cdot y_{\eta w} - DV1_w \cdot x_{\eta w} \quad (G.36)$$

$$V2_s = V2_s^* + DV2_s \cdot x_{\xi s} - DU2_s \cdot y_{\xi s} \quad (G.37)$$

or in terms of "I" and "J":

$$UC1(I, J) = UC1^*(I, J) + DU11 \cdot y_{\eta 1} - DV11 \cdot x_{\eta 1} \quad (G.38)$$

$$VC2(I, J) = VC2^*(I, J) + DV22 \cdot x_{\xi 2} - DU22 \cdot y_{\xi 2} \quad (G.39)$$

$$DU11 = -\frac{\Delta V}{APU1(I, J)} \left[\frac{(PC(I, J) - PC(I - 1, J))}{\Delta \xi} y_{\eta 1} - \frac{(PC(I - 1, J + 1) + PC(I, J + 1) - PC(I - 1, J - 1) - PC(I, J - 1))}{4\Delta \eta} y_{\xi 1} \right] \quad (G.40)$$

$$DV11 = -\frac{\Delta V}{APV1(I, J)} \left[\frac{(PC(I - 1, J + 1) + PC(I, J + 1) - PC(I - 1, J - 1) - PC(I, J - 1))}{4\Delta \eta} x_{\xi 1} - \frac{(PC(I, J) - PC(I - 1, J))}{\Delta \xi} x_{\eta 1} \right] \quad (G.41)$$

$$DV22 = -\frac{\Delta V}{APV2(I, J)} \left[\frac{(PC(I, J) - PC(I, J - 1))}{\Delta \eta} x_{\xi 2} - \frac{(PC(I + 1, J - 1) + PC(I + 1, J) - PC(I - 1, J) - PC(I - 1, J - 1))}{4\Delta \xi} x_{\eta 2} \right] \quad (G.42)$$

$$DU22 = -\frac{\Delta V}{APU2(I, J)} \left[\frac{(PC(I + 1, J - 1) + PC(I + 1, J) - PC(I - 1, J) - PC(I - 1, J - 1))}{4\Delta \xi} y_{\eta 2} - \frac{(PC(I, J) - PC(I, J - 1))}{\Delta \eta} y_{\xi 2} \right] \quad (G.43)$$

**G.3 CONTRAVARIANT VELOCITIES
NOT SATISFYING MASS-CONSERVATION**
(Figure G.5)

Contravariant Velocities Satisfying Mass-Conservation:
(denoted by *)

$$\begin{aligned} & UC1(I, J) \\ & UC1(I + 1, J) \\ & VC2(I, J) \\ & VC2(I, J + 1) \end{aligned}$$

Contravariant Velocities Not Satisfying Mass-Conservation:

$$\begin{aligned} & VC1(I, J) \\ & UC2(I, J) \\ & VC1(I + 1, J) \\ & UC2(I, J + 1) \end{aligned}$$

Relation for UC2(I,J) (Figure G.6)

$$UC2(I, J) = \frac{UC1(I, J) + UC1(I + 1, J) + UC1(I + 1, J - 1) + UC1(I, J - 1)}{4} \quad (G.44)$$

for $I = 2$ to $L2$ and $J = 3$ to $M2$

Relation for VC1(I,J) (Figure G.7)

$$VC1(I, J) = \frac{VC2(I, J) + VC2(I, J + 1) + VC2(I - 1, J + 1) + VC2(I - 1, J)}{4} \quad (G.45)$$

for $I = 3$ to $L2$ and $J = 2$ to $M2$

G.4 PHYSICAL VELOCITIES

$$U = uy_{\eta} - vx_{\eta} \quad (G.46)$$

$$V = -uy_{\xi} + vx_{\xi} \quad (G.47)$$

$$u = \frac{\begin{bmatrix} U & -x_\eta \\ V & x_\xi \end{bmatrix}}{\begin{bmatrix} y_\eta & -x_\eta \\ -y_\xi & x_\xi \end{bmatrix}} \quad (G.48)$$

and

$$v = \frac{\begin{bmatrix} y_\eta & U \\ -y_\xi & V \end{bmatrix}}{\begin{bmatrix} y_\eta & -x_\eta \\ -y_\xi & x_\xi \end{bmatrix}} \quad (G.49)$$

$$u = \frac{Ux_\xi + Vx_\eta}{y_\eta x_\xi - y_\xi x_\eta} \quad (G.50)$$

$$v = \frac{Vy_\eta + Uy_\xi}{y_\eta x_\xi - y_\xi x_\eta} \quad (G.51)$$

but

$$y_\eta x_\xi - y_\xi x_\eta = J \quad (G.52)$$

Therefore

$$\left. \begin{aligned} u &= \frac{1}{J}[Ux_\xi + Vx_\eta] \\ v &= \frac{1}{J}[Uy_\xi + Vy_\eta] \end{aligned} \right\} \quad (G.53)$$

u1 and v1 (Figure G.8)

$$u1(I, J) = \frac{1}{JAC1}(UC1(I, J) \cdot x_{\xi 1} + VC1(I, J) \cdot x_{\eta 1}) \quad (G.54)$$

$$v1(I, J) = \frac{1}{JAC1}(UC1(I, J) \cdot y_{\xi 1} + VC1(I, J) \cdot y_{\eta 1}) \quad (G.55)$$

u2 and v2 (Figure G.9)

$$u2(I, J) = \frac{1}{JAC2}(UC2(I, J) \cdot x_{\xi 2} + VC2(I, J) \cdot x_{\eta 2}) \quad (G.56)$$

$$v2(I, J) = \frac{1}{JAC2}(UC2(I, J) \cdot y_{\xi 2} + VC2(I, J) \cdot y_{\eta 2}) \quad (G.57)$$

G.5 APPLICATION OF RELAXATION FACTOR

Consider the general discretization equation (for momenta, pressure, energy and species):

$$AP_P \phi_P = \sum A_{(nb)P} \phi_{(nb)P} + B_P - L[\hat{P}_P] \Delta V \quad (G.58)$$

in which the term $L[\hat{P}_P] \Delta V$ appears only in momentum equations. Now write:

$$\dot{\phi}_P = \frac{\sum A_{(nb)P} \dot{\phi}_{(nb)P} + B_P}{AP_P} - \frac{L[\dot{P}_P] \Delta V}{AP_P} \quad (G.59)$$

or alternatively:

$$\dot{\phi}_P = \dot{\phi}_P^* + \frac{\sum A_{(nb)P} \dot{\phi}_{(nb)P} + B_P}{AP_P} - \dot{\phi}_P^* - \frac{L[\dot{P}_P] \Delta V}{AP_P} \quad (G.60)$$

Applying relaxation factor, α :

$$\dot{\phi}_P = \dot{\phi}_P^* + \alpha \left(\frac{\sum A_{(nb)P} \dot{\phi}_{(nb)P} + B_P}{AP_P} - \dot{\phi}_P^* - \frac{L[\dot{P}_P] \Delta V}{AP_P} \right) \quad (G.61)$$

$$\dot{\phi}_P = \dot{\phi}_P^* + \frac{\alpha}{AP_P} \sum A_{(nb)P} \dot{\phi}_{(nb)P} + \frac{\alpha B_P}{AP_P} - \alpha \dot{\phi}_P^* - \frac{\alpha L[\dot{P}_P] \Delta V}{AP_P} \quad (G.62)$$

$$\frac{AP_P}{\alpha} \dot{\phi}_P = \frac{AP_P}{\alpha} \dot{\phi}_P^* + \sum A_{(nb)P} \dot{\phi}_{(nb)P} + B_P - AP_P \dot{\phi}_P^* - L[\dot{P}_P] \Delta V \quad (G.63)$$

$$\frac{AP_P}{\alpha} \dot{\phi}_P = \sum A_{(nb)P} \dot{\phi}_{(nb)P} + B_P + \frac{(1-\alpha)AP_P}{\alpha} \dot{\phi}_P^* - L[\dot{P}_P] \Delta V \quad (G.64)$$

$$\text{let } \frac{AP_P}{\alpha} = AP(I, J) \quad (G.65)$$

$$\frac{(1-\alpha)}{\alpha} AP_P = (1-\alpha)AP(I, J) \quad (G.66)$$

$$B_P = B(I, J) \quad (G.67)$$

$$AP(I, J) \dot{\phi}(I, J) = \sum A_{(nb)}(I, J) \dot{\phi}_{(nb)}(I, J) + B(I, J) + (1-\alpha)AP(I, J) \dot{\phi}(I, J) - L[\dot{P}_P] \Delta V \quad (G.68)$$

Relations for $AP(I, J)$:

U1:

$$AP(I, J) = \frac{(AE(I, J) + AW(I, J) + AN(I, J) + AS(I, J) + AU(I, J))}{REL1} \quad (G.69)$$

V1:

$$AP(I, J) = \frac{(AE(I, J) + AW(I, J) + AN(I, J) + AS(I, J) + AU(I, J))}{REL2} \quad (G.70)$$

U2:

$$AP(I, J) = \frac{(AE(I, J) + AW(I, J) + AN(I, J) + AS(I, J) + AU(I, J))}{REL3} \quad (G.71)$$

V2:

$$AP(I, J) = \frac{(AE(I, J) + AW(I, J) + AN(I, J) + AS(I, J) + AU(I, J))}{REL4} \quad (G.72)$$

W:

$$AP(I, J) = \frac{(AE(I, J) + AW(I, J) + AN(I, J) + AS(I, J) + AU(I, J))}{REL10} \quad (G.73)$$

H:

$$AP(I, J) = \frac{(AE(I, J) + AW(I, J) + AN(I, J) + AS(I, J) + AU(I, J) - SP(I, J) \cdot DV)}{REL8} \quad (G.74)$$

M:

$$AP(I, J) = \frac{(AE(I, J) + AW(I, J) + AN(I, J) + AS(I, J) + AU(I, J) - SP(I, J) \cdot DV)}{REL9} \quad (G.75)$$

P:

$$AP(I, J) = \frac{(AE(I, J) + AW(I, J) + AN(I, J) + AS(I, J) + AU(I, J))}{REL6} \quad (G.76)$$

PC:

$$AP(I, J) = \frac{(AE(I, J) + AW(I, J) + AN(I, J) + AS(I, J) + AU(I, J))}{REL5} \quad (G.77)$$

Relations for $CON(I, J) = B(I, J) + (1 - \alpha)AP(I, J)\phi(I, J)$

$$U1: \quad CON(I, J) = B(I, J) + (1 - REL1)AP(I, J)U1(I, J) \quad (G.78)$$

$$V1: \quad CON(I, J) = B(I, J) + (1 - REL2)AP(I, J)V1(I, J) \quad (G.79)$$

$$U2: \quad CON(I, J) = B(I, J) + (1 - REL3)AP(I, J)U2(I, J) \quad (G.80)$$

$$V2: \quad CON(I, J) = B(I, J) + (1 - REL4)AP(I, J)V2(I, J) \quad (G.81)$$

$$W: \quad CON(I, J) = B(I, J) + (1 - REL10)AP(I, J)W(I, J) \quad (G.82)$$

$$H: \quad CON(I, J) = B(I, J) + (1 - REL8)AP(I, J)H(I, J) \quad (G.83)$$

$$M: \quad CON(I, J) = B(I, J) + (1 - REL9)AP(I, J)M(I, J) \quad (G.84)$$

$$P: \quad CON(I, J) = B(I, J) + (1 - REL6)AP(I, J)P(I, J) \quad (G.85)$$

$$PC: \quad CON(I, J) = B(I, J) + (1 - REL5)AP(I, J)PC(I, J) \quad (G.86)$$

G.6 PRESSURE-GRADIENT TERMS IN I AND J COORDINATES

U1 Momentum Equation

$$L[\hat{P}_w^u]\Delta V = \left\{ \frac{P_P - P_W}{\Delta\xi} y_{\eta w} - \frac{P_N + P_{NW} - P_S - P_{SW}}{4\Delta\eta} y_{\xi w} \right\} \Delta V \quad (G.87)$$

$$L[\hat{P}_w^u]\Delta V = \left\{ \left[\frac{P(I, J) - P(I-1, J)}{\Delta\xi} \right] y_{\eta 1} - \left[\frac{P(I, J+1) + P(I-1, J+1) - P(I, J-1) - P(I-1, J-1)}{4\Delta\eta} \right] y_{\xi 1} \right\} \Delta V \quad (G.88)$$

V1 Momentum Equation

$$L[\hat{P}_w^v]\Delta V = \left\{ \frac{P_N + P_{NW} - P_S - P_{SW}}{4\Delta\eta} x_{\xi w} - \frac{P_N - P_W}{\Delta\xi} x_{\eta w} \right\} \Delta V \quad (G.89)$$

$$L[\hat{P}_w^v]\Delta V = \left\{ \left[\frac{P(I, J+1) + P(I-1, J+1) - P(I, J-1) - P(I-1, J-1)}{4\Delta\eta} \right] x_{\xi 1} - \left[\frac{P(I, J) - P(I-1, J)}{\Delta\xi} \right] x_{\eta 1} \right\} \Delta V \quad (G.90)$$

U2 Momentum Equation

$$L[\hat{P}_s^u]\Delta V = \left\{ \frac{P_E + P_{SE} - P_W - P_{SW}}{4\Delta\xi} y_{\eta s} - \frac{P_P - P_S}{\Delta\eta} y_{\xi s} \right\} \Delta V \quad (G.91)$$

$$L[\hat{P}_s^u]\Delta V = \left\{ \left[\frac{P(I+1, J) + P(I+1, J-1) - P(I-1, J) - P(I-1, J-1)}{4\Delta\xi} \right] y_{\eta 2} - \left[\frac{P(I, J) - P(I, J-1)}{\Delta\eta} \right] y_{\xi 2} \right\} \Delta V \quad (G.92)$$

V2 Momentum Equation

$$L[\hat{P}_s^v]\Delta V = \left\{ \frac{P_P - P_S}{\Delta\eta} x_{\xi s} - \frac{P_E + P_{SE} - P_W - P_{SW}}{4\Delta\xi} x_{\eta s} \right\} \Delta V \quad (G.93)$$

$$L[\hat{P}_s^v]\Delta V = \left\{ \left[\frac{P(I, J) - P(I, J-1)}{\Delta\eta} \right] x_{\xi 2} - \left[\frac{P(I+1, J) + P(I+1, J-1) - P(I-1, J) - P(I-1, J-1)}{4\Delta\xi} \right] x_{\eta 2} \right\} \Delta V \quad (G.94)$$

**G.7 DERIVATION OF PRESSURE-GRADIENT TERM
FOR BOUNDARY CONTROL-VOLUMES ($J = 2$ AND $J = M2$)**

Range of Variations of I for Boundary Control-Volumes at $J = 2$ and $J = M2$. $I=3,L2$

U1 Velocity (Figure G.10)

@ $J = 2$ Control-volumes

$$CON(I, 2) = CON(I, 2) - L[\hat{P}_1^u] \Delta V \quad (G.95)$$

$$CON(I, 2) = CON(I, 2) - L[y_{\eta 1} \cdot P_{\xi 1} - y_{\xi 1} \cdot P_{\eta 1}] \Delta V \quad (G.96)$$

$$P_{\xi 1} = \left. \frac{\partial P}{\partial \xi} \right|_1 = \frac{P(I, 2) - P(I - 1, 2)}{\Delta \xi} \quad (G.97)$$

$$P_{\eta 1} = \left. \frac{\partial P}{\partial \eta} \right|_1 = \frac{1}{2} \left[\left. \frac{\partial P}{\partial \eta} \right|_2 + \left. \frac{\partial P}{\partial \eta} \right|_{wall} \right]$$

$$P_{\eta 1} = \frac{1}{2} \left[\frac{P_2' - P_1}{\Delta \eta} + \left. \frac{\partial P}{\partial \eta} \right|_{wall} \right] = \frac{1}{2} \frac{P_2' - P_1}{\Delta \eta} + \frac{1}{2} GG1 \quad (G.98)$$

$$P_{\eta 1} = \frac{\frac{P(I, 3) + P(I - 1, 3)}{2} - \frac{P(I, 2) + P(I - 1, 2)}{2}}{2 \Delta \eta} + \frac{1}{2} GG1$$

$$P_{\eta 1} = \frac{P(I, 3) + P(I - 1, 3) - P(I, 2) - P(I - 1, 2)}{4 \Delta \eta} + \frac{1}{2} GG1 \quad (G.99)$$

$$CON(I, 2) = CON(I, 2) - \left[\left(\frac{P(I, 2) - P(I - 1, 2)}{\Delta \xi} \right) y_{\eta 1} - \left(\frac{P(I, 3) + P(I - 1, 3) - P(I, 2) - P(I - 1, 2)}{4 \Delta \eta} + \frac{1}{2} GG1 \right) y_{\xi 1} \right] \Delta V \quad (G.100)$$

$$GG1 = \frac{P_1 - P_{wall}}{\left(\frac{\Delta \eta}{2} \right)} = \frac{\frac{1}{2}(P(I - 1, 2) + P(I, 2)) - \frac{1}{2}(P(I - 1, 1) + P(I, 1))}{\left(\frac{\Delta \eta}{2} \right)} \quad (G.101)$$

V1 Velocity (Figure G.10)

@ $J = 2$ Control-volumes

$$CON(I, 2) = CON(I, 2) - L[\hat{P}_1^v] \Delta V \quad (G.102)$$

$$CON(I, 2) = CON(I, 2) - L[x_{\xi 1} \cdot P_{\eta 1} - x_{\eta 1} \cdot P_{\xi 1}] \Delta V \quad (G.103)$$

$$CON(I, 2) = CON(I, 2) -$$

$$\left[\left(\frac{P(I, 3) + P(I - 1, 3) - P(I, 2) - P(I - 1, 2)}{4 \Delta \eta} + \frac{1}{2} GG1 \right) x_{\xi 1} - \left(\frac{P(I, 2) - P(I - 1, 2)}{\Delta \xi} \right) x_{\eta 1} \right] \Delta V \quad (G.104)$$

U1 Velocity (Figure G.10)

@ $J = M2$ Control-volumes

$$CON(I, M2) = CON(I, M2) - L[\dot{P}_1^u] \Delta V \quad (G.105)$$

$$CON(I, M2) = CON(I, M2) - L[y_{\eta 1} \cdot P_{\xi 1} - y_{\xi 1} \cdot P_{\eta 1}] \Delta V \quad (G.106)$$

$$P_{\xi 1} = \left. \frac{\partial P}{\partial \xi} \right|_1 = \frac{P(I, M2) - P(I-1, M2)}{\Delta \xi} \quad (G.107)$$

$$P_{\eta 1} = \left. \frac{\partial P}{\partial \eta} \right|_1 = \frac{1}{2} \left[\left. \frac{\partial P}{\partial \eta} \right|_2 + \left. \frac{\partial P}{\partial \eta} \right|_{wall} \right] = \frac{1}{2} \left[\frac{P_1 - P_2}{\Delta \eta} + \left. \frac{\partial P}{\partial \eta} \right|_{wall} \right]$$

$$P_{\eta 1} = \frac{1}{2} \frac{P_1 - P_2}{\Delta \eta} + \frac{1}{2} HH1 \quad (G.108)$$

$$P_{\eta 1} = \frac{\frac{P(I, M2) + P(I-1, M2)}{2} - \frac{P(I, M3) + P(I-1, M3)}{2}}{2 \Delta \eta} + \frac{1}{2} HH1$$

$$P_{\eta 1} = \frac{P(I, M2) + P(I-1, M2) - P(I, M3) - P(I-1, M3)}{4 \Delta \eta} + \frac{1}{2} HH1 \quad (G.109)$$

$$CON(I, M2) = CON(I, M2) - \left[\left(\frac{P(I, M2) - P(I-1, M2)}{\Delta \xi} \right) y_{\eta 1} - \left(\frac{P(I, M2) + P(I-1, M2) - P(I, M3) - P(I-1, M3)}{4 \Delta \eta} + \frac{1}{2} HH1 \right) y_{\xi 1} \right] \Delta V \quad (G.110)$$

$$\begin{aligned} HH1 &= \frac{P_{wall} - P_1}{\left(\frac{\Delta \eta}{2} \right)} \\ &= \frac{\frac{1}{2}(P(I-1, M1) + P(I, M1)) - \frac{1}{2}(P(I-1, M2) + P(I, M2))}{\left(\frac{\Delta \eta}{2} \right)} \end{aligned} \quad (G.111)$$

V1 Velocity (Figure G.10)

@ $J = M2$ Control-volumes

$$CON(I, M2) = CON(I, M2) - L[\dot{P}_1^v] \Delta V \quad (G.112)$$

$$CON(I, M2) = CON(I, M2) - (x_{\xi 1} \cdot P_{\eta 1} - x_{\eta 1} \cdot P_{\xi 1}) \Delta V \quad (G.113)$$

$$\begin{aligned} CON(I, M2) &= CON(I, M2) - \\ &\left[\left(\frac{P(I, M2) + P(I-1, M2) - P(I, M3) - P(I-1, M3)}{4 \Delta \eta} + \frac{1}{2} HH1 \right) x_{\xi 1} - \right. \\ &\left. \left(\frac{P(I, M2) - P(I-1, M2)}{\Delta \xi} \right) x_{\eta 1} \right] \Delta V \end{aligned} \quad (G.114)$$

**G.8 DERIVATION OF PRESSURE-GRADIENT TERM
FOR BOUNDARY CONTROL-VOLUMES ($I = 2$ AND $I = L2$)**

Range of Variations of J for Boundary Control-Volumes at $I = 2$ and $I = L2$. $J=3, M2$
U2 Velocity (Figure G.11)

@ $I = 2$ Control-volumes

$$CON(2, J) = CON(2, J) - L[\hat{P}_2^u] \Delta V \quad (G.115)$$

$$CON(2, J) = CON(2, J) - L[y_{\eta 2} \cdot P_{\xi 2} - y_{\xi 2} \cdot P_{\eta 2}] \Delta V \quad (G.116)$$

$$P_{\xi 2} = \left. \frac{\partial P}{\partial \xi} \right|_2 = \frac{1}{2} \left[\left. \frac{\partial P}{\partial \xi} \right|_3 + \left. \frac{\partial P}{\partial \xi} \right|_{wall} \right] = \frac{1}{2} \left[\frac{P_{3'} - P_2}{\Delta \xi} + \left. \frac{\partial P}{\partial \xi} \right|_{wall} \right]$$

$$P_{\xi 2} = \frac{1}{2} \frac{P_{3'} - P_2}{\Delta \xi} + \frac{1}{2} EE1 \quad (G.117)$$

$$P_{\xi 2} = \frac{\frac{P(3, J) + P(3, J-1)}{2} - \frac{P(2, J) + P(2, J-1)}{2}}{2 \Delta \xi} + \frac{1}{2} EE1$$

$$P_{\xi 2} = \frac{P(3, J) + P(3, J-1) - P(2, J) - P(2, J-1)}{4 \Delta \xi} + \frac{1}{2} EE1 \quad (G.118)$$

$$P_{\eta 2} = \left. \frac{\partial P}{\partial \eta} \right|_2 = \frac{P(2, J) - P(2, J-1)}{\Delta \eta} \quad (G.119)$$

$$CON(2, J) = CON(2, J) - \left[\left(\frac{P(3, J) + P(3, J-1) - P(2, J) - P(2, J-1)}{4 \Delta \xi} + \frac{1}{2} EE1 \right) y_{\eta 2} - \left(\frac{P(2, J) - P(2, J-1)}{\Delta \eta} \right) y_{\xi 2} \right] \Delta V \quad (G.120)$$

$$EE1 = \frac{P_2 - P_{wall}}{\left(\frac{\Delta \xi}{2} \right)} = \frac{\frac{1}{2}(P(2, J-1) + P(2, J)) - \frac{1}{2}(P(1, J-1) + P(1, J))}{\left(\frac{\Delta \xi}{2} \right)} \quad (G.121)$$

V2 Velocity (Figure G.11)

@ $I = 2$ Control-volumes

$$CON(2, J) = CON(2, J) - L[\hat{P}_2^v] \Delta V \quad (G.122)$$

$$CON(2, J) = CON(2, J) - (x_{\xi 2} \cdot P_{\eta 2} - x_{\eta 2} \cdot P_{\xi 2}) \Delta V \quad (G.123)$$

$$CON(2, J) = CON(2, J) - \left[\left(\frac{P(2, J) - P(2, J-1)}{\Delta\eta} \right) x_{\xi 2} \right. \\ \left. \left(\frac{P(3, J) + P(3, J-1) - P(2, J) - P(2, J-1)}{4\Delta\xi} + \frac{1}{2} EE1 \right) x_{\eta 2} \right] \Delta V \quad (G.124)$$

U2 Velocity (Figure G.11)

@ $I = L2$ Control-volumes

$$CON(L2, J) = CON(L2, J) - L[\hat{P}_2^u] \Delta V \quad (G.125)$$

$$CON(L2, J) = CON(L2, J) - L[y_{\eta 2} \cdot P_{\xi 2} - y_{\xi 2} \cdot P_{\eta 2}] \Delta V \quad (G.126)$$

$$P_{\xi 2} = \frac{\partial P}{\partial \xi} \Big|_2 = \frac{1}{2} \left[\frac{\partial P}{\partial \xi} \Big|_3 + \frac{\partial P}{\partial \xi} \Big|_{wall} \right] = \frac{1}{2} \left[\frac{P_2 - P_{3'}}{\Delta\xi} + \frac{\partial P}{\partial \xi} \Big|_{wall} \right]$$

$$P_{\xi 2} = \frac{1}{2} \frac{P_2 - P_{3'}}{\Delta\xi} + \frac{1}{2} FF1 \quad (G.127)$$

$$P_{\xi 2} = \frac{\frac{P(L2, J) + P(L2, J-1)}{2} - \frac{P(L3, J) - P(L3, J-1)}{2}}{2\Delta\xi} + \frac{1}{2} FF1$$

$$P_{\xi 2} = \frac{P(L2, J) + P(L2, J-1) - P(L3, J) - P(L3, J-1)}{4\Delta\xi} + \frac{1}{2} FF1 \quad (G.128)$$

$$P_{\eta 2} = \frac{\partial P}{\partial \eta} \Big|_2 = \frac{P(L2, J) - P(L2, J-1)}{\Delta\eta} \quad (G.129)$$

$$CON(L2, J) = CON(L2, J) -$$

$$\left[\left(\frac{P(L2, J) + P(L2, J-1) - P(L3, J) - P(L3, J-1)}{4\Delta\xi} + \frac{1}{2} FF1 \right) y_{\eta 2} - \right. \\ \left. \left(\frac{P(L2, J) - P(L2, J-1)}{\Delta\eta} \right) y_{\xi 2} \right] \Delta V \quad (G.130)$$

$$FF1 = \frac{P_{wall} - P_2}{\left(\frac{\Delta\xi}{2} \right)} \\ = \frac{\frac{1}{2}(P(L1, J) + P(L1, J-1)) - \frac{1}{2}(P(L2, J) + P(L2, J-1))}{\left(\frac{\Delta\xi}{2} \right)} \quad (G.131)$$

V2 Velocity (Figure G.11)

@ $I = L2$ Control-volumes

$$CON(L2, J) = CON(L2, J) - L[\hat{P}_2^v] \Delta V \quad (G.132)$$

$$CON(L2, J) = CON(L2, J) - (x_{\xi 2} \cdot P_{\eta 2} - x_{\eta 2} \cdot P_{\xi 2}) \Delta V \quad (G.133)$$

$$\begin{aligned}
CON(L2, J) = CON(L2, J) - \left[\left(\frac{P(L2, J) - P(L2, J - 1)}{\Delta\eta} \right) x_{\xi 2} - \right. \\
\left. \left(\frac{P(L2, J) + P(L2, J - 1) - P(L3, J) - P(L3, J - 1)}{4\Delta\xi} + \frac{1}{2} FF1 \right) x_{\eta 2} \right] \Delta V
\end{aligned} \tag{G.134}$$

G.9 BUOYANCY-TERM IN y-MOMENTUM EQUATION

Using $g_y = -g$, the y-momentum Eqn. (2.7) becomes:

$$\begin{aligned}
\frac{\partial}{\partial t}(\rho v) + \frac{\partial}{\partial x}(\rho uv) + \frac{\partial}{\partial y}(\rho v^2) + \frac{\partial}{\partial z}(\rho wv) \\
= -\frac{\partial P}{\partial y} - \left(\frac{\partial \tau_{xy}}{\partial x} + \frac{\partial \tau_{yy}}{\partial y} + \frac{\partial \tau_{zy}}{\partial z} \right) - \rho g
\end{aligned} \tag{G.135}$$

or

$$LHS = -\frac{\partial P}{\partial y} - \rho g - Q \tag{G.136}$$

for simplicity here. In order to introduce the buoyancy term into the y-momentum Eqn. (G.135), one may write:

$$P = P_S + P_D \tag{G.137}$$

where:

P_S = hydrostatic pressure

P_D = dynamic pressure

Therefore

$$LHS = -\frac{\partial P_S}{\partial y} - \frac{\partial P_D}{\partial y} - \rho g - Q \tag{G.138}$$

Now consider the special case that the fluid suddenly ceases to flow. The y-momentum Eqn. (G.136) for the no-flow condition becomes:

$$0 = -\frac{\partial P}{\partial y} - \rho g \quad \text{@ no-flow or hydrostatic condition} \tag{G.139}$$

or

$$-\frac{\partial P_S}{\partial y} - \rho_a g = 0 \tag{G.140}$$

in which ρ_a is the arithmetic mean density for a cross-section. From Eqn. (G.140)

$$-\frac{\partial P_S}{\partial y} = \rho_a g \quad (G.141)$$

Now substitute for $-\frac{\partial P_S}{\partial y}$ in Eqn. (G.138)

$$LHS = \rho_a g - \frac{\partial P_D}{\partial y} - \rho g - Q \quad (G.142)$$

or

$$LHS = -\frac{\partial P_D}{\partial y} - (\rho - \rho_a)g - Q \quad (G.143)$$

in which $(\rho - \rho_a)g$ is the buoyancy term. The y-momentum equation is therefore written as:

$$\begin{aligned} \frac{\partial}{\partial t}(\rho v) + \frac{\partial}{\partial x}(\rho uv) + \frac{\partial}{\partial y}(\rho v^2) + \frac{\partial}{\partial z}(\rho wv) \\ = -\frac{\partial P_D}{\partial y} - \left(\frac{\partial \tau_{xy}}{\partial x} + \frac{\partial \tau_{yy}}{\partial y} + \frac{\partial \tau_{zy}}{\partial z} \right) - (\rho - \rho_a)g \end{aligned} \quad (G.144)$$

The pressure is to be modified in other components of the momentum equation:

x-component:

$$LHS = -\frac{\partial P}{\partial x} - Q' \quad (G.145)$$

z-component:

$$LHS = -\frac{\partial P}{\partial z} - Q'' \quad (G.146)$$

Using

$$P = P_S + P_D \quad (G.147)$$

One can write:

$$\frac{\partial P_S}{\partial x} = 0 \quad (G.148)$$

$$\frac{\partial P_S}{\partial z} = 0 \quad (G.149)$$

Therefore

$$\frac{\partial P}{\partial x} = \frac{\partial P_D}{\partial x} \quad (G.150)$$

and

$$\frac{\partial P}{\partial z} = \frac{\partial P_D}{\partial z} \quad (G.151)$$

that is:

x-component

$$LHS = -\frac{\partial P_D}{\partial x} - Q' \quad (G.152)$$

z-component:

$$LHS = -\frac{\partial P_D}{\partial z} - Q'' \quad (G.153)$$

Using the buoyancy term in the y-momentum Eqn. (2.31), the pressure is modified to dynamic-pressure.

G.10 NUSSELT-NUMBER

From Bird³³ (page 423)

$$dQ = h_{loc}(\pi D dz)(T_o - T_b) \longrightarrow dQ = h_{loc}P dz(T_w - T_b) \quad G.154$$

in which P: perimeter, $T_o = T_w = T_{wall}$

$$dQ = \left(\frac{\pi D^2}{4}\right) \rho C_P [v] dT_b \longrightarrow dQ = A_c \rho C_P \bar{W} dT_b \quad G.155$$

in which A_c = cross-sectional area

$$h_{loc} = \frac{A_c}{P} (C_P \mu) \left(\frac{\rho \bar{W}}{\mu}\right) \frac{dT_b}{(T_w - T_b) dz} \quad G.156$$

$$Nu_{loc} = \frac{h_{loc}(DE)}{k} = \frac{A_c}{P} \left(\frac{C_P \mu}{k}\right) \left(\frac{\rho \bar{W}(DE)}{\mu}\right) \frac{dT_b}{(T_w - T_b) dz} \quad G.157$$

$$Nu_{loc} = \frac{A_c}{P} (Pr)(Re) \frac{dT_b}{(T_w - T_b) dz} \quad G.158$$

$$Nu_{loc} = \frac{A_c}{DE \cdot P} \left(\frac{dT_b}{T_w - T_b}\right) = \frac{1}{\left(\frac{dz}{DE \cdot Re \cdot Pr}\right)} \quad G.159$$

$$\frac{dT_b}{T_w - T_b} = -\frac{d(T_w - T_b)}{T_w - T_b} = -d\left(\frac{T_w - T_b}{T_w - T_b}\right) = -d\theta_b \quad G.160$$

in which

$$\theta_b = \frac{T_w - T_b}{T_w - T_b} \quad G.161$$

also

$$\frac{dz}{DE \cdot Re \cdot Pr} = d\left(\frac{z}{DE \cdot Re \cdot Pr}\right) = dz^{**} \quad G.162$$

and from the definition $DE = 4 \frac{A_c}{P}$, one can write $\frac{A_c}{DE \cdot P} = \frac{1}{4}$

therefore

$$Nu_{loc} = -\frac{1}{4\theta_b} \frac{d\theta_b}{dz^{**}} \quad G.163$$

$$\int_0^{z^{**}} Nu_{loc} \cdot dz^{**} = -\frac{1}{4} \int_1^{\theta_b} \frac{d\theta_b}{\theta_b} \quad G.164$$

$$Nu_{m,T}Z^{**} = -\frac{1}{4} \ln \theta_b \quad \text{G.165}$$

$$Nu_{m,T}Z^{**} = \frac{1}{4} \ln \frac{1}{\theta_b} \quad \text{G.166}$$

$$Nu_{m,T} = \frac{1}{4Z^{**}} \ln \frac{1}{\theta_b} \quad \text{G.167}$$

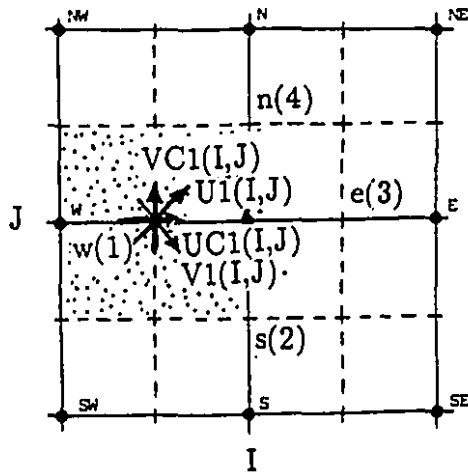


Fig. G.1

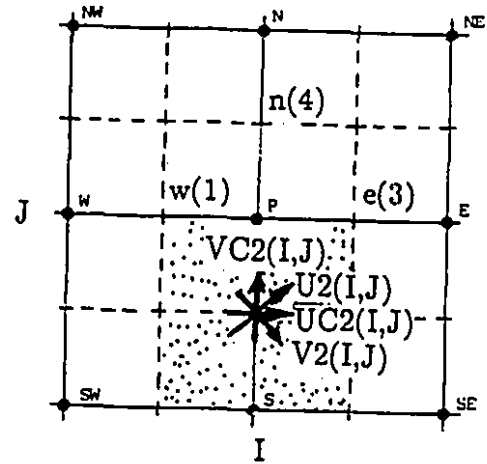


Fig. G.2

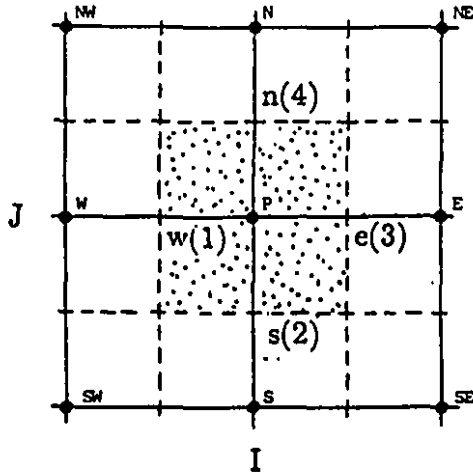


Fig. G.3

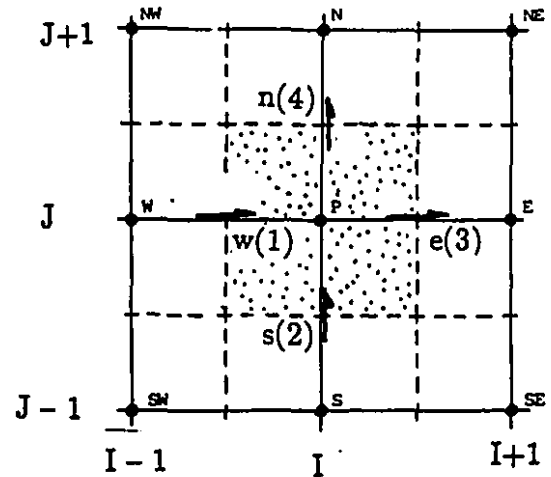


Fig. G.4

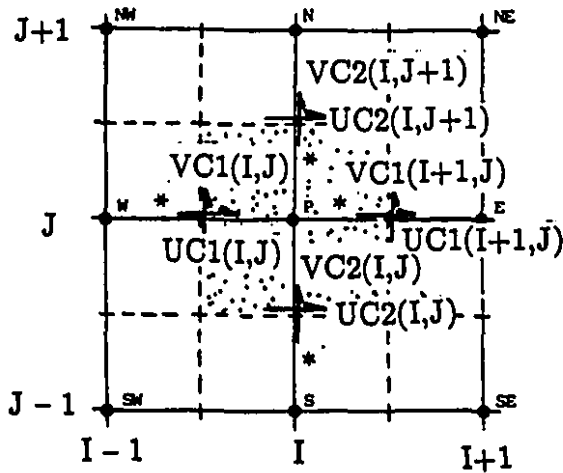


Fig. G.5

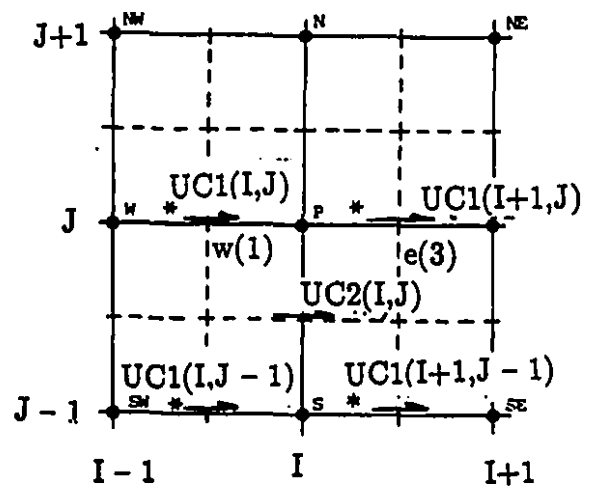


Fig. G.6

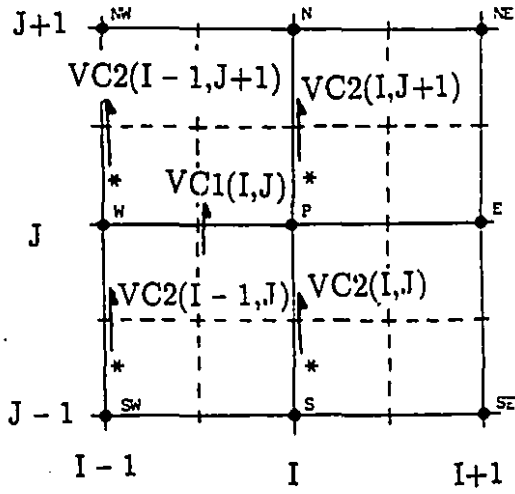


Fig. G.7

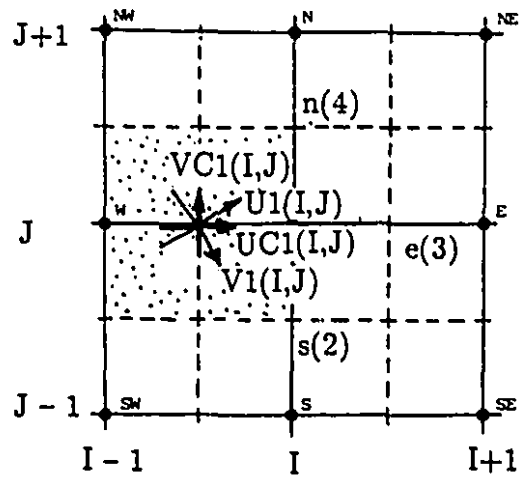


Fig. G.8

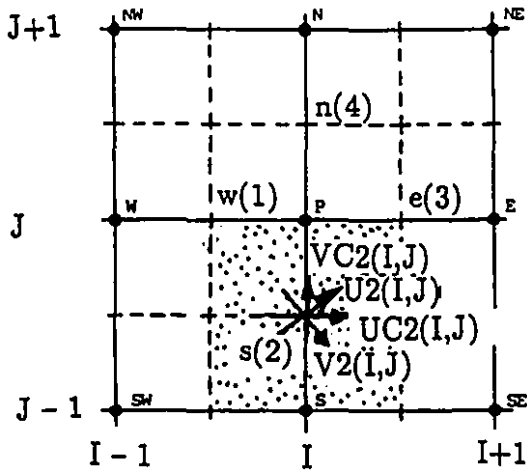


Fig. G.9

Range of variations of "I"
 for boundary control-volumes (@ J = 2 and J = M2)

J = 2 I = 3, L2

J = M2 I = 3, L2

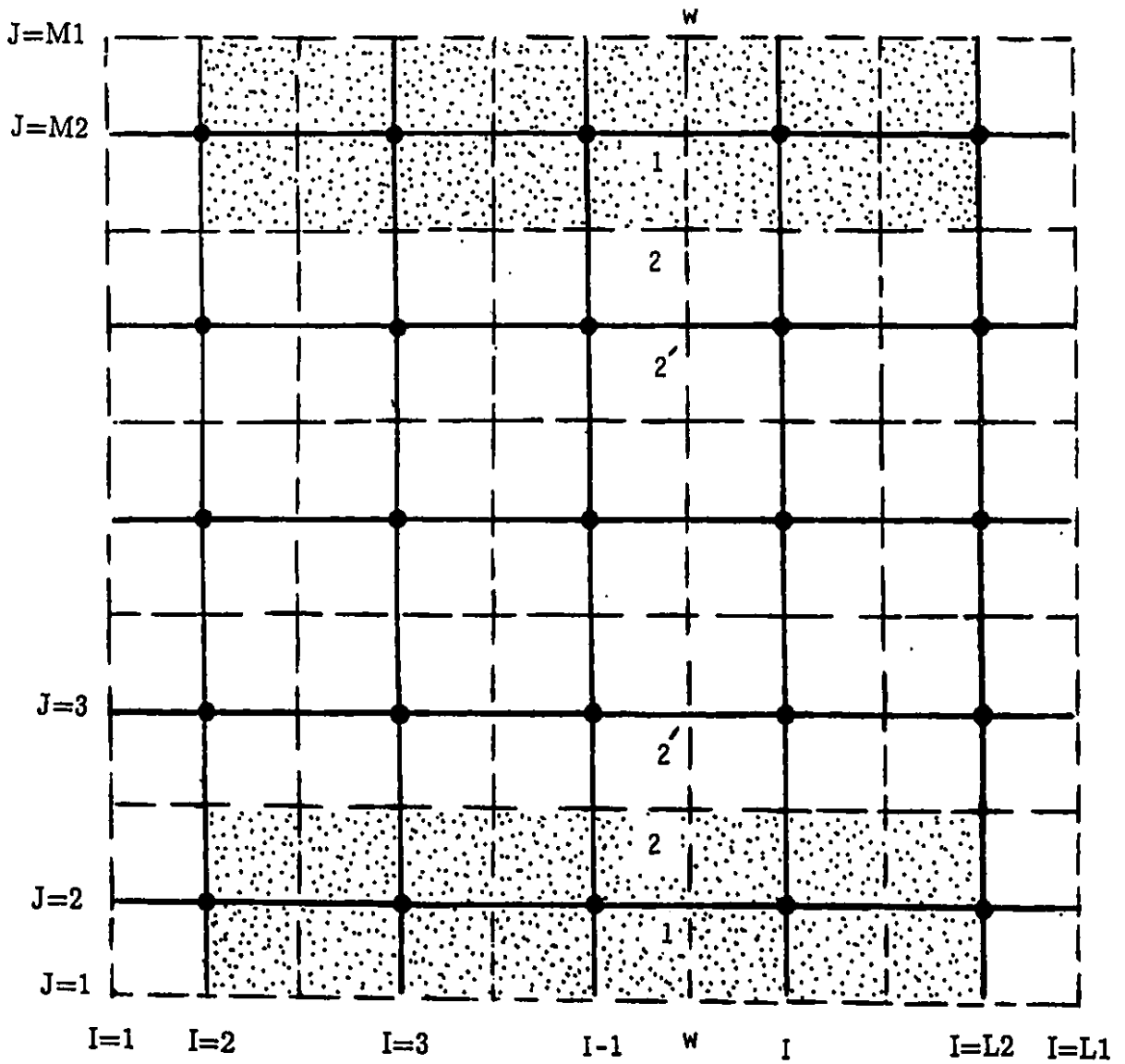


Fig. G.10

Range of variations of "J"

for boundary control-volumes @ $I = 2$ and $I = L2$

$I = 2$ $J = 3, M2$

$I = L2$ $J = 3, M2$

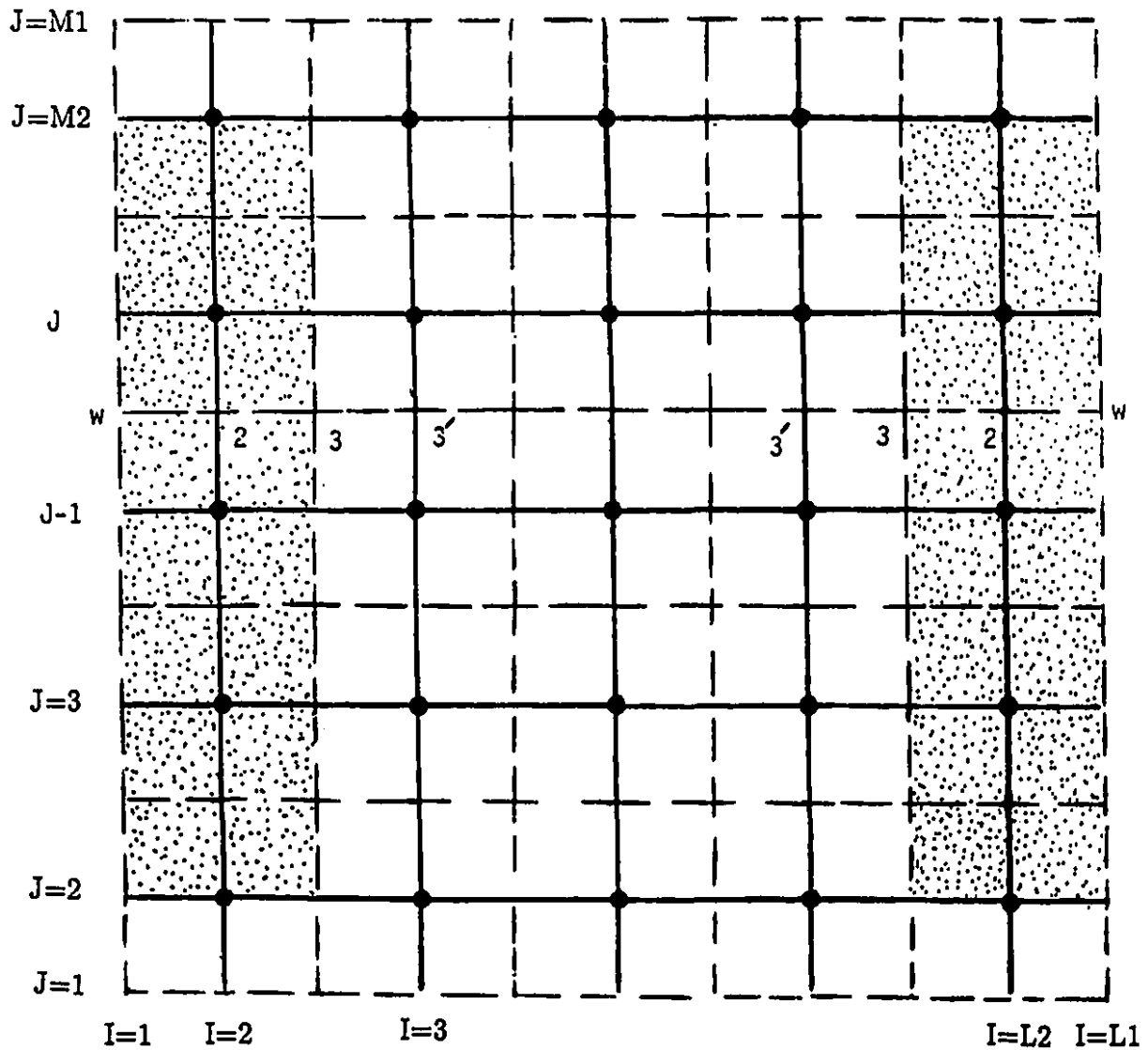
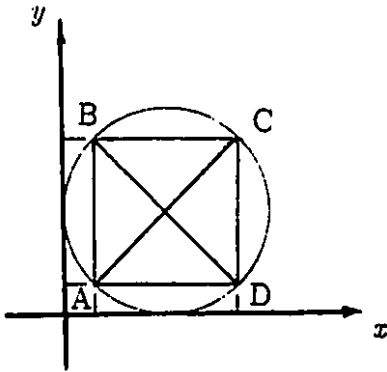


Fig. G.11

APPENDIX H
COMPUTER SOFTWARE

H.1 INPUT DATA AND FILE ALLOCATIONS FOR GRID PROGRAMMES

H.1.1 CIRCULAR-DUCT



$$\begin{aligned}
 A & \begin{cases} x = R(1 - \cos 45^\circ) \\ y = R(1 - \cos 45^\circ) \end{cases} \\
 B & \begin{cases} x = R(1 - \cos 45^\circ) \\ y = R(1 + \cos 45^\circ) \end{cases} \\
 C & \begin{cases} x = R(1 + \cos 45^\circ) \\ y = R(1 + \cos 45^\circ) \end{cases} \\
 D & \begin{cases} x = R(1 + \cos 45^\circ) \\ y = R(1 - \cos 45^\circ) \end{cases}
 \end{aligned}$$

EDIT AGRID.FOR OR BGRID.FOR PROGRAMMES:

FILES	AGRID.FOR:	BGRID.FOR:
	STAR 01	STAR 25
	STAR 02	STAR 26
	STAR 03	STAR 27
	STAR 04	STAR 28

/data

L1*	M1*	Tolerance	
0.2928932R	0.2928932R	0.2928932R	1.7071068R
1.7071068R	1.7071068R	1.7071068R	0.2928932R

1

R

/endrun

* This is for AGRID.FOR, for BGRID.FOR use (L1-1) & (M1-1)

EDIT PLOT.FOR PRIGRAMME:

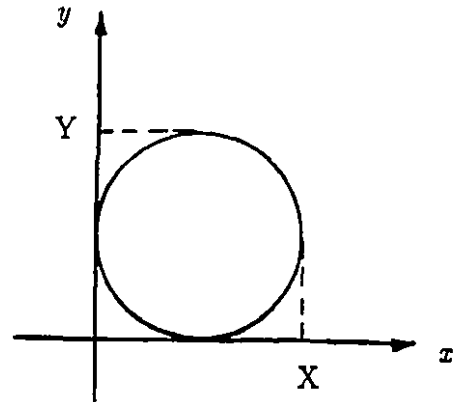
FOR $L1 \times M1 = 21 \times 21$

$$X = 6''$$

$$Y = \left(\frac{2R}{2R}\right) (6'') = 6''$$

$$\Delta X = \frac{6''}{21-1} = 0.3$$

$$\Delta Y = \frac{6''}{21-1} = 0.3$$



FILES FOR AGRID.FOR:

N(STAR 01) OLD

N(STAR 02) OLD

FOR BGRID.FOR:

N(STAR 25) OLD

N(STAR 26) OLD

PROGRAMME

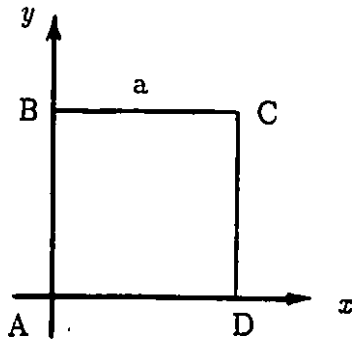
CALL PLOT(0.3, 0.3, -3)

CALL SCALE(X,6.0,441,1)

CALL SCALE(Y,6.0,441,1)

Note 1: numbers assigned to files are arbitrary.

H.1.2 SQUARE-DUCT



$$A \begin{cases} x = 0. \\ y = 0. \end{cases}$$

$$B \begin{cases} x = 0. \\ y = a \end{cases}$$

$$C \begin{cases} x = a \\ y = a \end{cases}$$

$$D \begin{cases} x = a \\ y = 0. \end{cases}$$

EDIT AGRID.FOR OR BGRID.FOR PROGRAMMES:

FILES	AGRID.FOR:	BGRID.FOR:
	STAR 05	STAR 29
	STAR 06	STAR 30
	STAR 07	STAR 31
	STAR 08	STAR 32

/data

L1*	M1*	Tolerance	
0.	0.	0.	a
a	a	a	0
2			

/endrun

* This is for AGRID.FOR, for BGRID.FOR use (L1-1) & (M1-1)

EDIT PLOT.FOR PRIGRAMME:

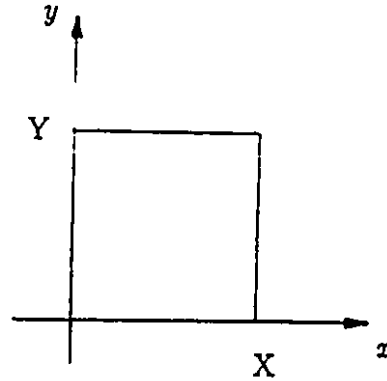
FOR $L1 \times M1 = 21 \times 21$

$$X = 6''$$

$$Y = \left(\frac{a}{a}\right) (6'') = 6''$$

$$\Delta X = \frac{6''}{21-1} = 0.3$$

$$\Delta Y = \frac{6''}{21-1} = 0.3$$



FILES FOR AGRID.FOR:

N(STAR 05) OLD

N(STAR 06) OLD

FOR BGRID.FOR:

N(STAR 29) OLD

N(STAR 30) OLD

PROGRAMME

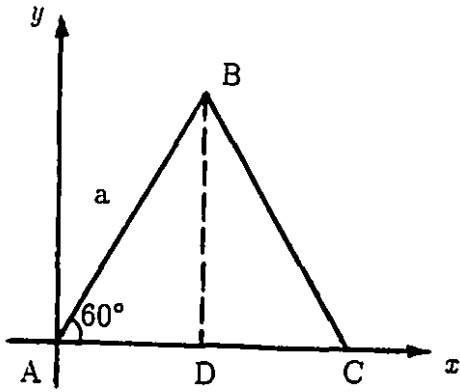
CALL PLOT(0.3, 0.3, -3)

CALL SCALE(X,6.0,441,1)

CALL SCALE(Y,6.0,441,1)

Refer to note 1 on page H.3.

H.1.3 TRIANGULAR-DUCT



$$A \begin{cases} x = 0. \\ y = 0. \end{cases}$$

$$B \begin{cases} x = a/2 \\ y = a \cdot \sin 60^\circ \end{cases}$$

$$C \begin{cases} x = a \\ y = 0. \end{cases}$$

$$D \begin{cases} x = a/2 \\ y = 0. \end{cases}$$

EDIT AGRID.FOR OR BGRID.FOR PROGRAMMES:

FILES	AGRID.FOR	BGRID.FOR
	STAR 09	STAR 33
	STAR 10	STAR 34
	STAR 11	STAR 35
	STAR 12	STAR 36

/data

L1*	M1*	Tolerance	
0.	0.	a/2	0.8660254a
a	0	a/2	0
3			
a			

/endrun

* This is for AGRID.FOR, for BGRID.FOR use (L1-1) & (M1-1)

EDIT PLOT.FOR PRIGRAMME:

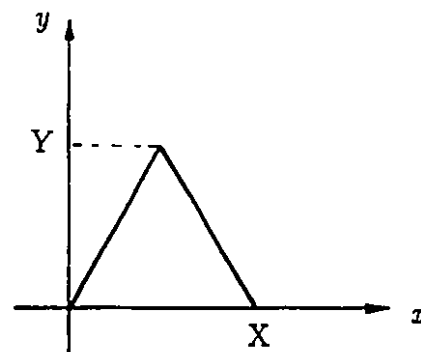
FOR $L1 \times M1 = 21 \times 21$

$$X = 6''$$

$$Y = \left(\frac{0.8660254a}{a} \right) (6'') = 5.1961524'' \quad \text{say } 5.2''$$

$$\Delta X = \frac{6''}{21 - 1} = 0.3$$

$$\Delta Y = \frac{5.2''}{21 - 1} = 0.26$$



FILES FOR AGRID.FOR:

N(STAR 09) OLD

N(STAR 10) OLD

FOR BGRID.FOR:

N(STAR 33) OLD

N(STAR 34) OLD

PROGRAMME

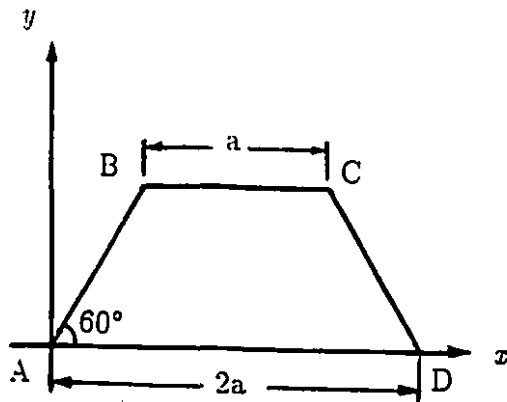
CALL PLOT(0.3, 0.26, -3)

CALL SCALE(X,6.0,441,1)

CALL SCALE(Y,5.2,441,1)

Refer to note 1 on page H.3.

H.1.4 TRAPEZOIDAL-DUCT



$$\begin{aligned}
 A & \begin{cases} x = 0. \\ y = 0. \end{cases} \\
 B & \begin{cases} x = a/2 \\ y = a \cdot \sin 60^\circ \end{cases} \\
 C & \begin{cases} x = 3a/2 \\ y = a \cdot \sin 60^\circ \end{cases} \\
 D & \begin{cases} x = 2a \\ y = 0. \end{cases}
 \end{aligned}$$

EDIT AGRID.FOR OR BGRID.FOR PROGRAMMES:

FILES	AGRID.FOR	BGRID.FOR
	STAR 13	STAR 37
	STAR 14	STAR 38
	STAR 15	STAR 39
	STAR 16	STAR 40

/data

L1*	M1*	Tolerance
0.	0.	a/2 0.8660254a
3a/2	0.8660254a	2a 0.
4		
tan 60°		
/endrun		

* This is for AGRID.FOR, for BGRID.FOR use (L1-1) & (M1-1)

EDIT PLOT.FOR PRIGRAMME:

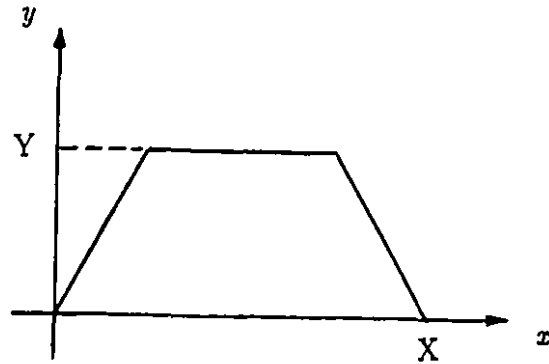
FOR $L1 \times M1 = 21 \times 21$

$$X = 12''$$

$$Y = \left(\frac{0.8660254a}{2a} \right) (12'') = 5.1961524 \text{ say } 5.2''$$

$$\Delta X = \frac{12''}{21 - 1} = 0.6$$

$$\Delta Y = \frac{5.2''}{21 - 1} = 0.26$$



FILES FOR AGRID.FOR

N(STAR 13) OLD

N(STAR 14) OLD

FOR BGRID.FOR

N(STAR 37) OLD

N(STAR 38) OLD

PROGRAMME

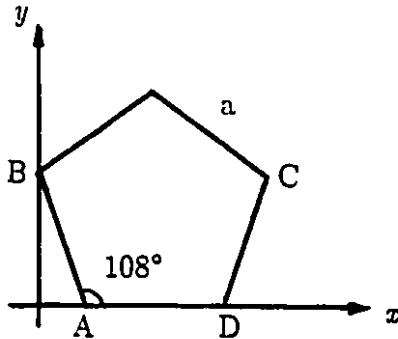
CALL PLOT(0.6, 0.26, -3)

CALL SCALE(X,12.0,441,1)

CALL SCALE(Y,5.2,441,1)

Refer to note 1 on page H.3.

H.1.5 PENTAGONAL-DUCT



$$A \begin{cases} x = a \cdot \cos 72^\circ \\ y = 0. \end{cases}$$

$$B \begin{cases} x = 0. \\ y = a \cdot \cos 18^\circ \end{cases}$$

$$C \begin{cases} x = a(1. + 2 \cdot \cos 72^\circ) \\ y = a \cdot \cos 18^\circ \end{cases}$$

$$D \begin{cases} x = a(1. + \cos 72^\circ) \\ y = 0. \end{cases}$$

EDIT AGRID.FOR OR BGRID.FOR PROGRAMMES:

FILES	AGRID.FOR	BGRID.FOR
	STAR 17	STAR 41
	STAR 18	STAR 42
	STAR 19	STAR 43
	STAR 20	STAR 44

/data

L1*	M1*	Tolerance	
0.3090169a	0.	0.	0.9510565a

1.6180338a	0.9510565a	1.3090169a	0.
------------	------------	------------	----

5

tan 72°

tan 36°

a

/endrun

* This is for AGRID.FOR, for BGRID.FOR use (L1-1) & (M1-1)

EDIT PLOT.FOR PRIGRAMME:

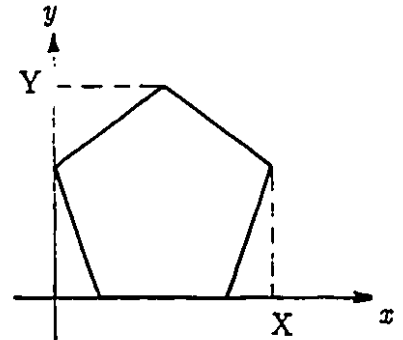
FOR $L1 \times M1 = 21 \times 21$

$$X = 6''$$

$$Y = \left(\frac{1.5388417a}{1.6180340a} \right) (6'') = 5.7063388'' \quad \text{say } 5.71''$$

$$\Delta X = \frac{6''}{21 - 1} = 0.3$$

$$\Delta Y = \frac{5.71''}{21 - 1} = 0.2855$$



FILES FOR AGRID.FOR

FOR BGRID.FOR

N(STAR 17) OLD

N(STAR 41) OLD

N(STAR 18) OLD

N(STAR 42) OLD

PROGRAMME

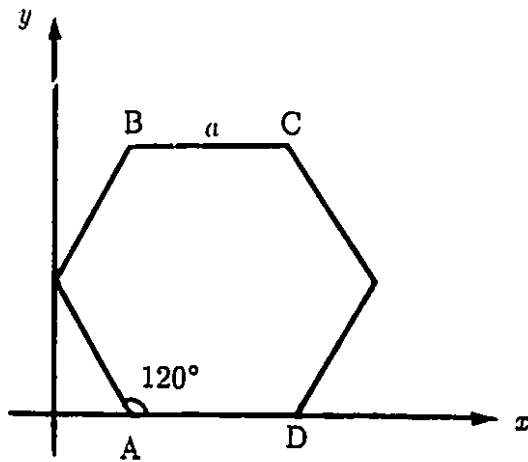
CALL PLOT(0.3, 0.2855, -3)

CALL SCALE(X,6.00,441,1)

CALL SCALE(Y,5.71,441,1)

Refer to note 1 on page H.3.

H.1.6 HEXAGONAL-DUCT



$$\begin{aligned}
 A & \begin{cases} x = a/2 \\ y = 0. \end{cases} \\
 B & \begin{cases} x = a/2 \\ y = a \cdot \tan 60^\circ \end{cases} \\
 C & \begin{cases} x = 3a/2 \\ y = a \cdot \tan 60^\circ \end{cases} \\
 D & \begin{cases} x = 3a/2 \\ y = 0. \end{cases}
 \end{aligned}$$

EDIT AGRID.FOR OR BGRID.FOR PROGRAMMES:

FILES	AGRID.FOR	BGRID.FOR
	STAR 21	STAR 45
	STAR 22	STAR 46
	STAR 23	STAR 47
	STAR 24	STAR 48

/data

L1* M1* Tolerance

a/2 0. a/2 1.7320508a

3a/2 1.7320508a 3a/2 0.

6

tan 60°

a

/endrun

* This is for AGRID.FOR, for BGRID.FOR use (L1-1) & (M1-1)

EDIT PLOT.FOR PRIGRAMME:

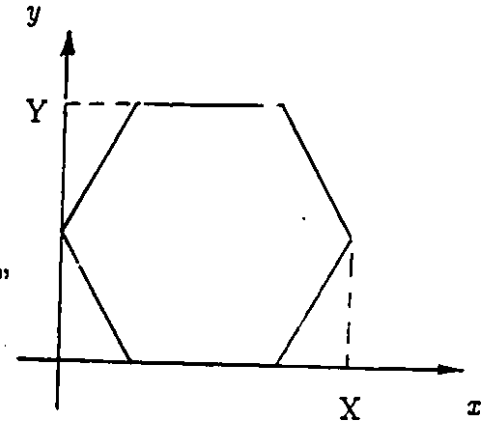
FOR $L1 \times M1 = 21 \times 21$

$$X = 6''$$

$$Y = \left(\frac{1.7320508}{2} \right) (6'') = 5.1961481'' \quad \text{say } 5.2''$$

$$\Delta X = \frac{6''}{21 - 1} = 0.3$$

$$\Delta Y = \frac{5.2''}{21 - 1} = 0.26$$



FILES FOR AGRID.FOR

FOR BGRID.FOR

N(STAR 21) OLD

N(STAR 45) OLD

N(STAR 22) OLD

N(STAR 46) OLD

PROGRAMME

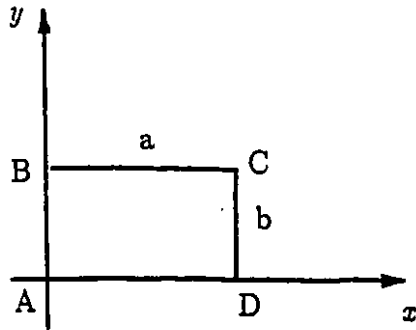
CALL PLOT(0.3, 0.26, -3)

CALL SCALE(X,6.00,441,1)

CALL SCALE(Y,5.2,441,1)

Refer to note 1 on page H.3.

H.1.7 RECTANGULAR-DUCTS



$$A \begin{cases} x = 0. \\ y = 0. \end{cases}$$

$$B \begin{cases} x = 0. \\ y = b \end{cases}$$

$$C \begin{cases} x = a \\ y = b \end{cases}$$

$$D \begin{cases} x = a \\ y = 0. \end{cases}$$

EDIT AGRID.FOR OR BGRID.FOR PROGRAMMES:

FILES	AGRID.FOR:	EGRID.FOR:
	STAR 100	STAR 200
	STAR 101	STAR 201
	STAR 102	STAR 202
	STAR 103	STAR 203

/data

L1*	M1*	Tolerance	
0.	0.	0.	b
a	b	a	0

/endrun

* This is for AGRID.FOR, for BGRID.FOR use (L1-1) & (M1-1)

AR = 1.5

EDIT PLOT.FOR PROGRAMME:

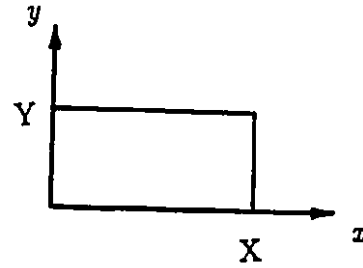
FOR L1 × M1 = 21 × 21

$$X = 6''$$

$$Y = \left(\frac{b}{a}\right)(6'') = \left(\frac{1}{1.5}\right)(6'') = 4''$$

$$\Delta X = \frac{6''}{21-1} = 0.3''$$

$$\Delta Y = \frac{4''}{21-1} = 0.2''$$



FILES FOR AGRID.FOR:

N(STAR 100) OLD

N(STAR 101) OLD

FOR BGRID.FOR:

N(STAR 200) OLD

N(STAR 201) OLD

PROGRAMME

CALL PLOT(0.3, 0.2, -3)

CALL SCALE(X,6,441,1)

CALL SCALE(Y,4,441,1)

Refer to note 1 on page H.3.

AR = 2.0

EDIT PLOT.FOR PRIGRAMME:

FOR $L1 \times M1 = 21 \times 21$

$$X = 6''$$

$$Y = \left(\frac{b}{a}\right) (6'') = \left(\frac{1}{2}\right) (6'') = 3''$$

$$\Delta X = \frac{6''}{21 - 1} = 0.3''$$

$$\Delta Y = \frac{3''}{21 - 1} = 0.15''$$

FILES	FOR AGRID.FOR:	FOR BGRID.FOR:
	N(STAR 104) OLD	N(STAR 204) OLD
	N(STAR 105) OLD	N(STAR 205) OLD

PROGRAMME

CALL PLOT(0.3, 0.15, -3)

CALL SCALE(X,6,441,1)

CALL SCALE(Y,3,441,1)

Refer to note 1 on page H.3.

Note: The sequence of steps followed on MUSIC-A operating system are as follows:

- (i) ZETAPURE
- (ii) EDIT AGRID.FOR OR BGRID.FOR
- (iii) EXECUTE AGRID.FOR OR BGRID.FOR
- (iv) EDIT PLOT.FOR
- (v) EXECUTE PLOT.FOR
- (vi) ZETASUBMIT

H.2 SEQUENCE OF STEPS ON MUSIC-A OPERATING SYSTEM FOR GRID GENERATION

- (i) ZETAPURGE
- (ii) EDIT AGRID.FOR OR BGRID.FOR
- (iii) EXECUTE AGRID.FOR OR BGRID.FOR
- (iv) EDIT PLOT.FOR
- (v) EXECUTE PLOT.FOR
- (vi) ZETASUBMIT

H.3 SEQUENCE OF STEPS ON MUSIC-A AND "OS" OPERATING SYSTEMS FOR SOLUTION OF DISCRETIZATION EQUATIONS

- (i) EDIT STAR30.JCL
- (ii) EDIT STAR30.FOR
- (iii) SUBMIT STAR30.JCL (ENTER "OS" PASSWORD)
- (iv) DISPLAY "OS" OUTPUT (ON MUSIC-"A") (Select View and/or Print)

H.4 A BRIEF USER'S GUIDE (INPUT INSTRUCTION) FOR STAR30.FOR PROGRAMME

- (a) Refer to SUPPLY1 subroutine:
 - (i) KK: choose desired geometry by its appropriate number specified in the programme
 - (ii) DSI: select axial-step size
 - (iii) IIM: number of planes in axial-direction
 - (iv) IIM1, IIM2, IIM3, IIM4 & IIM5: plane numbers for which printing of results re

desired

- (v) REL1 to REL10: relaxation-factors appropriately selected for the solution of their corresponding discretization equations
- (vi) DP: an initial guess for the pressure-gradient in the axial-direction
- (vii) IE: (1) for fluid-dynamics & heat-transfer (Newtonian)
(2) for fluid-dynamics & heat-transfer (non-Newtonian)
(3) for polymerization
- (viii) WINLET: specify duct inlet uniform velocity
TINLET: specify duct inlet uniform temperature
TWALL: specify duct wall temperature
NX: specify flow behaviour index (power-law exponent)
RHOINLET: specify fluid density at duct inlet
SPHTIN: specify fluid specific-heat at duct inlet
SPHTW: specify fluid specific-heat at duct wall
VISCIN: specify fluid viscosity at duct inlet
CONDIN: specify fluid thermal conductivity at duct inlet
- (b) Refer to PROPER subroutine
Make appropriate changes as required.
- (c) Select either SUPPLY2 or SUPPLY3 in the main programme
Make appropriate changes for the values of relaxation-factors inside SUPPLY2 or SUPPLY3 subroutines as required.
- (d) EDIT STAR30.JCL for file numbers as related to BGRID.FOR programme.

H.5 LIST OF COMPUTER-PROGRAMMES

- (i) BGRID.FOR
- (ii) PLOT.FOR
- (iii) STAR30.FOR
- (iv) GRAPH1.SAS

Note:

The computer programmes are available on a diskette and can be obtained from the following address on request:

Professor Arun S. Mujumdar,
Department of Chemical Engineering,
McGill University,
3480 University Street,
Montreal, Quebec,
Canada H3A 2A7